Coastal Evolution of the Rangitāiki Plains, Bay of Plenty, Aotearoa-New Zealand

A thesis

submitted in partial fulfilment.

of the requirements for the degree

of

Master of Science (Research) in Earth Sciences

At

The University of Waikato

By

Bailey Rackham

THE UNIVERSITY OF
WAIKATO
Te Whare Wānanga o Waikato

2025

Abstract

The Rangitāiki Plains is a tectonically active alluvial plain in the Eastern Bay of Plenty, New Zealand. Throughout the mid-late Holocene (8 ka to present), the Rangitāiki Plains have undergone substantial geomorphological change, with the coastline prograding approximately 10 km over the past 6.5 ka, leaving relic shoreline features known as beach ridges. Previous studies of the Rangitāiki Plains have utilised tephrochronology and radiocarbon dating to determine the ages of several palaeoshorelines. These dates provided minimum ages for beach ridges and resulted in aging constraints; furthermore, limited textural and geochemical characterisation of beach ridges has hampered understanding of sediment provenance and reworking changes. Addressing these research gaps is important as this knowledge is especially relevant in coastal management, modern climate change, and increasing anthropogenic impacts on the coastline.

Optically Stimulated Luminescence (OSL) dating on the Rangitāiki Plains produced older beach ridge ages than those derived via tephrochronology. OSL dating also showed that beach ridge ages coincided with volcanic eruption events. The OSL progradation rates extend to much older time frames than those based on tephrochronology, starting at 7.6 ka rather than 5.5 ka. New data concludes a prominent progradation peak up to 43.03 m yr^{-1} between 5.202±0.368 ka and 5.187±0.447 ka, around the time of the Whakatāne eruption. By 4 ka, progradation had slowed to only 1.14 m yr^{-1}, suggesting that longshore drift occurred earlier than previously calculated (2 ka), or that progradation slowed before longshore drift commenced. XRF and XRD analysis of sediments from Rangitāiki Plains confirms that beach ridge sediments comprise of intermediate igneous sediments that have been tephra fingerprinted to the Taupō Volcanic Zone.

Acknowledgements

First, I would like to thank the University of Waikato and University of Newcastle Partnership Seed Fund for funding this project and my supervisors, Dr Andrew La Croix and Dr Rafael Cabral Carvalho. You provided me with a project I loved and resonated deeply with my hometown, Whakatāne. I could not have asked for anything better. I appreciate your guidance and patience; I could not have completed this thesis without your encouragement and feedback.

Secondly, I would like to thank the other University of Waikato staff who helped me accomplish this study, including Dr Deonie Castle, Kirsty Vincent, and Annette Rodgers, whose knowledge of technical equipment and training was invaluable. I cannot express how grateful I am for your help; my thesis would have been impossible without you.

I would also like to thank Dave Gardiner (who might as well have been my third supervisor). Dave helped me operate the GPR, addressed my ArcGIS struggles, and was there in both Whakatāne and Stuarts Point to conduct fieldwork with me. Dave also ensured I got cake on my birthday while out of the country doing fieldwork. I appreciate your friendship, time and effort.

Following Dave, I would also like to thank Toshiyuki Kitazawa for his help during the New Zealand and Australian fieldwork and Toru Tamura for promptly undertaking OSL analysis on my samples.

I would also like to thank all my office buddies in F.2.02: Josh, Sarah, Nicole, Charlotte, Christine, and my other university friends, Zane, Kyra and Vinay. I could not have asked for better people to complete my studies with. Everyone is kind, understanding of the postgraduate struggles, and here for a laugh to cheer each other up. They also dealt with my computer rage and editing of my thesis. As Josh says, “He is the G.O.A.T. who took time out of his busy day to help out.”

To my other friends and family, thank you for your endless support. To Amy and Jade, you have been by my side throughout my undergraduate and postgraduate degrees. I could not have asked for better friends, thank you. To my family, Mum, Dad, Luke, and Obi, thank you for helping me survive my university career. I cherished my time visiting home and the love and support you provided me. I would also like to acknowledge my family, who did not get to see me finish my university career: Nana, Brady, Zane, Grandma and Granddad. I know you would be proud of me.

Contents

List of Figures

List of Tables

List of Equations

Chapter 1:
Introduction and Literature Review

1.1. Introduction

The Rangitāiki Plains is a tectonically active alluvial plain in the Eastern Bay of Plenty, New Zealand. Throughout the mid-late Holocene (8 ka to present), the region has undergone substantial geomorphological change (Figure 1.1). The coastline has prograded approximately 10 km over the past 6.5 ka, leaving relic shoreline features preserved in the sedimentary record (Beanland & Berryman, 1992). These features, whether wave or wind-formed, are referred to as prograded or stranded beach ridges (Otivos, 2000). These preserved beach ridge systems hold key sedimentary indicators that can be utilised to reconstruct past environmental conditions, offering insights into shoreline evolution, sediment supply, storm frequency, and sea-level fluctuations (Dougherty *et al.*, 2019).

Previous studies of the Rangitāiki Plains identified the primary cause of progradation as the subsiding Whakatāne Graben. The subsiding graben created accommodation space, which was infilled by abundant volcanic material transported by rivers (Beanland & Berryman, 1992; Pullar & Selby, 1971). Tephrochronology and radiocarbon dating were used in past studies to determine the ages of several palaeoshorelines (Pullar & Selby, 1971). Several beach ridge sets remain undated, or their age data remains constrained to tephrochronological correlations, resulting in gaps in the reconstruction of the Rangitāiki Plains evolution. Additionally, limited textural and geochemical characterisation of beach ridges has hampered understanding of sediment provenance and reworking processes occurring on the Rangitāiki Plains.

To address these limitations, Light Detection and Ranging (LiDAR), Ground-Penetrating Radar (GPR), Optically Stimulated Luminescence (OSL) dating, and geochemical analyses (X-ray fluorescence [XRF] and X-ray diffraction [XRD]) were integrated to investigate the timing, rates, and controlling mechanisms of the mid-late Holocene coastal progradation on the Rangitāiki Plains. These techniques help determine the age of prograding beach ridges and image their surface and subsurface structure. LiDAR for the Rangitāiki Plains uncovers the spatial extent of beach ridges, GPR provides subsurface stratigraphic imaging, OSL dating offers direct age estimates for the beach ridge deposits, XRF and XRD provide evidence of sediment type and provenance, and grain size explains sediment transport and deposition conditions. Together,

these techniques can improve our understanding of coastal evolution and beach ridge development across the Rangitāiki plains.

Addressing these research gaps is important as this knowledge is especially relevant in coastal management, modern climate change, and increasing anthropogenic impacts on the coastline. The Rangitāiki Plains are a low-lying, actively subsiding graben prone to flooding. The sandy beaches protect the Rangitāiki Plains from waves, storms, and flooding, making them an important feature in the preservation of the current coastal setting (Vousdoukas *et al.*, 2020). Coastal inundation from sea-level rise and shoreline erosion, and its effects on housing, resources, infrastructure, the economy, and local ecology, is becoming increasingly concerning to communities (Ali *et al.*, 2022; Dolan & Walker, 2006). A more detailed understanding of mid-late Holocene coastal dynamics can help predict future shoreline behaviour to inform coastal management and planning strategies in the Rangitāiki Plains and New Zealand.

By applying LiDAR, OSL, GPR and geochemical analysis techniques to the Rangitāiki Plains, this investigation seeks to address the following research questions:

1) What are the ages of the major beach ridge sets on the Rangitāiki Plains, and does OSL dating differ from existing tephrochronological estimates?
2) How do estimates of progradation rates based on new OSL age data compare to progradation rates estimated primarily based on tephrochronology? How do historical progradation rates compare with modern shoreline progradation rates?
3) Does XRF and XRD data help differentiate sediment sources, and how they changed through time?

1.2. Thesis Structure

This thesis is presented in a journal article format and structured into three main chapters. Chapter One introduces the study area and reviews the literature on relevant coastal sedimentary processes, the geomorphic history of the Rangitāiki Plains, and beach ridge analysis methods. Chapter Two is written in manuscript format and forms the core of the research. Chapter Three summarises the study's overall conclusions, links the conclusions to the research questions, and suggests directions for future research.

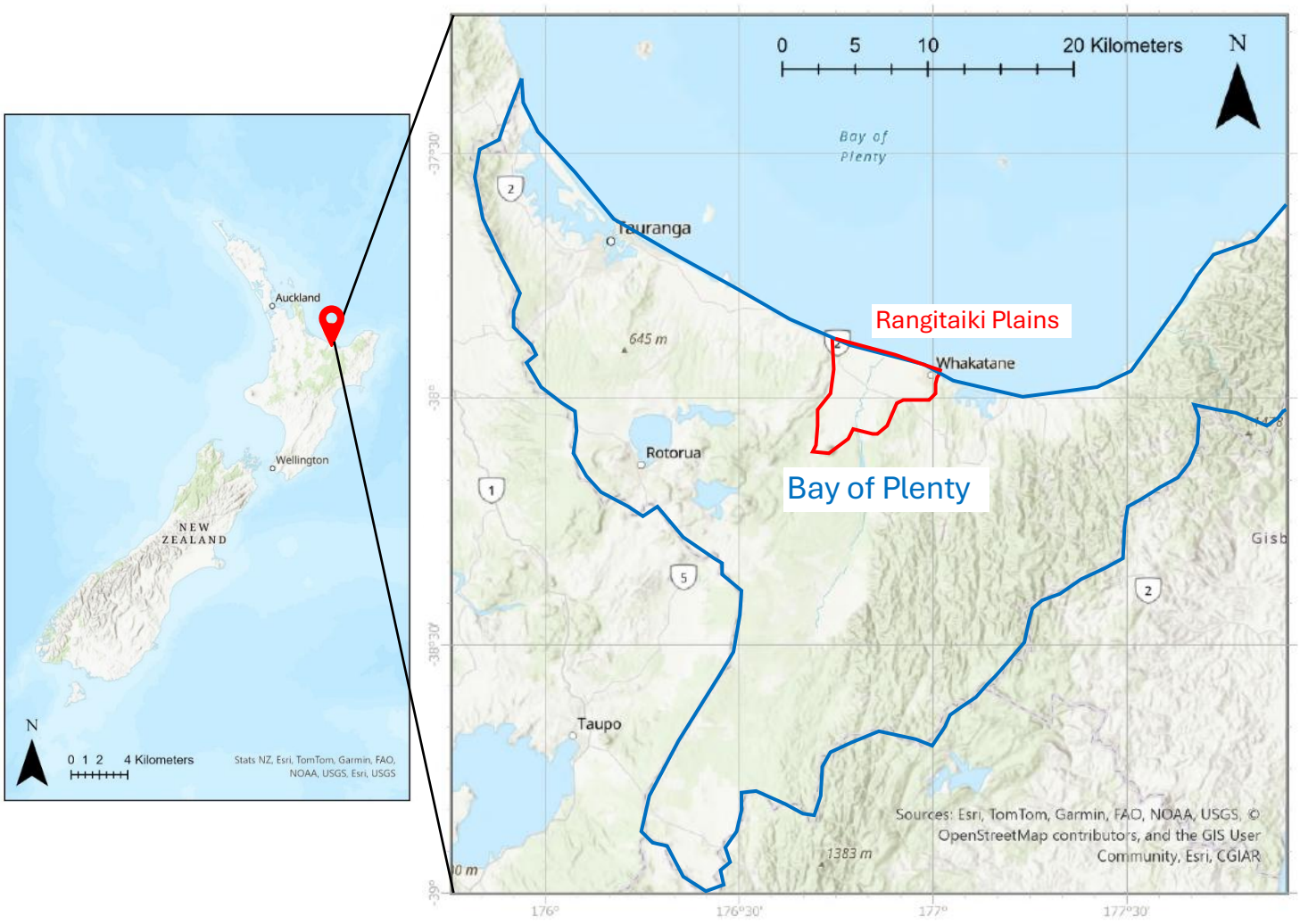

Figure 1.1: Location of the Rangitaiki Plains within the Bay of Plenty Region of New Zealand.

1.3. Background Literature

1.3.1. The State of Coastlines

Coastlines are dynamic natural transitions where land meets sea. The morphology and evolution of coastlines can vary depending on accommodation space and sediment supply changes driven by astronomical, geological and oceanographic factors (Muto & Steel, 1987). These factors cause all coastlines to exist in one of three states: equilibrium/stable, transgressional, or regressional. Equilibrium coastlines are characterised by stability and experience little movement over time (Muto & Steel, 1987). Such conditions occur when a coastline's constructive and destructive forces are balanced. Conversely, transgression refers to the landward shift of a coastline over time, resulting in the flooding of previously dry land (Bokuniewicz *et al.*, 2019). A regressing

coastline occurs when the land-sea boundary shifts seaward over time (Bokuniewicz *et al.*, 2019). When regression occurs due to high sediment accumulation, this is called progradation. Under certain progradation conditions, sediment can accumulate into new, distinct structures like seaward-building beach ridges.

Beach ridges are semi-shore-parallel wave or wind-built sediment accumulations deposited on coastlines (Otvos, 2000). These ridges develop as successive waves transport sediment onto the upper beach and deposit material near the high tide or storm limit, from aeolian-transported sand becoming trapped by vegetation, or a combination of both processes (Otvos, 2000). Beach ridges typically form during relative sea-level stability or rise accompanied by positive sediment budget phases (Taylor & Stone, 1996). When a shoreline undergoes significant progradation, beach ridges can become isolated from the active beach zone, forming stranded beach ridges (Otvos, 2000). Formation of these prograding beach ridges, like those seen on the Rangitāiki Plains, depends on several factors, including the eustatic and relative sea levels and sediment supply.

1.3.2. Eustatic and Relative Sea Level

Both eustatic and relative sea levels are critical in determining the state of a coastline. Eustatic, or absolute, sea level refers to the theoretical average global sea level height (Rovere *et al.*, 2016). Changes in eustatic sea level occur due to gravitational differences, changes in the volume of the world's oceans, or altered topography of ocean basins. These variations are typically driven by global-scale processes such as glacial-interglacial cycles, isostatic adjustments, and thermal expansion (Rovere *et al.*, 2016).

Conversely, relative sea level, also known as local sea level, refers to the height of the ocean surface in relation to a specific geographic location. Large-scale eustatic sea-level changes and regional factors influence relative sea levels, such as glacial isostatic adjustments, smaller-scale geological isostatic adjustments and tectonic movements. These changes lead to local coastline transgression, regression or stabilisation (Rovere *et al.*, 2016). Changes in eustatic and relative sea levels in response to the last glaciation event generated the oceanic conditions for the formation of the Rangitāiki Plains.

1.3.2.1. Glacial Eustacy and Isostatic Adjustment

Glacial cycles cause eustatic sea-level changes by altering global ocean volumes. These cycles consist of alternating long-term phases: colder glacial periods, with widespread ice sheets, and warmer interglacial periods, with reduced ice coverage (Berger & Loutre, 2010; Peltier, 1999). During glacial periods, eustatic sea level falls and coastlines regress, as colder temperatures

cause ocean water to be stored in expanding continental ice sheets (Rovere *et al.*, 2016). Conversely, continental ice sheets and glaciers melt during interglacial periods, returning water to the ocean, causing sea level to rise and shorelines to either transgress or prograde depending on sediment availability (Peltier, 1999; Rovere *et al.*, 2016). The combination of thermal expansion and glacial changes in water storage can cause the sea level to fluctuate by approximately 120 m over each glaciation cycle, causing significant global coastline shifts (Peltier, 1999).

Glacial cycles are also the primary drivers of changes in Earth's isostasy and relative sea levels. Isostatic adjustments refer to vertical movements of the Earth's crust resulting from changes in surface loading, such as the accumulation or removal of ice, water, or sediment. These adjustments occur because the crust's weight influences the crust's buoyancy on the semi-fluid mantle beneath (Rovere *et al.*, 2016). During glacial periods, the accumulation of large ice sheets adds significant weight to the continents, causing the crust to subside slowly into the mantle (Rovere *et al.*, 2016). The mantle material diverges to the ice sheet's margins, causing land uplift. These conditions cause transgression in some regions of the globe and shoreline regression in others.

1.3.2.2. Geological Eustacy and Tectonic Activity

Large-scale geological isostatic adjustments also affect the eustatic sea level. Geological isostatic processes occur predominantly from sea-floor spreading, but can also occur from large-scale sediment deposition and erosion (Rovere *et al.*, 2016). Sea-floor spreading occurs at divergent plate boundaries, where oceanic ridges form, altering the ocean basins' depth and shape (Rovere *et al.*, 2016). When oceanic ridges grow in size, they displace water by reducing the overall volume of the ocean basins, leading to an increase in eustatic sea level and shoreline transgression (Rovere *et al.*, 2016). Some of this displacement is combated by decreased buoyancy of the Earth's crust due to the accumulation of new oceanic crust material, causing crustal subsidence.

Tectonic activity is one of the most significant drivers of relative sea level change due to its ability to affect vertical land movement. Processes such as subsidence and uplift can significantly alter the elevation of coastal regions relative to the sea surface, resulting in localised sea-level changes. When tectonic subsidence occurs in coastal areas, the relative sea level increases. The rising sea level can transgress the coastline landwards, inundating low-lying areas and creating new accommodation space. This space may infill where the sediment budget permits, allowing the coastline to prograde seaward again, such as the Rangitāiki Plains (Rovere *et al.*, 2016). However, in cases where sediment supply is limited or disrupted, the coastline will continue to

retreat inland, resulting in long-term coastal erosion and land loss (Rovere *et al.*, 2016). Tectonic activity is one of the significant drivers of mid-late Holocene progradation on the Rangitāiki Plains.

1.3.2.3. New Zealand Sea Level Changes

New Zealand and the Rangitāiki Plains have experienced eustatic and relative sea-level variations throughout geological time. Reconstructions of Holocene sea levels in New Zealand have relied on the foundational work of Gibb (1986), who discovered that post-glacial sea-level rose from approximately 120m below present-day averages to reach its maximum and stabilised to present-day levels at approximately 6.5 ka. Clement *et al.* (2016) recently combined several previously isolated studies to produce a more comprehensive understanding of Holocene sea-level changes across New Zealand (Figure 1.2). Clement *et al.* (2016) found that the New Zealand Holocene marine transgression, the post-glacial rise in sea level, peaked earlier in the North Island than in the South Island. In the North Island, the highstand began around 8.1 to 7.34 ka, reaching up to 3 m above present sea level, dropping to present-day sea level around 4 ka (Clement *et al.*, 2016). In contrast, the South Island experienced its highstand later, around 7 to 6.4 ka, and the magnitudes were generally lower. For example, the Otago coast reached a maximum of approximately 1.4 m above present sea level (Clement *et al.*, 2016).

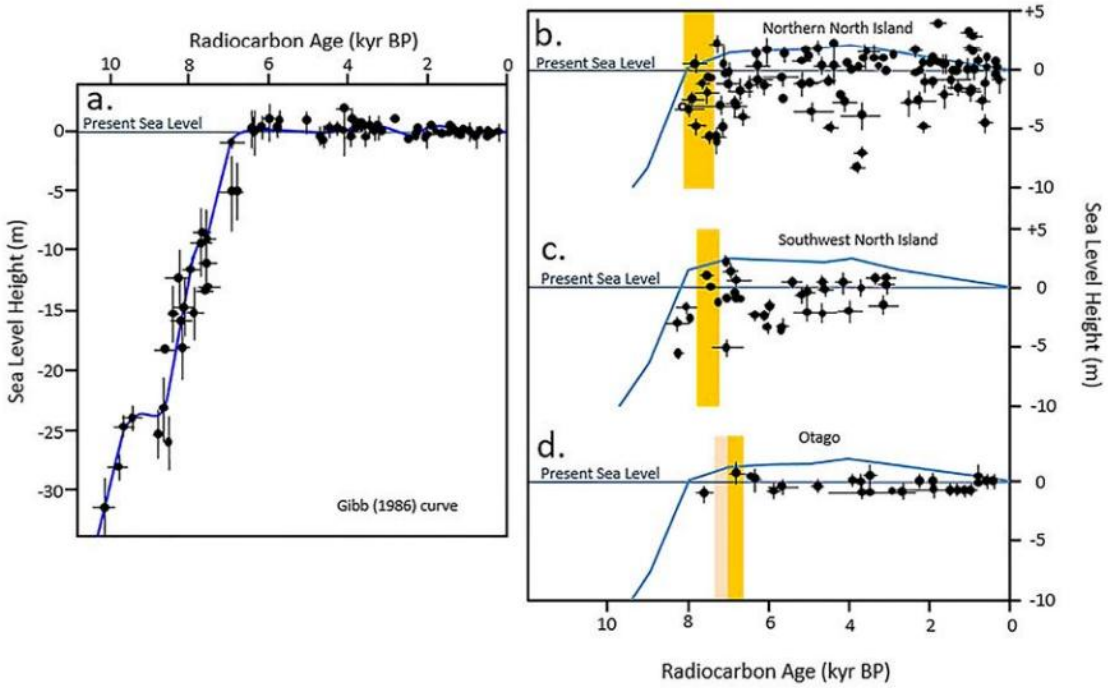

Figure 1.2: Relative sea-level curve for New Zealand as determined by (a) Gibb, 1986 and (b-d) Clement et al., 2016. The shaded region demonstrates the beginning of stable sea level period occurring presently, which started later in the South Island than the North Island (Sourced from King et al., 2021).

1.4. Rangitāiki Plains

1.4.1. Geographical Setting

The Rangitāiki Plains, located in the Bay of Plenty Region in New Zealand's North Island, borders the East coast and spans approximately 25 km from the township of Matatā in the west to Whakatāne in the east (Pullar, 1985) (Figure 1.3). The Rangitāiki Plains extend 22 km inland from the small town of Kawerau to the present-day shoreline, covering 400 km^2 (Pullar, 1985). Hilly terrain surrounds the Rangitāiki Plains, including the Mokoroa Hills to the east and the Manawahe Hills to the west. Notable cliff features include the Matatā Cliffs on the western coastal boundary, the Awakeri Sea Cliffs inland behind the Awakeri township, and the Whakatāne Headland at the eastern coastal boundary of the plains (Beanland & Berryman, 1992; Pullar, 1985). The Rangitāiki Plains reside within the Taupō Volcanic Zone and are surrounded by several continental and oceanic volcanoes, including Tarawera, Putauaki (Mount Edgecumbe), Moutohora (Whale Island), and Whakaari (White Island) off the coast (Beanland & Berryman, 1992).

Three rivers cross the Rangitāiki Plains, discharging into the ocean. The Tarawera River originates from Lake Tarawera and dominates the western margin of the plains, discharging near Matatā by the Tarawera Cut (Pullar, 1985). The Rangitāiki River headwaters are located near Lake Taupō and travel through the central Rangitāiki Plains, discharging approximately halfway between Whakatāne and Matatā at Thornton (Pullar, 1985). The Whakatāne River is located on the easternmost edge of the plains and originates from the Te Urewera National Park (Gibbson, 1990).

1.4.2. Tectonic Setting

New Zealand is located on the boundary of two tectonic plates, the Australian Plate to the west and the Pacific Plate to the east (Figure 1.4). The Pacific Plate converges on and subducts below the Australian Plate east of the North Island, forming the Hikurangi Trench, which connects to the oceanic Kermadec Trench in the north (Heads, 2017; King, 2000; Kingma, 1959). This subduction causes faulting and volcanism across the North Island. In the South Island, this tectonic margin shifts inland and becomes a transform boundary known as the Alpine Fault, which runs the length of the South Island (Heads, 2017; King, 2000; Kingma, 1959). South of the Alpine Fault, the Australian Plate subducts below the Pacific Plate and forms the Puysagur Trench (Heads, 2017; King, 2000; Kingma, 1959).

.

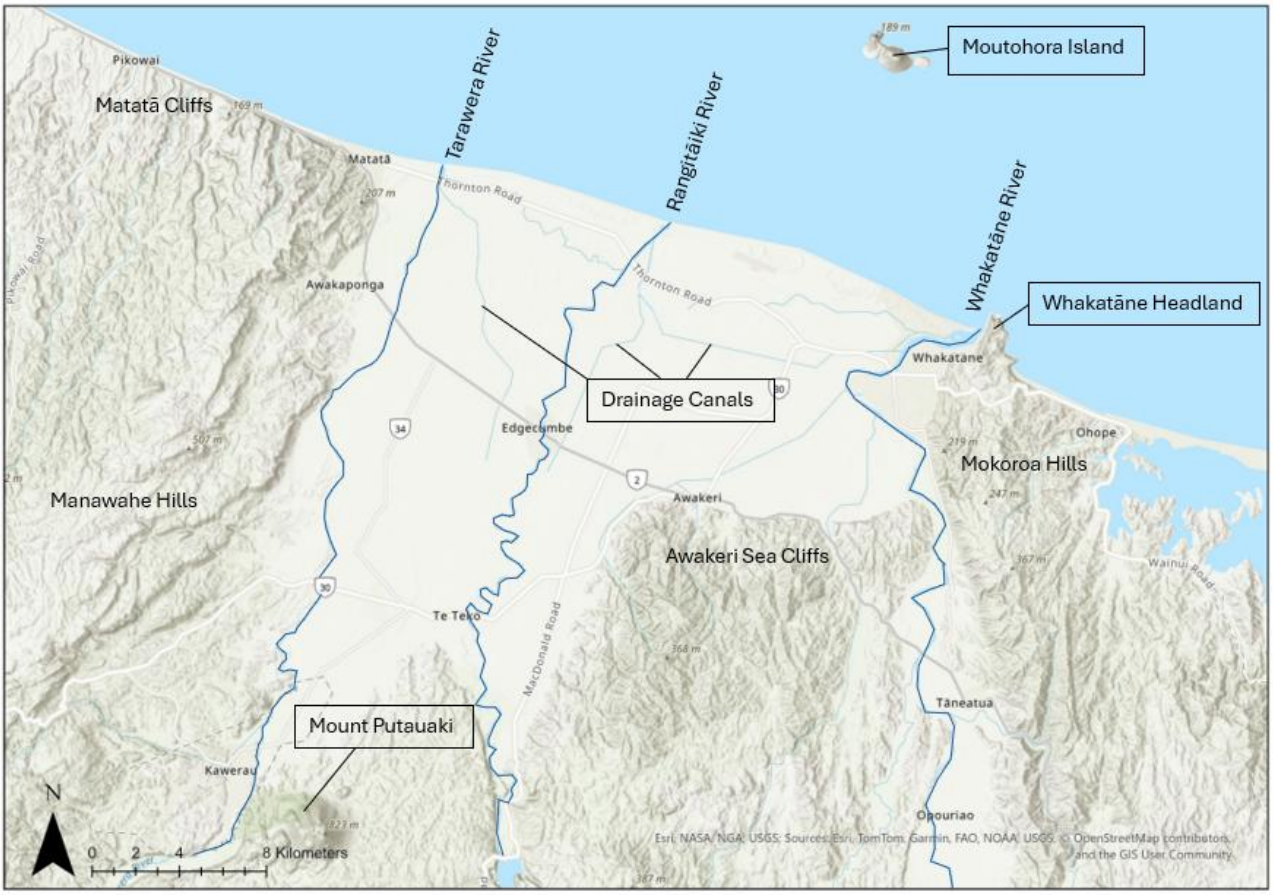

Figure 1.3: Map of the Rangitāiki Plains showing significant locations and geomorphological features

The tectonic setting of New Zealand has played a significant role in the evolution of the Rangitāiki Plains, shaping both the area's geomorphology and geology. The Rangitāiki Plains are located in an area of back-arc rifting, where the North Island Fault system and Taupō Rift Valley meet (Begg & Mouslopoulou, 2010; Mouslopoulou, 2007) (Figure 1.4). The Taupō Rift Valley extends 200 km northeast to southwest across the central North Island through the Taupō Volcanic Zone (Mouslopoulou, 2007; Beanland & Berryman, 1992; Begg & Mouslopoulou, 2010). Subduction of the oceanic Pacific Plate causes lithospheric extension at the surface, generating the rift valley and severe crustal faulting (Begg & Mouslopoulou, 2010; Mouslopoulou, 2007). Many of these faults are normal and experience slip during large-magnitude earthquake events (Beanland & Berryman, 1992; Begg & Mouslopoulou, 2010). Such faulting events have led to the formation of horst and graben structures.

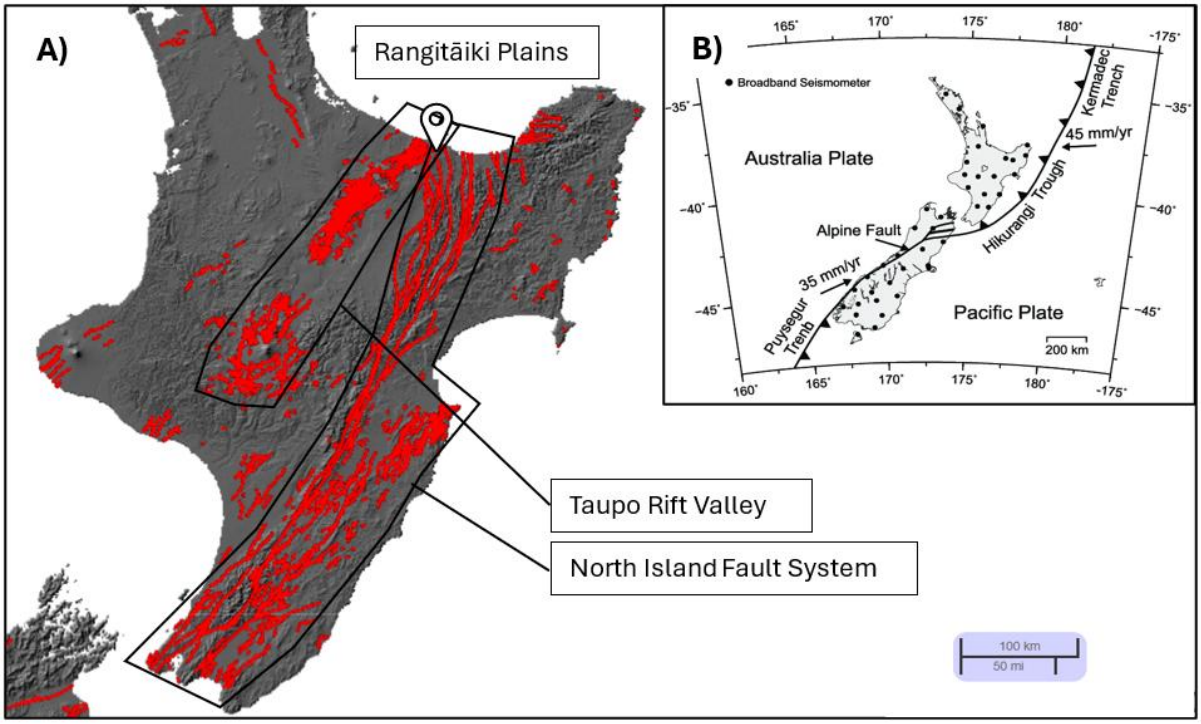

Figure 1.4: A) Tectonic setting in the Rangitāiki Plains, including the Taupo Rift Valley and North Island Fault Systems, which are significantly contributing to subsidence in the Rangitāiki Plains (adapted from Langridge et al., 2016); and B) New Zealand tectonic settling.

The Rangitāiki Plains are located within the Whakatāne Graben. The surrounding Mokoroa and Manawahe hills encasing the plains represent the horst. The graben experiences movement along several major fault lines and causes subsidence. Major faults include the Matatā, MacDonald, Te Teko, Awaiti, Omeheu, Otakiri, and the Edgcumbe Fault zones (Begg & Mouslopoulou, 2010). The downward movement of the graben structure created accommodation space for sediment infill, forming the modern Rangitāiki Plains (Figure 1.5). Subsidence of the graben began between 0.6 and 1 Ma (Beanland & Berryman, 1992). Presently, the long-term subsidence rate is approximately 1–2 mm yr^{-1}, with slower subsidence rates during the late Pleistocene of 0.4–0.8 mm yr^{-1}. The horst also experienced an uplift of approximately 1 mm yr^{-1} (Beanland & Berryman, 1992).

Present-day movement of the Whakatāne Graben and ongoing tectonic activity is evident through major earthquakes. One example of this is the 1987 Edgecumbe Earthquake. March 2nd 1987, saw a magnitude 6.5 earthquake occur at a shallow depth of 8 km along the Edgcumbe Fault on the Rangitāiki Plains. The major earthquake caused eleven surface ruptures, a 1.2 m extension in land area, and a land surface drop of 2 m to the northwest of the fault (Begg & Mouslopoulou, 2010). The earthquake also triggered displacements along five other fault lines in the area.

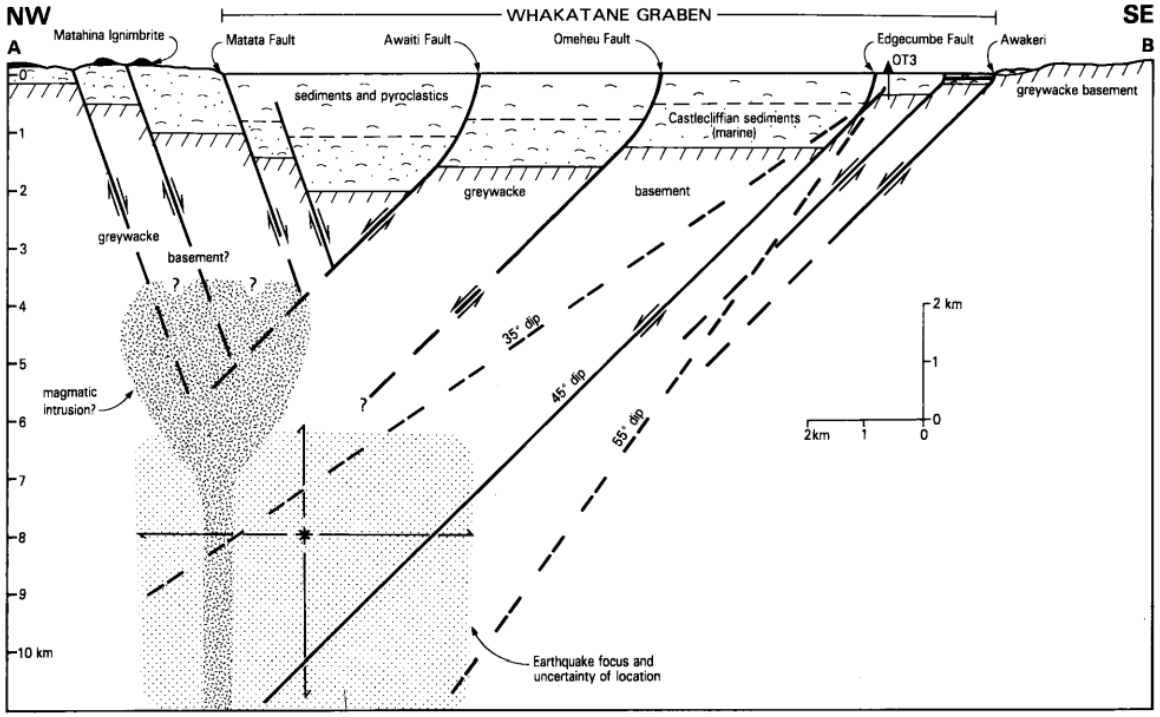

Figure 1.5: Cross section of the Whakatāne Graben running northwest to southeast, including associated faults and broad geological layers (sourced from Nairn & Beanland, 1989).

1.4.3. Geological Setting

1.4.3.1. Jurassic to Early Cretaceous

The geological composition of the Rangitāiki Plains was extensively studied in the 1970s and 1980s (Begg & Mouslopoulou, 2010). Seismic reflection and drillhole data were used to determine the subsurface geology across the plains. The dominant basement rock is greywacke, present at depths of up to 2.4 km, and is overlain by marine, volcanic, and fluvial deposits (Begg & Mouslopoulou, 2010).

The greywacke basement is part of the Waipapa and Torlesse composite terranes (Figure 1.6). The Torlesse Composite Terrane consists primarily of metasedimentary rocks, including greywacke and argillite, with bedding-parallel shear stress (Price *et al.*, 2015; White *et al.*, 2010). The Torlesse Composite Terrane underlies the eastern Rangitāiki Plains and crops out in the hills southeast of the plains (White *et al.*, 2010). The Waipapa Terrane is composed of hardened Manaia Hill Group sandstone and argillite, which are dated to the Late Jurassic period (White *et al.*, 2010). The Waipapa Terrane is thought to underlie the western Rangitāiki Plains and crops out at Otamarakau (White *et al.*, 2010). Both terranes formed as part of an accretionary wedge along Gondwana's convergent margin during the Mesozoic (Price *et al.*, 2015; White *et al.*, 2010).

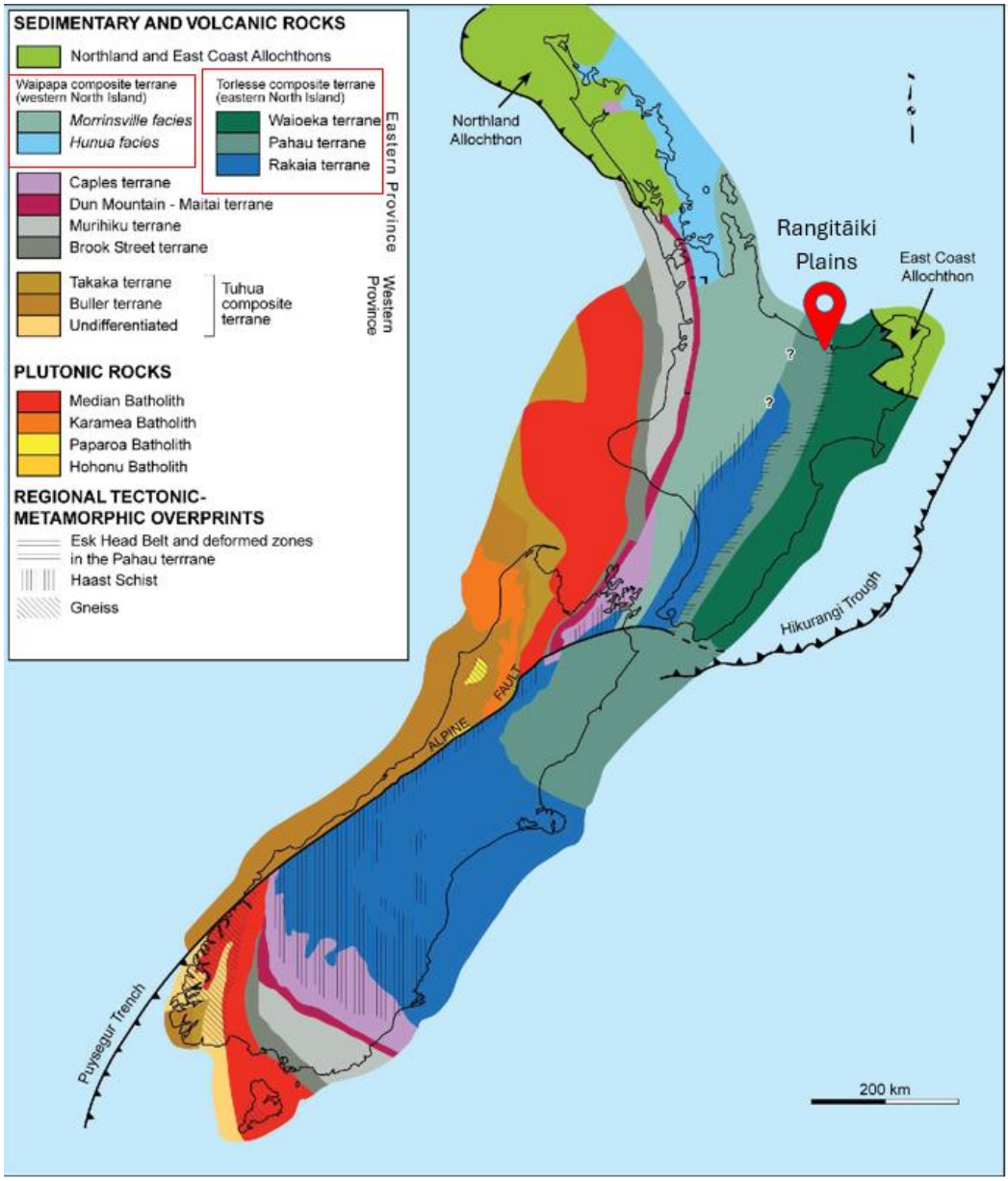

Figure 1.6: Map of New Zealand basement rock units, including the Waipapa and Torlesse composite terranes below the Rangitāiki Plains (sourced from Tripathi et al., 2008).

1.4.3.1. Late Cretaceous to Pliocene

After the diagenesis of the basement greywackes, the composite terranes experienced subsequent uplift, mountain building, subsidence, and then erosion caused by the Rangitata Orogeny mountain building event (150 and 100 Ma). The Rangitata Orogeny generated uplift until the Gondwana continent transitioned from converging to diverging at the tectonic margin around 100 Ma (Heads, 2017). Proto-New Zealand then underwent a period of rifting and subsidence until the late Oligocene, which caused most of the land to be submerged (Heads, 2017).

The Kaikoura Orogeny commenced in the Miocene. Tectonic extension came to an end, and a continental collision occurred between the Pacific and Australian tectonic plates, causing mountain building once more (Heads, 2017). This lifted the composite terranes above sea level, initiated subduction faulting and volcanics in New Zealand, and generated the groundwork for Quaternary deposits in the Rangitāiki Plains (Heads, 2017).

1.4.3.2. Quaternary

Quaternary deposits in the Rangitāiki Plains consist of volcanic, fluvial, and marine sediments. Several minor or discontinuous formations lack a clear definition above the basement greywacke (White *et al.*, 2010). Above these units, the next oldest prominent marker bed is the Matahina Ignimbrite (White *et al.*, 2010). The Matahina Formation is a thick and widespread formation that covers the entire Rangitāiki Plains and a large proportion of the surrounding horst (Figure 1.7). The Matahina Ignimbrite originated from the Haroharo Caldera within the Ōkataina Volcanic Centre and erupted at approximately 280 ka (Bailey & Carr, 1994). The eruption produced 120 km^3 of ignimbrite, primarily concentrated east of the caldera, covering an area of 2,000 km^2 and reaching depths of up to 200 m (Bailey & Carr, 1994). After the Matahina Ignimbrite, the geological layers up to the Holocene vary between non-marine and marine-dominated deposits influenced by glaciation cycles (Figure 1.7).

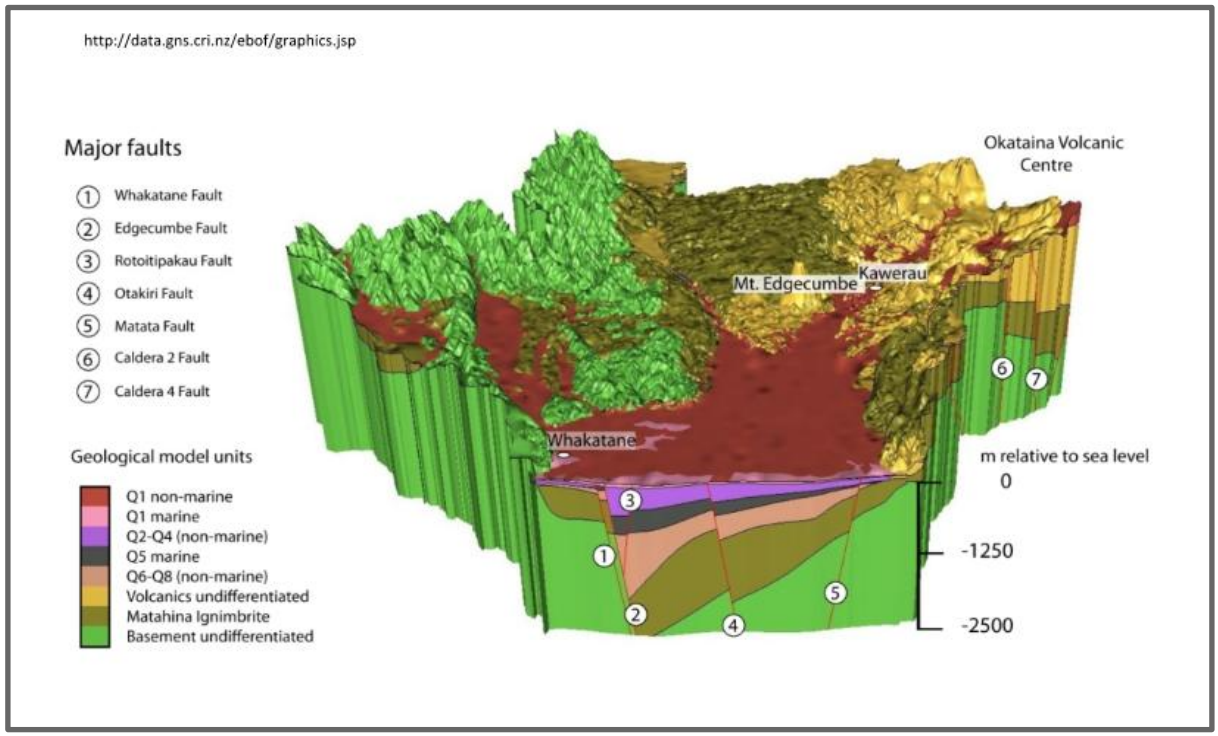

Figure 1.7: Three-dimensional model of the Rangitāiki Plains and the associated geological layers and faults (sourced from White et al., 2010). Q8–Q6 represent non-marine Pleistocene sediments deposited during a glacial period; Q5 consists of marine deposits from the last interglacial period when sea levels were higher; and Q2–Q4 contain terrestrial sediments from the previous Otiran glacial period and were deposited in the late Pleistocene.

1.4.3.3. Holocene

During the last glacial maximum before the Holocene, the sea level around New Zealand was 120 m below present (Gibb, 1986). Approximately 8.1 to 7.34 ka, a high stand occurred in the North Island, generating sea levels 3 m higher than the present-day average. This highstand caused erosion along the Awakeri Sea Cliffs until sea level fell and stabilised to the present-day level around 4 ka (Clement *et al.*, 2016). These stable oceanic conditions, in combination with a subsiding Whakatāne Graben and high sediment availability, allowed the Rangitāiki Plains to begin prograding due to an available accommodation space. Infilling did not occur uniformly due to these contributing factors. Approximately 6.5 km of progradation occurred in the last 5 ka and only 0.6–1.1 km over the past 1.8 ka (Pullar & Selby, 1971). This period saw the deposition of the marine and non-marine sediment (White *et al.*, 2010) (Figure 1.7). These sediments are further classified into linear beach ridges, volcanic outwash deposits, and background sedimentation from fluvial and swamp sources (Begg & Mouslopoulou, 2010; Nairn & Beanman,1989; Pullar, 1985) (Figure 1.8). Beach ridge deposits accumulated first, followed by peat formation and outflow of volcanic material directly onto the plain.

1.4.3.4. Holocene Sediment Provenance

Beach ridges are composed of volcanic material from the Taupō Volcanic Zone. Seven major eruptions allowed volcanic sediment to be transported to the Rangitāiki Plains through fluvial and airborne sources (Pullar & Selby, 1971). The aerial deposits were preserved best in peatlands between the beach ridge sets but appeared consecutively within ridge sediments (Pullar & Selby, 1971). The dominant volcanic marker beds and their associated ages include the Whakatāne Ash (5.526±0.145 ka), Taupō Supergroup members 11–12 (2.800±0.060 ka), Taupō Supergroup members 9–10 (2.059±0.118 ka), Taupō Pumice (1.718±0.010 ka), Kaharoa Ash (0.636±0.012 ka), and Tarawera Ash (0.064 ka) (Beanland & Berryman, 1992; Begg & Mouslopoulou, 2010; Lowe *et al.*, 2013; Pullar & Selby, 1971; Campbell, 1973)

1.4.3.5. Transport of Sediment

1.4.3.5.1. Riverine

The formation of mid-late Holocene sediments in the Rangitāiki Plains was strongly influenced by sediment transport from the Whakatāne, Rangitāiki, and Tarawera rivers. These rivers transported the material needed for progradation to the Rangitāiki Plains coastline. Once sediments reach the coastline, deposition occurs due to marine processes such as waves, wind, and current-driven sediment transport. The Whakatāne River originates in the Urewera region and carries

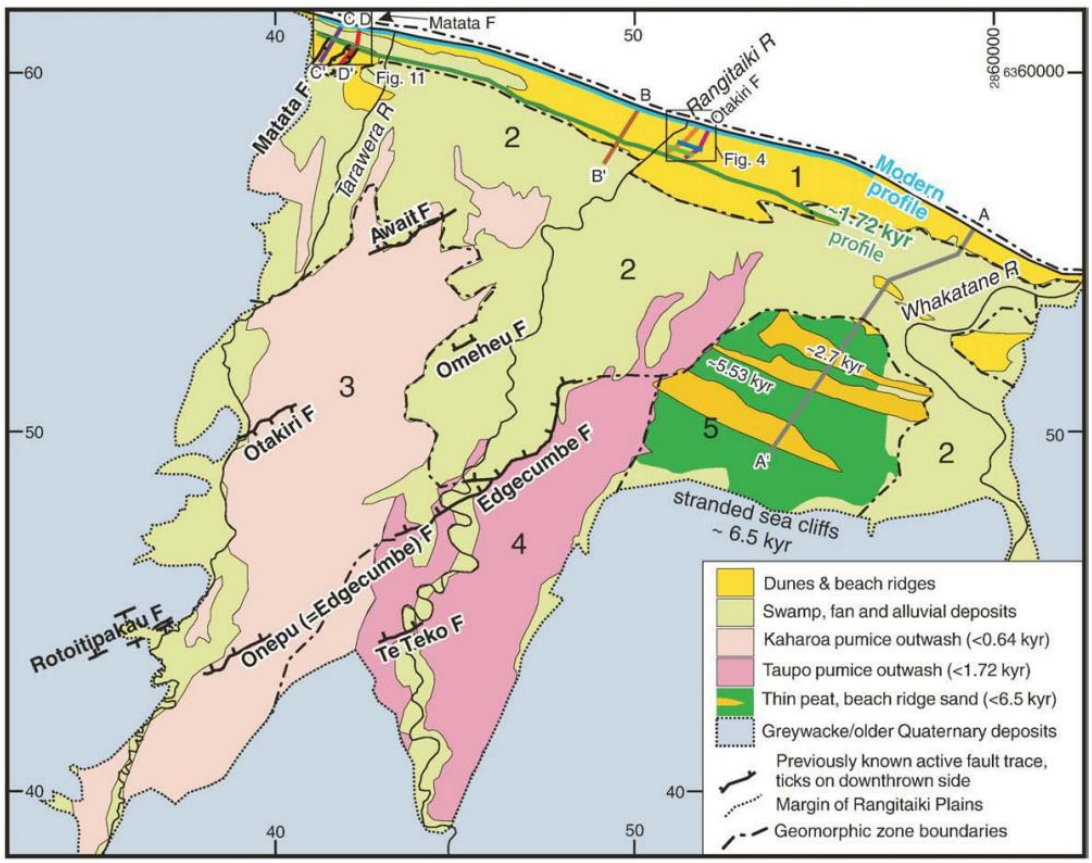

Figure 1.8: Geological map of the Holocene sediment deposits on the Rangitāiki Plains *(sourced from Begg & Mouslopoulou, 2010, who adapted it from Nairn & Beanman,1989 and Pullar, 1985).*

weathered greywacke into the Rangitāiki Plains (Gibbons, 1990). In contrast, the Rangitāiki River originates from the Ahimanawa Ranges southeast of Lake Taupō, and the Tarawera River from Lake Tarawera in the Ōkataina Volcanic Centre (Beanland & Berryman, 1992; Gibbons, 1990). These two rivers transport volcanic sediments, including large amounts of pumice, to the Rangitāiki Plains coastline, playing a significant role in shoreline progradation (Beanland & Berryman, 1992).

Riverine sediment supplies also generated outwash deposits on the Rangitāiki Plains (Figure 1.8). The Rangitāiki and Tarawera Rivers have elevated riverbeds, known as perched rivers, which make them prone to bank failure (Gibbons, 1990). The Taupō and Kaharoa pumice outwash events occurred as heavy rainfall brought large amounts of volcanic material down the rivers after the eruption events, causing riverbanks to burst and volcanic material to be deposited directly on the Rangitāiki Plains (Begg & Mouslopoulou, 2010; Gibbons, 1990; Pullar, 1985).

1.4.3.5.2. Wave-Driven Transport

Once volcanic sediment reached the ocean, marine processes deposited material onto the coast of the Rangitāiki Plains. Beach sediment is deposited primarily by bedload and subordinately by suspended load transport through waves, currents, and winds. Sediment deposition by waves depends on several factors, including wave energy and dominant wave direction. Waves without significant energy will not carry sediment. Shields Law (1936) describes this notion in its simplest form, giving the bed shear stress needed for sediment entrainment (Equation 1).

$$\theta = \frac{\tau_b}{(\rho_s - \rho) g d} \qquad \textit{Equation 1}$$

Shield's parameter (θ) is determined by bed shear stress (τ), sediment density (ρ_s), fluid density (ρ), gravitational acceleration (g), and sediment diameter (d). When the Shields parameter is less than the critical parameter for a particular sediment, the sediment will remain stationary or cease movement; when the Shields parameter is greater, the fluid force of the water overcomes the gravity and drag acting on sediment particles to generate transport (Shields, 1936). Other factors can also affect bedload and suspended load transport, such as tidal currents, longshore currents, grain sorting and shape, bed structure, and sudden changes in turbulence typical of surf zones; however, there is no one equation to encompass all these factors.

New Zealand experiences significant wind wave action from the surrounding seas. The dominant wind in New Zealand is the westerly trade wind, which produces predominantly westerly waves (Ivamy & Kench, 2006). The Rangitāiki Plains are located on the East coast of New Zealand and are thus sheltered from these waves, as the westerlies must cross over the North Island before reaching the east coast, reducing wind energy and wave size (Macky *et al.*, 1995) (Figure 1.9). The eastern coast typically experiences swell waves of 0.5–1.5 m with a 5–7 second period. Beach waves range from 0.4–0.8 m with a 9–12 second period (Macky *et al.*, 1995). These shorter-period waves are generated by local weather. In contrast, swell waves in the Bay of Plenty are formed by long-distance northerly to easterly winds from atmospheric depressions north of New Zealand (Ivamy & Kench, 2006). Swells from these directions develop due to the large wind fetch, which allows them to travel with minimal energy loss. These conditions create an overall low-energy wave environment around the Bay of Plenty and Rangitāiki Plains (Macky *et al.*, 1995; Pickett, 2004).

These waves are the primary source of sediment deposition on the Rangitāiki Plains coast (Iremonger, 2007). The Rangitāiki Plains beaches experience erosion during storm events and accretion from waves during fair weather (Iremonger, 2007). Bay of Plenty beaches operate in a

cycle known as cut and fill. This is when swell conditions associated with summer conditions generate wave-driven swash deposition known as constructive swash, which accretes beaches, whereas in winter storm waves remove this sediment and store the material in offshore bars till the summer, where sediment is reintegrated into the coast (Iremonger, 2007).

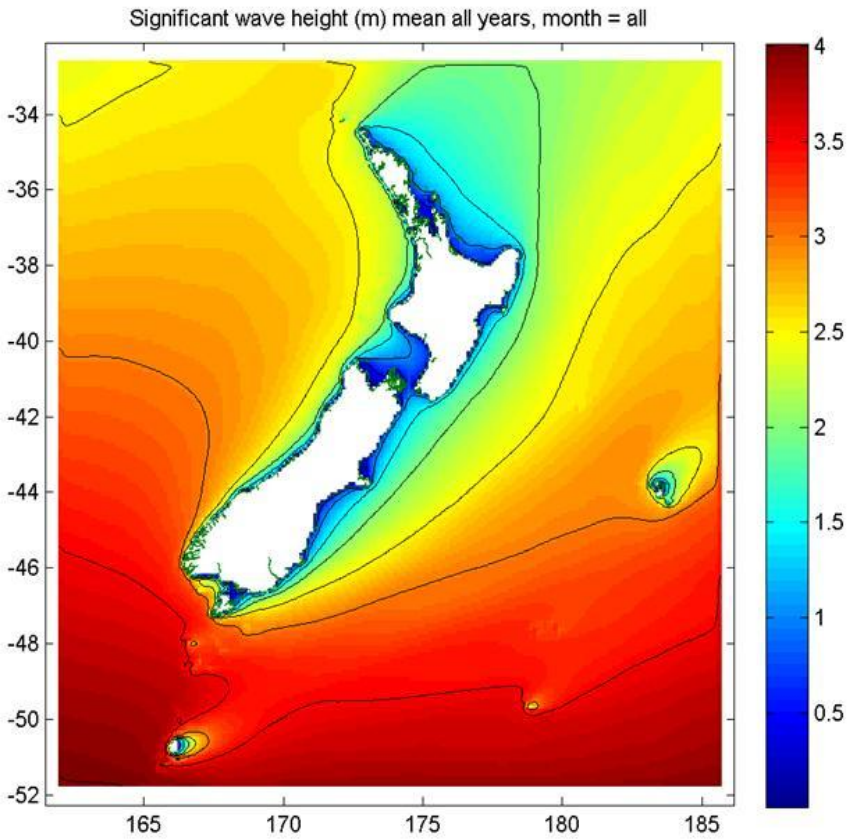

Figure 1.9: Significant wave height around New Zealand showing a smaller average wave height in the Bay of Plenty area (sourced from NIWA, 2024).

1.4.3.5.3. Littoral Drift

In addition to waves, the Rangitāiki Plains also experience current-driven sediment transport onto its beaches. Littoral drift, or longshore drift, is one of the dominant currents affecting sediment transport on the Rangitāiki Plains coastline. Littoral drift is a coastal current that moves sediment along the shoreline within the surf zone (Garrison, 2015). This process creates a current parallel to the coastline, redistributing sediment away from sources such as river mouths (Garrison, 2015). Regions with active littoral drift often experience beach ridge formation due to an abundant sediment supply, while erosion can occur in areas where littoral drift is weak or absent.

Approximately 2 ka, the Rangitāiki Plains had prograded far enough for sediment to bypass the Whakatāne Headland (Kohi Point) and accumulate in the Ōhiwa Harbour estuary (Beanland & Berryman, 1992). Previously, the Whakatāne Headland acted as a barrier to littoral drift, trapping

sediment within the Rangitāiki Plains area. Presently, littoral drift still occurs in a north-west to south-east direction across the Rangitāiki Plains and continues to transport material past the Whakatāne Headland.

1.4.3.5.4. Astronomical Tides

In addition to littoral drift, the Rangitāiki Plains also experience current-driven sediment transport from tides. Two main tidal constituents affect New Zealand: the semi-diurnal solar tide (S2) and the semi-diurnal lunar tide (M2). These tidal constituents produce two tides daily of differing heights (Walters *et al.*, 2001). Interactions between the S2 and M2 tides and their superposition with other ocean waves cause larger tides in western New Zealand and smaller tides in eastern New Zealand (Stephens *et al.*, 2020; Walters *et al.*, 2001).

Because of the weakened S2 tidal effect on the east coast, the Bay of Plenty experiences a range of tidal heights. The average range of a Bay of Plenty spring tide is 1.6m, while the neap tide average is 1.2m (Ivamy & Kench, 2006). Furthermore, 27% of tides exceed the elevation of the mean spring tide (Bell & Lewis, 2006). The overall nature of surface tidal currents in New Zealand limits their effect on sediment transport (Carter & Heath, 1975). Tidal currents in the Bay of Plenty cannot directly move sediments, as tidal water velocity is too slow and does not generate enough energy to overcome the entrainment threshold to start moving sediment readily, however, increased water levels during high tides allow waves that carry sediment further up the shore for sediment deposition (Carter & Heath, 1975). Furthermore, under some combined conditions, like storm events, sediments may move with the tides as waves, winds, and currents resonate and superimpose.

1.4.3.5.5. Storms and Meteorological Tides

The Bay of Plenty experiences an average of approximately 1.3 storms per year (between 1873 and 1990) (Hay *et al.*, 1991), originating from either occluded fronts, tropical cyclones, and Tasman depressions (De Lange & Gibb, 2000). The frequency of each storm event differs temporally. Different storm types are more common in certain months due to climatic conditions: tropical cyclones peak in February, Tasman depressions in May, and occluded fronts in July (Hay *et al.*, 1991). While the dominant storm type can vary with season, the Bay of Plenty is most affected by blocking events when extreme weather systems remain stationary or slow-moving over New Zealand (Stephens *et al.*, 2020). These storm events influence ocean sediment circulation by generating high-energy waves, strong winds, and meteorological tides/storm surges.

When atmospheric pressure differences are significant, high-energy winds form that transfer energy into surface waters and generate larger waves. For example, Cyclone Gabrielle, which impacted New Zealand in 2023, produced winds of over 90 km/h and waves of over 6.8 m high in the Bay of Plenty (Bay of Plenty Times, 2023). At the Rangitāiki Plains, these high-energy waves have an increased velocity and interact more with the seabed than low-energy waves, allowing them to overcome the critical forces opposing sediment transport. These conditions generate stronger beach swash and backwash during storms, leading to overall sediment loss from Rangitāiki Plains beaches. High energy wave conditions also left behind storm deposits on the Rangitaiki Plains consisting of heavy metals, more coarse and unsorted sediment, and organic matter.

Meteorological tides, also known as storm surges, also affect sediment transport. Storm surges are high water levels above the astronomical tide height caused by low-pressure atmospheric events. Due to New Zealand's deep and narrow continental shelf, storm surges are limited to about 0.5 m, or 25% of the tidal range (Stephens *et al.*, 2020). Storm surges increase the effects of tidal currents and waves (De Lange *et al.*, 2000). For example, storm surges generate larger tidal heights and increased tidal currents, which have the energy to move bottom sediment. Furthermore, meteorological tides allow larger surface waves to reach the shore due to the reduced energy loss from seabed friction.

Ultimately, storm-generated waves, winds, and surges are highly effective at transporting sediment due to their large energy transfer over a short period (Carter & Heath, 1975). In the Bay of Plenty, sediment is typically eroded from the coast during storms but is accreted again soon after the storm events due to the combination of surface waves and longshore drift (Pullar & Selby, 1971).

1.4.3.5.6. Wind-Driven Transport

Once sediment is deposited on the beach by waves and currents, wind plays an important role in redistributing the sediment through aeolian transport. Like water, wind can transport sediment through bedload and suspended modes. Aeolian transport is especially important in dune formation on top of beach ridges, also known as aeolian capping, as sediment is transported inland and trapped by vegetation and other obstructions. The amount of aeolian sedimentation along coastlines depends on factors such as the dominant wind direction and average wind velocity. Typically, sand sediment transport can occur when winds reach 5-10 m/s, however, the transport mechanisms are slightly different from wave-driven transport, as wind-driven transport is governed by not only wind condition but sediment availability due to sediment moisture

content, beach slope, beach width, vegetation and lag deposit presence (de Vries *et al.*, 2014; de Vries *et al.*, 2012). For example, strong winds will not initiate aeolian transport during storm events if accompanied by rain, as sand saturation increases the threshold wind speed for sediment movement too significantly (de Vries *et al.*, 2012). Similar to Shield's equation (1936), no one equation accounts for all the factors affecting aeolian beach transport.

1.4.3.5.7. El Niño Southern Oscillation

As the Rangitāiki Plains' dominant cause of coastline erosion is storm events, long-term climatic cycles also affect sediment deposition by influencing the frequency of storm events. Examples of these climatic cycles include the Pacific Decadal Oscillation and the El Niño-Southern Oscillation (ENSO). ENSO is an equatorial Pacific climate pattern that occurs periodically, approximately every five years, alternating between three phases of differing characteristics: neutral, El Niño and La Niña.

In New Zealand, El Niño conditions result in south-westerly onshore winds, drier weather with reduced extratropical cyclone activity, and warmer air temperatures (De Lange, 2001; Gordon, 1986; Philander, 1983). During La Niña, New Zealand experiences increased air and water temperatures, north-westerly onshore winds, more frequent storms such as extratropical cyclones, and rising sea levels (De Lange, 2001; Gordon, 1986; Philander, 1983). In comparison, neutral conditions have oceanic and climatic conditions near the long-term average.

The effects of ENSO in the Bay of Plenty are well-documented compared to the rest of New Zealand (De Lange, 2001). Tide gauge data from the Moturiki Island site show a correlation between sea behaviour and ENSO phases. The data indicate that the Bay of Plenty experiences larger and steeper wave conditions during La Niña (De Lange, 2001). The data suggest sediment erosion is more pronounced during La Niña, when storm events are more frequent, while sediment accretion occurs during El Niño (De Lange & Gibb, 2000).

1.4.4. Anthropogenic Effects

1.4.4.1. Pre-European Arrival

The Eastern Bay of Plenty was one of the first areas settled by Polynesians after voyaging from Hawaiki over 1,000 years ago (Whakatāne District Council, 2010). During Māori settlement, the Rangitāiki Plains consisted primarily of peatlands and swamps, prone to flooding due to poor river drainage (Pullar, 1985). Approximately 100 years ago, the Rangitāiki River did not have its own river mouth (Gibbons, 1990). Instead, the Rangitāiki River flowed behind coastal beach ridge sets,

joining the Tarawera River, before reaching the sea at Matatā. Several branches connected the Rangitāiki River to the adjacent Tarawera and Whakatāne River systems (Pullar, 1985). The Whakatāne branch, known as the Orini Stream, was located 5 km inland, while the Tarawera branch, the Awaiti Stream, was 6.5 km inland (Gibbons, 1990). The perched nature of the Rangitāiki and Tarawera rivers also led to frequent flooding, often washing away crops planted along riverbanks (Gibbons, 1990).

1.4.4.2. European Arrival and Drainage

By 1830, Europeans had settled in the Bay of Plenty, bringing whalers, sealers, fishers, traders, and missionaries into the Whakatāne area (Pullar, 1985). By the late 1880s, government politicians were under pressure to find more suitable land for settlement (Gibbons, 1990). The Rangitāiki Plains' swampy lands showed the promise of fertile soil if drained. After much debate over how to successfully drain the swamps, the Rangitāiki Drainage District and the first Drainage Board were established in December 1894 (Gibbons, 1990). However, the Drainage Board was short-lived and ultimately failed in its goal to drain the plains. After two more failed drainage boards, due to ongoing disagreements, complaints, and a lack of public, governmental and economic support, the government's Lands Department took over draining the Rangitāiki Plains (Gibbons, 1990). With a government loan of £50,000 (equivalent to NZ$12.4 million in 2025), a new outlet for the Rangitāiki River was proposed to carry sediment and pumice directly out to sea while lowering the river's water level (Gibbons, 1990). Plans also included dredging, straightening, and widening the Tarawera outlet, expanding several existing drains and installing stopbanks (Gibbons, 1990). By May 1914, the new channel for the Rangitāiki River was completed and operational (Gibbons, 1990). Within hours of the new channels opening, water levels in the Rangitāiki River receded below recorded summer levels, successfully draining thousands of acres of land (Gibbons, 1990). This was the beginning of the alteration of sedimentation on the Rangitāiki Plains by anthropogenic effects.

1.4.4.3. Hydroelectric Dams

In recent history, sedimentation on the Rangitāiki Plains has been altered by the construction of hydroelectric dams, including the Matahina and Aniwhenua dams. The Matahina and Aniwhenua dams reduce the Rangitāiki River's flow velocity and cause sediment to settle behind the dam. Where the Rangitāiki River meets the Matahina Lake, water velocity drops below 20 cm/s, causing a large delta to form at the dam's inlet (Phillips & Nelson, 1981). The water entering the Matahina Lake has a high concentration of suspended sediment, over 100 mg/L (Phillips & Nelson, 1981). During the materials' passage through the lake, deposition decreases the suspended sediment

load by 71–98%. Research indicates that the dam retains 100% of the bedload and 64% of the suspended sediments, accumulating approximately 235,000 m^3 of sediment annually in the Matahina Lake (Phillips & Nelson, 1981). Before the construction of the Matahina Dam, the river discharged approximately 201,000 tonnes of suspended sediment and 188,000 tonnes of bedload sediment into the ocean annually (Phillips & Nelson, 1981). After the dam's construction, these figures dropped to 65,000 tonnes and 10,000 tonnes, respectively (Phillips & Nelson, 1981). Furthermore, the Rangitāiki Plains have also lost sediment due to the Matahina Dam's use as flood mitigation. The dam pre-emptively releases water when severe weather is predicted, lowering the dam levels to reduce flood peaks and sediment transport onto the plains (Gibbons, 1990). The large retention of sediment by the Matahina Dam and the use of the dam as flood protection reduces the transport of coastal sediments critical for beach ridge building. Phillips & Nelson (1981) have suggested that the decrease in sediment delivery has reduced coastal progradation and may be exacerbating coastal instability in the region, as the Rangitāiki River was the plain's greatest sediment provider.

1.4.5. Current Coastal State

The Rangitāiki Plains coastline has reached an equilibrium or near-equilibrium state over the late Holocene (Beanland & Berryman, 1992). This near-equilibrium state resulted from transporting materials away from the Rangitāiki Plains coastline via littoral drift (Beanland & Berryman, 1992). This equilibrium is evident from past research (Beanland & Berryman, 1992; Pullar & Selby, 1971) and ongoing coastal monitoring by the Bay of Plenty Regional Council. The Council has been monitoring dune morphology and sand volumes since 1976 across 54 sites in the Bay of Plenty (Healy, 1978). Nine of these monitoring sites are spread across the Rangitāiki Plains, with one west of Matatā, three between the Tarawera and Rangitāiki River mouths, and five between the Rangitāiki and Whakatāne river mouths (Healy, 1978). Monitoring from 1990 to 2019, four of the sites were considered stable, four accreting, and one semi-eroded (Bay of Plenty Regional Council, 2019).

1.5. Beach Ridges Investigation Methods

1.5.1. Beach Ridge Dating

Dating is critical to understanding palaeoenvironmental change, such as the progradation of beach ridge systems. Determining the age of sediments helps reconstruct timescales for coastal changes, including fluctuations in sediment budgets, deposition histories, and storm event

frequencies. Three main techniques are commonly used to date beach sediments: radiocarbon dating, tephrochronology, and OSL.

1.5.1.1. Radiocarbon Dating

Radiocarbon dating relies on the radioactive carbon isotope, carbon-14 (^{14}C), to determine the age of organic materials such as wood, charcoal, peat, bones, or shells. This technique only works on organic matter, as living organisms continuously absorb atmospheric carbon (Bowman, 1990; Libby & Johnson, 1955). When an organism dies, the individual stops absorbing carbon, and its internal ^{14}C begins decaying into ^{12}N, with a half-life of 5,730 years (Bowman, 1990; Libby & Johnson, 1955). ^{14}C decays because of its nuclear instability, as ^{14}C has more neutrons than protons. During decay, a neutron emits a high-energy electron (a beta particle) and is converted into a proton, changing the atom from carbon (six protons) to nitrogen (seven protons) (Hajdas, 2008). By measuring the amount of ^{14}C in a sample, scientists can calculate the material's age based on the known half-life using Equation 2 (Libby, 1949).

$$t = \left(\frac{t_{1/2}}{ln(2)}\right) * ln(N_0/N_t) \qquad \textit{Equation 2}$$

Where the age of the sample (t) is calculated using the half-life of the sample ($t_{1/2}$), the number of ^{14}C atoms remaining (N_t), and the initial number of ^{14}C (N_0). This method is effective for dating organic materials up to approximately 50,000 years old; beyond that, the ^{14}C content is typically too depleted for accurate measurement (Hajdas, 2008). Radiocarbon dating can be helpful in coastal environments with abundant organic remains, including shell fragments, marine and terrestrial vegetation, and peat from coastal wetlands. However, there are limitations when dating beach ridges. Because beach ridges are primarily composed of sand grains, organic matter for dating can be difficult to find preserved or may be well reworked, meaning dating will not reflect the time of deposition. For these reasons, other dating methods can better suit beach ridges on the Rangitāiki Plains.

1.5.1.2. Tephrochronology

Tephrochronology is a chronological dating method that uses volcanic ash layers as time markers. Individual tephra layers are typically dated by: radiocarbon dating of organic material bracketing the tephra layer, K-Ar dating, Ar-Ar dating, zircon fission-track, isothermal plateau fission-track of volcanic minerals, or relative dating by correlation with previously dated tephra (Lowe, 2011; Shane, 2000). Tephra is particularly useful in dating due to its ability to spread across large areas within hours of eruption and its easy preservation in diverse sedimentary

environments (Shane, 2000). These factors made tephrochronology the ideal dating method used by previous investigators on the Rangitāiki Plains (Pullar & Selby, 1971)

Pullar and Selby (1971) used tephrochronology and radiocarbon dating to determine beach ridge sets' ages and interpret sediment accumulation on the Rangitāiki Plains. Seven major eruptions deposited significant volcanic material on the Rangitāiki Plains (Pullar & Selby, 1971). The material was preserved best in peatlands between the beach ridge sets but appeared consecutively within ridge sediments (Pullar & Selby, 1971). Marker beds were identified and aged based on other sources' radiocarbon dating of the eruption. The dominant volcanic marker beds and their associated ages include the Whakatāne Ash (5.526±0.145 ka), Taupō Supergroup members 11–12 (2.800±0.060 ka), Taupō Supergroup members 9–10 (2.059±0.118 ka), Taupō Pumice (1.718±0.010 ka), Kaharoa Ash (0.636±0.012 ka), and Tarawera Ash (0.064 ka) (Beanland & Berryman, 1992; Begg & Mouslopoulou, 2010; Lowe *et al.*, 2013; Pullar & Selby, 1971; Campbell, 1973). Locations where volcanic marker beds ceased to exist were identified as potential palaeoshorelines. This tephrochronology allowed for the estimation of beach ridge ages and the reconstruction of past coastline positions at the times of volcanic eruptions (Beanland & Berryman, 1992; Begg & Mouslopoulou, 2010; Pullar & Selby, 1971) (Figure 1.10).

1.5.1.1. Optically Stimulated Luminescence

OSL is a method used to determine when quartz or feldspar minerals were last exposed to sunlight (Huntley *et al.*, 1985; Aitken, 1998). OSL measures the accumulated radiation in these minerals due to exposure to natural radioisotopes such as ^{234}U, ^{40}K, ^{232}Th, and cosmic rays (Aitken, 1998; Wintle, 1987). When quartz and feldspar minerals are buried, they accumulate trapped electrons caused by ionising radiation. These electrons become lodged within defects in the mineral's crystal lattice called traps. When exposed to light in a laboratory, the trapped electrons are released, emitting photons (luminescence) as they return to a lower energy state (Aitken, 1998; Wintle, 1987; Wintle & Adamiec, 2017). Measuring this luminescence reveals the amount of stored energy. This equivalent exposure is divided by the environmental dose rate obtained by measuring U, Th and K radioactive elements, to determine the last time the sediment was exposed to sunlight (Aitken, 1998; Wintle & Adamiec, 2017).

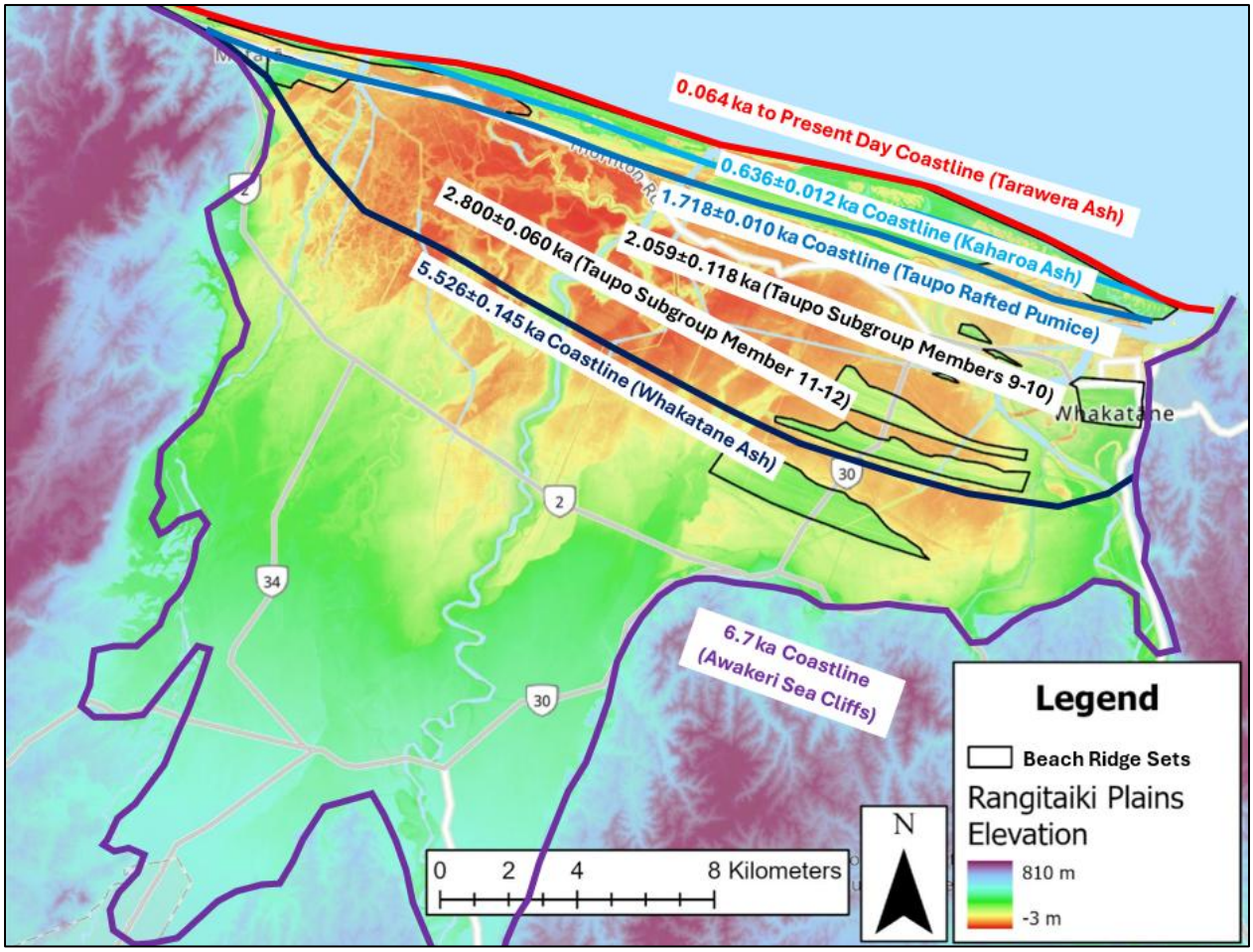

Figure 1.10: Estimated positions of palaeoshorelines at the times of significant volcanic eruptions and approximate age of beach ridge sets from various Rangitāiki Plains research papers, including Pullar & Selby (1971), Beanland & Berryman (1992) and Begg & Mouslopoulou (2010).

Quartz OSL is commonly utilised for sediment dating, as quartz is abundant, quick to bleach and has a stable signal; however, quartz OSL is not ideal for older dating as the environmental dose saturates the mineral's signal (Duller, 1997; Zhang & Li, 2020). Instead, techniques like Feldspar Infrared Stimulated Luminescence (IRSL) and Post-IR Infrared Stimulated Luminescence (pIRIR) are utilised. IRSL stimulates luminescence at low temperatures, targeting shallower, less stable traps, while PIRIR stimulates luminescence at low temperatures and then at higher temperatures, targeting deeper, more stable traps (Zhang & Li, 2020). These methods have more stable signals not hampered by environmental dose radiation (Devi *et al.*, 2024). However, IRSL is subject to anomalous fading, which causes age estimates to be too young (Devi *et al.*, 2024; Duller, 1997; Zhang & Li, 2020). pIRIR has minor anomalous fading, making pIRIR suitable for dating a wide range of sediments (Devi *et al.*, 2024; Zhang & Li, 2020). Quartz and feldspar mineral grains in beach ridges make this an ideal dating technique for beach ridges on the Rangitāiki Plains.

1.5.2. Imaging Beach Ridges

1.5.2.1. Light Detection and Ranging

LiDAR is a remote sensing method that uses lasers to create high-resolution three-dimensional models of surface topography. When helicopters, aeroplanes, drones, or satellites are equipped with lasers that emit pulses toward the ground, LiDAR is known as airborne laser scanning (Doyle & Woodroffe, 2018; Dougherty *et al.*, 2019). These pulses are reflected to a sensor, and the time taken for the signal to return and the signal intensity are recorded (Wang *et al.*, 2024). The characteristics of the returned signal can be used to distinguish between vegetation, bare ground, and other surface features (Doyle & Woodroffe, 2018). This spatial information can be translated into useful maps, such as digital elevation models, which can identify beach ridges' presence, morphology, and extent, including features like the number of ridges, location of stranded ridge sets, position, orientation, elevation and truncations (Dougherty *et al.*, 2019).

1.5.2.2. Ground Penetrating Radar

GPR is a subsurface imaging technique that can detect beach ridge structures. GPR transmits high-frequency electromagnetic (microwave) pulses into the ground via a transmitter (Jol *et al.*, 1996; Jol, 2008; Dougherty *et al.*, 2019). These waves reflect, refract, or scatter upon encountering materials with differing electrical properties (Jol *et al.*, 1996). The response depends on the materials' dielectric permittivity, which is their ability to store electrical energy in an electric field (Jol, 2008; Dougherty *et al.*, 2019).

Variations in dielectric permittivity cause differences in the return time and pattern of energy signals, enabling the interpretation of different sedimentary facies. The return signal is recorded as wave amplitude, in time rather than depth. Low amplitudes typically indicate homogeneous materials, while high amplitudes signal contrasts in mineralogy, sorting, grain size, or moisture content (Jol, 2008; Dougherty *et al.*, 2019). These reflections undergo a time-depth conversion based on the velocity of electromagnetic waves travelling through the sediment and are plotted into vertical profiles that reveal lithological changes with depth. This time-depth conversion introduced uncertainty into the data as the conversion relies on accurately knowing the wave velocity, which is altered by small changes in sediment moisture, composition, and grain size.

GPR is especially effective in sand-rich barrier systems, as dry sand is highly resistive and has low conductivity (Jol, 2008). Furthermore, heavy metal deposits occur during storms, creating prominent reflectors in GPR profiles between sand deposits. This makes visualising the

stratigraphic layer on GPR easy and is especially useful on prograding beach ridge systems like the Rangitāiki Plains.

1.5.3. Beach Ridge Sediment Analysis

1.5.3.1. X-Ray Fluorescence

XRF is utilised to determine the elemental composition of sediments. XRF exposes sediments to X-rays, which causes electrons to become ionised. Ionisation is the process in which an electron is displaced from electron shells to form ions. XRF removes electrons from the inner rings of an atom, causing instability and electrons from outer shells to move inwards to regain stability (Weltje & Tjallingii, 2008). This displacement emits each element's secondary (fluorescent) X-ray energy characteristic (Weltje & Tjallingii, 2008). This fluorescence is measured and processed to give quantitative data on the elements present in the sample.

XRF is a viable way to determine the sedimentary origin of beach ridge material, as the presence and relative abundance of various elements show different sedimentary origins. For example, at the simplest level, a higher proportion of CaO to SiO indicates calcareous marine sediments, whereas a higher proportion of SiO to CaO indicates siliciclastic sediments. Elements like these can be incorporated into elemental ratios and principal equations to determine factors like rock origin and weathering. Allowing for a comparison between adjacent and successive beach ridges to provide information on sediment source and transport dynamics.

1.5.3.1.1. SandClass System

Several beach and beach ridge studies have utilised the SandClass System to classify sediments (Hernandez-Hinojosa et al., 2018; Svendsen et al., 2007; Yalcin et al., 2022). Herron (1984) generated a scale that utilised elemental ratios to classify sands and sandstones into the respective subcategories of: Fe-shale, Fe-sand, shale, wacke, litharenite, sublitharenite, arkose, subarkose and quartz arenite (Figure 1.11). $Log_{10}(SiO_2/Al_2O_3)$ delimited the silica-rich mature quartz (quartzarenites) from aluminium-rich mudstones or shales (Herron, 1984). $Log_{10}(Fe_2O_3/K_2O)$ separates iron-rich shales from iron-rich sands (Herron, 1984). CaO is also utilised in the spectrum but is omitted from graphical representations. CaO concentrates are utilised to classify sediments and sedimentary rocks as calcareous. Samples with a weight % less than 4% are noncalcareous (Herron, 1984).

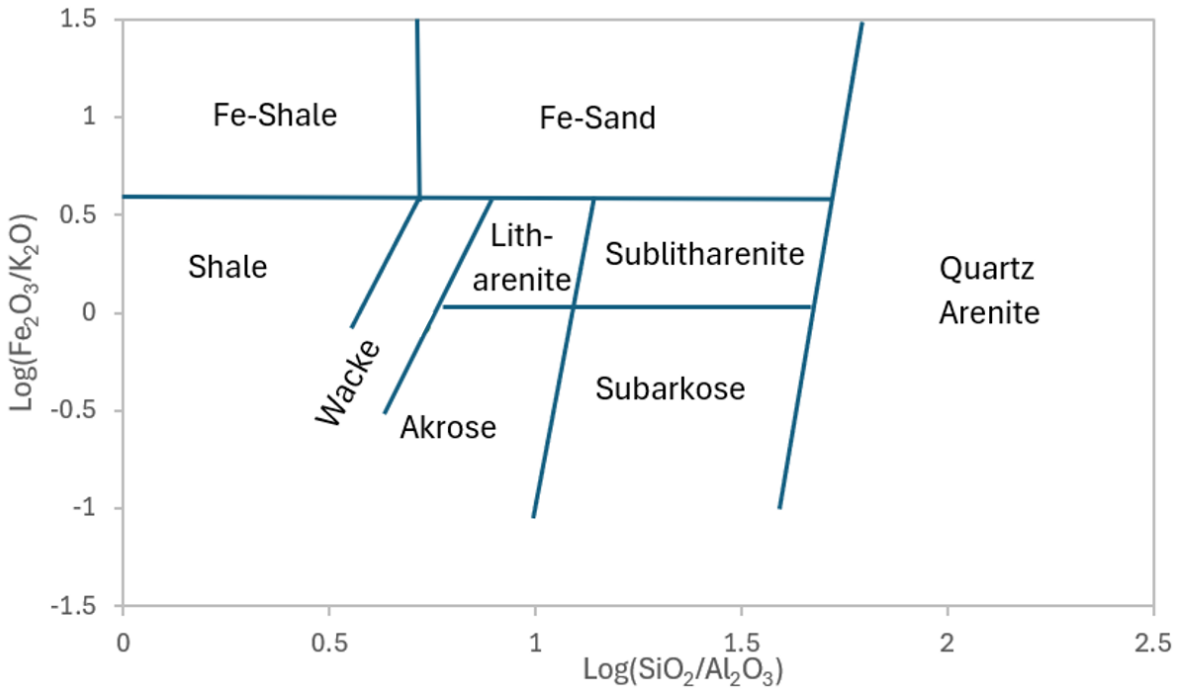

Figure 1.11: SandClass diagram used to classify sands and sandstones (Herron, 1984).

1.5.3.1.2. Discriminant Function for Provenance

The discriminant function diagram categorises sedimentary rocks and sediments into four major groups based on major geochemistry: felsic igneous provenance, intermediate igneous provenance, mafic igneous provenance and quartzose sedimentary provenance (Roser & Korsch, 1988) (Figure 1.12). The discriminant functions are calculated using elemental oxides, including TiO_2, Al_2O_3, Fe_2O_3T, MgO, CaO, Na_2O, and K_2O. These elements were chosen and used in particular ratios in the discriminant functions based on the result of various linear equations captured from individual trends in major elements from the different provenance classifications (Roser & Korsch, 1988) (Equation 3 & Equation 4).

$$DF1 = -1.773TiO_2 + 0.607Al_2O_3 + 0.760Fe_2O_3 - 1.500MgO$$
$$+0.616CaO + 0.509Na_2O - 1.224K_2O - 9.09$$

Equation 3

$$DF2 = 0.445\,TiO_2 + 0.070\,Al_2O_3 - 0.250\,Fe_2O_3 - 1.142\,MgO$$
$$+0.438\,CaO + 1.475\,Na_2O + 1.426\,K_2O - 6.861$$

Equation 4

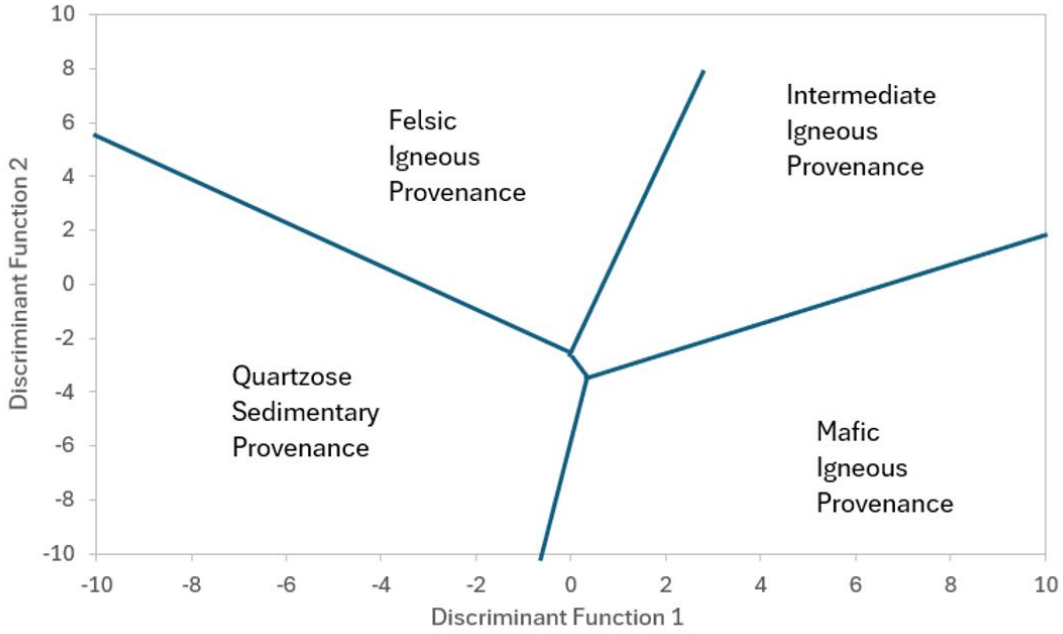

Figure 1.12: Discriminant function diagram of Roser & Korsch (1988) used to classify sand and sandstones by provenance.

1.5.3.1.3. Alteration and Weathering Indices

Several indices can be utilised to determine the degree of alteration or weathering in sediments and sedimentary rocks. The most commonly used ones are: Chemical Index of Alteration (CIA), Plagioclase Index of Alteration (PIA), and the Chemical Index of Weathering (CIW) (Adeigbe & Oyekola, 2020) (Equation 5, Equation 6 & Equation 7). All these indices evaluate sedimentary alteration based on primary elemental ratios from XRF. These indices were formed based on the sequence of rock minerals that break down based on the Glodich Stability Series (1938). The indices follow the weathering of these minerals based on their common elements, which are easily leached from materials (Fedo *et al.*, 1995; Harnois, 1988; Nesbitt & Young, 1982). The CIW was constructed after the CIA had errors associated with potassium being added back into the rock form from illite clay, whereas the PIA was made only to track weathering in sediments dominated by plagioclase (Fedo *et al.*, 1995; Harnois, 1988).

$$CIA = [Al_2O_3 / (Al_2O_3 + CaO* + Na_2O + K_2O)] * 100$$ *Equation 5*

$$CIW = [Al_2O_3 / (Al_2O_3 + CaO* + Na_2O)] * 100$$ *Equation 6*

$$PIA = [(Al_2O_3 - K_2O) / (Al_2O_3 + CaO* + Na_2O - K_2O)] * 100$$ *Equation 7*

CIA, PIA and CIW are all interpreted very similarly, with results ranging from 1-100, indicating varying degrees of weathering. In sands, a CIA of approximately <50 indicate fresh source rock with no weathering, 50-60 indicates weathering has started, while 60-80 is intermediate and 80-100 is extreme (Hernandez-Hinojosa, 2018; Malick & Ishiga, 2016; Yalcin *et al.*, 2022). Similarly, for PIA and CIW, 50 indicates unweathered material, while 100 is extremely weathered (Adeigbe & Oyekola, 2020; Fedo *et al.*, 1995; Malick & Ishiga, 2016; Yalcin *et al.*, 2022).

1.5.3.2. X-Ray Diffraction

XRD is a geochemical technique used to determine the mineralogy of a sediment sample based on mineral crystal structure. This method works by directly X-raying a sedimentary sample and measuring the scattering or diffraction of X-rays due to the mineral's crystal lattice (Chauhan & Chauhan, 2014). Bragg's Law describes that each mineral has a specific crystalline structure, following Equation 8 (Bragg, 1913).

$$n\lambda = 2d\sin(\theta) \qquad \textit{Equation 8}$$

Where the order of reflection (n) multiplied by the wavelength of X-rays (λ) is calculated based on interplanar/d-spacing between crystal planes (d), and angle of reflection of X-rays (θ). Each mineral has atomic planes of differing d-spacings that cause X-rays to diffract at different angles based on the mineral structure (Chauhan & Chauhan, 2014). Constructive interference occurs when diffracted x-rays are in phase, generating a detectable intensity peak (Chauhan & Chauhan, 2014). This data is collected and forms unique graphs plotting X-ray angles with diffraction intensity to identify minerals (Chauhan & Chauhan, 2014). XRD can be utilised to identify minerals in coastal and beach ridge settings, and mineral makeup can hint at sediment provinces and reworking due to the Glodich Stability Series (1938).

1.5.3.3. Laser Particle Size Analysis

Beach ridge sediment can also be analysed using a laser particle sizer. This method measures sediment particle size by detecting the angle at which the particles scatter light. Sediment is placed into a water solution, which is rapidly stirred by the machine, and light is then passed through the sample while the sediment is in suspension (McCave *et al.*, 1986). Sensors detect the angle and intensity of scattered light, and the measurements are interpreted into grain size based on the Fraunhofer approximation or Mie theory (McCave *et al.*, 1986). For example, smaller particles scatter light at wider angles, while larger particles scatter light at smaller angles (McCave *et al.*, 1986).

1.6. Summary

Beach ridges are semi-shore-parallel wave or wind-built sediment accumulations deposited on coastlines (Otvos, 2000). Beach ridges often form when coastlines are in one of two states, regressing (shifting seaward) or equilibrium (Taylor & Stone, 1996). Various factors influence these states, including eustatic sea level, relative sea level, and sediment supply. In the North Island of New Zealand, the post-glacial sea level highstand began around 8.1 to 7.34 ka, reaching up to 3 m above present sea level, dropping to present-day sea level around 4 ka (Clement *et al.*, 2016). These sea-level changes initiated the beginning of progradation on the Rangitāiki Plains.

The Rangitāiki Plains form part of the eastern Bay of Plenty graben and have undergone significant subsidence (4.7 m) during the Holocene as part of the Taupō Rift Valley (Begg & Mouslopoulou, 2010). This subsidence, combined with volcanic activity from the Taupō Volcanic Zone, riverine sediment transport, and wave-dominated coastal accretion conditions, allowed sediment to accumulate and prograde the coastline (Pullar & Selby, 1975). The result is a layer of Holocene sediment overlying greywacke basement rock and intermittent glacial/interglacial deposits. As a result of progradation, the Rangitāiki Plains have extensive beach ridge sets, both stranded inland and at the modern coastline.

Progradation rates have varied over time as the coastline developed. Progradation was highest before 2 ka (Beanland & Berryman, 1992; Pullar & Selby, 1975). Around 2 ka, progradation is thought to have slowed due to the initiation of littoral drift past the Whakatāne headland (Beanland & Berryman, 1992). Since then, human activities such as drainage and dam construction have further modified the plains, causing additional changes in sedimentation patterns (Gibb, 1986). Today, the coastline has shifted from prograding to near-equilibrium (Bay of Plenty Regional Council, 2019; Beanland & Berryman, 1992; Pullar & Selby, 1971).

Several geophysical and geochemical techniques are available to investigate beach ridges like those on the Rangitaiki Plains. Dating methods include radiocarbon dating, tephrochronology, and OSL, while imaging techniques include LiDAR and GPR. XRF is used for elemental classification of sediments, whose ratios can be utilised in further classifications such as the SandClass system, the Discriminant Function for Provenance, and indices for weathering such as CIA, PIA and CIW. XRD also provides mineralogy, and laser particle sizing generates grain size and sediment sorting data.

References

Ali, I., Shaik, R., Azman, A., Singh, P., Bala, J. D., Ao, A., ... Hossain, K. (2022). Impacts of climate change on coastal communities. In the Research anthology on environmental and societal impacts of climate change (pp. 1659–1671). IGI Global Scientific Publishing.

Adeigbe, O. C., & Oyekola, C. B. (2020). Geology and geochemistry of sediments from Lewumeji and Idogun wells, Eastern Dahomey Basin, Southwestern Nigeria. Geology, 10(5).

Aitken, M. J. (1998). Introduction to optical dating: The dating of Quaternary sediments by the use of photon-stimulated luminescence. Oxford: Clarendon Press.

Bailey, R. A., & Carr, R. G. (1994). Physical geology and eruptive history of the Matahina ignimbrite, Taupō volcanic zone, North Island, New Zealand. New Zealand Journal of Geology and Geophysics, 37(3), 319–344.

Bay of Plenty Regional Council. (2019). Physical coastal monitoring 2019. Whakatāne, New Zealand: Bay of Plenty Regional Council, Toi Moana. Retrieved from https://atlas.boprc.govt.nz/api/v1/edms/document/A3312176/content

Bay of Plenty Times. (2023). Cyclone Gabrielle: Coromandel cut off, national state of emergency declared as Bay of Plenty begins clean-up. NZ Herald. Retrieved from https://www.nzherald.co.nz/bay-of-plenty-times/news/cyclone-gabrielle-coromandel-cut-off-national-state-of-emergency-declared-as-bay-of-plenty-begins-clean-up/UAJ27GHAYFAWLHHXZTGV4XJA4Q/

Beanland, S., & Berryman, K. R. (1992). Holocene coastal evolution in a continental rift setting: Bay of Plenty, New Zealand. Quaternary International, 15, 151–158.

Begg, J. G., & Mouslopoulou, V. (2010). Analysis of late Holocene faulting within an active rift using LiDAR, Taupō Rift, New Zealand. Journal of Volcanology and Geothermal Research, 190(1–2), 152–167.

Bell, R., & Lewis, M. (2006). *MHWS level for the Bay of Plenty*. National Institute of Water & Atmospheric Research Ltd. Hamilton, New Zealand.

Berger, A., & Loutre, M. F. (2010). Modelling the 100-kyr glacial–interglacial cycles. Global and Planetary Change, 72(4), 275–281.

Bokuniewicz, H., Makowski, C., & Finkl, C. W. (2019). Ingression, regression, and transgression. In Encyclopedia of coastal science (pp. 1037–1039). Cham, Switzerland: Springer International Publishing. doi:10.1007/978-3-319-93806-6_181

Bowman, S. (1990). Radiocarbon dating (Vol. 1). Berkeley: University of California Press.

Bragg, W. L. (1913). The reflection of short electromagnetic waves by a crystal. *Proceedings of the Cambridge Philosophical Society*, *17*, 43–57.

Carter, L., & Heath, R. A. (1975). Role of mean circulation, tides, and waves in the transport of bottom sediment on the New Zealand continental shelf. New Zealand Journal of Marine and Freshwater Research, 9(4), 423–448.

Chauhan, A., & Chauhan, P. (2014). Powder XRD technique and its applications in science and technology. Journal of Analytical & Bioanalytical Techniques, 5(5), 1–5.

Chiswell, S. M., Bostock, H. C., Sutton, P. J. H., & Williams, M. J. M. (2015). Physical oceanography of the deep seas around New Zealand: A review. New Zealand Journal of Marine and Freshwater Research, 49(2), 286–317. doi:10.1080/00288330.2014.99291

Clement, A. J., Whitehouse, P. L., & Sloss, C. R. (2016). An examination of spatial variability in the timing and magnitude of Holocene relative sea-level changes in the New Zealand archipelago. Quaternary Science Reviews, 131, 73–101. Retrieved from http://sciencedirect.com/science/article/pii/S0277379115301232

De Lange, W. P., & Gibb, J. G. (2000). Seasonal, interannual, and decadal variability of storm surges at Tauranga, New Zealand. New Zealand Journal of Marine and Freshwater Research, 34(3), 419–434.

De Lange, W. P. (2001). Interdecadal Pacific Oscillation (IPO): A mechanism for forcing decadal scale coastal change on the northeast coast of New Zealand? Journal of Coastal Research, 657–664.

Devi, M., Chauhan, N., & Singhvi, A. K. (2024). Post-violet infrared stimulated luminescence (pVIRSL) dating protocol for potassium feldspar. Quaternary Geochronology, 79, 101487.

De Vries, S., Arens, S. M., De Schipper, M. A., & Ranasinghe, R. (2014). Aeolian sediment transport on a beach with a varying sediment supply. *Aeolian Research*, *15*, 235-244.

De Vries, S., Southgate, H. N., Kanning, W., & Ranasinghe, R. (2012). Dune behavior and aeolian transport on decadal timescales. *Coastal Engineering (Amsterdam)*, *67*, 41–53. https://doi.org/10.1016/j.coastaleng.2012.04.002

Dolan, A. H., & Walker, I. J. (2006). Understanding vulnerability of coastal communities to climate change related risks. Journal of Coastal Research, 1316–1323.

Dougherty, A. J., Choi, J., Turney, C. M., & Dosseto, A. (2019). Technical note: Optimizing the utility of combined GPR, OSL, and LiDAR (GOaL) to extract paleoenvironmental records and decipher shoreline evolution. Climate of the Past, 15(1), 389–404.

Doyle, T. B., & Woodroffe, C. D. (2018). The application of LiDAR to investigate foredune morphology and vegetation. Geomorphology, 303, 106–121.

Duller, G. A. T. (1997). Behavioural studies of stimulated luminescence from feldspars. Radiation Measurements, 27(5–6), 663–694.

Fedo, C. M., Nesbitt, H. W., & Young, G. M. (1995). Unraveling the effects of potassium metasomatism in sedimentary rocks and paleosols, with implications for paleoweathering conditions and provenance. Geology, 23(10), 921–924. doi:10.1130/0091-7613(1995)023<0921:UTEOPM>2.3.CO;2

Garrison, T. S. (2015). Oceanography (9th ed.). Belmont, CA: Cengage Learning.

Gibb, J. G. (1986). A New Zealand regional Holocene eustatic sea-level curve and its application to determination of vertical tectonic movements. Royal Society of New Zealand Bulletin, 24, 377–395.

Gibbons, W. H. (1990). The Rangitāiki, 1890–1900: Settlement and drainage on the Rangitāiki. Whakatāne: Whakatāne & District Historical Society.

Gordon, N. D. (1986). The southern oscillation and New Zealand weather. Monthly Weather Review, 114(2), 371–387.

Hajdas, I. (2008). Radiocarbon dating and its applications in Quaternary studies. E&G Quaternary Science Journal, 57(1/2), 2–24. Retrieved from https://egqsj.copernicus.org/articles/57/2/2008/egqsj-57-2-2008.pdf

Harnois, L. (1988). The CIW index: A new chemical index of weathering. Sedimentary Geology, 55(3–4), 319–322. doi:10.1016/0037-0738(88)90137-6

Hay, D. N., de Lange, W. P., & Healy, T. R. (1991, January). Storm and oceanographic databases for the Western Bay of Plenty. In Australasian Conference on Coastal and Ocean Engineering (pp. 139–143). Hamilton, New Zealand: Water Quality Centre, DSIR Marine and Freshwater.

Heads, M. (2017). Biogeography and Neogene geology of mainland New Zealand: Alpine Fault strike-slip, Kaikoura orogeny, and Pleistocene glaciation. In Biogeography and evolution in New Zealand (pp. 291–338). Boca Raton, FL: CRC Press. doi:10.1201/9781315368177-17

Healy, T. R. (1978). Bay of Plenty coastal survey report 78/3: Nearshore hydrographic survey of beach bars. Whakatāne, New Zealand: Bay of Plenty Catchment Commission.

Healy, T., & De Lange, W. (2014). Reliability of geomorphic indicators of littoral drift: Examples from the Bay of Plenty, New Zealand. [Unpublished report].

Hernandez-Hinojosa, V., Montiel-Garcia, P. C., Armstrong-Altrin, J. S., Nagarajan, R., & Kasper-Zubillaga, J. J. (2018). Textural and geochemical characteristics of beach sands along the western Gulf of Mexico, Mexico. Carpathian Journal of Earth and Environmental Sciences, 13(1), 161–174.

Herron, M. M. (1988). Geochemical classification of terrigenous sands and shales from core or log data. *Journal of Sedimentary Research*, *58*(5), 820-829.

Huntley, D. J., Godfrey-Smith, D. I., & Thewalt, M. L. (1985). Optical dating of sediments. Nature, 313(5998), 105–107.

Iremonger, S. D. (2007). *NERMN beach profile monitoring (Environmental Publication 2007/08)*. Whakatāne, New Zealand: Environment Bay of Plenty.

Ivamy, M. C., & Kench, P. S. (2006). Hydrodynamics and morphological adjustment of a mixed sand and gravel beach, Torere, Bay of Plenty, New Zealand. *Marine Geology, 228*(1–4), 137–152.

Jol, H. M., Smith, D. G., & Meyers, R. A. (1996). Digital ground penetrating radar (GPR): A new geophysical tool for coastal barrier research (examples from the Atlantic, Gulf and Pacific Coasts, USA). *Journal of Coastal Research,* 960–968.

Jol, H. M. (Ed.). (2008). *Ground penetrating radar theory and applications.* Amsterdam: Elsevier.

King, P. R. (2000). Tectonic reconstructions of New Zealand: 40 Ma to the present. *New Zealand Journal of Geology and Geophysics, 43*(4), 611–638.

King, D. J., Newnham, R. M., Gehrels, W. R., & Clark, K. J. (2021). Late Holocene sea-level changes and vertical land movements in New Zealand. *New Zealand Journal of Geology and Geophysics, 64*(1), 21–36. doi:10.1080/00288306.2020.1761839

Kingma, J. T. (1959). The tectonic history of New Zealand. *New Zealand Journal of Geology and Geophysics, 2*(1), 1–55.

Langridge, R. M., Ries, W. F., Litchfield, N. J., Villamor, P., Van Dissen, R. J., Barrell, D. J. A., ... Stirling, M. W. (2016). The New Zealand Active Faults Database. *New Zealand Journal of Geology and Geophysics, 59*, 86–96. doi:10.1080/00288306.2015.1112818

Libby, W. F. (1949). *Radiocarbon dating*. Chicago: University of Chicago Press.

Libby, W. F., & Johnson, F. (1955). *Radiocarbon dating* (Vol. 2). Chicago: University of Chicago Press.

Lowe, D. J. (2011). Tephrochronology and its application: A review. *Quaternary Geochronology, 6*(2), 107–153.

Lundquist, C. J., Ramsay, D., Bell, R., Swales, A., & Kerr, S. (2011). Predicted impacts of climate change on New Zealand's biodiversity. *Pacific Conservation Biology, 17*(3), 179–191.

Macky, G. H., Latimer, G. J., & Smith, R. K. (1995). Wave climate of the western Bay of Plenty, New Zealand, 1991–93. *New Zealand Journal of Marine and Freshwater Research, 29*(3), 311–327.

Malick, B. M. L., & Ishiga, H. (2016). Geochemical classification and determination of maturity source weathering in beach sands of eastern San'in Coast, Tango Peninsula, and Wakasa Bay, Japan. *Earth Science Research, 5*(1), 44–56.

Marshak, S. (2015). *Earth: Portrait of a planet* (5th ed.). New York: W. W. Norton & Company.

McCave, I. N., Bryant, R. J., Cook, H. F., & Coughanowr, C. A. (1986). Evaluation of a laser-diffraction-size analyzer for use with natural sediments. *Journal of Sedimentary Petrology, 56*(4), 561–564.

Montaño, M. M., Suanda, S. H., & de Souza, J. M. A. C. (2023). Modelled coastal circulation and Lagrangian statistics from a large coastal embayment: The case of Bay of Plenty, Aotearoa New Zealand. *Estuarine, Coastal and Shelf Science, 281,* 108212.

Mouslopoulou, V., Nicol, A., Little, T. A., & Walsh, J. J. (2007). Displacement transfer between intersecting regional strike-slip and extensional fault systems. *Journal of Structural Geology, 29*(1), 100–116.

Muto, T., & Steel, R. J. (1997). Principles of regression and transgression: The nature of the interplay between accommodation and sediment supply. *Journal of Sedimentary Research, 67*(6), 994–1000.

Nairn, I. A., & Beanland, S. (1989). Geological setting of the 1987 Edgecumbe earthquake, New Zealand. *New Zealand Journal of Geology and Geophysics, 32*(1), 1–13.

Nesbitt, H. W., & Young, G. M. (1982). Early Proterozoic climates and plate motions inferred from major element chemistry of lutites. *Nature, 299*(5885), 715–717. doi:10.1038/299715a0

NIWA. (2024). *Waves*. Wellington: National Institute of Water and Atmospheric Research. Retrieved from https://niwa.co.nz/hazards/waves

Otvos, E. G. (2000). Beach ridges—Definitions and significance. *Geomorphology, 32*(1–2), 83–108. doi:10.1016/S0169-555X(99)00075-6

Peltier, W. R. (1999). Global sea-level rise and glacial isostatic adjustment. *Global and Planetary Change, 20*(2–3), 93–123.

Philander, S. G. H. (1983). El Niño Southern Oscillation phenomena. *Nature, 302*(5906), 295–301.

Phillips, C. J., & Nelson, C. S. (1981). Sedimentation in an artificial lake—Lake Matahina, Bay of Plenty. *New Zealand Journal of Marine and Freshwater Research, 15*(4), 459–473.

Pickett, V. (2004). *The application of equilibrium beach profile theory to coastal hazard identification in the Bay of Plenty* (Master's thesis). University of Waikato, Hamilton, New Zealand.

Price, R. C., Mortimer, N., Smith, I. E. M., & Maas, R. (2015). Whole-rock geochemical reference data for Torlesse and Waipapa terranes, North Island, New Zealand. *New Zealand Journal of Geology and Geophysics, 58*(3), 213–228. doi:10.1080/00288306.2015.1026832

Prentice, L. (2008). *Coastal systems: Waves, tides, sediments, cells* (GeoFile 575). Retrieved from https://www.thegeographeronline.net/uploads/2/6/6/2/26629356/geofile_575_coastal_systems.pdf

Pullar, W. A., & Selby, M. J. (1971). Coastal progradation of Rangitāiki Plains, New Zealand. *New Zealand Journal of Science, 14,* 419–434.

Pullar, W. A. (1985). *Soils and land use of Rangitāiki Plains, North Island, New Zealand* (New Zealand Soil Survey Report 86). Wellington: New Zealand Soil Bureau.

Roser, B. P., & Korsch, R. J. (1988). Provenance signatures of sandstone-mudstone suites determined using discriminant function analysis of major-element data. *Chemical geology*, *67*(1-2), 119-139.

Rovere, A., Stocchi, P., & Vacchi, M. (2016). Eustatic and relative sea-level changes. *Current Climate Change Reports, 2,* 221–231. Retrieved from https://link.springer.com/content/pdf/10.1007/s40641-016-0045-7.pdf

Shane, P. (2000). Tephrochronology: A New Zealand case study. *Earth-Science Reviews, 49*(1–4), 223–259.

Shields, A. (1936). *Application of similarity principles and turbulence research to bed-load movement* (W. P. Ott & J. C. van Uchelen, Trans.). Pasadena, CA: California Institute of Technology, Soil Conservation Service Cooperative Laboratory.

Stephens, S. A., Bell, R. G., & Haigh, I. D. (2020). Spatial and temporal analysis of extreme storm-tide and skew-surge events around the coastline of New Zealand. *Natural Hazards and Earth System Sciences, 20*(3), 783–800.

Sutton, P. J., Chiswell, S. M., Bowen, M. M., & Williams, M. J. (2003). *A summary of physical oceanography around New Zealand.* Wellington: NIWA.

Svendsen, J., Friis, H., Stollhofen, H., & Hartley, N. (2007). Facies discrimination in a mixed fluvio-eolian setting using elemental whole-rock geochemistry—Applications for reservoir characterization. *Journal of Sedimentary Research, 77*(1), 23–33.

Taylor, M., & Stone, G. W. (1996). Beach-ridges: A review. *Journal of Coastal Research,* 612–621.

Tripathi, A. R. P., Kamp, P. J., & Nelson, C. S. (2008). Te Kuiti Group (Late Eocene–Oligocene) lithostratigraphy east of Taranaki Basin in central-western North Island, New Zealand. *New Zealand Journal of Geology and Geophysics, 51*(2), 125–143.

Vousdoukas, M. I., Ranasinghe, R., Mentaschi, L., Plomaritis, T. A., Athanasiou, P., Luijendijk, A., & Feyen, L. (2020). Sandy coastlines under threat of erosion. *Nature Climate Change, 10*(3), 260–263.

Walters, R. A., Goring, D. G., & Bell, R. G. (2001). Ocean tides around New Zealand. *New Zealand Journal of Marine and Freshwater Research*, *35*(3), 567-579. https://doi.org/10.1080/00288330.2001.9517023

Wang, C., Yang, X., Xi, X., Nie, S., & Dong, P. (2024). *Introduction to LiDAR remote sensing.* Boca Raton, FL: CRC Press.

Weltje, G. J., & Tjallingii, R. (2008). Calibration of XRF core scanners for quantitative geochemical logging of sediment cores: Theory and application. *Earth and Planetary Science Letters*, *274*(3-4), 423-438.

Wentworth, C. K. (1922). A scale of grade and class terms for clastic sediments. *The Journal of Geology, 30*(5), 377–392. doi:10.1086/622910

Whakatāne District Council. (2010). *Ports operation plan: History of the Whakatāne District's port and harbour areas*. Retrieved from https://www.Whakatāne.govt.nz/sites/www.Whakatāne.govt.nz/files/documents/documents-section/council-plans/ports-operational-plan/WDC%20PORTS%20DOC%20Appendicies%20web%20section%20one.pdf

White, P., Raiber, M., Begg, J., Freeman, J., & Thorstad, J. (2010). *Groundwater resource investigations of the Rangitāiki Plains stage 1: Conceptual geological model, groundwater budget and preliminary groundwater allocation assessment*. Whakatāne, New Zealand: Bay of Plenty Regional Council. Retrieved from https://www.boprc.govt.nz/media/101224/cr_2010-113_-_groundwater_resource_investigations_of_the_Rangitāiki_plains_stage_1-_web_download_copy.pdf

Wintle, A. G. (1997). Luminescence dating: Laboratory procedures and protocols. *Radiation Measurements, 27*(5–6), 769–817.

Wintle, A. G., & Adamiec, G. (2017). Optically stimulated luminescence signals from quartz: A review. *Radiation Measurements, 98,* 10–33.

Yalcin, M. G., Nyamsari, D. G., Ozer Atakoglu, O., & Yalcin, F. U. S. U. N. (2022). Chemical and statistical characterization of beach sand sediments: Implication for natural and anthropogenic origin and paleo-environment. *International Journal of Environmental Science and Technology, 19*(3), 1335–1356.

Zhang, J., & Li, S. H. (2020). Review of the post-IR IRSL dating protocols of K-feldspar. *Methods and Protocols, 3*(1), 7.

Chapter 2:

Reconstructing Holocene Coastal Evolution of the Rangitāiki Plains, Aotearoa-New Zealand, Using Geophysical and Geochemical Approaches

2.1. Introduction

The Rangitāiki Plains, situated in the eastern Bay of Plenty, New Zealand, form a tectonically active alluvial plain deposited throughout the mid-late Holocene (~8 ka to present). Over the past ~6,500 years, the coastline has prograded approximately 10 km due to a combination of tectonic subsidence and high sediment supply (Beanland & Berryman, 1992). This progradation has resulted in the formation of successive sandy beach ridge sets, often termed prograded or stranded beach ridges on the Rangitāiki Plains. In this thesis, all relict sand ridges are referred to as beach ridges regardless of whether their formation history is wave-dominated, aeolian-dominated, or a combination of both (following Otvos, 2000). These preserved beach sediments are crucial for understanding environmental changes, offering insights into shoreline evolution, sediment supply, storm activity, and sea-level fluctuations. Understanding coastal evolution is especially relevant in the context of modern climate change and increasing anthropogenic impacts on the coastline. A more detailed understanding of past coastal dynamics can help forecast future shoreline behaviour and inform coastal management and planning strategies in the Rangitāiki Plains and New Zealand. A thorough reconstruction of Holocene coastal progradation is needed to support these efforts.

Previous studies of the Rangitāiki Plains have investigated progradation rates, sediment accumulation, and faulting, identifying the primary driver of progradation as the subsiding Whakatāne Graben, which created the accommodation space that has been infilled by volcaniclastic material transported by rivers (Beanland & Berryman, 1992; Begg & Mouslopoulou, 2010; Pullar & Selby, 1971). Pullar & Selby (1971) previously applied tephrochronology and radiocarbon dating to determine the ages of several palaeoshorelines, and therefore, minimum ages of beach ridge sets. However, several beach ridge sets remain undated, or their age data remains constrained by uncertain tephrochronological correlations, resulting in gaps in the reconstruction of progradation rates. Additionally, limited textural and geochemical

characterisation of beach ridges has hampered understanding of sediment provenance and reworking processes occurring on the Rangitāiki Plains. To address these limitations, Light Detection and Ranging (LiDAR), Ground-Penetrating Radar (GPR), Optically Stimulated Luminescence (OSL) dating, and geochemical analyses (X-ray fluorescence [XRF] and X-ray diffraction [XRD]) were integrated. This study aimed to investigate the timing, rates, and controlling mechanisms of mid-late Holocene coastal progradation on the Rangitāiki Plains by studying the age and surface and subsurface structure of prograding beach ridge sets.

2.2. Regional Background

The Rangitāiki Plains are located in the Bay of Plenty Region on New Zealand's North Island and span approximately 22 km from the township of Matatā in the west to Whakatāne in the east (Pullar, 1985) (Figure 1.1). The plains extend 20 km inland from the coast to the small town of Kawerau, covering 400 km^2 (Pullar & Selby, 1973; Pullar, 1985). Hilly terrain surrounds the plains, including the Mokoroa Hills to the east and the Manawahe Hills to the west.

Located at the intersection of the Taupō Rift Valley and the North Island Fault System, the plains lie within a seismically active graben (Beanland & Berryman, 1992; Begg & Mouslopoulou, 2010). The Rangitāiki Plains are formed from sediment accumulation within the Whakatāne Graben and are underlain by greywacke basement rocks (Beanland & Berryman, 1992; Begg & Mouslopoulou, 2010). Subsequent sedimentary sequences reflect alternating marine and non-marine deposits from interglacial and glacial periods (White *et al.*, 2010). During the last glacial period (115 ka to 11.7 ka), sea level was 120m above the present-day average (Gibb, 1986). At the start of the Holocene, sea level rose to 3 m above present-day average by 8.1 ka to 7.34 ka, falling slowly to stabilise its current level around 4 ka (Clement *et al.*, 2016). Since this Holocene sea-level stabilisation, sedimentation has been dominantly riverine, with sediment supplied from the Rangitāiki, Tarawera, and Whakatāne rivers (Gibbons, 1990; White *et al.*, 2010). Sediment provenance varies regionally: the Whakatāne River transports predominantly weathered greywacke from the Urewera Ranges, while the Rangitāiki and Tarawera rivers deliver volcanic-derived sediments from Taupō and Tarawera catchments (Beanland & Berryman, 1992; Gibbons, 1990).

Materials transported down these rivers were discharged to the Pacific Ocean and subsequently deposited on the coastline via wave action, causing progradation and the construction of beach ridges. Deposition has been largely restricted to the Whakatāne Graben due to the headlands

blocking sediment transport from the bay. Progradation continued until about 2 ka, when the shoreline extended far enough out to sea for sediment to bypass the Whakatāne Headland under longshore drift (Beanland & Berryman, 1992). This longshore drift removed sediment from the bay and reduced progradation (Beanland & Berryman, 1992). After European arrival in the 1800s, human activities such as river damming and extensive drainage modifications further impacted this trend, disrupting sediment supply. These conditions ultimately lead to a modern near-equilibrium coastline position (Beanland & Berryman, 1992).

2.2.1. Study Area

This study focused on the portion of the Rangitāiki Plains east of Whakatāne Graben, situated across the Whakatāne River from Whakatāne township. Between November 5th and 7th, 2024, field work was undertaken to investigate four major and one minor beach ridge set. The major beach ridge sets were named Set 1 (landward-most) through to Set 4 (seaward-most), while the minor was named RANGI24-6B (Figure 2.1). Sediment samples, OSL samples and GPR transects were collected across each beach ridge set. Access, property boundaries and landowner permissions constrained site selection. Sites were chosen to allow both sediment samples and GPR surveying in proximity, enabling optimal comparison between datasets. In addition to beach ridge sampling sites, samples were taken from the swash zone along the modern Rangitāiki Plains coastline (Figure 2.1). These sites were located along the coast depending on beach accessibility.

2.3. Methods

2.3.1. Light Detection and Ranging

LiDAR data was sourced from the Bay of Plenty 1 m digital elevation model (DEM) dataset (2019–2022) provided by Land Information New Zealand (2021). Tiles were merged using the mosaic tool in ArcGIS Pro (Esri, 2023) to create a continuous raster. Once symbology was applied, beach ridge sets were identifiable due to their elevation above the surrounding peat and alluvial plains. These maps guided field sampling for GPR and OSL analyses. Furthermore, LiDAR images were also combined with OSL dating to determine the progradation rate between beach ridge sets. This was done by measuring the distances between the beach ridges on which sediment sampling for OSL occurred and dividing the horizontal distances by the temporal difference between the OSL samples.

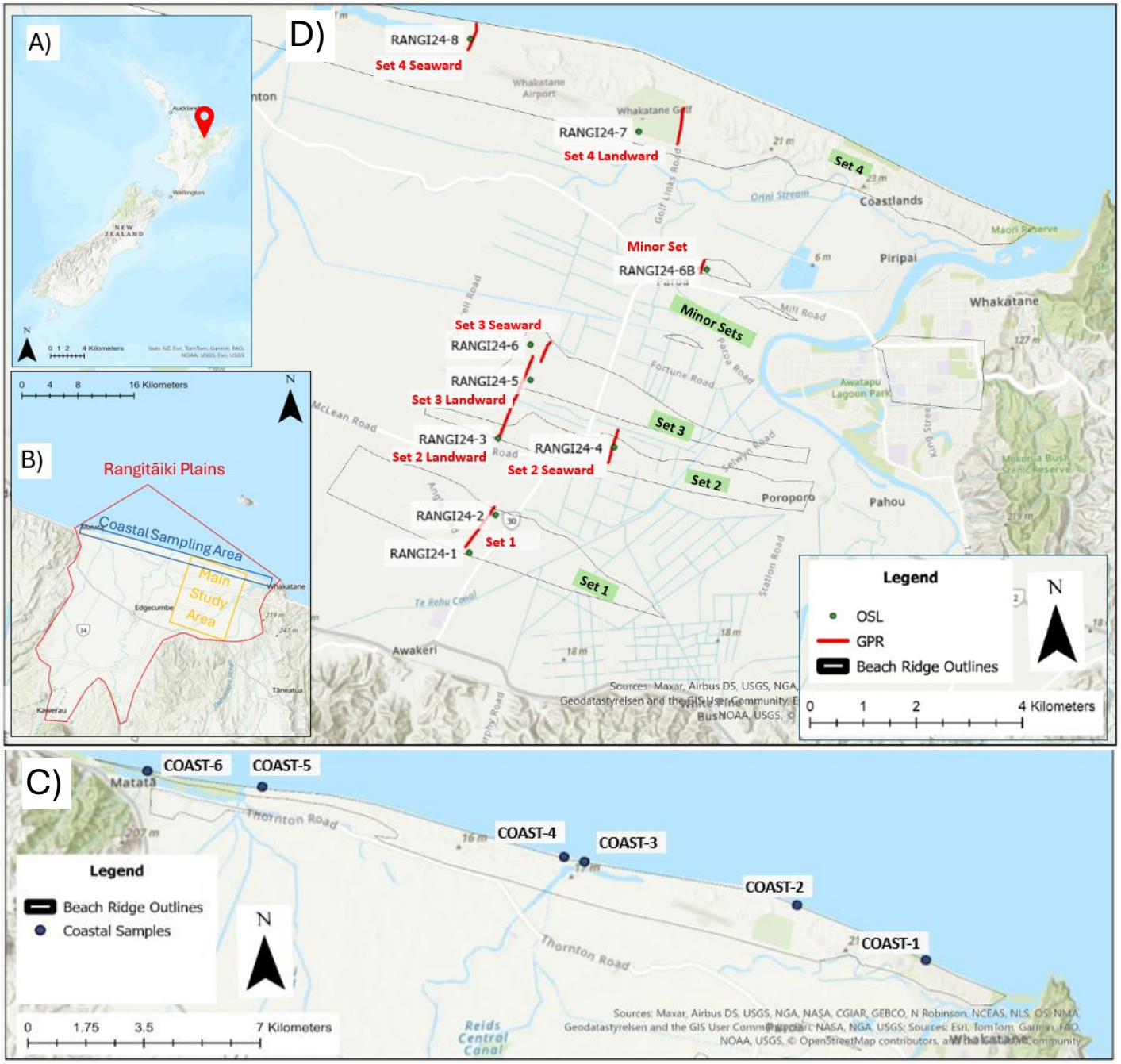

Figure 2.1: Rangitaiki Plains study area including names of data and locations where OSL and modern coastal samples were taken, as well as the location of GPR transects.

2.3.2. Ground Penetrating Radar

GPR surveys were carried out to image the internal stratigraphy of beach ridges. A COBRA CBD wireless penta-antenna GPR unit was combined with a Leica GS18 Real Time Kinematic (RTK) GPS for positional data. The system was configured for sandy sediments and operated on two channels simultaneously: Channel 1 was 100 ns (6.99 m depth) and Channel 2 was 50 ns (3.50 m depth).

GPR transects were collected across the four major beach ridge sets and the minor beach ridge, resulting in nine profiles in total (Figure 2.1). GPR transects were named based on their respective beach ridge sets and whether they were taken from the seaward or landward extent. Transect locations were selected on properties with semi-modified surfaces, such as cattle raceways, farm roads, and tracks, which showed no evidence of artificial modification flattening the beach ridges in the LiDAR DEM and were confirmed in the field based on topographic observations. These surfaces were preferred due to the need for smooth terrain to maintain close ground contact for the GPR.

The RTK GPS, mounted on the GPR unit, recorded latitude, longitude, and elevation every 5 m (±0.1 m). A synchronised waypoint was created on the RTK and GPR units to confirm alignment for processing in PRISM2 (Radar Systems, Inc. & RadarTeam Sweden AB, 2018) software.

Following GPR surveys, RTK data were modified in ArcGIS Pro (Esri, 2023) to produce accurate lines of the GPR transects. These GPR coordinates were input into the topographic correction function of PRISM2 (Radar Systems, Inc. & RadarTeam Sweden AB, 2018) to adjust the GPR lines for elevation. The GPR lines were then analysed for distinct characteristics such as seaward/landward dipping stratigraphy, erosional surfaces, and other reflectors.

2.3.3. Optically Stimulated Luminescence

Sediment samples for OSL age-determinations were collected at the nine sites depicted in Figure 2.1. These sites were located on prominent beach ridges crests at the landward and seaward ends of the four major sets and the one minor set (Figure 2.1). Samples were collected using a hand auger approximately 80 cm below the apparent crest of each beach ridge. A change in colour and sediment texture between soil and sand marked the tops of beach ridges. When the appropriate sampling depth was reached, a metal tube replaced the auger head for sample collection. The auger was carefully inserted back into the auger hole and hammered into the sediment with a mallet. Once the sampling tube was full of sediment, the tube was pulled back

to the surface and sealed with end-caps and duct tape to prevent light exposure at the centre of each core.

Samples were opened in a darkroom at the University of Waikato. Under red light, the central portion of each sample tube was removed and double-sealed in black plastic for OSL dating. Sediment at the tube ends was retained to analyse environmental dose rates, moisture content, grain size, elemental and mineral composition. OSL samples were sent to the Geological Survey of Japan, National Institute of Advanced Industrial Science and Technology for dating. The environmental dose rate was analysed at Intertek in Maddington, Western Australia, and textual and geochemical analyses were conducted at the University of Waikato.

Standard procedures for the National Institute of Advanced Industrial Science and Technology were followed when preparing the OSL samples. Upon testing three different OSL signals (Quartz OSL, Feldspar Infrared Stimulated Luminescence [IRSL], and Post-IR Infrared Stimulated Luminescence [pIRIR]), results showed that Quartz OSL did not perform appropriately due to the volcanic nature of the sediment. Consequently, feldspar IRSL and pIRIR signals were used to determine the age of the beach ridge sediments. Due to decreased error in pIRIR dating compared to the IRSL dating, pIRIR was utilised for the final Rangitāiki Plains OSL ages.

2.3.4. Geochemical and Textual Analysis

Sediment samples for geochemical analysis were collected from auger sampling at 20 cm intervals up to the depth of the OSL samples. Sediment samples were also collected from the swash zone along the modern coastline to track longshore drift direction. These samples were taken at Coastlands, Thornton, and Matatā beaches (Figure 2.1). Modern coastal sediment samples (MCS) were labelled COAST-1 (east) through COAST-6 (west). OSL and sediment samples were labelled RANGI24-1 (landward) through RANGI24-8 (seaward). These samples were all analysed at the University of Waikato for their elemental composition, mineralogy, and grain size.

2.3.4.1. X-Ray Fluorescence

XRF was used to determine the elemental composition of all the sediment samples collected on the Rangitāiki Plains. Samples were dried at 105 °C for 24 hours and then milled to a fine powder using a tungsten carbide ring mill. Loss on ignition (LOI) for both organic matter and carbonate content was measured for all the samples by combusting approximately 0.1–0.2 g of sample at 1100 °C overnight and calculating the mass loss. For major element analysis, fusion beads were prepared by combining 0.8 g of sample with 8 g of a 12:22 lithium borate flux and lithium iodide,

then melting the mixture at 1100 °C. Pressed pellets for trace element analysis were formed by mixing the powdered sample with 16% ethanol PVA glue, compressing the mixture in a hydraulic press at 200 bar, and drying the pressed pellets at 70 °C in an oven. These processes were summarised in Figure 2.2.

Samples were analysed using a Bruker WDXRF S8 Tiger XRF. Major elemental results were reported as weight percent (wt%) in oxides including Na_2O, MgO, Al_2O_3, SiO_2, P_2O_5, SO_3, K_2O, CaO, TiO_2, MnO, and Fe_2O_3. Trace elements, reported in parts per million (PPM), included Sc, V, Cr, Co, Ni, Cu, Zn, Ga, As, Rb, Sr, Y, Zr, Nb, Mo, Sn, Sb, Cs, Ba, La, Ce, Nd, Tl, Pb, Th, U, F, S, and Cl. Standards GSP-2 (granodiorite), AGV-2 (andesite), and RGM-2 (coarse-grained granite) were used to calibrate the XRF instrument and ensure quality control. Results from this analysis were composed into tables and analysed for specific elemental ratios.

2.3.4.2. X-Ray Diffraction

XRD was used to determine the mineralogy of all the sediment samples taken on the Rangitāiki Plains. Samples were dried at 105 °C overnight, milled, and packed into sample holders (Figure 2.2). They were then analysed using a PANalytical Empyrean XRD system. A quartz standard (NIST SRM 1878) was used for calibration.

XRD results were analysed using HighScore Plus (PANalytical, 2012). This software identified peaks in the XRD diffractograms and associated the most likely minerals with each set of peaks. Data Viewer (Malvern Panalytical, 2020) was used to compare results across different samples and to produce XRD graphs.

2.3.4.3. Laser Particle Sizer

The grain size of sediments was measured using a Malvern Mastersizer 3000 laser diffraction particle size analyser. Samples were dried at 105 °C, and organic matter was removed using 10% and 30% hydrogen peroxide. Once bubbling from hydrogen peroxide reactions in the sediment samples ceased, hexametaphosphate (Calgon) was added and left to deflocculate particles for 24 hours. Samples were then run through the Mastersizer on a sediment setting. The particle sizer used a stir speed of 2410 RPM, ultrasound at 50%, and a laser obstruction between 5% and 20%. The data collection software used was Mastersizer Xplorer (Malvern Panalytical, 2024). Results were processed using GRADISTAT (Blott & Pye, 2001), which calculates statistical parameters, including mean, sorting, skewness, and kurtosis using the Folk and Ward (1957) method.

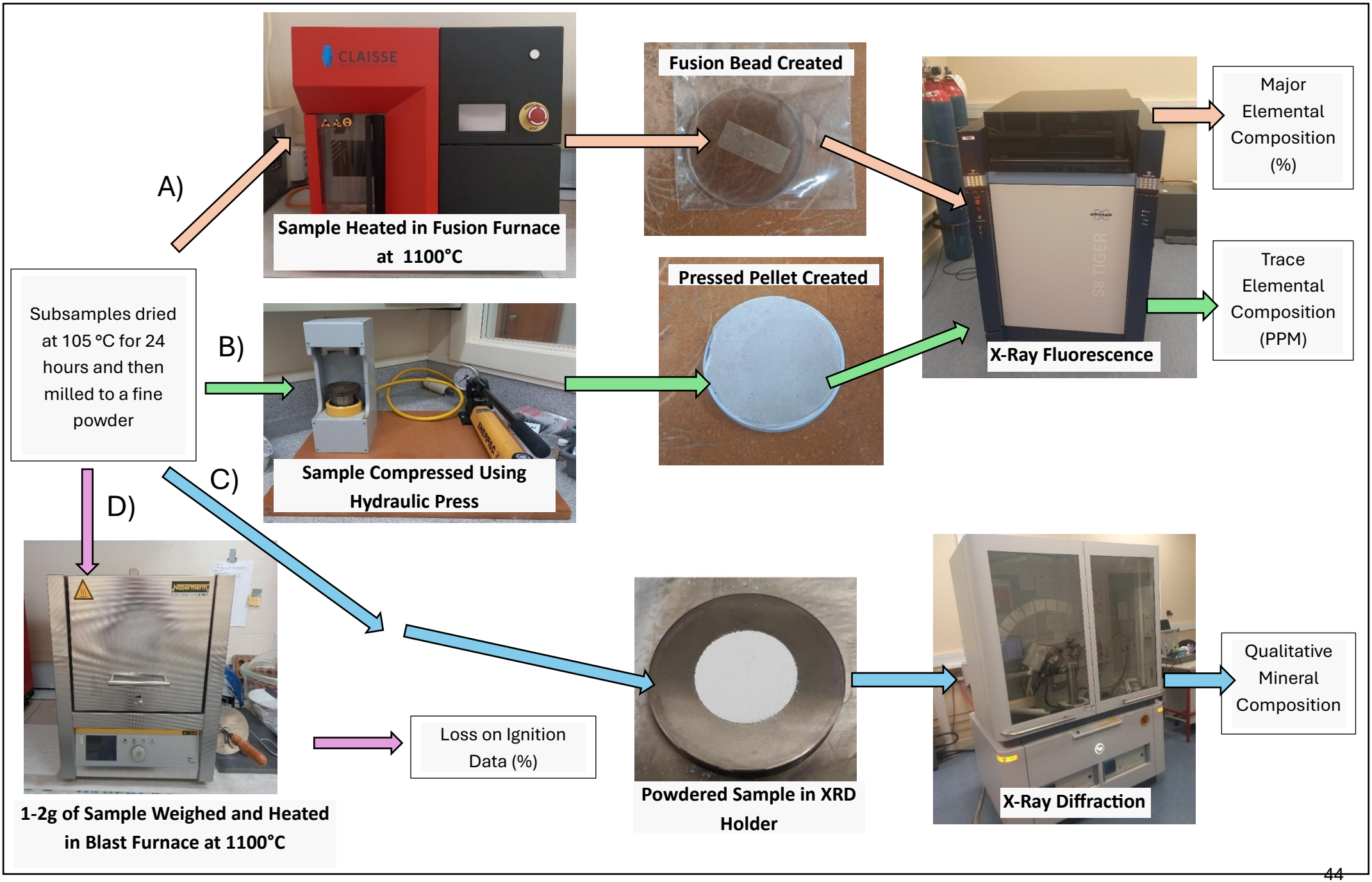

Figure 2.2: Summarised process of geochemical analysis of samples taken on the Rangitaiki Plains. A) Process for Major XRF data collection; B) process for trace XRF data collection; C) process for XRD data collection; D) process for LOI data collection.

2.3.4.4. Munsell Colour Chart

Samples were visually analysed for colour while field moist using the Munsell Soil Colour Chart (Munsell Colour, 2009). Secondary observers confirmed colours in the laboratory to ensure consistent interpretation across samples.

2.4. Results and Interpretations

2.4.1. Light Detection and Ranging

The Rangitāiki Plains LiDAR data depicts the varying spatial extent of the beach ridges (Figure 2.3 & Table 2.1). The LiDAR shows that all the beach ridges vary in width and length, as well as the number of ridges present. Beach Ridge Sets 1, 2 and 3 (BRS 1-3) are all located in the eastern Rangitāiki Plains and all have similar morphologies. They are cut off at their western margin by meandering arms of sediment with a greater elevation than the surrounding flood plains (Figure 2.3). The landward side of all the ridges is a straight boundary, while the seaward sides vary significantly in shape, creating an uneven boundary. The Taupō washout event, a significant deposition of volcanic material from the 1.718±0.010 ka Taupō eruption onto the plains, caused the lobes of sediment cutting off the western margin of BRS 1-3 (Figure 2.3). The inconsistent seaward sides of the beach ridges suggest erosion between each subsequent development of beach ridges.

The beach ridges vary in maximum and average elevation from landward to seaward. The second-highest elevation occurs at BRS 1, before declining from BRS 2 to BRS 3 and increasing again to the maximum elevation at BRS 4. BRS 1 is located 10.180-9.332 km inland of the modern coastline and is 1.41 km inland of BRS 2. This beach ridge has a slight concave shape, with no truncations, nine beach ridges and a maximum elevation of 5.48 m. BRS 2 is located 7.922-7.468 km from the modern coastline and 2.06 km from BRS 3. BRS 2 also has no truncations, seven beach ridges, and a maximum elevation of 4.4 m. BRS 3 is 6.852-6.198 km inland from the modern coastline and 3.67 km from the minor beach ridge set. BRS 3 also has no truncations, eight beach ridges, and a maximum elevation of 5.04 m. The decrease in BRS 1-3 beach ridge height over time suggests the relative sea level has decreased.

The minor beach ridge set (RANGI24-6B) has similar morphology to BRS 1-3; however, it is a scattering of three small ridges divided by lower elevation areas (Figure 2.3). The minor beach ridge set is located 2.1 km inland of RANGI24-7 and has a max elevation of 7.54 m. Due to its

discontinuity, the set has an unknown number of ridges. However, based on RANGI24-6B's parallel position to the unsampled beach ridge set under the Whakatāne township, RANGI24-6B is likely an eroded proportion of that beach ridge.

Beach Ridge Set 4 (BRS 4) spanned the entire length of the Rangitāiki Plains coastline and has a slight convex orientation of ridges with no truncations. BRS 4 has scattered depressions that appear as non-uniform circular inclusions within the beach ridges, typically featuring a raised landward margin before returning to the standard beach ridge topography. These features are aeolian blowouts, regions where intense aeolian transport has blown sediment from the beach ridge system and generated depressions. This suggests BRS 4 experiences more erosive aeolian transport than BRS 1-3.

BRS 4 exhibits the highest elevation of all the beach ridge sets, reaching over 9.3 m. BRS 4 also displays the most well-defined ridges on the plains, consisting of 19 individual ridges. The taller beach ridges suggest a higher relative mean sea level during the formation of BRS 4 compared to the previous beach ridge sets, likely the result of tectonic subsidence.

Table 2.1: Characteristics of beach ridge sets on the Rangitāiki Plains, including distance from the coast, width, elevation, number of ridges and whether truncations are present.

Ridge Name	Distance From Coast (km)	Ridge Width (m)	Max Elevation (m)	Average Elevation (m)	Number of Ridges	Truncations
Set 1	10.18-9.33	850	5.48	4.60	9	No
Set 2	7.92-7.47	450	4.40	3.48	7	No
Set 3	6.85-6.20	650	5.04	3.14	8	No
Minor	3.68	N/A	7.54	3.24	N/A	No
Set 4	1.57-0.46	1110	9.30	6.20	19	No

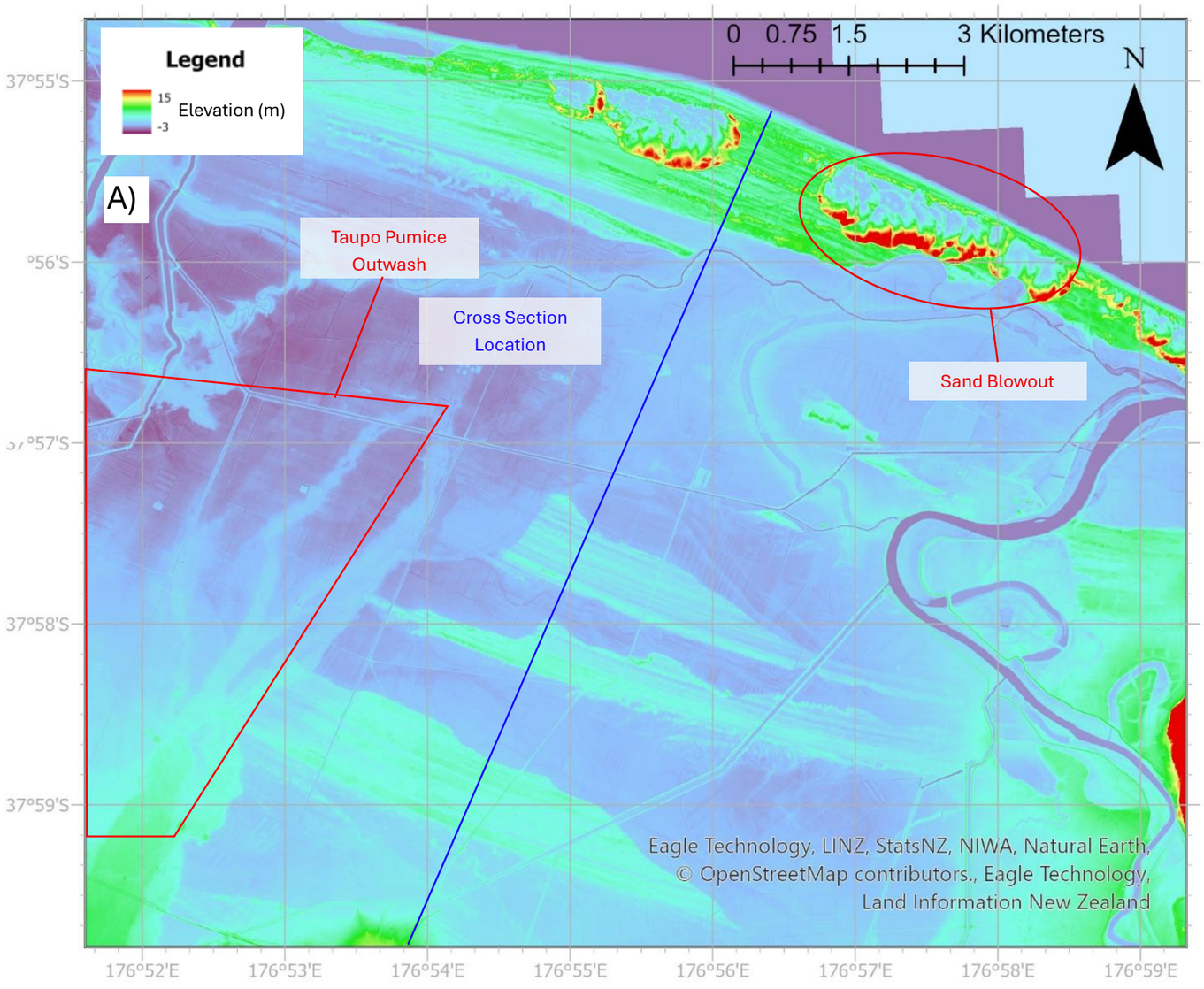

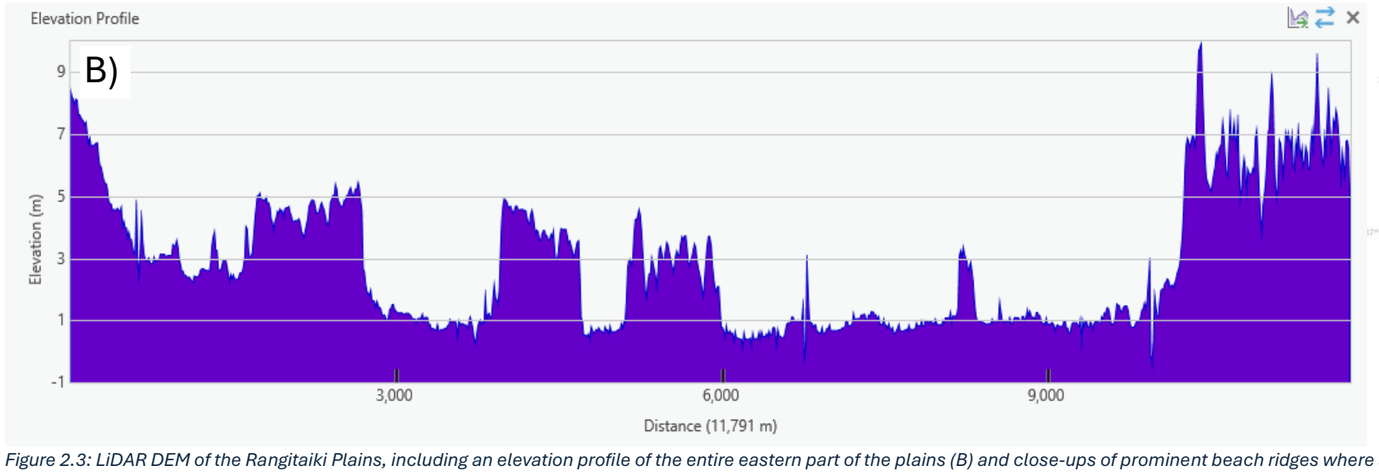

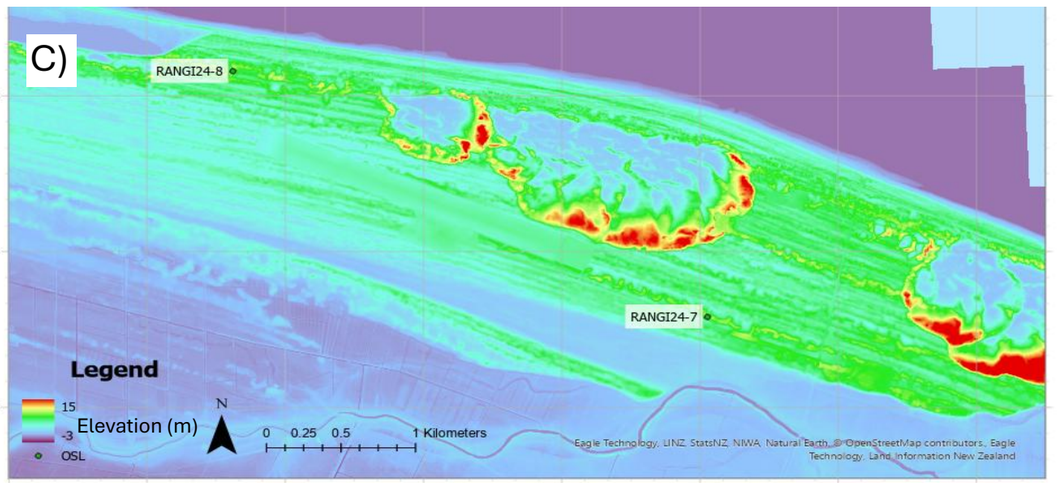

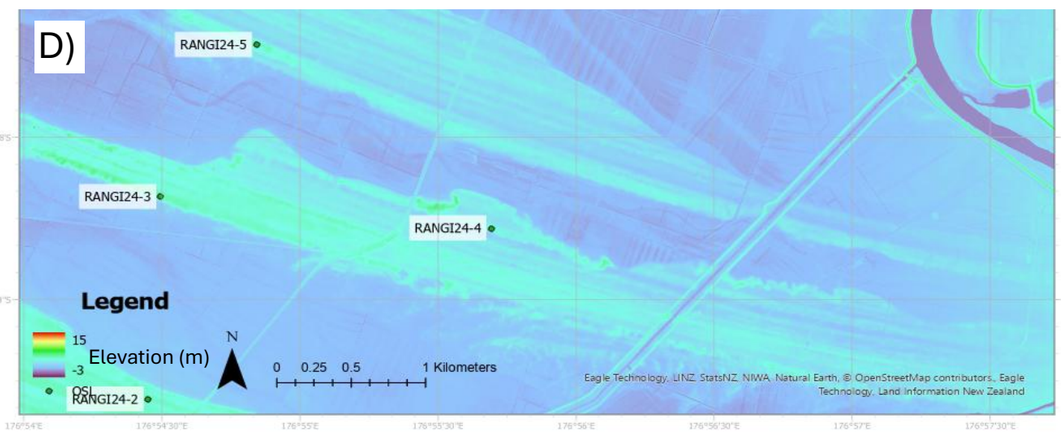

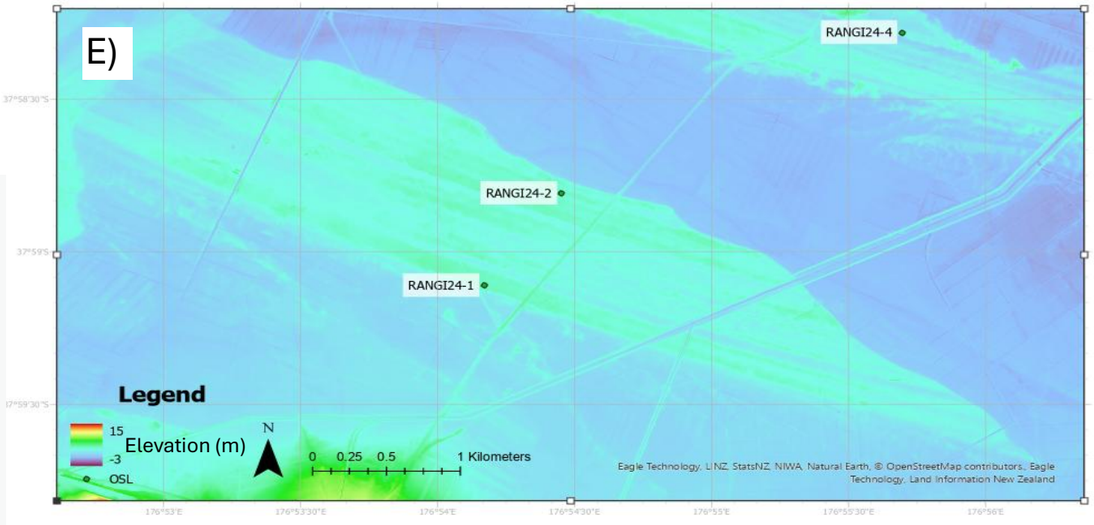

Figure 2.3: LiDAR DEM of the Rangitaiki Plains, including an elevation profile of the entire eastern part of the plains (B) and close-ups of prominent beach ridges where sediment augering occurred. C) Beach Ridge Set 4; D) Beach Ridge Set 3 and 2; E) Beach Ridge Set 1.

2.4.2. Ground Penetrating Radar

The GPR provided subsurface imaging of the Rangitāiki Plains. Imaging was most effective near the coast (BRS 4), where only a thin soil layer (up to 10 cm) covered the preserved beach ridges. Imaging quality and detail declined inland, and correspondingly, the Set 4 Seaward GPR transect was the most suitable for detailed examination (Figure 2.4). All GPR transects are presented in Appendix B.

The Set 4 Seaward transect was 551 m long and imaged approximately 2.5 m deep from the ground surface. Several sections of the transect show crossbedding with reflectors of low to intermediate intensity (Figure 2.4A). Figure 2.4A shows reflectors sloping from southeast to northwest away from a central ridge peak at 11-12 m from the start of the transect. Crossbed directions indicate seaward progradation of sediment from wave and wind-driven transport.

Figure 2.4A also highlights areas where layers dip northwest to southeast of the beach ridge peak. The reflectors immediately southeast of the ridge peak have a higher intensity than seaward sloping reflectors and form concave patterns up to 1.25 m below the ground surface. The direction of these crossbeds is landward-dipping, and the stronger and contrasting reflectors indicate that materials with distinctly different dialectic properties have been deposited. The strong reflectors may indicate the deposition of coarser, more poorly sorted material or other materials such as shells, organic debris and heavy metals under high-energy conditions, such as storms, making this GPR feature a washover deposit.

Figure 2.4B shows another section of the Set 4 Seaward GPR transect, ranging from 72 m to 116 m. This section contains a mix of southeast to northwest and northwest to southeast sloping reflectors, which have a shorter continuity than those seen in Figure 2.4A. These reflectors are of low to intermediate intensity and experience distinct boundaries where the orientation of the sediment layers abruptly shifts slope direction. The orientation of these landward and seaward sloping reflectors could indicate the direction of progradation. When progradation is imaged on an angle (not parallel) to the progradation direction, the image can produce concave lobes instead of seaward sloping reflectors, like those seen in Figure 2.4B. This insinuates that the progradation of BRS 4 was not always perpendicular to the present-day coastline.

Between 412 m and 456 m, the BRS 4 seaward GPR track has a distinctive high-intensity reflector sloping southeast to northwest (Figure 2.4C). The reflector originates at the surface at 418 m and travels to a depth of 1.5 m from the surface by 450 m. Reflectors below this boundary are seaward sloping of low to intermediate intensity, while those above the boundary are bunched together

and exhibit a higher intensity than those reflectors below. This feature is an erosional surface because of the high-intensity, distinct reflector that crosscuts bedding. These erosional surfaces are typical of storm events, causing sediment transport off beach ridges and deposition of heavy metals. The ridge has a strong reflector, indicating a storm deposit with a differing makeup from the rest of the beach ridge before progradation resumed.

2.4.3. Core Stratigraphy

Eight lithological profiles were created using the textural data collected from the auger sites on the Rangitāiki Plains. These sites all show similar patterns in grain size, sorting, Munsell Colour Chart, and loss on ignition (LOI) between the soil (sediment above the beach ridge crest), beach ridge (sediment below the beach ridge crest) and MCS. Figure 2.5 shows representative profiles from one of the landward-most (RANGI24-1), the remaining profiles are displayed in Appendix N.

The oldest sediment samples from the base of the cores are moderately to moderately well-sorted medium sand with a Munsell Colour Chart consisting of brown, dull yellowish-brown, and, at the deeper levels, some greys or olive-brown hues. The LOI in these units declined marginally with depth but stayed relatively consistent. The layer ranged from 1.4 m and below at RANGI24-1 to below 0.1 m at RANGI24-8, consistent in its properties from landward to seaward extents. This unit was identified as beach ridge material.

Above the beach ridge material is a second layer composed of very poorly to poorly sorted, coarse silt to fine sand with a Munsell Colour Chart of shades of black sediment at the surface, quickly fading into dark brown and brown with increasing depth. The LOI of this unit decreased rapidly with depth. For example, RANGI24-1 LOI values decreased from 10.62% at the surface to 0.99% at the top of the beach ridge (Figure 2.5). These layers ranged from above 1.4 m in RANGI24-1 to above 0.1 m at RANGI24-8 and are consistent in their properties from landward to seaward extents. These characteristics gave this unit a soil classification.

There are several reasons for the differences in characteristics between beach ridge and soil material. The soils are likely finer than beach ridge deposits due to increased sediment deposition by aeolian transport and the breakdown of materials through physical, chemical, and biological weathering over time. Furthermore, soil sediment is darker at the surface due to increased organic matter, which is typically darker than volcano-felsic sands. The decrease in LOI with depth is also due to organic matter content. Organic matter is higher in the soil because of swampy peat deposits and surface vegetation. The beach ridge sediment still showed low LOI, likely due to some marine carbonates being present.

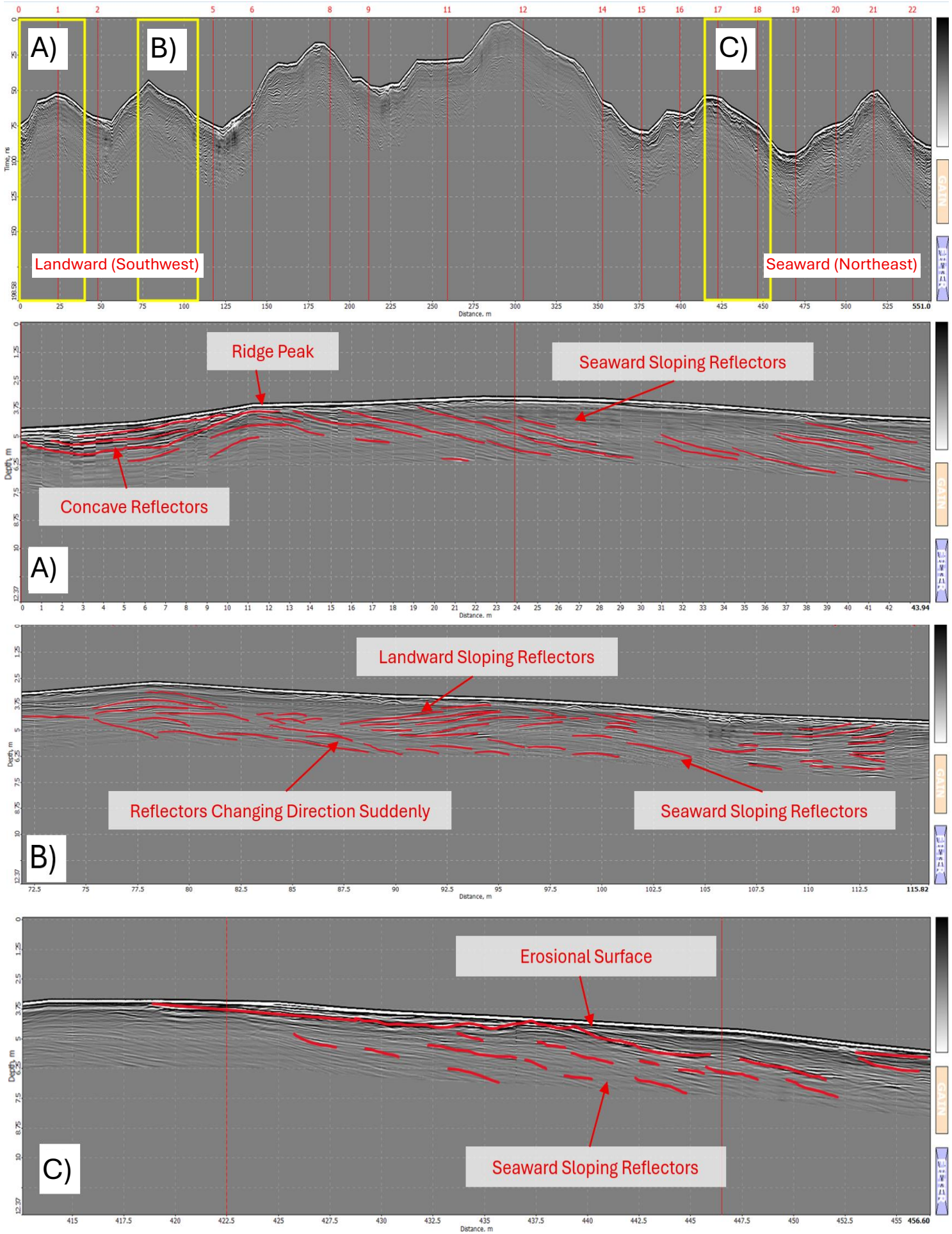

Figure 2.4: A) Full GPR transect of Set 4 Seawards, highlighted in yellow are the areas annotated in A, B and C. A) GPR transect from 0 m to 44 m; B) GPR transect from 72 m to 116 m; C) GPR transect from 412 m to 456 m.

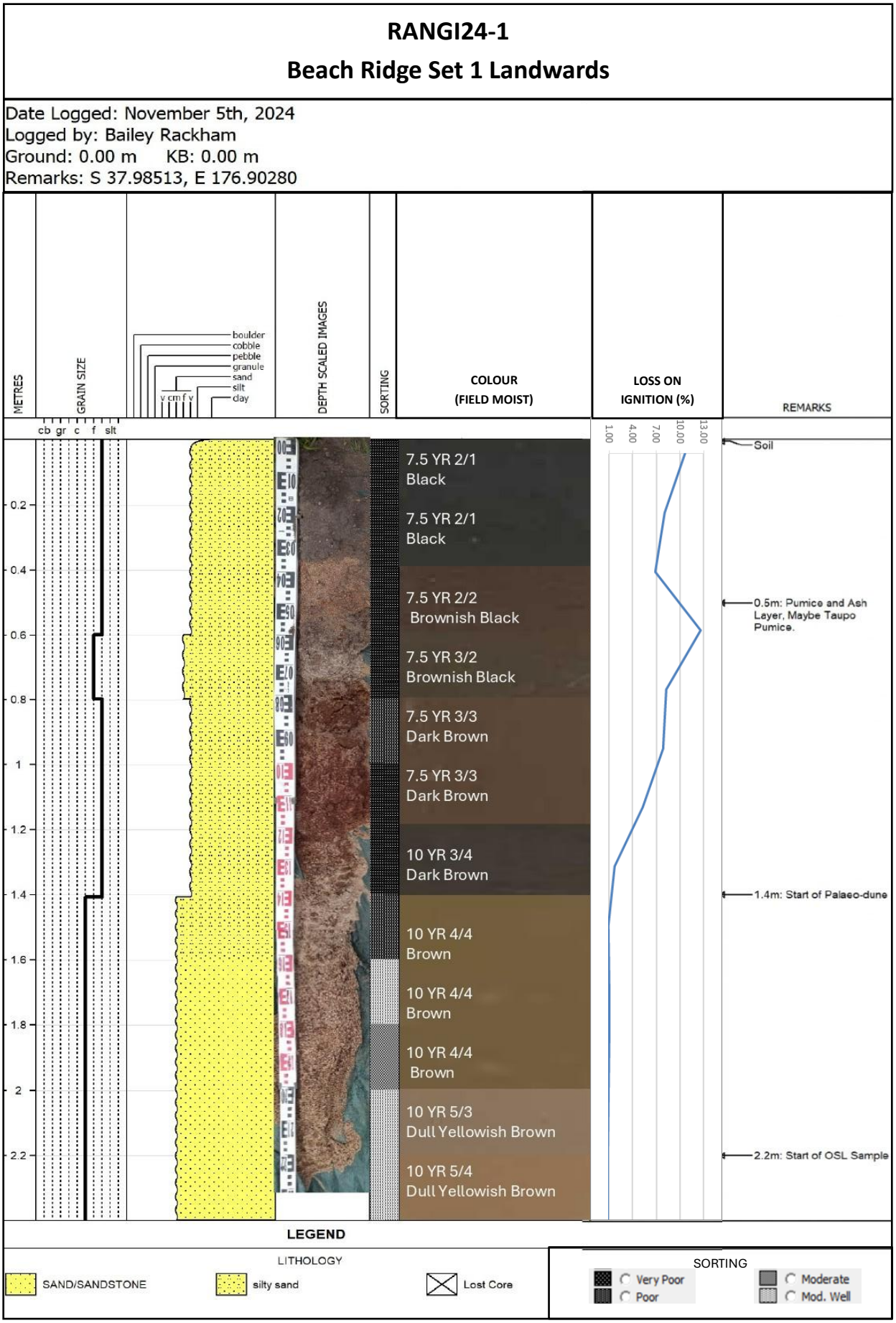

Figure 2.5: Lithological column showing changes in textural components of the sample site RANGI24-1 with depth. Features include sediment classification, grain size, sorting, Munsell Colour Chart and LOI.

2.4.4. Modern Coastal Sediments

Textual analysis of MCS from the Rangitāiki Plains showed varying properties from beach ridge samples. The Munsell Colour Chart of MCS is dominantly shades of grey with hints of brown rather than brown to dull yellowish brown. The grain size also appears coarser than that of beach ridge samples, with most MCS classified as coarse sand compared to the medium sand of beach ridges. The degree of sorting in MCS is the same as that of the beach ridges; all sites comprised of moderately well-sorted grains. Most of these textual differences occurred due to the conditions of the MCS site. The duller shades of sediment based on the Munsell Colour Chart are due to the waterlogged environment of the swash zone, preventing oxidation. Beach ridges are unsaturated above the water table, allowing minerals like iron to oxidise and produce red/brown pigments. The difference in grain size between the beach ridge and the modern coastline is also likely due to the swash zone sampling environment. MCS were taken at the low tide swash zone; there is much more energy in waves at this zone than further up the shore, where beach ridges form, meaning a slightly larger grain size was not unexpected. Overall, only slight textural differences existed between beach ridge and MCS, indicating that sedimentary processes are still behaving similarly.

In addition to differences between beach ridge and MCS, the grain size and sorting of the MCS trend varied along the Rangitāiki Plains coastline. Grain size is greatest immediately east of river mouths and decreases eastwards. For example, the average grain size is 828.9 μm immediately east of the Rangitāiki River Mouth (Coast 3), travelling eastwards, the average grain size depletes to 657.3 μm (COAST 2), then to 435.0 μm at Whakatāne (COAST 1). Coast 3 is also the only site with gravel present (Appendix M). These conditions reflect longshore drift from west to east across the Rangitāiki Plains.

2.4.5. Geochemical Analysis

2.4.5.1. X-Ray Diffraction

Results obtained by XRD show that all samples taken on the Rangitāiki Plains are composed of quartz and plagioclase (Figure 2.6). There was also the detection of a mica mineral scattered throughout the sites (Appendix K). This mineral has no distinct pattern between landward and seaward beach ridge sets or when compared to the MCS. The diffractogram graphs produced by the XRD show trends in volcanic glass in the form of amorphous humps. When comparing beach ridge and soil diffractograms, all soil samples have amorphous humps, while all beach ridges do not (Figure 2.6). RANGI24-1 is utilised as an exemplar for this differentiation, but the same trend is seen across all sampling sites. Volcanic glass in soils is likely to be directly deposited from

tephras, while in beach ridges, the volcanic glass was detrital and mixed due to wave and tidal processes.

2.4.5.2. X-Ray Fluorescence

XRF results were tabulated, showing average soil (sediment above the beach ridge crest), beach ridge (sediment below the beach ridge crest), and MCS values for each site (Appendix I). Beach ridges have slightly higher concentrations of SiO_2 than the overlying soil, ranging from 69.8% to 73.9% in beach ridges, compared to 65.6% to 70.5% in soils. The next most abundant oxide is Al_2O_3, with concentrations ranging from 14.6% to 16.5% in beach ridges and from 12.7% to 15.4% in soils. LOI's showed a notable difference between soil and beach ridge sands. Soils have LOI values ranging from 2.7% to 9.6%, while LOI in beach ridges remained below 2.3% in all cases. In order of abundance, the following most abundant oxides across all samples are Na_2O, CaO, K_2O, and Fe_2O_3. Several elements are also present in concentrations below 1% by weight. Ba, Sr, and Cl consistently have the highest concentrations of the trace elements across all soil and beach ridge samples, with values in the hundreds of parts per million (PPM). For example, Ba ranged from 374 PPM to 584 PPM in beach ridges and from 488 PPM to 656 PPM in soils.

Although major elements varied between beach ridge sediments and soil, composition remained relatively similar between landward and seaward samples within these two classes. Nevertheless, one element that increases from landward to seaward is Fe_2O_3. In beach ridges at RANGI24-1, Fe_2O_3 is 1.44%; at RANGI24-7, Fe_2O_3 content doubled to 2.80%. Furthermore, P content increased 180% from landward to seaward in beach ridges, starting at 0.04% at RANGI24-1 and shifting to 2.19% at the modern coast. Zr rose from 59.75 PPM at RANGI24-1 to 105.5 PPM at RANGI24-8, Y doubled from 6.75 PPM to 14.25 PPM across the plains, Rb concentrations rose from 25.25 PPM to 67.75 PPM and La from 0PPM to 6PPM. Ba also rose from 374.25 PPM to 584.25 PPM, and F from 37.75 PPM to 200.00 PPM. Furthermore, from RANGI24-1 to the MCS, S changed from 35 PPM to 2477 PPM and Cl from 226 PPM to 2593 PPM.

These changes in elemental composition occur due to depositional and post-depositional conditions. Several elements, including Fe, Zr, Y, and La, likely increased closer to the modern coastline as they are found in heavy metal minerals. As progradation has slowed, younger beaches experience more storm events, allowing for increased deposits of these heavy minerals, causing their concentrations to increase over time. Elements like Rb and Ba are commonly found in feldspar and their derived clays. Younger beach ridges likely have higher concentrations as feldspars are less weathered, and these materials are less leached. Elements like Cl, S, F, and P are greater at the coast due to salt spray directly from the ocean.

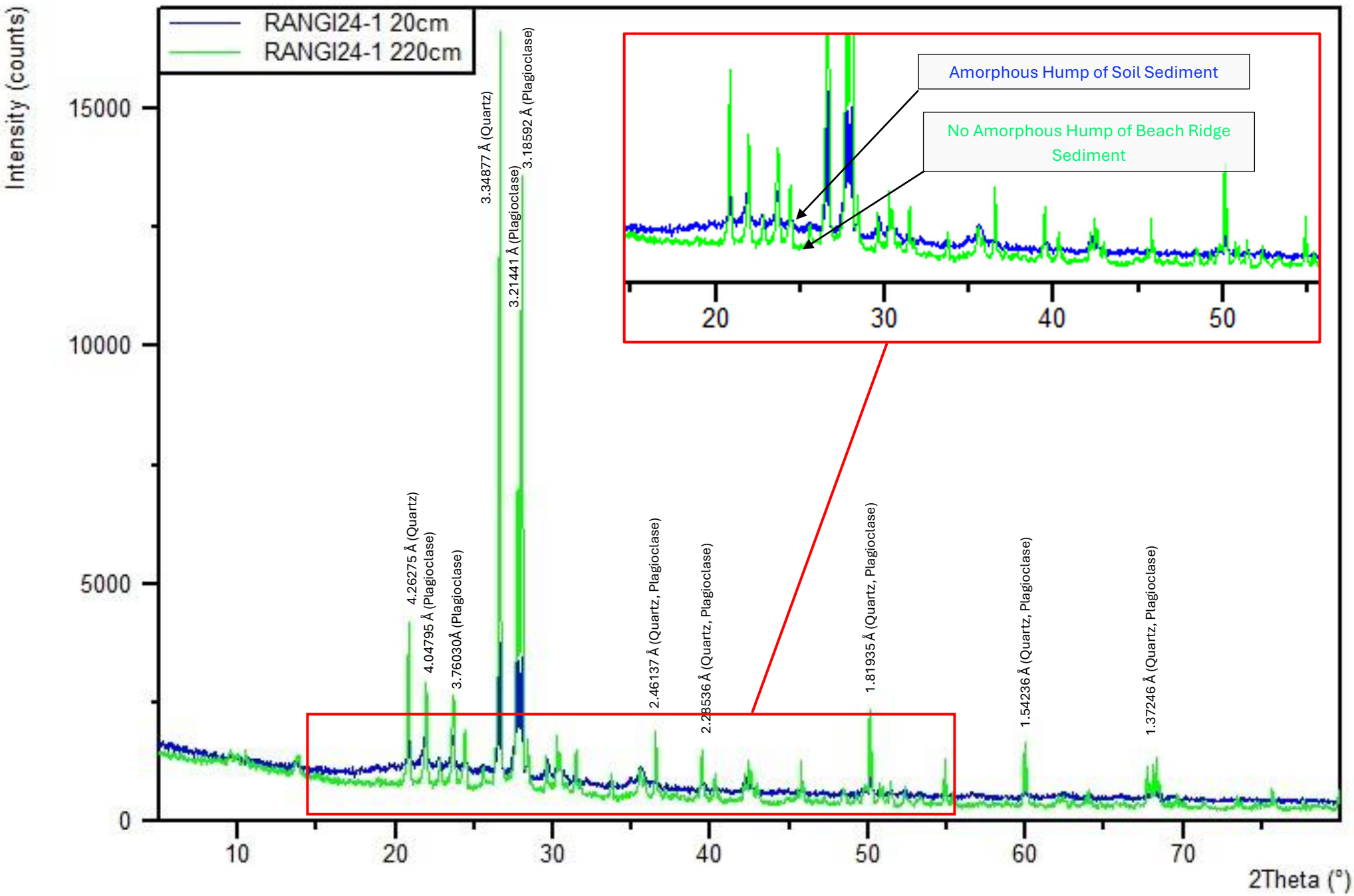

Figure 2.6: XRD diffractogram for RANGI24-1 20cm (a soil sample) and RANGI24-1 220cm (a beach ridge sample) showing D-spacing of significant peaks used to identify quartz and plagioclase mineral presence as well as an amorphous hump between soil and beach ridge samples.

2.4.5.2.1. SandClass Analysis

The SandClass system classified almost all the Rangitāiki Plains soil, beach ridge and MCS into the wacke sedimentary group (Herron, 1984) (Figure 2.7). These samples have low Fe_2O_3/K_2O ratios and intermediate to low SiO_2/Al_2O_3 ratios. There is little distinct pattern within the beach ridges and soil sample groupings in the Wacke category. For beach ridges RANGI24-1 to RANGI24-5 has a linear negative trend from wacke to shale; however, after RANGI24-5, the results are scattered throughout the wacke classification with no distinct order. There is no pattern at all for soil samples.

This wacke classification can infer the samples' proportion of quartz, feldspars, and lithics. The low Fe_2O_3/K_2O suggests an intermediate to low percentage of lithic fragments and a high concentration of stable minerals. Similarly, the SiO_2/Al_2O_3 ratio is intermediate to low, indicating a higher proportion of feldspar than quartz. Classifying all these samples into the same wacke group indicates a relatively similar sediment supply between beach ridges.

The MCS average is on the border of Wacke and Arkose (Figure 2.7). Arkose suggests the sediment is more sorted and has a high proportion of quartz. This suggests that the MCS is more reworked than the older beach ridge sediment.

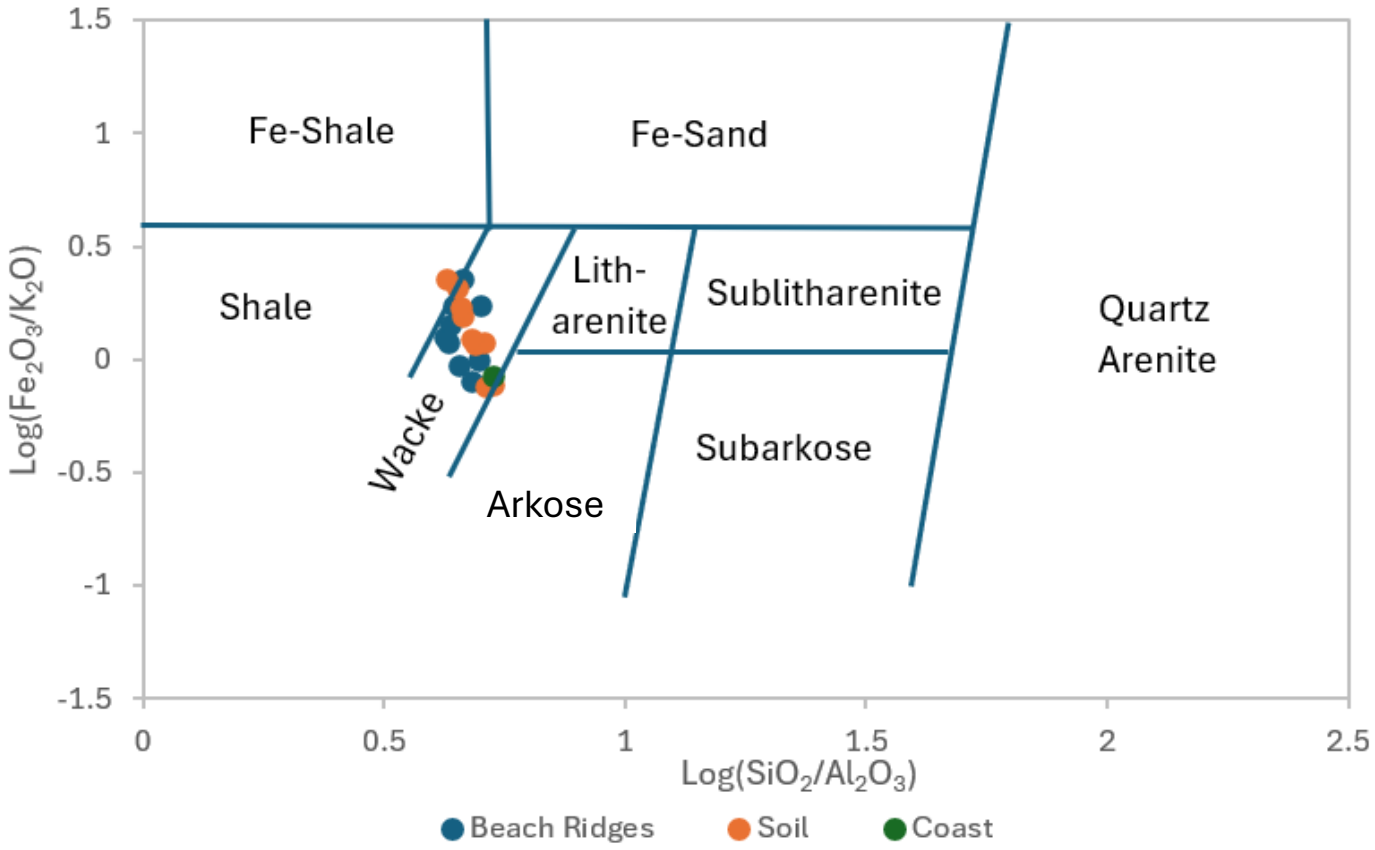

Figure 2.7: SandClass classification of the Rangitaiki Plains soil, beach ridge and modern coastal sediment samples following Herron (1984).

2.4.5.2.2. Discriminant Function for Provenance

The discriminant function for provenance classified the Rangitāiki Plains sediment samples as felsic igneous to intermediate igneous (Roser & Korsch, 1988) (Figure 2.8). While there is no distinct pattern within the beach ridges and soil sample groupings, there is a classification difference between the soil and beach ridge groups. Beach ridges are dominantly intermediate igneous, while soils are between felsic and intermediate. Soils contained direct felsic and intermediate tephra deposits, which could explain this mixed classification. The classification of beach ridges in one provenance grouping indicates their source material likely did not change significantly from the mid to late Holocene. Conversely, MCS deposits are classified as felsic igneous. This could indicate increased reworking, which results in a higher quartz concentration, which may produce a felsic provenance. This classification matches the wacke-arkose SandClass classification and indicates MCS has likely undergone more reworking before final deposition than older beach ridges.

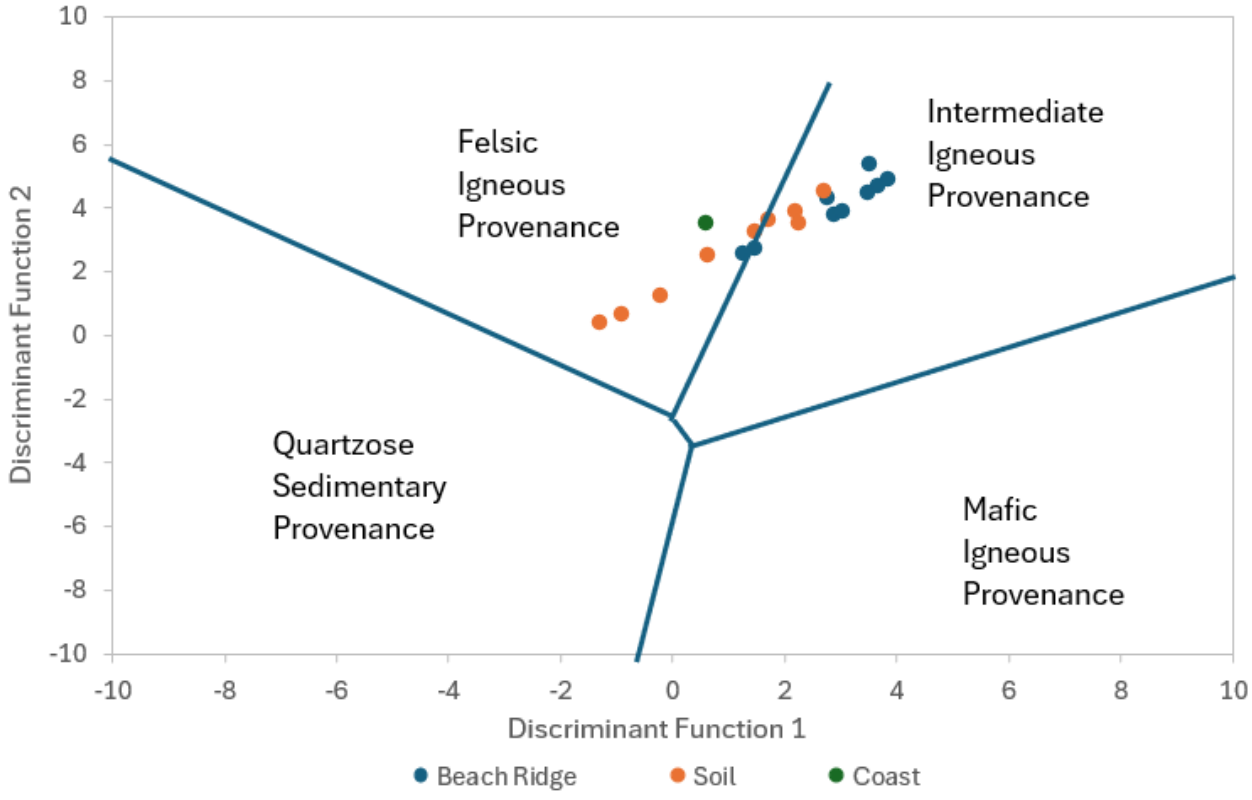

Figure 2.8: Discriminant function for provenance classification of the Rangitaiki Plains soil, beach ridge and modern coastal sediment samples following Roser & Korsch (1988).

2.4.5.2.3. Alteration and Weathering Indices

Calculations of the Chemical Index of Alteration (CIA), Plagioclase Index of Alteration (PIA), and Chemical Index of Weathering (CIW) reveal values between 50 and 75 (Table 2.2). Beach ridge samples averaged 61.76 for CIA, 63.45 for PIA and 65.81for CIW. Meanwhile, soils have averages of 63.39, 66.34, and 69.78, respectively, and MCS of 59.27, 61.65, and 66.00, respectively. The indices establishes that weathering intensity, from highest to lowest, is soils, beach ridges, then MCS. Soils display higher CIA, PIA and CIW values than beach ridge sediment, demonstrating that soils are more chemically weathered than beach ridges. Beach ridges have higher CIA, PIA, and CIW values than the MCS, indicating that MCS samples are less weathered than the beach ridges. There is no distinct increase or decrease in these indices with proximity to the modern coastline. For example, RANGI24-2 has the lowest CIA, PIA and CIW for beach ridges, while RANGI24-3 has the highest. Ultimately, the results of these indices between 50 and 75 suggest the sediment has only experienced a light degree of weathering. This is consistent with fresh volcanic material sources, like those transported down the Rangitāiki and Tarawera Rivers.

Table 2.2: Average CIA, PIA and CIW calculated for the soil, beach ridge and coastal sediment samples taken on the Rangitāiki Plains.

Sample	Type	CIA	PIA	CIW
RANGI24-1	Beach Ridge	60.69	61.55	63.03
RANGI24-2	Beach Ridge	58.94	59.61	61.05
RANGI24-3	Beach Ridge	62.86	65.43	68.58
RANGI24-4	Beach Ridge	62.33	63.63	65.45
RANGI24-5	Beach Ridge	62.48	64.51	67.18
RANGI24-6	Beach Ridge	63.01	64.69	66.83
RANGI24-6B	Beach Ridge	62.21	63.87	66.18
RANGI24-7	Beach Ridge	61.93	63.82	66.46
RANGI24-8	Beach Ridge	61.38	63.92	67.53
Average	Beach Ridge	61.76	63.45	65.81
RANGI24-1	Soil	60.95	64.52	69.49
RANGI24-2	Soil	61.20	64.71	69.49
RANGI24-3	Soil	63.01	65.99	69.49
RANGI24-4	Soil	65.08	67.81	70.49
RANGI24-5	Soil	64.67	67.26	69.90
RANGI24-6	Soil	62.00	65.33	69.55
RANGI24-6B	Soil	66.01	68.49	70.75
RANGI24-7	Soil	64.65	67.30	70.01
RANGI24-8	Soil	62.95	65.63	68.86
Average	Soil	63.39	66.34	69.78
Average	Coastal	59.27	61.65	66.00

2.4.6. Optically Stimulated Luminescence

The pIRIR170 OSL dating procedure produced the most reliable age results for the Rangitāiki Plains due to limited anomalous fading (Table 2.3). Beach Ridge ages ranged from 7.602±0.59 ka at RANGI24-1, located 10.18 km from the modern coastline, to 0.776±0.084 ka at RANGI24-8, just 0.45 km from the modern coast (Figure 2.9). OSL established the following dates for the distinct beach ridge sets: BRS 1 (7.602±0.587 to 7.038±0.577 ka), BRS 2 (5.620±0.368 to 5.742±0.464 ka), BRS 3 (5.202±0.368 to 5.187±0.447 ka), Minor Set (2.965±0.225 ka), and BRS 4 (2.047±0.128 to 0.776±0.084 ka). There is one instance of a slight age reversal at site RANGI24-3. The OSL age is 0.122 ka younger than the successive seaward OSL date; however, the dating uncertainties overlap and do not ensure this age reversal.

OSL data was used to generate progradation rates for the Rangitāiki Plains (Table 2.4). The overall average progradation rate for the Rangitāiki Plains was calculated to be 1.43 m yr^{-1}. When examined over shorter periods, the OSL data showed relatively stable progradation rates ranging from 1.50 to 2.56 m yr^{-1} between 7.602±0.587 ka and 5.202±0.368 ka. Immediately following this period, a sharp increase in progradation was observed, with rates reaching 43.03 m yr^{-1} between 5.202±0.368 ka and 5.187±0.447 ka, before declining to 1.14 m yr^{-1}. From 5.187±0.447 ka, the progradation rate declined to 0.09 m yr^{-1}. Average beach ridge lifetimes calculated for these periods also showed a similar trend, with beach ridge lifetime decreasing where progradation increased. For example, the longest beach ridge lifetimes are experienced at BRS 1 (6.27 years) and BRS 4 (6.69 years) when progradation was slowest.

Table 2.3: OSL dating results and environmental doses for the Rangitaiki Plains.

Sample ID	K (%)	U (ppm)	Th (ppm)	Water content (%)	Dose rate (Gy/ka)	Equivalent dose (Gy/ka)	Uncorrected age (ka)	g2days-value (%/decade)	Corrected age (ka)
RGT24-1	0.64	0.48	1.96	3.7	1.826 ± 0.136	12.799 ± 0.239	7.008 ± 0.537	1.150 ± 0.310	7.602 ± 0.587
RGT24-2	0.66	0.42	1.82	3.7	1.828 ± 0.136	11.862 ± 0.321	6.490 ± 0.513	1.170 ± 0.340	7.038 ± 0.577
RGT24-3	1.53	1.35	5.76	5.6	3.158 ± 0.173	16.383 ± 0.522	5.188 ± 0.328	0.990 ± 0.340	5.620 ± 0.368
RGT24-4	0.90	0.75	3.16	4.6	2.236 ± 0.144	11.848 ± 0.621	5.300 ± 0.441	1.570 ± 0.350	5.742 ± 0.464
RGT24-5	1.30	1.14	4.80	4.4	2.840 ± 0.162	13.643 ± 0.485	4.804 ± 0.323	1.330 ± 0.310	5.202 ± 0.368
RGT24-6	0.91	0.70	2.95	4.1	2.215 ± 0.144	10.611 ± 0.643	4.790 ± 0.426	1.140 ± 0.370	5.187 ± 0.447
RGT24-6B	1.12	0.96	4.11	1.5	2.626 ± 0.157	7.209 ± 0.360	2.745 ± 0.213	0.920 ± 0.380	2.965 ± 0.225
RGT24-7	1.32	1.16	4.79	3.3	2.888 ± 0.164	5.480 ± 0.138	1.898 ± 0.118	0.690 ± 0.350	2.047 ± 0.128
RGT24-8	1.52	1.41	5.73	4.9	3.181 ± 0.174	2.299 ± 0.222	0.723 ± 0.080	0.050 ± 0.370	0.776 ± 0.084

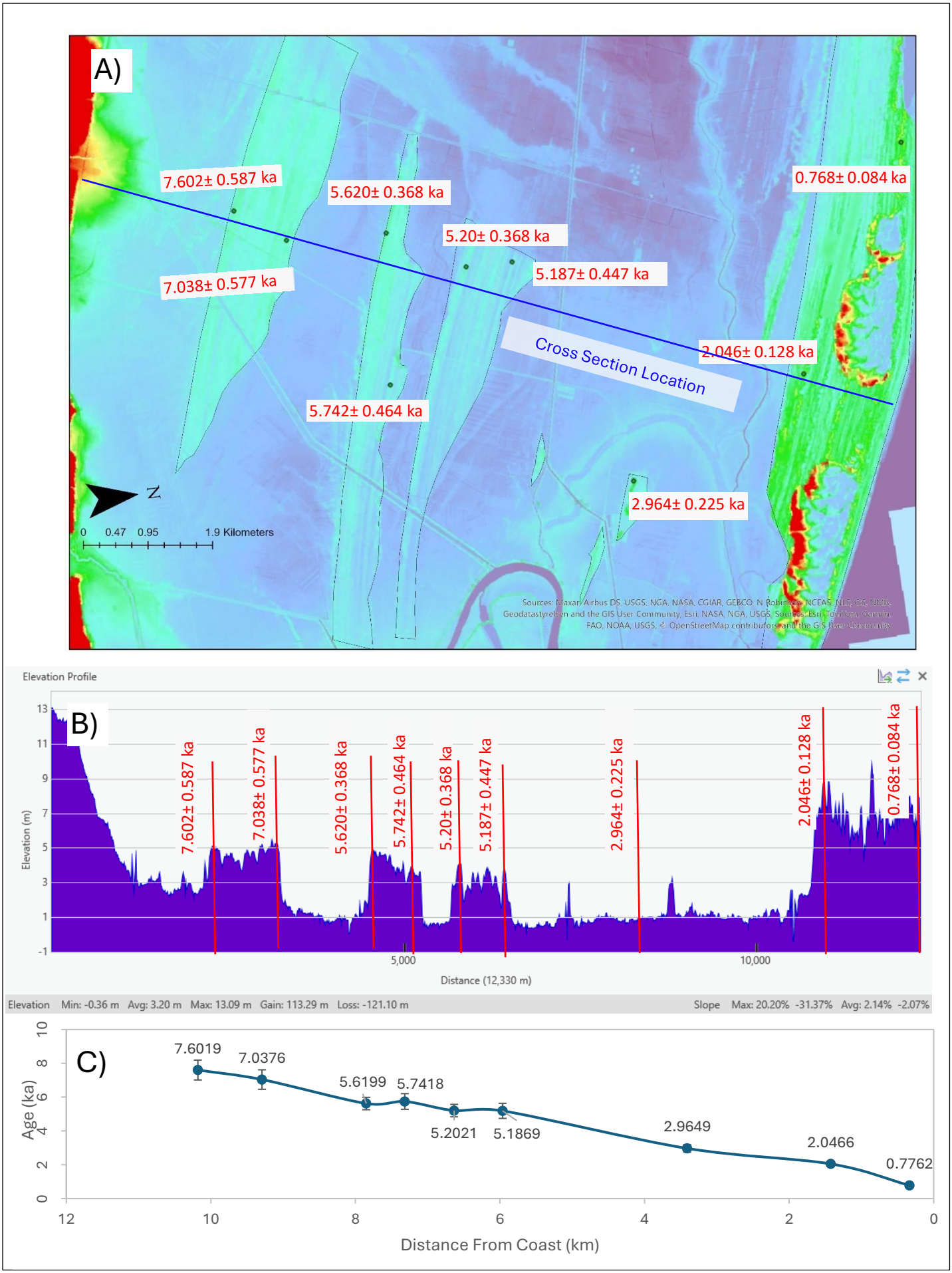

Figure 2.9: A) Location of OSL dates for beach ridges on a DEM of the Rangitaiki Plains; B) location of OSL dates on an elevation profile of the Rangitāiki Plains; C) change in age of sediments with distance from the coastline for the Rangitaiki Plains OSL samples.

Table 2.4: Progradation rates calculated for the Rangitāiki Plains based on OSL dating. RANGI24-4 is not included in the calculation to remove the effects of the minor age reversal. The distance between sites is measured between beach ridges from which OSL sites originated rather than directly between OSL sites that do not line up.

Site	Age (ka)	Age Difference (ka)	Age Difference (yrs)	Distance From Coast (km)	Distance Between Sites (m)	Progradation (m/yr)	Average Ridge Lifetime (yr)
RANGI24-1	7.6019			10.180			
		0.5643	564.3		848	1.503	6.27
RANGI24-2	7.0376			9.332			
		1.4177	1417.7		1410	0.995	1.74
RANGI24-3	5.6199			7.922			
							N/A
		0.4178	417.8		1070	2.561	
RANGI24-5	5.2021			6.852			
		0.0152	15.2		654	43.026	0.19
RANGI24-6	5.1869			6.198			
		2.222	2222.0		2522	1.135	
RANGI24-6B	2.9649			3.676			N/A
		0.9183	918.3		2102	2.289	
RANGI24-7	2.0466			1.574			
		1.2704	1270.4		1117	0.092	6.69
RANGI24-8	0.7762			0.457			

2.5. Discussion

2.5.1. Optically Stimulating Luminescence

OSL dating from this study aligns with previous investigations on the Rangitāiki Plains. In the past, Pullar and Selby (1971) determined several possible palaeoshorelines by identifying the extent of tephra layers across the Rangitāiki Plains and estimating their ages based on the radiocarbon dating of Fergusson and Rafter (1955). Since the publication of Pullar and Selby's (1971) tephrochronology dates, new dates for volcanic eruptions via radiocarbon dating by Lowe *et al*. (2013) have been published. Figure 2.10 compares palaeoshoreline age dates determined by OSL against Pullar and Selby's (1971) estimates and the adjusted estimates by Lowe *et al*. (2013).

OSL demonstrated older ages than those derived via tephrochronology for the same beach ridge units. The older OSL dates are expected as tephra mantles beach ridges, and are deposited after beach ridge formation. Therefore, tephrochronology ages given seawards of beach ridges give the minimum age for the beach ridge sets.

In addition to tephrochronology only supplying a minimum age for beach ridge deposits, there are several other reasons why OSL dating on the Rangitāiki Plains is a more accurate estimate of the palaeoshoreline positions. One major contributor was the accuracy of identifying the extent of tephra layers when conducting tephrochronological dating. Pullar and Selby (1971) claimed the best place to identify tephra in the Rangitāiki Plains was in peat swamps between beach ridge sets, due to the colour and textural contrast between tephra and peat, and that they were not easily distinguishable in beach ridges. These conditions led to tephra being identified in peat zones or troughs of beach ridges. It is possible that tephra was challenging to distinguish outside these zones, which led to tephrochronological palaeoshorelines being dated younger than the actual shoreline.

Furthermore, the OSL dates are more reliable as tephra can be eroded from beach ridges and redistributed by waves and winds. As past shoreline dates were based on the location of tephra closest to the present-day coastline, movement of these materials could have easily skewed tephrochronological dating. Evidence of coastline erosion is evident from LiDAR and GPR images. LiDAR demonstrated periods of erosion between each major beach ridge set, while GPR images show erosion surfaces cutting across beach ridge formations, suggesting erosional cycles. Washover and aeolian deposits were also evident, suggesting sediment could be readily transported by wind and waves after deposition. Pullar and Selby (1971) found evidence of such movement in their tephrochronological study. Evidence of aeolian transport was suggested by the absence of volcanic material in the trough between beach ridges but not on crests. For these reasons, Pullar and Selby (1971) classified all the tephra palaeoshorelines as “possible” shorelines to reflect the uncertainty that the current tephra extents might not represent where tephra was initially deposited.

Previously, investigations assumed that progradation from the Awakeri Sea Cliffs occurred ~6.5 ka (6.7±0.100 cal ka, Clement *et al.*, 2016), based on the sea level change initially determined by Gibb (1986); however, OSL dating of BRS 1 spans from 7.602±0.587 ka to 7.038±0.577 ka (Pullar & Selby, 1971). Because the landward margin of BRS 1 is dated 0.315 to 1.49 ka older than the interpreted age of the Awakeri Sea Cliffs of 6.5 ka, new OSL data suggests that the Awakeri Sea Cliffs' outcropping and the progradation of the Rangitāiki Plains began earlier than previously expected (Pullar & Selby, 1971). This aligns with new Holocene highstand dates established by Clement *et al.* (2016), which state the North Island highstand occurred between 8.1 ka and 7.34 ka rather than at 6.7 ka.

BRS 1-3 has OSL dates older than tephra deposits that overlaid the beach ridges. The minimum age for BRS 1 determined by the tephrochronology was 5.526±0.145 ka based on the deposition of the Whakatāne ash over BRS 1. As stated previously, the OSL dating of BRS 1 spans from 7.602±0.587 ka to 7.038±0.577 ka, which is older than this date. The timing of this beach ridge within the same age range as the post-glacial highstand suggests this material was deposited due to this event.

The minimum age determined by tephrochronology for BRS 2 was 2.800±0.060 ka. The OSL ages for BRS 2 ranged from 5.620±0.368 ka to 5.742±0.464 ka. The nearby palaeoshoreline estimate of 5.526±0.145 ka, which is approximately 400 m landward of the ridge set, falls within the uncertainty intervals of these dates (Figure 2.10). This indicates that the deposition of BRS 2 occurred rapidly after the Whakatāne eruption.

The minimum age determined by tephrochronology for BRS 3 was 2.059±0.118 ka based on the closest palaeoshoreline determined by Pullar and Selby (1971) seaward of the beach ridge set. BRS 3 has OSL dates of 5.20±0.368 ka to 5.187±0.447 ka. Pullar and Selby (1971) had also estimated the age of the ridge set to be 2.800±0.060 ka based on the seaward-most extent of the Taupō supergroup members 11-12 ending in the landward third of the ridge set (Figure 2.10). 2.800±0.060 ka is much younger than the OSL date of BRS 3, indicating that this tephra was likely subject to movement or erosion after its initial deposition, removing it from areas of the plain seaward of BRS 3.

Similarly, the Minor Beach Ridge's (RANGI24-6B) minimum age determined by tephrochronology was also 2.059±0.118 ka (Pullar & Selby, 1971). OSL ages for RANGI24-6B are 2.964±0.225 ka. While the uncertainties between OSL dating and the 2.059±0.118 ka tephra deposit do not overlap, the 2.800±0.060 ka deposit, approximately 3 km between RANGI24-6B, overlaps. These dates further insinuate that the spatial extent of the Taupō Supergroup members 11-12 has been altered. Ultimately, the two Taupō eruption events likely produced the material for RANGI24-6B, and the undated beach ridge set below the Whakatāne township.

Based on the Tarawera eruption event, the BRS 4 minimum age determined by tephrochronology was 0.064 ka. BRS 4 has OSL ages of 2.046±0.128 ka to 0.768±0.084 ka. The Taupō pumice tephra is found 200 m before BRS 4, indicating the ridge set likely formed after the eruption from increased sediment supplies. Kaharoa Ash (0.636±0.012 ka) also occurred in the centre of BRS 4, while Tarawera Ash (0.064 ka) occurred near the seaward extent of BRS 4. The BRS 4 seaward extent age of 0.768±0.084 ka was located seaward of the Tarawera Ash deposit, meaning the Tarawera Ash has likely shifted or eroded over time, disrupting its original extent.

Based on the inherent advantages of directly dating beach ridge sediments, as opposed to the relative nature of tephrochronology, in addition to the struggles faced when finding and identifying tephra by Pullar and Selby (1971), this study concludes that OSL dating provides a more reliable representation of the depositional evolution of the Rangitāiki Plains.

2.5.2. Progradation Rates

Since establishing more direct dates for mid-late Holocene sediment, the progradation rate for the Rangitāiki Plains also varied compared to past tephrochronology estimates. As discussed earlier, tephrochronology only provides the minimum date for beach ridges as they are deposited blanketing beach ridges, biasing calculations of progradation rates. Past progradation rates calculated by Pullar and Selby (1971) were situated earlier than 5.526±0.145 ka. The data show a peak in progradation to a maximum of 3.85 m yr^{-1} between the two Taupō Supergroup members, approximately 2.800±0.060 ka and 2.059±0.118 ka (Figure 2.11). After this peak, the progradation rate declines and reaches a minimum between the Kaharoa Ash (0.636±0.012 ka) deposit and the Tarawera deposit (0.064 ka) of 0.23 m yr^{-1} (Figure 2.11).

When comparing OSL and Pullar and Selby (1971) progradation rates, the OSL progradation rates extend to much older time frames, starting at 7.60±0.587 ka rather than 5.526±0.145 ka. This was expected as tephrochronology dates only provide a minimum age for beach ridges. The OSL dating concludes a prominent progradation peak up to 43.03 m yr^{-1} between RANGI24-5 (5.202±0.368 ka) and RANGI24-6 (5.187±0.447 ka). This sudden progradation peak likely occurred due to a pulse of volcanic sediment from the Whakatāne eruption, around 5.526±0.145 ka. Previously, Pullar and Selby (1971) noted a misalignment between increased progradation and increased volcanic eruption size, where proximal, significant eruptions, such as Whakatāne and Kaharoa, did not correspond with high progradation rates. For example, the highest progradation rate of 3.85 m yr^{-1} found at approximately 2.5 ka did not align with any significant events. These events are expected to align as volcanic eruptions are the primary sediment source to the Rangitāiki Plains. New OSL ages better align with volcanic events, generating a closer correlation between propagation and eruption size. This is consistent with the Whakatāne Ash's position 400 m behind the start of BRS 2. The prominent progradation peak is a stark difference from the rest of the OSL progradation rates, of which the highest is 2.56 m yr^{-1} (Figure 2.11).

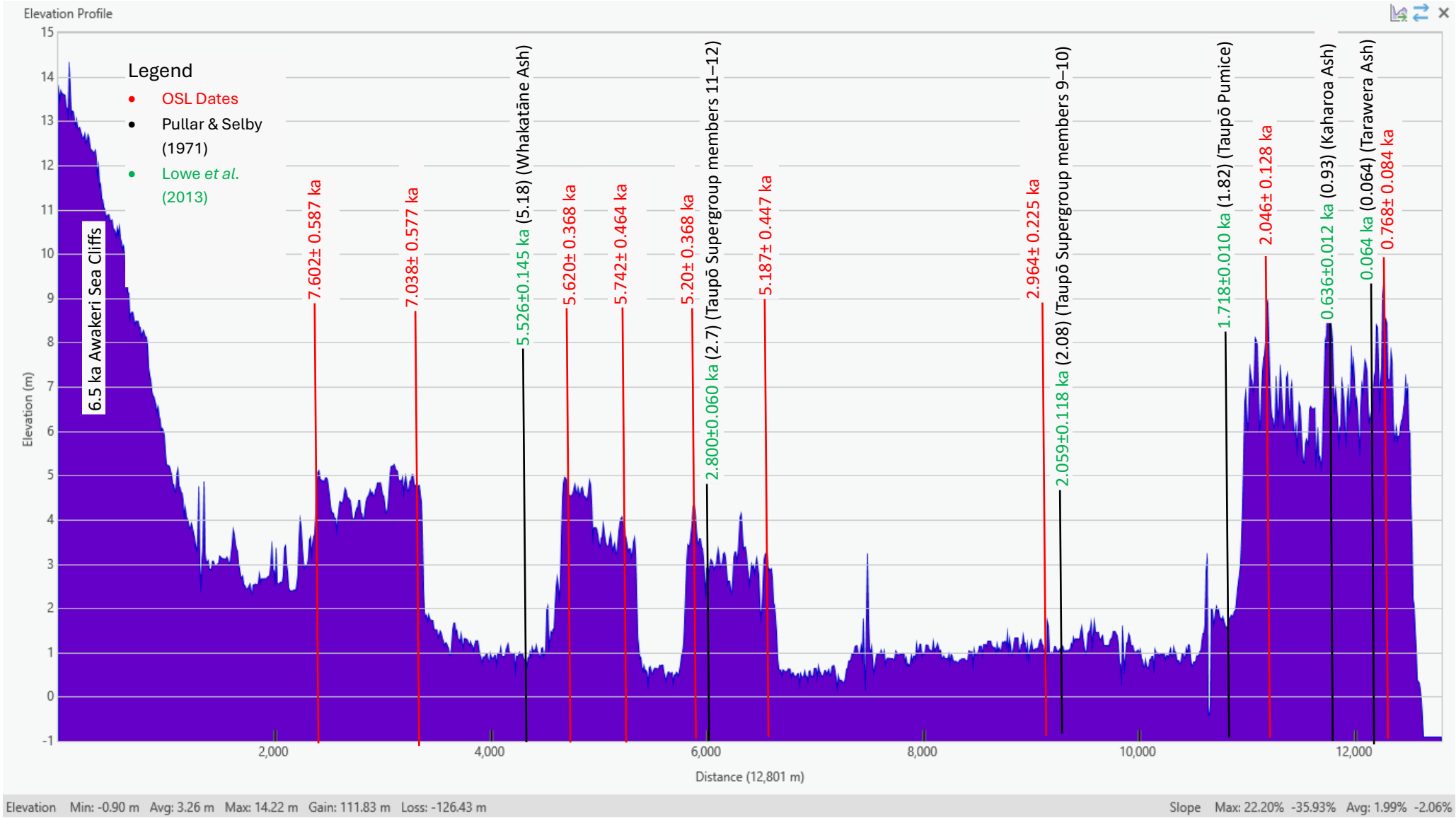

Figure 2.10: Cross-section of the eastern Rangitaiki Plains showing beach ridge sets and their associated ages from new OSL data (red), Pullar and Selby's (1971) tephrochronology (black), and Pullar and Selby's adjusted dates for new radiocarbon dating by Lowe et al. (2013) (green).

By 4 ka, progradation had slowed to only 1.14 m yr^{-1}. Previously, Beanland and Berryman (1992) indicated that progradation rates slowed down around 2 ka, when longshore drift began past the Whakatāne Headland. Longshore drift started after the Rangitāiki Plains built out far enough for sediment to bypass the Whakatāne Headland. This occurred when the length of the headland was less than or equal to the width of the nearshore zone (Healy & De Lange, 2014). Additionally, for sediment exchange to occur, the perimeter of the headland had to reach a distance of less than 2 km (Healy & De Lange, 2014). The OSL progradation rates either indicate that longshore drift occurred earlier than 2 ka or that progradation slowed before longshore drift commenced in 2 ka.

The initiation of longshore drift may help explain the misalignment between Puller and Selby's (1971) progradation rates and eruption events. Significant eruptions like the Taupō and Kaharoa eruptions occurred when longshore drift was already initiated. As the Taupō and Kaharoa eruption events occurred after Beanland and Berryman's (1992) suggested time of longshore drift starting, longshore drift likely carried a large proportion of the new sediment away from the Rangitāiki Plains, preventing significant progradation after the events.

Based on the increased accuracy of OSL dating compared to tephrochronology and the correlation between new progradation rates and observations by Pullar and Selby (1971) and Beanland and Berryman (1992), this thesis concludes that the new progradation rates better reflect the evolution of the Rangitāiki Plains.

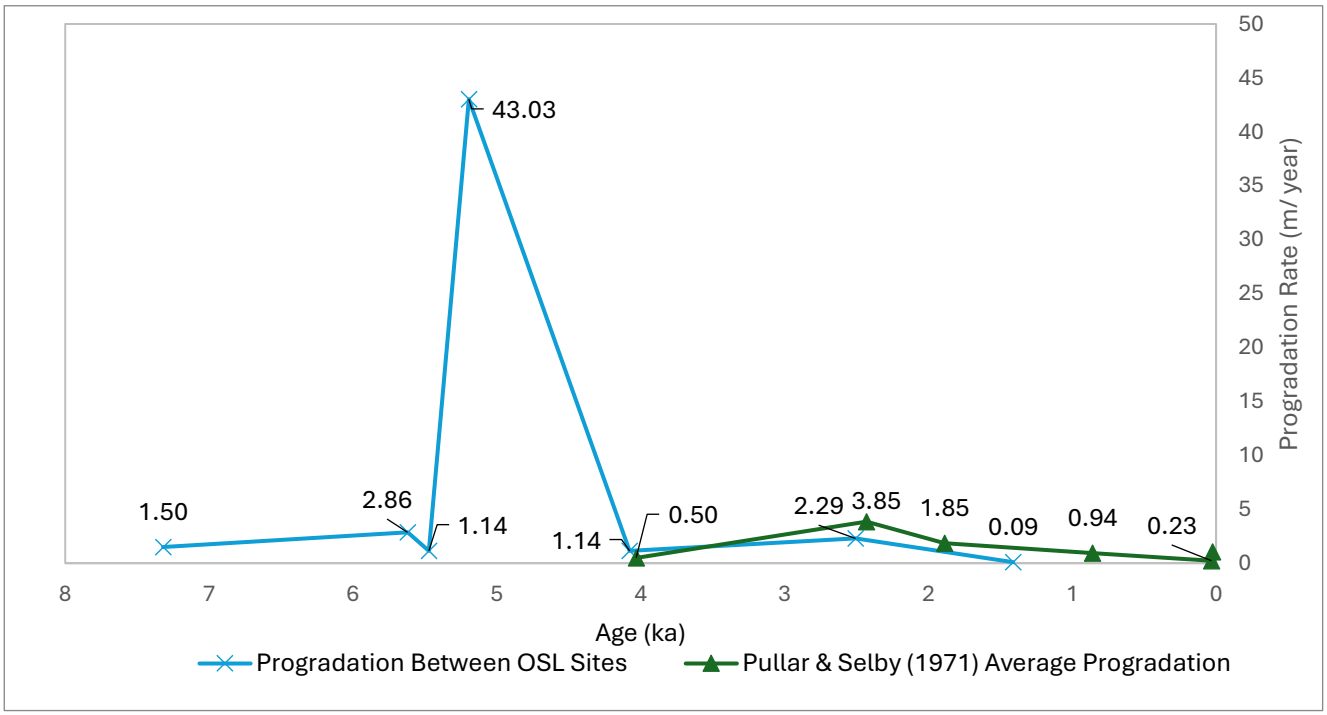

Figure 2.11:Progradation rates calculated from OSL samples vs progradation rates calculated by Pullar and Selby (1971) for the Rangitāiki Plains.

When comparing OSL progradation rates to modern coastline progradation rates measured by the Bay of Plenty Regional Council (2025), it is evident that shoreline progradation has continued declining. The overall modern coastal progradation is 0.14 m yr^{-1} based on the toe of foredune position over the last 35 years across ten beach monitoring sites on the Rangitāiki Plains (Bay of Plenty Regional Council, 2025) (Figure 2.12). These measurements follow trends in OSL data, which set the most recent progradation rate from approximately 2.047±0.128 ka to only 0.09 m yr^{-1}. Modern progradation rates are also consistent with progradation averages from Pullar and Selby (1971), which show the most recent progradation rate of 0.30 m yr^{-1} from 0.064 ka in the east of the Rangitāiki Plains. While this shows the shoreline may still be prograding, the coast has undergone several fluctuations in sediment volume and toe of foredune position during the last 35 years (Bay of Plenty Regional Council, 2025). The shoreline is probably more accurately described as being in dynamic equilibrium, as claimed by prior researchers (Beanland & Berryman, 1992; Begg & Mouslopoulou, 2010).

Trend analysis of Bay of Plenty Regional Council (2025) sites via linear regression describes overall and 5-yearly beach trends, endorsing this conclusion (Table 2.5). The 5-year average showed an overwhelmingly stable trend, which endorsed the claim of dynamic equilibrium (Bay of Plenty Regional Council, 2025). However, all 35 years of data showed a majority accretion between Whakatāne and Tarawera since 1990. Some sites have a distinctly different trend between dune volume and toe of foredune position, where dune volume increased but the toe of foredune position eroded, which may indicate that aeolian transport across the dunes is increasing while shoreline progradation has slowed. Evidence of this aeolian transport was seen and previously described in LiDAR images.

Based on the alignment of this thesis's observations and data with previous studies and current Bay of Plenty Regional Council monitoring, this study concluded that the current Rangitāiki Plains shoreline is likely in a state of equilibrium or very slow progradation, with increased aeolian transport compared to mid-late Holocene beach ridges due to decreased sediment supply to the coast and increased longshore drift. These conditions, however, are subject to change if sediment supply increases from another volcanic eruption. Short-term, decadal trends should not be expected to continue under changing environmental conditions.

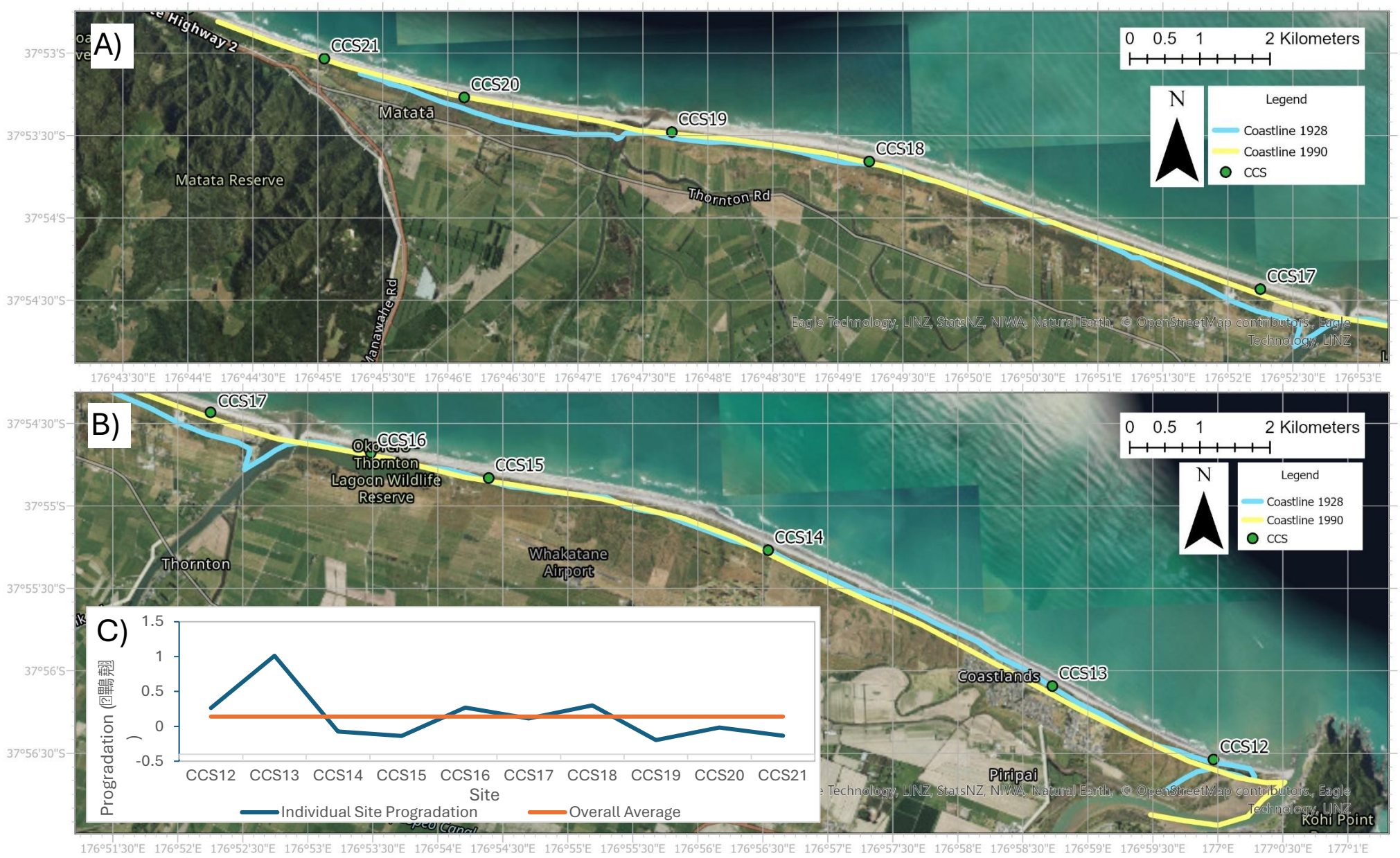

Figure 2.12: Averaged toe of foredune position for 1928 and 1990 compared to the present-day coastline on the Rangitaiki Plains. A) western Rangitaiki Plains; B) eastern Rangitaiki Plains; C) progradation calculated between 1990 and 2025 for Bay of Plenty Regional Council (2025) sites CCS12 to CCS22.

Table 2.5: Linear regression trend analyses for the state of coastal monitoring sites on the Rangitāiki Plains, including progradation trends for all data since 1990 and a five-yearly average (Sourced from Bay of Plenty Regional Council, 2025). Results labelled 'inconclusive' represents discrepancies between the dune volume and toe of foredune progression, causing the beach trend to be unknown. Results labelled with a '?' have one stable condition and another accreting or eroding.

		Trend Analysis					
		All Data			Last 5 Years		
Beach	**Coastal Profile**	**Volume**	**TOD**	**Trend**	**Volume**	**TOD**	**Trend**
Whakatāne	CCS12	Stable	Stable	Stable	Stable	Stable	Stable
Whakatāne	CCS13	Accretion	Accretion	Accretion	Stable	Stable	Stable
Whakatāne	CCS14	Accretion	Stable	Accretion?	Stable	Stable	Stable
Rangitāiki	CCS15	Stable	Stable	Stable	Stable	Stable	Stable
Rangitāiki	CCS16	Accretion	Accretion	Accretion	Stable	Stable	Stable
Rangitāiki	CCS17	Accretion	Stable	Accretion?	Stable	Erosion	Erosion?
Tarawera	CCS18	Accretion	Accretion	Accretion	Stable	Stable	Stable
Tarawera	CCS19	Accretion	Erosion	Inconclusive	Stable	Stable	Stable
Tarawera	CCS20	Erosion	Erosion	Erosion	Stable	Stable	Stable
Matatā	CCS21	Accretion	Erosion	Inconclusive	Stable	Stable	Stable
Matatā	CCS22	Accretion	Accretion	Accretion	Stable	Stable	Stable

2.5.3. X-Ray Fluorescence and X-Ray Diffraction

XRF and XRD analysis of sediments from Rangitāiki Plains suggests that beach ridge sediments comprise of intermediate volcanic sediments. This corresponds with the continuous volcanic eruption from the Taupō Volcanic Zone and Ōkataina Volcanic Centre over the time of the Rangitāiki Plains progradation. This confirms that sediment forming the Rangitāiki Plains can be attributed to the Whakatāne Ash (5.526±0.145 ka), Taupō Supergroup members 11–12 (2.800±0.060 ka), Taupō Supergroup members 9–10 (2.059±0.118 ka), Taupō Pumice (1.718±0.010 ka), Kaharoa Ash (0.636±0.012 ka), and Tarawera Ash (0.064 ka) eruptions. Despite beach ridge material appearing intermediate igneous in composition, most of these eruption events were felsic, producing rhyolite. The leading cause of the differentiation between felsic source and intermediate sediment deposited on the Rangitāiki Plains is alteration and reworking after the eruptions. This volcanic sediment had to travel 10s to 100s of kilometres downstream and be reworked by waves before forming beach ridges. These processes break down rhyolitic volcanic glass, and at the coast, these sediments can become mixed with other minor sediment sources such as greywacke from the Urewera ranges from the Whakatāne river. These conditions decrease ratios of felsic minerals and make sediment appear intermediate in nature.

Soil deposits are similarly volcanic in origin but range from intermediate to felsic composition and are more mature and weathered than beach ridge deposits. RANGI24-1, 2, 3, 4 and 6 are classified as felsic, while the remaining soil samples are classified as intermediate. These sites are some of the oldest measured on the Rangitāiki Plains, dating between 7.602±0.587 ka and 5.187±0.447 ka, meaning they have deeper soil layers than seaward sites. For example, soil depth spanned 1.4 m on RANGI24-1; however, in RANGI24-8, soil depth was only 0.1 m deep. Several volcanic deposits have occurred on top of these landward beach ridges compared to seaward sites, accumulating more felsic material, and giving them a felsic igneous provenance despite weathering effects. As these deposits are deposited directly onto the plain by airfall and are not reworked, they are also found on top of each ridge, are not contaminated by peat, and are more likely to reflect the source material. Furthermore, another potential reason for this is the leaching of elements like Fe, Mg, Na, and Ca inland, which leaves behind more felsic silicic minerals than those closer to the coast. For example, on the Rangitāiki Plains, Fe_2O_3 concentrations doubled from landward to seaward.

While variation between landward and seaward beach ridges is minimal, beach ridge composition varied from MCS. MCS has a more felsic provenance and a wacke-arkose sedimentary type, with an increased presence of quartz and sorting compared to beach ridge samples. These indicators suggested that MCS experiences more reworking than past beach ridges. This is consistent with slower progradation rates and increased longshore drift. Ultimately, these trends reflect those previously discussed by prior researchers on the Rangitāiki Plains and correspond to sediment size, sorting and XRD results.

In addition to classifying Rangitāiki Plains sediment as felsic to intermediate in provenance by the discriminant function for provenance, the Taupō volcanic zone can further be proven as the dominant sediment source through tephra fingerprinting. When comparing the Rangitāiki Plains Major XRF data to XRF analysis for significant eruptions that supplied material to the plains (Whakatāne, Taupō, Kaharoa), the proportion of each element present on the Rangitāiki Plains is very similar to the elemental ratios measured from these eruptions in other studies (Table 2.6). These results further confirm that sediment is dominantly from these eruptive episodes rather than from another regional rock source or offshore marine sediment.

Similarly, the XRD minerology also reflects those of volcanic origins. Marine minerals are absent, and quartz, plagioclase and micas are the most dominant minerals present. These are all typical of Taupō Volcanic Zone eruptions. For example, studies by Smith *et al.* (2006) determined that the dominant minerals present in the Whakatāne tephra were quartz> plagioclase> hornblende;

other minerals present included cummingtonite, pyroxenes and Fe-Ti oxides. Kaharoa and Taupō eruptions were also found to have the same minerals (Smith *et al.*, 2005).

Based on the correspondence of XRF and XRD data to volcanics in the Taupō Volcanic Zone, this thesis concludes that the Rangitāiki Plains Holocene sediment progradation was dominantly volcanic in provenance from this source.

Table 2.6: Major elemental geochemistry obtained for eruption events affecting the Rangitāiki Plains (Whakatāne, Taupō and Kaharoa) from various studies.

Source	**(Smith *et al.*, 2005)**	**(Hopkins *et al.*, 2021)**		**(Newnham *et al.*, 1995)**	**(Lowe *et al.*, 2008)**	**(Hopkins *et al.*, 2021)**		**(Newnham *et al.*, 1995)**	**(Newnham *et al.*, 1998)**	**(Smith *et al.*, 2005)**	**(Hopkins *et al.*, 2021)**	
Eruption	Whakatāne	Whakatāne	**Average**	Taupō	Taupō	Taupō	**Average**	Kaharoa	Kaharoa	Kaharoa	Kaharoa	**Average**
SiO_2	77.833	77.850	**77.842**	76.505	75.040	76.000	**75.848**	78.400	78.000	77.680	77.900	**77.995**
Al_2O_3	12.207	12.600	**12.403**	12.975	13.450	13.200	**13.208**	12.405	12.550	12.355	12.700	**12.503**
TiO_2	0.173	0.135	**0.154**	0.225	0.300	0.200	**0.242**	0.125	0.110	0.125	0.100	**0.115**
FeO	0.850	1.120	**0.985**	1.780	1.990	1.800	**1.857**	0.840	0.810	0.805	0.900	**0.839**
MnO	0.070	0.030	**0.050**		0.070	0.100	**0.085**			0.075	0.100	**0.088**
MgO	0.100	0.110	**0.105**	0.220	0.220	0.200	**0.213**	0.100	0.100	0.050	0.100	**0.088**
CaO	0.770	0.860	**0.815**	1.360	1.470	1.400	**1.410**	0.665	0.550	0.545	0.600	**0.590**
Na_2O	4.170	3.685	**3.928**	3.655	4.490	4.100	**4.082**	3.395	3.670	4.025	3.800	**3.723**
K_2O	3.687	3.540	**3.613**	2.915	2.850	3.000	**2.922**	3.995	4.050	4.195	4.000	**4.060**
Cl	0.160	0.180	**0.170**	0.150	0.190	0.200	**0.180**	0.155	0.160	0.150	0.200	**0.166**

References

Bay of Plenty Regional Council. (2025). *Coastal profile analysis 2025* [Data set]. Available upon request from the Bay of Plenty Regional Council.

Beanland, S., & Berryman, K. R. (1992). Holocene coastal evolution in a continental rift setting: Bay of Plenty, New Zealand. *Quaternary International, 15,* 151–158.

Begg, J. G., & Mouslopoulou, V. (2010). Analysis of late Holocene faulting within an active rift using lidar, Taupō Rift, New Zealand. *Journal of Volcanology and Geothermal Research, 190*(1–2), 152–167.

Blott, S. J., & Pye, K. (2001). *Gradistat: A grain size distribution and statistics package for analysing unconsolidated sediments* (Version 4) [Computer software]. Staffordshire University. http://www.s-j-blott.co.uk/gradistat.html

Dougherty, A. J., Choi, J., Turney, C. M., & Dosseto, A. (2019). Technical note: Optimizing the utility of combined GPR, OSL, and Lidar (GOaL) to extract paleoenvironmental records and decipher shoreline evolution. *Climate of the Past, 15*(1), 389–404.

Esri. (2023). *ArcGIS Pro* (Version 3.1) [Computer software]. Environmental Systems Research Institute. https://www.esri.com/en-us/arcgis/products/arcgis-pro/overview

Fergusson, G. J., & Rafter, T. A. (1955). New Zealand ^{14}C age measurements—2. *New Zealand Journal of Science and Technology. B, 36,* 371–374.

Folk, R. L., & Ward, W. C. (1957). Brazos River bar: A study in the significance of grain size parameters. *Journal of Sedimentary Research, 27*(1), 3–26. https://doi.org/10.1306/74D70646-2B21-11D7-8648000102C1865D

Froggatt, P. C., & Lowe, D. J. (1990). A review of late Quaternary silicic and some other tephra formations from New Zealand: Their stratigraphy, nomenclature, distribution, volume, and age. *New Zealand Journal of Geology and Geophysics, 33*(1), 89–109.

Gibbons, W. H. (1990). *The Rangitāiki, 1890–1900: Settlement and drainage on the Rangitāiki.* Whakatāne & District Historical Society.

Healy, T., & De Lange, W. (2014). Reliability of geomorphic indicators of littoral drift: Examples from the Bay of Plenty, New Zealand. [Unpublished manuscript].

Herron, M. M. (1988). Geochemical classification of terrigenous sands and shales from core or log data. *Journal of Sedimentary Research, 58*(5), 820–829.

Hopkins, J. L., Bidmead, J. E., Lowe, D. J., Wysoczanski, R. J., Pillans, B. J., Ashworth, L., … & Tuckett, F. (2020). TephraNZ: A major and trace element reference dataset for prominent Quaternary rhyolitic tephras in New Zealand and implications for correlation. *Geochronology Discussions, 2020,* 1–63.

Jain, M., Murray, A. S., & Botter-Jensen, L. (2004). Optically stimulated luminescence dating: How significant is incomplete light exposure in fluvial environments? *Quaternaire, 15*(1), 143–157.

Land Information New Zealand. (2021, updated June 20, 2023). *Bay of Plenty LiDAR 1 m DEM (2019–2022)* [Digital elevation model]. LINZ Data Service. https://data.linz.govt.nz/layer/105690-bay-of-plenty-lidar-1m-dem-2019-2022/

Lowe, D. J., Shane, P. A., Alloway, B. V., & Newnham, R. M. (2008). Fingerprints and age models for widespread New Zealand tephra marker beds erupted since 30,000 years ago: A framework for NZ-INTIMATE. *Quaternary Science Reviews, 27*(1–2), 95–126.

Lowe, D. J., Blaauw, M., Hogg, A. G., & Newnham, R. M. (2013). Ages of 24 widespread tephras erupted since 30,000 years ago in New Zealand, with re-evaluation of the timing and palaeoclimatic implications of the Lateglacial cool episode recorded at Kaipo bog. *Quaternary Science Reviews, 74,* 170–194.

Malvern Panalytical. (2020). *Data Viewer* [Computer software]. Malvern Panalytical.

Malvern Panalytical. (2024). *Mastersizer Xplorer* (Version 5.02) [Computer software]. Malvern Panalytical.

Manville, V., Newton, E. H., & White, J. D. L. (2005). Fluvial responses to volcanism: Resedimentation of the 1800a Taupō ignimbrite eruption in the Rangitāiki River catchment, North Island, New Zealand. *Geomorphology, 65,* 49–70.

Munsell Colour. (2009). *Munsell soil color charts* (2009 rev. ed.). Munsell Color, a division of X-Rite, Incorporated.

Murray, A. S., Olley, J. M., & Caitcheon, G. G. (1995). Measurement of equivalent doses in quartz from contemporary water-lain sediments using optically stimulated luminescence. *Quaternary Science Reviews, 14*(4), 365–371.

Nairn, I. A., & Beanland, S. (1989). Geological setting of the 1987 Edgecumbe earthquake, New Zealand. *New Zealand Journal of Geology and Geophysics, 32,* 1–13.

Newnham, R. M., Lowe, D. J., & Wigley, G. N. A. (1995). Late Holocene palynology and palaeovegetation of tephra-bearing mires at Papamoa and Waihi Beach, western Bay of Plenty, North Island, New Zealand. *Journal of the Royal Society of New Zealand, 25*(2), 283–300.

Newnham, R. M., Lowe, D. J., McGlone, M. S., Wilmshurst, J. M., & Higham, T. F. G. (1998). The Kaharoa Tephra is a critical datum for the earliest human impact in northern New Zealand. *Journal of Archaeological Science, 25*(6), 533–544. https://doi.org/10.1006/jasc.1997.0217

Otvos, E. G. (2000). Beach ridges—Definitions and significance. *Geomorphology, 32*(1–2), 83–108. doi:10.1016/S0169-555X(99)00075-6

PANalytical. (2012). *HighScore Plus* (Version 3.0e [3.0.5]) [Computer software]. PANalytical.

Pullar, W. A., & Selby, M. J. (1971). Coastal progradation of Rangitāiki Plains, New Zealand. *New Zealand Journal of Science, 14,* 419–434.

Pullar, W. A. (1985). *Soils and land use of Rangitāiki Plains, North Island, New Zealand.* New Zealand Soil Survey Report 86.

Radar Systems, Inc., & RadarTeam Sweden AB. (2018). *Prism* (Version 2.60.05.RT) [Computer software]. Radar Systems, Inc.

Roser, B. P., & Korsch, R. J. (1988). Provenance signatures of sandstone–mudstone suites determined using discriminant function analysis of major-element data. *Chemical Geology, 67*(1–2), 119–139.

Smith, V. C., Shane, P., & Nairn, I. A. (2005). Trends in rhyolite geochemistry, mineralogy, and magma storage during the last 50 Kyr at Ōkataina and Taupō volcanic centres, Taupō Volcanic Zone, New Zealand. *Journal of Volcanology and Geothermal Research, 148*(3–4), 372–406.

Smith, V. C., Shane, P., Nairn, I. A., & Williams, C. M. (2006). Geochemistry and magmatic properties of eruption episodes from Haroharo linear vent zone, Ōkataina Volcanic Centre, New Zealand, during the last 10 Kyr. *Bulletin of Volcanology, 69*(1), 57–88. https://doi.org/10.1007/s00445-006-0056-7

Wentworth, C. K. (1922). A scale of grade and class terms for clastic sediments. *The Journal of Geology, 30*(5), 377–392. doi:10.1086/622910

White, P., Raiber, M., Begg, J., Freeman, J., & Thorstad, J. (2010). *Groundwater resource investigations of the Rangitāiki Plains stage 1: Conceptual geological model, groundwater budget and preliminary groundwater allocation assessment*. Whakatāne, New Zealand: Bay of Plenty Regional Council. Retrieved from https://www.boprc.govt.nz/media/101224/cr_2010-113_-_groundwater_resource_investigations_of_the_Rangitāiki_plains_stage_1-_web_download_copy.pdf

Woodroffe, C. D. (2021). The turnaround from transgression to regression of Holocene barrier systems in south-eastern Australia: Geomorphology, geological framework and geochronology. *Sedimentology, 68*(3), 943–986.

Chapter 3:
Conclusions and Future Study

3.1. Conclusions

The overall aim of the thesis was to investigate the progradation of the Rangitāiki Plains over the mid-late Holocene and determine if applying new investigation techniques to the area would provide alternative dating of beach ridge sets, rates of progradation and sediment provenance than previous studies. This was achieved by applying geophysical, geochemical and sedimentological techniques to the Holocene beach ridge systems on the Rangitāiki Plains. Light Detection and Ranging (LiDAR) uncovered morphological characteristics of beach ridges, including the number of ridges, elevation and width. Ground penetrating radar (GPR) provided subsurface stratigraphic imaging of beach ridges, including indications of seaward and landward sloping deposits, washover deposits and storm erosional surfaces. Optically Stimulated Luminescence (OSL) dating gave ages of landward and seaward extents of major beach ridge sets and updated progradation rates. X-ray fluorescence (XRF), X-ray diffraction (XRD) and laser particle size analysis identified a Taupō Volcanic Zone igneous provenance for beach ridge material, and that beach ridge sediment did not change significantly with age.

The significance of this study lies in the vulnerability of the low-lying, tectonically subsiding Rangitāiki Plains to change in the coastline induced by climate change-related sea level rise and anthropogenic alteration of sediment budgets. A more detailed understanding of past coastal dynamics and how they compare to current ones could help predict future shoreline behaviour and inform coastal management and planning strategies in the Rangitāiki Plains and New Zealand. This chapter aims to conclude the investigation findings, evaluate the investigation methods and produce recommendations for future research and sea level conditions.

1) **What are the ages of the major beach ridge sets on the Rangitāiki Plains, and does OSL dating differ from existing tephrochronological estimates?**

OSL established the following approximate dates for the distinct beach ridge sets on the Rangitāiki Plains: Beach Ridge Set 1 (7.602±0.587 to 7.038±0.577 ka), Set 2 (5.620±0.368 to 5.742±0.464 ka), Set 3 (5.202±0.368 to 5.187±0.447 ka), Minor Set (2.965±0.235 ka), and Set 4 (2.047±0.128 to 0.776±0.084 ka).

OSL dating produced older ages than those derived via tephrochronology for the same beach ridge units. Pullar and Selby (1971) produced the Tephrochronology ages, which ranged from 5.526±0.145 ka

to 0.064 ka, whereas OSL dating ranged from 7.602±0.587 ka to 0.776±0.084 ka. This was expected as tephra deposits mantle the beach ridges and give the minimum age for the beach ridge sets. While tephra did not directly date beach ridges, tephra did provide evidence of sediment sources. Several OSL ages and eruption dates occurred in proximity and had overlapping uncertainties, suggesting that the formation of beach ridge sets did coincide with eruption events. For example, the Whakatāne eruption (5.526±0.145 ka) overlaps with Beach Ridge Set 2 (.620±0.368 to 5.742±0.464 ka), and the Taupō Supergroup members 11–12 (2.800±0.060 ka) overlaps with the Minor Beach Ridge Set (2.965±0.235 ka), and Taupō Supergroup members 9-10 (2.059±0.118 ka) and Beach Ridge Set 4 (2.047±0.128 to 0.776±0.084 ka). Overall, the OSL data does coincide with tephrochronology; however, OSL gives more accurate dates for the beach ridges as sediment is dated directly, removing uncertainties related to the tephrochronology methods.

2) **How do estimates of progradation rates based on new OSL age data compare to progradation rates estimated primarily based on tephrochronology? How do historical progradation rates compare with modern shoreline progradation rates?**

Since establishing direct dates for mid-late Holocene beach ridges, the progradation rates for the Rangitāiki Plains have also changed. As discussed earlier, tephrochronology only provides the minimum date for beach ridge deposits, biasing calculations of progradation rates. OSL progradation rates extended to much older time frames than estimates by Pullar and Selby (1971), starting at 7.6 ka rather than 5.5 ka. The OSL dating concludes a prominent progradation peak up to 43.03 m yr^{-1} between RANGI24-5 (5.202 ka) and RANGI24-6 (5.1869 ka). Previously, the highest progradation calculated via tephrochronology was 3.85 m yr^{-1} between 2.80±0.06 ka and 2.06±0.12 ka. By 4 ka, progradation had slowed to only 1.14 m yr^{-1}. Previously, Beanland and Berryman (1992) indicated that progradation rates slowed down around 2 ka, when longshore drift began past the Whakatāne Headland. However, the OSL progradation rates either indicate that longshore drift occurred earlier than 2 ka or that progradation slowed before longshore drift commenced 2 ka.

When comparing OSL progradation rates to modern coastline progradation rates measured by the Bay of Plenty Regional Council (2025), it is evident that shoreline progradation has continued declining. The overall modern coastal progradation is 0.14 m yr^{-1} based on the toe of foredune position over the last 35 years across ten beach monitoring sites on the Rangitāiki Plains (Bay of Plenty Regional Council, 2025). These measurements follow trends in OSL data, which set the most recent progradation rate from approximately 1.5 ka to only 0.09 m yr^{-1}. This study concluded that the current Rangitāiki Plains shoreline is likely in a state of equilibrium or very slow progradation, with increased aeolian transport compared to mid-late Holocene beach ridges due to decreased sediment supply to the coast and increased longshore drift.

3) **Does XRF and XRD data help differentiate sediment sources, and how they changed over time?**

XRF and XRD identified the primary sediment source on the Rangitaiki Plains as volcanic eruption material from the Taupō Volcanic Zone and Ōkataina Volcanic Centre. The SandClass system classified all sediment as a wacke and non-calcareous, containing high feldspar and fewer quartz and lithic fragments, which matches XRD results of quartz, plagioclase and little/no volcanic glass. The discriminant function of provenance classified all beach ridge sediments as intermediate igneous and soils as intermediate to felsic igneous, while alteration indexes describe the sediment as slightly weathered. Overall, beach ridge sediment was classified as a medium sand with moderate to moderately well sorting, with a Munsell Colour Chart classification of dull-yellowish brown to brown.

While sedimentary characteristics between Beach Ridge Sets 1-4 remained constant, indicating little to no change in sediment source, the modern coastal sediment samples differed slightly. Modern coastal samples had a more felsic provenance and a wacke-arkose sedimentary type, suggesting an increased presence of quartz and sorting compared to beach ridge samples. These indicators suggest that modern coastal sediment experiences more reworking than stranded beach ridges. This is consistent with slower progradation rates and increased longshore drift. Ultimately, these sediment characteristic trends reflect those previously discussed by prior researchers on the Rangitāiki Plains (Beanland & Berryman, 1992; Begg & Mouslopoulou, 2010; Pullar & Selby, 1971). The geochemical data also rule out marine sediments as a dominant sediment source and suggest that sediment contributing to the Holocene progradation of the Rangitāiki Plains was relatively unchanged and consistent throughout history.

3.2. Study Limitations and Future Research

While this study provided a range of new data and generated updated and improved insights on the nature of beach ridge systems, this investigation was not without limitations. The first limitation encountered when planning the Rangitāiki Plains study was how sampleable the land was. Some key areas could not be sampled due to infrastructure or land ownership. For example, due to development, the beach ridge system under the Whakatāne township could not be sampled. Furthermore, several potential augering sites were ruled out due to a lack of land ownership contact or permissions. The landowners who let field work occur on their property were very helpful and gracious. Future studies could benefit from a more extended reconnaissance period, where meetings with landowners could be set up and better contact could be established to gain a more complete data set for the entire Rangitāiki Plains.

Another limitation related to OSL data collection was the number of samples taken. Both equipment and budget were limited. This meant that only nine samples could be taken on the Rangitāiki Plains. A clearer picture of the progradation could be painted with more samples, especially at the western end of the plains. Future investigations could help build on the existing OSL data and create a clearer picture of how the coast evolved, not just the eastern bounds.

Outside of OSL dating, limitations were also experienced with the GPR data collection. GPR transects were limited to cattle raceways, trails, and farm paths due to the difficulty of the GPR in rough terrain. Tall grass, loose sand, mud and potholes all prevent the GPR from being pushed smoothly along a surface. This can cause jumps in the data and poor signal penetration as the unit is knocked around. Furthermore, GPR was also limited by its signal strength through the soil above the beach ridges. While GPR signals travel well through sand, as demonstrated by the BRS 4 Seaward transect, they are absorbed and diminished in soils with high dielectric properties. This meant the GPR imaging capabilities decreased rapidly the further inland one travelled. A higher-end GPR unit could solve these issues and provide better imaging of beach ridge deposits. For example, drone and car-mounted units with higher signal strength could potentially beat these issues.

In addition to solving these limitations, future studies may benefit from making three-dimensional GPR profiles. This is done by taking GPR transects in a grid-like system to build a three-dimensional model of sedimentary layers in various software. This may provide more information on the internal structure of beach ridges, including the direction of progradation, which was uncertain from standalone GPR transects. This might also help identify more unique features, such as storm erosional surfaces, which could be OSL dated for a more complete progradation history. In future studies, understanding storm erosion and how the Rangitāiki Plains respond to storms over time could be valuable to coastal management as storm events are set to become more frequent and extreme in the face of climate change (Lundquist *et al.*, 2011).

Studies of local and regional sediment budgets could help determine how much sea level rise the plains could withstand based on how much sediment is transported to and from the Rangitāiki Plains. This is especially significant now due to the increased effect of longshore drift on the sediment budget. This knowledge gap could be filled by taking sediment samples along the historic beach ridges and analysing their size, sorting, and XRF ratios for longshore drift markers to determine how quickly progradation was reduced after longshore drift commenced.

3.3. Summary and Recommendation for the Rangitāiki Plains

Based on the results of this thesis, there are several complex contributing factors controlled the progradation of beach ridge systems on the Rangitāiki Plains. New OSL data refined the dating and historic progradation of the Rangitāiki Plains, while new geochemical data confirm felsic to intermediate volcanic sediment sources and an increase in sediment reworking at the modern coastline. The investigation has uncovered new knowledge gaps in the progradation of the Rangitāiki Plains and expresses the need to continue studying the area to gain the best understanding of its formation and the potential effects of anthropogenic changes and sea level rise. Some possible future scenarios and recommendations include:

1) **The Rangitāiki Plains successfully prograde under sea level rise.**

   Coastlines are unpredictable environments governed by many intermingling processes with uncertain and complex behaviours and interactions. Slowed progradation now does not mean progradation will cease due to increased relative sea levels. If sediment supply is high enough to outpace the available accommodation space generated by subsidence and sea-level rise, the shoreline will advance and extend the coastal plain. Tectonics and volcanism are unpredictable and could provide the sediment needed for this to occur. Progradation will likely continue in the form of beach ridges rather than another feature like a river delta, as waves and longshore drift redistribute sediment faster than material is being brought downriver.

2) **The Rangitāiki Plains fail to prograde due to anthropogenic alteration of sedimentation.**

   Anthropogenic alteration of the sediment feeder systems on the Rangitāiki Plains, such as damming the Rangitāiki River, has altered sediment supply routes. River damming reduces sediment supply to the coast, and land draining causes the peat deposits to dehydrate and subside. These factors increase the Rangitāiki Plains' vulnerability to sea level rise by decreasing sediment supply for progradation, increasing the likelihood of inundation. For these reasons, the shoreline may not prograde when faced with increased relative sea level caused by climate change.

3) **The Rangitāiki Plains fail to prograde due to tectonic subsidence**

   Between the Whakatāne Grabens active tectonic subsidence and the estimated relative sea level rise for New Zealand predicted to be between 0.18 – 0.59 m by 2100, the relative increase in sea level may be too much for the Rangitāiki Plains slowed progradation rate, especially if another significant earthquake subsidence event occurs (Lundquist *et al.*, 2011). After the

Edgecumbe earthquake in March 1987, the shoreline retreated 45 m in response to just a 0.4 m rise in sea level due to subsidence (Iremonger, 2007). To withstand a rise of 0.59 m in sea level, the coastline must prograde by approximately 66 m. Over the last 35 years, the coastline collectively prograded 49 m; however, some sites experienced 35 m of progradation, while others experienced 5 m of erosion. These conditions indicate that the predicted inundation is not impossible. For the best chance of mitigation and adaptation, the Bay of Plenty Regional Council should continue monitoring the condition of the coastline. The New Zealand government should also continue recommending and implementing climate change mitigation tactics to lessen potential impacts on the local community and economy.

References

Bay of Plenty Regional Council. (2025). *Coastal profile analysis 2025* [Data set]. Available upon request from the Bay of Plenty Regional Council.

Beanland, S., & Berryman, K. R. (1992). Holocene coastal evolution in a continental rift setting: Bay of Plenty, New Zealand. *Quaternary International, 15,* 151–158.

Begg, J. G., & Mouslopoulou, V. (2010). Analysis of late Holocene faulting within an active rift using lidar, Taupō Rift, New Zealand. *Journal of Volcanology and Geothermal Research, 190*(1–2), 152–167.

Iremonger, S. D. (2007). *NERMN beach profile monitoring (Environmental Publication 2007/08)*. Whakatāne, New Zealand: Environment Bay of Plenty.

Lundquist, C. J., Ramsay, D., Bell, R., Swales, A., & Kerr, S. (2011). Predicted impacts of climate change on New Zealand's biodiversity. *Pacific Conservation Biology, 17*(3), 179–191.

Pullar, W. A., & Selby, M. J. (1971). Coastal progradation of Rangitāiki Plains, New Zealand. New Zealand Journal of Science, 14, 419–434.

Appendices

Appendix A: GPR Transect Coordinates

ID	Location	Latitude	Longitude	Height (m)
Rangi 6b 0001	Minor (Half)	-37.947299	176.943998	29.826315
Rangi 6b 0002	Minor (Half)	-37.947342	176.943978	30.124834
Rangi 6b 0003	Minor (Half)	-37.947386	176.943963	29.381708
Rangi 6b 0004	Minor (Half)	-37.947428	176.943939	30.157408
Rangi 6b 0005	Minor (Half)	-37.947470	176.943917	29.983171
Rangi 6b 0006	Minor (Half)	-37.947513	176.943896	30.205887
Rangi 6b 0007	Minor (Half)	-37.947558	176.943882	30.240264
Rangi 6b 0008	Minor (Half)	-37.947602	176.943864	30.268551
Rangi 6b 0009	Minor (Half)	-37.947647	176.943845	30.184079
Rangi 6b 0010	Minor (Half)	-37.947689	176.943824	29.988271
Rangi 6b 0011	Minor (Half)	-37.947732	176.943802	30.610442
Rangi 6b 0012	Minor (Half)	-37.947775	176.943780	30.483244
Rangi 6b 0013	Minor (Half)	-37.947818	176.943762	30.385054
Rangi 6b 0014	Minor (Half)	-37.947860	176.943742	30.246131
Rangi 6b 0015	Minor (Half)	-37.947905	176.943724	30.111928
Rangi 6b 0016	Minor (Half)	-37.947948	176.943707	29.933938
Rangi 6b 0017	Minor (Half)	-37.947992	176.943691	29.778401
Rangi 6b 0018	Minor (Half)	-37.948008	176.943683	29.661664
Rangi 6b ROAD 01	Minor (Perpendicular)	-37.947358	176.944007	31.327732
Rangi 6b ROAD 02	Minor (Perpendicular)	-37.947341	176.943954	31.407282
Rangi 6b ROAD 03	Minor (Perpendicular)	-37.947324	176.943900	31.342479
Rangi 6b ROAD 04	Minor (Perpendicular)	-37.947315	176.943865	31.176101
Rangi 6b ROAD 05	Minor (Perpendicular)	-37.947310	176.943845	30.969824
Rangi 6b ROAD 06	Minor (Perpendicular)	-37.947297	176.943791	30.183957
Rangi 6b ROAD 07	Minor (Perpendicular)	-37.947283	176.943736	29.720344
Rangi 6b ROAD 08	Minor (Perpendicular)	-37.947269	176.943681	29.600041
Rangi 6b ROAD 09	Minor (Perpendicular)	-37.947258	176.943624	29.439891
Rangi 6b ROAD 10	Minor (Perpendicular)	-37.947250	176.943593	29.309991
Rangi 6b ROAD 11	Minor (Perpendicular)	-37.947246	176.943570	29.168698

Rangi 6b ROAD 12	Minor (Perpendicular)	-37.947237	176.943513	28.938949
Rangi 6b ROAD 13	Minor (Perpendicular)	-37.947228	176.943457	28.817552
Rangi 6b ROAD 14	Minor (Perpendicular)	-37.947226	176.943438	28.802083

Rangi 6b2 0001	Minor (Whole)	-37.948008	176.943683	29.673306
Rangi 6b2 0002	Minor (Whole)	-37.947965	176.943701	29.764395
Rangi 6b2 0003	Minor (Whole)	-37.947922	176.943719	29.902222
Rangi 6b2 0004	Minor (Whole)	-37.947917	176.943722	29.926775
Rangi 6b2 0005	Minor (Whole)	-37.947880	176.943739	30.104383
Rangi 6b2 0006	Minor (Whole)	-37.947837	176.943759	30.260305
Rangi 6b2 0007	Minor (Whole)	-37.947795	176.943782	30.410147
Rangi 6b2 0008	Minor (Whole)	-37.947770	176.943791	30.551629
Rangi 6b2 0009	Minor (Whole)	-37.947752	176.943798	30.617568
Rangi 6b2 0010	Minor (Whole)	-37.947710	176.943818	30.762576
Rangi 6b2 0011	Minor (Whole)	-37.947667	176.943836	30.853308
Rangi 6b2 0012	Minor (Whole)	-37.947623	176.943852	30.966035
Rangi 6b2 0013	Minor (Whole)	-37.947610	176.943857	30.992812
Rangi 6b2 0014	Minor (Whole)	-37.947580	176.943870	31.060666
Rangi 6b2 0015	Minor (Whole)	-37.947537	176.943887	31.125161
Rangi 6b2 0016	Minor (Whole)	-37.947494	176.943904	31.192885
Rangi 6b2 0017	Minor (Whole)	-37.947451	176.943921	31.290682
Rangi 6b2 0018	Minor (Whole)	-37.947431	176.943931	31.258062
Rangi 6b2 0019	Minor (Whole)	-37.947407	176.943941	31.305530
Rangi 6b2 0020	Minor (Whole)	-37.947364	176.943959	31.307904
Rangi 6b2 0021	Minor (Whole)	-37.947322	176.943980	31.312059
Rangi 6b2 0022	Minor (Whole)	-37.947279	176.944002	31.268223
Rangi 6b2 0023	Minor (Whole)	-37.947237	176.944024	31.223567
Rangi 6b2 0024	Minor (Whole)	-37.947219	176.944032	31.169741
Rangi 6b2 0025	Minor (Whole)	-37.947219	176.944032	31.112056
Rangi 6b2 0026	Minor (Whole)	-37.947194	176.944044	31.123831
Rangi 6b2 0027	Minor (Whole)	-37.947152	176.944066	31.065534
Rangi 6b2 0028	Minor (Whole)	-37.947109	176.944086	31.017932
Rangi 6b2 0029	Minor (Whole)	-37.947066	176.944107	31.023968
Rangi 6b2 0030	Minor (Whole)	-37.947023	176.944128	31.042840
Rangi 6b2 0031	Minor (Whole)	-37.946980	176.944147	31.040980
Rangi 6b2 0032	Minor (Whole)	-37.946935	176.944161	30.950464
Rangi 6b2 0033	Minor (Whole)	-37.946894	176.944188	30.806896
Rangi 6b2 0034	Minor (Whole)	-37.946854	176.944214	30.851510
Rangi 6b2 0035	Minor (Whole)	-37.946823	176.944230	30.837454
Rangi 6b2 0036	Minor (Whole)	-37.946812	176.944235	30.797350
Rangi 6b2 0037	Minor (Whole)	-37.946769	176.944255	30.641012
Rangi 6b2 0038	Minor (Whole)	-37.946734	176.944270	30.568307
Rangi 6b2 0039	Minor (Whole)	-37.946726	176.944275	30.534872

Rangi 6b2 0040	Minor (Whole)	-37.946684	176.944297	30.456180
Rangi 6b2 0041	Minor (Whole)	-37.946642	176.944317	30.390541
Rangi 6b2 0042	Minor (Whole)	-37.946641	176.944318	30.398310
Rangi 6b2 0043	Minor (Whole)	-37.946599	176.944339	30.361791
Rangi 6b2 0044	Minor (Whole)	-37.946556	176.944358	30.414108
Rangi 6b2 0045	Minor (Whole)	-37.946513	176.944379	30.444264
Rangi 6b2 0046	Minor (Whole)	-37.946470	176.944397	30.478465
Rangi 6b2 0047	Minor (Whole)	-37.946439	176.944411	30.512294
Rangi 6b2 0048	Minor (Whole)	-37.946427	176.944416	30.517526
Rangi 6b2 0049	Minor (Whole)	-37.946384	176.944436	30.585269
Rangi 6b2 0050	Minor (Whole)	-37.946358	176.944449	30.608510
Rangi 6b2 0051	Minor (Whole)	-37.946341	176.944458	30.642292
Rangi 6b2 0052	Minor (Whole)	-37.946299	176.944479	30.699152
Rangi 6b2 0053	Minor (Whole)	-37.946256	176.944499	30.705181
Rangi 6b2 0054	Minor (Whole)	-37.946214	176.944521	30.615108
Rangi 6b2 0055	Minor (Whole)	-37.946196	176.944530	30.587606
Rangi 6b2 0056	Minor (Whole)	-37.946196	176.944530	30.591050
RANGI AIR 0001	Set 4 Seaward	-37.916795	176.904783	32.735068
RANGI AIR 0002	Set 4 Seaward	-37.916761	176.904814	33.015463
RANGI AIR 0003	Set 4 Seaward	-37.916722	176.904843	33.803753
RANGI AIR 0004	Set 4 Seaward	-37.916681	176.904869	33.891366
RANGI AIR 0005	Set 4 Seaward	-37.916651	176.904887	34.057575
RANGI AIR 0006	Set 4 Seaward	-37.916641	176.904894	33.944016
RANGI AIR 0007	Set 4 Seaward	-37.916601	176.904921	33.656018
RANGI AIR 0008	Set 4 Seaward	-37.916560	176.904946	33.311735
RANGI AIR 0009	Set 4 Seaward	-37.916535	176.904959	33.098474
RANGI AIR 0010	Set 4 Seaward	-37.916518	176.904969	33.008636
RANGI AIR 0011	Set 4 Seaward	-37.916477	176.904992	32.935519
RANGI AIR 0012	Set 4 Seaward	-37.916436	176.905016	33.521862
RANGI AIR 0013	Set 4 Seaward	-37.916410	176.905031	33.992189
RANGI AIR 0014	Set 4 Seaward	-37.916394	176.905041	34.300661
RANGI AIR 0015	Set 4 Seaward	-37.916354	176.905065	34.785977
RANGI AIR 0016	Set 4 Seaward	-37.916312	176.905088	34.448494
RANGI AIR 0017	Set 4 Seaward	-37.916291	176.905102	34.213852
RANGI AIR 0018	Set 4 Seaward	-37.916270	176.905111	34.086530
RANGI AIR 0019	Set 4 Seaward	-37.916228	176.905132	33.814032
RANGI AIR 0020	Set 4 Seaward	-37.916187	176.905157	33.427778
RANGI AIR 0021	Set 4 Seaward	-37.916167	176.905169	33.180560
RANGI AIR 0022	Set 4 Seaward	-37.916144	176.905180	32.956458
RANGI AIR 0023	Set 4 Seaward	-37.916102	176.905203	32.807861
RANGI AIR 0024	Set 4 Seaward	-37.916067	176.905239	33.150798
RANGI AIR 0025	Set 4 Seaward	-37.916045	176.905251	33.349619
RANGI AIR 0026	Set 4 Seaward	-37.916026	176.905265	33.617107
RANGI AIR 0027	Set 4 Seaward	-37.915984	176.905288	34.494241
RANGI AIR 0028	Set 4 Seaward	-37.915942	176.905310	35.159551

RANGI AIR 0029	Set 4 Seaward	-37.915921	176.905322	35.412547
RANGI AIR 0030	Set 4 Seaward	-37.915900	176.905336	35.250662
RANGI AIR 0031	Set 4 Seaward	-37.915857	176.905359	35.274128
RANGI AIR 0032	Set 4 Seaward	-37.915814	176.905379	35.742324
RANGI AIR 0033	Set 4 Seaward	-37.915772	176.905401	36.092570
RANGI AIR 0034	Set 4 Seaward	-37.915769	176.905402	36.090221
RANGI AIR 0035	Set 4 Seaward	-37.915731	176.905425	35.736502
RANGI AIR 0036	Set 4 Seaward	-37.915689	176.905447	35.079678
RANGI AIR 0037	Set 4 Seaward	-37.915647	176.905471	34.399933
RANGI AIR 0038	Set 4 Seaward	-37.915645	176.905472	34.374741
RANGI AIR 0039	Set 4 Seaward	-37.915606	176.905498	34.018413
RANGI AIR 0040	Set 4 Seaward	-37.915565	176.905523	33.956065
RANGI AIR 0041	Set 4 Seaward	-37.915525	176.905546	34.135619
RANGI AIR 0042	Set 4 Seaward	-37.915524	176.905546	34.151964
RANGI AIR 0043	Set 4 Seaward	-37.915482	176.905569	34.628290
RANGI AIR 0044	Set 4 Seaward	-37.915441	176.905593	35.117481
RANGI AIR 0045	Set 4 Seaward	-37.915399	176.905614	35.052355
RANGI AIR 0046	Set 4 Seaward	-37.915398	176.905615	35.056966
RANGI AIR 0047	Set 4 Seaward	-37.915357	176.905639	35.074835
RANGI AIR 0048	Set 4 Seaward	-37.915315	176.905661	35.090575
RANGI AIR 0049	Set 4 Seaward	-37.915272	176.905682	35.072774
RANGI AIR 0050	Set 4 Seaward	-37.915231	176.905709	35.420990
RANGI AIR 0051	Set 4 Seaward	-37.915188	176.905729	35.963372
RANGI AIR 0052	Set 4 Seaward	-37.915146	176.905751	36.476221
RANGI AIR 0053	Set 4 Seaward	-37.915143	176.905753	36.576956
RANGI AIR 0054	Set 4 Seaward	-37.915106	176.905776	36.640606
RANGI AIR 0055	Set 4 Seaward	-37.915064	176.905799	36.350579
RANGI AIR 0056	Set 4 Seaward	-37.915022	176.905821	36.096402
RANGI AIR 0057	Set 4 Seaward	-37.915004	176.905830	35.872297
RANGI AIR 0058	Set 4 Seaward	-37.914979	176.905844	35.512617
RANGI AIR 0059	Set 4 Seaward	-37.914938	176.905868	35.348842
RANGI AIR 0060	Set 4 Seaward	-37.914897	176.905893	35.198537
RANGI AIR 0061	Set 4 Seaward	-37.914882	176.905903	35.087263
RANGI AIR 0062	Set 4 Seaward	-37.914857	176.905920	34.716047
RANGI AIR 0063	Set 4 Seaward	-37.914816	176.905945	34.101866
RANGI AIR 0064	Set 4 Seaward	-37.914774	176.905970	33.419650
RANGI AIR 0065	Set 4 Seaward	-37.914765	176.905975	33.272617
RANGI AIR 0066	Set 4 Seaward	-37.914732	176.905994	32.765338
RANGI AIR 0067	Set 4 Seaward	-37.914690	176.906017	32.423662
RANGI AIR 0068	Set 4 Seaward	-37.914648	176.906040	32.309977
RANGI AIR 0069	Set 4 Seaward	-37.914645	176.906042	32.336273
RANGI AIR 0070	Set 4 Seaward	-37.914606	176.906063	32.840878
RANGI AIR 0071	Set 4 Seaward	-37.914565	176.906085	33.402931
RANGI AIR 0072	Set 4 Seaward	-37.914531	176.906103	33.405332
RANGI AIR 0073	Set 4 Seaward	-37.914523	176.906108	33.411060
RANGI AIR 0074	Set 4 Seaward	-37.914480	176.906130	33.766564

RANGI AIR 0075	Set 4 Seaward	-37.914437	176.906152	34.388713
RANGI AIR 0076	Set 4 Seaward	-37.914412	176.906166	34.491425
RANGI AIR 0077	Set 4 Seaward	-37.914395	176.906175	34.517046
RANGI AIR 0078	Set 4 Seaward	-37.914353	176.906196	34.214934
RANGI AIR 0079	Set 4 Seaward	-37.914311	176.906220	33.997412
RANGI AIR 0080	Set 4 Seaward	-37.914292	176.906230	33.803983
RANGI AIR 0081	Set 4 Seaward	-37.914270	176.906243	33.620610
RANGI AIR 0082	Set 4 Seaward	-37.914228	176.906267	33.126344
RANGI AIR 0083	Set 4 Seaward	-37.914188	176.906294	32.634943
RANGI AIR 0084	Set 4 Seaward	-37.914166	176.906308	32.424183
RANGI AIR 0085	Set 4 Seaward	-37.914148	176.906320	32.348450
RANGI AIR 0086	Set 4 Seaward	-37.914103	176.906335	32.522424
RANGI AIR 0087	Set 4 Seaward	-37.914058	176.906329	32.955568
RANGI AIR 0088	Set 4 Seaward	-37.914019	176.906300	33.090012
RANGI AIR 0089	Set 4 Seaward	-37.913992	176.906277	33.167602
RANGI AIR 0090	Set 4 Seaward	-37.913979	176.906270	33.165413
RANGI AIR 0091	Set 4 Seaward	-37.913934	176.906259	33.401790
RANGI AIR 0092	Set 4 Seaward	-37.913888	176.906260	33.934539
RANGI AIR 0093	Set 4 Seaward	-37.913843	176.906268	34.241207
RANGI AIR 0094	Set 4 Seaward	-37.913811	176.906272	34.252700
RANGI AIR 0095	Set 4 Seaward	-37.913797	176.906273	34.206230
RANGI AIR 0096	Set 4 Seaward	-37.913752	176.906270	33.597492
RANGI AIR 0097	Set 4 Seaward	-37.913706	176.906270	32.942988
RANGI AIR 0098	Set 4 Seaward	-37.913662	176.906257	32.460860
RANGI AIR 0099	Set 4 Seaward	-37.913637	176.906280	32.223521
RANGI AIR 0100	Set 4 Seaward	-37.913629	176.906296	32.157135
RANGI AIR 0101	Set 4 Seaward	-37.913592	176.906330	32.363899
RANGI AIR 0102	Set 4 Seaward	-37.913546	176.906324	32.544007
RANGI AIR 0103	Set 4 Seaward	-37.913507	176.906292	32.693049
RANGI AIR 0104	Set 4 Seaward	-37.913489	176.906281	32.531314
RANGI AIR 0105	Set 4 Seaward	-37.913466	176.906267	32.157796
RANGI AIR 0106	Set 4 Seaward	-37.913420	176.906261	31.691094
RANGI AIR 0107	Set 4 Seaward	-37.913374	176.906267	31.503203
RANGI AIR 0108	Set 4 Seaward	-37.913329	176.906276	31.169574
RANGI AIR 0109	Set 4 Seaward	-37.913289	176.906290	30.706190
RANGI AIR 0110	Set 4 Seaward	-37.913289	176.906290	30.710422

rangi golf 0001	Set 4 Landward	-37.930326	176.940405	34.127406
rangi golf 0002	Set 4 Landward	-37.930279	176.940408	35.283994
rangi golf 0003	Set 4 Landward	-37.930233	176.940415	36.051687
rangi golf 0004	Set 4 Landward	-37.930189	176.940432	36.064685
rangi golf 0005	Set 4 Landward	-37.930148	176.940455	35.983517
rangi golf 0006	Set 4 Landward	-37.930108	176.940484	35.671278
rangi golf 0007	Set 4 Landward	-37.930098	176.940489	35.551310
rangi golf 0008	Set 4 Landward	-37.930064	176.940499	35.178572
rangi golf 0009	Set 4 Landward	-37.930020	176.940510	34.625107

rangi golf 0010	Set 4 Landward	-37.929975	176.940518	33.917079
rangi golf 0011	Set 4 Landward	-37.929929	176.940528	33.372454
rangi golf 0012	Set 4 Landward	-37.929894	176.940540	33.177280
rangi golf 0013	Set 4 Landward	-37.929886	176.940543	33.151327
rangi golf 0014	Set 4 Landward	-37.929842	176.940558	32.993342
rangi golf 0015	Set 4 Landward	-37.929797	176.940569	32.921562
rangi golf 0016	Set 4 Landward	-37.929752	176.940586	33.505503
rangi golf 0017	Set 4 Landward	-37.929703	176.940600	33.784091
rangi golf 0018	Set 4 Landward	-37.929659	176.940614	33.884592
rangi golf 0019	Set 4 Landward	-37.929615	176.940610	34.592824
rangi golf 0020	Set 4 Landward	-37.929614	176.940609	34.617886
rangi golf 0021	Set 4 Landward	-37.929568	176.940608	34.916849
rangi golf 0022	Set 4 Landward	-37.929522	176.940616	35.169237
rangi golf 0023	Set 4 Landward	-37.929481	176.940640	35.026094
rangi golf 0024	Set 4 Landward	-37.929437	176.940656	34.749051
rangi golf 0025	Set 4 Landward	-37.929392	176.940670	34.041092
rangi golf 0026	Set 4 Landward	-37.929348	176.940689	33.952678
rangi golf 0027	Set 4 Landward	-37.929305	176.940709	34.380751
rangi golf 0028	Set 4 Landward	-37.929296	176.940713	34.461334
rangi golf 0029	Set 4 Landward	-37.929261	176.940725	34.776344
rangi golf 0030	Set 4 Landward	-37.929215	176.940737	34.996317
rangi golf 0031	Set 4 Landward	-37.929171	176.940751	34.989711
rangi golf 0032	Set 4 Landward	-37.929126	176.940763	34.739338
rangi golf 0033	Set 4 Landward	-37.929082	176.940775	34.376396
rangi golf 0034	Set 4 Landward	-37.929038	176.940790	34.107135
rangi golf 0035	Set 4 Landward	-37.929017	176.940800	33.920849
rangi golf 0036	Set 4 Landward	-37.928993	176.940808	33.648049
rangi golf 0037	Set 4 Landward	-37.928948	176.940819	33.372621
rangi golf 0038	Set 4 Landward	-37.928902	176.940831	33.333516
rangi golf 0039	Set 4 Landward	-37.928857	176.940839	33.784468
rangi golf 0040	Set 4 Landward	-37.928813	176.940848	34.385525
rangi golf 0041	Set 4 Landward	-37.928766	176.940853	34.788684
rangi golf 0042	Set 4 Landward	-37.928748	176.940860	34.947719
rangi golf 0043	Set 4 Landward	-37.928723	176.940869	34.845539
rangi golf 0044	Set 4 Landward	-37.928679	176.940886	34.600085
rangi golf 0045	Set 4 Landward	-37.928635	176.940904	34.392731
rangi golf 0046	Set 4 Landward	-37.928590	176.940918	34.109576
rangi golf 0047	Set 4 Landward	-37.928546	176.940932	33.959502
rangi golf 0048	Set 4 Landward	-37.928533	176.940936	33.994355
rangi golf 0049	Set 4 Landward	-37.928502	176.940948	34.093857
rangi golf 0050	Set 4 Landward	-37.928457	176.940964	34.376940
rangi golf 0051	Set 4 Landward	-37.928413	176.940978	35.081628
rangi golf 0052	Set 4 Landward	-37.928367	176.940989	34.951545
rangi golf 0053	Set 4 Landward	-37.928322	176.940997	34.714620
rangi golf 0054	Set 4 Landward	-37.928277	176.941006	35.101151
rangi golf 0055	Set 4 Landward	-37.928234	176.941015	35.196459

rangi golf 0056	Set 4 Landward	-37.928232	176.941015	35.184279
rangi golf 0057	Set 4 Landward	-37.928187	176.941021	34.780593
rangi golf 0058	Set 4 Landward	-37.928140	176.941027	34.557148
rangi golf 0059	Set 4 Landward	-37.928095	176.941034	34.583148
rangi golf 0060	Set 4 Landward	-37.928080	176.941036	34.561830
rangi golf 0061	Set 4 Landward	-37.928050	176.941040	34.526979
rangi golf 0062	Set 4 Landward	-37.928005	176.941046	34.386010
rangi golf 0063	Set 4 Landward	-37.927958	176.941054	34.251417
rangi golf 0064	Set 4 Landward	-37.927913	176.941063	34.175604
rangi golf 0065	Set 4 Landward	-37.927896	176.941068	34.127869
rangi golf 0066	Set 4 Landward	-37.927869	176.941074	34.042161
rangi golf 0067	Set 4 Landward	-37.927823	176.941086	33.844802
rangi golf 0068	Set 4 Landward	-37.927779	176.941099	33.550817
rangi golf 0069	Set 4 Landward	-37.927734	176.941111	33.268372
rangi golf 0070	Set 4 Landward	-37.927719	176.941114	33.193606
rangi golf 0071	Set 4 Landward	-37.927688	176.941121	33.088996
rangi golf 0072	Set 4 Landward	-37.927642	176.941132	33.099706
rangi golf 0073	Set 4 Landward	-37.927597	176.941138	33.574388
rangi golf 0074	Set 4 Landward	-37.927551	176.941145	34.065821
rangi golf 0075	Set 4 Landward	-37.927505	176.941153	34.188413
rangi golf 0076	Set 4 Landward	-37.927473	176.941156	34.039340
rangi golf 0077	Set 4 Landward	-37.927460	176.941158	33.900653
rangi golf 0078	Set 4 Landward	-37.927414	176.941162	33.532624
rangi golf 0079	Set 4 Landward	-37.927367	176.941162	33.193979
rangi golf 0080	Set 4 Landward	-37.927320	176.941165	33.058616
rangi golf 0081	Set 4 Landward	-37.927274	176.941171	33.267411
rangi golf 0082	Set 4 Landward	-37.927230	176.941184	33.911884
rangi golf 0083	Set 4 Landward	-37.927210	176.941192	34.079538
rangi golf 0084	Set 4 Landward	-37.927187	176.941202	34.129346
rangi golf 0085	Set 4 Landward	-37.927144	176.941222	34.158283
rangi golf 0086	Set 4 Landward	-37.927100	176.941238	34.153731
rangi golf 0087	Set 4 Landward	-37.927056	176.941255	34.179223
rangi golf 0088	Set 4 Landward	-37.927012	176.941270	34.140006
rangi golf 0089	Set 4 Landward	-37.926968	176.941283	34.186824
rangi golf 0090	Set 4 Landward	-37.926923	176.941293	34.224217
rangi golf 0091	Set 4 Landward	-37.926898	176.941297	34.233960
rangi golf 0092	Set 4 Landward	-37.926879	176.941304	34.271570
rangi golf 0093	Set 4 Landward	-37.926835	176.941322	34.364324
rangi golf 0094	Set 4 Landward	-37.926790	176.941334	34.305558
rangi golf 0095	Set 4 Landward	-37.926746	176.941343	33.817662
rangi golf 0096	Set 4 Landward	-37.926700	176.941350	33.182121
rangi golf 0097	Set 4 Landward	-37.926654	176.941359	32.906190
rangi golf 0098	Set 4 Landward	-37.926620	176.941363	33.166008
rangi golf 0099	Set 4 Landward	-37.926608	176.941364	33.309723
rangi golf 0100	Set 4 Landward	-37.926563	176.941371	33.702688
rangi golf 0101	Set 4 Landward	-37.926517	176.941378	33.959619

rangi golf 0102	Set 4 Landward	-37.926471	176.941382	34.307050
rangi golf 0103	Set 4 Landward	-37.926443	176.941384	34.745628
rangi golf 0104	Set 4 Landward	-37.926425	176.941384	34.776890
rangi golf 0105	Set 4 Landward	-37.926379	176.941383	34.503478
rangi golf 0106	Set 4 Landward	-37.926333	176.941384	34.141471
rangi golf 0107	Set 4 Landward	-37.926287	176.941387	33.764203
rangi golf 0108	Set 4 Landward	-37.926242	176.941388	33.513289
rangi golf 0109	Set 4 Landward	-37.926196	176.941389	33.394111
rangi golf 0110	Set 4 Landward	-37.926170	176.941391	33.518310
rangi golf 0111	Set 4 Landward	-37.926150	176.941390	33.792491
rangi golf 0112	Set 4 Landward	-37.926103	176.941385	34.664553
rangi golf 0113	Set 4 Landward	-37.926058	176.941377	36.112591
rangi golf 0114	Set 4 Landward	-37.926012	176.941380	36.501802
rangi golf 0115	Set 4 Landward	-37.925984	176.941387	36.386029
rangi golf 0116	Set 4 Landward	-37.925967	176.941392	36.230504
rangi golf 0117	Set 4 Landward	-37.925924	176.941410	35.679063
rangi golf 0118	Set 4 Landward	-37.925880	176.941426	35.423115
rangi golf 0119	Set 4 Landward	-37.925836	176.941442	35.583558
rangi golf 0120	Set 4 Landward	-37.925816	176.941448	35.868271
rangi golf 0121	Set 4 Landward	-37.925792	176.941458	35.930196
rangi golf 0122	Set 4 Landward	-37.925747	176.941470	35.387181
rangi golf 0123	Set 4 Landward	-37.925702	176.941473	34.902818
rangi golf 0124	Set 4 Landward	-37.925658	176.941488	34.308560
rangi golf 0125	Set 4 Landward	-37.925648	176.941496	34.206225
rangi golf 0126	Set 4 Landward	-37.925623	176.941524	33.991734
rangi golf 0127	Set 4 Landward	-37.925588	176.941561	33.714661
rangi golf 0128	Set 4 Landward	-37.925550	176.941594	33.790066
rangi golf 0129	Set 4 Landward	-37.925511	176.941623	34.223503
rangi golf 0130	Set 4 Landward	-37.925474	176.941656	34.224915
rangi golf 0131	Set 4 Landward	-37.925440	176.941685	34.145235

rangi1 0008	Set 1	-37.984357	176.902193	32.857650
rangi1 0009	Set 1	-37.984289	176.902262	32.706685
rangi1 0010	Set 1	-37.984283	176.902268	32.703095
rangi1 0011	Set 1	-37.984252	176.902295	32.653040
rangi1 0012	Set 1	-37.984212	176.902322	32.567880
rangi1 0013	Set 1	-37.984202	176.902329	32.579004
rangi1 0014	Set 1	-37.984173	176.902355	32.503127
rangi1 0015	Set 1	-37.984138	176.902391	32.281503
rangi1 0016	Set 1	-37.984101	176.902426	32.072253
rangi1 0017	Set 1	-37.984066	176.902462	31.890523
rangi1 0018	Set 1	-37.984030	176.902497	31.756057
rangi1 0019	Set 1	-37.984029	176.902499	31.749713
rangi1 0020	Set 1	-37.983995	176.902535	31.651337
rangi1 0021	Set 1	-37.983958	176.902568	31.594399
rangi1 0022	Set 1	-37.983945	176.902579	31.572630

rangi1 0023	Set 1	-37.983945	176.902579	31.569058
rangi1 0024	Set 1	-37.983920	176.902600	31.547598
rangi1 0025	Set 1	-37.983886	176.902637	31.568161
rangi1 0026	Set 1	-37.983873	176.902650	31.610506
rangi1 0027	Set 1	-37.983850	176.902675	31.681152
rangi1 0028	Set 1	-37.983815	176.902712	31.874269
rangi1 0029	Set 1	-37.983792	176.902734	32.127250
rangi1 0030	Set 1	-37.983779	176.902747	32.289953
rangi1 0031	Set 1	-37.983745	176.902785	32.570460
rangi1 0032	Set 1	-37.983728	176.902803	32.513269
rangi1 0033	Set 1	-37.983709	176.902820	32.574071
rangi1 0034	Set 1	-37.983671	176.902852	32.501974
rangi1 0035	Set 1	-37.983658	176.902865	32.490116
rangi1 0036	Set 1	-37.983638	176.902891	32.489276
rangi1 0037	Set 1	-37.983601	176.902925	32.526276
rangi1 0038	Set 1	-37.983601	176.902925	32.516197
rangi1 0039	Set 1	-37.983565	176.902960	32.405986
rangi1 0040	Set 1	-37.983530	176.902994	32.369611
rangi1 0041	Set 1	-37.983529	176.902996	32.370037
rangi1 0042	Set 1	-37.983494	176.903033	32.157145
rangi1 0043	Set 1	-37.983474	176.903050	32.098016
rangi1 0044	Set 1	-37.983456	176.903064	32.078072
rangi1 0045	Set 1	-37.983418	176.903094	32.026830
rangi1 0046	Set 1	-37.983409	176.903102	32.019115
rangi1 0047	Set 1	-37.983381	176.903127	32.017296
rangi1 0048	Set 1	-37.983354	176.903151	32.006790
rangi1 0049	Set 1	-37.983343	176.903160	32.070298
rangi1 0050	Set 1	-37.983305	176.903192	32.069662
rangi1 0051	Set 1	-37.983285	176.903208	32.084799
rangi1 0052	Set 1	-37.983266	176.903224	32.029822
rangi1 0053	Set 1	-37.983231	176.903260	32.023380
rangi1 0054	Set 1	-37.983217	176.903274	32.014555
rangi1 0055	Set 1	-37.983195	176.903294	32.049212
rangi1 0056	Set 1	-37.983160	176.903330	32.130945
rangi1 0057	Set 1	-37.983157	176.903333	32.099951
rangi1 0058	Set 1	-37.983124	176.903367	32.023689
rangi1 0059	Set 1	-37.983089	176.903403	31.964625
rangi1 0060	Set 1	-37.983082	176.903410	31.955006
rangi1 0061	Set 1	-37.983054	176.903441	31.842721
rangi1 0062	Set 1	-37.983020	176.903480	31.778950
rangi1 0063	Set 1	-37.983016	176.903484	31.775930
rangi1 0064	Set 1	-37.982987	176.903518	31.759923
rangi1 0065	Set 1	-37.982953	176.903555	31.656135
rangi1 0066	Set 1	-37.982951	176.903557	31.666188
rangi1 0067	Set 1	-37.982914	176.903586	31.678688
rangi1 0068	Set 1	-37.982878	176.903622	31.760808

rangi1 0069	Set 1	-37.982848	176.903653	31.742163
rangi1 0070	Set 1	-37.982843	176.903659	31.739719
rangi1 0071	Set 1	-37.982807	176.903695	31.772691
rangi1 0072	Set 1	-37.982775	176.903727	31.754493
rangi1 0073	Set 1	-37.982771	176.903730	31.770767
rangi1 0074	Set 1	-37.982735	176.903766	31.825883
rangi1 0075	Set 1	-37.982700	176.903804	31.879212
rangi1 0076	Set 1	-37.982680	176.903827	31.922029
rangi1 0077	Set 1	-37.982666	176.903843	31.939155
rangi1 0078	Set 1	-37.982632	176.903881	32.061769
rangi1 0079	Set 1	-37.982599	176.903920	32.114525
rangi1 0080	Set 1	-37.982583	176.903936	32.114281
rangi1 0081	Set 1	-37.982564	176.903957	32.104091
rangi1 0082	Set 1	-37.982528	176.903992	32.026592
rangi1 0083	Set 1	-37.982492	176.904027	31.955580
rangi1 0084	Set 1	-37.982455	176.904059	31.859435
rangi1 0085	Set 1	-37.982451	176.904063	31.848801
rangi1 0086	Set 1	-37.982418	176.904095	31.782481
rangi1 0087	Set 1	-37.982382	176.904130	31.788720
rangi1 0088	Set 1	-37.982354	176.904156	31.790106
rangi1 0089	Set 1	-37.982345	176.904165	31.802304
rangi1 0090	Set 1	-37.982310	176.904202	31.808542
rangi1 0091	Set 1	-37.982276	176.904239	31.857228
rangi1 0092	Set 1	-37.982276	176.904239	31.857749
rangi1 0093	Set 1	-37.982240	176.904276	31.974689
rangi1 0094	Set 1	-37.982206	176.904313	32.121173
rangi1 0095	Set 1	-37.982171	176.904351	32.135864
rangi1 0096	Set 1	-37.982162	176.904360	32.194125
rangi1 0097	Set 1	-37.982136	176.904387	32.239400
rangi1 0098	Set 1	-37.982100	176.904423	32.245113
rangi1 0099	Set 1	-37.982075	176.904449	32.252943
rangi1 0100	Set 1	-37.982064	176.904458	32.274623
rangi1 0101	Set 1	-37.982027	176.904489	32.303467
rangi1 0102	Set 1	-37.981990	176.904525	32.303541
rangi1 0103	Set 1	-37.981970	176.904544	32.338474
rangi1 0104	Set 1	-37.981953	176.904559	32.374770
rangi1 0105	Set 1	-37.981916	176.904592	32.424232
rangi1 0106	Set 1	-37.981883	176.904623	32.330310
rangi1 0107	Set 1	-37.981879	176.904626	32.316520
rangi1 0108	Set 1	-37.981844	176.904662	32.266889
rangi1 0109	Set 1	-37.981806	176.904693	32.290382
rangi1 0110	Set 1	-37.981792	176.904708	32.265865
rangi1 0111	Set 1	-37.981770	176.904730	32.281488
rangi1 0112	Set 1	-37.981735	176.904766	32.297281
rangi1 0113	Set 1	-37.981712	176.904786	32.298722
rangi1 0114	Set 1	-37.981697	176.904799	32.321557

rangi1 0115	Set 1	-37.981662	176.904835	32.253659
rangi1 0116	Set 1	-37.981637	176.904865	32.318667
rangi1 0117	Set 1	-37.981628	176.904873	32.315141
rangi1 0118	Set 1	-37.981591	176.904907	32.304503
rangi1 0119	Set 1	-37.981553	176.904939	32.308000
rangi1 0120	Set 1	-37.981532	176.904956	32.329379
rangi1 0121	Set 1	-37.981516	176.904972	32.359125
rangi1 0122	Set 1	-37.981480	176.905007	32.355751
rangi1 0123	Set 1	-37.981453	176.905034	32.398373
rangi1 0124	Set 1	-37.981445	176.905042	32.389718
rangi1 0125	Set 1	-37.981408	176.905077	32.336435
rangi1 0126	Set 1	-37.981386	176.905102	32.329502
rangi1 0127	Set 1	-37.981373	176.905114	32.278678
rangi1 0128	Set 1	-37.981336	176.905148	32.292243
rangi1 0129	Set 1	-37.981300	176.905183	32.205455
rangi1 0130	Set 1	-37.981283	176.905199	32.212260
rangi1 0131	Set 1	-37.981263	176.905217	32.171704
rangi1 0132	Set 1	-37.981227	176.905253	32.179317
rangi1 0133	Set 1	-37.981190	176.905286	32.098535
rangi1 0134	Set 1	-37.981186	176.905290	32.095102
rangi1 0135	Set 1	-37.981154	176.905322	32.054134
rangi1 0136	Set 1	-37.981118	176.905358	32.041772
rangi1 0137	Set 1	-37.981103	176.905373	32.033884
rangi1 0138	Set 1	-37.981083	176.905393	32.048331
rangi1 0139	Set 1	-37.981048	176.905429	32.093507
rangi1 0140	Set 1	-37.981020	176.905453	32.118471
rangi1 0141	Set 1	-37.981011	176.905462	32.138900
rangi1 0142	Set 1	-37.980977	176.905500	32.202238
rangi1 0143	Set 1	-37.980943	176.905535	32.274507
rangi1 0144	Set 1	-37.980942	176.905536	32.279997
rangi1 0145	Set 1	-37.980904	176.905570	32.420165
rangi1 0146	Set 1	-37.980867	176.905603	32.477487
rangi1 0147	Set 1	-37.980839	176.905629	32.521235
rangi1 0148	Set 1	-37.980831	176.905637	32.539488
rangi1 0149	Set 1	-37.980794	176.905670	32.543208
rangi1 0150	Set 1	-37.980766	176.905697	32.553651
rangi1 0151	Set 1	-37.980757	176.905705	32.547734
rangi1 0152	Set 1	-37.980720	176.905738	32.506189
rangi1 0153	Set 1	-37.980702	176.905757	32.508033
rangi1 0154	Set 1	-37.980685	176.905776	32.567029
rangi1 0155	Set 1	-37.980648	176.905809	32.599195
rangi1 0156	Set 1	-37.980626	176.905832	32.621235
rangi1 0157	Set 1	-37.980612	176.905845	32.605339
rangi1 0158	Set 1	-37.980575	176.905879	32.485687
rangi1 0159	Set 1	-37.980555	176.905895	32.465942
rangi1 0160	Set 1	-37.980538	176.905913	32.437804

rangi1 0161	Set 1	-37.980503	176.905949	32.391042
rangi1 0162	Set 1	-37.980487	176.905965	32.354492
rangi1 0163	Set 1	-37.980468	176.905985	32.329929
rangi1 0164	Set 1	-37.980430	176.906017	32.309343
rangi1 0165	Set 1	-37.980399	176.906041	32.313177
rangi1 0166	Set 1	-37.980391	176.906048	32.320634
rangi1 0167	Set 1	-37.980356	176.906087	32.400457
rangi1 0168	Set 1	-37.980321	176.906125	32.558075
rangi1 0169	Set 1	-37.980315	176.906131	32.568187
rangi1 0170	Set 1	-37.980285	176.906163	32.568904
rangi1 0171	Set 1	-37.980251	176.906201	32.609016
rangi1 0172	Set 1	-37.980216	176.906238	32.623847
rangi1 0173	Set 1	-37.980212	176.906242	32.614577
rangi1 0174	Set 1	-37.980182	176.906275	32.647387
rangi1 0175	Set 1	-37.980147	176.906312	32.655749
rangi1 0176	Set 1	-37.980121	176.906335	32.640935
rangi1 0177	Set 1	-37.980109	176.906346	32.634211
rangi1 0178	Set 1	-37.980073	176.906383	32.634067
rangi1 0179	Set 1	-37.980039	176.906420	32.686061
rangi1 0180	Set 1	-37.980007	176.906450	32.712893
rangi1 0181	Set 1	-37.980002	176.906455	32.713007
rangi1 0182	Set 1	-37.979968	176.906493	32.811251
rangi1 0183	Set 1	-37.979934	176.906532	32.648486
rangi1 0184	Set 1	-37.979911	176.906554	32.534496
rangi1 0185	Set 1	-37.979898	176.906567	32.529361
rangi1 0186	Set 1	-37.979865	176.906605	32.525531
rangi1 0187	Set 1	-37.979843	176.906629	32.659471
rangi1 0188	Set 1	-37.979828	176.906641	32.779807
rangi1 0189	Set 1	-37.979791	176.906675	32.830123
rangi1 0190	Set 1	-37.979754	176.906709	32.886083
rangi1 0191	Set 1	-37.979747	176.906714	32.842358
rangi1 0192	Set 1	-37.979714	176.906734	32.899007
rangi1 0193	Set 1	-37.979669	176.906735	32.809813
rangi1 0194	Set 1	-37.979668	176.906735	32.800619
rangi1 0195	Set 1	-37.979627	176.906760	32.831464
rangi1 0196	Set 1	-37.979587	176.906789	32.824759
rangi1 0197	Set 1	-37.979547	176.906815	32.832230
rangi1 0198	Set 1	-37.979510	176.906847	32.893009
rangi1 0199	Set 1	-37.979473	176.906882	32.809411
rangi1 0200	Set 1	-37.979464	176.906893	32.776146
rangi1 0201	Set 1	-37.979439	176.906918	32.744858
rangi1 0202	Set 1	-37.979403	176.906955	32.604471
rangi1 0203	Set 1	-37.979394	176.906966	32.548652
rangi1 0204	Set 1	-37.979370	176.906994	32.423162
rangi1 0205	Set 1	-37.979331	176.907025	32.214340
rangi1 0206	Set 1	-37.979324	176.907031	32.174497

rangi1 0207	Set 1	-37.979297	176.907063	32.171428
rangi1 0208	Set 1	-37.979262	176.907101	31.793069
rangi1 0209	Set 1	-37.979254	176.907109	31.703708
rangi1 0210	Set 1	-37.979226	176.907136	31.436759
rangi1 0211	Set 1	-37.979190	176.907171	31.137454
rangi1 0212	Set 1	-37.979183	176.907176	31.081965
rangi1 0213	Set 1	-37.979152	176.907203	30.824990
rangi1 0214	Set 1	-37.979116	176.907237	30.557035
rangi1 0215	Set 1	-37.979089	176.907259	30.415824
rangi1 0216	Set 1	-37.979078	176.907270	30.348715
rangi1 0217	Set 1	-37.979040	176.907303	30.242537
rangi1 0218	Set 1	-37.979004	176.907331	30.150820

RANGI4 00001	Set 2 Sewards	-37.973378	176.927135	31.288955
RANGI4 00002	Set 2 Sewards	-37.973306	176.927163	31.275458
RANGI4 00003	Set 2 Sewards	-37.973278	176.927175	31.359274
RANGI4 00004	Set 2 Sewards	-37.973263	176.927181	31.439511
RANGI4 00005	Set 2 Sewards	-37.973220	176.927201	31.661134
RANGI4 00006	Set 2 Sewards	-37.973200	176.927210	31.732716
RANGI4 00007	Set 2 Sewards	-37.973176	176.927219	31.797849
RANGI4 00008	Set 2 Sewards	-37.973133	176.927237	31.843270
RANGI4 00009	Set 2 Sewards	-37.973111	176.927247	31.827101
RANGI4 00010	Set 2 Sewards	-37.973089	176.927257	31.826743
RANGI4 00011	Set 2 Sewards	-37.973045	176.927275	31.690151
RANGI4 00012	Set 2 Sewards	-37.973035	176.927280	31.647520
RANGI4 00013	Set 2 Sewards	-37.973003	176.927293	31.535483
RANGI4 00014	Set 2 Sewards	-37.972971	176.927307	31.429984
RANGI4 00015	Set 2 Sewards	-37.972959	176.927312	31.396236
RANGI4 00016	Set 2 Sewards	-37.972916	176.927330	31.273729
RANGI4 00017	Set 2 Sewards	-37.972907	176.927335	31.259557
RANGI4 00018	Set 2 Sewards	-37.972873	176.927347	31.173559
RANGI4 00019	Set 2 Sewards	-37.972836	176.927365	31.025265
RANGI4 00020	Set 2 Sewards	-37.972830	176.927367	30.999921
RANGI4 00021	Set 2 Sewards	-37.972786	176.927385	30.851697
RANGI4 00022	Set 2 Sewards	-37.972761	176.927396	30.826057
RANGI4 00023	Set 2 Sewards	-37.972742	176.927405	30.802937
RANGI4 00024	Set 2 Sewards	-37.972698	176.927423	30.825311
RANGI4 00025	Set 2 Sewards	-37.972683	176.927429	30.853648
RANGI4 00026	Set 2 Sewards	-37.972655	176.927441	30.909670
RANGI4 00027	Set 2 Sewards	-37.972617	176.927458	31.015651
RANGI4 00028	Set 2 Sewards	-37.972612	176.927460	31.031431
RANGI4 00029	Set 2 Sewards	-37.972570	176.927478	31.015182
RANGI4 00030	Set 2 Sewards	-37.972530	176.927495	30.914933
RANGI4 00031	Set 2 Sewards	-37.972526	176.927497	30.899578
RANGI4 00032	Set 2 Sewards	-37.972483	176.927515	30.734243
RANGI4 00033	Set 2 Sewards	-37.972449	176.927529	30.667989

RANGI4 00034	Set 2 Sewards	-37.972439	176.927533	30.654042
RANGI4 00035	Set 2 Sewards	-37.972396	176.927553	30.608972
RANGI4 00036	Set 2 Sewards	-37.972365	176.927567	30.624645
RANGI4 00037	Set 2 Sewards	-37.972354	176.927571	30.602785
RANGI4 00038	Set 2 Sewards	-37.972310	176.927587	30.443022
RANGI4 00039	Set 2 Sewards	-37.972266	176.927598	30.486329
RANGI4 00040	Set 2 Sewards	-37.972263	176.927598	30.482738
RANGI4 00041	Set 2 Sewards	-37.972220	176.927600	30.604833
RANGI4 00042	Set 2 Sewards	-37.972175	176.927597	30.743155
RANGI4 00043	Set 2 Sewards	-37.972167	176.927596	30.560019
RANGI4 00044	Set 2 Sewards	-37.972129	176.927595	30.972146
RANGI4 00045	Set 2 Sewards	-37.972084	176.927606	31.402674
RANGI4 00046	Set 2 Sewards	-37.972047	176.927622	31.246051
RANGI4 00047	Set 2 Sewards	-37.972041	176.927625	31.221781
RANGI4 00048	Set 2 Sewards	-37.971997	176.927640	30.869468
RANGI4 00049	Set 2 Sewards	-37.971956	176.927662	30.855051
RANGI4 00050	Set 2 Sewards	-37.971955	176.927662	30.755673
RANGI4 00051	Set 2 Sewards	-37.971912	176.927680	30.559242
RANGI4 00052	Set 2 Sewards	-37.971872	176.927699	30.390987
RANGI4 00053	Set 2 Sewards	-37.971870	176.927701	30.380881
RANGI4 00054	Set 2 Sewards	-37.971826	176.927718	30.252123
RANGI4 00055	Set 2 Sewards	-37.971820	176.927721	30.220696
RANGI4 00056	Set 2 Sewards	-37.971783	176.927736	30.133001
RANGI4 00057	Set 2 Sewards	-37.971739	176.927753	30.058881
RANGI4 00058	Set 2 Sewards	-37.971731	176.927756	30.055820
RANGI4 00059	Set 2 Sewards	-37.971696	176.927771	30.007275
RANGI4 00060	Set 2 Sewards	-37.971668	176.927783	30.014710
RANGI4 00061	Set 2 Sewards	-37.971653	176.927790	30.052523
RANGI4 00062	Set 2 Sewards	-37.971609	176.927809	30.023205
RANGI4 00063	Set 2 Sewards	-37.971600	176.927813	30.039634
RANGI4 00064	Set 2 Sewards	-37.971566	176.927827	30.081725
RANGI4 00065	Set 2 Sewards	-37.971522	176.927843	30.128993
RANGI4 00066	Set 2 Sewards	-37.971500	176.927853	30.119646
RANGI4 00067	Set 2 Sewards	-37.971478	176.927861	30.165943
RANGI4 00068	Set 2 Sewards	-37.971435	176.927877	30.328722
RANGI4 00069	Set 2 Sewards	-37.971407	176.927890	30.557695
RANGI4 00070	Set 2 Sewards	-37.971391	176.927897	30.718381
RANGI4 00071	Set 2 Sewards	-37.971348	176.927913	31.181134
RANGI4 00072	Set 2 Sewards	-37.971341	176.927916	31.246606
RANGI4 00073	Set 2 Sewards	-37.971303	176.927932	31.503800
RANGI4 00074	Set 2 Sewards	-37.971268	176.927948	31.640039
RANGI4 00075	Set 2 Sewards	-37.971260	176.927952	31.616777
RANGI4 00076	Set 2 Sewards	-37.971215	176.927971	31.573898
RANGI4 00077	Set 2 Sewards	-37.971172	176.927989	31.453005
RANGI4 00078	Set 2 Sewards	-37.971165	176.927992	31.414923
RANGI4 00079	Set 2 Sewards	-37.971128	176.928007	31.297611

RANGI4 00080	Set 2 Sewards	-37.971085	176.928025	31.077562
RANGI4 00081	Set 2 Sewards	-37.971066	176.928033	30.981697
RANGI4 00082	Set 2 Sewards	-37.971041	176.928042	30.855289
RANGI4 00083	Set 2 Sewards	-37.970998	176.928061	30.762532
RANGI4 00084	Set 2 Sewards	-37.970983	176.928067	30.751700
RANGI4 00085	Set 2 Sewards	-37.970954	176.928078	30.696021
RANGI4 00086	Set 2 Sewards	-37.970912	176.928097	30.656017
RANGI4 00087	Set 2 Sewards	-37.970910	176.928098	30.669719
RANGI4 00088	Set 2 Sewards	-37.970867	176.928114	30.663162
RANGI4 00089	Set 2 Sewards	-37.970825	176.928133	30.653450
RANGI4 00090	Set 2 Sewards	-37.970813	176.928139	30.615812
RANGI4 00091	Set 2 Sewards	-37.970782	176.928153	30.637307
RANGI4 00092	Set 2 Sewards	-37.970739	176.928173	30.646299
RANGI4 00093	Set 2 Sewards	-37.970696	176.928187	30.614311
RANGI4 00094	Set 2 Sewards	-37.970668	176.928199	30.607180
RANGI4 00095	Set 2 Sewards	-37.970653	176.928206	30.623076
RANGI4 00096	Set 2 Sewards	-37.970609	176.928227	30.814473
RANGI4 00097	Set 2 Sewards	-37.970589	176.928237	30.794765
RANGI4 00098	Set 2 Sewards	-37.970566	176.928245	30.792461
RANGI4 00099	Set 2 Sewards	-37.970521	176.928265	29.838792
RANGI4 00100	Set 2 Sewards	-37.970503	176.928280	30.736502
RANGI4 00101	Set 2 Sewards	-37.970481	176.928291	30.797199
RANGI4 00102	Set 2 Sewards	-37.970437	176.928313	30.620516
RANGI4 00103	Set 2 Sewards	-37.970395	176.928335	30.708985
RANGI4 00104	Set 2 Sewards	-37.970384	176.928341	30.672727
RANGI4 00105	Set 2 Sewards	-37.970352	176.928358	31.202603
RANGI4 00106	Set 2 Sewards	-37.970311	176.928380	31.232067
RANGI4 00107	Set 2 Sewards	-37.970273	176.928400	31.218107
RANGI4 00108	Set 2 Sewards	-37.970269	176.928402	31.241389
RANGI4 00109	Set 2 Sewards	-37.970226	176.928424	31.179162
RANGI4 00110	Set 2 Sewards	-37.970184	176.928446	31.165263
RANGI4 00111	Set 2 Sewards	-37.970166	176.928457	31.119927
RANGI4 00112	Set 2 Sewards	-37.970141	176.928469	31.079521
RANGI4 00113	Set 2 Sewards	-37.970099	176.928492	31.093493
RANGI4 00114	Set 2 Sewards	-37.970058	176.928516	31.133161
RANGI4 00115	Set 2 Sewards	-37.970052	176.928519	31.152226
RANGI4 00116	Set 2 Sewards	-37.970016	176.928538	31.199387
RANGI4 00117	Set 2 Sewards	-37.969974	176.928558	31.040519
RANGI4 00118	Set 2 Sewards	-37.969963	176.928562	30.952685
RANGI4 00119	Set 2 Sewards	-37.969930	176.928575	30.558338
RANGI4 00120	Set 2 Sewards	-37.969888	176.928592	30.087579
RANGI4 00121	Set 2 Sewards	-37.969887	176.928592	30.086460
RANGI4 00122	Set 2 Sewards	-37.969843	176.928607	29.546894
RANGI4 00123	Set 2 Sewards	-37.969800	176.928623	29.059819
RANGI4 00124	Set 2 Sewards	-37.969800	176.928624	29.053647
RANGI4 00125	Set 2 Sewards	-37.969756	176.928639	28.769985

RANGI4 00126	Set 2 Sewards	-37.969712	176.928657	28.477115
RANGI4 00127	Set 2 Sewards	-37.969710	176.928658	28.482253
RANGI4 00128	Set 2 Sewards	-37.969667	176.928673	28.449144
RANGI4 00129	Set 2 Sewards	-37.969624	176.928691	28.393824
RANGI4 00130	Set 2 Sewards	-37.969612	176.928696	28.386752
RANGI4 00131	Set 2 Sewards	-37.969581	176.928710	28.378263
RANGI4 00132	Set 2 Sewards	-37.969538	176.928728	28.400241
RANGI4 00133	Set 2 Sewards	-37.969495	176.928746	28.285979
RANGI4 00134	Set 2 Sewards	-37.969489	176.928749	28.297989
RANGI4 00135	Set 2 Sewards	-37.969451	176.928766	28.338195
RANGI4 00136	Set 2 Sewards	-37.969407	176.928784	28.354403
RANGI4 00137	Set 2 Sewards	-37.969365	176.928807	28.363129
RANGI4 00138	Set 2 Sewards	-37.969352	176.928813	28.380472
RANGI4 00139	Set 2 Sewards	-37.969320	176.928823	28.414277
RANGI4 00140	Set 2 Sewards	-37.969277	176.928842	28.278251
RANGI4 00141	Set 2 Sewards	-37.969235	176.928861	28.322479
RANGI4 00142	Set 2 Sewards	-37.969195	176.928878	28.312900
RANGI4 00143	Set 2 Sewards	-37.969191	176.928880	28.306521
RANGI4 00144	Set 2 Sewards	-37.969148	176.928899	28.332651
RANGI4 00145	Set 2 Sewards	-37.969104	176.928918	28.281677
RANGI4 00146	Set 2 Sewards	-37.969086	176.928924	28.250930
RANGI4 00147	Set 2 Sewards	-37.969061	176.928940	28.336879
RANGI4 00148	Set 2 Sewards	-37.969018	176.928960	28.285730
RANGI4 00149	Set 2 Sewards	-37.968983	176.928975	28.308508

RANGI-6 0001	Set 3 Sewards	-37.956816	176.917715	31.348860
RANGI-6 0002	Set 3 Sewards	-37.956854	176.917683	31.295239
RANGI-6 0003	Set 3 Sewards	-37.956888	176.917645	31.121377
RANGI-6 0004	Set 3 Sewards	-37.956921	176.917603	30.900897
RANGI-6 0005	Set 3 Sewards	-37.956950	176.917560	30.747181
RANGI-6 0006	Set 3 Sewards	-37.956967	176.917540	30.701344
RANGI-6 0007	Set 3 Sewards	-37.956981	176.917518	30.651633
RANGI-6 0008	Set 3 Sewards	-37.957007	176.917470	30.608648
RANGI-6 0009	Set 3 Sewards	-37.957036	176.917425	30.580964
RANGI-6 0010	Set 3 Sewards	-37.957065	176.917381	30.573626
RANGI-6 0011	Set 3 Sewards	-37.957082	176.917359	30.564506
RANGI-6 0012	Set 3 Sewards	-37.957096	176.917338	30.560650
RANGI-6 0013	Set 3 Sewards	-37.957127	176.917295	30.589923
RANGI-6 0014	Set 3 Sewards	-37.957159	176.917254	30.620296
RANGI-6 0015	Set 3 Sewards	-37.957192	176.917216	30.692924
RANGI-6 0016	Set 3 Sewards	-37.957227	176.917187	30.809120
RANGI-6 0017	Set 3 Sewards	-37.957230	176.917185	30.833017
RANGI-6 0018	Set 3 Sewards	-37.957271	176.917156	31.049265
RANGI-6 0019	Set 3 Sewards	-37.957312	176.917133	31.044527
RANGI-6 0020	Set 3 Sewards	-37.957355	176.917109	30.768265
RANGI-6 0021	Set 3 Sewards	-37.957396	176.917087	30.390437

RANGI-6 0022	Set 3 Sewards	-37.957420	176.917074	30.236475
RANGI-6 0023	Set 3 Sewards	-37.957438	176.917064	30.149314
RANGI-6 0024	Set 3 Sewards	-37.957480	176.917038	30.037330
RANGI-6 0025	Set 3 Sewards	-37.957521	176.917015	30.034843
RANGI-6 0026	Set 3 Sewards	-37.957564	176.916991	30.044529
RANGI-6 0027	Set 3 Sewards	-37.957591	176.916976	30.069135
RANGI-6 0028	Set 3 Sewards	-37.957605	176.916967	30.098311
RANGI-6 0029	Set 3 Sewards	-37.957646	176.916943	30.183793
RANGI-6 0030	Set 3 Sewards	-37.957688	176.916920	30.307582
RANGI-6 0031	Set 3 Sewards	-37.957730	176.916895	30.558800
RANGI-6 0032	Set 3 Sewards	-37.957759	176.916878	30.687044
RANGI-6 0033	Set 3 Sewards	-37.957772	176.916871	30.773419
RANGI-6 0034	Set 3 Sewards	-37.957814	176.916846	30.956129
RANGI-6 0035	Set 3 Sewards	-37.957855	176.916822	31.057450
RANGI-6 0036	Set 3 Sewards	-37.957898	176.916803	31.150956
RANGI-6 0037	Set 3 Sewards	-37.957941	176.916782	30.973019
RANGI-6 0038	Set 3 Sewards	-37.957952	176.916776	30.893798
RANGI-6 0039	Set 3 Sewards	-37.957979	176.916750	30.709854
RANGI-6 0040	Set 3 Sewards	-37.958019	176.916720	30.395970
RANGI-6 0041	Set 3 Sewards	-37.958061	176.916695	30.143724
RANGI-6 0042	Set 3 Sewards	-37.958104	176.916671	29.975946
RANGI-6 0043	Set 3 Sewards	-37.958139	176.916652	29.953444
RANGI-6 0044	Set 3 Sewards	-37.958146	176.916648	29.969311
RANGI-6 0045	Set 3 Sewards	-37.958188	176.916626	30.034902
RANGI-6 0046	Set 3 Sewards	-37.958229	176.916603	30.056748
RANGI-6 0047	Set 3 Sewards	-37.958271	176.916579	30.132883
RANGI-6 0048	Set 3 Sewards	-37.958313	176.916558	30.254274
RANGI-6 0049	Set 3 Sewards	-37.958355	176.916537	30.394258
RANGI-6 0050	Set 3 Sewards	-37.958371	176.916527	30.439517
RANGI-6 0051	Set 3 Sewards	-37.958397	176.916515	30.502182
RANGI-6 0052	Set 3 Sewards	-37.958441	176.916497	30.540593
RANGI-6 0053	Set 3 Sewards	-37.958483	176.916473	30.572004
RANGI-6 0054	Set 3 Sewards	-37.958526	176.916449	30.611095
RANGI-6 0055	Set 3 Sewards	-37.958568	176.916428	30.692093
RANGI-6 0056	Set 3 Sewards	-37.958610	176.916404	30.814154
RANGI-6 0057	Set 3 Sewards	-37.958625	176.916396	30.872010
RANGI-6 0058	Set 3 Sewards	-37.958652	176.916381	30.945097
RANGI-6 0059	Set 3 Sewards	-37.958695	176.916357	31.023432
RANGI-6 0060	Set 3 Sewards	-37.958738	176.916334	31.004852
RANGI-6 0061	Set 3 Sewards	-37.958779	176.916312	30.875329
RANGI-6 0062	Set 3 Sewards	-37.958822	176.916287	30.708139
RANGI-6 0063	Set 3 Sewards	-37.958863	176.916261	30.599597
RANGI-6 0064	Set 3 Sewards	-37.958872	176.916255	30.579668
RANGI-6 0065	Set 3 Sewards	-37.958905	176.916238	30.601634
RANGI-6 0066	Set 3 Sewards	-37.958948	176.916216	30.682529
RANGI-6 0067	Set 3 Sewards	-37.958990	176.916194	30.777323

RANGI-6 0068	Set 3 Sewards	-37.959033	176.916174	30.938141
RANGI-6 0069	Set 3 Sewards	-37.959077	176.916158	31.088388
RANGI-6 0070	Set 3 Sewards	-37.959122	176.916144	31.201020
RANGI-6 0071	Set 3 Sewards	-37.959133	176.916140	31.220860
RANGI-6 0072	Set 3 Sewards	-37.959165	176.916126	31.288475
RANGI-6 0073	Set 3 Sewards	-37.959209	176.916107	31.403951
RANGI-6 0074	Set 3 Sewards	-37.959252	176.916086	31.601511
RANGI-6 0075	Set 3 Sewards	-37.959295	176.916068	31.753252
RANGI-6 0076	Set 3 Sewards	-37.959316	176.916056	31.792282
RANGI-6 0077	Set 3 Sewards	-37.959337	176.916044	31.785383
RANGI-6 0078	Set 3 Sewards	-37.959378	176.916021	31.802813
RANGI-6 0079	Set 3 Sewards	-37.959421	176.916000	31.888772
RANGI-6.2 0001	Set 3 Landwards	-37.958736	176.914613	31.645575
RANGI-6.2 0002	Set 3 Landwards	-37.958777	176.914585	31.755305
RANGI-6.2 0003	Set 3 Landwards	-37.958817	176.914556	31.686348
RANGI-6.2 0004	Set 3 Landwards	-37.958860	176.914540	31.569063
RANGI-6.2 0005	Set 3 Landwards	-37.958903	176.914517	31.494341
RANGI-6.2 0006	Set 3 Landwards	-37.958932	176.914501	31.499199
RANGI-6.2 0007	Set 3 Landwards	-37.958945	176.914494	31.508988
RANGI-6.2 0008	Set 3 Landwards	-37.958986	176.914467	31.528373
RANGI-6.2 0009	Set 3 Landwards	-37.959027	176.914443	31.414768
RANGI-6.2 0010	Set 3 Landwards	-37.959069	176.914420	31.231652
RANGI-6.2 0011	Set 3 Landwards	-37.959111	176.914396	31.052924
RANGI-6.2 0012	Set 3 Landwards	-37.959152	176.914370	30.985340
RANGI-6.2 0013	Set 3 Landwards	-37.959193	176.914345	31.038917
RANGI-6.2 0014	Set 3 Landwards	-37.959235	176.914321	31.045134
RANGI-6.2 0015	Set 3 Landwards	-37.959257	176.914308	31.111149
RANGI-6.2 0016	Set 3 Landwards	-37.959277	176.914297	31.147910
RANGI-6.2 0017	Set 3 Landwards	-37.959319	176.914272	31.153620
RANGI-6.2 0018	Set 3 Landwards	-37.959360	176.914249	31.069323
RANGI-6.2 0019	Set 3 Landwards	-37.959402	176.914225	30.926570
RANGI-6.2 0020	Set 3 Landwards	-37.959444	176.914203	30.782668
RANGI-6.2 0021	Set 3 Landwards	-37.959486	176.914179	30.756026
RANGI-6.2 0022	Set 3 Landwards	-37.959528	176.914156	30.730020
RANGI-6.2 0023	Set 3 Landwards	-37.959564	176.914135	30.788506
RANGI-6.2 0024	Set 3 Landwards	-37.959569	176.914132	30.792893
RANGI-6.2 0025	Set 3 Landwards	-37.959612	176.914108	30.793901
RANGI-6.2 0026	Set 3 Landwards	-37.959655	176.914085	30.765406
RANGI-6.2 0027	Set 3 Landwards	-37.959697	176.914062	30.817632
RANGI-6.2 0028	Set 3 Landwards	-37.959738	176.914038	30.871310
RANGI-6.2 0029	Set 3 Landwards	-37.959779	176.914016	31.005210
RANGI-6.2 0030	Set 3 Landwards	-37.959821	176.913993	31.136952
RANGI-6.2 0031	Set 3 Landwards	-37.959830	176.913988	31.160171
RANGI-6.2 0032	Set 3 Landwards	-37.959863	176.913969	31.185272
RANGI-6.2 0033	Set 3 Landwards	-37.959904	176.913945	31.183280

RANGI-6.2 0034	Set 3 Landwards	-37.959945	176.913919	31.172278
RANGI-6.2 0035	Set 3 Landwards	-37.959986	176.913892	31.157748
RANGI-6.2 0036	Set 3 Landwards	-37.960028	176.913870	31.211467
RANGI-6.2 0037	Set 3 Landwards	-37.960071	176.913850	31.159965
RANGI-6.2 0038	Set 3 Landwards	-37.960097	176.913838	31.134291
RANGI-6.2 0039	Set 3 Landwards	-37.960113	176.913830	31.116320
RANGI-6.2 0040	Set 3 Landwards	-37.960155	176.913807	31.140124
RANGI-6.2 0041	Set 3 Landwards	-37.960197	176.913783	31.140001
RANGI-6.2 0042	Set 3 Landwards	-37.960238	176.913758	31.070235
RANGI-6.2 0043	Set 3 Landwards	-37.960279	176.913735	30.976486
RANGI-6.2 0044	Set 3 Landwards	-37.960299	176.913725	30.933528
RANGI-6.2 0045	Set 3 Landwards	-37.960321	176.913712	30.849320
RANGI-6.2 0046	Set 3 Landwards	-37.960363	176.913689	30.671288
RANGI-6.2 0047	Set 3 Landwards	-37.960405	176.913666	30.533844
RANGI-6.2 0048	Set 3 Landwards	-37.960447	176.913643	30.431073
RANGI-6.2 0049	Set 3 Landwards	-37.960490	176.913621	30.381389
RANGI-6.2 0050	Set 3 Landwards	-37.960507	176.913613	30.354842
RANGI-6.2 0051	Set 3 Landwards	-37.960533	176.913599	30.373809
RANGI-6.2 0052	Set 3 Landwards	-37.960575	176.913576	30.418498
RANGI-6.2 0053	Set 3 Landwards	-37.960617	176.913554	30.510010
RANGI-6.2 0054	Set 3 Landwards	-37.960659	176.913531	30.525763
RANGI-6.2 0055	Set 3 Landwards	-37.960692	176.913511	30.544913
RANGI-6.2 0056	Set 3 Landwards	-37.960700	176.913507	30.554274
RANGI-6.2 0057	Set 3 Landwards	-37.960742	176.913483	30.604332
RANGI-6.2 0058	Set 3 Landwards	-37.960783	176.913458	30.607584
RANGI-6.2 0059	Set 3 Landwards	-37.960824	176.913434	30.623770
RANGI-6.2 0060	Set 3 Landwards	-37.960865	176.913407	30.582310
RANGI-6.2 0061	Set 3 Landwards	-37.960870	176.913404	30.564609
RANGI-6.2 0062	Set 3 Landwards	-37.960908	176.913387	30.476459
RANGI-6.2 0063	Set 3 Landwards	-37.960952	176.913367	30.405747
RANGI-6.2 0064	Set 3 Landwards	-37.960994	176.913346	30.348650
RANGI-6.2 0065	Set 3 Landwards	-37.961036	176.913322	30.370231
RANGI-6.2 0066	Set 3 Landwards	-37.961058	176.913310	30.381190
RANGI-6.2 0067	Set 3 Landwards	-37.961077	176.913299	30.412774
RANGI-6.2 0068	Set 3 Landwards	-37.961120	176.913276	30.458285
RANGI-6.2 0069	Set 3 Landwards	-37.961161	176.913252	30.570431
RANGI-6.2 0070	Set 3 Landwards	-37.961202	176.913228	30.831113
RANGI-6.2 0071	Set 3 Landwards	-37.961244	176.913206	31.016118
RANGI-6.2 0072	Set 3 Landwards	-37.961273	176.913189	31.134631
RANGI-6.2 0073	Set 3 Landwards	-37.961286	176.913182	31.182059
RANGI-6.2 0074	Set 3 Landwards	-37.961328	176.913158	31.357066
RANGI-6.2 0075	Set 3 Landwards	-37.961369	176.913133	31.565416
RANGI-6.2 0076	Set 3 Landwards	-37.961409	176.913105	31.847163
RANGI-6.2 0077	Set 3 Landwards	-37.961448	176.913074	32.021038
RANGI-6.2 0078	Set 3 Landwards	-37.961458	176.913066	32.098471
RANGI-6.2 0079	Set 3 Landwards	-37.961487	176.913045	32.209638

RANGI-6.2 0080	Set 3 Landwards	-37.961529	176.913019	32.239452
RANGI-6.2 0081	Set 3 Landwards	-37.961571	176.912993	32.290420
RANGI-6.2 0082	Set 3 Landwards	-37.961610	176.912967	32.265792
RANGI-6.2 0083	Set 3 Landwards	-37.961652	176.912942	32.221793
RANGI-6.2 0084	Set 3 Landwards	-37.961692	176.912920	32.191322
RANGI-6.2 0085	Set 3 Landwards	-37.961694	176.912919	32.176443
RANGI-6.2 0086	Set 3 Landwards	-37.961733	176.912889	32.022448
RANGI-6.2 0087	Set 3 Landwards	-37.961776	176.912867	31.821768
RANGI-6.2 0088	Set 3 Landwards	-37.961818	176.912845	31.571664
RANGI-6.2 0089	Set 3 Landwards	-37.961860	176.912820	31.378772
RANGI-6.2 0090	Set 3 Landwards	-37.961901	176.912796	31.282970
RANGI-6.2 0091	Set 3 Landwards	-37.961904	176.912794	31.276806
RANGI-6.2 0092	Set 3 Landwards	-37.961943	176.912771	31.123085
RANGI-6.2 0093	Set 3 Landwards	-37.961985	176.912746	31.048758
RANGI-6.2 0094	Set 3 Landwards	-37.962019	176.912727	30.986425
RANGI-6.2 0095	Set 3 Landwards	-37.962026	176.912723	30.963556
RANGI-6.2 0096	Set 3 Landwards	-37.962068	176.912701	30.927741
RANGI-6.2 0097	Set 3 Landwards	-37.962110	176.912676	30.769558
RANGI-6.2 0098	Set 3 Landwards	-37.962151	176.912651	30.466494
RANGI-6.2 0099	Set 3 Landwards	-37.962193	176.912627	30.201785
RANGI-6.2 0100	Set 3 Landwards	-37.962210	176.912618	30.090192
RANGI-6.2 0101	Set 3 Landwards	-37.962236	176.912604	29.966947
RANGI-6.2 0102	Set 3 Landwards	-37.962278	176.912584	29.829643
RANGI-6.2 0103	Set 3 Landwards	-37.962321	176.912562	29.757160
RANGI-6.2 0104	Set 3 Landwards	-37.962364	176.912541	29.673774
RANGI-6.2 0105	Set 3 Landwards	-37.962405	176.912518	29.579487
RANGI-6.2 0106	Set 3 Landwards	-37.962427	176.912506	29.540908
RANGI-6.2 0107	Set 3 Landwards	-37.962447	176.912494	29.500668
RANGI-6.2 0108	Set 3 Landwards	-37.962488	176.912471	29.361920
RANGI-6.2 0109	Set 3 Landwards	-37.962530	176.912447	29.189514
RANGI-6.2 0110	Set 3 Landwards	-37.962573	176.912424	29.130625
RANGI-6.2 0111	Set 3 Landwards	-37.962604	176.912403	29.128309
RANGI-6.2 0112	Set 3 Landwards	-37.962614	176.912398	29.127321
RANGI-6.2 0113	Set 3 Landwards	-37.962658	176.912382	29.081292
RANGI-6.2 0114	Set 3 Landwards	-37.962702	176.912365	28.943998
RANGI-6.2 0115	Set 3 Landwards	-37.962744	176.912345	28.884436
RANGI-6.2 0116	Set 3 Landwards	-37.962786	176.912321	28.801487
RANGI-6.2 0117	Set 3 Landwards	-37.962808	176.912308	28.812044
RANGI-6.2 0118	Set 3 Landwards	-37.962827	176.912299	28.846078
RANGI-6.2 0119	Set 3 Landwards	-37.962870	176.912278	28.766035
RANGI-6.2 0120	Set 3 Landwards	-37.962913	176.912256	28.794293
RANGI-6.2 0121	Set 3 Landwards	-37.962955	176.912235	28.878938
RANGI-6.2 0122	Set 3 Landwards	-37.962972	176.912223	28.856287
RANGI-6.2 0123	Set 3 Landwards	-37.962996	176.912209	28.817385
RANGI-6.2 0124	Set 3 Landwards	-37.963039	176.912188	28.848919
RANGI-6.2 0125	Set 3 Landwards	-37.963081	176.912167	28.922143

RANGI-6.2 0126	Set 3 Landwards	-37.963123	176.912144	28.932806
RANGI-6.2 0127	Set 3 Landwards	-37.963164	176.912119	28.832509
RANGI-6.2 0128	Set 3 Landwards	-37.963165	176.912119	28.834964
RANGI-6.2 0129	Set 3 Landwards	-37.963207	176.912096	28.808119
RANGI-6.2 0130	Set 3 Landwards	-37.963249	176.912073	28.797849
RANGI-6.2 0131	Set 3 Landwards	-37.963291	176.912048	28.828310
RANGI-6.2 0132	Set 3 Landwards	-37.963332	176.912023	28.775646
RANGI-6.2 0133	Set 3 Landwards	-37.963358	176.912009	28.799394
RANGI-6.2 0134	Set 3 Landwards	-37.963374	176.911999	28.799344
RANGI-6.2 0135	Set 3 Landwards	-37.963416	176.911978	28.802863
RANGI-6.2 0136	Set 3 Landwards	-37.963458	176.911956	28.762535
RANGI-6.2 0137	Set 3 Landwards	-37.963500	176.911933	28.749042
RANGI-6.2 0138	Set 3 Landwards	-37.963533	176.911913	28.769987
RANGI-6.2 0139	Set 3 Landwards	-37.963541	176.911907	28.768652
RANGI-6.2 0140	Set 3 Landwards	-37.963584	176.911886	28.790779
RANGI-6.2 0141	Set 3 Landwards	-37.963625	176.911862	28.820021
RANGI-6.2 0142	Set 3 Landwards	-37.963667	176.911840	28.825449
RANGI-6.2 0143	Set 3 Landwards	-37.963708	176.911816	28.778955
RANGI-6.2 0144	Set 3 Landwards	-37.963718	176.911809	28.770818
RANGI-6.2 0145	Set 3 Landwards	-37.963750	176.911795	28.740442
RANGI-6.2 0146	Set 3 Landwards	-37.963793	176.911773	28.710426
RANGI-6.2 0147	Set 3 Landwards	-37.963836	176.911751	28.738261
RANGI-6.2 0148	Set 3 Landwards	-37.963879	176.911730	28.732481
RANGI-6.2 0149	Set 3 Landwards	-37.963920	176.911704	28.726858
RANGI-6.2 0150	Set 3 Landwards	-37.963960	176.911677	28.674562
RANGI-6.2 0151	Set 3 Landwards	-37.964002	176.911654	28.621057
RANGI-6.2 0152	Set 3 Landwards	-37.964044	176.911631	28.643124
RANGI-6.2 0153	Set 3 Landwards	-37.964066	176.911619	28.643543
RANGI-6.2 0154	Set 3 Landwards	-37.964086	176.911608	28.710158
RANGI-6.2 0155	Set 3 Landwards	-37.964129	176.911585	28.664101
RANGI-6.2 0156	Set 3 Landwards	-37.964168	176.911561	28.665126
RANGI-6.2 0157	Set 3 Landwards	-37.964169	176.911561	28.664459
RANGI-6.2 0158	Set 3 Landwards	-37.964210	176.911534	28.618002
RANGI-6.2 0159	Set 3 Landwards	-37.964252	176.911513	28.814818
RANGI-6.2 0160	Set 3 Landwards	-37.964295	176.911491	28.837489
RANGI-6.2 0161	Set 3 Landwards	-37.964336	176.911467	28.771183
RANGI-6.2 0162	Set 3 Landwards	-37.964337	176.911467	28.766631
RANGI-6.30001	Set 2 Landwards	-37.964294	176.911317	28.728284
RANGI-6.30002	Set 2 Landwards	-37.964337	176.911294	28.666858
RANGI-6.30003	Set 2 Landwards	-37.964378	176.911268	28.610249
RANGI-6.30004	Set 2 Landwards	-37.964419	176.911242	28.641875
RANGI-6.30005	Set 2 Landwards	-37.964459	176.911214	28.697560
RANGI-6.30006	Set 2 Landwards	-37.964460	176.911214	28.693537
RANGI-6.30007	Set 2 Landwards	-37.964500	176.911189	28.759772
RANGI-6.30008	Set 2 Landwards	-37.964543	176.911167	28.763020

RANGI-6.30009	Set 2 Landwards	-37.964586	176.911145	28.753471
RANGI-6.30010	Set 2 Landwards	-37.964627	176.911121	28.747558
RANGI-6.30011	Set 2 Landwards	-37.964668	176.911098	28.683526
RANGI-6.30012	Set 2 Landwards	-37.964681	176.911091	28.653492
RANGI-6.30013	Set 2 Landwards	-37.964709	176.911076	28.665851
RANGI-6.30014	Set 2 Landwards	-37.964752	176.911054	28.580777
RANGI-6.30015	Set 2 Landwards	-37.964794	176.911033	28.566061
RANGI-6.30016	Set 2 Landwards	-37.964836	176.911010	28.550743
RANGI-6.30017	Set 2 Landwards	-37.964878	176.910988	28.519859
RANGI-6.30018	Set 2 Landwards	-37.964921	176.910967	28.477608
RANGI-6.30019	Set 2 Landwards	-37.964953	176.910950	28.444297
RANGI-6.30020	Set 2 Landwards	-37.964963	176.910945	28.457861
RANGI-6.30021	Set 2 Landwards	-37.965006	176.910921	28.414478
RANGI-6.30022	Set 2 Landwards	-37.965048	176.910898	28.421419
RANGI-6.30023	Set 2 Landwards	-37.965089	176.910875	28.505959
RANGI-6.30024	Set 2 Landwards	-37.965133	176.910852	28.521660
RANGI-6.30025	Set 2 Landwards	-37.965172	176.910828	28.651075
RANGI-6.30026	Set 2 Landwards	-37.965173	176.910827	28.662217
RANGI-6.30027	Set 2 Landwards	-37.965217	176.910805	28.715929
RANGI-6.30028	Set 2 Landwards	-37.965259	176.910781	28.732775
RANGI-6.30029	Set 2 Landwards	-37.965302	176.910758	28.736483
RANGI-6.30030	Set 2 Landwards	-37.965344	176.910738	28.694474
RANGI-6.30031	Set 2 Landwards	-37.965370	176.910723	28.681149
RANGI-6.30032	Set 2 Landwards	-37.965387	176.910713	28.687949
RANGI-6.30033	Set 2 Landwards	-37.965430	176.910691	28.707239
RANGI-6.30034	Set 2 Landwards	-37.965472	176.910668	28.742265
RANGI-6.30035	Set 2 Landwards	-37.965514	176.910644	28.713568
RANGI-6.30036	Set 2 Landwards	-37.965557	176.910623	28.724873
RANGI-6.30037	Set 2 Landwards	-37.965598	176.910600	28.706631
RANGI-6.30038	Set 2 Landwards	-37.965600	176.910599	28.705120
RANGI-6.30039	Set 2 Landwards	-37.965640	176.910577	28.726006
RANGI-6.30040	Set 2 Landwards	-37.965681	176.910555	28.678429
RANGI-6.30041	Set 2 Landwards	-37.965724	176.910532	28.698135
RANGI-6.30042	Set 2 Landwards	-37.965767	176.910511	28.761068
RANGI-6.30043	Set 2 Landwards	-37.965808	176.910487	28.817460
RANGI-6.30044	Set 2 Landwards	-37.965808	176.910487	28.808789
RANGI-6.30045	Set 2 Landwards	-37.965851	176.910464	28.773447
RANGI-6.30046	Set 2 Landwards	-37.965893	176.910445	28.769328
RANGI-6.30047	Set 2 Landwards	-37.965935	176.910420	28.728336
RANGI-6.30048	Set 2 Landwards	-37.965978	176.910397	28.782662
RANGI-6.30049	Set 2 Landwards	-37.966007	176.910381	28.746023
RANGI-6.30050	Set 2 Landwards	-37.966019	176.910374	28.761242
RANGI-6.30051	Set 2 Landwards	-37.966062	176.910354	28.767059
RANGI-6.30052	Set 2 Landwards	-37.966104	176.910331	28.758559
RANGI-6.30053	Set 2 Landwards	-37.966146	176.910307	28.719110
RANGI-6.30054	Set 2 Landwards	-37.966189	176.910286	28.736517

RANGI-6.30055	Set 2 Landwards	-37.966232	176.910262	28.735533
RANGI-6.30056	Set 2 Landwards	-37.966259	176.910248	28.756023
RANGI-6.30057	Set 2 Landwards	-37.966275	176.910241	28.777626
RANGI-6.30058	Set 2 Landwards	-37.966316	176.910218	28.812001
RANGI-6.30059	Set 2 Landwards	-37.966359	176.910197	28.794237
RANGI-6.30060	Set 2 Landwards	-37.966402	176.910174	28.766133
RANGI-6.30061	Set 2 Landwards	-37.966444	176.910151	28.789361
RANGI-6.30062	Set 2 Landwards	-37.966460	176.910142	28.797320
RANGI-6.30063	Set 2 Landwards	-37.966460	176.910142	28.793186
RANGI-6.30064	Set 2 Landwards	-37.966486	176.910126	28.838616
RANGI-6.30065	Set 2 Landwards	-37.966528	176.910104	28.855299
RANGI-6.30066	Set 2 Landwards	-37.966570	176.910080	28.850817
RANGI-6.30067	Set 2 Landwards	-37.966613	176.910059	28.877548
RANGI-6.30068	Set 2 Landwards	-37.966655	176.910034	28.865260
RANGI-6.30069	Set 2 Landwards	-37.966696	176.910011	28.880544
RANGI-6.30070	Set 2 Landwards	-37.966727	176.909995	28.889663
RANGI-6.30071	Set 2 Landwards	-37.966739	176.909988	28.910935
RANGI-6.30072	Set 2 Landwards	-37.966782	176.909969	28.958015
RANGI-6.30073	Set 2 Landwards	-37.966824	176.909946	28.928279
RANGI-6.30074	Set 2 Landwards	-37.966867	176.909922	28.960628
RANGI-6.30075	Set 2 Landwards	-37.966910	176.909900	28.958951
RANGI-6.30076	Set 2 Landwards	-37.966930	176.909889	28.964255
RANGI-6.30077	Set 2 Landwards	-37.966952	176.909877	28.979178
RANGI-6.30078	Set 2 Landwards	-37.966995	176.909855	28.977989
RANGI-6.30079	Set 2 Landwards	-37.967037	176.909833	29.006319
RANGI-6.30080	Set 2 Landwards	-37.967080	176.909809	29.041997
RANGI-6.30081	Set 2 Landwards	-37.967122	176.909787	29.061037
RANGI-6.30082	Set 2 Landwards	-37.967139	176.909777	29.041515
RANGI-6.30083	Set 2 Landwards	-37.967165	176.909763	29.034925
RANGI-6.30084	Set 2 Landwards	-37.967207	176.909740	29.054849
RANGI-6.30085	Set 2 Landwards	-37.967249	176.909717	29.061421
RANGI-6.30086	Set 2 Landwards	-37.967292	176.909694	29.085478
RANGI-6.30087	Set 2 Landwards	-37.967334	176.909669	29.126521
RANGI-6.30088	Set 2 Landwards	-37.967377	176.909646	29.145945
RANGI-6.30089	Set 2 Landwards	-37.967419	176.909624	29.174950
RANGI-6.30090	Set 2 Landwards	-37.967431	176.909618	29.146970
RANGI-6.30091	Set 2 Landwards	-37.967461	176.909602	29.193038
RANGI-6.30092	Set 2 Landwards	-37.967502	176.909579	29.253274
RANGI-6.30093	Set 2 Landwards	-37.967545	176.909554	29.299828
RANGI-6.30094	Set 2 Landwards	-37.967575	176.909539	29.344131
RANGI-6.30095	Set 2 Landwards	-37.967587	176.909532	29.375085
RANGI-6.30096	Set 2 Landwards	-37.967630	176.909508	29.416628
RANGI-6.30097	Set 2 Landwards	-37.967673	176.909484	29.450883
RANGI-6.30098	Set 2 Landwards	-37.967715	176.909461	29.518384
RANGI-6.30099	Set 2 Landwards	-37.967757	176.909438	29.555776
RANGI-6.30100	Set 2 Landwards	-37.967787	176.909421	29.638252

RANGI-6.30101	Set 2 Landwards	-37.967798	176.909414	29.678121
RANGI-6.30102	Set 2 Landwards	-37.967841	176.909391	29.933800
RANGI-6.30103	Set 2 Landwards	-37.967885	176.909369	30.265765
RANGI-6.30104	Set 2 Landwards	-37.967927	176.909345	30.951751
RANGI-6.30105	Set 2 Landwards	-37.967961	176.909329	31.376048
RANGI-6.30106	Set 2 Landwards	-37.967970	176.909325	31.414801
RANGI-6.30107	Set 2 Landwards	-37.968013	176.909301	31.376423
RANGI-6.30108	Set 2 Landwards	-37.968057	176.909279	31.497925
RANGI-6.30109	Set 2 Landwards	-37.968100	176.909259	31.656519
RANGI-6.30110	Set 2 Landwards	-37.968142	176.909240	31.715800
RANGI-6.30111	Set 2 Landwards	-37.968164	176.909230	31.787228
RANGI-6.30112	Set 2 Landwards	-37.968186	176.909219	31.741097
RANGI-6.30113	Set 2 Landwards	-37.968229	176.909200	31.937464
RANGI-6.30114	Set 2 Landwards	-37.968271	176.909178	31.952135
RANGI-6.30115	Set 2 Landwards	-37.968312	176.909152	32.024558
RANGI-6.30116	Set 2 Landwards	-37.968340	176.909135	32.060130
RANGI-6.30117	Set 2 Landwards	-37.968354	176.909127	32.083895
RANGI-6.30118	Set 2 Landwards	-37.968396	176.909105	32.170530
RANGI-6.30119	Set 2 Landwards	-37.968436	176.909079	32.246967
RANGI-6.30120	Set 2 Landwards	-37.968439	176.909077	32.258696
RANGI-6.30121	Set 2 Landwards	-37.968478	176.909054	32.357897
RANGI-6.30122	Set 2 Landwards	-37.968519	176.909029	32.370364
RANGI-6.30123	Set 2 Landwards	-37.968561	176.909006	32.315608
RANGI-6.30124	Set 2 Landwards	-37.968584	176.908992	32.260558
RANGI-6.30125	Set 2 Landwards	-37.968602	176.908980	32.215756
RANGI-6.30126	Set 2 Landwards	-37.968643	176.908956	32.214320
RANGI-6.30127	Set 2 Landwards	-37.968685	176.908932	32.167899
RANGI-6.30128	Set 2 Landwards	-37.968727	176.908908	32.132564
RANGI-6.30129	Set 2 Landwards	-37.968761	176.908888	32.135254
RANGI-6.30130	Set 2 Landwards	-37.968761	176.908888	32.133192
RANGI-6.30131	Set 2 Landwards	-37.968769	176.908883	32.135812
RANGI-6.30132	Set 2 Landwards	-37.968811	176.908861	32.155113
RANGI-6.30133	Set 2 Landwards	-37.968852	176.908836	32.164813
RANGI-6.30134	Set 2 Landwards	-37.968893	176.908812	32.175719
RANGI-6.30135	Set 2 Landwards	-37.968919	176.908798	32.221671
RANGI-6.30136	Set 2 Landwards	-37.968936	176.908790	32.267412
RANGI-6.30137	Set 2 Landwards	-37.968978	176.908770	32.365088
RANGI-6.30138	Set 2 Landwards	-37.969021	176.908747	32.422497
RANGI-6.30139	Set 2 Landwards	-37.969064	176.908727	32.368943
RANGI-6.30140	Set 2 Landwards	-37.969072	176.908723	32.405067
RANGI-6.30141	Set 2 Landwards	-37.969105	176.908703	32.431137
RANGI-6.30142	Set 2 Landwards	-37.969147	176.908678	32.468532
RANGI-6.30143	Set 2 Landwards	-37.969189	176.908653	32.464177
RANGI-6.30144	Set 2 Landwards	-37.969206	176.908645	32.467671
RANGI-6.30145	Set 2 Landwards	-37.969232	176.908630	32.464870
RANGI-6.30146	Set 2 Landwards	-37.969274	176.908608	32.440208

RANGI-6.30147	Set 2 Landwards	-37.969315	176.908582	32.453506
RANGI-6.30148	Set 2 Landwards	-37.969358	176.908557	32.454583
RANGI-6.30149	Set 2 Landwards	-37.969399	176.908535	32.394022
RANGI-6.30150	Set 2 Landwards	-37.969441	176.908512	32.445170
RANGI-6.30151	Set 2 Landwards	-37.969441	176.908512	32.443079
RANGI-6.30152	Set 2 Landwards	-37.969483	176.908489	32.513033
RANGI-6.30153	Set 2 Landwards	-37.969525	176.908466	32.620624
RANGI-6.30154	Set 2 Landwards	-37.969566	176.908441	32.727475
RANGI-6.30155	Set 2 Landwards	-37.969568	176.908440	32.723244
RANGI-6.30156	Set 2 Landwards	-37.969608	176.908420	32.763335
RANGI-6.30157	Set 2 Landwards	-37.969650	176.908395	32.742438

Appendix B: GPR Transects

Beach Ridge Set 4 Seawards GPR Transect (Channel 1)

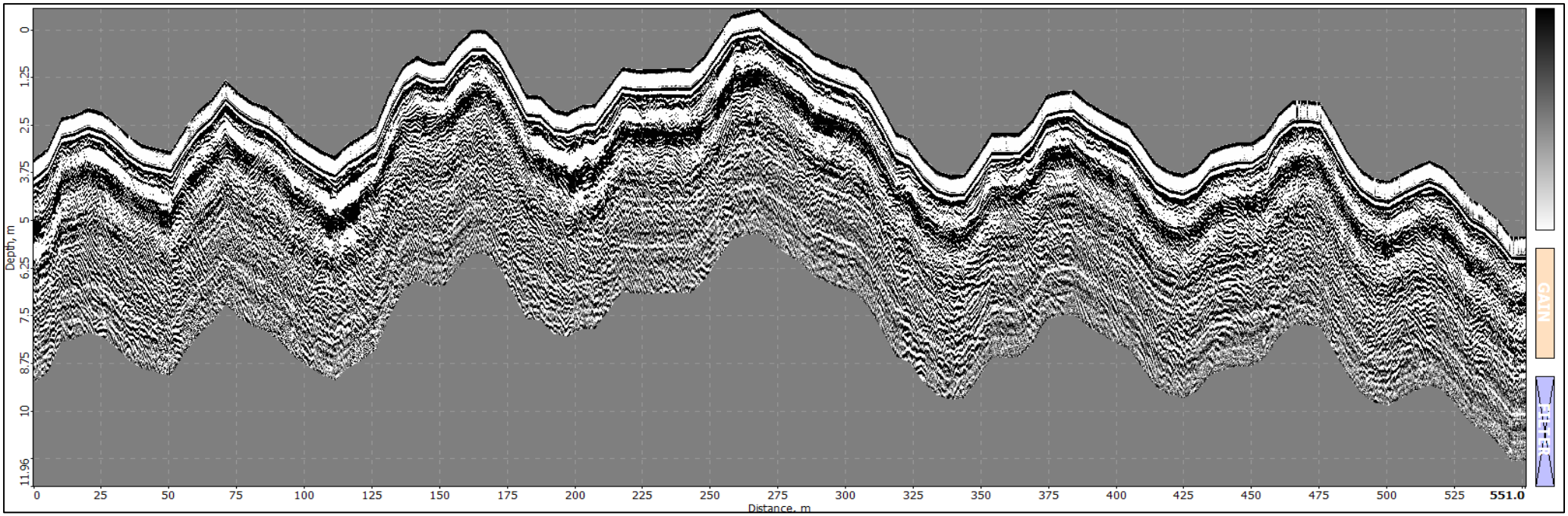

Beach Ridge Set 4 Seawards GPR Transect (Channel 2)

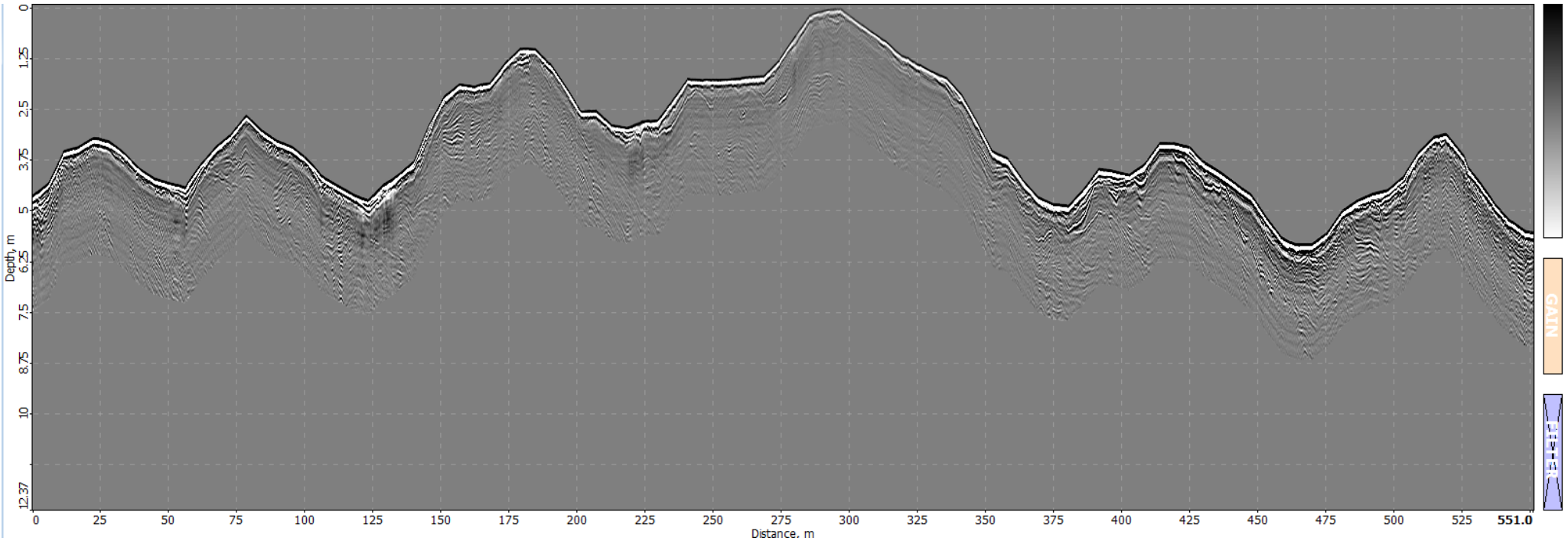

Beach Ridge Set 4 Landwards GPR Transect (Channel 1)

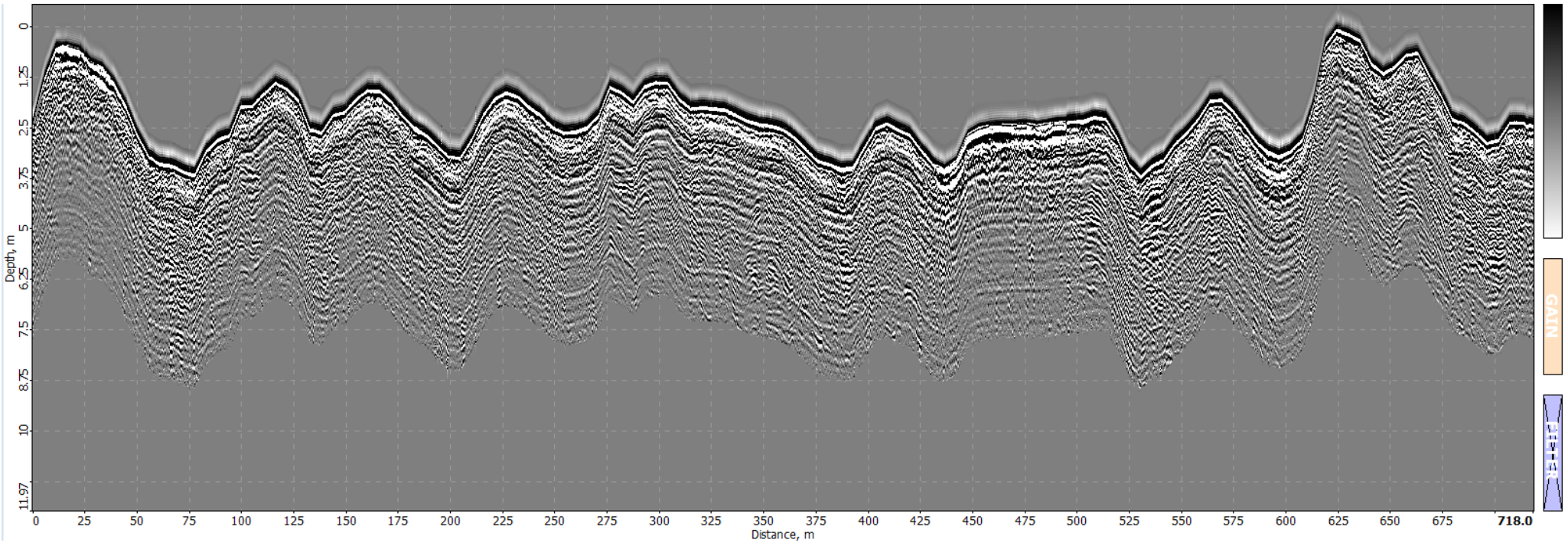

Beach Ridge Set 4 Landwards GPR Transect (Channel 2)

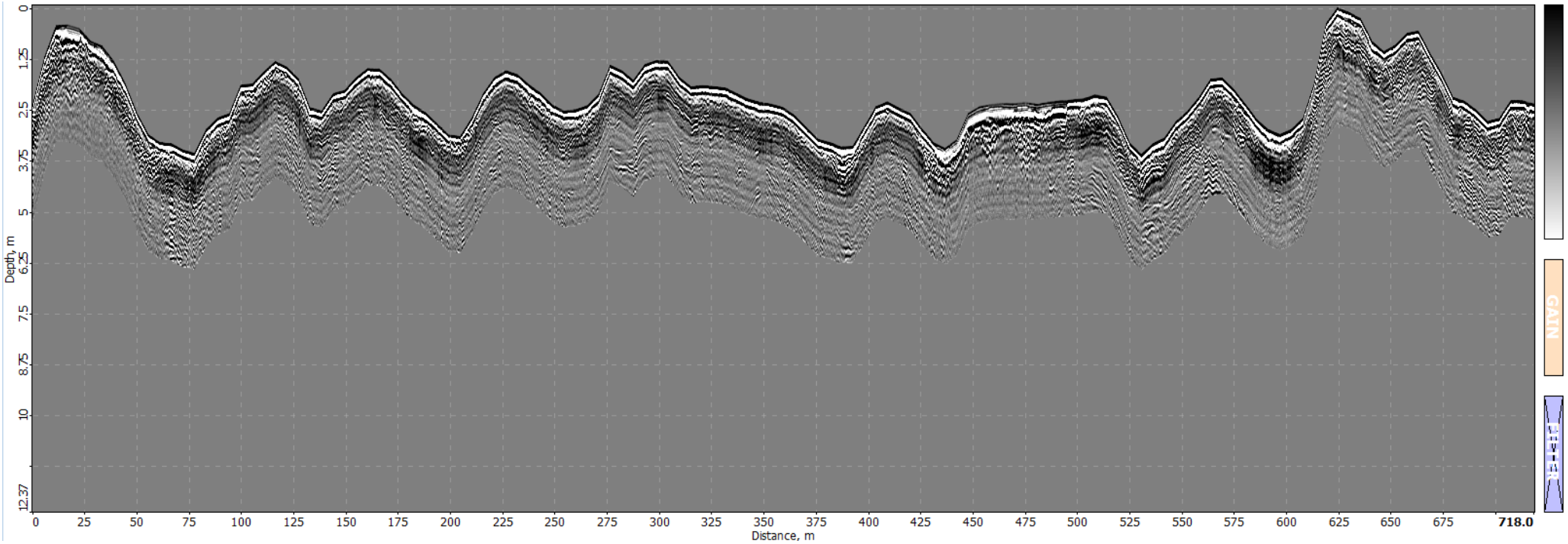

Beach Ridge Set 3 Seawards GPR Transect (Channel 1)

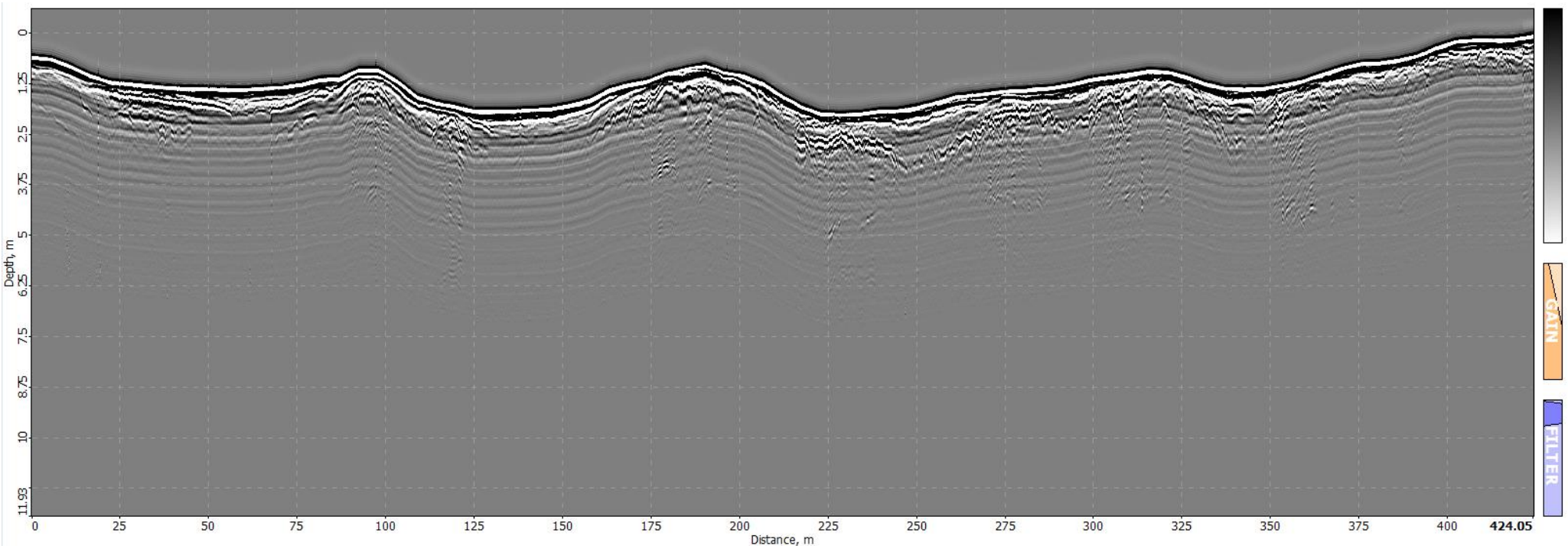

Beach Ridge Set 3 Seawards GPR Transect (Channel 2)

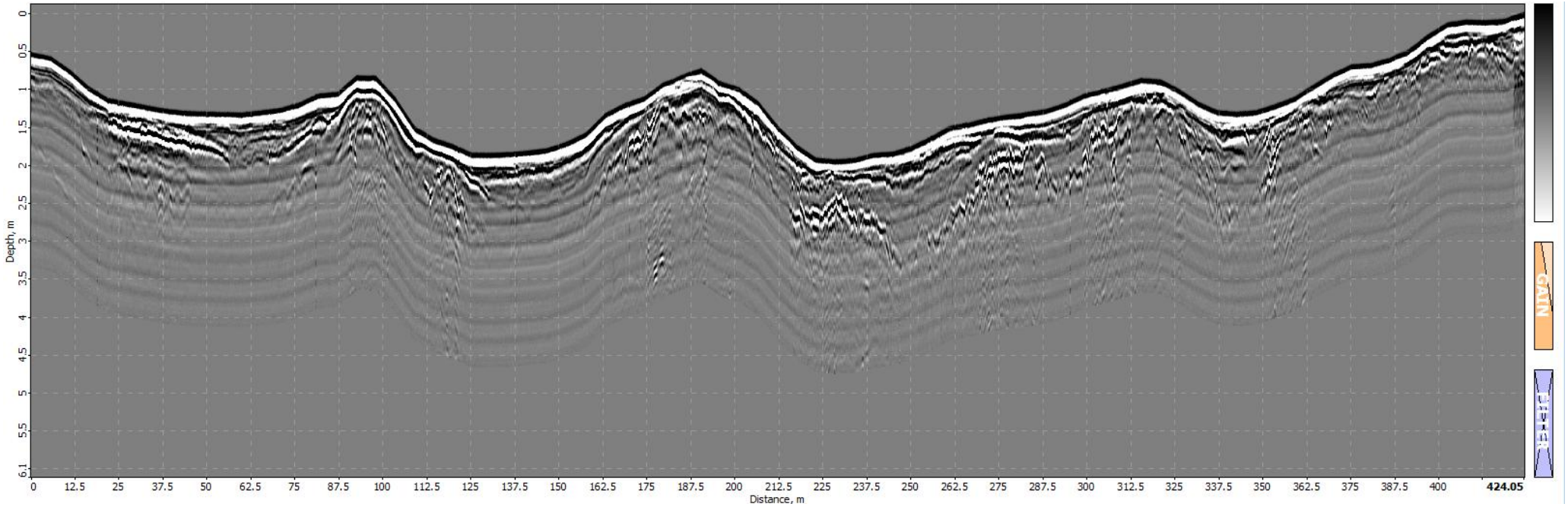

Beach Ridge Set 3 Landwards GPR Transect (Channel 1)

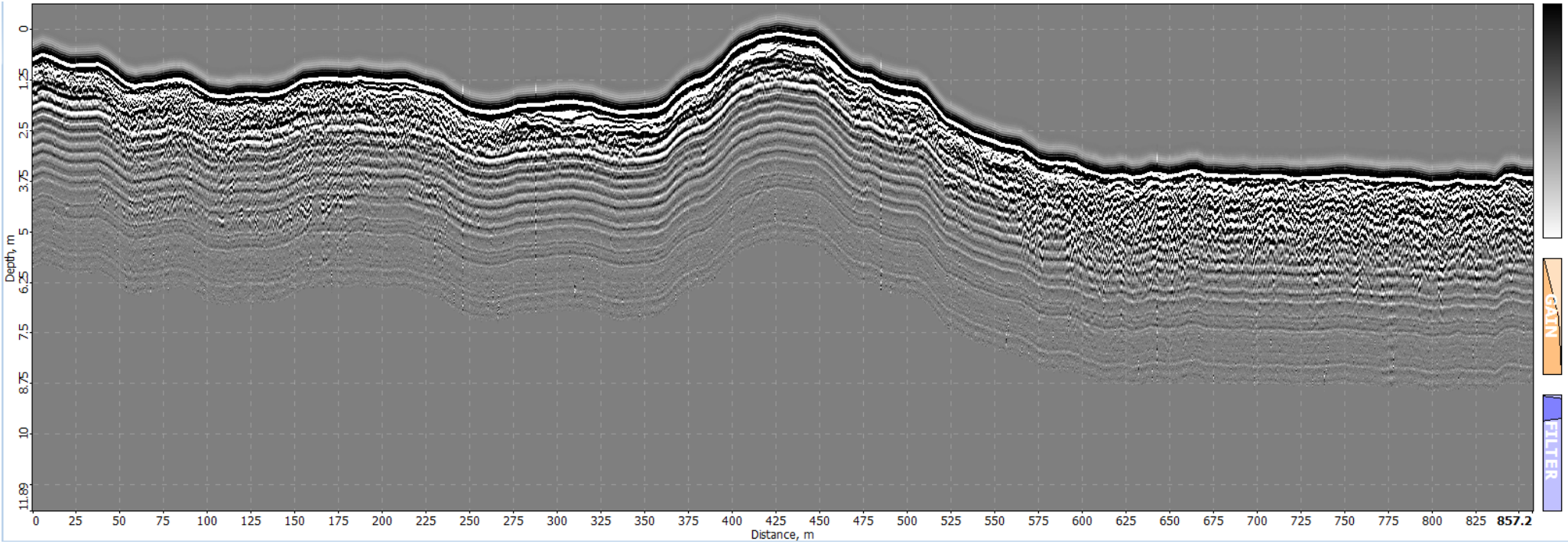

Beach Ridge Set 3 Landwards GPR Transect (Channel 2)

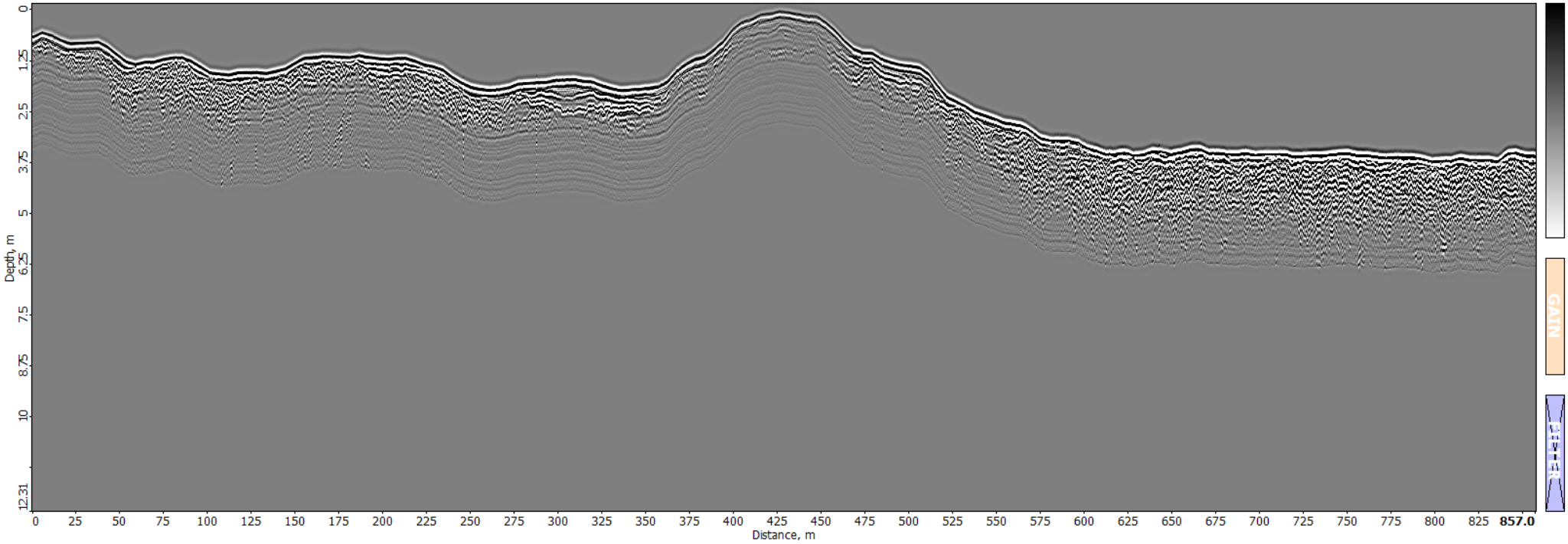

Beach Ridge Set 2 Seawards GPR Transect (Channel 1)

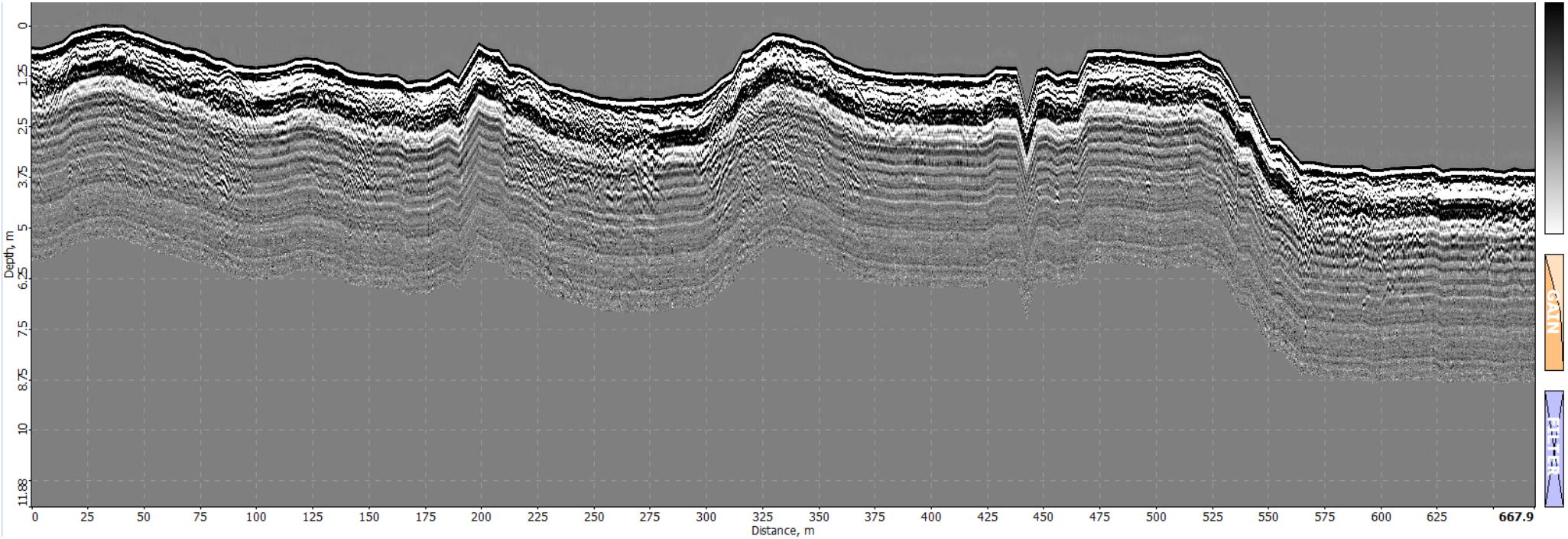

Beach Ridge Set 2 Seawards GPR Transect (Channel 2)

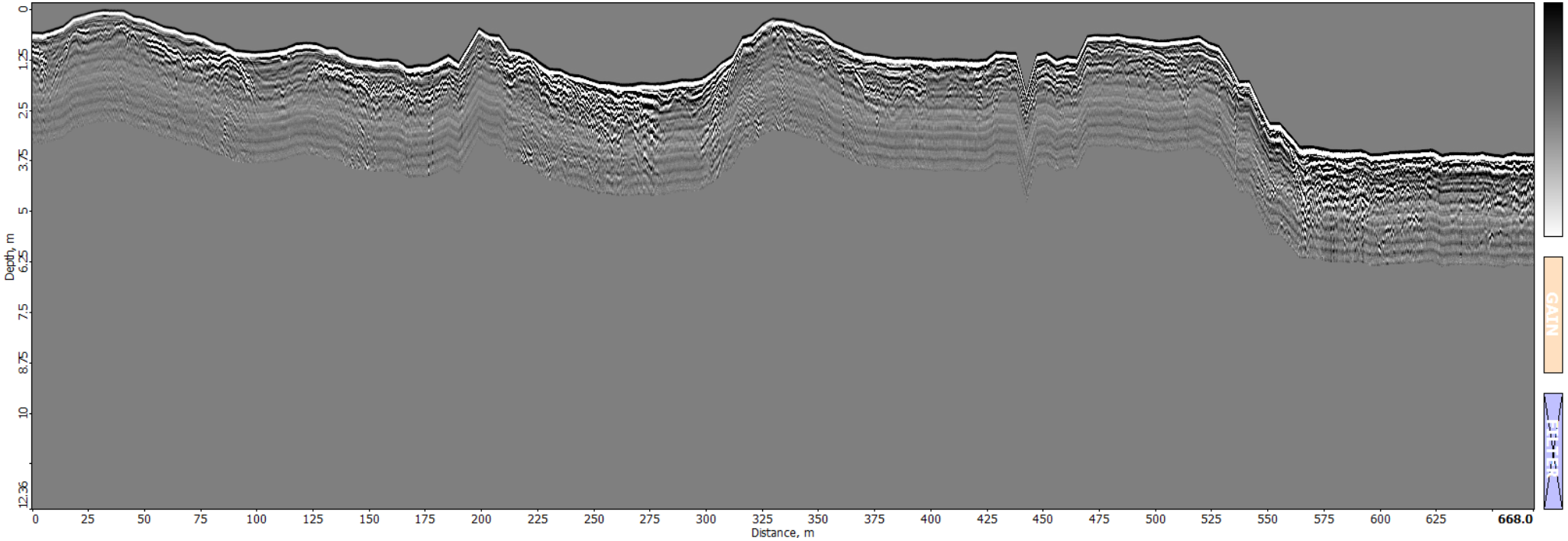

Beach Ridge Set 2 Landwards GPR Transect (Channel 1)

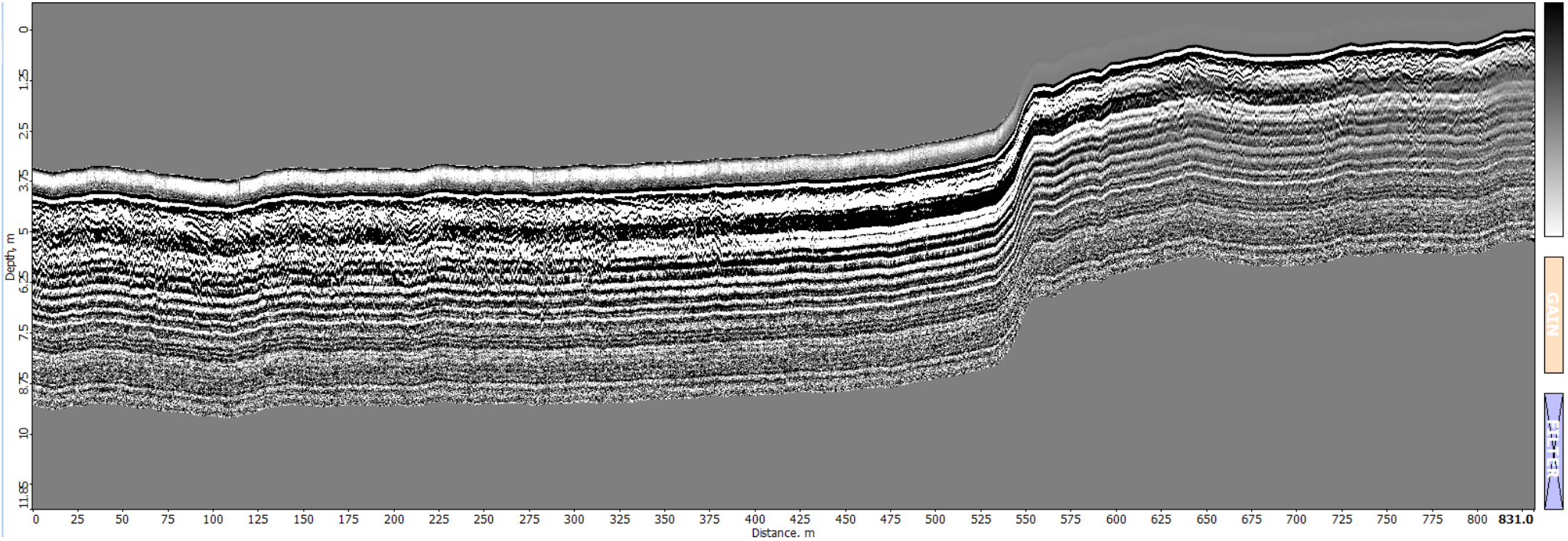

Beach Ridge Set 2 Landwards GPR Transect (Channel 2)

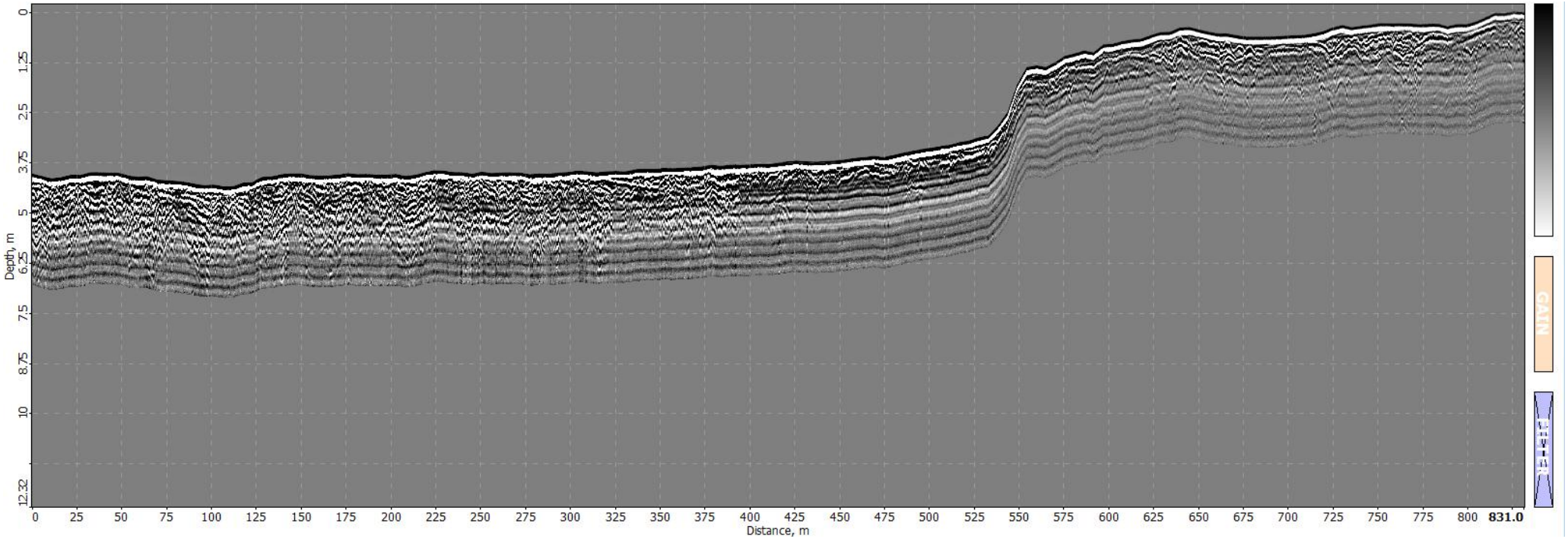

Half Minor Beach Ridge Set GPR Transect (Channel 1)

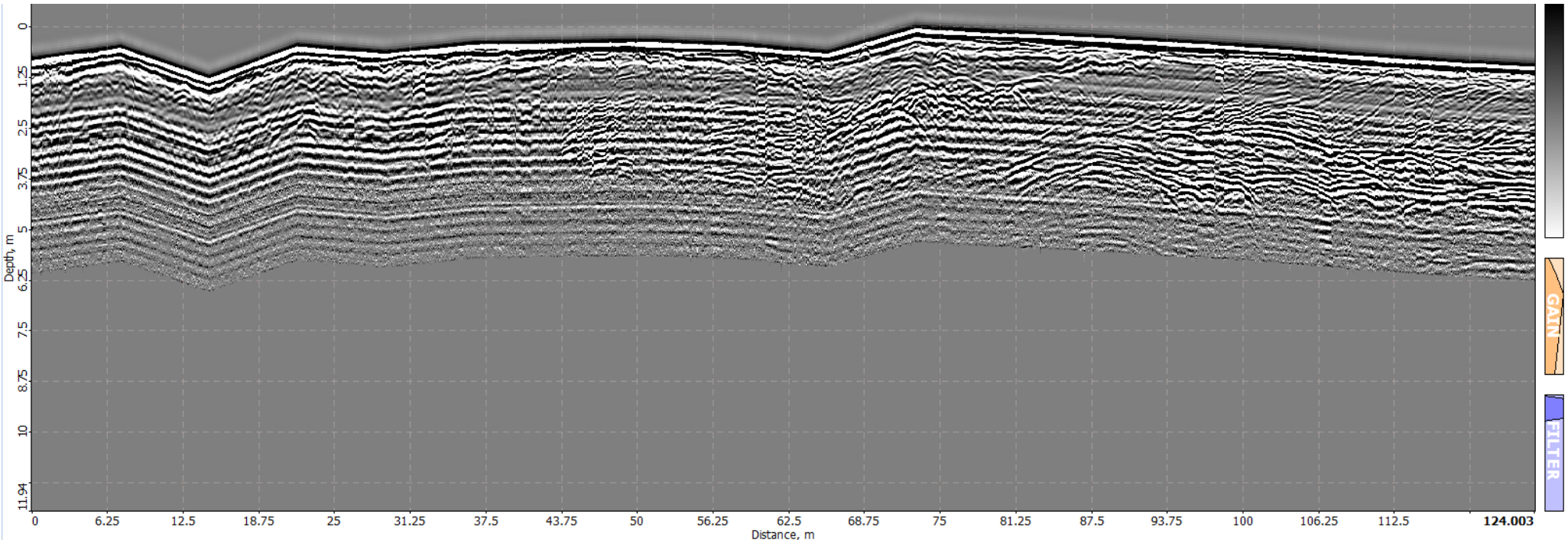

Half Minor Beach Ridge Set GPR Transect (Channel 2)

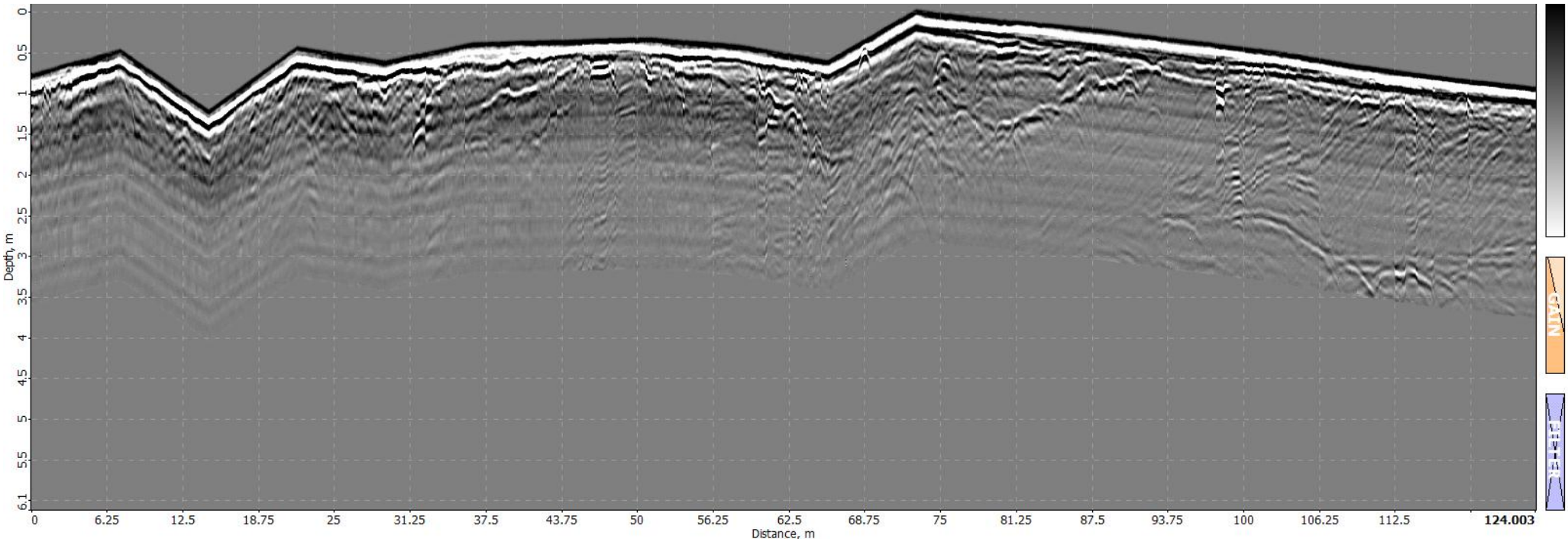

Whole Minor Beach Ridge Set GPR Transect (Channel 1)

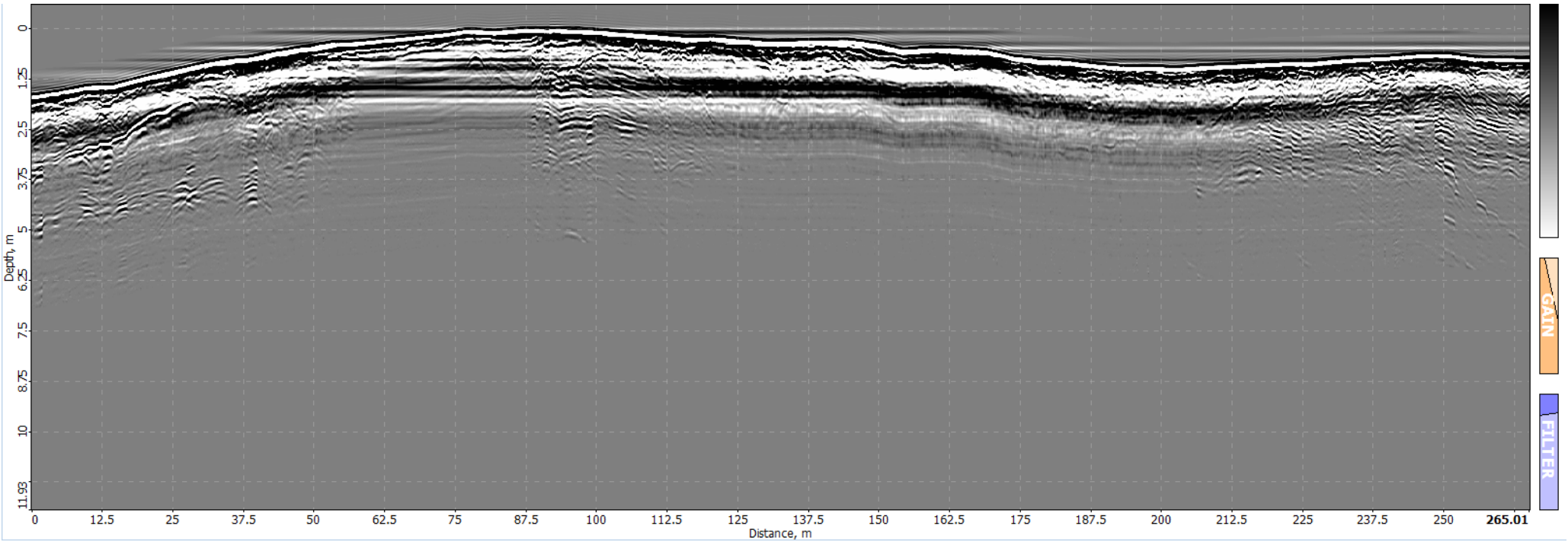

Whole Minor Beach Ridge Set GPR Transect (Channel 2)

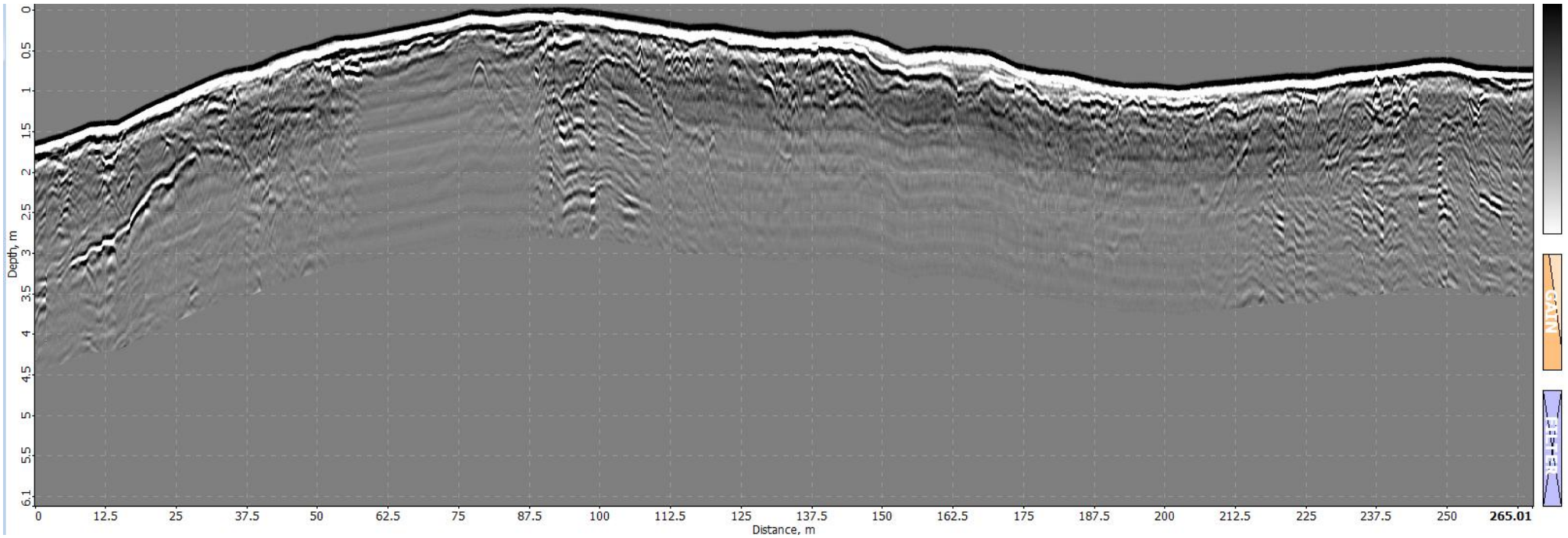

Road Minor Beach Ridge Set GPR Transect (Channel 1)

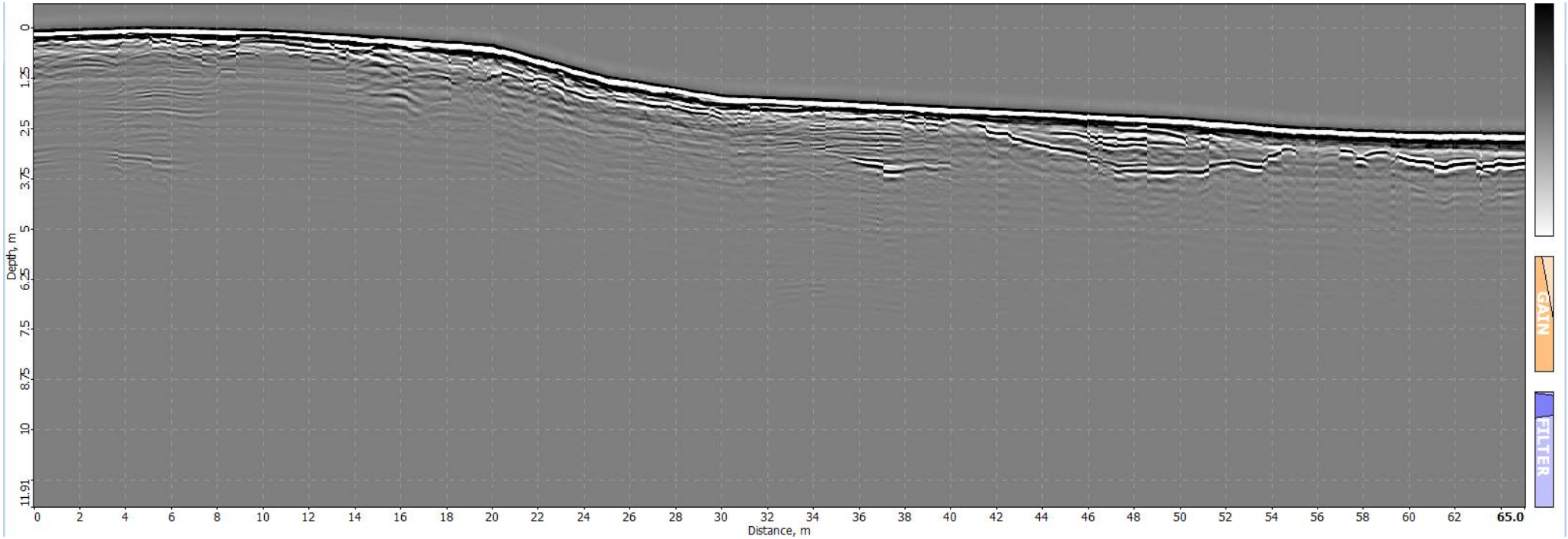

Road Minor Beach Ridge Set GPR Transect (Channel 2)

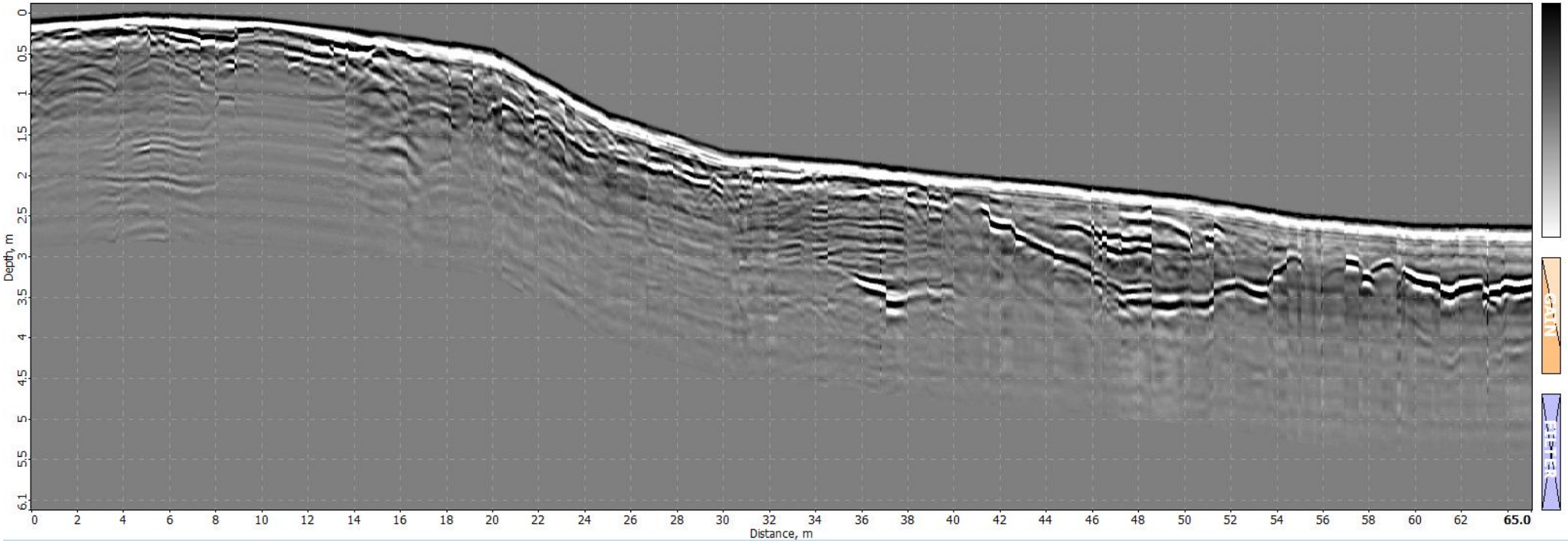

Beach Ridge Set 1 GPR Transect (Channel 1)

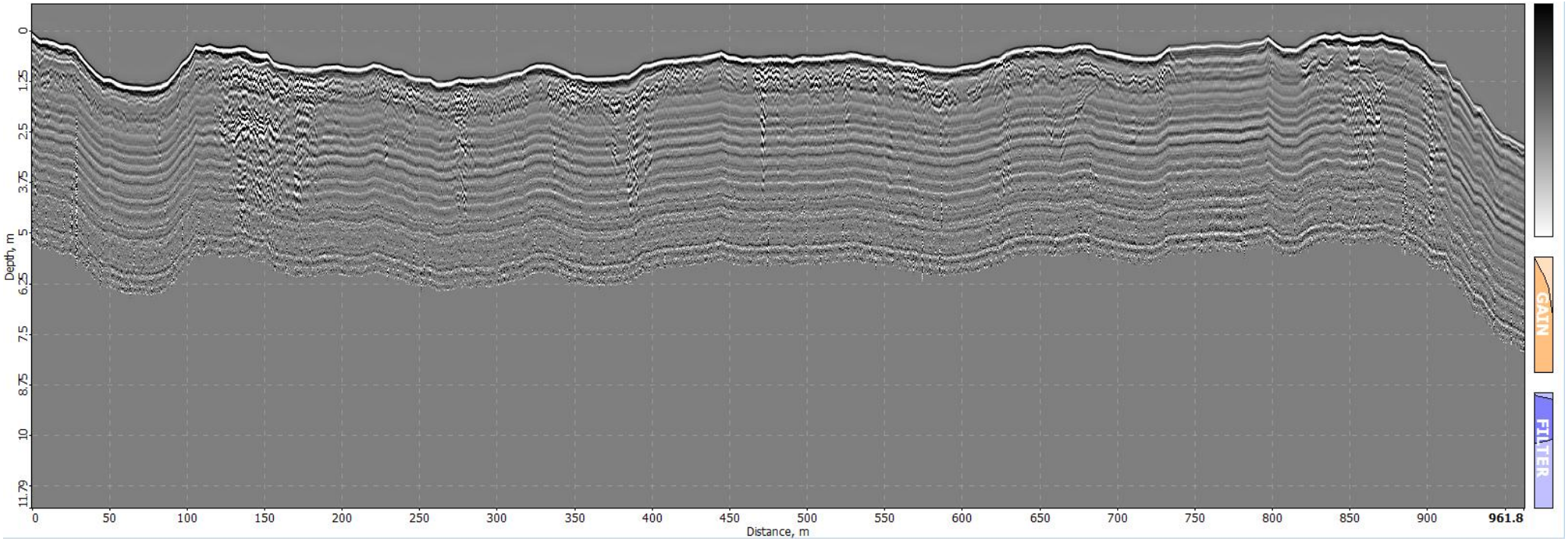

Beach Ridge Set 1 GPR Transect (Channel 2)

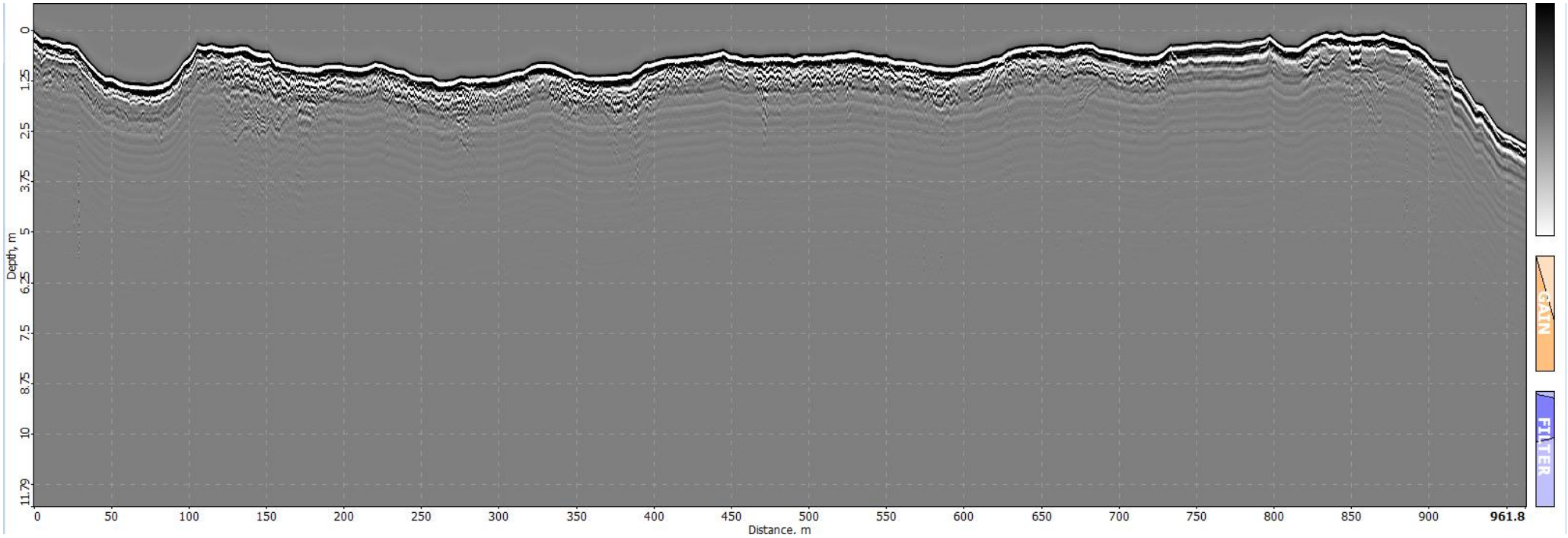

Appendix C: OSL Data

Sample Name	Location	Ridge Elevation from Sea Level (m)	Distance From Coast (km)	Sample Distance from Sea Level (m)	Top of Ridge Depth (m)	OSL Depth from Surface (m)	Age (ka)		Error (ka)	Lower Limit (ka)	Upper Limit (ka)
RANGI24-1	Set 1 Landward	5.07	10.180	2.87	3.67	2.2	7.6019	±	0.587	8.1889	7.0149
RANGI24-2	Set 1 Seward	4.90	9.292	2.65	3.45	2.25	7.0376	±	0.5767	7.6143	6.4609
RANGI24-3	Set 2 Landward	5.20	7.849	3.50	4.30	1.7	5.6199	±	0.3675	5.9874	5.2524
RANGI24-4	Set 2 Seward	3.90	7.317	2.40	3.20	1.5	5.7418	±	0.4638	6.2056	5.278
RANGI24-5	Set 3 Landward	4.44	6.634	3.14	3.94	1.3	5.2021	±	0.3677	5.5698	4.8344
RANGI24-6	Set 3 Seward	3.13	5.964	1.83	2.63	1.3	5.1869	±	0.4468	5.6337	4.7401
RANGI24-6B	Minor Set	8.67	3.410	7.67	8.47	1	2.9649	±	0.2254	3.1903	2.7395
RANGI24-7	Set 4 Landward	9.30	1.424	8.40	9.20	0.9	2.0466	±	0.1283	2.1749	1.9183
RANGI24-8	Set 4 Seward	8.68	0.334	7.78	8.58	0.9	0.7762	±	0.0844	0.8606	0.6918

	Sample ID	Depth (m)	Total dose rate (Gy/ka)			n	Equivalent dose (Gy/ka)			Uncorrected age (ka)			g2days-value (%/decade)			Corrected age (ka)		
IR50	RGT24-1	0.8	1.83	±	0.14	6	7.9	±	0.2	4.30	±	0.3	6.4	±	0.3	7.63	±	0.6
	RGT24-2	0.75	1.83	±	0.14	6	7.6	±	0.2	4.17	±	0.3	6.0	±	0.3	7.40	±	0.6
	RGT24-3	0.8	3.16	±	0.17	6	11.8	±	0.3	3.75	±	0.2	6.2	±	0.3	6.62	±	0.4
	RGT24-4	0.8	2.24	±	0.14	6	8.1	±	0.2	3.63	±	0.3	7.0	±	0.3	6.39	±	0.5
	RGT24-5	0.8	2.84	±	0.16	5	9.6	±	0.1	3.38	±	0.2	6.3	±	0.3	5.94	±	0.4
	RGT24-6	0.8	2.22	±	0.14	6	7.0	±	0.4	3.17	±	0.3	6.6	±	0.3	5.55	±	0.5
	RGT24-6B	0.8	2.63	±	0.16	4	5.4	±	0.1	2.05	±	0.1	6.3	±	0.3	3.52	±	0.2
	RGT24-7	0.8	2.89	±	0.16	6	3.6	±	0.1	1.24	±	0.1	5.7	±	0.3	2.10	±	0.2
	RGT24-8	0.8	3.18	±	0.17	4	1.2	±	0.03	0.37	±	0.0	5.4	±	0.3	0.59	±	0.04
pIRIR170	RGT24-1	0.8	1.83	±	0.14	5	12.8	±	0.2	7.01	±	0.5	1.15	±	0.3	7.60	±	0.6
	RGT24-2	0.75	1.83	±	0.14	6	11.9	±	0.3	6.49	±	0.5	1.17	±	0.3	7.04	±	0.6
	RGT24-3	0.8	3.16	±	0.17	6	16.4	±	0.5	5.19	±	0.3	0.99	±	0.3	5.62	±	0.4
	RGT24-4	0.8	2.24	±	0.14	6	11.8	±	0.6	5.30	±	0.4	1.57	±	0.4	5.74	±	0.5
	RGT24-5	0.8	2.84	±	0.16	6	13.6	±	0.5	4.80	±	0.3	1.33	±	0.3	5.20	±	0.4
	RGT24-6	0.8	2.22	±	0.14	6	10.6	±	0.6	4.79	±	0.4	1.14	±	0.4	5.19	±	0.4
	RGT24-6B	0.8	2.63	±	0.16	6	7.2	±	0.4	2.75	±	0.2	0.92	±	0.4	2.96	±	0.2
	RGT24-7	0.8	2.89	±	0.16	5	5.5	±	0.1	1.90	±	0.1	0.69	±	0.4	2.05	±	0.1
	RGT24-8	0.8	3.18	±	0.17	6	2.3	±	0.2	0.72	±	0.1	0.05	±	0.4	0.78	±	0.1

Sample ID	Laboratory	Depth	K	U	Th	Water content	Dose rate
	code	(m)	(%)	(ppm)	(ppm)	(%)	(Gy/ka)
RGT24-1	gsj25065	0.8	0.64	0.48	1.96	3.7	1.83 ± 0.14
RGT24-2	gsj25066	0.75	0.66	0.42	1.82	3.7	1.83 ± 0.14
RGT24-3	gsj25067	0.8	1.53	1.35	5.76	5.6	3.16 ± 0.17
RGT24-4	gsj25068	0.8	0.90	0.75	3.16	4.6	2.24 ± 0.14
RGT24-5	gsj25069	0.8	1.30	1.14	4.80	4.4	2.84 ± 0.16
RGT24-6	gsj25070	0.8	0.91	0.70	2.95	4.1	2.22 ± 0.14
RGT24-6B	gsj25073	0.8	1.12	0.96	4.11	1.5	2.63 ± 0.16
RGT24-7	gsj25071	0.8	1.32	1.16	4.79	3.3	2.89 ± 0.16
RGT24-8	gsj25072	0.8	1.52	1.41	5.73	4.9	3.18 ± 0.17

Appendix D: OSL Moisture Content Data

		After Drying (40°C)	
Sample:	**Tray + Sample**	**Sample**	**Difference (%)**
RANGI24-1 OSL	61.5903	59.5417	3.6654
RANGI24-2 OSL	57.4781	55.4327	3.7349
RANGI24-3 OSL	50.1173	48.0640	5.6001
RANGI24-4 OSL	61.0271	58.9641	4.5698
RANGI24-5 OSL	57.5043	55.4659	4.3625
RANGI24-6 OSL	58.2220	56.1984	4.0863
RANGI24-6B OSL	60.9962	58.9619	1.5097
RANGI24-7 OSL	55.7378	53.6897	3.2865
RANGI24-8 OSL	54.4379	52.3991	4.8787
		Repeated Drying (40°C)	
Sample:	**Tray + Sample**	**Sample**	**Difference (%)**
RANGI24-1 OSL	61.5724	59.5238	3.6944
RANGI24-2 OSL	57.4500	55.4046	3.7837
RANGI24-3 OSL	50.0937	48.0404	5.6464
RANGI24-4 OSL	60.9957	58.9327	4.6207
RANGI24-5 OSL	57.4529	55.4145	4.4512
RANGI24-6 OSL	58.1748	56.1512	4.1669
RANGI24-6B OSL	60.9460	58.9117	1.5936
RANGI24-7 OSL	55.6997	53.6516	3.3552
RANGI24-8 OSL	54.3997	52.3609	4.9480

Appendix E: Progradation Rates

Site	Age (ka)	Age Difference (ka)	Age Difference (yrs)	Distance Between Ridges (m)	Progradation (m/yr)
RANGI24-1	7.6019				
		0.5643	564.3	848	1.50
RANGI24-2	7.0376				
		1.4177	1417.7	1410	0.995
RANGI24-3	5.6199				
RANGI24-4	5.7418	0.4178	417.8	1070	2.56
RANGI24-5	5.2021				
		0.0152	15.2	654	43.03
RANGI24-6	5.1869				
		2.2220	2222.0	2522	1.14
RANGI24-6B	2.9649				
		0.9183	918.3	2102	2.29
RANGI24-7	2.0466				
		1.2704	1270.4	117	0.09
RANGI24-8	0.7762				

Total Distance (m)	**9754**
Total Time (yr)	6825.7
Total Progradation (m/yr)	1.429010944

Appendix F: Loss on Ignition

Sample	Depth	LOI (%)	Sample	Depth	LOI (%)
COAST 1	0cm	1.8669	**RANGI24-4**	20cm	10.9378
COAST 2	0cm	2.0213	**RANGI24-4**	40cm	8.0875
COAST 3	0cm	1.3286	**RANGI24-4**	60cm	2.3801
COAST 4	0cm	1.4611	**RANGI24-4**	80cm	1.6679
COAST 5	0cm	2.1934	**RANGI24-4**	100cm	1.8991
COAST 6	0cm	1.9882	**RANGI24-4**	120cm	1.6828
RANGI24-1	20cm	10.6207	**RANGI24-4**	140cm	1.6793
RANGI24-1	40cm	8.0276	**RANGI24-4**	OSL	1.5646
RANGI24-2	50cm (Taupo)	6.8488	**RANGI24-5**	0cm	6.8377
RANGI24-1	60cm	12.655	**RANGI24-5**	20cm	5.4941
RANGI24-1	80cm	8.2388	**RANGI24-5**	40cm	2.3884
RANGI24-1	100cm	7.8617	**RANGI24-5**	60cm	2.1786
RANGI24-1	120cm	5.2547	**RANGI24-5**	80cm	2.2432
RANGI24-1	140cm	1.7645	**RANGI24-5**	100cm	1.8268
RANGI24-1	160cm	0.9607	**RANGI24-5**	120cm	2.0481
RANGI24-1	180cm	0.9955	**RANGI24-5**	OSL	2.0276
RANGI24-1	180cm	1.0641	**RANGI24-5**	OUTCROP	1.6479
RANGI24-1	200cm	0.9650	**RANGI24-6**	0cm	15.0497
RANGI24-1	220cm	0.8482	**RANGI24-6**	20cm	8.3782
RANGI24-1	OSL	0.8323	**RANGI24-6**	40cm	5.5921
RANGI24-2	20cm	10.1612	**RANGI24-6**	40cm	5.9066
RANGI24-2	40cm	12.2758	**RANGI24-6**	60cm	3.2509
RANGI24-2	60cm	17.0213	**RANGI24-6**	80cm	1.9053
RANGI24-2	80cm	4.8045	**RANGI24-6**	100cm	1.6437
RANGI24-2	100cm	7.1971	**RANGI24-6**	120cm	1.4665
RANGI24-2	120cm	4.1236	**RANGI24-6**	OSL	1.2994
RANGI24-2	140cm	2.8097	**RANGI24-6B**	0cm	5.8069
RANGI24-2	160cm	0.7731	**RANGI24-6B**	20cm	4.1864
RANGI24-2	180cm	0.6932	**RANGI24-6B**	40cm	1.9606
RANGI24-2	200cm	0.6847	**RANGI24-6B**	60cm	1.8284
RANGI24-2	220cm	0.6548	**RANGI24-6B**	80cm	1.9277
RANGI24-2	OSL	0.8250	**RANGI24-6B**	100cm	1.5525
RANGI24-3	0cm	12.452	**RANGI24-6B**	OSL	1.8316
RANGI24-3	20cm	8.1022	**RANGI24-7**	0cm	3.2665
RANGI24-3	40cm	6.051915	**RANGI24-7**	20cm	1.8611
RANGI24-3	60cm	3.31146	**RANGI24-7**	40cm	1.7067
RANGI24-3	60cm	3.294801	**RANGI24-7**	60cm	1.5905
RANGI24-3	80cm	3.128377	**RANGI24-7**	80cm	1.4163
RANGI24-3	100cm	2.654824	**RANGI24-7**	OSL	1.0257
RANGI24-3	120cm	2.002991	**RANGI24-8**	0cm	2.7284
RANGI24-3	140cm	2.390211	**RANGI24-8**	20cm	1.9363
RANGI24-3	140cm	2.558197	**RANGI24-8**	40cm	2.1594
RANGI24-3	160cm	1.666116	**RANGI24-8**	60cm	1.7114
RANGI24-3	OSL	1.970731	**RANGI24-8**	80cm	1.5498
			RANGI24-8	OSL	1.8877

Appendix G: XRF Major Element Composition

Name:	COAST 1	COAST 2	COAST 3	COAST 4	COAST 5	COAST 6
Depth:	0cm	0cm	0cm	0cm	0cm	0cm
Date:	18/12/2024	18/12/2024	10/01/2025	8/01/2025	21/12/2024	18/12/2024
Time:	15:50	16:08	16:25	19:31	14:46	16:26
SiO2 (%)	72.28	72.61	74.35	73.10	74.57	72.19
Al2O3 (%)	14.21	13.52	13.49	14.31	12.72	14.55
TiO2 (%)	0.24	0.22	0.22	0.18	0.18	0.14
MnO (%)	0.05	0.07	0.07	0.06	0.08	0.04
Fe2O3 (%)	2.16	2.16	2.01	1.68	1.68	1.49
MgO (%)	0.66	0.69	0.61	0.51	0.43	0.49
CaO (%)	2.52	2.09	2.61	2.80	1.91	4.41
Na2O (%)	4.21	4.13	3.94	4.34	3.95	4.24
K2O (%)	2.22	2.86	1.95	1.94	2.90	1.28
P2O5 (%)	0.06	0.06	0.06	0.05	0.05	0.05
SO3 (%)	0.02	0.01	0.01	0.02	0.00	0.01
SrO (%)	0.02	0.01	0.02	0.02	0.01	0.03
BaO (%)	0.06	0.07	0.05	0.06	0.08	0.05
CO2 (%)	1.87	2.02	1.33	1.46	2.19	1.99
Sum (%)	100.60	100.52	100.71	100.54	100.75	100.97
Specimen mass (g)	0.80	0.80	0.80	0.80	0.80	0.80
Additive mass (g)	8.00	8.00	8.00	8.00	8.00	8.00

Name:	RANGI24-1	RANGI24-1	RANGI24-1	RANGI24-1	RANGI24-1	RANGI24-1	RANGI24-1	RANGI24-1	RANGI24-1	RANGI24-1	RANGI24-1
Depth:	**20cm**	**40cm**	**60cm**	**80cm**	**100cm**	**120cm**	**140cm**	**160cm**	**180cm**	**200cm**	**220cm**
Date:	18/12/20	21/12/20	18/12/20	21/12/20	8/01/202	18/12/20	18/12/20	8/01/202	18/12/20	18/12/202	21/12/20
Time:	24 16:43	24 15:21	24 17:01	24 11:13	5 20:24	24 17:19	24 17:36	5 22:10	24 17:54	4 18:12	24 11:31
SiO2 (%)	61.010	69.860	66.480	69.890	69.880	72.070	73.270	73.760	74.610	74.150	73.790
Al2O3 (%)	12.600	12.260	11.800	12.950	13.380	13.650	15.240	14.600	14.360	14.620	14.700
TiO2 (%)	0.420	0.270	0.275	0.232	0.214	0.208	0.165	0.302	0.228	0.239	0.259
MnO (%)	0.100	0.056	0.049	0.049	0.052	0.052	0.030	0.055	0.043	0.046	0.054
Fe2O3 (%)	4.635	1.639	1.529	1.130	1.123	1.040	1.034	1.721	1.381	1.438	1.611
MgO (%)	2.140	0.486	0.247	0.210	0.232	0.221	0.431	0.861	0.635	0.679	0.803
CaO (%)	4.623	1.849	1.383	1.201	1.199	1.388	3.609	3.797	3.633	3.741	3.827
Na2O (%)	2.568	3.394	3.433	3.628	3.625	3.803	4.048	3.981	3.933	3.996	4.025
K2O (%)	1.530	2.260	2.420	2.730	2.740	2.610	0.920	0.780	0.830	0.830	0.790
P2O5 (%)	0.242	0.104	0.089	0.065	0.069	0.055	0.034	0.044	0.045	0.046	0.048
SO3 (%)	0.050	0.040	0.030	0.060	0.060	0.030	0.000	0.000	0.000	0.000	0.000
SrO (%)	0.016	0.012	0.011	0.009	0.009	0.012	0.029	0.030	0.029	0.029	0.029
BaO (%)	0.045	0.0578	0.0676	0.0745	0.0756	0.0728	0.0414	0.0414	0.035	0.0389	0.0321
CO2 (%)	10.620	8.030	12.650	8.240	7.860	5.250	1.760	0.960	1.000	0.960	0.850
Sum (%)	100.601	100.325	100.479	100.479	100.520	100.481	100.624	100.938	100.773	100.828	100.830
Specimen mass:	0.800	0.799	0.800	0.799	0.801	0.800	0.801	0.800	0.801	0.802	0.801
Additive mass:	8.001	8.002	8.002	8.000	8.003	8.001	8.002	8.002	8.002	8.001	8.002

Name:	RANGI24-2	RANGI24-2	RANGI24-2	RANGI24-2	RANGI24-2	RANGI24-2	RANGI24-2	RANGI24-2	RANGI24-2	RANGI24-2	RANGI24-2
Depth:	**20cm**	**40cm**	**60cm**	**80cm**	**100cm**	**120cm**	**140cm**	**160cm**	**180cm**	**200cm**	**220cm**
Date:	18/12/20	18/12/20	18/12/20	18/12/20	21/12/20	18/12/20	21/12/20	21/12/20	21/12/20	18/12/20	21/12/20
Time:	24 18:30	24 19:57	24 20:15	24 20:33	24 11:49	24 20:51	24 12:06	24 12:24	24 12:42	24 21:08	24 12:59
SiO2 (%)	63.140	62.100	60.560	72.660	69.980	73.700	74.870	71.980	72.400	72.250	71.050
Al2O3 (%)	12.730	13.710	12.770	13.350	13.880	13.230	12.930	15.460	15.510	15.520	15.970
TiO2 (%)	0.393	0.381	0.321	0.256	0.206	0.179	0.188	0.344	0.269	0.308	0.300
MnO (%)	0.093	0.087	0.064	0.056	0.049	0.051	0.054	0.061	0.050	0.059	0.071
Fe2O3 (%)	3.794	2.747	1.927	1.222	1.008	1.011	1.036	1.970	1.640	1.891	2.146
MgO (%)	1.756	0.858	0.428	0.325	0.202	0.165	0.193	0.992	0.797	0.964	1.164
CaO (%)	4.010	2.728	1.822	1.764	1.228	1.100	1.286	4.032	4.028	4.075	4.290
Na2O (%)	2.828	3.410	3.241	3.839	3.621	3.832	3.942	4.261	4.283	4.294	4.379
K2O (%)	1.700	1.890	2.110	2.380	2.710	3.050	2.840	0.880	0.850	0.840	0.810
P2O5 (%)	0.219	0.168	0.153	0.055	0.063	0.044	0.044	0.035	0.038	0.037	0.038
SO3 (%)	0.050	0.060	0.030	0.020	0.030	0.000	0.000	0.000	0.000	0.000	0.000
SrO (%)	0.015	0.018	0.013	0.014	0.009	0.009	0.010	0.031	0.031	0.031	0.032
BaO (%)	0.0521	0.0495	0.0614	0.062	0.068	0.0709	0.0768	0.0358	0.0382	0.0355	0.0361
CO2 (%)	10.160	12.280	17.020	4.800	7.200	4.120	2.810	0.770	0.690	0.680	0.650
Sum (%)	100.934	100.483	100.545	100.818	100.263	100.571	100.286	100.866	100.640	101.008	100.948
Specimen mass:	0.801	0.800	0.799	0.800	0.801	0.799	0.800	0.801	0.800	0.802	0.800
Additive mass:	8.000	8.000	8.001	8.001	8.001	8.001	8.002	8.002	8.001	8.001	8.002

Name:	RANGI24-3	RANGI24-3	RANGI24-3	RANGI24-3	RANGI24-3	RANGI24-3	RANGI24-3	RANGI24-3	RANGI24-3
Depth:	0cm	20cm	40cm	60cm	80cm	100cm	120cm	140cm	160cm
Date:	18/12/2024	18/12/2024	21/12/2024	18/12/2024	8/01/2025	13/01/2025	8/01/2025	18/12/2024	18/12/2024
Time:	21:26	21:44	13:17	22:01	20:59	16:00	21:17	22:19	22:37
SiO2 (%)	62.480	64.910	69.120	71.380	71.190	71.370	72.420	72.810	72.160
Al2O3 (%)	12.620	13.420	13.640	14.750	15.130	15.410	14.980	14.550	15.030
TiO2 (%)	0.322	0.364	0.322	0.283	0.237	0.228	0.238	0.186	0.245
MnO (%)	0.081	0.086	0.065	0.046	0.048	0.047	0.048	0.044	0.058
Fe2O3 (%)	2.793	3.310	2.057	1.514	1.506	1.509	1.497	1.259	1.652
MgO (%)	1.085	1.341	0.671	0.499	0.529	0.562	0.515	0.357	0.687
CaO (%)	3.255	3.535	2.568	2.627	2.654	2.855	2.689	2.173	3.042
Na2O (%)	3.186	3.309	3.738	4.150	4.184	4.200	4.164	4.156	4.179
K2O (%)	1.810	1.900	2.050	1.870	1.880	1.700	1.810	2.310	1.540
P2O5 (%)	0.496	0.398	0.208	0.075	0.055	0.053	0.047	0.047	0.042
SO3 (%)	0.050	0.060	0.050	0.010	0.020	0.030	0.020	0.010	0.000
SrO (%)	0.017	0.017	0.017	0.022	0.022	0.025	0.023	0.019	0.027
BaO (%)	0.0511	0.0516	0.0582	0.0582	0.0531	0.0576	0.0588	0.068	0.0443
CO2 (%)	12.450	8.100	6.050	3.310	3.130	2.650	2.000	2.560	1.670
Sum (%)	100.710	100.813	100.621	100.614	100.650	100.713	100.519	100.565	100.380
Specimen mass:	0.799	0.801	0.799	0.799	0.803	0.801	0.801	0.799	0.800
Additive mass:	8.002	8.000	8.000	8.002	8.003	8.001	8.002	8.000	8.000

Name:	RANGI24-4	RANGI24-4	RANGI24-4	RANGI24-4	RANGI24-4	RANGI24-4	RANGI24-4
Depth:	20cm	40cm	60cm	80cm	100cm	120cm	140cm
Date:	18/12/2024 22:55	18/12/2024 23:12	10/01/2025 17:18	10/01/2025 17:54	18/12/2024 23:30	18/12/2024 23:48	19/12/2024 0:06
Time:							
SiO2 (%)	61.290	67.010	70.760	71.100	71.080	70.460	70.760
Al2O3 (%)	13.170	14.280	15.820	16.360	16.420	16.620	16.380
TiO2 (%)	0.401	0.350	0.298	0.223	0.183	0.217	0.195
MnO (%)	0.093	0.060	0.048	0.043	0.035	0.043	0.052
Fe2O3 (%)	3.877	1.892	1.609	1.418	1.250	1.409	1.454
MgO (%)	1.664	0.624	0.652	0.588	0.493	0.614	0.680
CaO (%)	4.019	2.747	3.449	3.774	3.725	3.823	3.770
Na2O (%)	2.996	3.758	4.259	4.433	4.407	4.494	4.436
K2O (%)	1.670	1.740	1.300	1.110	1.150	1.180	1.210
P2O5 (%)	0.302	0.123	0.056	0.042	0.047	0.041	0.042
SO3 (%)	0.060	0.030	0.010	0.020	0.030	0.020	0.010
SrO (%)	0.016	0.021	0.029	0.032	0.031	0.032	0.031
BaO (%)	0.0528	0.0486	0.0504	0.0385	0.0512	0.0455	0.0427
CO2 (%)	10.940	8.090	2.380	1.670	1.900	1.680	1.680
Sum (%)	100.555	100.786	100.732	100.867	100.810	100.688	100.748
Specimen mass:	0.800	0.800	0.802	0.802	0.800	0.799	0.801
Additive mass:	8.001	8.001	7.999	8.000	8.002	8.001	8.001

Name:	RANGI24-5	RANGI24-5	RANGI24-5	RANGI24-5	RANGI24-5	RANGI24-5	RANGI24-5	RANGI24-5
Depth:	0cm	20cm	40cm	60cm	80cm	100cm	120cm	OUTCROP
Date:	8/01/2025	19/12/2024	19/12/2024	21/12/2024	19/12/2024	15/01/2025	19/12/2024	19/12/2024
Time:	21:52	0:23	0:41	15:39	0:59	3:03	1:34	19:50
SiO2 (%)	65.880	65.900	70.550	70.930	71.450	71.360	71.150	71.990
Al2O3 (%)	14.320	14.380	15.750	15.830	15.880	15.830	15.850	15.570
TiO2 (%)	0.322	0.378	0.235	0.230	0.155	0.162	0.174	0.192
MnO (%)	0.070	0.088	0.047	0.043	0.040	0.038	0.040	0.039
Fe2O3 (%)	2.759	3.488	1.896	1.793	1.444	1.402	1.508	1.498
MgO (%)	0.975	1.405	0.540	0.477	0.363	0.380	0.423	0.441
CaO (%)	3.521	3.860	3.407	3.202	3.193	3.329	3.107	2.996
Na2O (%)	3.733	3.563	4.337	4.348	4.388	4.363	4.394	4.393
K2O (%)	1.580	1.730	1.440	1.600	1.620	1.480	1.730	1.740
P2O5 (%)	0.272	0.191	0.055	0.052	0.050	0.049	0.049	0.045
SO3 (%)	0.030	0.040	0.000	0.000	0.000	0.000	0.000	0.000
SrO (%)	0.022	0.020	0.028	0.027	0.026	0.027	0.026	0.026
BaO (%)	0.0503	0.0511	0.0552	0.0535	0.0514	0.0491	0.0592	0.0539
CO2 (%)	6.840	5.490	2.390	2.180	2.240	1.830	2.050	1.650
Sum (%)	100.384	100.601	100.743	100.781	100.917	100.304	100.569	100.631
Specimen mass:	0.799	0.802	0.802	0.800	0.799	0.802	0.800	0.801
Additive mass:	8.000	8.000	8.002	8.002	8.000	8.000	8.000	8.000

Name:	RANGI 24-6	RANGI 24-6	RANGI 24-6	RANGI 24-6	RANGI 24-6	RANGI 24-6	RANGI 24-6	RANGI 24-6	RANGI 24-6	RANGI 24-6	RANGI 24-6	RANGI 24-6	RANGI 24-6
Depth:	0cm	20cm	40cm	60cm	80cm	100cm	120cm	B 0cm	B 20cm	B 40cm	B 60cm	B 80cm	B 100cm
Date:	10/01/	21/12/	19/12/	19/12/	19/12/	10/01/	8/01/2	10/01/	21/12/	19/12/	19/12/	8/01/2	8/01/2
Time:	2025 15:50	2024 13:35	2024 20:08	2024 20:26	2024 20:43	2025 16:43	025 20:42	2025 17:36	2024 14:10	2024 21:01	2024 21:19	025 20:06	025 21:35
SiO2 (%)	60.430	67.240	70.130	69.230	69.880	70.110	69.660	64.890	66.430	69.910	70.320	69.760	69.990
Al2O3 (%)	12.350	13.060	13.440	16.320	16.690	16.680	16.620	15.270	15.570	16.270	16.240	16.120	16.270
TiO2 (%)	0.295	0.288	0.281	0.257	0.247	0.263	0.322	0.399	0.374	0.229	0.215	0.257	0.299
MnO (%)	0.081	0.083	0.066	0.043	0.043	0.054	0.058	0.081	0.080	0.051	0.053	0.058	0.063
Fe2O3 (%)	2.827	2.539	2.094	1.732	1.711	1.751	1.841	3.322	3.208	1.980	1.865	2.096	2.303
MgO (%)	0.874	0.649	0.473	0.524	0.578	0.673	0.770	1.330	1.289	0.661	0.595	0.689	0.757
CaO (%)	2.920	2.215	2.008	3.408	3.668	3.667	3.801	3.902	3.936	3.485	3.472	3.445	3.528
Na2O (%)	3.070	3.493	3.774	4.360	4.543	4.524	4.507	3.790	3.961	4.444	4.460	4.396	4.447
K2O (%)	1.710	2.240	2.340	1.450	1.390	1.410	1.310	1.430	1.460	1.450	1.460	1.470	1.410
P2O5 (%)	0.353	0.213	0.133	0.059	0.046	0.049	0.047	0.113	0.099	0.062	0.059	0.059	0.051
SO3 (%)	0.050	0.060	0.040	0.030	0.010	0.020	0.010	0.030	0.020	0.000	0.000	0.000	0.000
SrO (%)	0.016	0.014	0.015	0.028	0.031	0.030	0.031	0.026	0.027	0.029	0.029	0.029	0.030
BaO (%)	0.0519	0.0629	0.0647	0.0488	0.0503	0.0459	0.0431	0.0487	0.0536	0.0499	0.042	0.046	0.0432
CO2 (%)	15.050	8.380	5.590	3.250	1.910	1.640	1.470	5.810	4.190	1.960	1.830	1.930	1.550
Sum (%)	100.100	100.545	100.459	100.754	100.809	100.934	100.495	100.444	100.702	100.593	100.657	100.370	100.759
Specimen mass:	0.801	0.803	0.800	0.800	0.800	0.800	0.801	0.800	0.801	0.800	0.802	0.801	0.800
Additive mass:	8.003	8.001	8.002	8.002	8.002	8.002	8.001	8.001	8.001	8.001	8.000	8.001	8.003

Name:	RANGI24-7	RANGI24-7	RANGI24-7	RANGI24-7	RANGI24-7	RANGI24-8	RANGI24-8	RANGI24-8	RANGI24-8	RANGI24-8
Depth:	**0cm**	**20cm**	**40cm**	**60cm**	**80cm**	**0cm**	**20cm**	**40cm**	**60cm**	**80cm**
Date:	10/01/20	10/01/20	10/01/20	19/12/20	19/12/20	19/12/20	19/12/20	21/12/20	21/12/20	21/12/20
Time:	25 17:01	25 16:07	25 18:11	24 21:37	24 21:54	24 22:12	24 22:30	24 13:53	24 14:28	24 15:04
SiO2 (%)	68.020	69.170	69.470	70.260	70.300	70.520	72.650	72.000	72.250	73.130
Al2O3 (%)	15.170	15.880	15.970	15.880	15.920	14.750	14.690	14.630	14.690	14.500
TiO2 (%)	0.440	0.381	0.362	0.288	0.321	0.246	0.226	0.287	0.269	0.222
MnO (%)	0.090	0.091	0.085	0.070	0.077	0.055	0.051	0.061	0.055	0.055
Fe2O3 (%)	3.460	3.078	2.981	2.440	2.699	2.312	1.832	2.226	2.124	1.864
MgO (%)	1.139	0.942	0.937	0.710	0.793	0.849	0.513	0.650	0.596	0.506
CaO (%)	3.279	3.270	3.318	3.180	3.281	3.282	2.643	2.587	2.525	2.562
Na2O (%)	3.950	4.236	4.262	4.328	4.303	4.054	4.231	4.157	4.186	4.169
K2O (%)	1.660	1.580	1.580	1.700	1.610	1.860	1.990	1.990	2.040	2.000
P2O5 (%)	0.102	0.068	0.065	0.058	0.060	0.076	0.059	0.058	0.055	0.052
SO3 (%)	0.010	0.000	0.000	0.000	0.000	0.000	0.000	0.000	0.000	0.000
SrO (%)	0.026	0.029	0.030	0.028	0.029	0.023	0.023	0.023	0.023	0.022
BaO (%)	0.0511	0.0464	0.0515	0.0481	0.0499	0.0538	0.058	0.0556	0.0561	0.056
CO2 (%)	3.270	1.860	1.710	1.590	1.420	2.730	1.940	2.160	1.710	1.550
Sum (%)	100.675	100.638	100.827	100.586	100.868	100.834	100.908	100.894	100.593	100.708
Specimen mass:	0.801	0.802	0.801	0.800	0.801	0.803	0.801	0.800	0.801	0.800
Additive mass:	8.003	8.000	8.002	8.002	8.001	8.002	8.000	8.002	8.002	8.001

Appendix H: Trace Element Composition from XRF

Name:	COAST 1	COAST 2	COAST 3	COAST 4	COAST 5	COAST 6
Depth:	0cm	0cm	0cm	0cm	0cm	0cm
Date:	12/01/2025	12/01/2025	13/01/2025	10/01/2025	8/01/2025	22/12/2024
Time:	20:13	23:06	2:00	8:52	18:10	0:19
Sc (PPM)	8.0	8.0	7.0	7.0	6.0	5.0
V (PPM)	30.0	27.0	28.0	22.0	17.0	15.0
Cr (PPM)	4.0	0.0	3.0	13.0	0.0	0.0
Co (PPM)	53.0	71.0	60.0	48.0	71.0	76.0
Ni (PPM)	7.0	4.0	7.0	5.0	6.0	6.0
Cu (PPM)	6.0	5.0	5.0	5.0	5.0	5.0
Zn (PPM)	42.0	43.0	37.0	35.0	40.0	27.0
Ga (PPM)	15.0	15.0	15.0	15.0	14.0	15.0
As (PPM)	9.0	11.0	10.0	9.0	11.0	11.0
Rb (PPM)	73.0	93.0	65.0	63.0	96.0	39.0
Sr (PPM)	215.0	140.0	211.0	225.0	127.0	311.0
Y (PPM)	17.0	23.0	14.0	14.0	23.0	10.0
Zr (PPM)	111.0	123.0	100.0	93.0	112.0	64.0
Nb (PPM)	5.0	6.0	5.0	4.0	6.0	3.0
Mo (PPM)	4.0	4.0	4.0	4.0	4.0	4.0
Sn (PPM)	2.0	3.0	2.0	2.0	3.0	4.0
Sb (PPM)	1.0	1.0	1.0	1.0	3.0	2.0
Cs (PPM)	1.0	1.0	1.0	3.0	1.0	1.0
Ba (PPM)	589.0	717.0	554.0	576.0	759.0	473.0

La (PPM)	11.0	15.0	7.0	7.0	12.0	0.0
Ce (PPM)	39.0	54.0	36.0	45.0	61.0	30.0
Nd (PPM)	17.0	22.0	18.0	17.0	22.0	15.0
Tl (PPM)	0.0	1.0	0.0	0.0	1.0	0.0
Pb (PPM)	9.0	11.0	8.0	7.0	12.0	5.0
Th (PPM)	9.0	10.0	7.0	6.0	11.0	4.0
U (PPM)	3.0	3.0	3.0	3.0	3.0	3.0
SiO2 (%)	72.1	72.5	74.1	73.0	74.3	71.7
Al2O3 (%)	14.2	13.5	13.5	14.3	12.7	14.5
TiO2 (%)	0.3	0.2	0.2	0.2	0.2	0.1
MnO (PPM)	560.0	715.0	732.0	620.0	752.0	439.0
Fe2O3 (%)	2.2	2.2	2.0	1.7	1.7	1.5
Na2O (%)	4.2	4.1	3.9	4.3	3.9	4.2
MgO (%)	0.7	0.7	0.6	0.5	0.4	0.5
K2O (%)	2.2	2.9	1.9	1.9	2.9	1.3
CaO (%)	2.5	2.1	2.6	2.8	1.9	4.4
P2O5 (%)	0.1	0.1	0.1	0.1	0.1	0.1
S (PPM)	3713.0	2895.0	3693.0	2602.0	435.0	1525.0
F (PPM)	241.0	183.0	151.0	209.0	145.0	124.0
Cl (PPM)	3121.0	2219.0	1879.0	4951.0	1712.0	1676.0
CO2 (%)	1.9	2.0	1.3	1.5	2.2	2.0
Sum (%)	101.2	101.0	101.0	101.2	100.6	100.6
Compton (%)	103.0	103.1	103.2	102.7	103.3	104.1

Name:	RANGI24-1	RANGI24-1	RANGI24-1	RANGI24-1	RANGI24-1	RANGI24-1	RANGI24-1	RANGI24-1	RANGI24-1	RANGI24-1	RANGI24-1
Depth:	**20cm**	**40cm**	**60cm**	**80cm**	**100cm**	**120cm**	**140cm**	**160cm**	**180cm**	**200cm**	**220cm**
Date:	9/01/2025	9/01/2025	20/12/2024	7/01/2025	10/01/2025	20/12/2024	20/12/2024	11/01/2025	6/01/2025	24/01/2025	6/01/2025
Time:	15:31	6:51	7:10	12:02	21:58	12:57	15:51	0:52	17:02	11:15	22:48
Sc (PPM)	15.0	8.0	8.0	5.0	5.0	5.0	6.0	7.0	6.0	6.0	7.0
V (PPM)	99.0	22.0	15.0	9.0	9.0	6.0	12.0	18.0	15.0	17.0	16.0
Cr (PPM)	0.0	0.0	0.0	0.0	0.0	7.0	17.0	16.0	27.0	6.0	15.0
Co (PPM)	48.0	36.0	52.0	20.0	37.0	45.0	49.0	50.0	50.0	42.0	55.0
Ni (PPM)	5.0	4.0	4.0	3.0	4.0	3.0	4.0	6.0	6.0	4.0	5.0
Cu (PPM)	11.0	6.0	7.0	5.0	5.0	5.0	6.0	5.0	5.0	5.0	5.0
Zn (PPM)	58.0	38.0	42.0	35.0	34.0	34.0	23.0	30.0	27.0	28.0	30.0
Ga (PPM)	14.0	14.0	15.0	15.0	16.0	15.0	16.0	16.0	16.0	15.0	16.0
As (PPM)	11.0	7.0	8.0	7.0	7.0	6.0	6.0	5.0	5.0	5.0	4.0
Rb (PPM)	54.0	79.0	84.0	93.0	92.0	86.0	30.0	24.0	26.0	26.0	25.0
Sr (PPM)	160.0	127.0	114.0	101.0	97.0	122.0	299.0	301.0	294.0	303.0	306.0
Y (PPM)	17.0	20.0	25.0	23.0	23.0	21.0	6.0	7.0	6.0	7.0	7.0
Zr (PPM)	99.0	127.0	172.0	136.0	131.0	131.0	56.0	62.0	58.0	59.0	60.0
Nb (PPM)	4.0	6.0	6.0	7.0	7.0	7.0	3.0	3.0	3.0	3.0	3.0
Mo (PPM)	4.0	4.0	4.0	4.0	4.0	4.0	4.0	4.0	4.0	4.0	4.0
Sn (PPM)	2.0	4.0	3.0	3.0	4.0	4.0	3.0	4.0	3.0	4.0	2.0
Sb (PPM)	2.0	3.0	2.0	1.0	2.0	2.0	2.0	2.0	2.0	3.0	2.0
Cs (PPM)	2.0	5.0	1.0	1.0	1.0	1.0	1.0	2.0	2.0	2.0	2.0
Ba (PPM)	444.0	613.0	645.0	738.0	737.0	751.0	407.0	362.0	381.0	379.0	375.0
La (PPM)	8.0	7.0	12.0	14.0	11.0	10.0	0.0	0.0	0.0	0.0	0.0
Ce (PPM)	32.0	47.0	57.0	49.0	52.0	48.0	24.0	24.0	18.0	21.0	21.0
Nd (PPM)	20.0	19.0	25.0	22.0	23.0	19.0	9.0	7.0	11.0	8.0	11.0

Tl (PPM)	0.0	1.0	1.0	1.0	1.0	1.0	0.0	0.0	0.0	0.0	0.0
Pb (PPM)	5.0	11.0	14.0	14.0	13.0	12.0	4.0	5.0	4.0	3.0	4.0
Th (PPM)	5.0	9.0	11.0	12.0	12.0	11.0	4.0	4.0	4.0	4.0	4.0
U (PPM)	3.0	3.0	3.0	3.0	3.0	3.0	3.0	3.0	3.0	3.0	3.0
SiO2 (%)	61.0	69.9	66.5	69.9	69.8	72.0	73.0	73.4	74.3	73.8	73.5
Al2O3 (%)	12.6	12.3	11.8	13.0	13.4	13.6	15.2	14.5	14.3	14.6	14.6
TiO2 (%)	0.4	0.3	0.3	0.2	0.2	0.2	0.2	0.3	0.2	0.2	0.3
MnO (PPM)	995.0	586.0	569.0	530.0	540.0	539.0	312.0	528.0	403.0	417.0	466.0
Fe2O3 (%)	4.6	1.6	1.5	1.1	1.1	1.0	1.0	1.7	1.4	1.4	1.6
Na2O (%)	2.6	3.4	3.4	3.6	3.6	3.8	4.0	4.0	3.9	4.0	4.0
MgO (%)	2.1	0.5	0.2	0.2	0.2	0.2	0.4	0.9	0.6	0.7	0.8
K2O (%)	1.5	2.3	2.4	2.7	2.7	2.6	0.9	0.8	0.8	0.8	0.8
CaO (%)	4.6	1.8	1.4	1.2	1.2	1.4	3.6	3.8	3.6	3.7	3.8
P2O5 (%)	0.2	0.1	0.1	0.1	0.1	0.1	0.0	0.0	0.0	0.0	0.0
S (PPM)	1685.0	1343.0	2039.0	1258.0	981.0	634.0	254.0	30.0	56.0	24.0	30.0
F (PPM)	264.0	264.0	88.0	105.0	105.0	188.0	85.0	15.0	19.0	74.0	43.0
Cl (PPM)	597.0	779.0	957.0	995.0	928.0	984.0	226.0	161.0	272.0	245.0	228.0
CO2 (%)	10.6	8.0	12.7	8.2	7.9	5.3	1.8	1.0	1.0	1.0	0.8
Sum (%)	100.9	100.6	100.8	100.7	100.6	100.6	100.4	100.5	100.4	100.4	100.4
Compton (%)	102.7	101.8	100.9	101.9	102.4	102.1	102.8	103.1	102.4	102.6	102.3

Name:	RANGI24-2	RANGI24-2	RANGI24-2	RANGI24-2	RANGI24-2	RANGI24-2	RANGI24-2	RANGI24-2	RANGI24-2	RANGI24-2	RANGI24-2
Depth:	20cm	40cm	60cm	80cm	100cm	120cm	140cm	160cm	180cm	200cm	220cm
Date:	20/12/2024	20/12/2024	9/01/2025	7/01/2025	7/01/2025	9/01/2025	7/01/2025	7/01/2025	7/01/2025	21/12/2024	7/01/2025
Time:	18:44	21:37	9:45	1:42	12:02	12:38	4:35	7:29	12:02	6:18	16:09
Sc (PPM)	15.0	12.0	12.0	5.0	5.0	5.0	3.0	9.0	8.0	7.0	10.0
V (PPM)	88.0	36.0	24.0	14.0	13.0	7.0	5.0	20.0	17.0	18.0	22.0
Cr (PPM)	4.0	2.0	0.0	0.0	3.0	0.0	0.0	4.0	11.0	11.0	9.0
Co (PPM)	41.0	39.0	41.0	48.0	16.0	36.0	73.0	51.0	46.0	52.0	44.0
Ni (PPM)	5.0	4.0	4.0	4.0	4.0	3.0	3.0	7.0	6.0	5.0	6.0
Cu (PPM)	13.0	8.0	11.0	6.0	6.0	5.0	5.0	5.0	6.0	5.0	5.0
Zn (PPM)	61.0	64.0	55.0	37.0	35.0	35.0	37.0	46.0	37.0	36.0	39.0
Ga (PPM)	14.0	17.0	16.0	15.0	15.0	15.0	15.0	17.0	16.0	15.0	17.0
As (PPM)	10.0	9.0	9.0	7.0	7.0	8.0	8.0	5.0	5.0	5.0	4.0
Rb (PPM)	60.0	70.0	78.0	79.0	91.0	101.0	94.0	28.0	26.0	26.0	25.0
Sr (PPM)	157.0	178.0	135.0	144.0	103.0	94.0	114.0	315.0	321.0	319.0	333.0
Y (PPM)	18.0	23.0	25.0	20.0	22.0	24.0	21.0	8.0	8.0	7.0	9.0
Zr (PPM)	109.0	167.0	190.0	125.0	119.0	125.0	122.0	77.0	65.0	69.0	70.0
Nb (PPM)	5.0	6.0	7.0	6.0	7.0	7.0	7.0	3.0	3.0	3.0	4.0
Mo (PPM)	4.0	4.0	4.0	4.0	4.0	4.0	4.0	4.0	4.0	4.0	4.0
Sn (PPM)	4.0	2.0	3.0	4.0	5.0	4.0	5.0	2.0	3.0	4.0	3.0
Sb (PPM)	2.0	2.0	2.0	3.0	2.0	2.0	3.0	1.0	1.0	2.0	2.0
Cs (PPM)	5.0	3.0	1.0	1.0	1.0	3.0	1.0	1.0	1.0	2.0	1.0
Ba (PPM)	487.0	494.0	590.0	682.0	742.0	814.0	786.0	398.0	395.0	394.0	388.0
La (PPM)	4.0	10.0	14.0	13.0	13.0	16.0	11.0	0.0	0.0	0.0	0.0
Ce (PPM)	37.0	46.0	49.0	50.0	49.0	55.0	48.0	23.0	25.0	22.0	28.0
Nd (PPM)	16.0	22.0	23.0	22.0	22.0	23.0	21.0	11.0	9.0	12.0	8.0

Tl (PPM)	0.0	1.0	1.0	0.0	1.0	1.0	1.0	0.0	0.0	0.0	0.0
Pb (PPM)	8.0	11.0	14.0	10.0	13.0	12.0	13.0	3.0	4.0	3.0	3.0
Th (PPM)	7.0	9.0	9.0	9.0	12.0	11.0	11.0	4.0	4.0	4.0	5.0
U (PPM)	3.0	3.0	3.0	3.0	3.0	3.0	3.0	3.0	3.0	3.0	3.0
SiO2 (%)	62.9	62.1	60.5	72.4	70.0	73.5	74.9	71.7	72.2	71.9	70.7
Al2O3 (%)	12.7	13.7	12.8	13.3	13.9	13.2	12.9	15.4	15.5	15.4	15.9
TiO2 (%)	0.4	0.4	0.3	0.3	0.2	0.2	0.2	0.3	0.3	0.3	0.3
MnO (PPM)	966.0	851.0	644.0	526.0	506.0	543.0	553.0	574.0	478.0	558.0	641.0
Fe2O3 (%)	3.8	2.7	1.9	1.2	1.0	1.0	1.0	2.0	1.6	1.9	2.1
Na2O (%)	2.8	3.4	3.2	3.8	3.6	3.8	3.9	4.2	4.3	4.3	4.4
MgO (%)	1.8	0.9	0.4	0.3	0.2	0.2	0.2	1.0	0.8	1.0	1.2
K2O (%)	1.7	1.9	2.1	2.4	2.7	3.0	2.8	0.9	0.8	0.8	0.8
CaO (%)	4.0	2.7	1.8	1.8	1.2	1.1	1.3	4.0	4.0	4.1	4.3
P2O5 (%)	0.2	0.2	0.2	0.1	0.1	0.0	0.0	0.0	0.0	0.0	0.0
S (PPM)	1625.0	1930.0	2988.0	393.0	711.0	142.0	38.0	0.0	124.0	43.0	0.0
F (PPM)	224.0	221.0	141.0	127.0	292.0	197.0	194.0	49.0	68.0	27.0	0.0
Cl (PPM)	681.0	899.0	897.0	937.0	1012.0	1022.0	1176.0	280.0	207.0	190.0	219.0
CO2 (%)	10.1	12.3	17.0	4.8	7.2	4.1	2.8	0.8	0.7	0.7	0.7
Sum (%)	100.9	100.8	100.9	100.6	100.5	100.5	100.5	100.5	100.5	100.5	100.5
Compton (%)	102.3	101.3	100.3	103.5	102.2	102.2	103.2	102.8	103.4	103.4	102.8

Name:	RANGI24-3	RANGI24-3	RANGI24-3	RANGI24-3	RANGI24-3	RANGI24-3	RANGI24-3	RANGI24-3	RANGI24-3
Depth:	0cm	20cm	40cm	60cm	80cm	100cm	120cm	140cm	160cm
Date:	7/01/2025	21/12/2024	22/12/2024	7/01/2025	11/01/2025	13/01/2025	9/01/2025	9/01/2025	10/01/2025
Time:	19:03	9:11	3:13	21:56	3:45	16:11	18:25	21:18	0:12
Sc (PPM)	10.0	11.0	8.0	7.0	7.0	7.0	6.0	5.0	8.0
V (PPM)	53.0	67.0	31.0	17.0	17.0	18.0	17.0	11.0	17.0
Cr (PPM)	23.0	1.0	0.0	3.0	10.0	9.0	0.0	5.0	11.0
Co (PPM)	39.0	40.0	40.0	43.0	34.0	47.0	44.0	53.0	47.0
Ni (PPM)	6.0	4.0	4.0	4.0	5.0	6.0	7.0	6.0	5.0
Cu (PPM)	18.0	13.0	9.0	7.0	5.0	6.0	6.0	6.0	5.0
Zn (PPM)	88.0	62.0	51.0	41.0	40.0	35.0	33.0	34.0	36.0
Ga (PPM)	15.0	14.0	16.0	17.0	16.0	16.0	15.0	16.0	15.0
As (PPM)	9.0	10.0	8.0	6.0	6.0	6.0	6.0	5.0	6.0
Rb (PPM)	68.0	70.0	71.0	62.0	62.0	56.0	59.0	77.0	51.0
Sr (PPM)	178.0	179.0	184.0	229.0	234.0	254.0	238.0	193.0	268.0
Y (PPM)	17.0	18.0	18.0	14.0	14.0	12.0	13.0	16.0	11.0
Zr (PPM)	109.0	116.0	130.0	114.0	107.0	100.0	97.0	101.0	105.0
Nb (PPM)	5.0	5.0	5.0	6.0	5.0	5.0	4.0	6.0	4.0
Mo (PPM)	4.0	4.0	4.0	4.0	4.0	4.0	4.0	4.0	4.0
Sn (PPM)	5.0	3.0	3.0	3.0	5.0	4.0	5.0	5.0	3.0
Sb (PPM)	2.0	1.0	3.0	2.0	1.0	2.0	3.0	1.0	1.0
Cs (PPM)	3.0	1.0	3.0	3.0	1.0	1.0	1.0	1.0	1.0
Ba (PPM)	537.0	553.0	579.0	566.0	579.0	550.0	561.0	672.0	520.0
La (PPM)	5.0	7.0	14.0	2.0	2.0	1.0	0.0	11.0	0.0
Ce (PPM)	39.0	42.0	45.0	35.0	35.0	29.0	36.0	46.0	30.0
Nd (PPM)	16.0	19.0	21.0	18.0	13.0	15.0	14.0	16.0	12.0

Tl (PPM)	0.0	0.0	0.0	0.0	0.0	0.0	0.0	1.0	0.0
Pb (PPM)	8.0	7.0	9.0	8.0	8.0	7.0	8.0	10.0	7.0
Th (PPM)	6.0	7.0	8.0	8.0	7.0	5.0	7.0	9.0	6.0
U (PPM)	3.0	3.0	3.0	3.0	3.0	3.0	3.0	3.0	3.0
SiO2 (%)	62.4	64.8	69.1	71.3	71.0	71.2	72.3	72.7	72.2
Al2O3 (%)	12.6	13.4	13.6	14.7	15.1	15.4	15.0	14.5	15.0
TiO2 (%)	0.3	0.4	0.3	0.3	0.2	0.2	0.2	0.2	0.3
MnO (PPM)	806.0	890.0	654.0	500.0	482.0	468.0	464.0	472.0	515.0
Fe2O3 (%)	2.8	3.3	2.1	1.5	1.5	1.5	1.5	1.3	1.7
Na2O (%)	3.2	3.3	3.7	4.1	4.2	4.2	4.2	4.1	4.2
MgO (%)	1.1	1.3	0.7	0.5	0.5	0.6	0.5	0.4	0.7
K2O (%)	1.8	1.9	2.0	1.9	1.9	1.7	1.8	2.3	1.5
CaO (%)	3.2	3.5	2.6	2.6	2.6	2.8	2.7	2.2	3.0
P2O5 (%)	0.5	0.4	0.2	0.1	0.1	0.1	0.0	0.0	0.0
S (PPM)	2122.0	1279.0	779.0	313.0	336.0	683.0	320.0	355.0	180.0
F (PPM)	128.0	158.0	182.0	139.0	244.0	138.0	170.0	145.0	125.0
Cl (PPM)	705.0	653.0	715.0	655.0	526.0	536.0	501.0	767.0	408.0
CO2 (%)	12.4	8.1	6.1	3.3	3.1	2.7	2.0	2.6	1.7
Sum (%)	100.8	100.8	100.7	100.6	100.5	100.5	100.5	100.5	100.5
Compton (%)	101.5	102.3	102.3	103.1	102.4	102.8	103.0	102.7	102.8

Name:	RANGI24-4	RANGI24-4	RANGI24-4	RANGI24-4	RANGI24-4	RANGI24-4	RANGI24-4
Depth:	20cm	40cm	60cm	80cm	100cm	120cm	140cm
Date:	11/01/2025	11/01/2025	11/01/2025	11/01/2025	11/01/2025	11/01/2025	8/01/2025
Time:	6:38	9:32	12:25	15:19	18:12	21:06	0:50
Sc (PPM)	14.0	10.0	8.0	6.0	5.0	7.0	8.0
V (PPM)	78.0	26.0	28.0	20.0	18.0	18.0	15.0
Cr (PPM)	6.0	0.0	18.0	22.0	46.0	0.0	9.0
Co (PPM)	42.0	45.0	60.0	51.0	47.0	45.0	46.0
Ni (PPM)	4.0	4.0	6.0	5.0	7.0	6.0	6.0
Cu (PPM)	11.0	8.0	6.0	6.0	5.0	6.0	6.0
Zn (PPM)	62.0	46.0	37.0	32.0	31.0	34.0	33.0
Ga (PPM)	15.0	16.0	17.0	17.0	17.0	17.0	17.0
As (PPM)	10.0	7.0	5.0	5.0	5.0	5.0	5.0
Rb (PPM)	62.0	63.0	45.0	36.0	37.0	38.0	39.0
Sr (PPM)	171.0	206.0	292.0	320.0	318.0	325.0	316.0
Y (PPM)	19.0	19.0	10.0	8.0	9.0	9.0	10.0
Zr (PPM)	115.0	150.0	97.0	79.0	69.0	77.0	77.0
Nb (PPM)	5.0	6.0	4.0	3.0	3.0	3.0	3.0
Mo (PPM)	4.0	4.0	4.0	4.0	4.0	4.0	4.0
Sn (PPM)	5.0	4.0	4.0	5.0	4.0	4.0	3.0
Sb (PPM)	2.0	2.0	3.0	4.0	3.0	2.0	2.0
Cs (PPM)	1.0	7.0	2.0	1.0	1.0	1.0	1.0
Ba (PPM)	524.0	532.0	474.0	448.0	447.0	457.0	465.0
La (PPM)	10.0	6.0	0.0	0.0	0.0	0.0	4.0

Ce (PPM)	36.0	37.0	32.0	23.0	31.0	24.0	26.0
Nd (PPM)	17.0	20.0	13.0	10.0	12.0	11.0	10.0
Tl (PPM)	0.0	1.0	0.0	0.0	0.0	0.0	0.0
Pb (PPM)	8.0	11.0	6.0	5.0	7.0	6.0	5.0
Th (PPM)	8.0	7.0	4.0	4.0	4.0	4.0	4.0
U (PPM)	3.0	3.0	3.0	3.0	3.0	3.0	3.0
SiO2 (%)	61.3	66.8	70.6	70.8	70.8	70.2	70.5
Al2O3 (%)	13.2	14.3	15.8	16.3	16.3	16.6	16.3
TiO2 (%)	0.4	0.4	0.3	0.2	0.2	0.2	0.2
MnO (PPM)	956.0	613.0	450.0	396.0	365.0	418.0	476.0
Fe2O3 (%)	3.9	1.9	1.6	1.4	1.2	1.4	1.4
Na2O (%)	3.0	3.7	4.2	4.4	4.4	4.5	4.4
MgO (%)	1.7	0.6	0.7	0.6	0.5	0.6	0.7
K2O (%)	1.7	1.7	1.3	1.1	1.1	1.2	1.2
CaO (%)	4.0	2.7	3.4	3.8	3.7	3.8	3.8
P2O5 (%)	0.3	0.1	0.1	0.0	0.0	0.0	0.0
S (PPM)	1495.0	906.0	203.0	343.0	256.0	389.0	157.0
F (PPM)	304.0	278.0	150.0	111.0	80.0	106.0	66.0
Cl (PPM)	696.0	702.0	319.0	252.0	280.0	271.0	380.0
CO2 (%)	10.9	8.1	2.4	1.7	1.9	1.7	1.7
Sum (%)	100.8	100.7	100.5	100.5	100.4	100.5	100.4
Compton (%)	101.6	101.6	102.7	103.2	102.4	102.6	102.8

Name:	RANGI24-5	RANGI24-5	RANGI24-5	RANGI24-5	RANGI24-5	RANGI24-5	RANGI24-5	RANGI24-5
Depth:	0cm	20cm	40cm	60cm	80cm	100cm	120cm	OUTCROP
Date:	12/01/2025	12/01/2025	8/01/2025	12/01/2025	12/01/2025	16/01/2025	10/01/2025	11/01/2025
Time:	8:39	11:33	3:43	14:26	17:20	9:41	5:59	23:59
Sc (PPM)	9.0	13.0	7.0	7.0	5.0	6.0	6.0	5.0
V (PPM)	43.0	63.0	23.0	19.0	15.0	16.0	17.0	19.0
Cr (PPM)	4.0	3.0	4.0	7.0	4.0	1.0	0.0	9.0
Co (PPM)	37.0	47.0	31.0	43.0	34.0	51.0	44.0	60.0
Ni (PPM)	4.0	4.0	4.0	4.0	4.0	5.0	5.0	6.0
Cu (PPM)	10.0	8.0	5.0	5.0	5.0	5.0	5.0	5.0
Zn (PPM)	53.0	53.0	31.0	31.0	29.0	28.0	31.0	32.0
Ga (PPM)	17.0	16.0	17.0	16.0	16.0	16.0	16.0	15.0
As (PPM)	8.0	10.0	7.0	7.0	8.0	7.0	7.0	7.0
Rb (PPM)	60.0	63.0	50.0	54.0	53.0	49.0	57.0	58.0
Sr (PPM)	232.0	208.0	284.0	273.0	270.0	285.0	270.0	267.0
Y (PPM)	15.0	18.0	11.0	11.0	11.0	10.0	12.0	12.0
Zr (PPM)	105.0	118.0	88.0	90.0	80.0	76.0	84.0	92.0
Nb (PPM)	5.0	5.0	4.0	4.0	4.0	4.0	4.0	4.0
Mo (PPM)	4.0	4.0	4.0	4.0	4.0	4.0	4.0	4.0
Sn (PPM)	5.0	5.0	4.0	4.0	4.0	3.0	4.0	4.0
Sb (PPM)	3.0	3.0	3.0	2.0	3.0	3.0	3.0	3.0
Cs (PPM)	4.0	3.0	3.0	8.0	3.0	1.0	1.0	1.0
Ba (PPM)	514.0	521.0	512.0	538.0	541.0	525.0	570.0	570.0

La (PPM)	2.0	5.0	4.0	0.0	3.0	0.0	0.0	5.0
Ce (PPM)	30.0	42.0	25.0	25.0	27.0	31.0	34.0	41.0
Nd (PPM)	15.0	18.0	10.0	14.0	15.0	16.0	16.0	16.0
Tl (PPM)	0.0	0.0	0.0	0.0	0.0	0.0	0.0	0.0
Pb (PPM)	9.0	7.0	6.0	8.0	6.0	6.0	7.0	7.0
Th (PPM)	7.0	6.0	5.0	5.0	6.0	5.0	5.0	5.0
U (PPM)	3.0	3.0	3.0	3.0	3.0	3.0	3.0	3.0
SiO2 (%)	65.9	65.9	70.3	70.6	71.0	71.4	71.0	71.8
Al2O3 (%)	14.3	14.4	15.7	15.8	15.8	15.8	15.8	15.5
TiO2 (%)	0.3	0.4	0.2	0.2	0.2	0.2	0.2	0.2
MnO (PPM)	695.0	851.0	454.0	453.0	409.0	392.0	441.0	409.0
Fe2O3 (%)	2.8	3.5	1.9	1.8	1.4	1.4	1.5	1.5
Na2O (%)	3.7	3.6	4.3	4.3	4.4	4.4	4.4	4.4
MgO (%)	1.0	1.4	0.5	0.5	0.4	0.4	0.4	0.4
K2O (%)	1.6	1.7	1.4	1.6	1.6	1.5	1.7	1.7
CaO (%)	3.5	3.9	3.4	3.2	3.2	3.3	3.1	3.0
P2O5 (%)	0.3	0.2	0.1	0.1	0.0	0.0	0.0	0.0
S (PPM)	909.0	569.0	159.0	111.0	100.0	75.0	87.0	157.0
F (PPM)	246.0	262.0	154.0	154.0	158.0	106.0	190.0	173.0
Cl (PPM)	538.0	646.0	524.0	442.0	453.0	414.0	488.0	468.0
CO2 (%)	6.8	5.5	2.4	2.2	2.2	1.8	2.0	1.6
Sum (%)	100.6	100.7	100.5	100.5	100.4	100.4	100.4	100.5
Compton (%)	101.9	103.4	102.9	102.9	102.8	102.8	102.5	103.2

Name:	RANGI24-6	RANGI24-6	RANGI24-6	RANGI24-6	RANGI24-6	RANGI24-6	RANGI24-6B	RANGI24-6B	RANGI24-6B	RANGI24-6B	RANGI24-6B	RANGI24-6B	RANGI24-6B
Depth:	0cm	20cm	40cm	60cm	80cm	100cm	120cm	0cm	20cm	40cm	60cm	80cm	100cm
Date: Time:	13/01/2025 4:54	22/12/2024 9:00	8/01/2025 6:36	13/01/2025 7:47	13/01/2025 10:41	14/01/2025 0:40	14/01/2025 3:38	14/01/2025 6:31	8/01/2025 9:30	14/01/2025 9:24	14/01/2025 12:18	14/01/2025 15:11	14/01/2025 18:05
Sc (PPM)	9.0	8.0	7.0	6.0	7.0	7.0	7.0	12.0	12.0	7.0	6.0	9.0	7.0
V (PPM)	44.0	32.0	22.0	26.0	23.0	21.0	18.0	59.0	54.0	22.0	19.0	23.0	26.0
Cr (PPM)	7.0	3.0	2.0	17.0	16.0	10.0	22.0	4.0	8.0	1.0	18.0	23.0	16.0
Co (PPM)	34.0	37.0	47.0	51.0	54.0	37.0	49.0	36.0	47.0	47.0	49.0	39.0	43.0
Ni (PPM)	5.0	5.0	5.0	6.0	4.0	6.0	5.0	5.0	7.0	5.0	6.0	6.0	3.0
Cu (PPM)	16.0	11.0	8.0	7.0	6.0	5.0	6.0	8.0	7.0	6.0	6.0	6.0	5.0
Zn (PPM)	112.0	66.0	49.0	35.0	34.0	37.0	41.0	53.0	47.0	36.0	38.0	38.0	40.0
Ga (PPM)	15.0	16.0	16.0	17.0	17.0	17.0	17.0	17.0	17.0	16.0	17.0	18.0	17.0
As (PPM)	9.0	11.0	9.0	8.0	8.0	6.0	7.0	9.0	10.0	8.0	6.0	8.0	8.0
Rb (PPM)	67.0	79.0	80.0	49.0	47.0	46.0	42.0	53.0	51.0	49.0	48.0	49.0	47.0
Sr (PPM)	171.0	145.0	152.0	285.0	309.0	310.0	316.0	269.0	271.0	301.0	297.0	297.0	306.0
Y (PPM)	18.0	21.0	20.0	11.0	10.0	11.0	11.0	12.0	12.0	10.0	10.0	11.0	10.0
Zr (PPM)	111.0	129.0	134.0	96.0	87.0	88.0	102.0	102.0	100.0	85.0	84.0	88.0	90.0
Nb (PPM)	5.0	6.0	6.0	4.0	4.0	5.0	4.0	4.0	4.0	4.0	4.0	4.0	4.0
Mo (PPM)	4.0	4.0	4.0	4.0	4.0	4.0	4.0	4.0	4.0	4.0	4.0	4.0	4.0
Sn (PPM)	5.0	3.0	4.0	4.0	3.0	4.0	2.0	3.0	2.0	4.0	5.0	3.0	4.0
Sb (PPM)	3.0	2.0	2.0	2.0	1.0	2.0	2.0	2.0	1.0	2.0	2.0	2.0	2.0
Cs (PPM)	0.0	3.0	1.0	1.0	1.0	1.0	1.0	1.0	8.0	1.0	1.0	6.0	1.0
Ba (PPM)	545.0	627.0	654.0	512.0	506.0	502.0	487.0	485.0	492.0	499.0	500.0	509.0	489.0
La (PPM)	4.0	8.0	5.0	2.0	0.0	0.0	0.0	0.0	3.0	0.0	0.0	0.0	0.0
Ce (PPM)	39.0	52.0	44.0	32.0	27.0	35.0	29.0	35.0	30.0	33.0	35.0	28.0	35.0

Nd (PPM)	13.0	20.0	21.0	14.0	12.0	11.0	12.0	10.0	11.0	12.0	13.0	14.0	15.0
Tl (PPM)	1.0	1.0	1.0	0.0	0.0	0.0	0.0	0.0	0.0	0.0	0.0	0.0	0.0
Pb (PPM)	13.0	11.0	11.0	6.0	6.0	6.0	4.0	9.0	6.0	7.0	6.0	6.0	5.0
Th (PPM)	8.0	9.0	10.0	5.0	5.0	4.0	4.0	6.0	5.0	5.0	5.0	5.0	5.0
U (PPM)	3.0	3.0	3.0	3.0	3.0	3.0	3.0	3.0	3.0	3.0	3.0	3.0	3.0
SiO2 (%)	60.4	67.2	70.1	69.0	69.6	69.8	69.6	64.9	66.3	69.8	70.1	69.8	69.8
Al2O3 (%)	12.4	13.1	13.4	16.3	16.6	16.6	16.6	15.3	15.6	16.2	16.2	16.1	16.2
TiO2 (%)	0.3	0.3	0.3	0.3	0.2	0.3	0.3	0.4	0.4	0.2	0.2	0.3	0.3
MnO (PPM)	829.0	823.0	679.0	451.0	449.0	499.0	569.0	822.0	780.0	538.0	529.0	590.0	601.0
Fe2O3 (%)	2.8	2.5	2.1	1.7	1.7	1.7	1.8	3.3	3.2	2.0	1.9	2.1	2.3
Na2O (%)	3.1	3.5	3.8	4.3	4.5	4.5	4.5	3.8	4.0	4.4	4.4	4.4	4.4
MgO (%)	0.9	0.6	0.5	0.5	0.6	0.7	0.8	1.3	1.3	0.7	0.6	0.7	0.8
K2O (%)	1.7	2.2	2.3	1.4	1.4	1.4	1.3	1.4	1.5	1.5	1.5	1.5	1.4
CaO (%)	2.9	2.2	2.0	3.4	3.7	3.6	3.8	3.9	3.9	3.5	3.5	3.4	3.5
P2O5 (%)	0.4	0.2	0.1	0.1	0.0	0.0	0.0	0.1	0.1	0.1	0.1	0.1	0.1
S (PPM)	2747.0	1067.0	571.0	344.0	198.0	296.0	147.0	740.0	509.0	30.0	51.0	25.0	45.0
F (PPM)	126.0	214.0	160.0	150.0	129.0	179.0	52.0	107.0	123.0	179.0	175.0	95.0	103.0
Cl (PPM)	605.0	809.0	959.0	408.0	337.0	345.0	309.0	415.0	554.0	328.0	338.0	357.0	304.0
CO2 (%)	15.1	8.4	5.6	3.2	1.9	1.6	1.5	5.8	4.2	2.0	1.8	1.9	1.6
Sum (%)	100.4	100.7	100.6	100.5	100.5	100.5	100.5	100.6	100.7	100.5	100.5	100.5	100.5
Compton (%)	99.9	102.0	102.8	102.9	102.5	102.3	103.2	101.9	102.7	103.4	104.0	102.9	103.3

Name:	RANGI24-7	RANGI24-7	RANGI24-7	RANGI24-7	RANGI24-7	RANGI24-8	RANGI24-8	RANGI24-8	RANGI24-8	RANGI24-8
Depth:	**0cm**	**20cm**	**40cm**	**60cm**	**80cm**	**0cm**	**20cm**	**40cm**	**60cm**	**80cm**
Date: Time:	14/01/2025 20:58	15/01/2025 5:56	15/01/2025 8:49	15/01/2025 11:43	15/01/2025 14:36	15/01/2025 17:30	15/01/2025 20:23	15/01/2025 23:17	8/01/2025 12:23	8/01/2025 15:17
Sc (PPM)	11.0	10.0	9.0	8.0	9.0	9.0	7.0	7.0	6.0	6.0
V (PPM)	43.0	34.0	32.0	27.0	28.0	37.0	21.0	28.0	22.0	20.0
Cr (PPM)	55.0	14.0	17.0	13.0	6.0	70.0	13.0	10.0	0.0	0.0
Co (PPM)	42.0	46.0	39.0	55.0	44.0	66.0	60.0	48.0	45.0	53.0
Ni (PPM)	7.0	7.0	6.0	7.0	7.0	8.0	6.0	7.0	5.0	7.0
Cu (PPM)	5.0	6.0	6.0	6.0	6.0	6.0	6.0	5.0	5.0	5.0
Zn (PPM)	51.0	51.0	52.0	45.0	45.0	42.0	37.0	42.0	41.0	38.0
Ga (PPM)	17.0	17.0	17.0	17.0	17.0	15.0	16.0	16.0	16.0	15.0
As (PPM)	9.0	8.0	8.0	8.0	8.0	10.0	8.0	9.0	9.0	9.0
Rb (PPM)	58.0	54.0	55.0	58.0	55.0	64.0	67.0	67.0	68.0	68.0
Sr (PPM)	261.0	298.0	302.0	290.0	297.0	240.0	241.0	243.0	236.0	235.0
Y (PPM)	13.0	11.0	12.0	13.0	12.0	14.0	14.0	14.0	15.0	14.0
Zr (PPM)	118.0	105.0	105.0	104.0	102.0	92.0	100.0	111.0	110.0	101.0
Nb (PPM)	5.0	5.0	4.0	4.0	4.0	5.0	5.0	5.0	5.0	5.0
Mo (PPM)	4.0	4.0	4.0	4.0	4.0	4.0	4.0	4.0	4.0	4.0
Sn (PPM)	3.0	3.0	3.0	3.0	3.0	3.0	3.0	5.0	3.0	3.0
Sb (PPM)	2.0	2.0	3.0	2.0	2.0	2.0	2.0	3.0	1.0	2.0
Cs (PPM)	2.0	1.0	1.0	3.0	4.0	3.0	1.0	1.0	1.0	1.0
Ba (PPM)	499.0	484.0	488.0	513.0	489.0	554.0	583.0	573.0	592.0	589.0
La (PPM)	2.0	0.0	0.0	3.0	0.0	6.0	5.0	5.0	4.0	10.0

Ce (PPM)	32.0	28.0	29.0	37.0	38.0	38.0	33.0	37.0	40.0	43.0
Nd (PPM)	11.0	12.0	13.0	15.0	15.0	18.0	17.0	18.0	15.0	17.0
Tl (PPM)	0.0	0.0	0.0	0.0	0.0	0.0	0.0	0.0	0.0	0.0
Pb (PPM)	6.0	6.0	7.0	7.0	8.0	7.0	9.0	7.0	7.0	9.0
Th (PPM)	5.0	6.0	6.0	5.0	6.0	6.0	7.0	6.0	6.0	7.0
U (PPM)	3.0	3.0	3.0	3.0	3.0	3.0	3.0	3.0	3.0	3.0
SiO2 (%)	68.0	69.1	69.3	70.2	70.0	70.2	72.3	71.7	72.1	72.9
Al2O3 (%)	15.2	15.9	15.9	15.9	15.9	14.7	14.6	14.6	14.7	14.5
TiO2 (%)	0.4	0.4	0.4	0.3	0.3	0.3	0.2	0.3	0.3	0.2
MnO (PPM)	843.0	874.0	820.0	718.0	748.0	593.0	513.0	563.0	563.0	552.0
Fe2O3 (%)	3.5	3.1	3.0	2.4	2.7	2.3	1.8	2.2	2.1	1.9
Na2O (%)	3.9	4.2	4.3	4.3	4.3	4.0	4.2	4.1	4.2	4.2
MgO (%)	1.1	0.9	0.9	0.7	0.8	0.8	0.5	0.6	0.6	0.5
K2O (%)	1.7	1.6	1.6	1.7	1.6	1.9	2.0	2.0	2.0	2.0
CaO (%)	3.3	3.3	3.3	3.2	3.3	3.3	2.6	2.6	2.5	2.6
P2O5 (%)	0.1	0.1	0.1	0.1	0.1	0.1	0.1	0.1	0.1	0.1
S (PPM)	250.0	95.0	23.0	0.0	11.0	124.0	75.0	45.0	55.0	19.0
F (PPM)	164.0	182.0	158.0	133.0	181.0	94.0	226.0	193.0	180.0	201.0
Cl (PPM)	385.0	286.0	275.0	338.0	292.0	505.0	516.0	465.0	552.0	588.0
CO2 (%)	3.3	1.9	1.7	1.6	1.4	2.7	1.9	2.2	1.7	1.5
Sum (%)	100.7	100.7	100.6	100.5	100.6	100.5	100.5	100.5	100.5	100.5
Compton (%)	101.5	102.8	102.7	103.0	103.3	102.4	103.4	102.9	103.2	102.8

Appendix I: Elemental Averages from XRF

		SiO2 (%)	Al2O3 (%)	TiO2 (%)	MnO (%)	Fe2O3 (%)	MgO (%)	CaO (%)	Na2O (%)	P2O5 (%)	SO3 (%)	SrO (%)	BaO (%)	CO2 (%)
RANGI24-1	Ridge	73.92	14.70	0.24	0.05	1.44	0.68	3.72	4.00	0.04	0.00	0.03	0.04	1.11
RANGI24-2	Ridge	71.92	15.62	0.31	0.06	1.91	0.98	4.11	4.30	0.04	0.00	0.03	0.04	0.70
RANGI24-3	Ridge	72.19	14.99	0.22	0.05	1.48	0.53	2.69	4.17	0.05	0.02	0.02	0.06	2.22
RANGI24-4	Ridge	70.85	16.45	0.20	0.04	1.38	0.59	3.77	4.44	0.04	0.02	0.03	0.04	1.73
RANGI24-5	Ridge	71.38	15.79	0.18	0.04	1.53	0.42	3.17	4.38	0.05	0.00	0.03	0.05	1.99
RANGI24-6	Ridge	69.72	16.58	0.27	0.05	1.76	0.64	3.64	4.48	0.05	0.02	0.03	0.05	2.07
RANGI24-6B	Ridge	70.00	16.23	0.25	0.06	2.06	0.68	3.48	4.44	0.06	0.00	0.03	0.05	1.82
RANGI24-7	Ridge	69.80	15.91	0.34	0.08	2.80	0.85	3.26	4.28	0.06	0.00	0.03	0.05	1.65
RANGI24-8	Ridge	72.51	14.63	0.25	0.06	2.01	0.57	2.58	4.19	0.06	0.00	0.02	0.06	1.84
Average	Ridge	71.36	15.65	0.25	0.05	1.82	0.66	3.38	4.30	0.05	0.01	0.03	0.05	1.68
RANGI24-1	Soil	68.20	12.77	0.27	0.06	1.85	0.59	1.94	3.41	0.10	0.05	0.01	0.07	8.78
RANGI24-2	Soil	68.14	13.23	0.27	0.06	1.82	0.56	1.99	3.53	0.11	0.03	0.01	0.06	8.34
RANGI24-3	Soil	67.82	13.91	0.31	0.07	2.24	0.83	2.93	3.71	0.25	0.04	0.02	0.05	6.61
RANGI24-4	Soil	66.35	14.42	0.35	0.07	2.46	0.98	3.41	3.67	0.16	0.03	0.02	0.05	7.14
RANGI24-5	Soil	67.44	14.82	0.31	0.07	2.71	0.97	3.60	3.88	0.17	0.02	0.02	0.05	4.91
RANGI24-6	Soil	65.93	12.95	0.29	0.08	2.49	0.67	2.38	3.45	0.23	0.05	0.02	0.06	9.67
RANGI24-6B	Soil	65.66	15.42	0.39	0.08	3.27	1.31	3.92	3.88	0.11	0.03	0.03	0.05	5.00
RANGI24-7	Soil	68.02	15.17	0.44	0.09	3.46	1.14	3.28	3.95	0.10	0.01	0.03	0.05	3.27
RANGI24-8	Soil	70.52	14.75	0.25	0.06	2.31	0.85	3.28	4.05	0.08	0.00	0.02	0.05	2.73
Average	Soil	67.57	14.16	0.32	0.07	2.51	0.88	2.97	3.73	0.15	0.03	0.02	0.06	6.27
Average	Coast	73.18	13.80	0.20	0.06	1.86	0.56	2.72	4.13	2.19	0.06	0.01	0.02	0.06

		Sc (PPM)	V (PPM)	Cr (PPM)	Co (PPM)	Ni (PPM)	Cu (PPM)	Zn (PPM)	Ga (PPM)	As (PPM)	Rb (PPM)	Sr (PPM)	Y (PPM)	Zr (PPM)	Nb (PPM)	Mo (PPM)	Sn (PPM)
RANGI24-1	Ridge	6.50	16.50	16.00	49.25	5.25	5.00	28.75	15.75	4.75	25.25	301.00	6.75	59.75	3.00	4.00	3.25
RANGI24-2	Ridge	8.50	19.25	8.75	48.25	6.00	5.25	39.50	16.25	4.75	26.25	322.00	8.00	70.25	3.25	4.00	3.00
RANGI24-3	Ridge	6.50	15.75	6.25	47.75	6.00	5.75	34.50	15.50	5.75	60.75	238.25	13.00	100.75	4.75	4.00	4.25
RANGI24-4	Ridge	6.50	17.75	19.25	47.25	6.00	5.75	32.50	17.00	5.00	37.50	319.75	9.00	75.50	3.00	4.00	4.00
RANGI24-5	Ridge	6.00	16.75	3.00	43.00	4.50	5.00	29.75	16.00	7.25	53.25	274.50	11.00	82.50	4.00	4.00	3.75
RANGI24-6	Ridge	6.75	23.00	11.25	47.25	5.25	6.50	38.75	16.75	7.75	55.50	264.00	13.00	101.25	4.75	4.00	3.75
RANGI24-6B	Ridge	7.25	22.50	14.50	44.50	5.00	5.75	38.00	17.00	7.50	48.25	300.25	10.25	86.75	4.00	4.00	4.00
RANGI24-7	Ridge	9.00	30.25	12.50	46.00	6.75	6.00	48.25	17.00	8.00	55.50	296.75	12.00	104.00	4.25	4.00	3.00
RANGI24-8	Ridge	6.50	22.75	5.75	51.50	6.25	5.25	39.50	15.75	8.75	67.50	238.75	14.25	105.50	5.00	4.00	3.50
Average	Ridge	7.06	20.50	10.81	47.19	5.67	5.58	36.61	16.33	6.61	47.75	283.92	10.81	87.36	4.00	4.00	3.61
RANGI24-1	Soil	7.43	24.57	3.43	41.00	3.86	6.43	37.71	15.00	7.43	74.00	145.71	19.29	121.71	5.71	4.00	3.29
RANGI24-2	Soil	8.14	26.71	1.29	42.00	3.86	7.71	46.29	15.29	8.29	81.86	132.14	21.86	136.71	6.43	4.00	3.86
RANGI24-3	Soil	8.60	37.00	7.40	39.20	4.60	10.40	56.40	15.60	7.80	66.60	200.80	16.20	115.20	5.20	4.00	3.80
RANGI24-4	Soil	10.67	44.00	8.00	49.00	4.67	8.33	48.33	16.00	7.33	56.67	223.00	16.00	120.67	5.00	4.00	4.33
RANGI24-5	Soil	9.67	43.00	3.67	38.33	4.00	7.67	45.67	16.67	8.33	57.67	241.33	14.67	103.67	4.67	4.00	4.67
RANGI24-6	Soil	8.00	32.67	4.00	39.33	5.00	11.67	75.67	15.67	9.67	75.33	156.00	19.67	124.67	5.67	4.00	4.00
RANGI24-6B	Soil	12.00	56.50	6.00	41.50	6.00	7.50	50.00	17.00	9.50	52.00	270.00	12.00	101.00	4.00	4.00	2.50
RANGI24-7	Soil	11.00	43.00	55.00	42.00	7.00	5.00	51.00	17.00	9.00	58.00	261.00	13.00	118.00	5.00	4.00	3.00
RANGI24-8	Soil	9.00	37.00	70.00	66.00	8.00	6.00	42.00	15.00	10.00	64.00	240.00	14.00	92.00	5.00	4.00	3.00
Average	Soil	9.39	38.27	17.64	44.26	5.22	7.86	50.34	15.91	8.59	65.12	207.78	16.30	114.85	5.19	4.00	3.60
Average	Coast	6.83	23.17	3.33	63.17	5.83	5.17	37.33	14.83	10.17	71.50	204.83	16.83	100.50	4.83	4.00	2.67

		Sb (PPM)	Cs (PPM)	Ba (PPM)	La (PPM)	Ce (PPM)	Nd (PPM)	Tl (PPM)	Pb (PPM)	Th (PPM)	U (PPM)	S (PPM)	F (PPM)	Cl (PPM)
RANGI24-1	Ridge	2.25	2.00	374.25	0.00	21.00	9.25	0.00	4.00	4.00	3.00	35.00	37.75	226.50
RANGI24-2	Ridge	1.50	1.25	393.75	0.00	24.50	10.00	0.00	3.25	4.25	3.00	41.75	36.00	224.00
RANGI24-3	Ridge	1.75	1.00	575.75	3.00	35.25	14.25	0.25	8.00	6.75	3.00	384.50	144.50	553.00
RANGI24-4	Ridge	2.75	1.00	454.25	1.00	26.00	10.75	0.00	5.75	4.00	3.00	286.25	90.75	295.75
RANGI24-5	Ridge	2.75	3.25	543.50	0.75	29.25	15.25	0.00	6.75	5.25	3.00	93.25	152.00	449.25
RANGI24-6	Ridge	1.75	1.00	543.50	1.75	34.50	14.50	0.25	7.25	6.00	3.00	352.25	154.50	512.25
RANGI24-6B	Ridge	2.00	2.25	499.25	0.00	32.75	13.50	0.00	6.00	5.00	3.00	37.75	138.00	331.75
RANGI24-7	Ridge	2.25	2.25	493.50	0.75	33.00	13.75	0.00	7.00	5.75	3.00	32.25	163.50	297.75
RANGI24-8	Ridge	2.00	1.00	584.25	6.00	38.25	16.75	0.00	8.00	6.50	3.00	48.50	200.00	530.25
Average	Ridge	2.11	1.67	495.78	1.47	30.50	13.11	0.06	6.22	5.28	3.00	145.72	124.11	380.06
RANGI24-1	Soil	2.00	1.71	619.29	8.86	44.14	19.57	0.71	10.43	9.14	3.00	1170.57	157.00	780.86
RANGI24-2	Soil	2.29	2.14	656.43	11.57	47.71	21.29	0.71	11.57	9.71	3.00	1118.14	199.43	946.29
RANGI24-3	Soil	1.80	2.20	562.80	6.00	39.20	17.40	0.00	8.00	7.20	3.00	965.80	170.20	650.80
RANGI24-4	Soil	2.33	3.33	510.00	5.33	35.00	16.67	0.33	8.33	6.33	3.00	868.00	244.00	572.33
RANGI24-5	Soil	3.00	3.33	515.67	3.67	32.33	14.33	0.00	7.33	6.00	3.00	545.67	220.67	569.33
RANGI24-6	Soil	2.33	1.33	608.67	5.67	45.00	18.00	1.00	11.67	9.00	3.00	1461.67	166.67	791.00
RANGI24-6B	Soil	1.50	4.50	488.50	1.50	32.50	10.50	0.00	7.50	5.50	3.00	624.50	115.00	484.50
RANGI24-7	Soil	2.00	2.00	499.00	2.00	32.00	11.00	0.00	6.00	5.00	3.00	250.00	164.00	385.00
RANGI24-8	Soil	2.00	3.00	554.00	6.00	38.00	18.00	0.00	7.00	6.00	3.00	124.00	94.00	505.00
Average	Soil	2.14	2.62	557.15	5.62	38.43	16.31	0.31	8.65	7.10	3.00	792.04	170.11	631.68
Average	Coast	1.50	1.33	611.33	8.67	44.17	18.50	0.33	8.67	7.83	3.00	2477.17	175.50	2593.00

Appendix J: X-Ray Diffraction Diffractograms

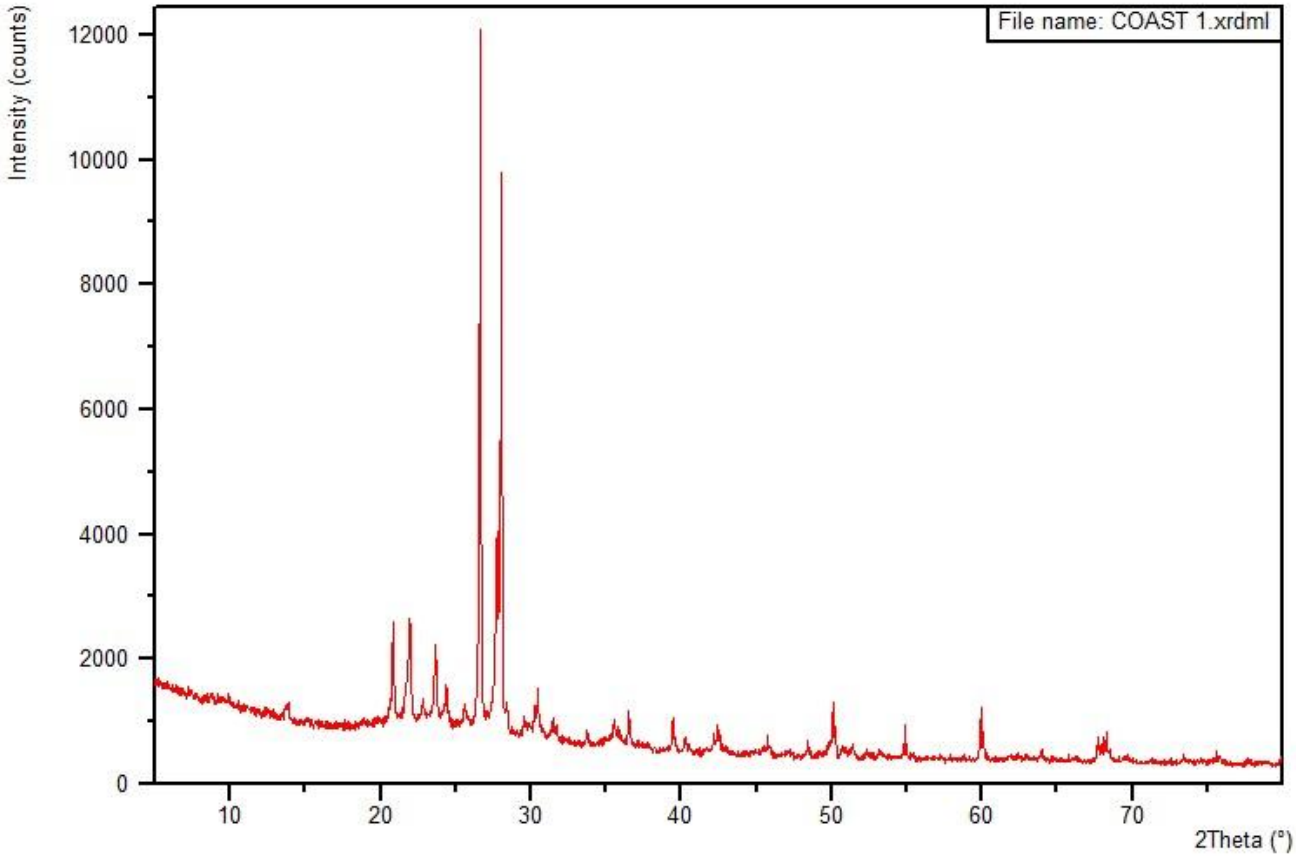

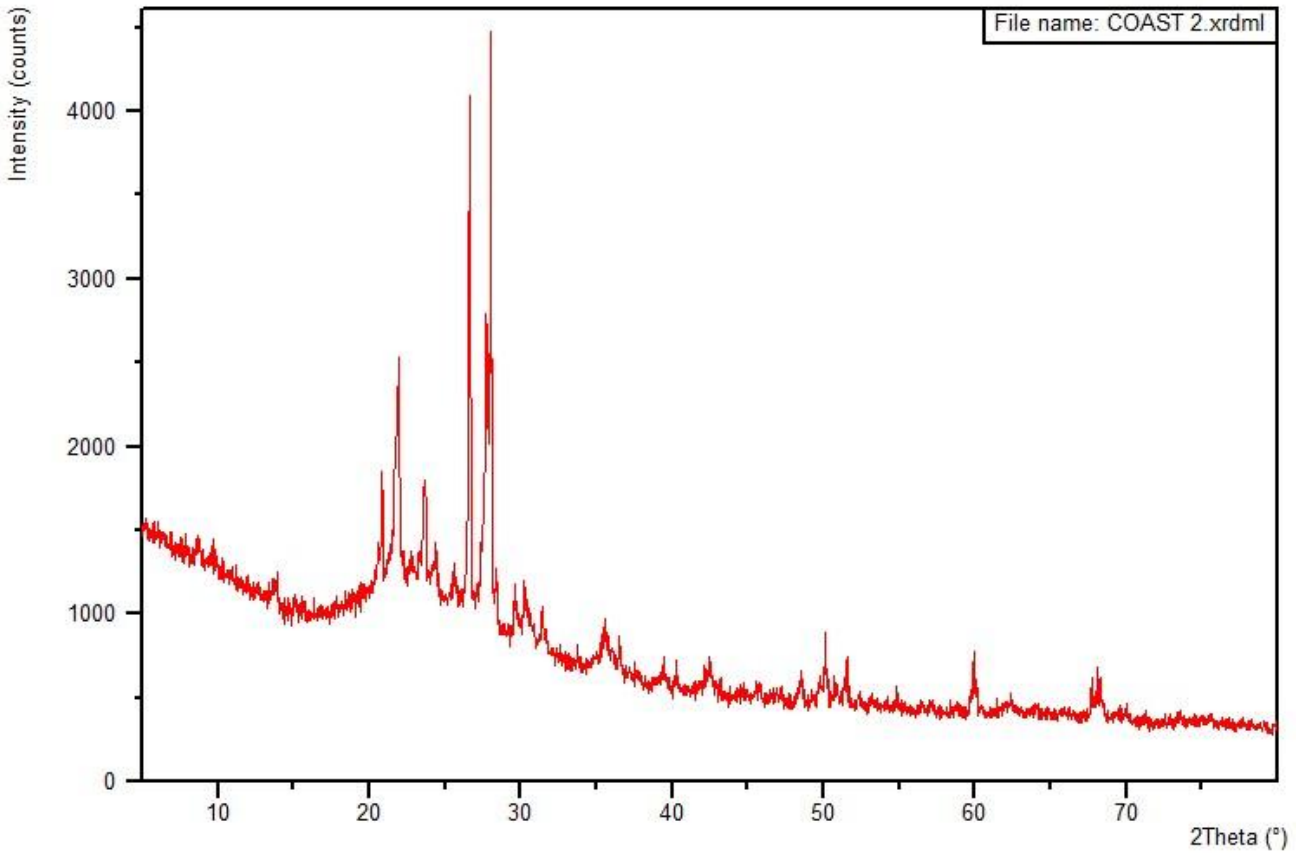

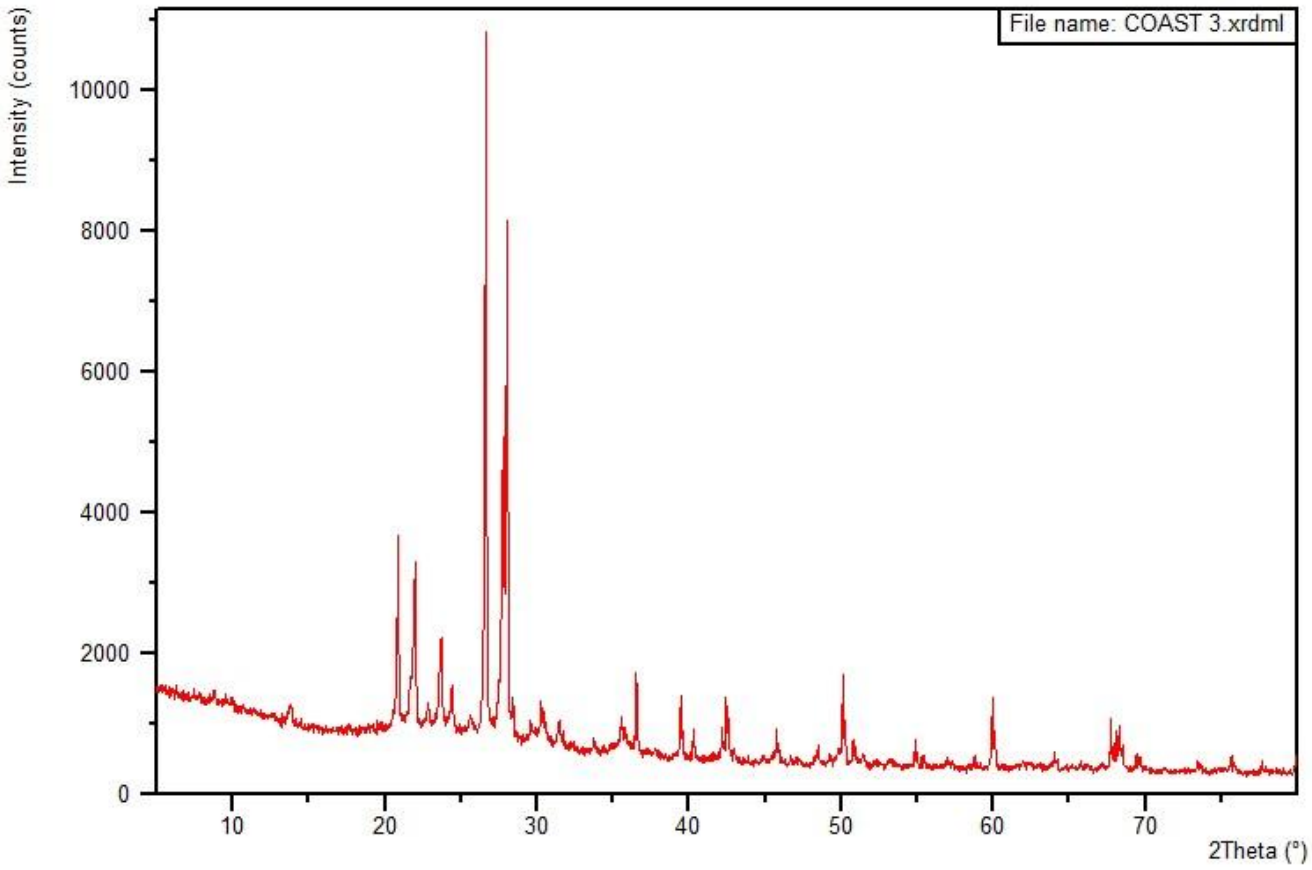
File name: COAST 3.xrdml
Intensity (counts)
10000
8000
6000
4000
2000
0
10
20
30
40
50
60
70
2Theta (°)

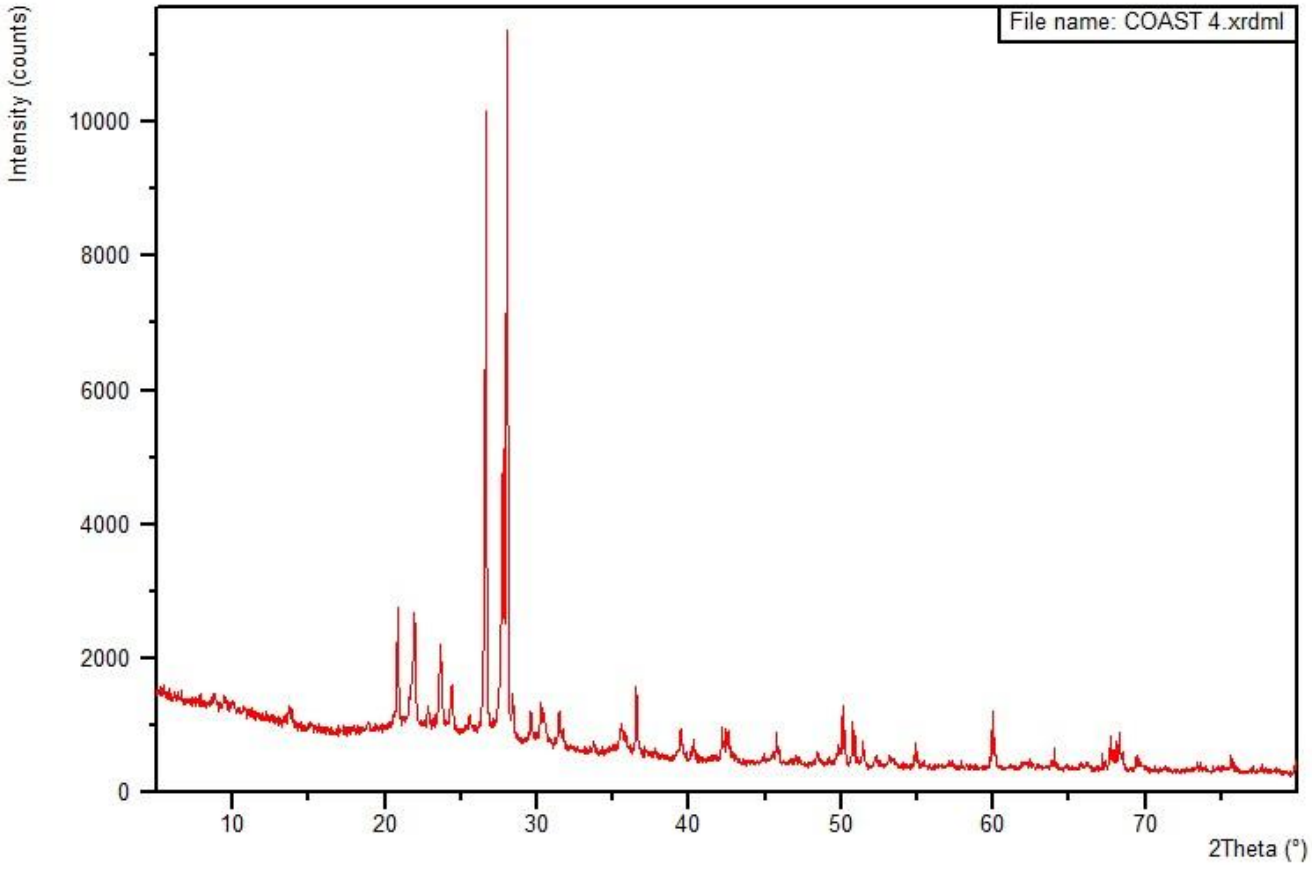
File name: COAST 4.xrdml
Intensity (counts)
10000
8000
6000
4000
2000
0
10
20
30
40
50
60
70
2Theta (°)

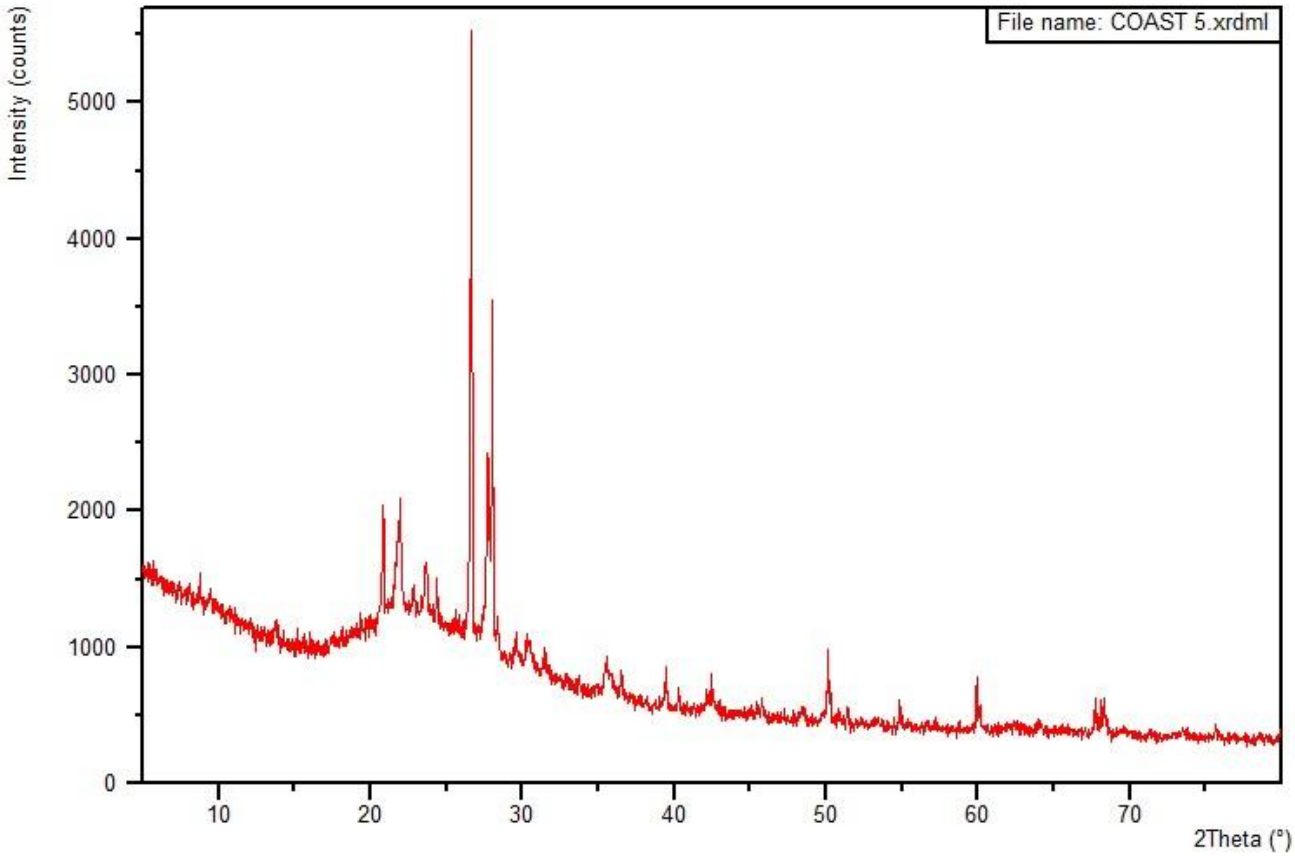
File name: COAST 5.xrdml
Intensity (counts)
5000
4000
3000
2000
1000
0
10
20
30
40
50
60
70
2Theta (°)

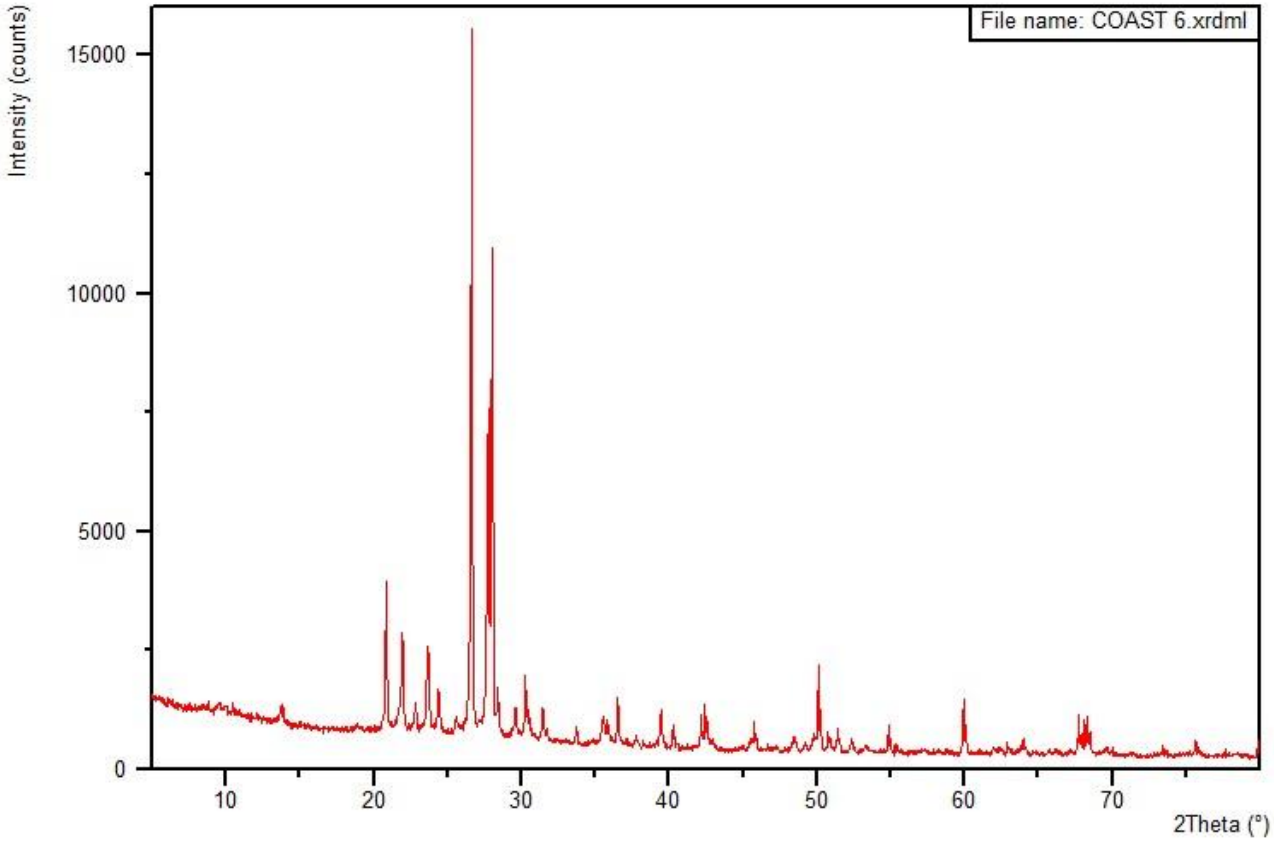
File name: COAST 6.xrdml
Intensity (counts)
15000
10000
5000
0
10
20
30
40
50
60
70
2Theta (°)

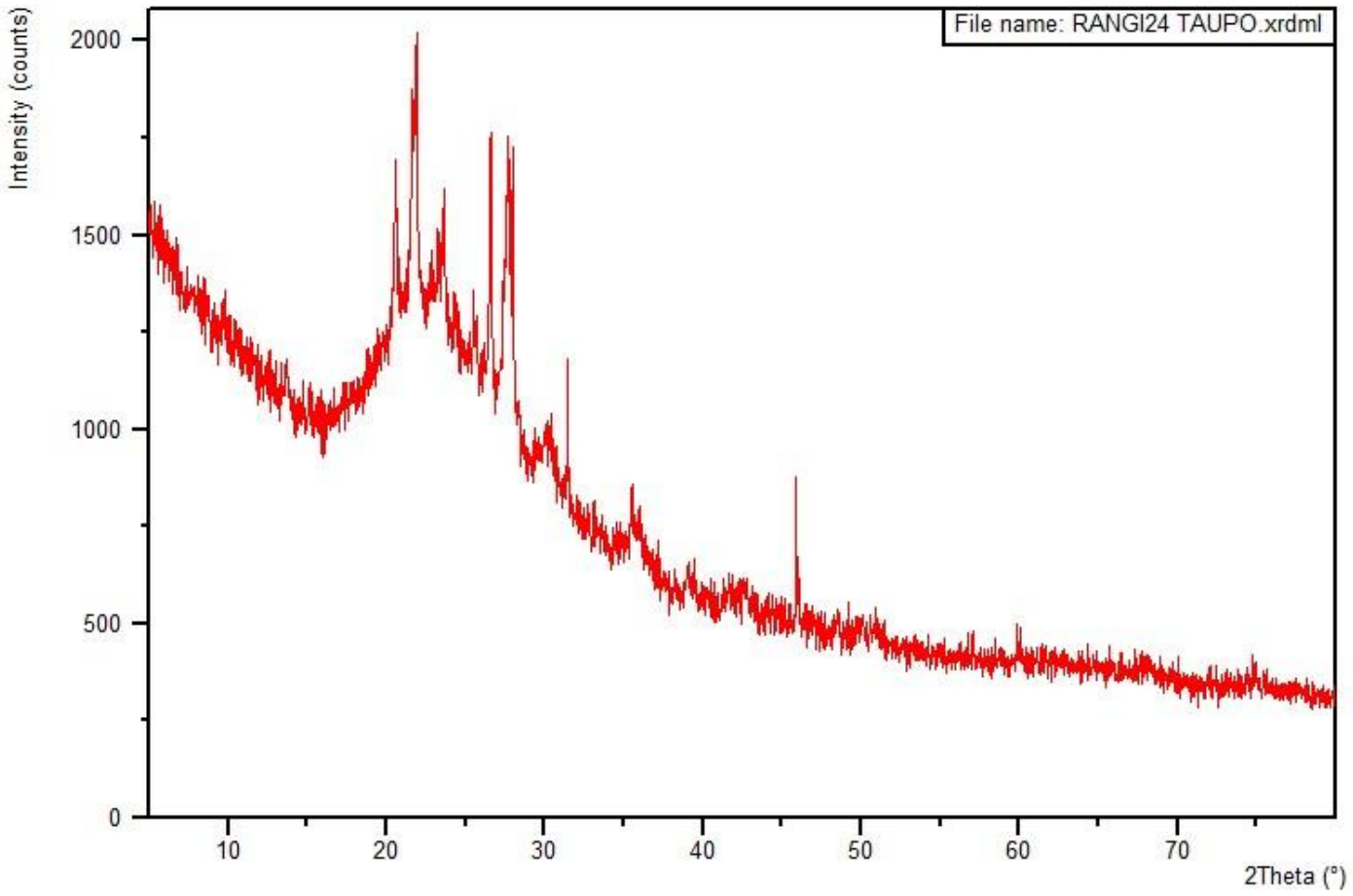
File name: RANGI24 TAUPO.xrdml
Intensity (counts)
2000
1500
1000
500
0
10
20
30
40
50
60
70
2Theta (°)

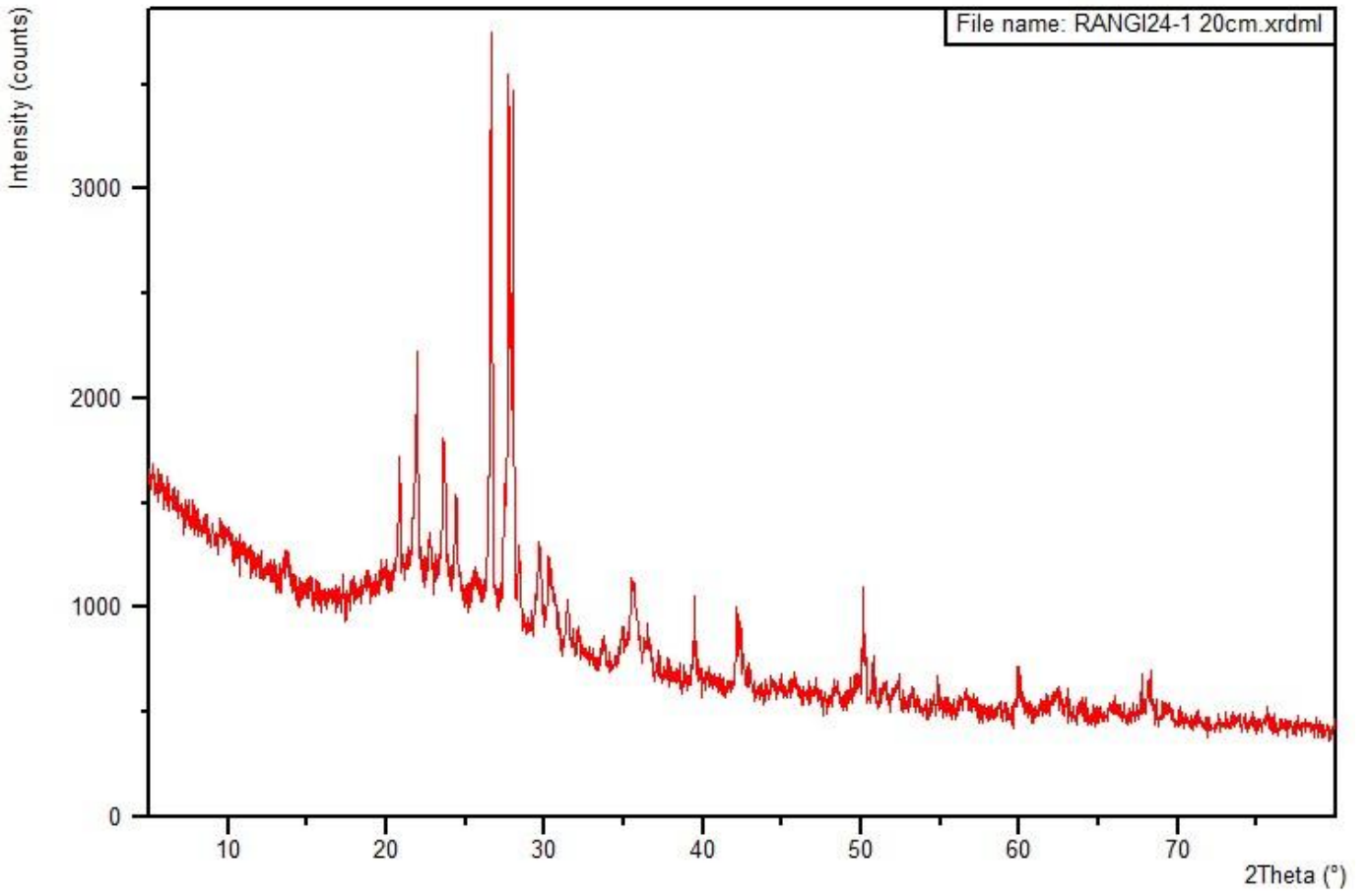
File name: RANGI24-1 20cm.xrdml
Intensity (counts)
3000
2000
1000
0
10
20
30
40
50
60
70
2Theta (°)

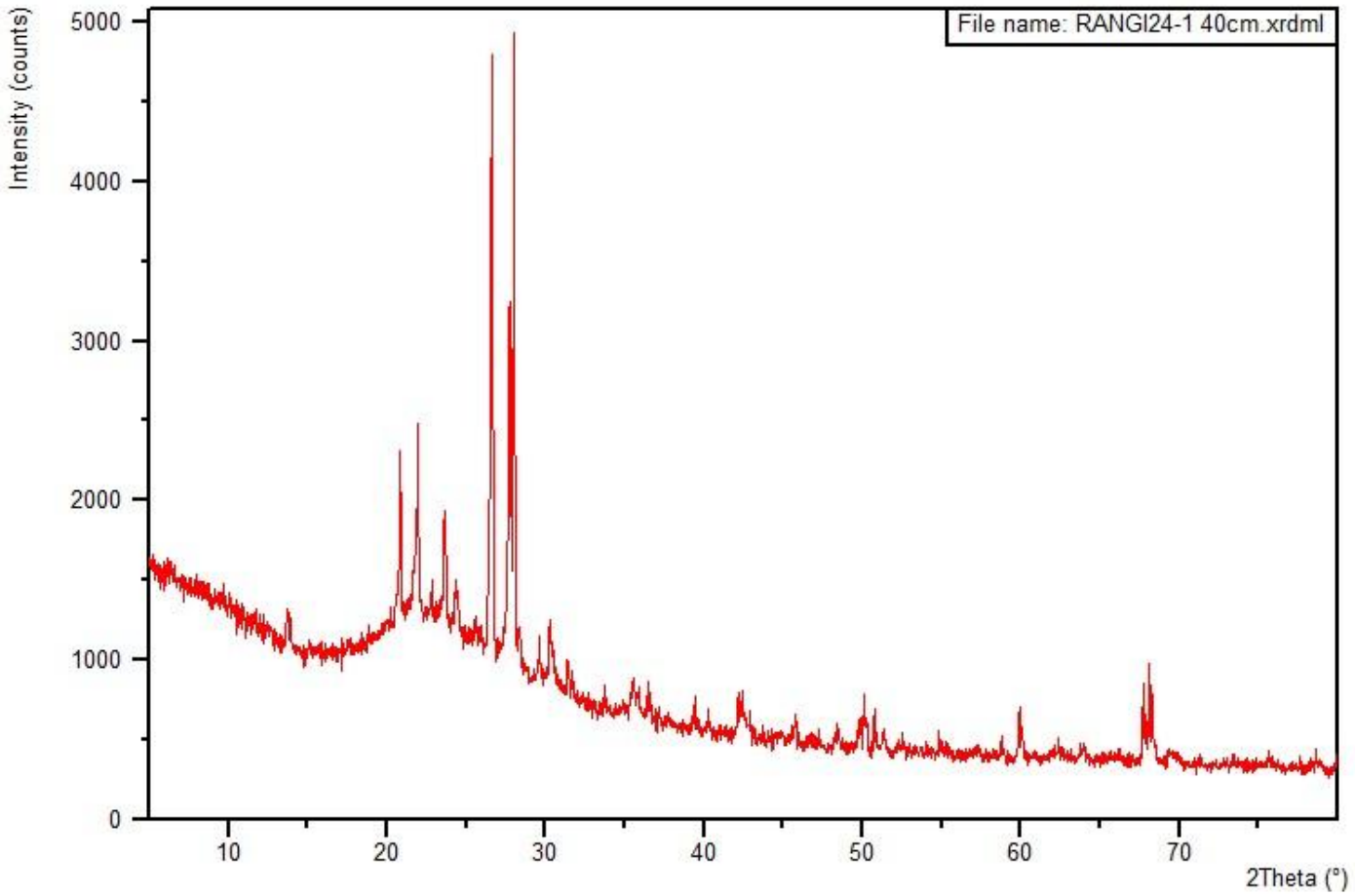
File name: RANGI24-1 40cm.xrdml
Intensity (counts)
5000
4000
3000
2000
1000
0
10
20
30
40
50
60
70
2Theta (°)

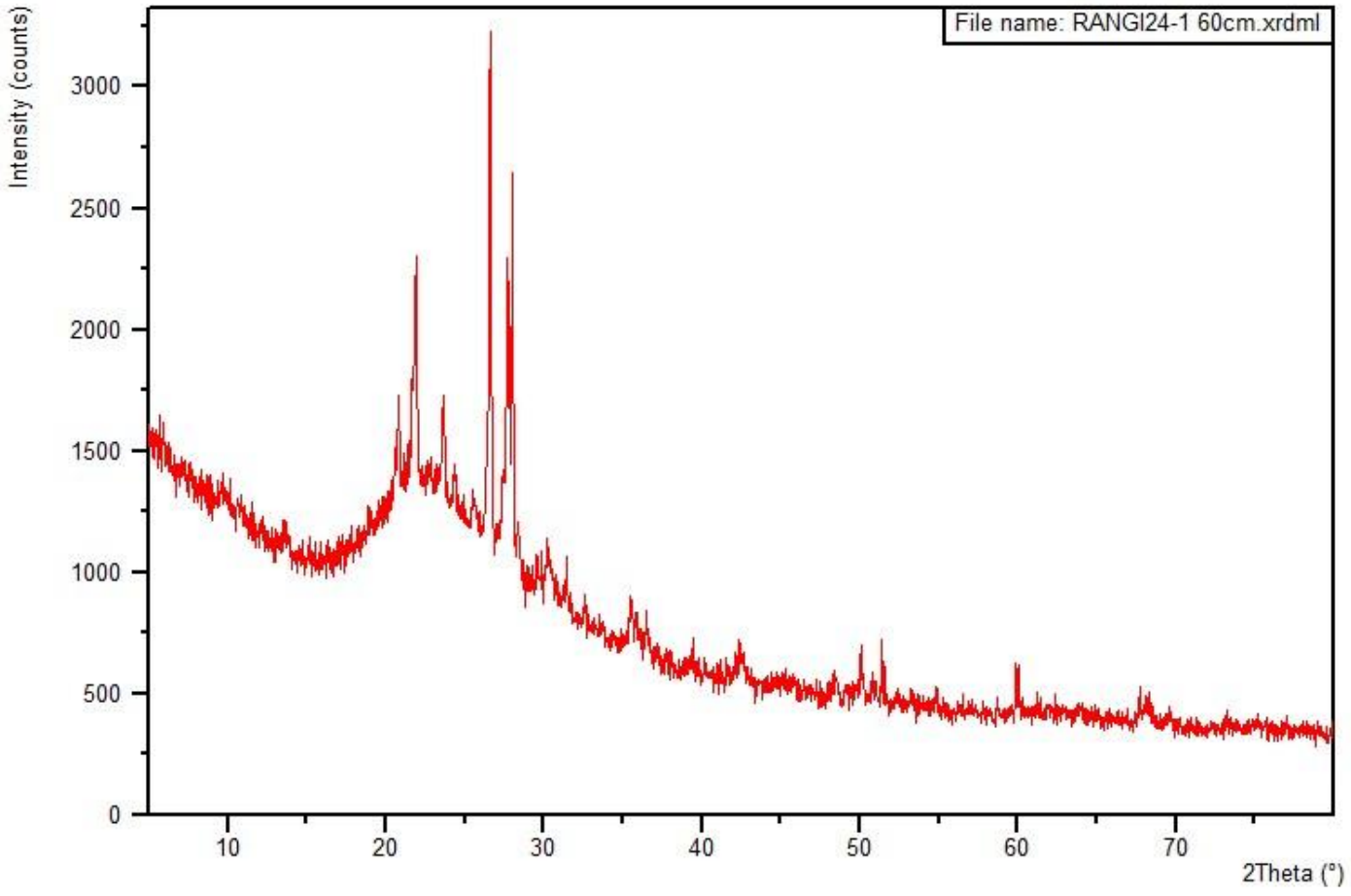
File name: RANGI24-1 60cm.xrdml
Intensity (counts)
3000
2500
2000
1500
1000
500
0
10
20
30
40
50
60
70
2Theta (°)

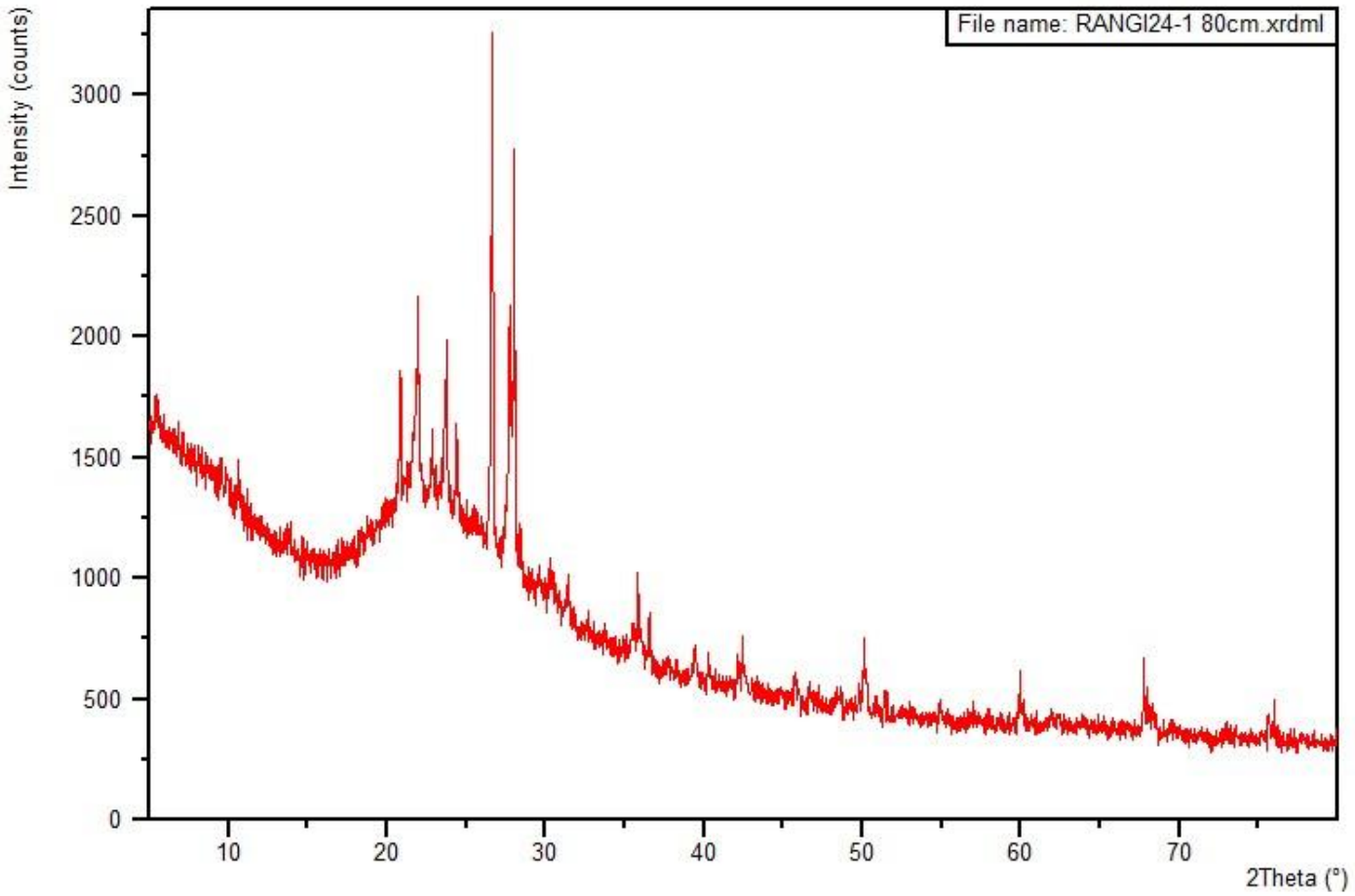
File name: RANGI24-1 80cm.xrdml
Intensity (counts)
3000
2500
2000
1500
1000
500
0
10
20
30
40
50
60
70
2Theta (°)

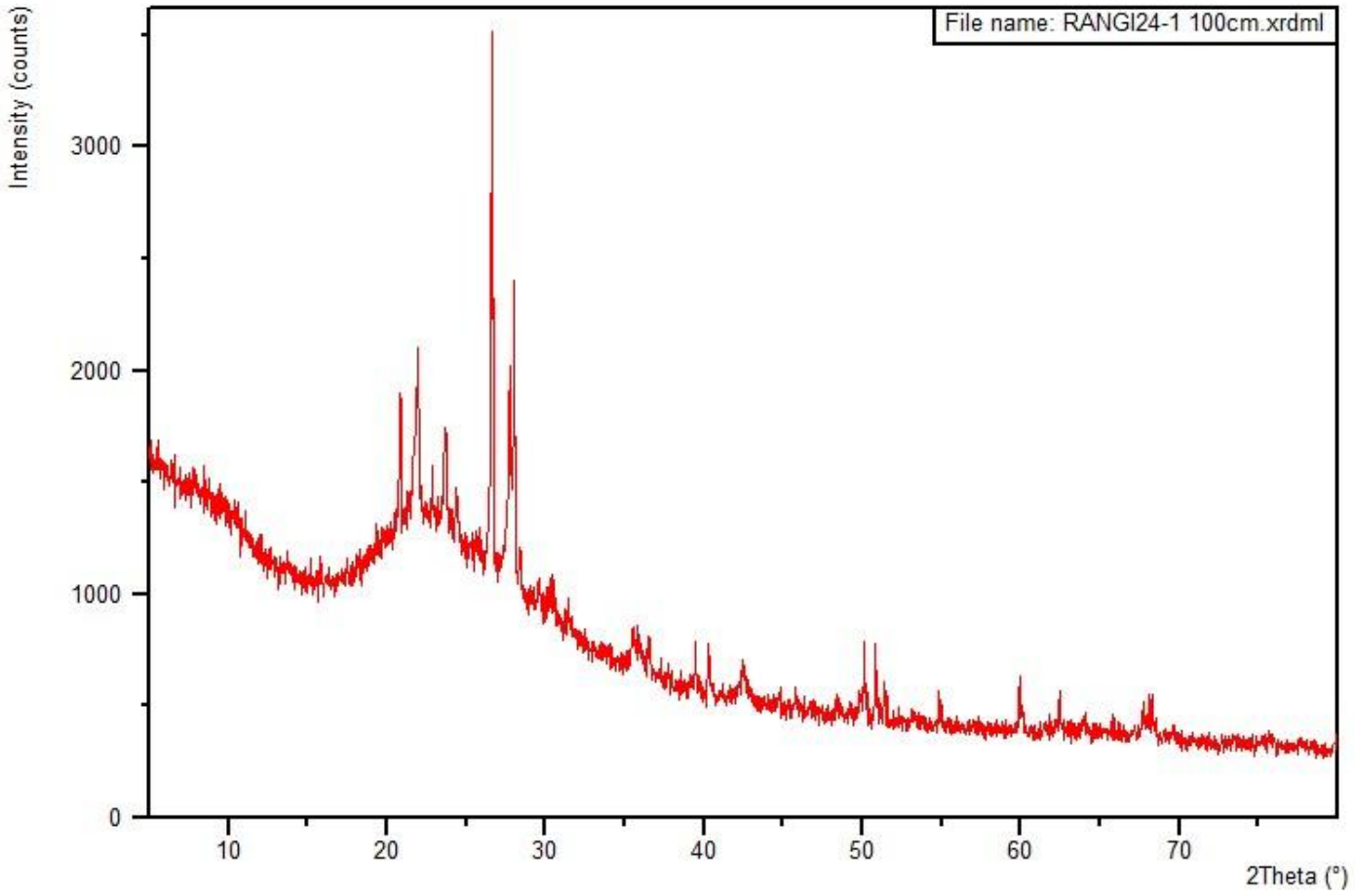
File name: RANGI24-1 100cm.xrdml
Intensity (counts)
3000
2000
1000
0
10
20
30
40
50
60
70
2Theta (°)

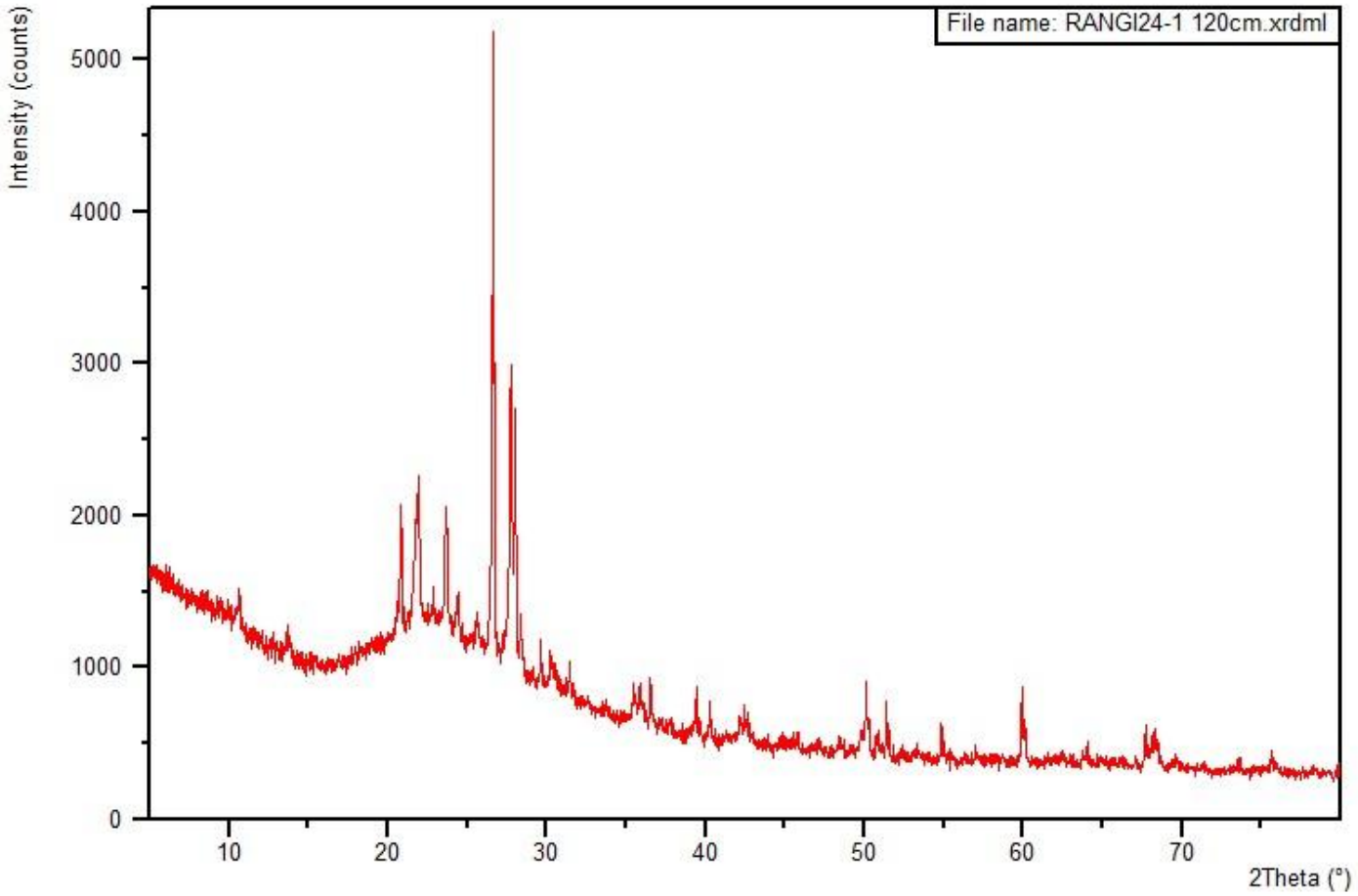
File name: RANGI24-1 120cm.xrdml
Intensity (counts)
5000
4000
3000
2000
1000
0
10
20
30
40
50
60
70
2Theta (°)

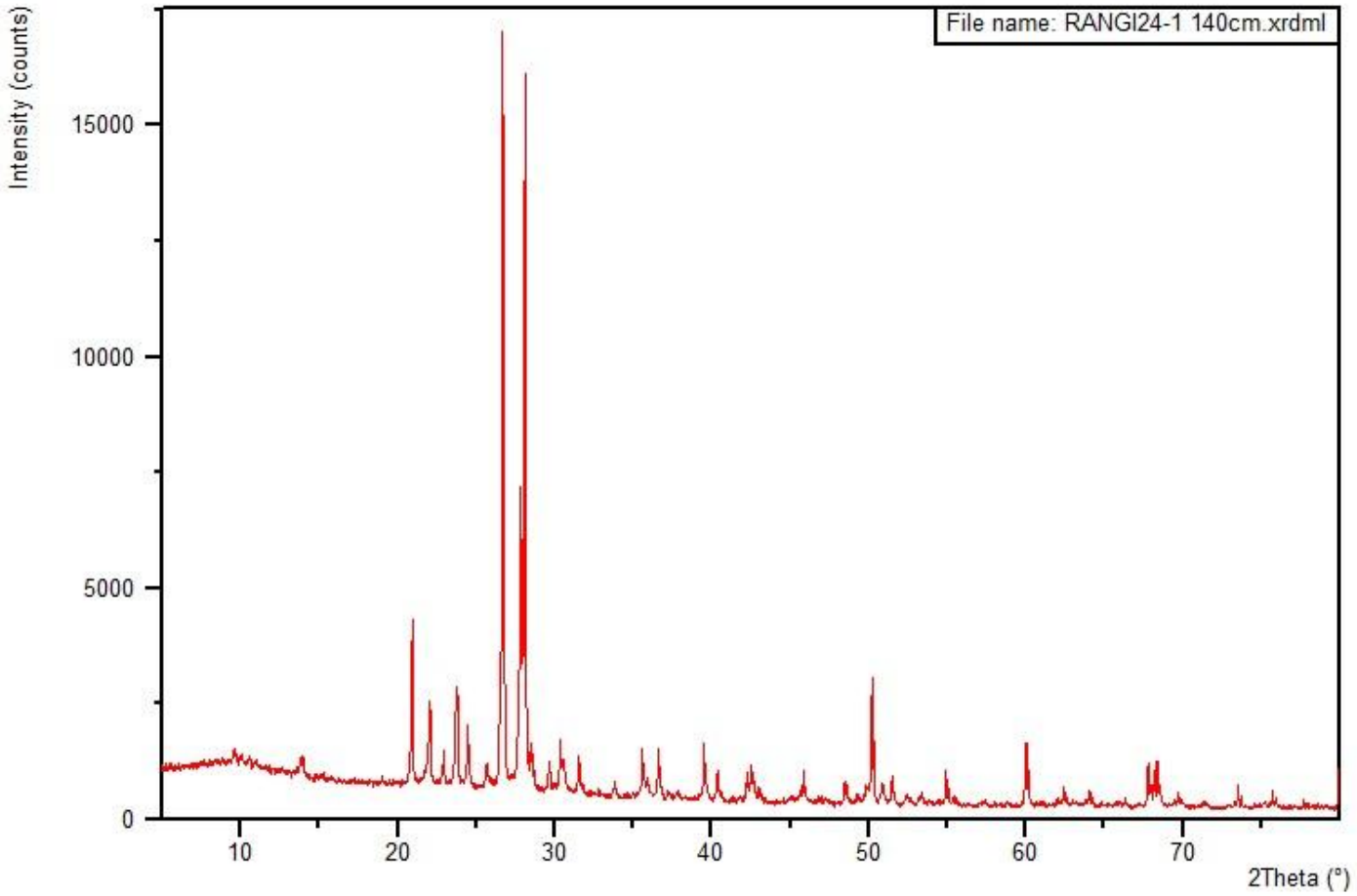
File name: RANGI24-1 140cm.xrdml
Intensity (counts)
15000
10000
5000
0
10
20
30
40
50
60
70
2Theta (°)

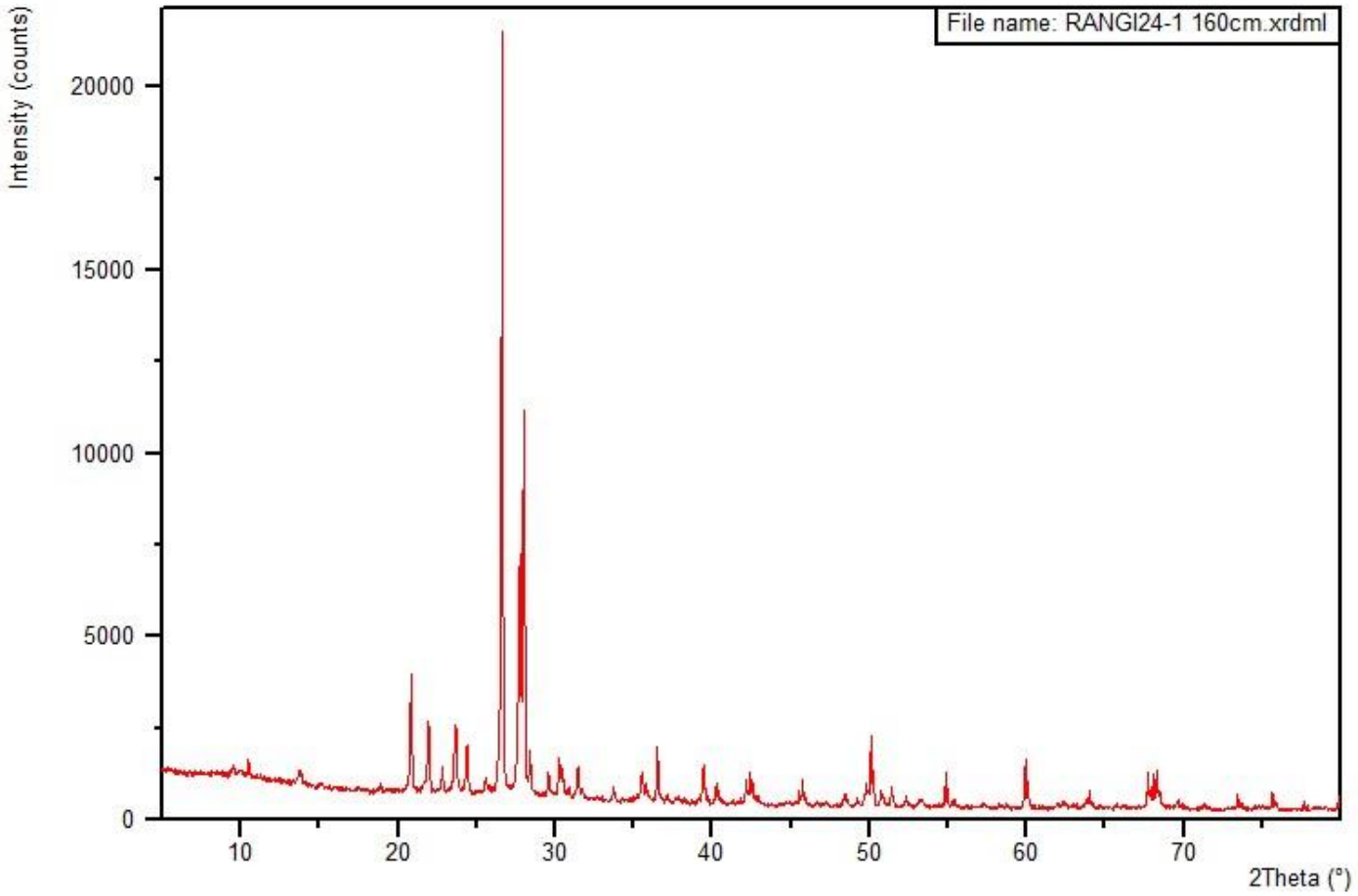
File name: RANGI24-1 160cm.xrdml
Intensity (counts)
20000
15000
10000
5000
0
10
20
30
40
50
60
70
2Theta (°)

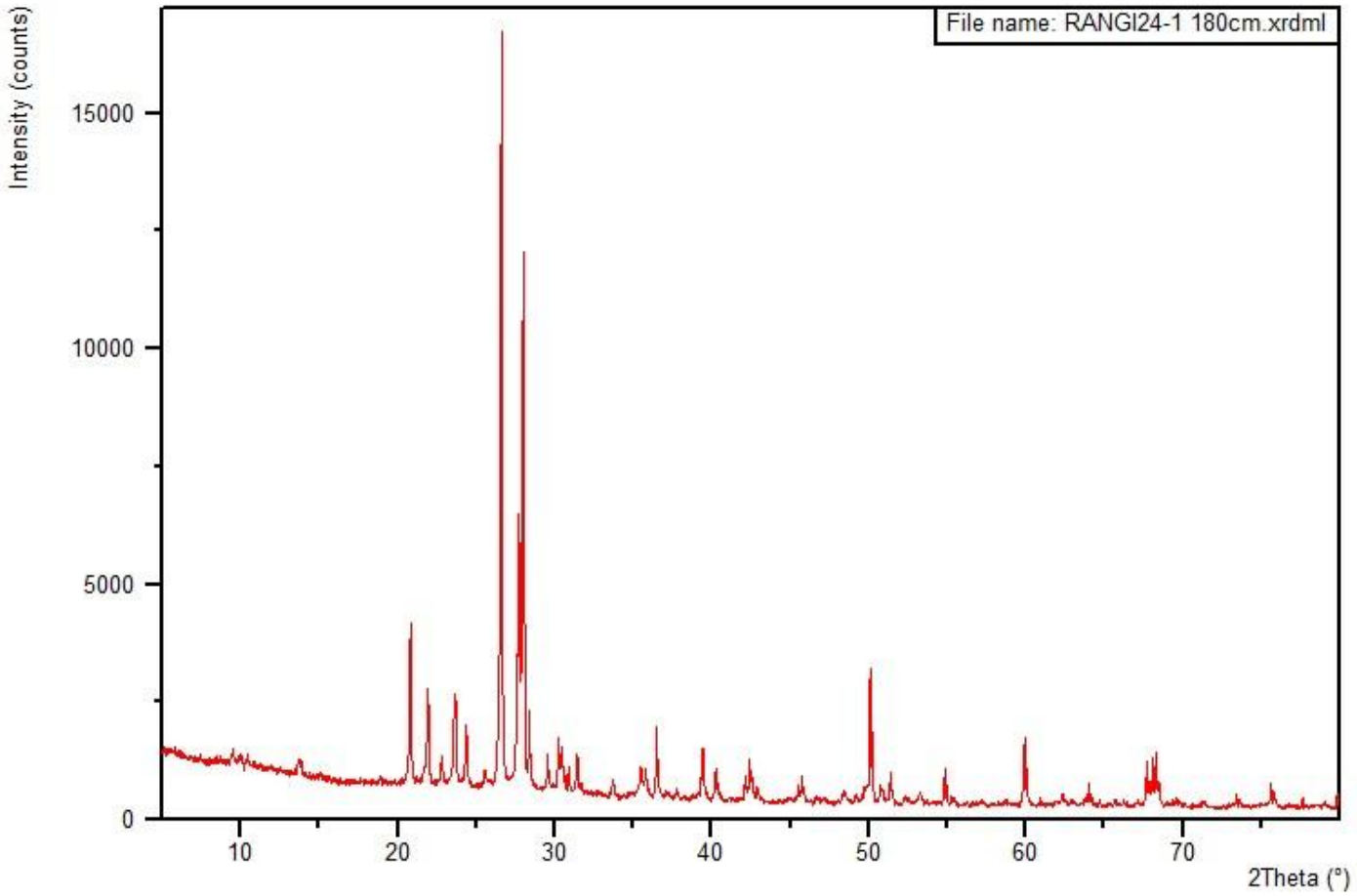
File name: RANGI24-1 180cm.xrdml
Intensity (counts)
15000
10000
5000
0
10
20
30
40
50
60
70
2Theta (°)

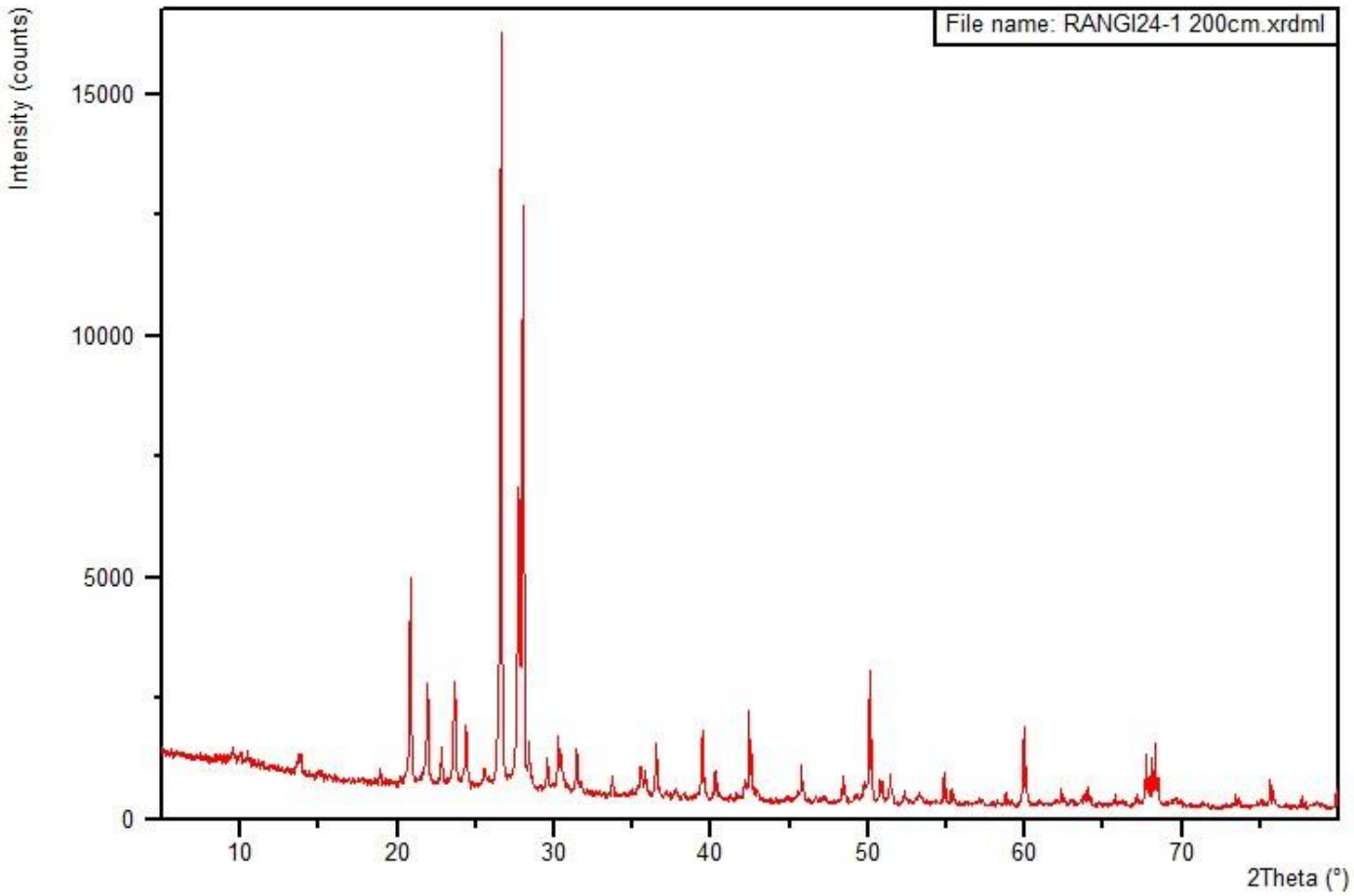
File name: RANGI24-1 200cm.xrdml
Intensity (counts)
15000
10000
5000
0
10
20
30
40
50
60
70
2Theta (°)

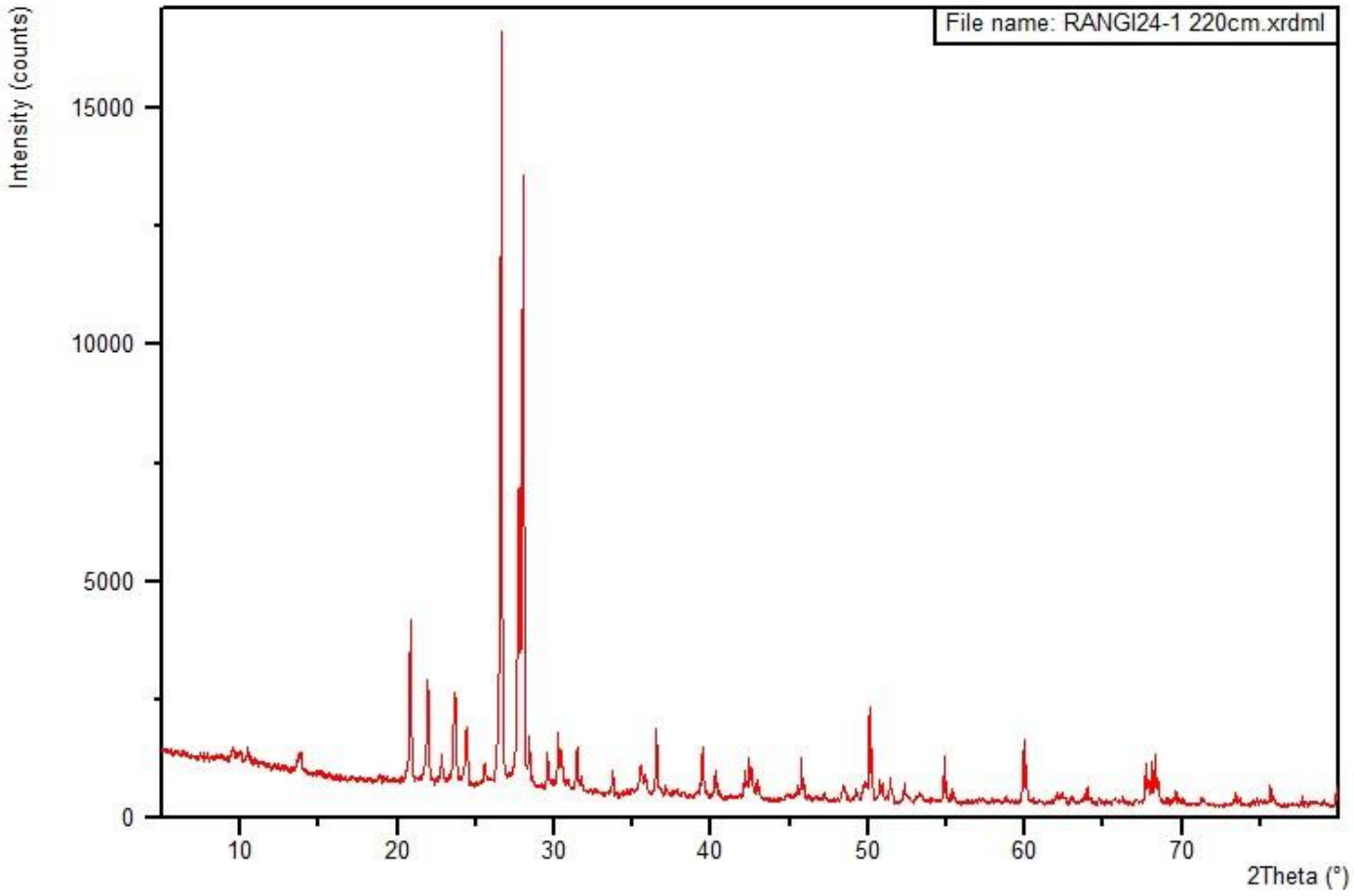
File name: RANGI24-1 220cm.xrdml
Intensity (counts)
15000
10000
5000
0
10
20
30
40
50
60
70
2Theta (°)

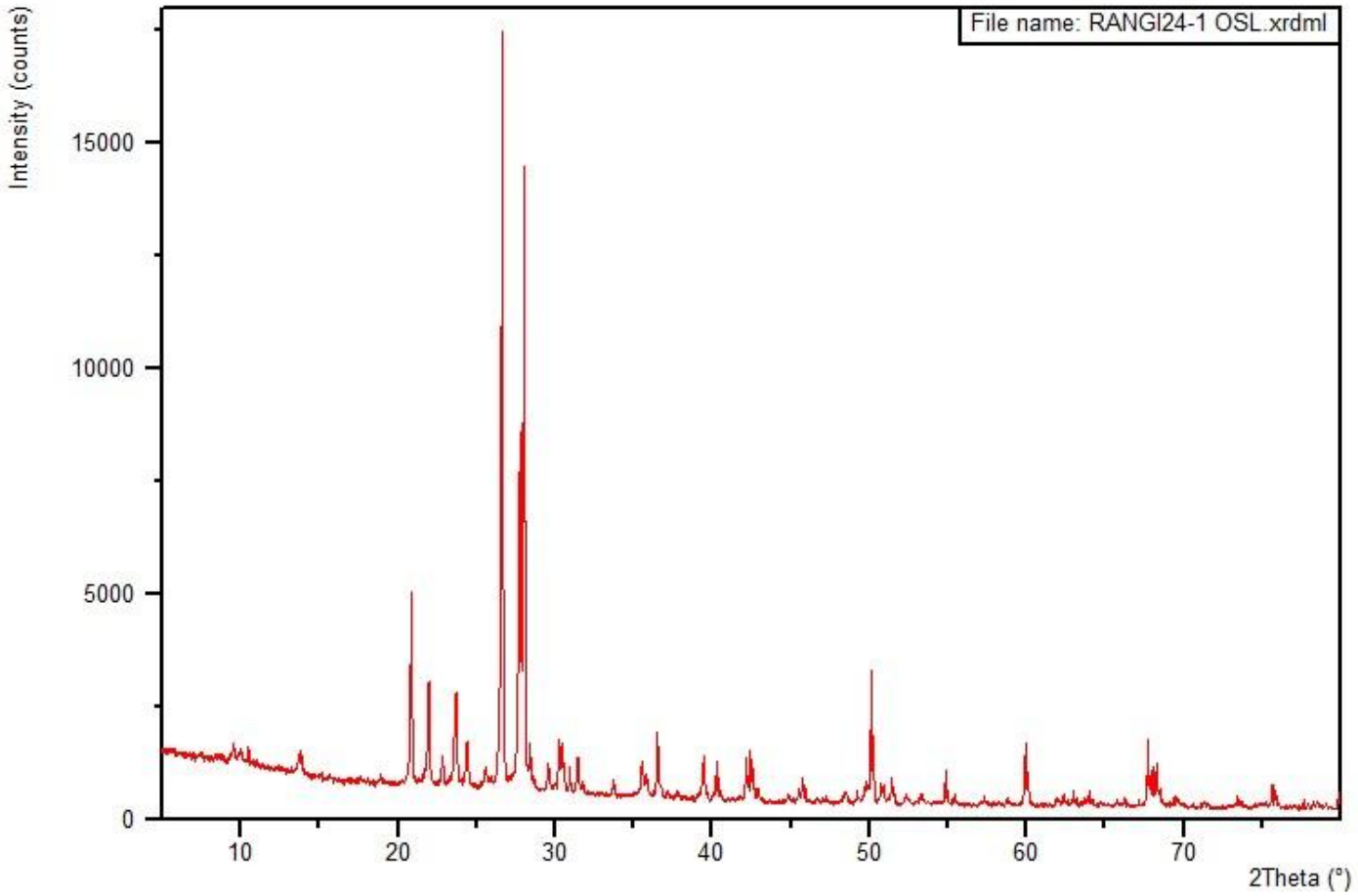
File name: RANGI24-1 OSL.xrdml
Intensity (counts)
15000
10000
5000
0
10
20
30
40
50
60
70
2Theta (°)

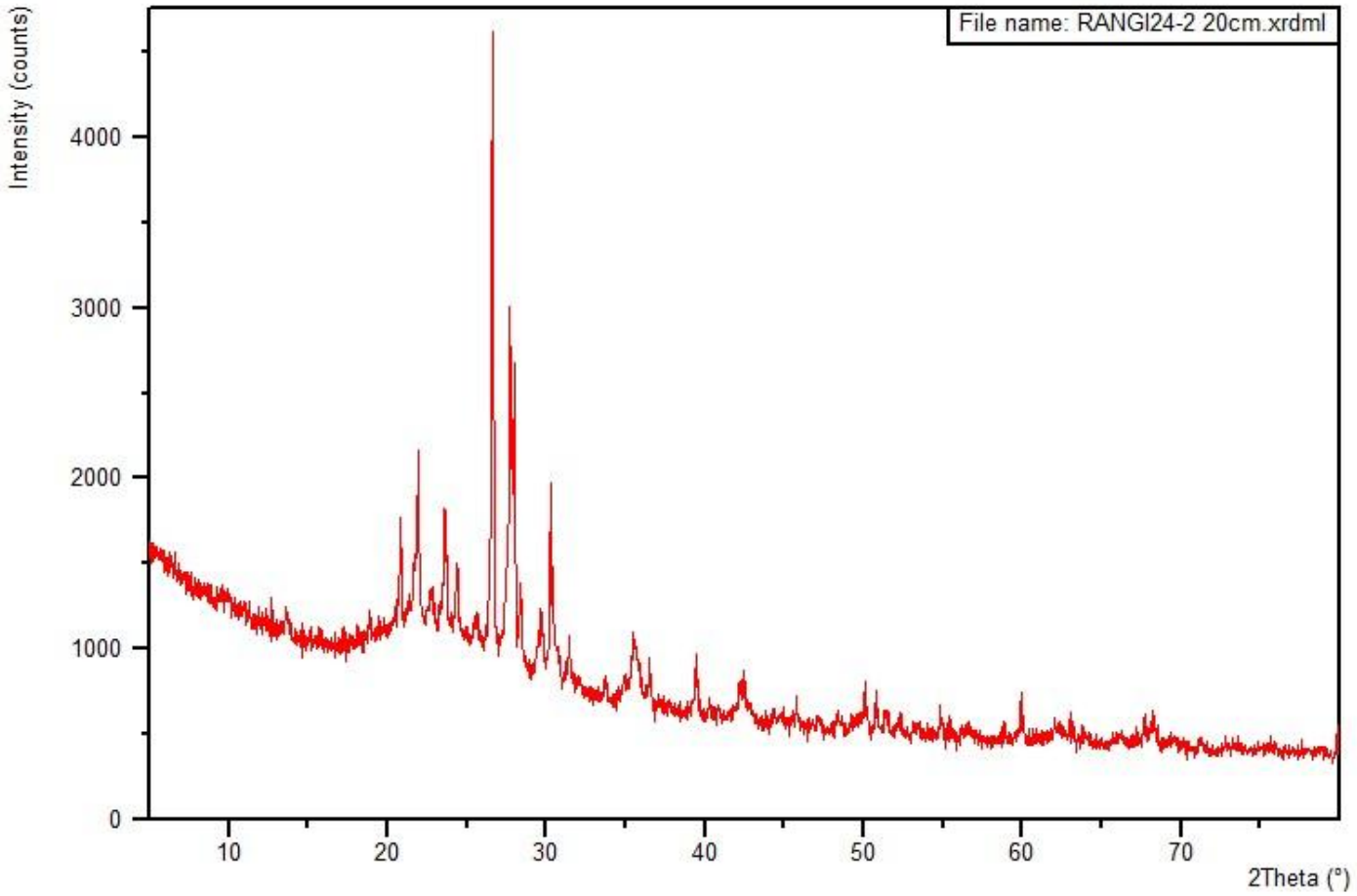
File name: RANGI24-2 20cm.xrdml
Intensity (counts)
4000
3000
2000
1000
0
10
20
30
40
50
60
70
2Theta (°)

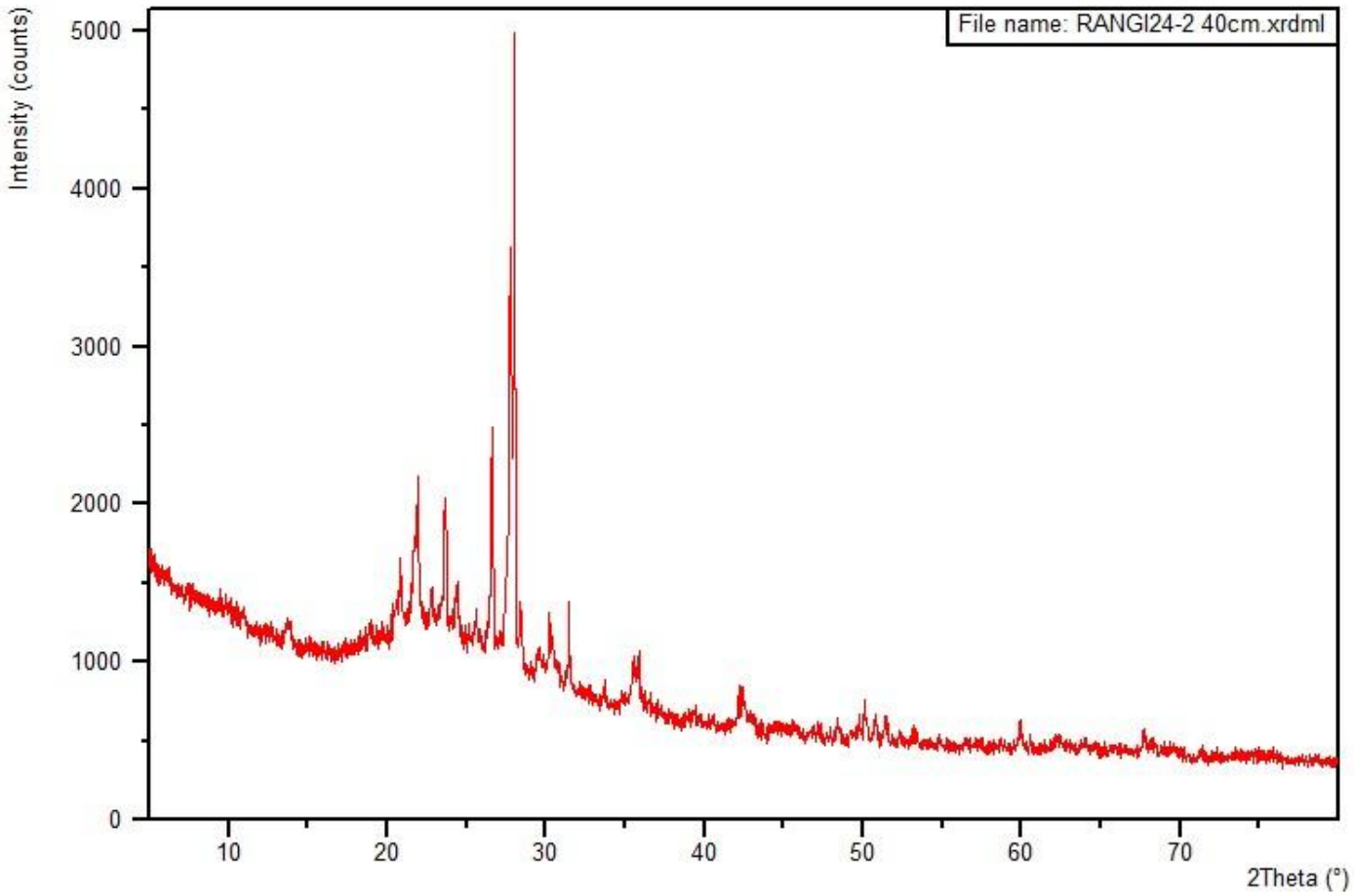
File name: RANGI24-2 40cm.xrdml
Intensity (counts)
5000
4000
3000
2000
1000
0
10
20
30
40
50
60
70
2Theta (°)

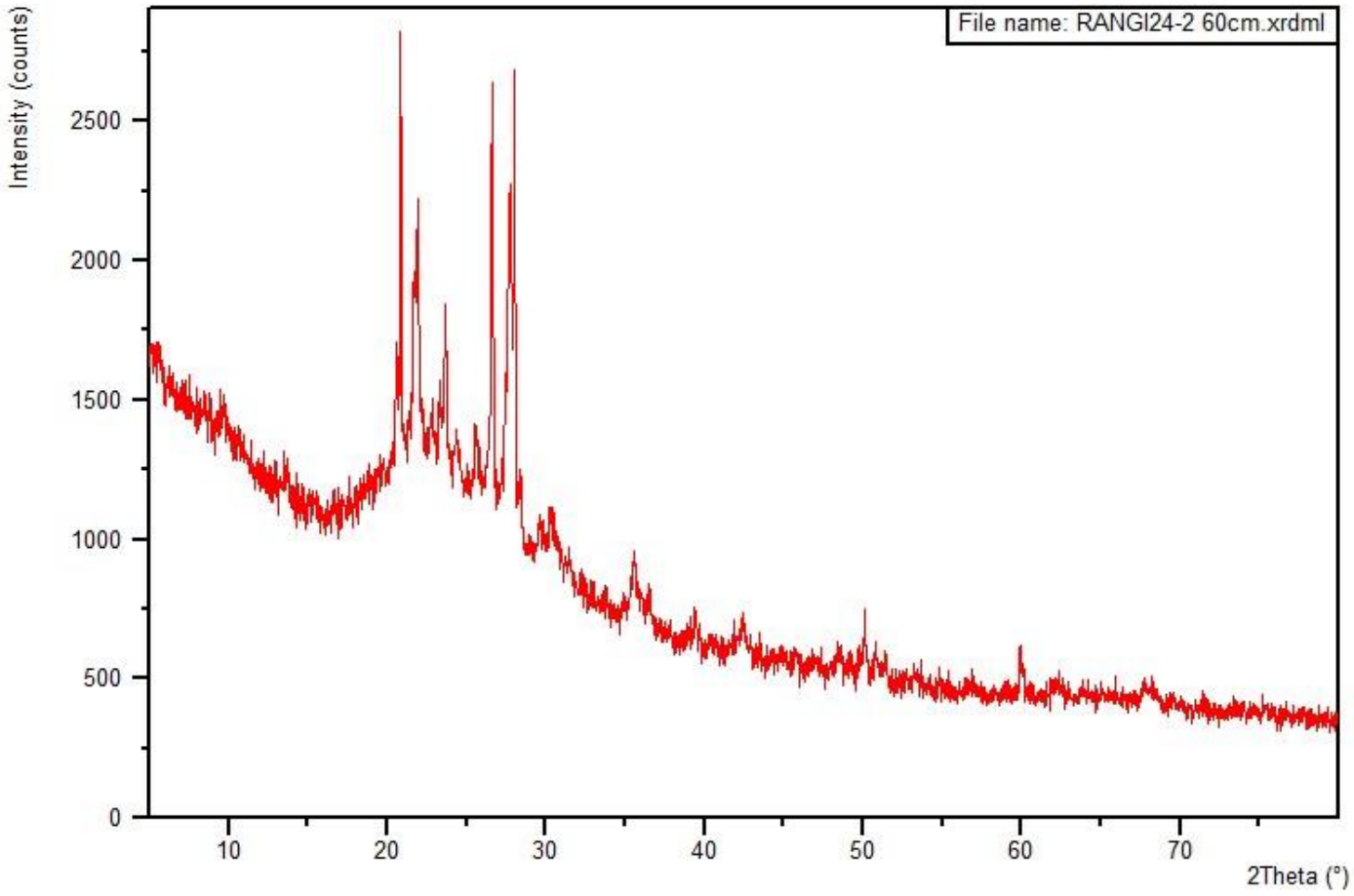
File name: RANGI24-2 60cm.xrdml
Intensity (counts)
2500
2000
1500
1000
500
0
10
20
30
40
50
60
70
2Theta (°)

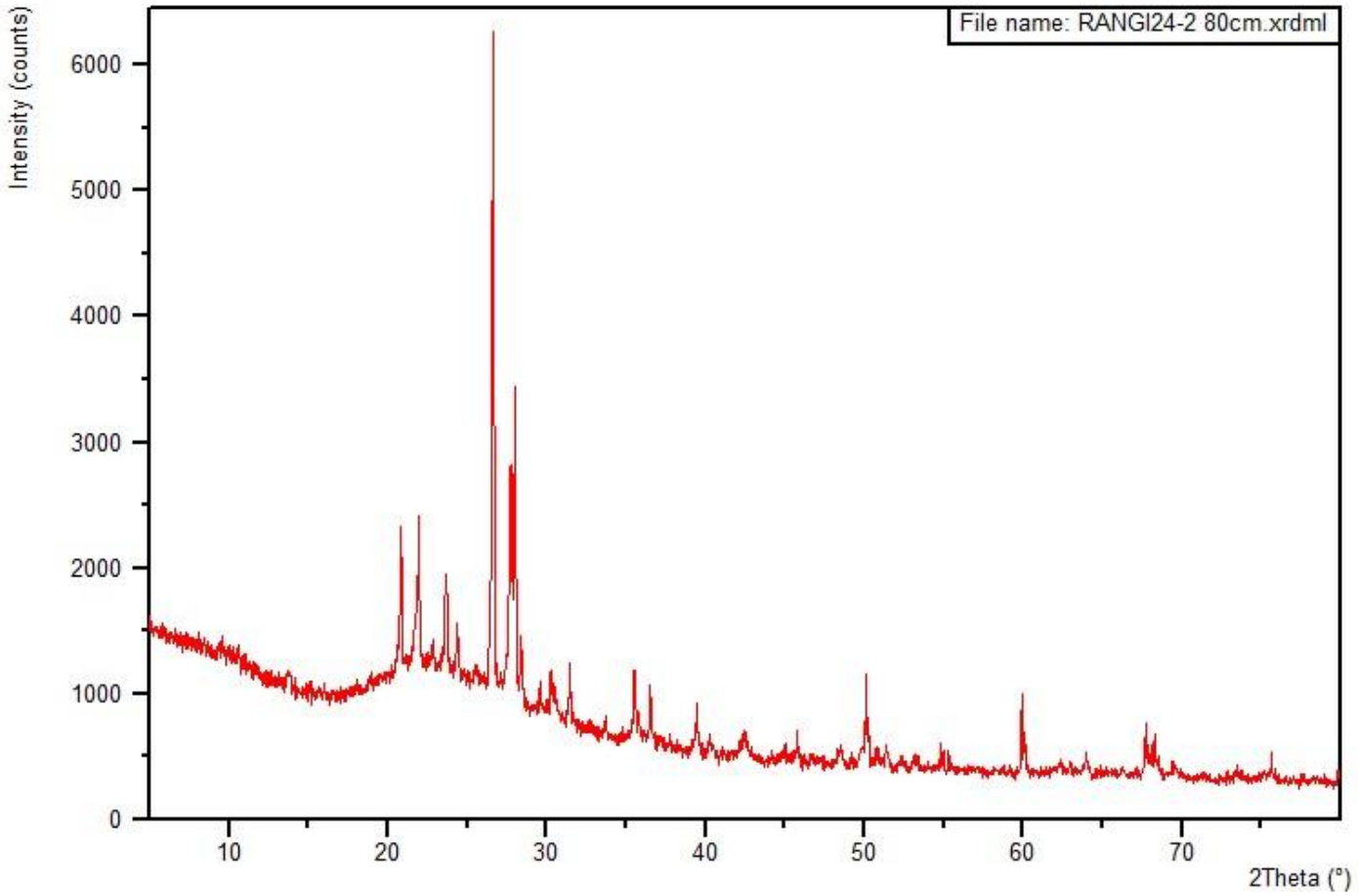
File name: RANGI24-2 80cm.xrdml
Intensity (counts)
6000
5000
4000
3000
2000
1000
0
10
20
30
40
50
60
70
2Theta (°)

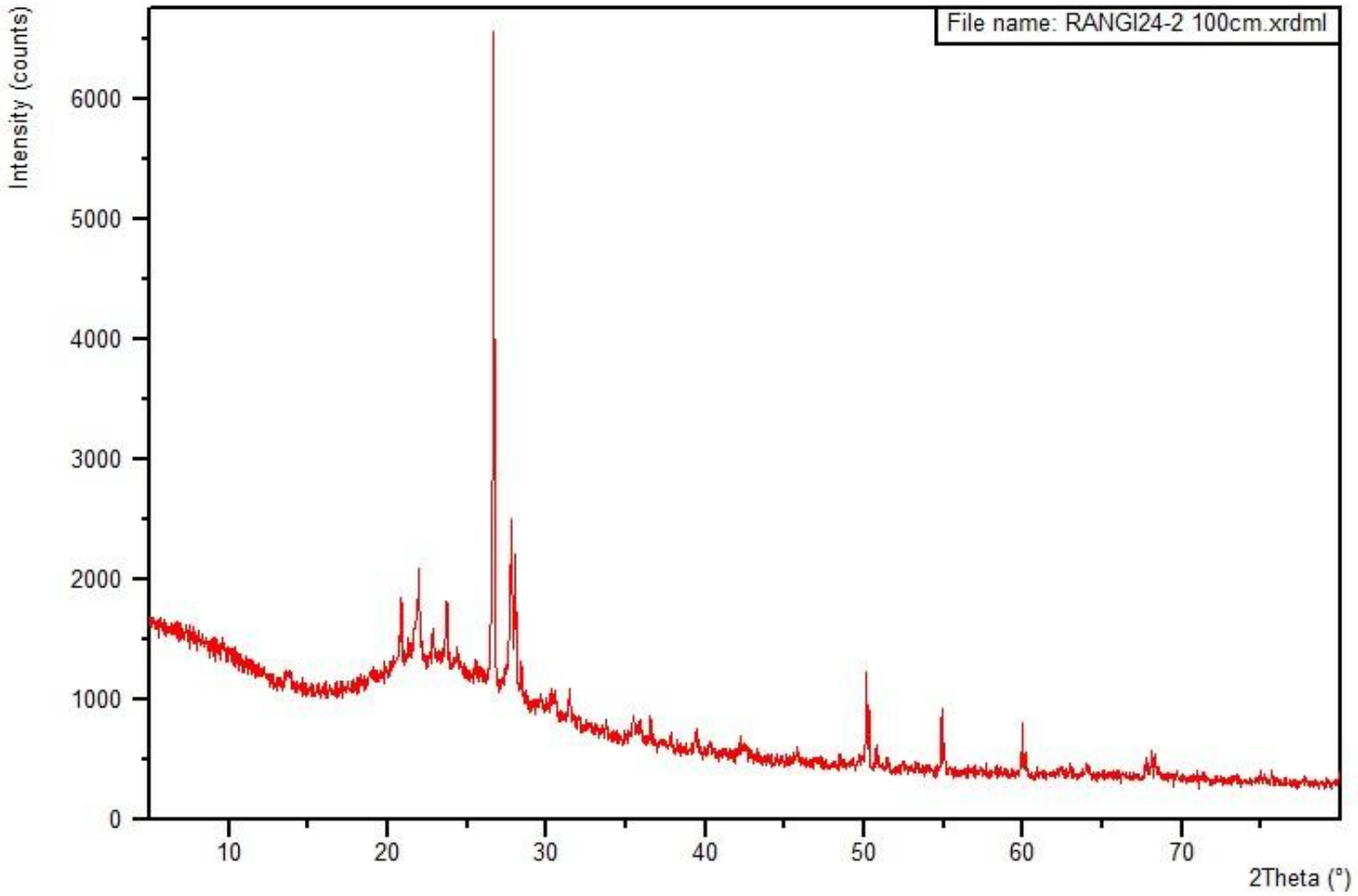
File name: RANGI24-2 100cm.xrdml
Intensity (counts)
6000
5000
4000
3000
2000
1000
0
10
20
30
40
50
60
70
2Theta (°)

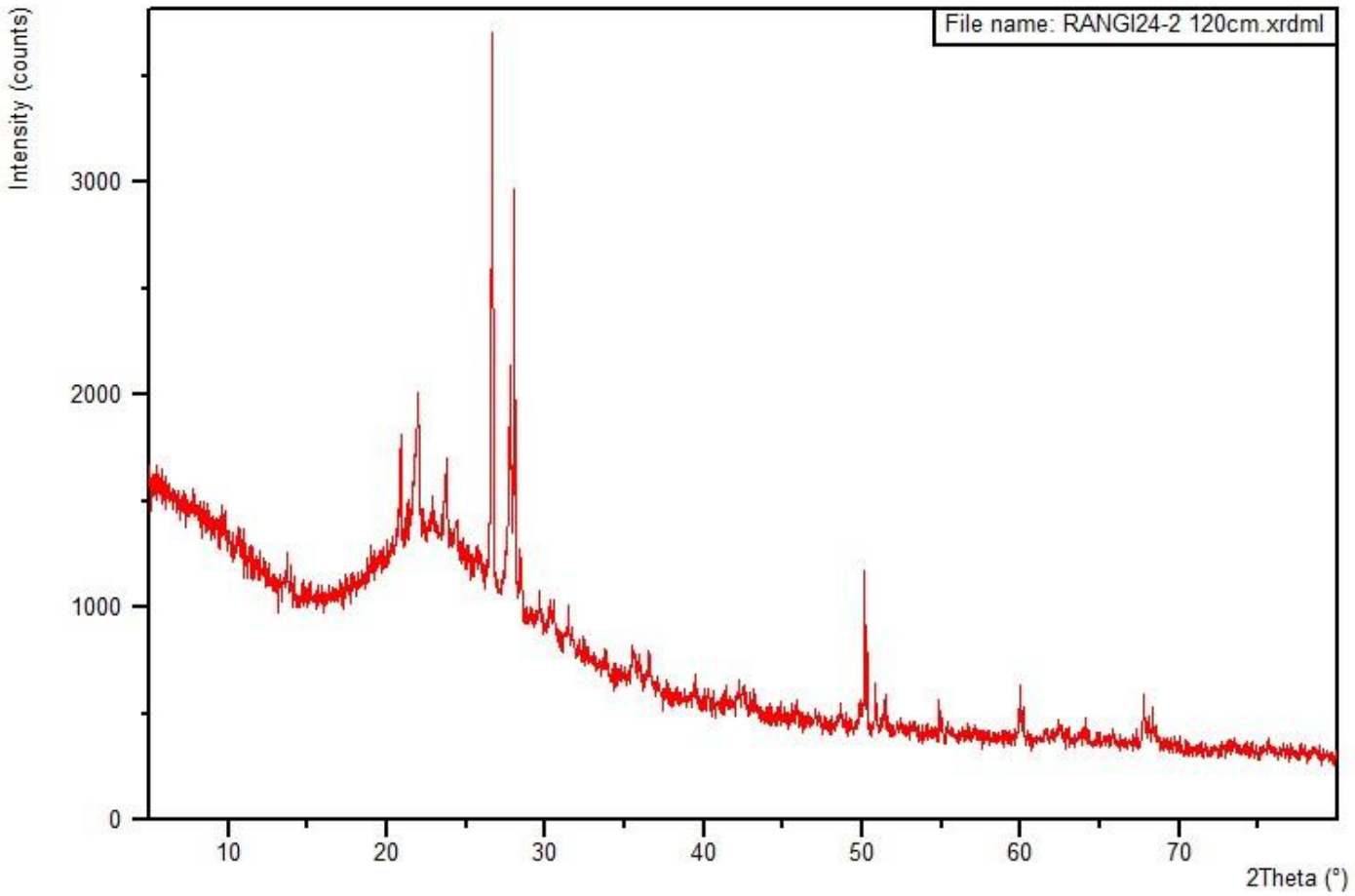
File name: RANGI24-2 120cm.xrdml
Intensity (counts)
0
1000
2000
3000
10
20
30
40
50
60
70
2Theta (°)

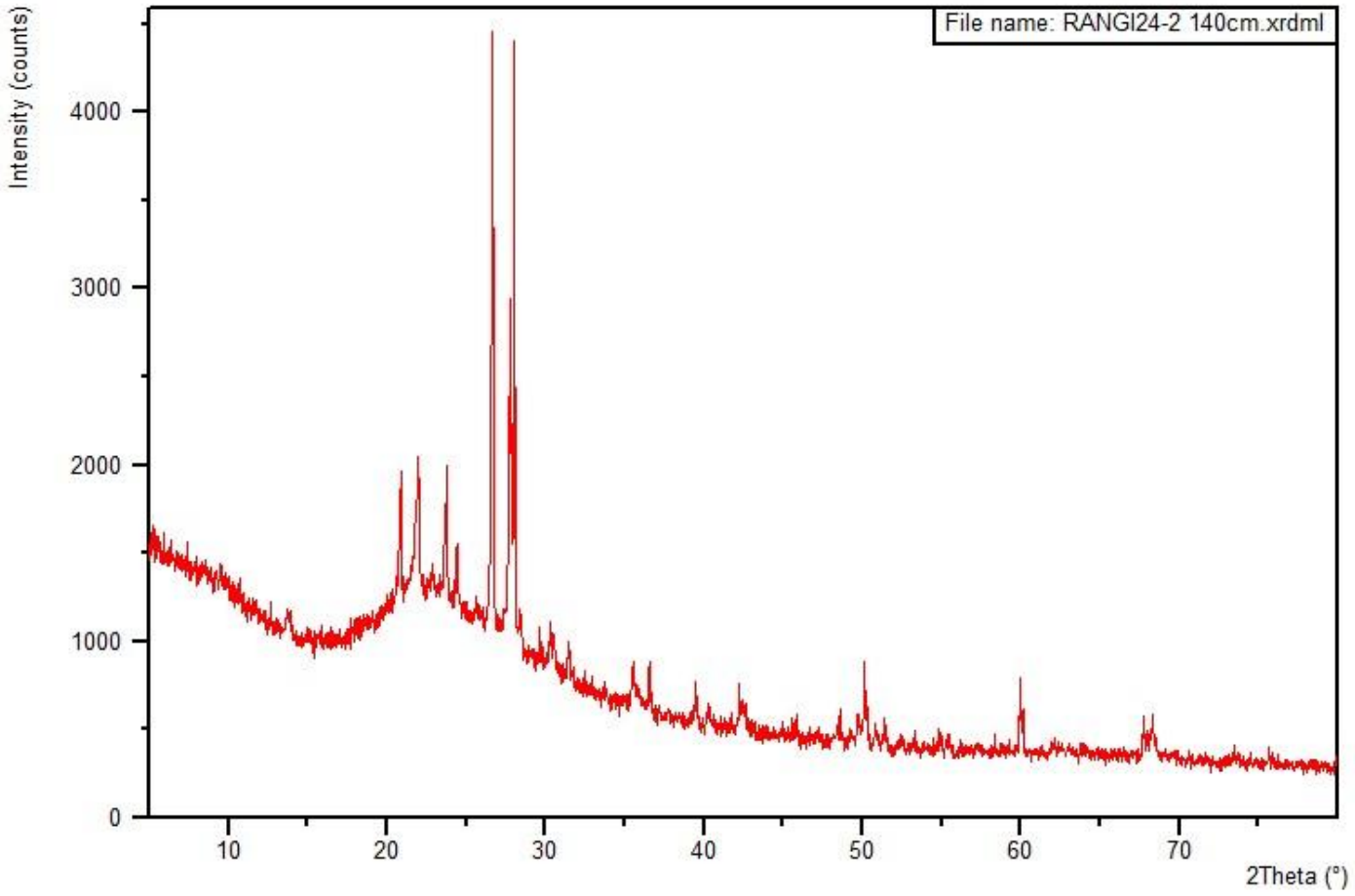
File name: RANGI24-2 140cm.xrdml
Intensity (counts)
0
1000
2000
3000
4000
10
20
30
40
50
60
70
2Theta (°)

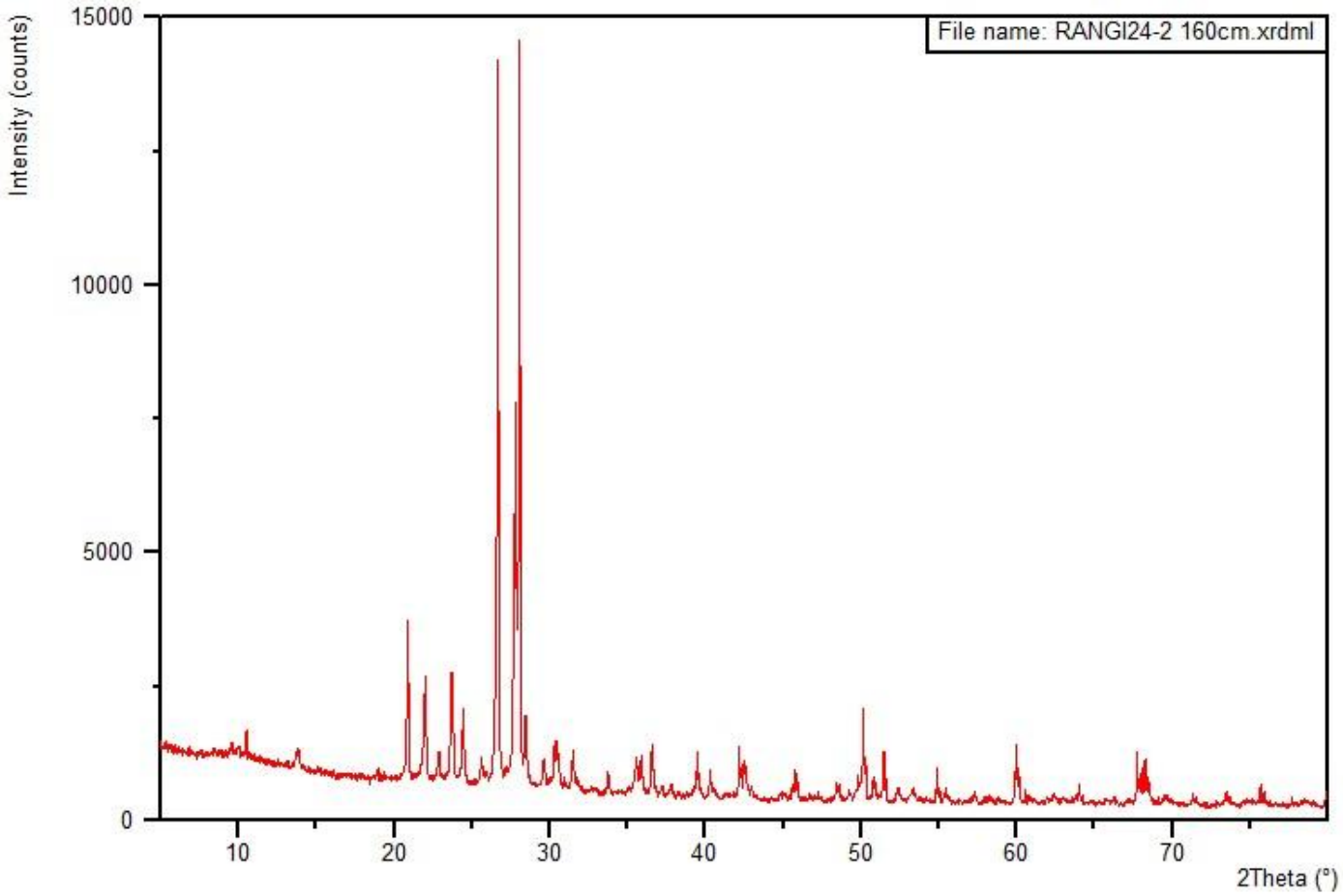
File name: RANGI24-2 160cm.xrdml
Intensity (counts)
15000
10000
5000
0
10
20
30
40
50
60
70
2Theta (°)

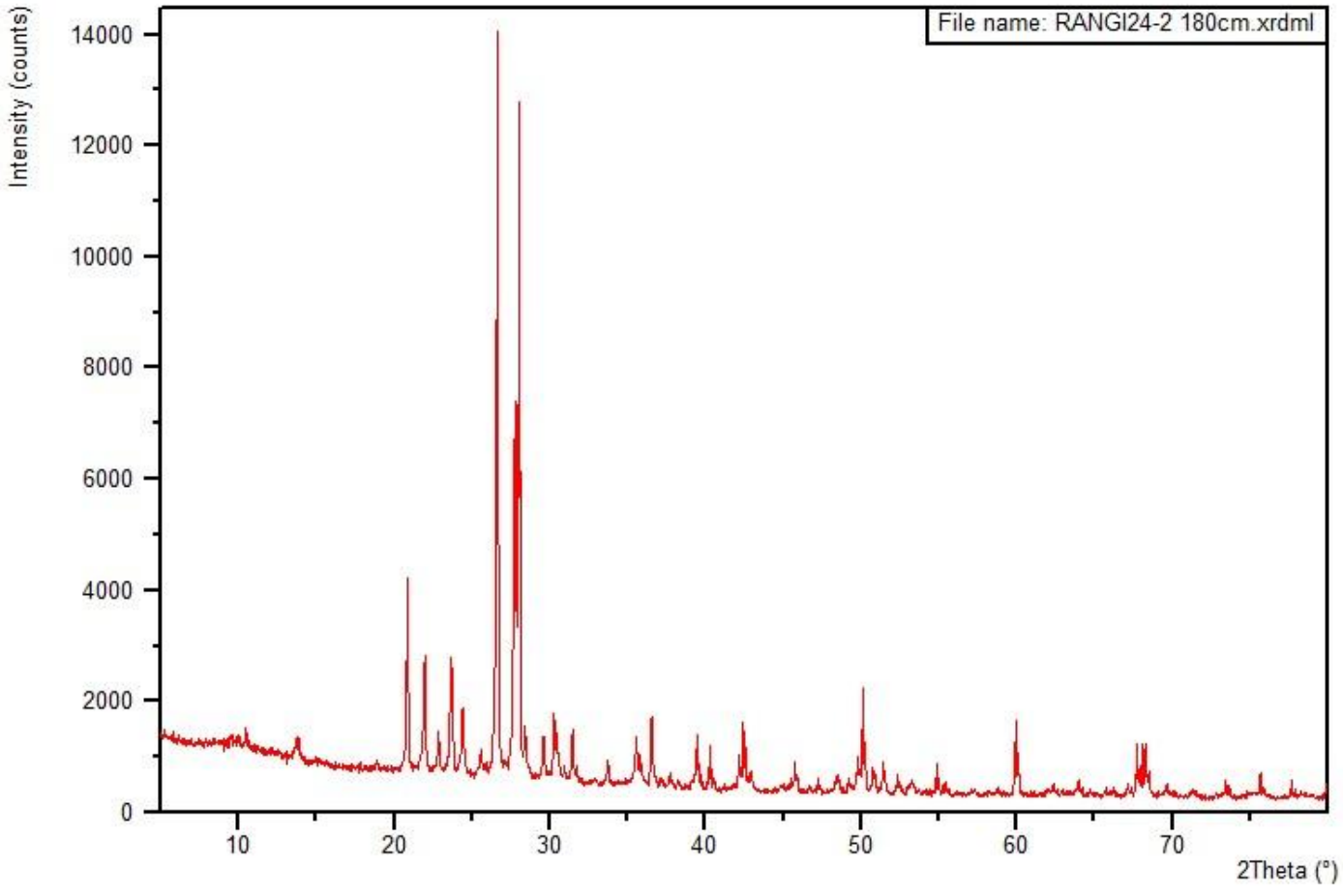
File name: RANGI24-2 180cm.xrdml
Intensity (counts)
14000
12000
10000
8000
6000
4000
2000
0
10
20
30
40
50
60
70
2Theta (°)

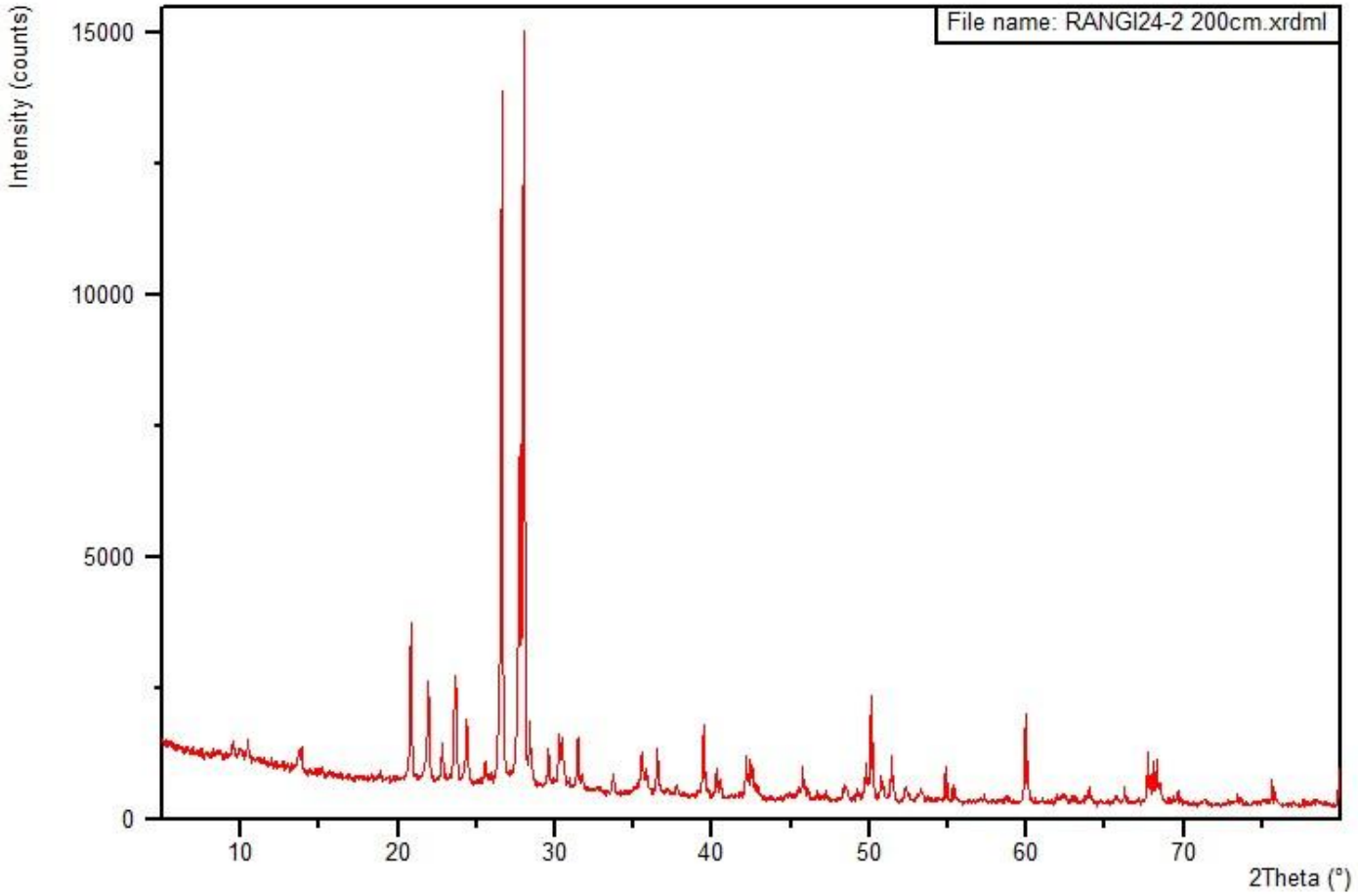
File name: RANGI24-2 200cm.xrdml
Intensity (counts)
15000
10000
5000
0
10
20
30
40
50
60
70
2Theta (°)

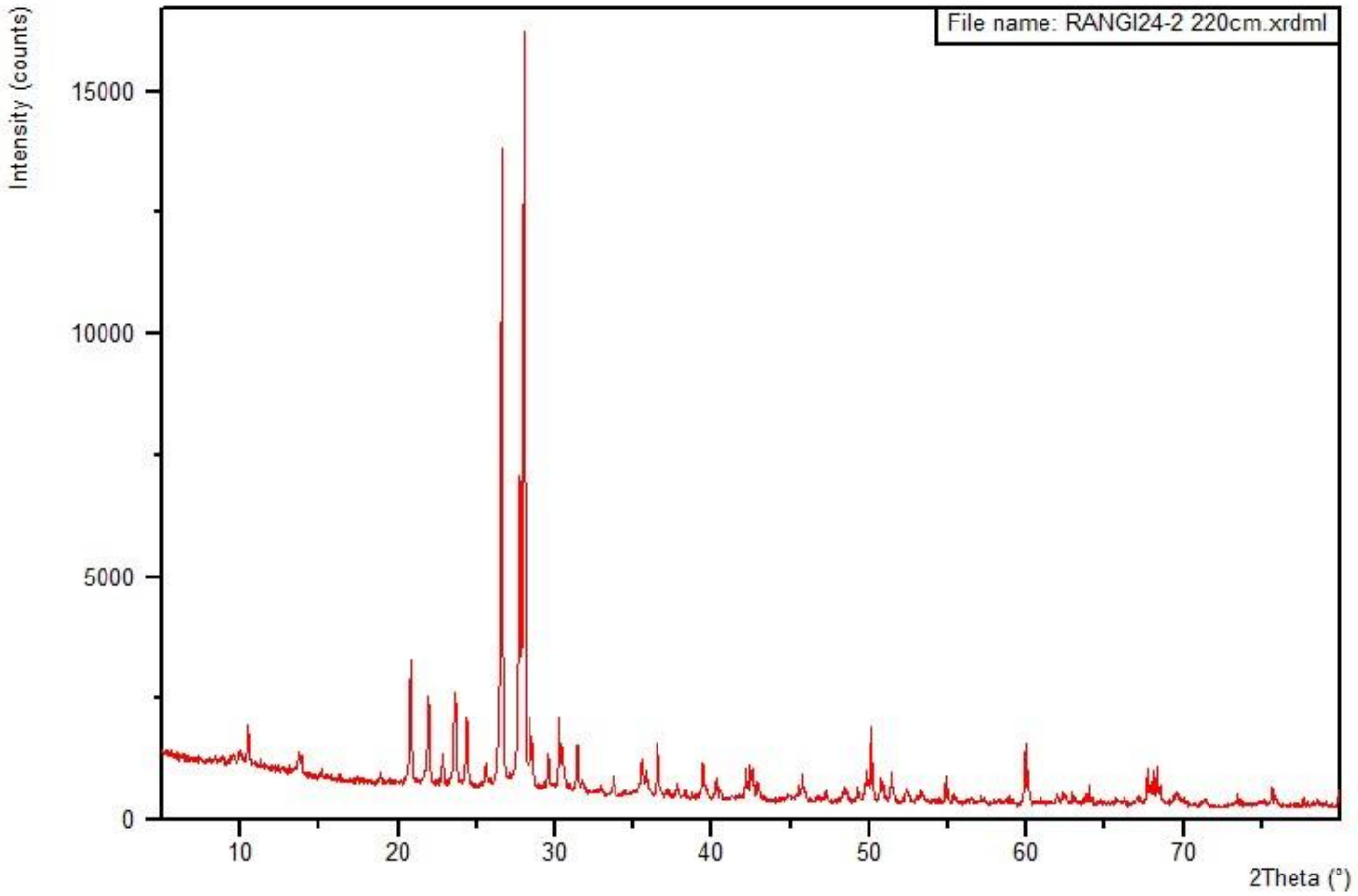
File name: RANGI24-2 220cm.xrdml
Intensity (counts)
15000
10000
5000
0
10
20
30
40
50
60
70
2Theta (°)

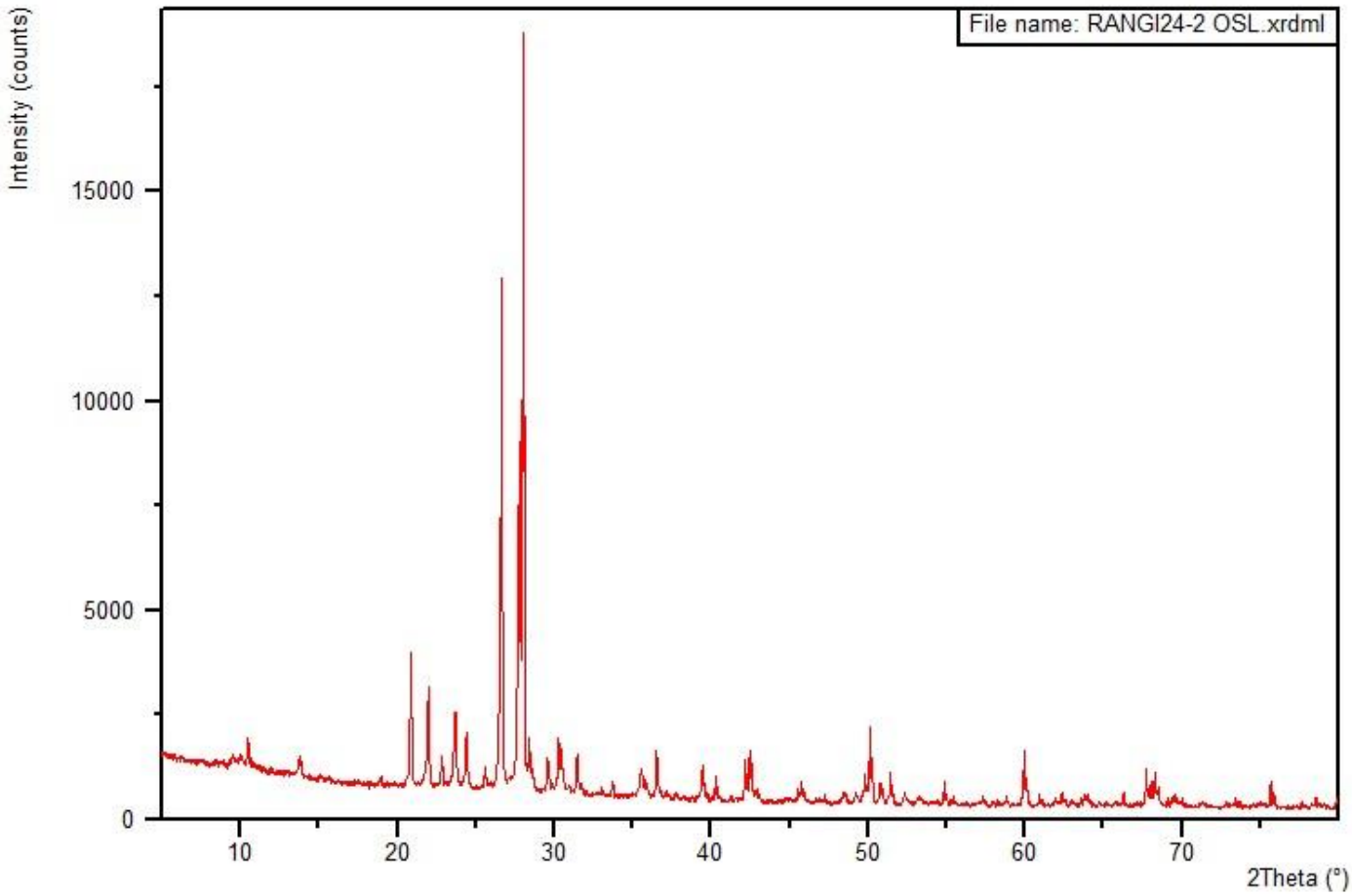
File name: RANGI24-2 OSL.xrdml
Intensity (counts)
15000
10000
5000
0
10
20
30
40
50
60
70
2Theta (°)

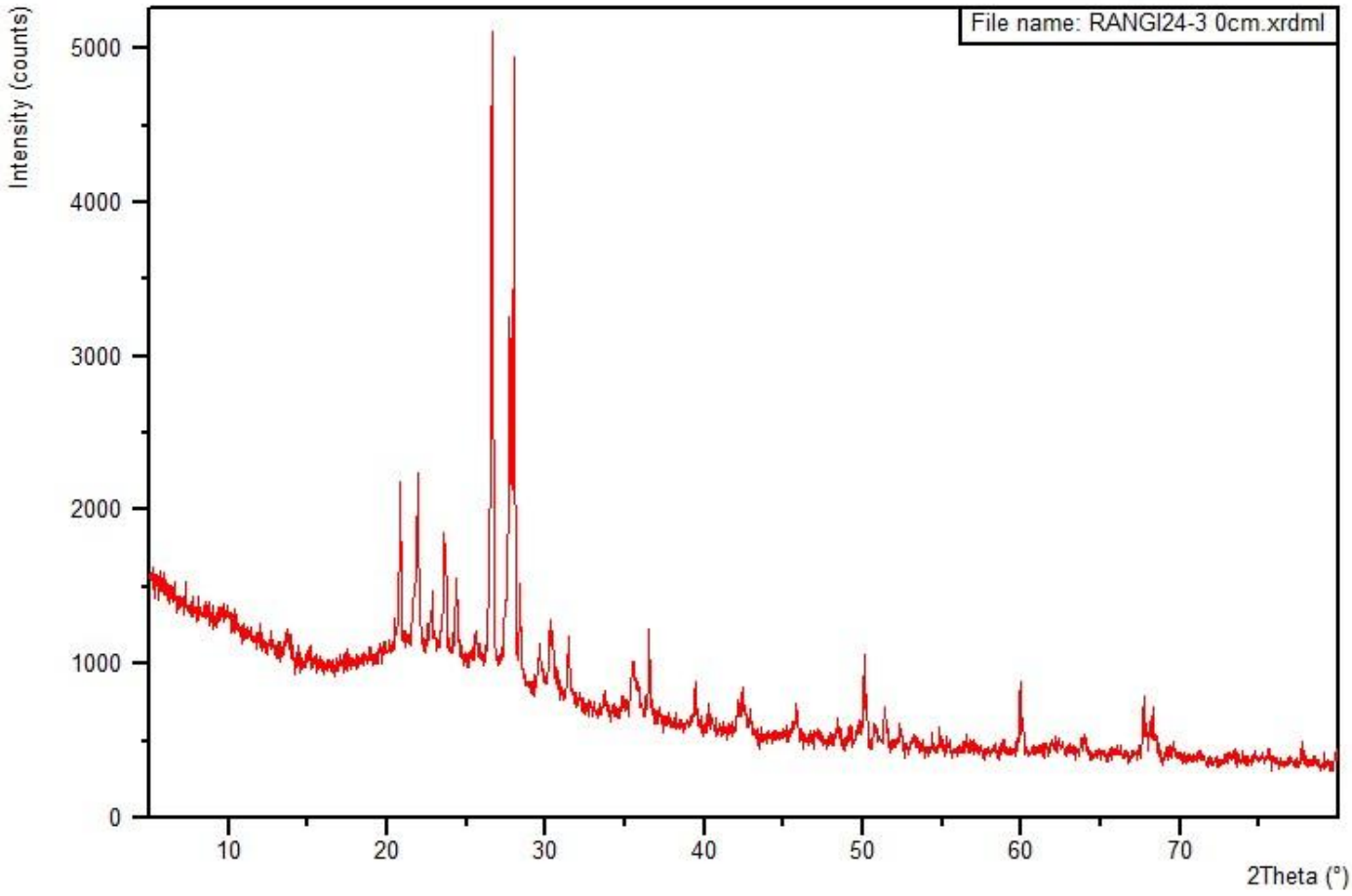
File name: RANGI24-3 0cm.xrdml
Intensity (counts)
5000
4000
3000
2000
1000
0
10
20
30
40
50
60
70
2Theta (°)

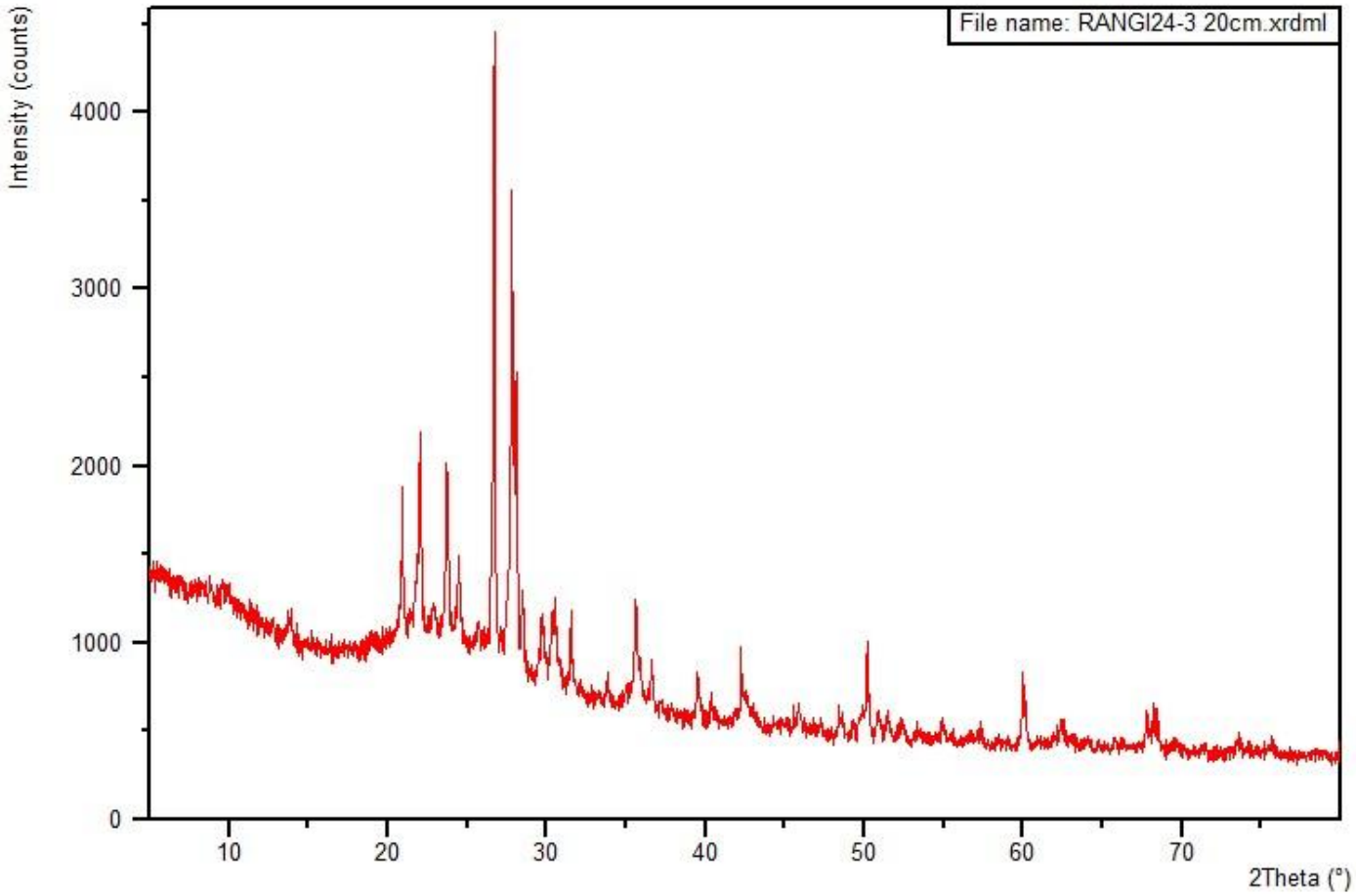
File name: RANGI24-3 20cm.xrdml
Intensity (counts)
0
1000
2000
3000
4000
10
20
30
40
50
60
70
2Theta (°)

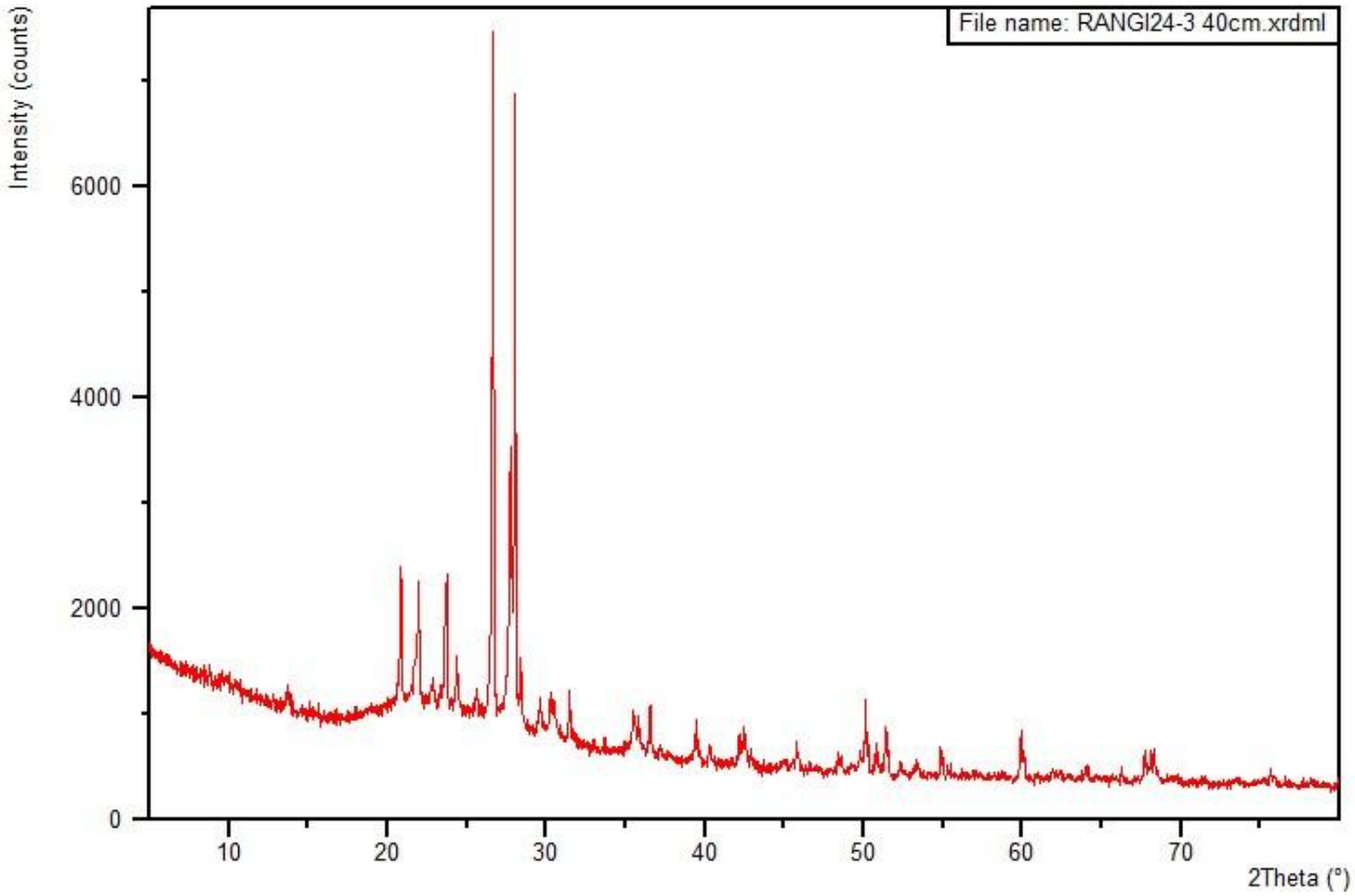
File name: RANGI24-3 40cm.xrdml
Intensity (counts)
0
2000
4000
6000
10
20
30
40
50
60
70
2Theta (°)

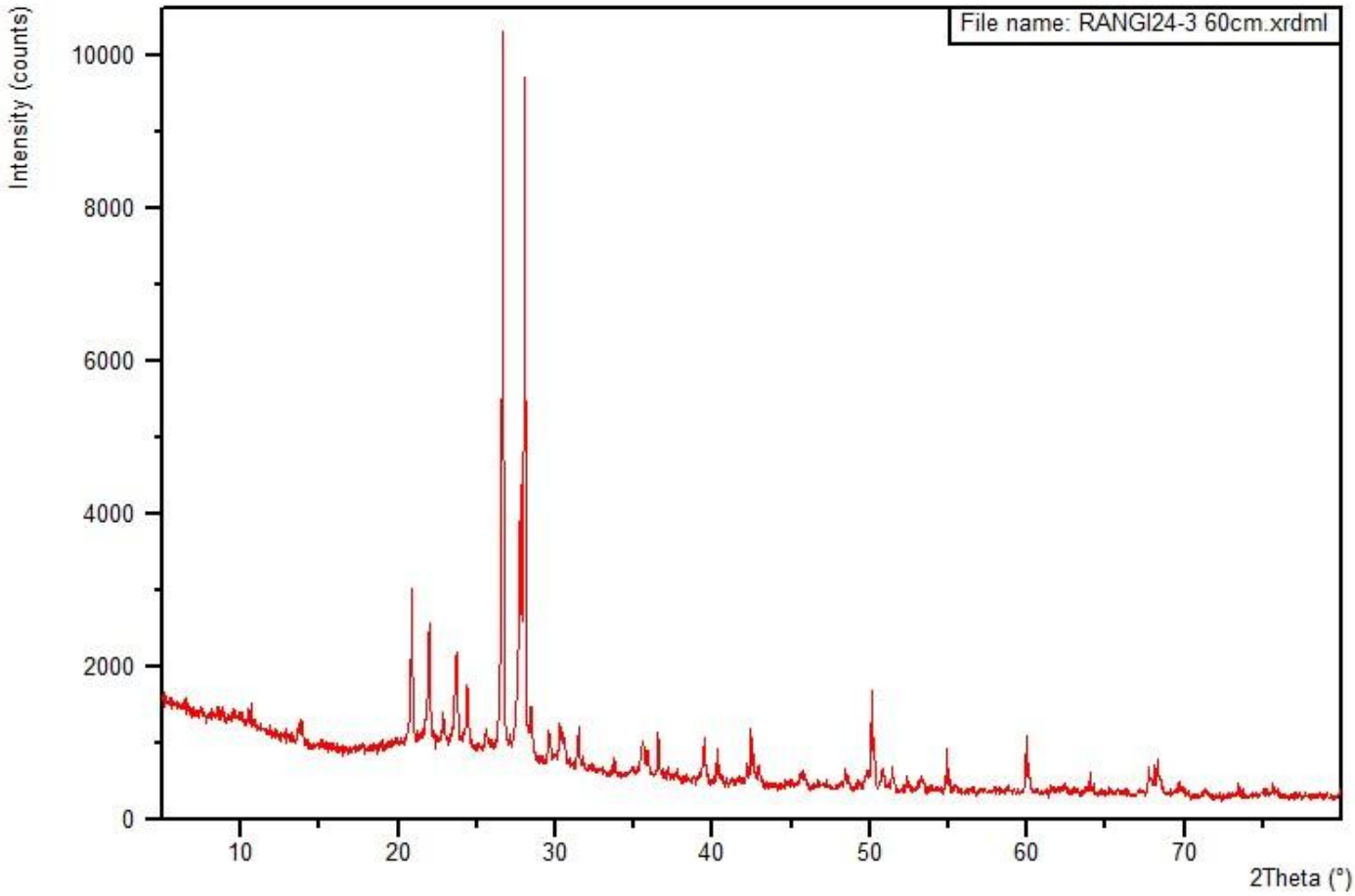
File name: RANGI24-3 60cm.xrdml
Intensity (counts)
10000
8000
6000
4000
2000
0
10
20
30
40
50
60
70
2Theta (°)

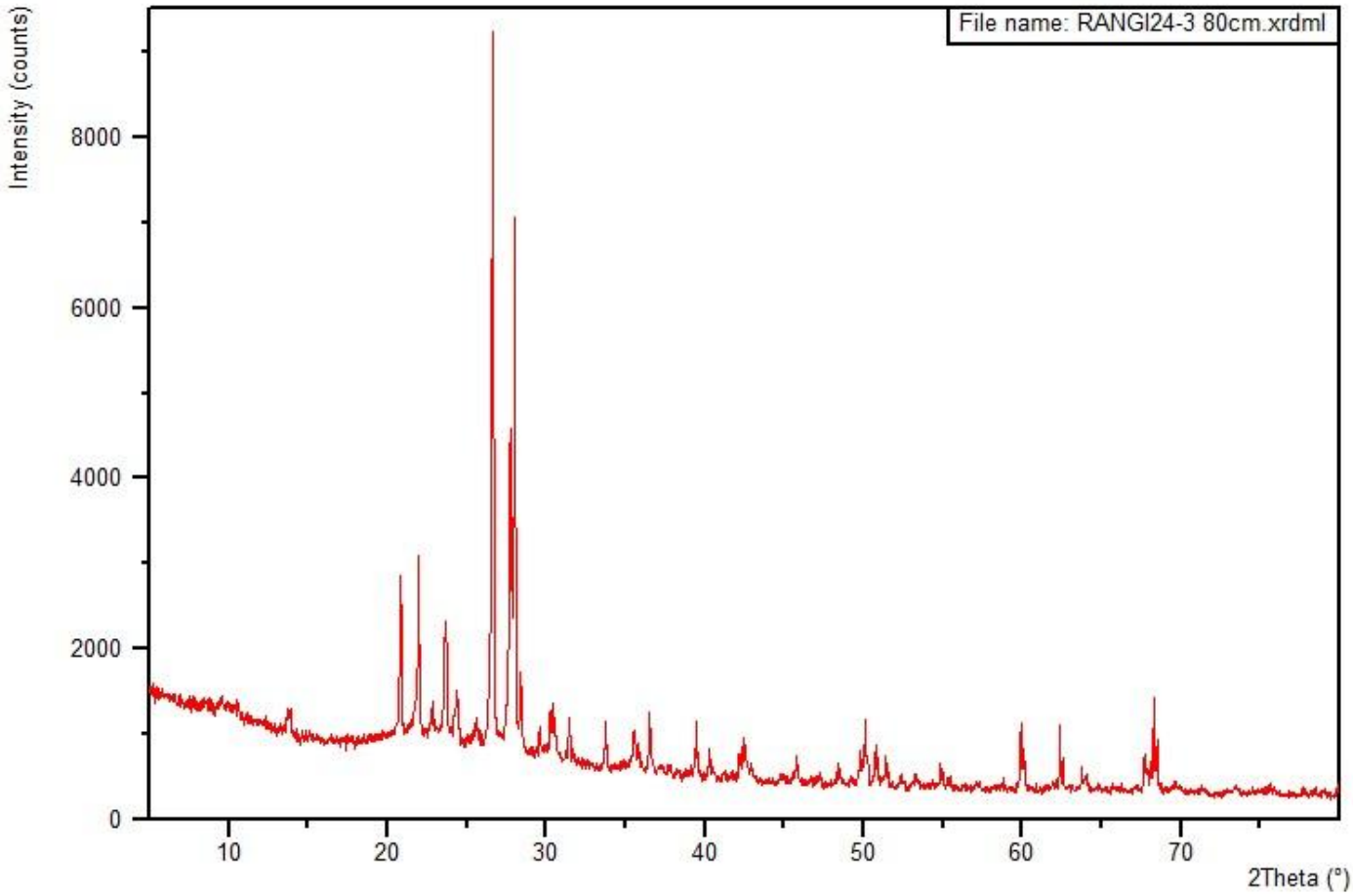
File name: RANGI24-3 80cm.xrdml
Intensity (counts)
8000
6000
4000
2000
0
10
20
30
40
50
60
70
2Theta (°)

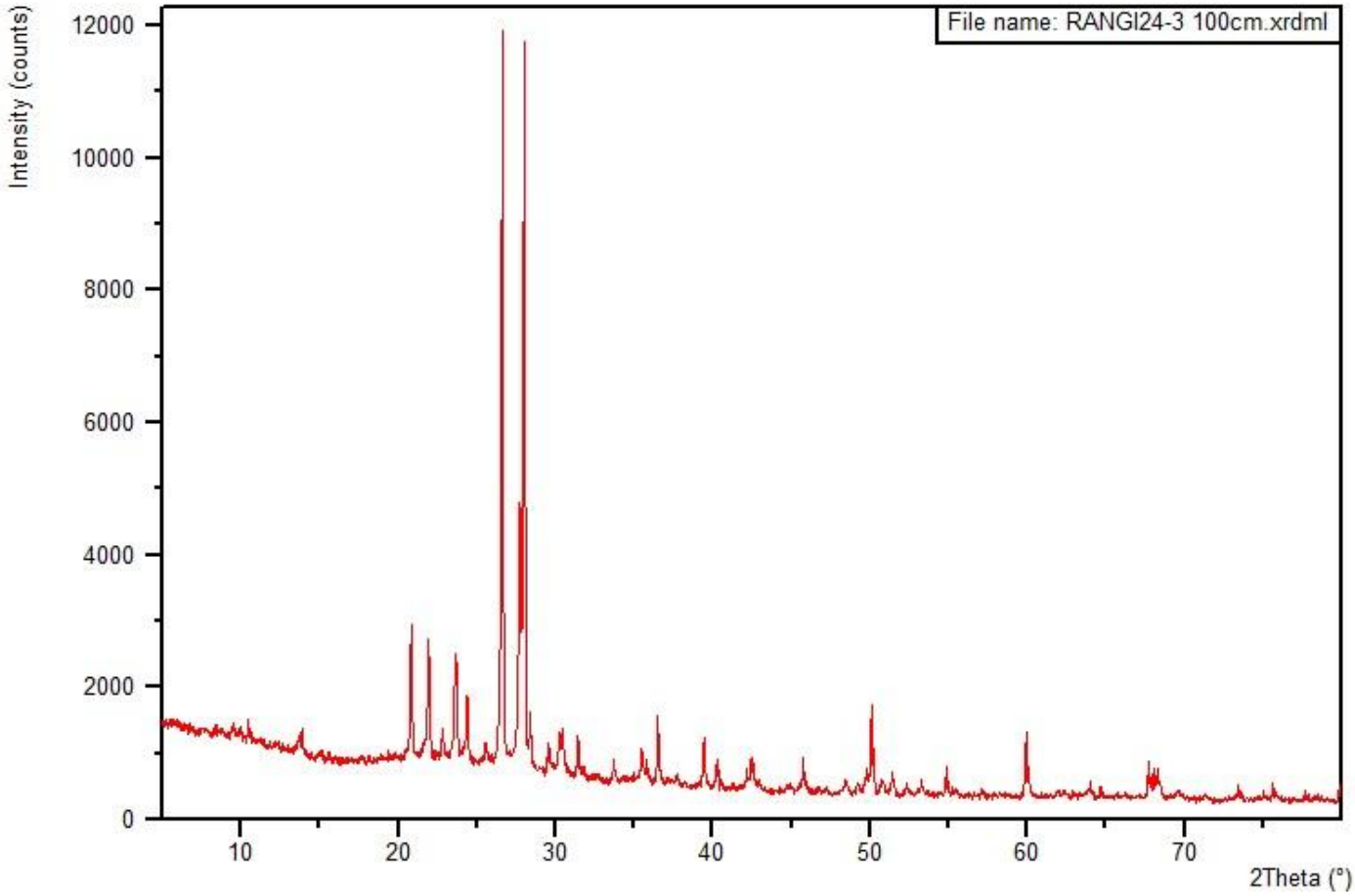
File name: RANGI24-3 100cm.xrdml
Intensity (counts)
12000
10000
8000
6000
4000
2000
0
10
20
30
40
50
60
70
2Theta (°)

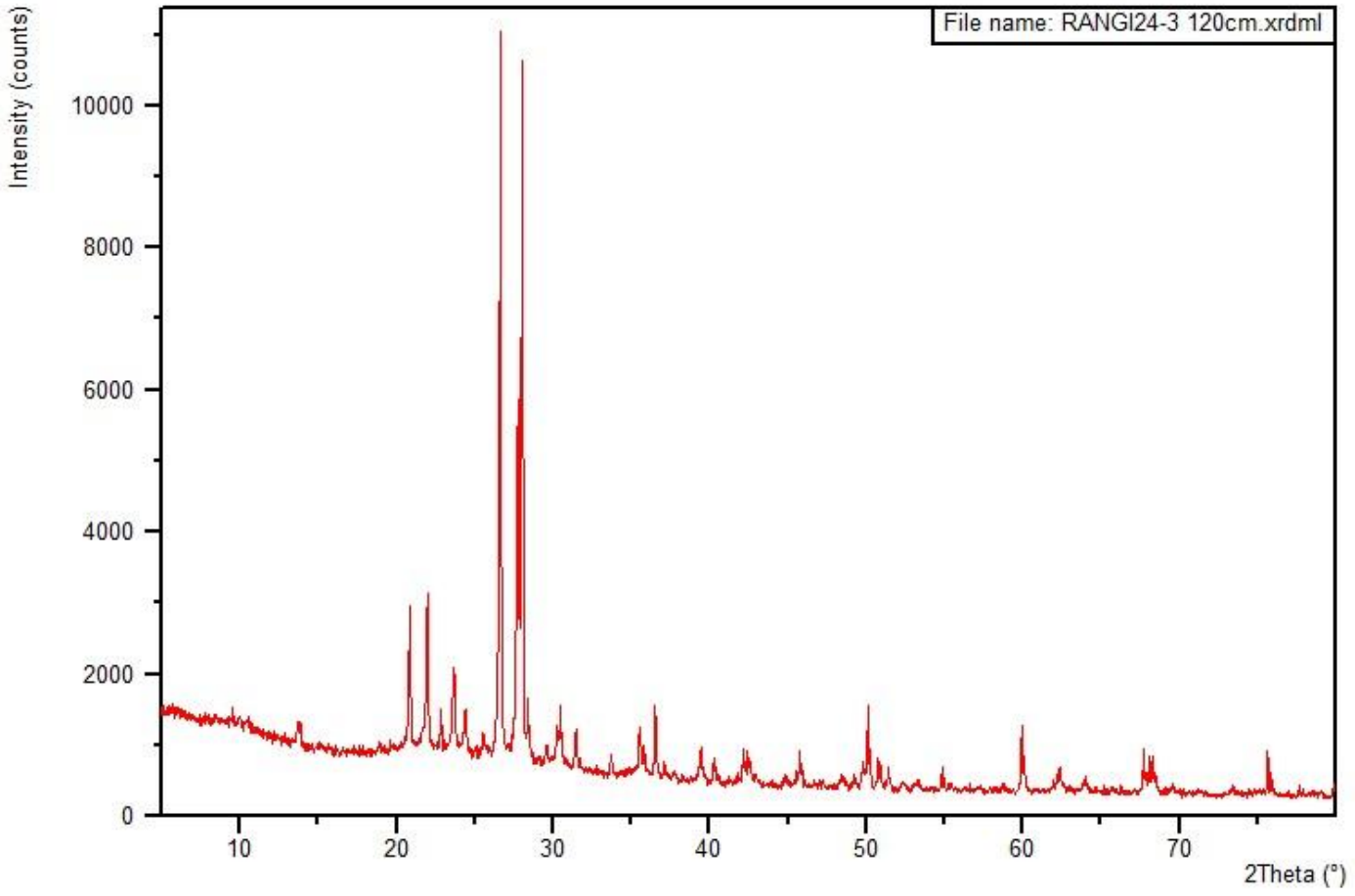
File name: RANGI24-3 120cm.xrdml
Intensity (counts)
10000
8000
6000
4000
2000
0
10
20
30
40
50
60
70
2Theta (°)

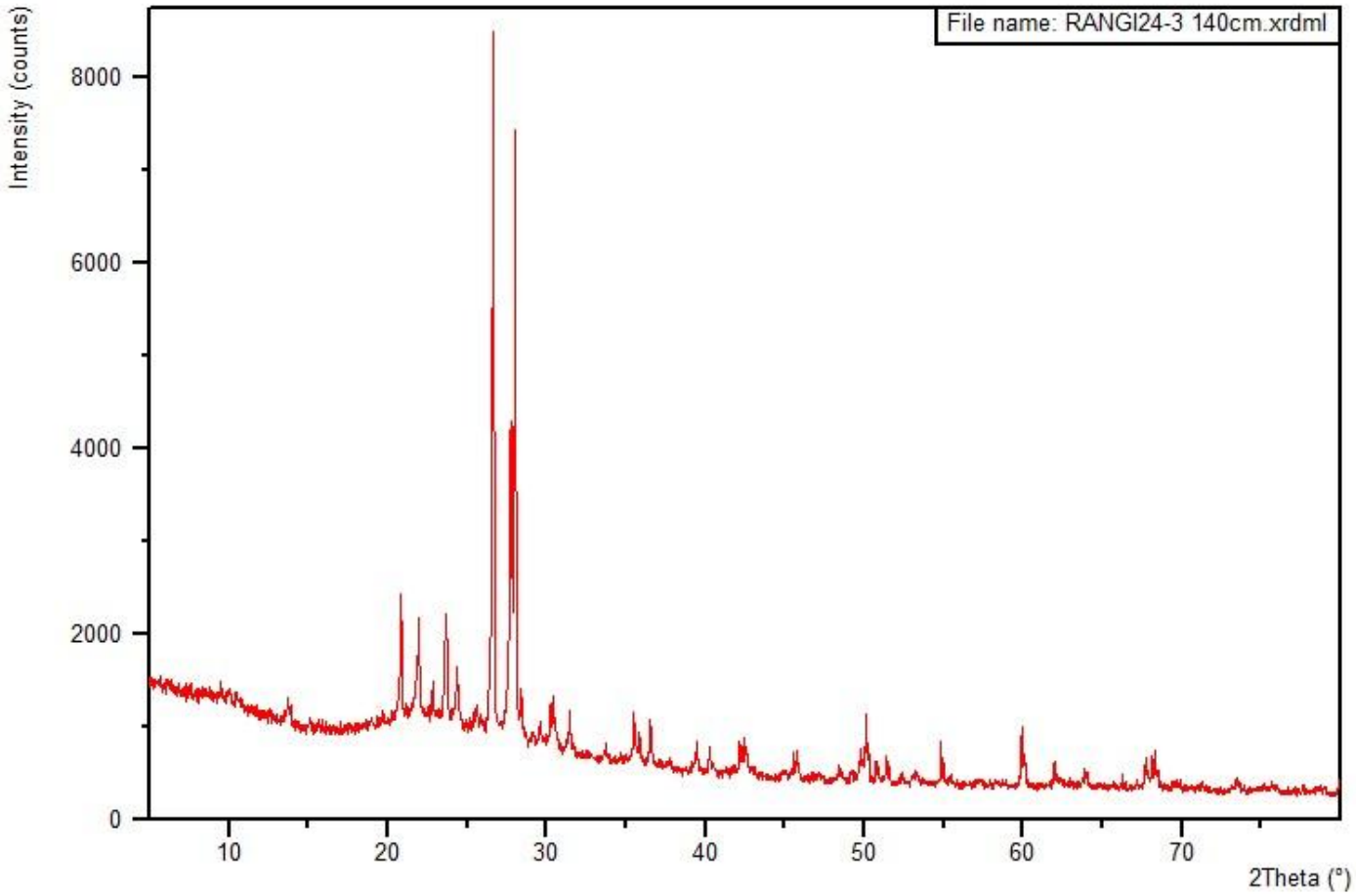
File name: RANGI24-3 140cm.xrdml
Intensity (counts)
8000
6000
4000
2000
0
10
20
30
40
50
60
70
2Theta (°)

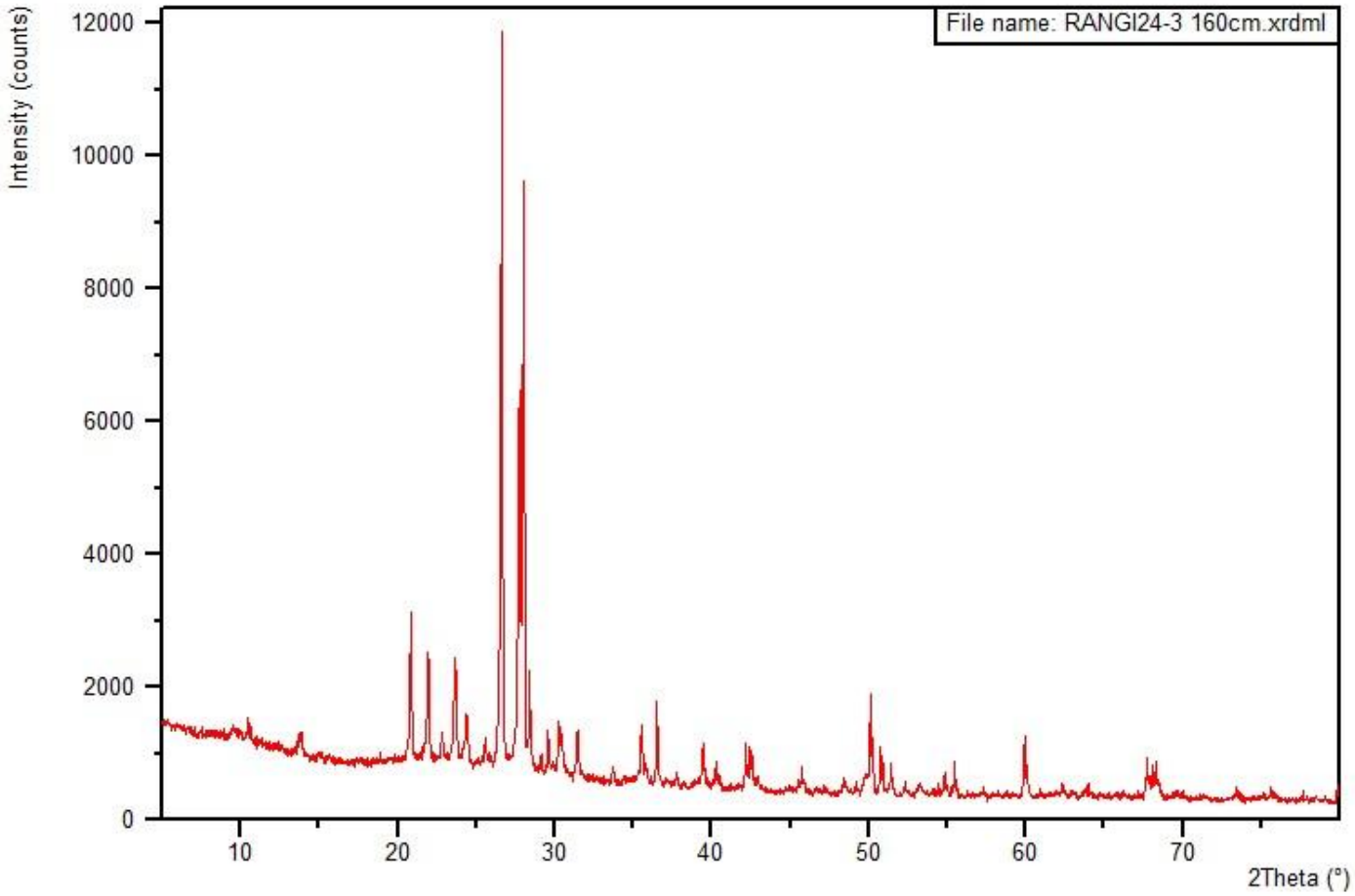
File name: RANGI24-3 160cm.xrdml
Intensity (counts)
12000
10000
8000
6000
4000
2000
0
10
20
30
40
50
60
70
2Theta (°)

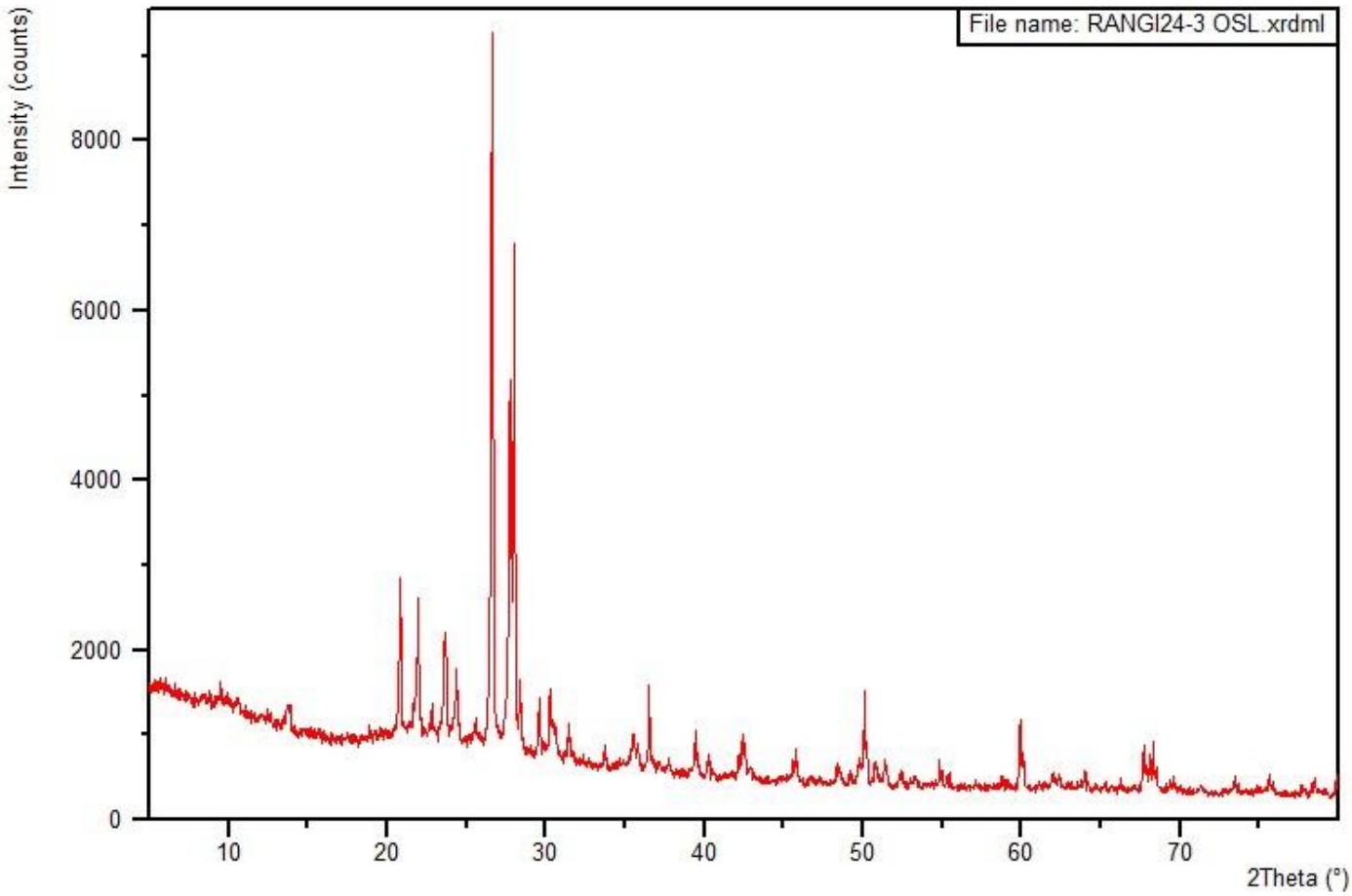
File name: RANGI24-3 OSL.xrdml
Intensity (counts)
8000
6000
4000
2000
0
10
20
30
40
50
60
70
2Theta (°)

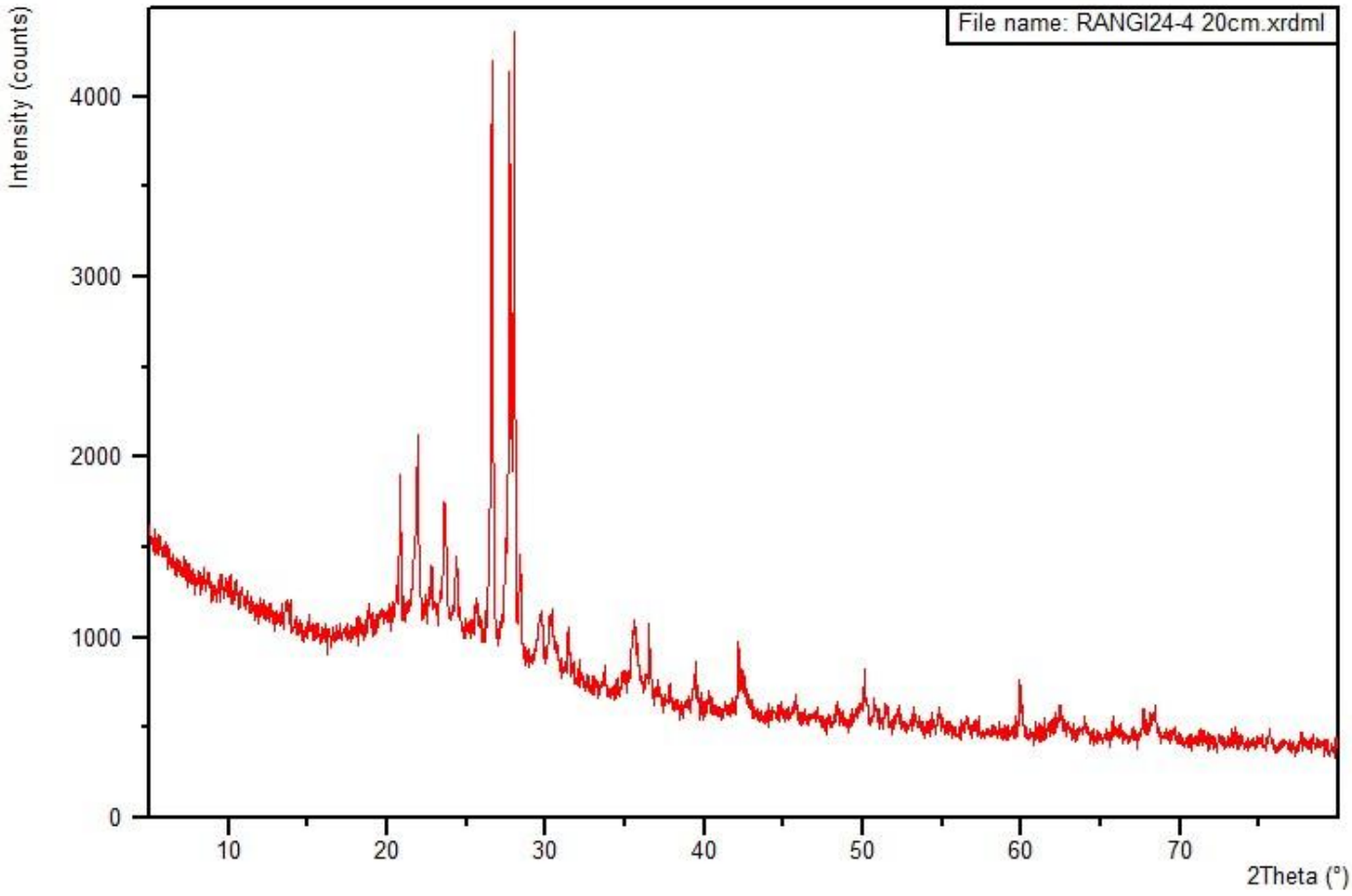
File name: RANGI24-4 20cm.xrdml
Intensity (counts)
4000
3000
2000
1000
0
10
20
30
40
50
60
70
2Theta (°)

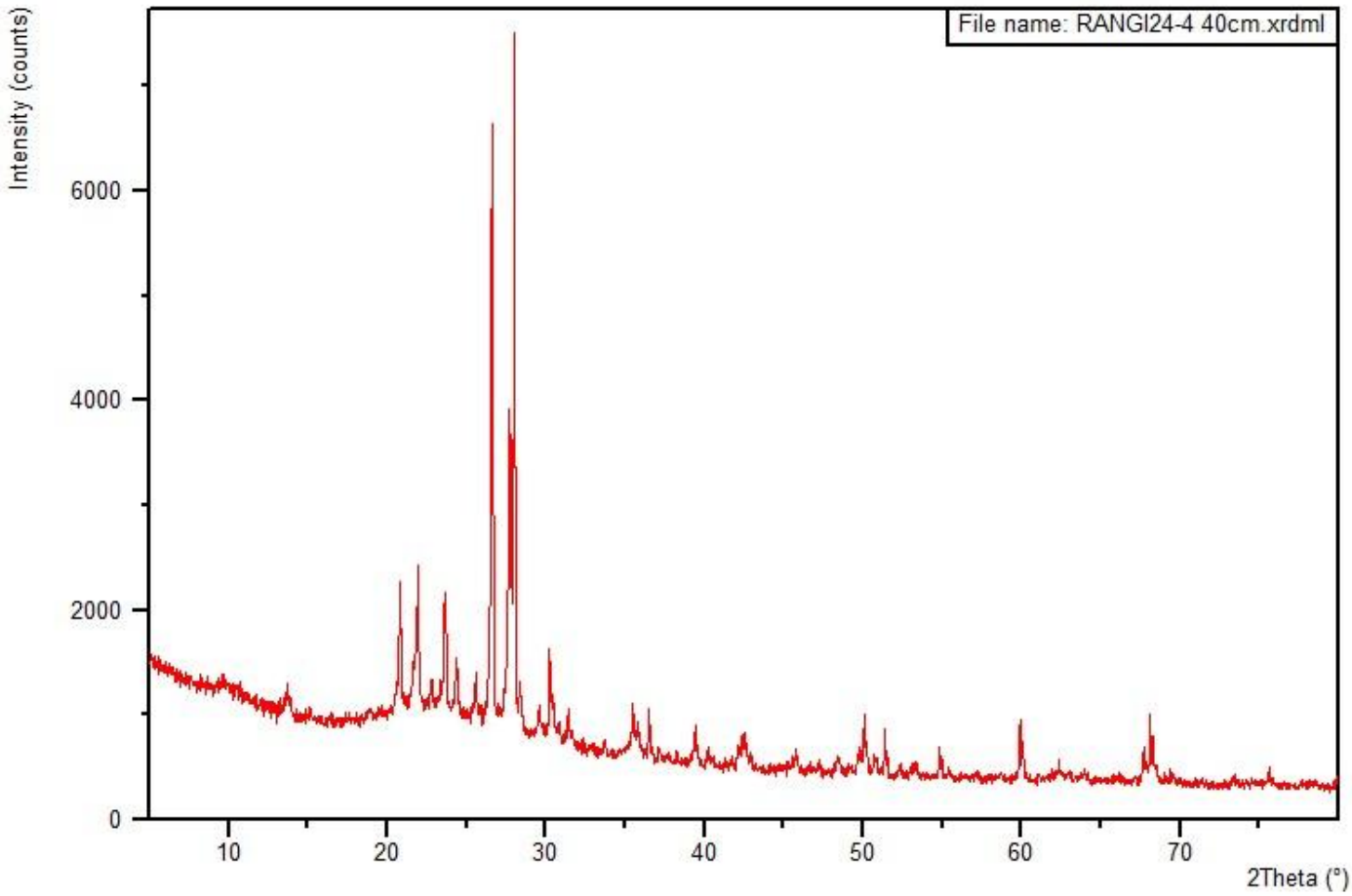
File name: RANGI24-4 40cm.xrdml
Intensity (counts)
0
2000
4000
6000
10
20
30
40
50
60
70
2Theta (°)

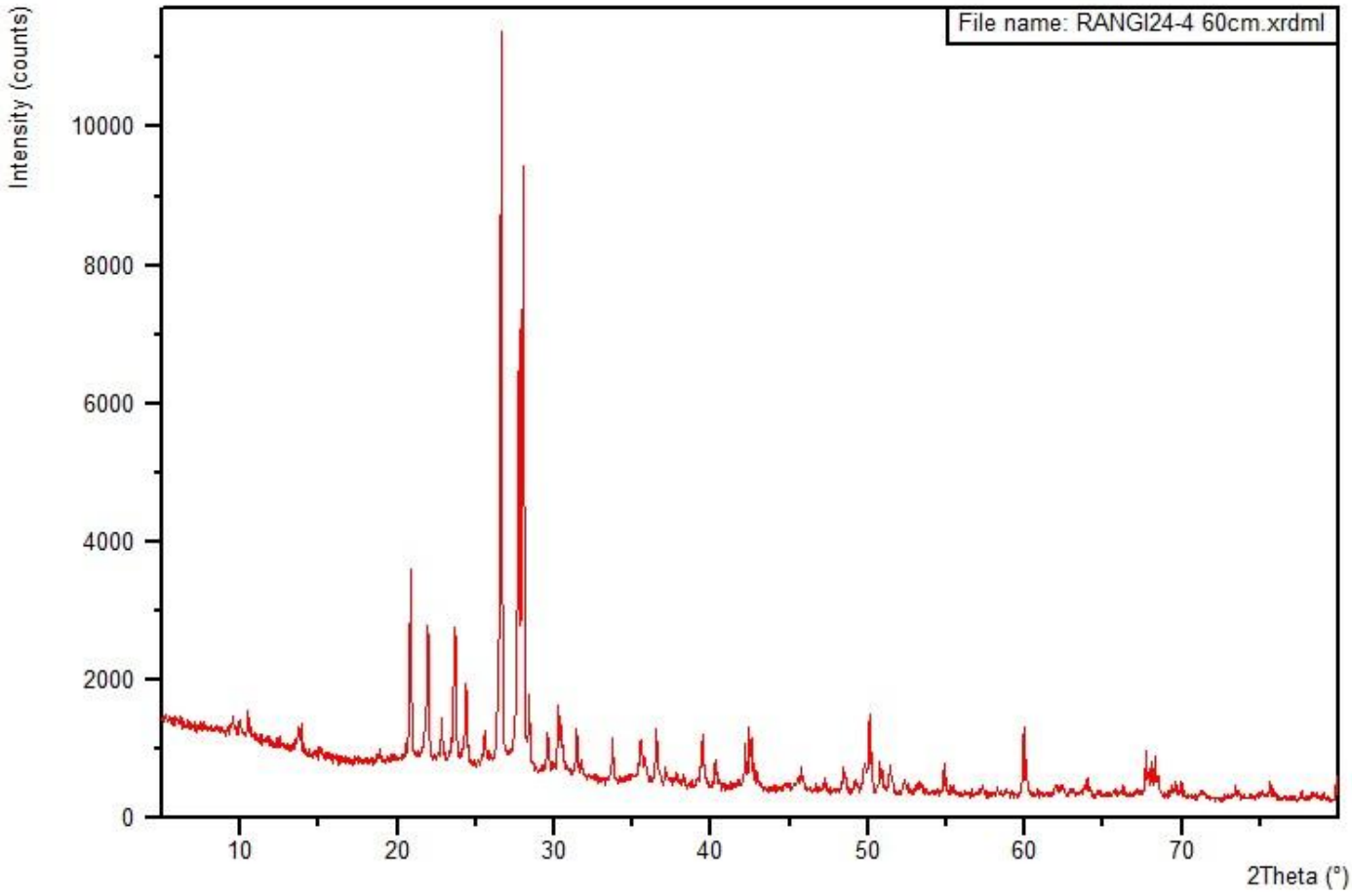
File name: RANGI24-4 60cm.xrdml
Intensity (counts)
0
2000
4000
6000
8000
10000
10
20
30
40
50
60
70
2Theta (°)

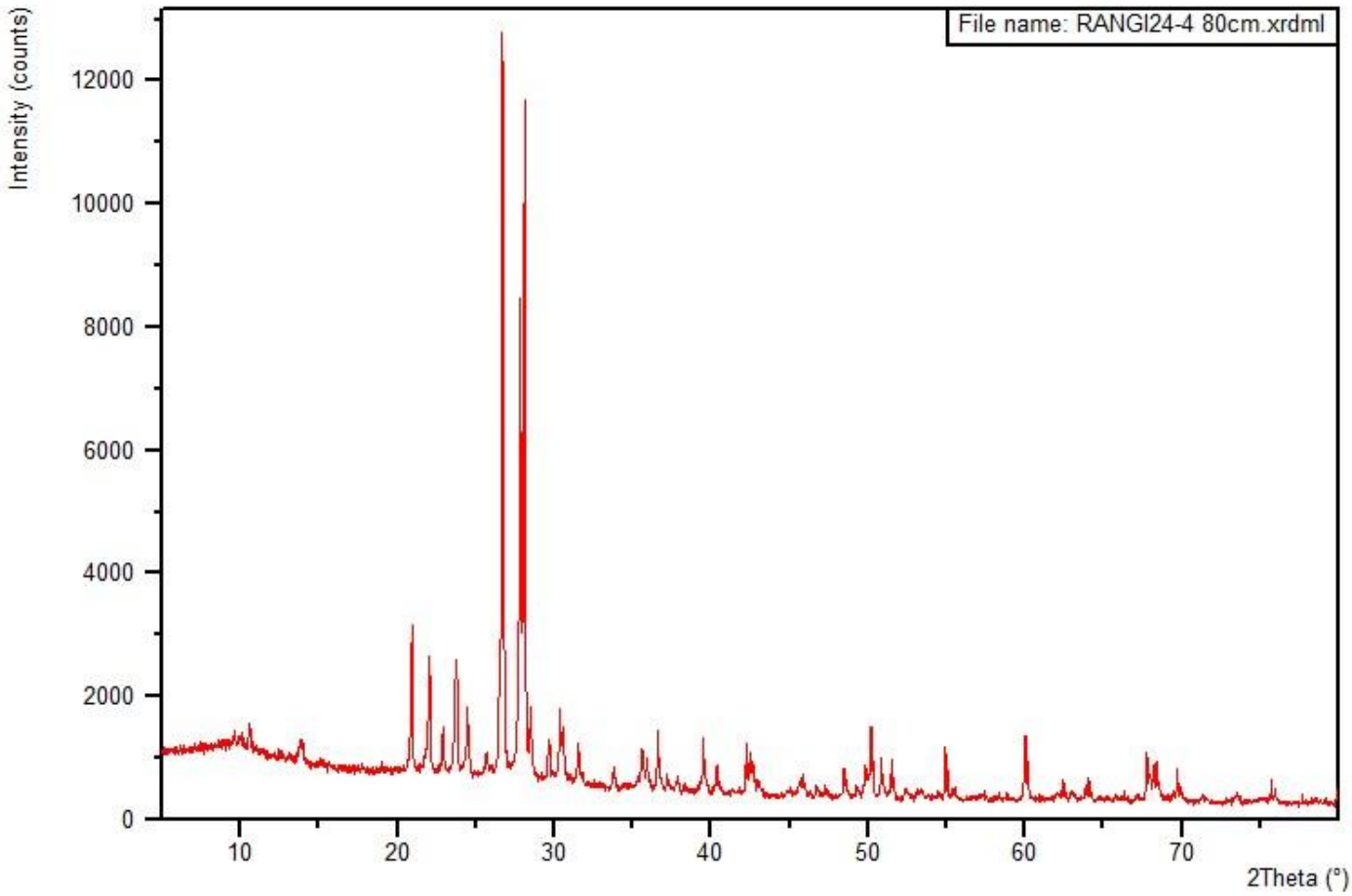
File name: RANGI24-4 80cm.xrdml
Intensity (counts)
12000
10000
8000
6000
4000
2000
0
10
20
30
40
50
60
70
2Theta (°)

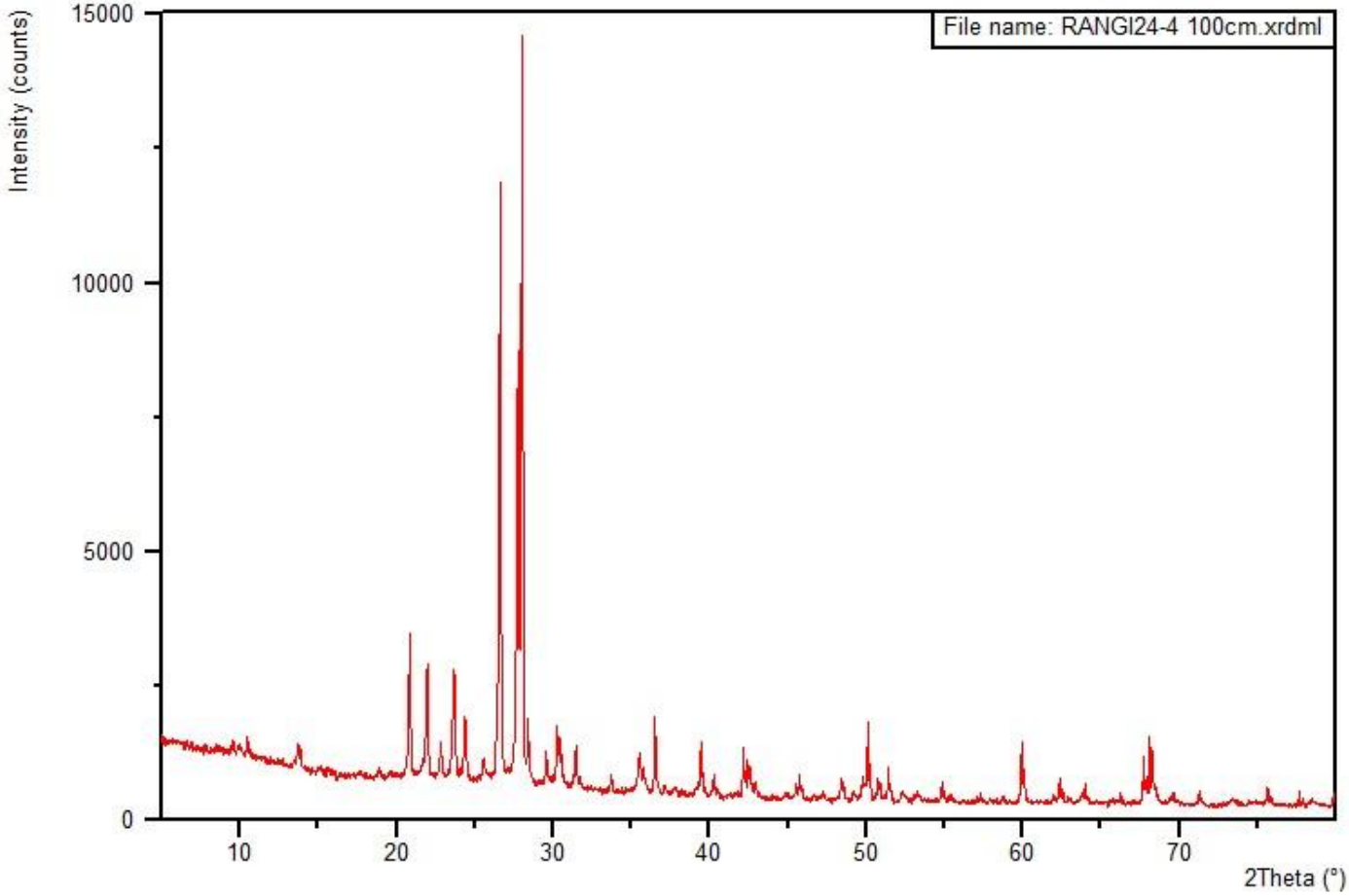
File name: RANGI24-4 100cm.xrdml
Intensity (counts)
15000
10000
5000
0
10
20
30
40
50
60
70
2Theta (°)

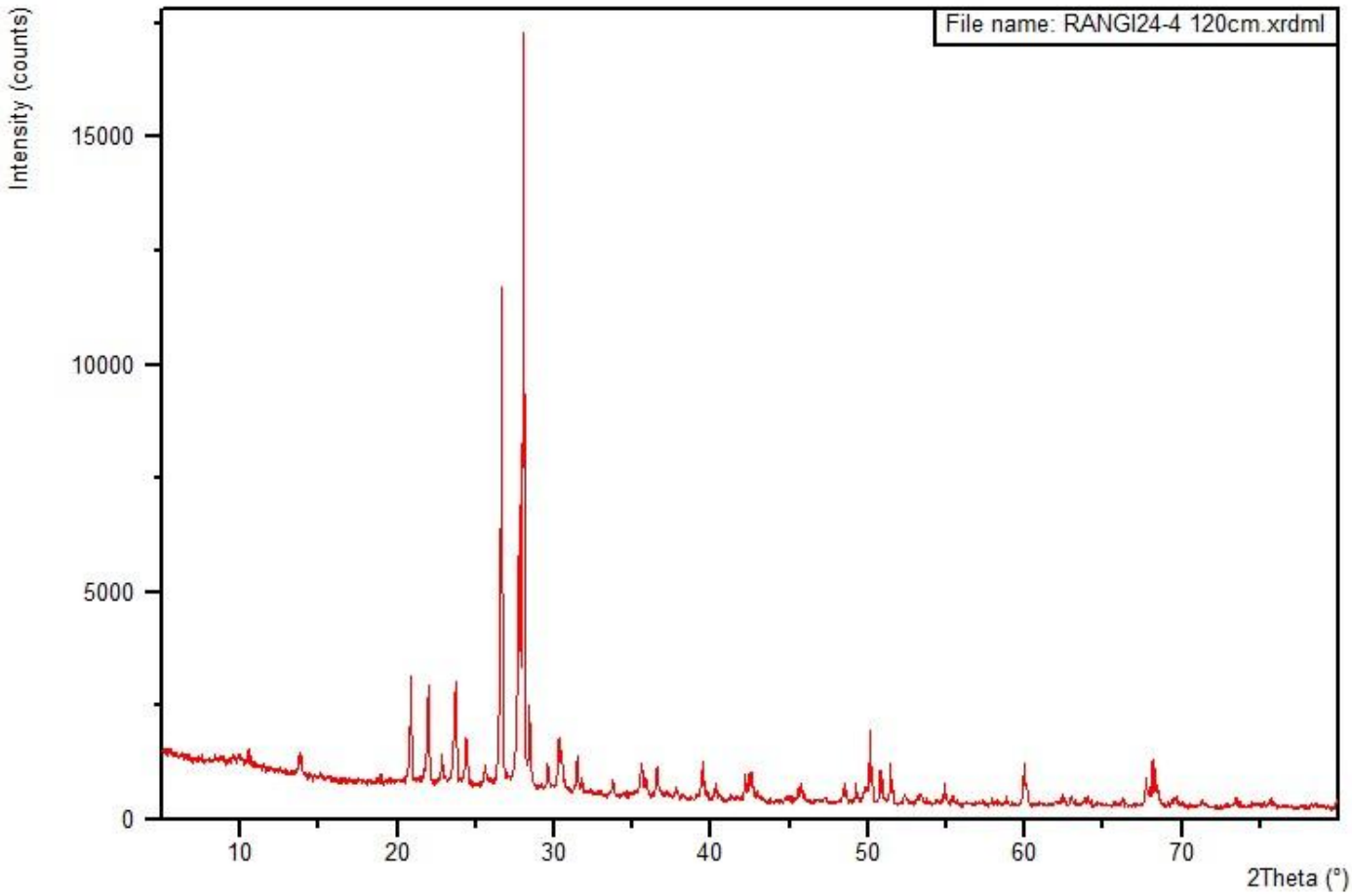
File name: RANGI24-4 120cm.xrdml
Intensity (counts)
15000
10000
5000
0
10
20
30
40
50
60
70
2Theta (°)

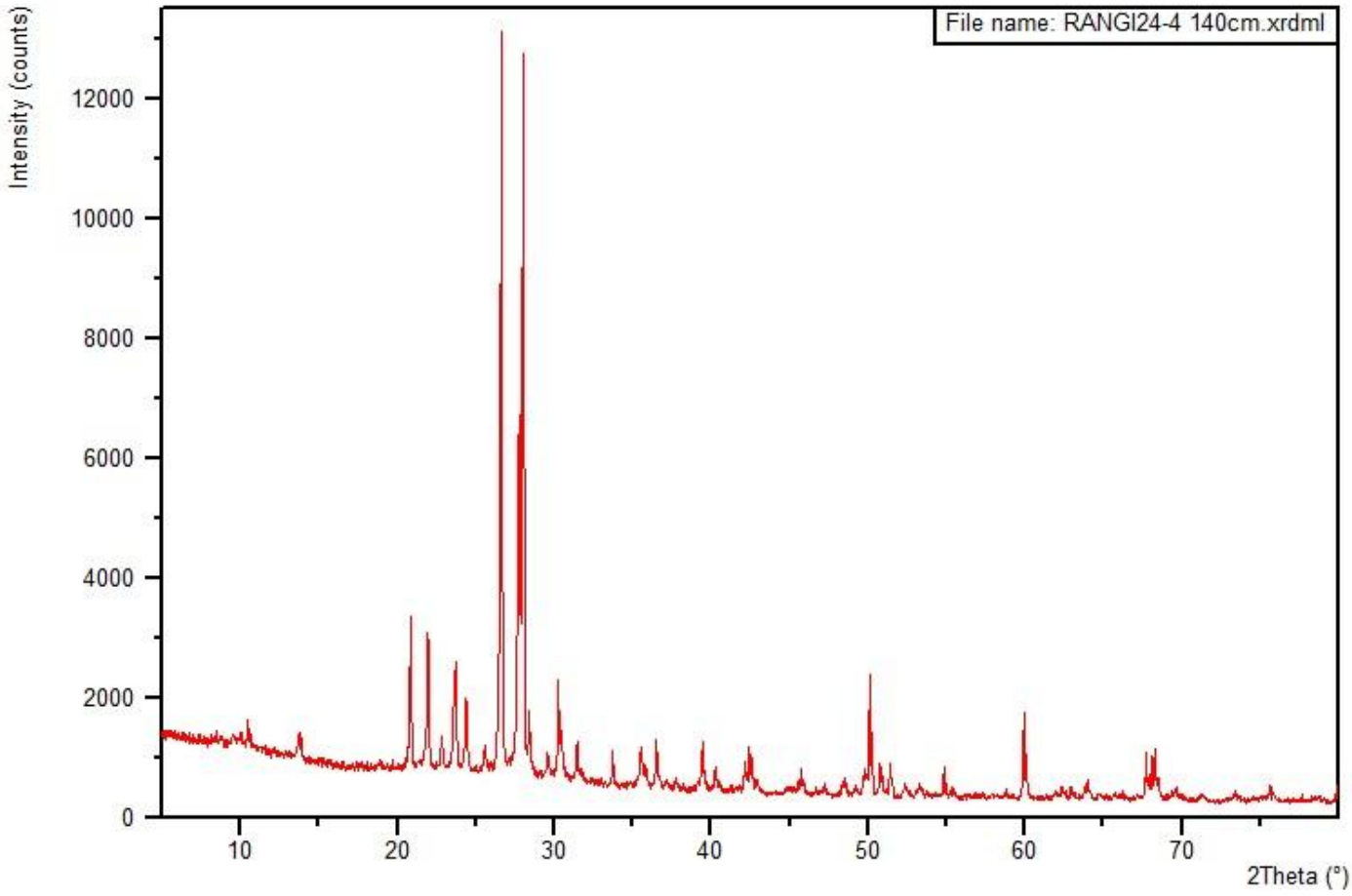
File name: RANGI24-4 140cm.xrdml
Intensity (counts)
12000
10000
8000
6000
4000
2000
0
10
20
30
40
50
60
70
2Theta (°)

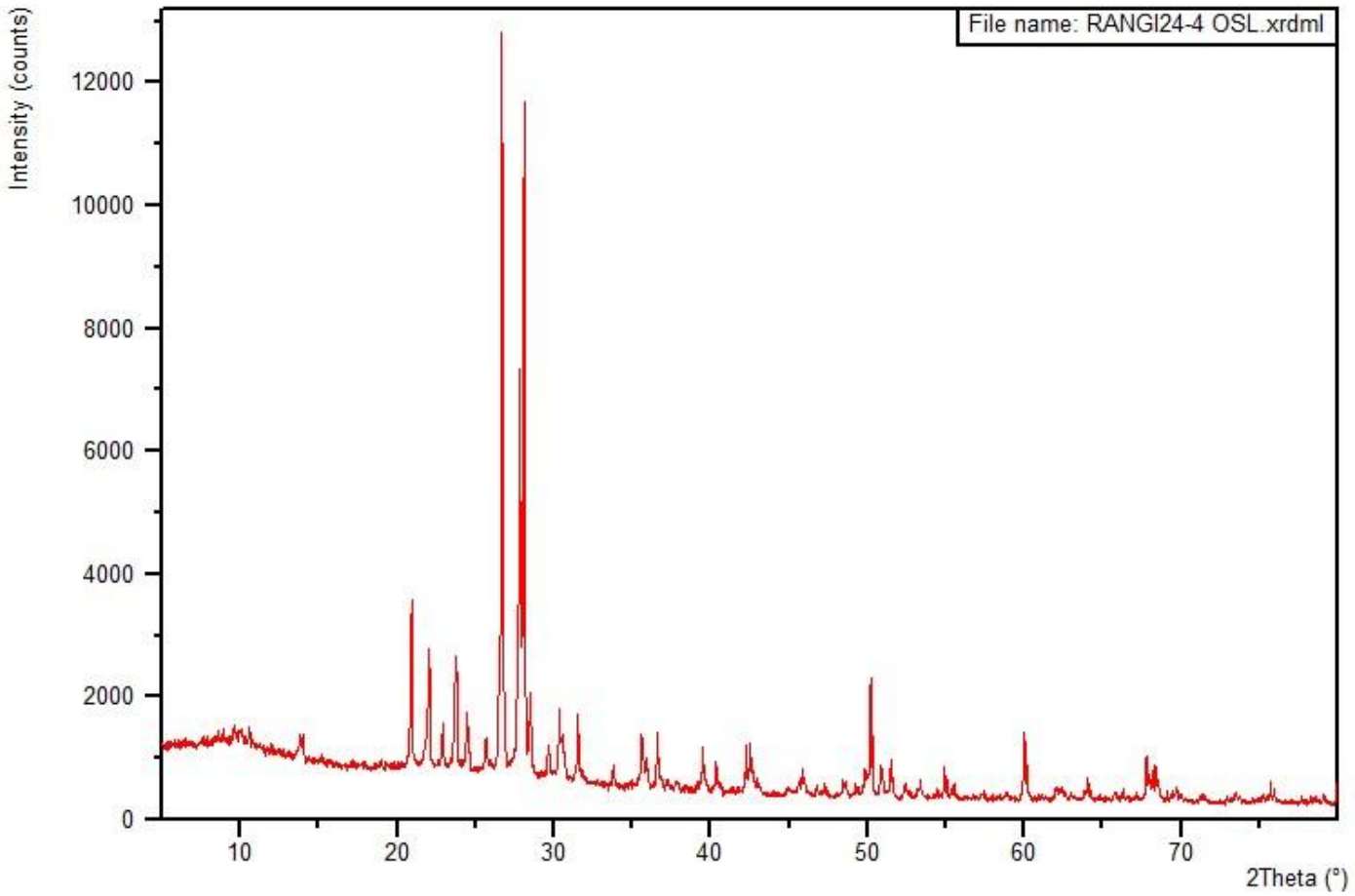
File name: RANGI24-4 OSL.xrdml
Intensity (counts)
12000
10000
8000
6000
4000
2000
0
10
20
30
40
50
60
70
2Theta (°)

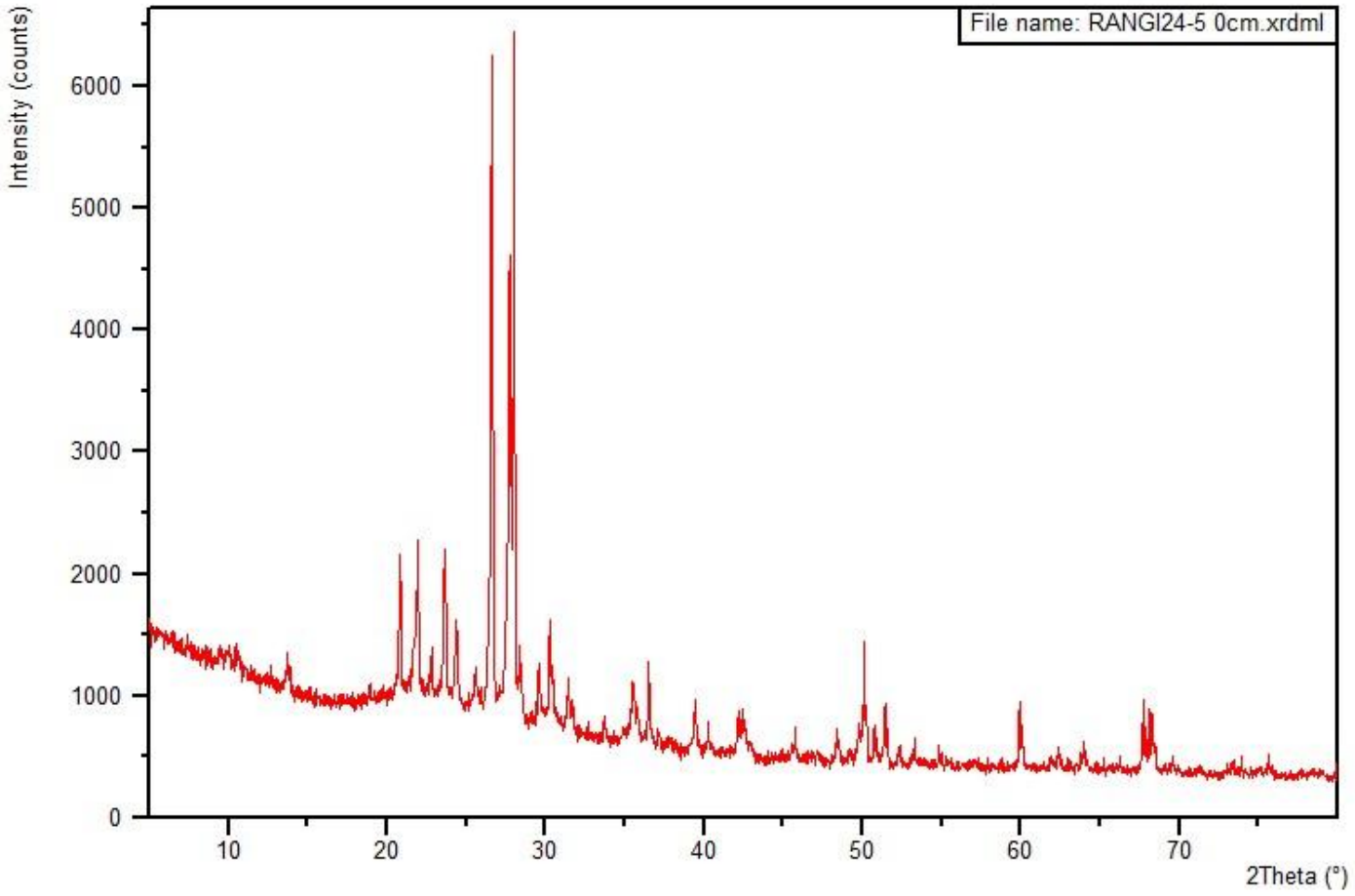
File name: RANGI24-5 0cm.xrdml
Intensity (counts)
6000
5000
4000
3000
2000
1000
0
10
20
30
40
50
60
70
2Theta (°)

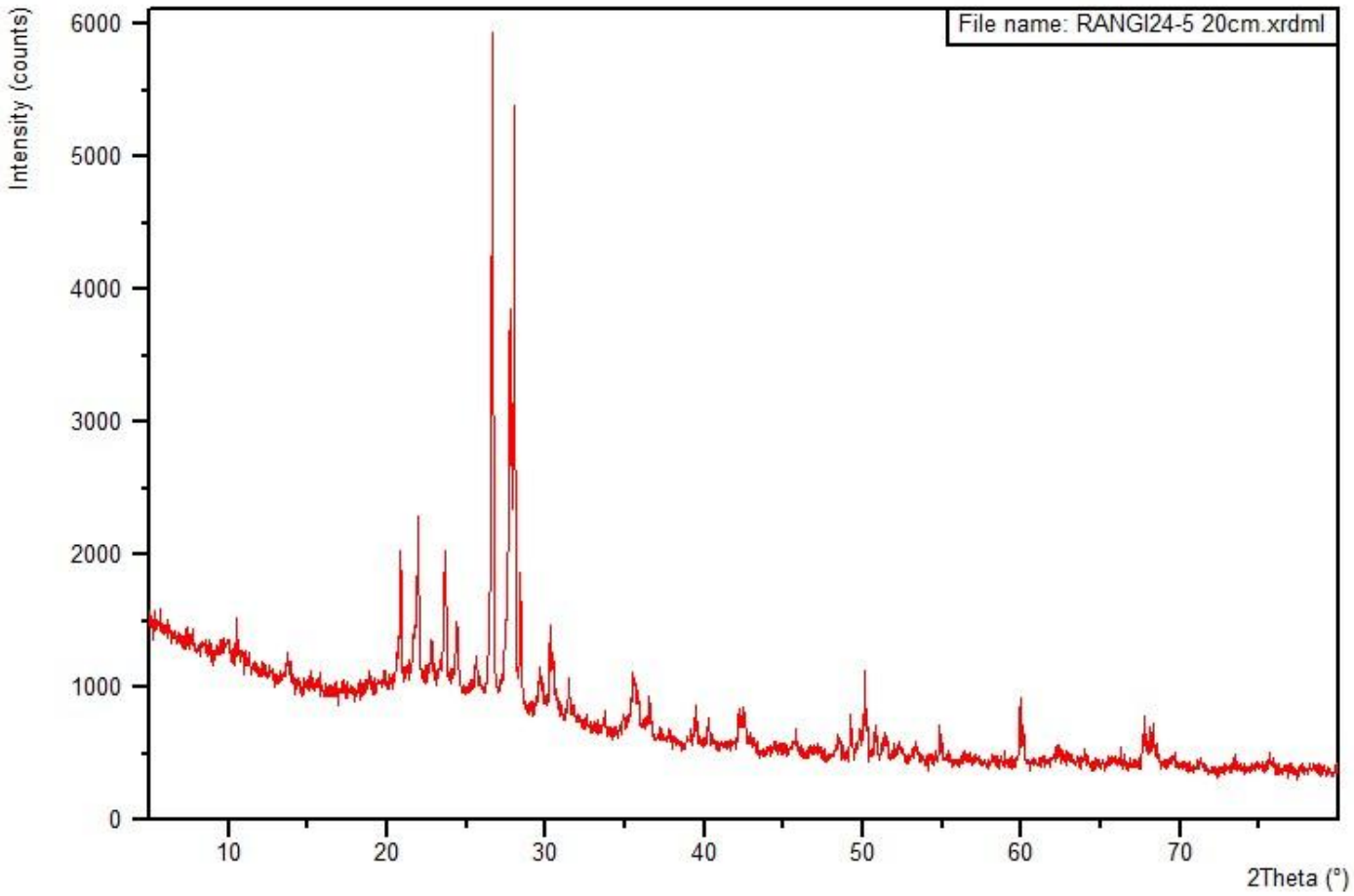
File name: RANGI24-5 20cm.xrdml
Intensity (counts)
6000
5000
4000
3000
2000
1000
0
10
20
30
40
50
60
70
2Theta (°)

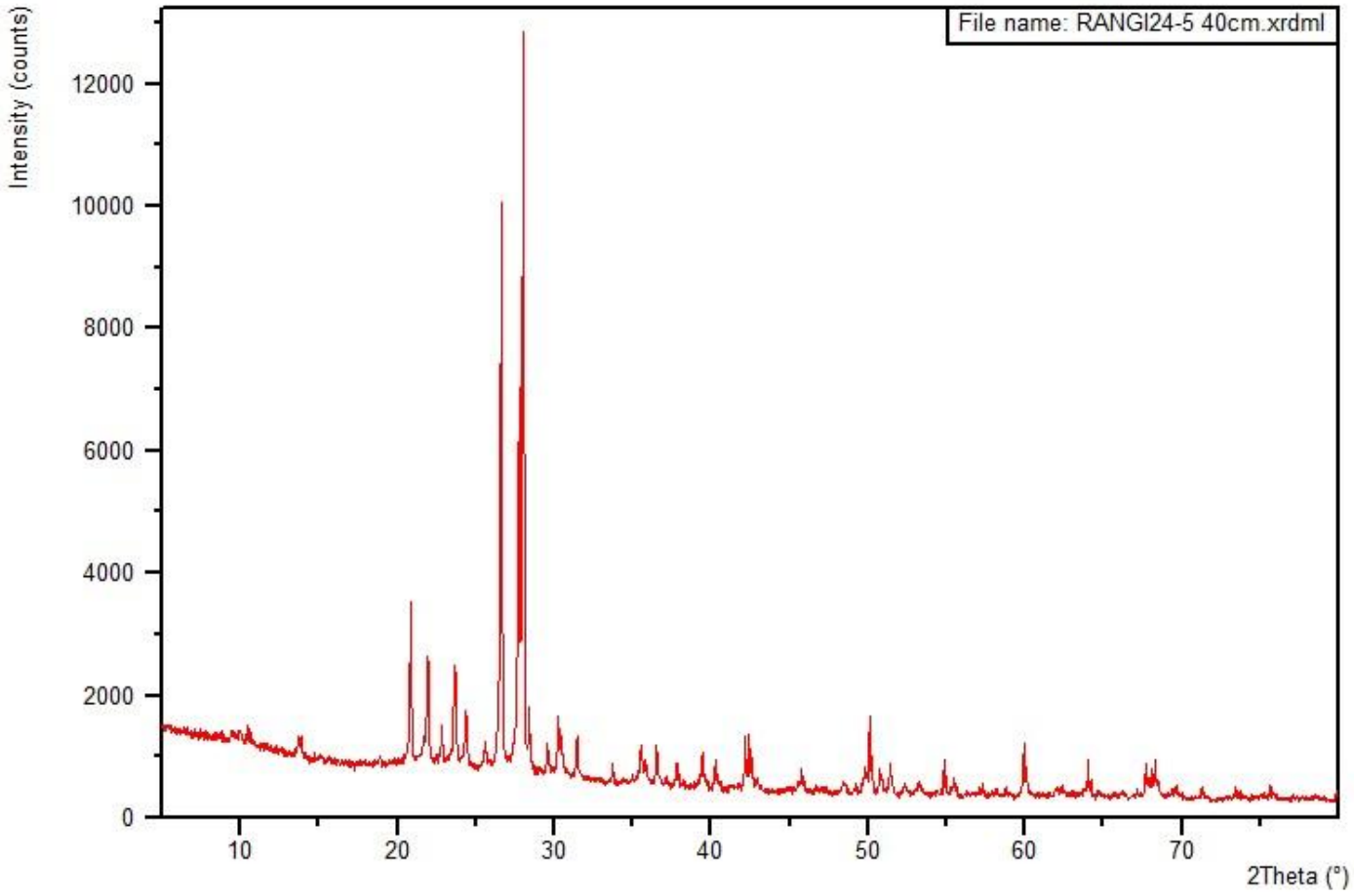
File name: RANGI24-5 40cm.xrdml
Intensity (counts)
12000
10000
8000
6000
4000
2000
0
10
20
30
40
50
60
70
2Theta (°)

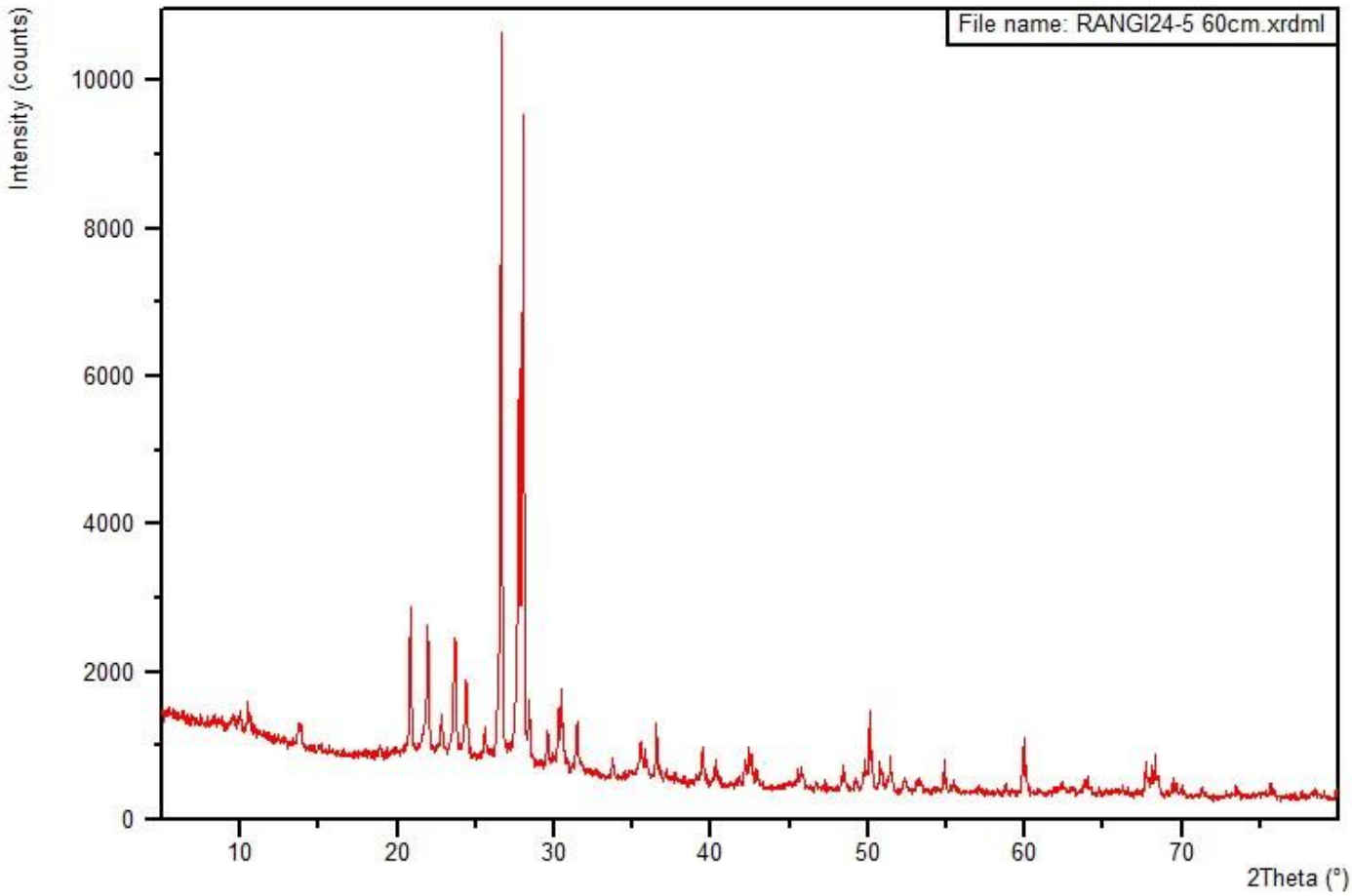
File name: RANGI24-5 60cm.xrdml
Intensity (counts)
10000
8000
6000
4000
2000
0
10
20
30
40
50
60
70
2Theta (°)

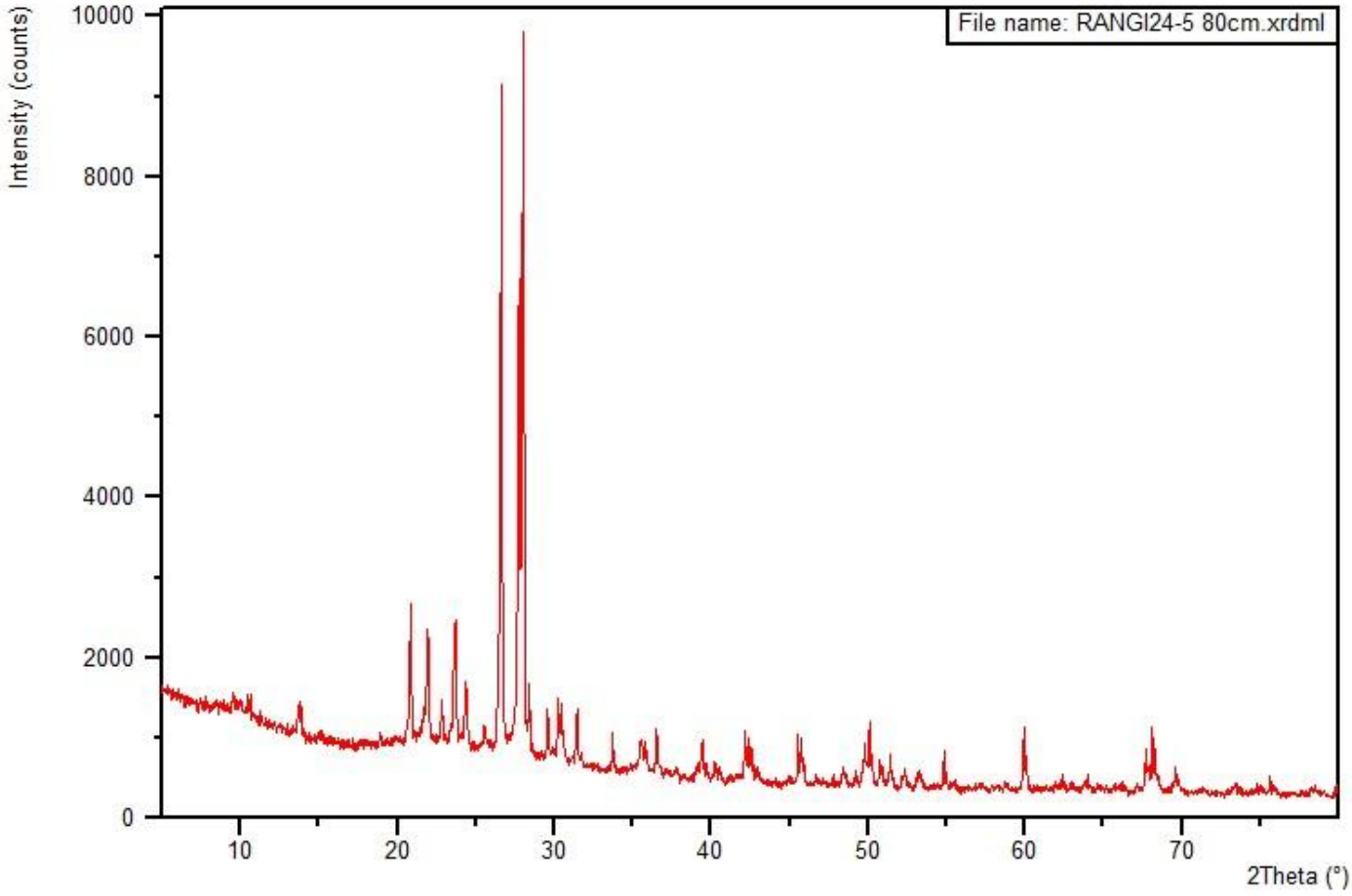
File name: RANGI24-5 80cm.xrdml
Intensity (counts)
10000
8000
6000
4000
2000
0
10
20
30
40
50
60
70
2Theta (°)

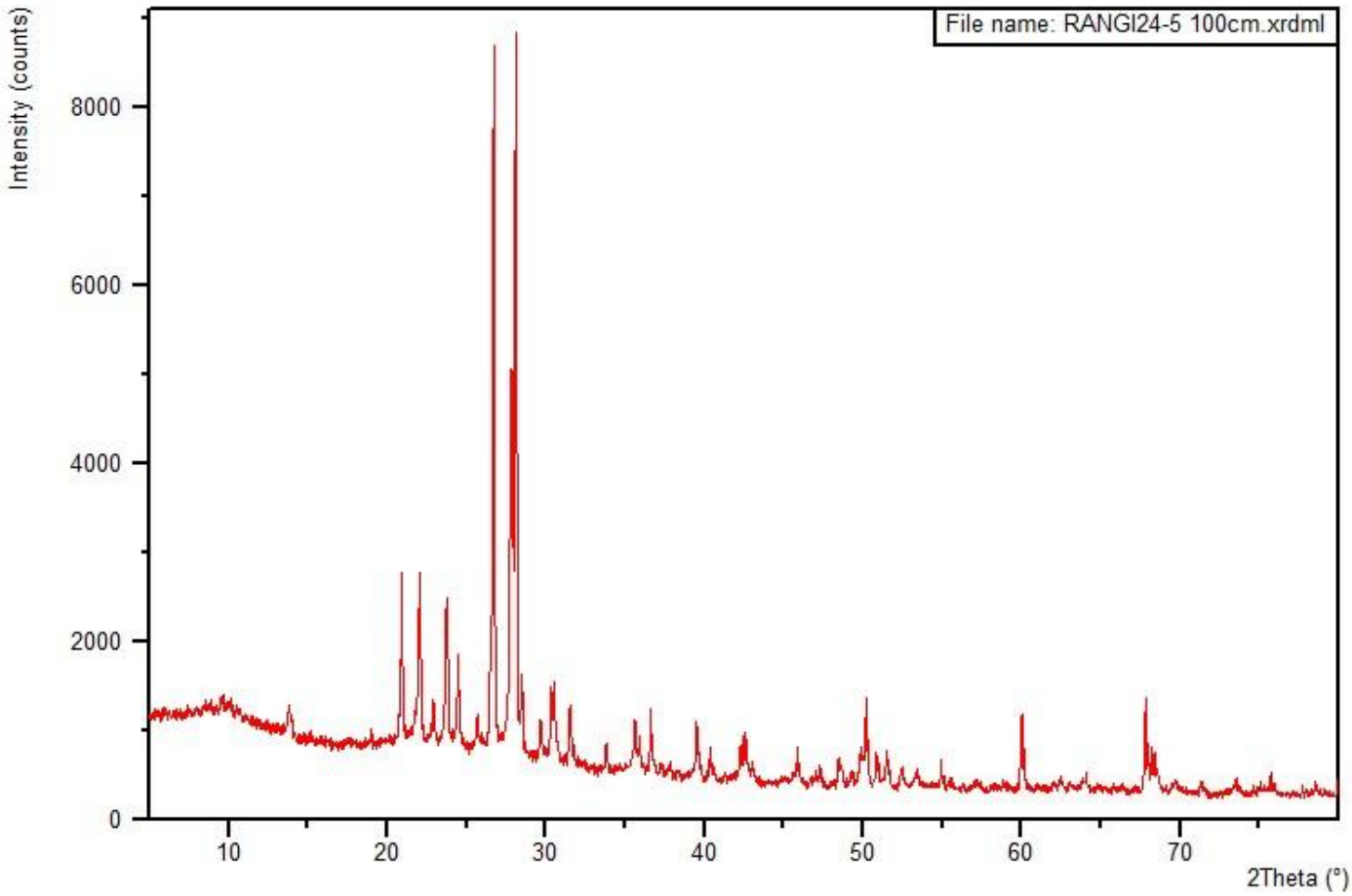
File name: RANGI24-5 100cm.xrdml
Intensity (counts)
8000
6000
4000
2000
0
10
20
30
40
50
60
70
2Theta (°)

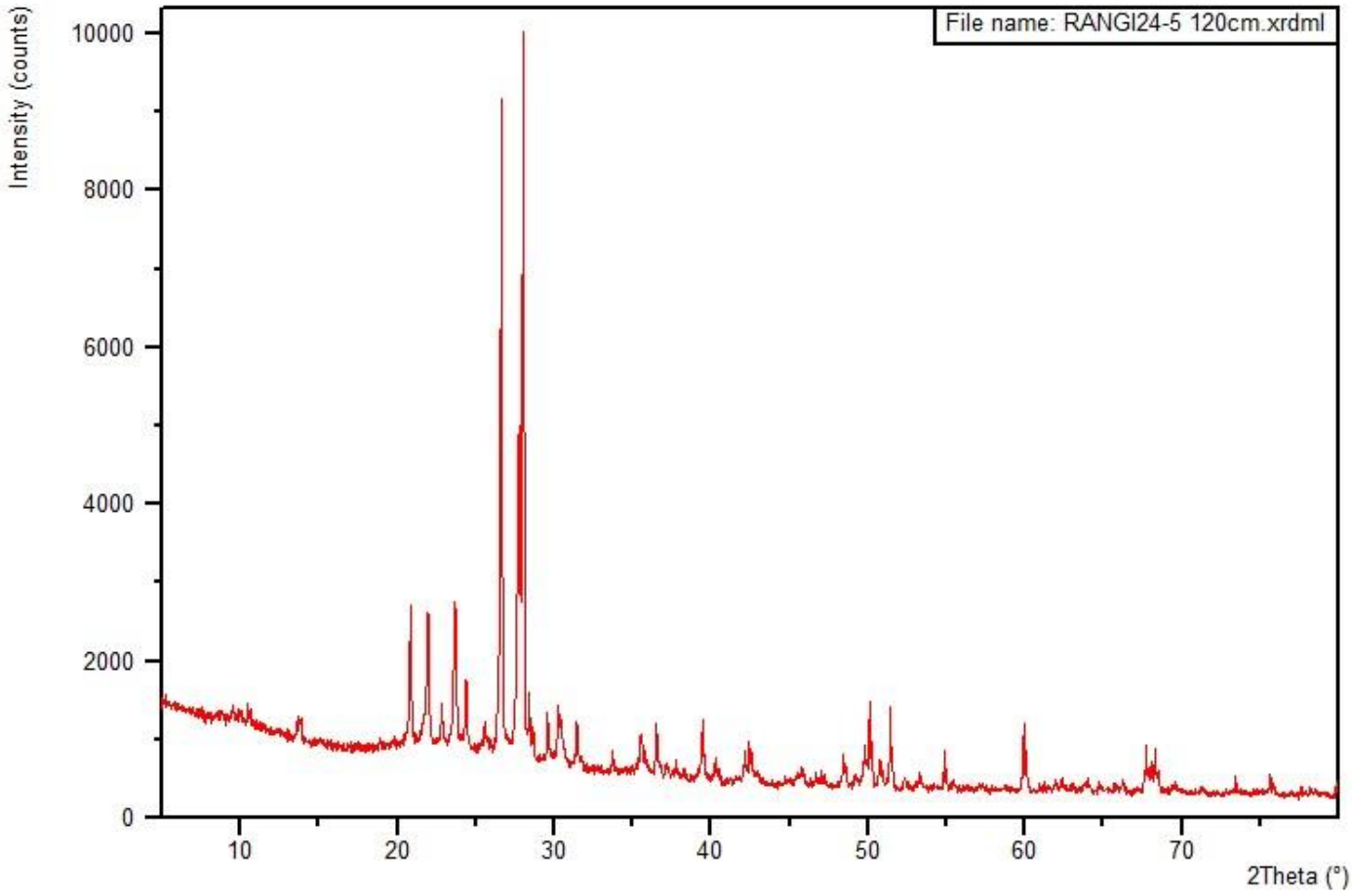
File name: RANGI24-5 120cm.xrdml
Intensity (counts)
10000
8000
6000
4000
2000
0
10
20
30
40
50
60
70
2Theta (°)

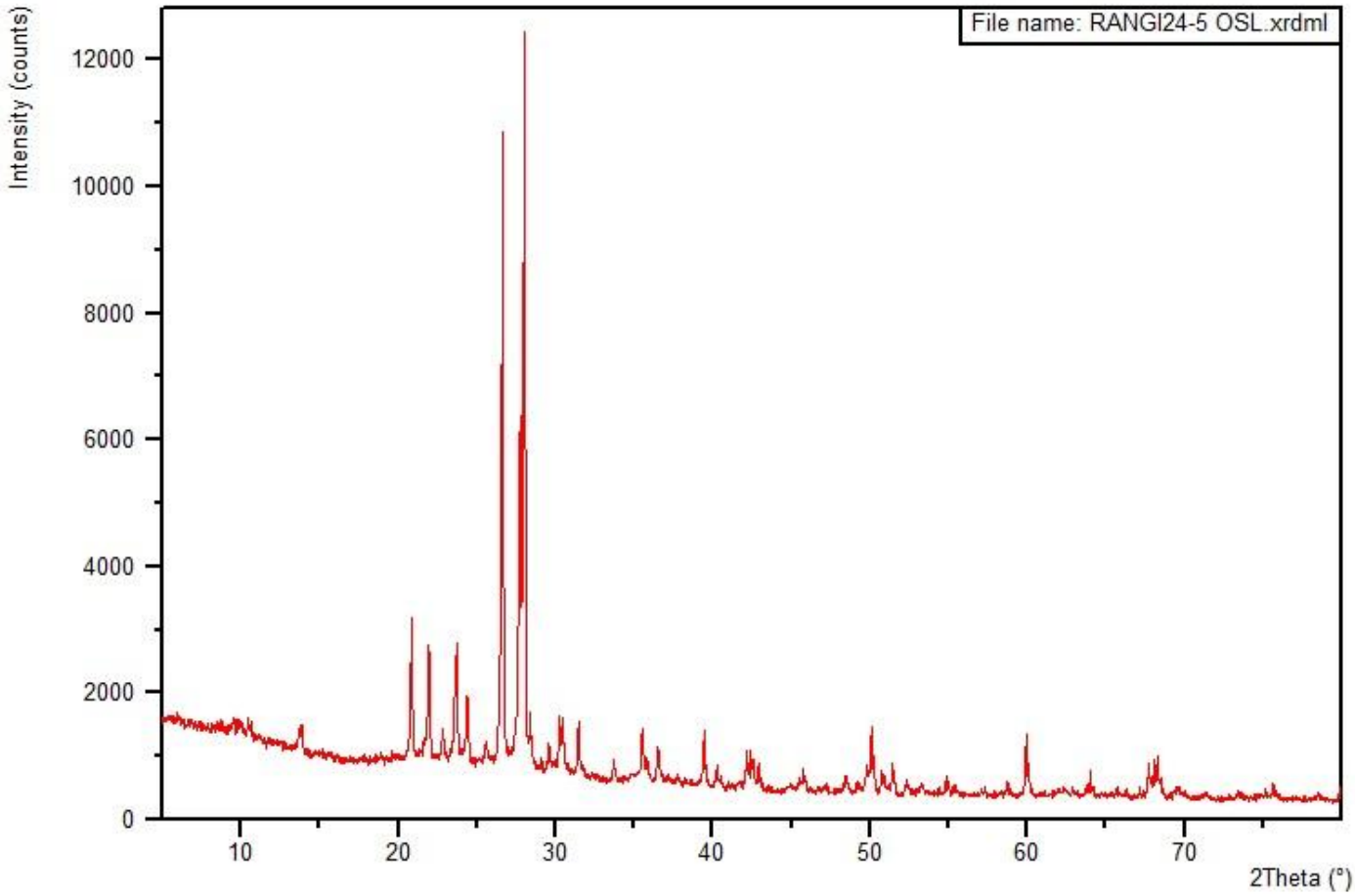
File name: RANGI24-5 OSL.xrdml
Intensity (counts)
12000
10000
8000
6000
4000
2000
0
10
20
30
40
50
60
70
2Theta (°)

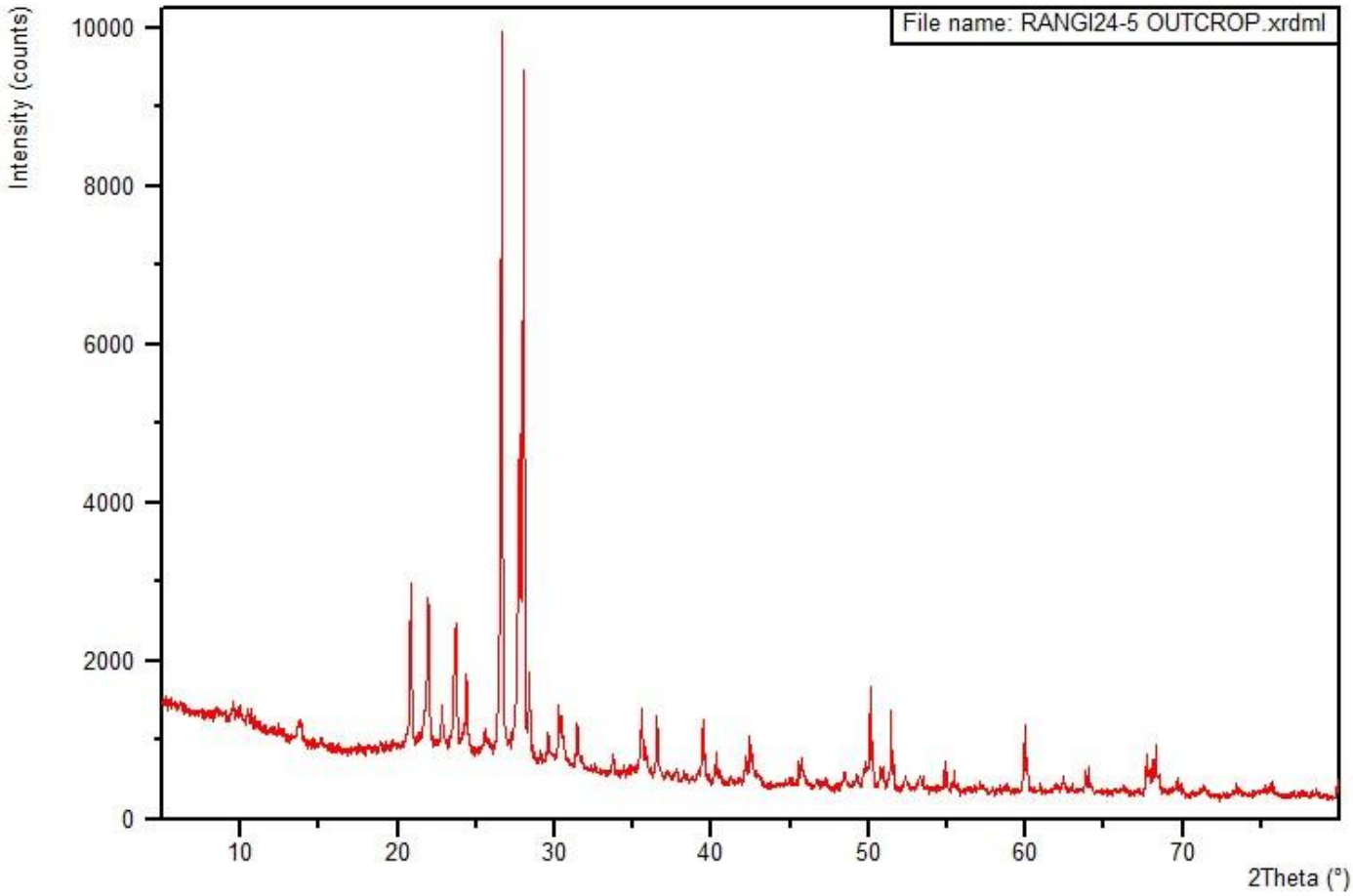
File name: RANGI24-5 OUTCROP.xrdml
Intensity (counts)
10000
8000
6000
4000
2000
0
10
20
30
40
50
60
70
2Theta (°)

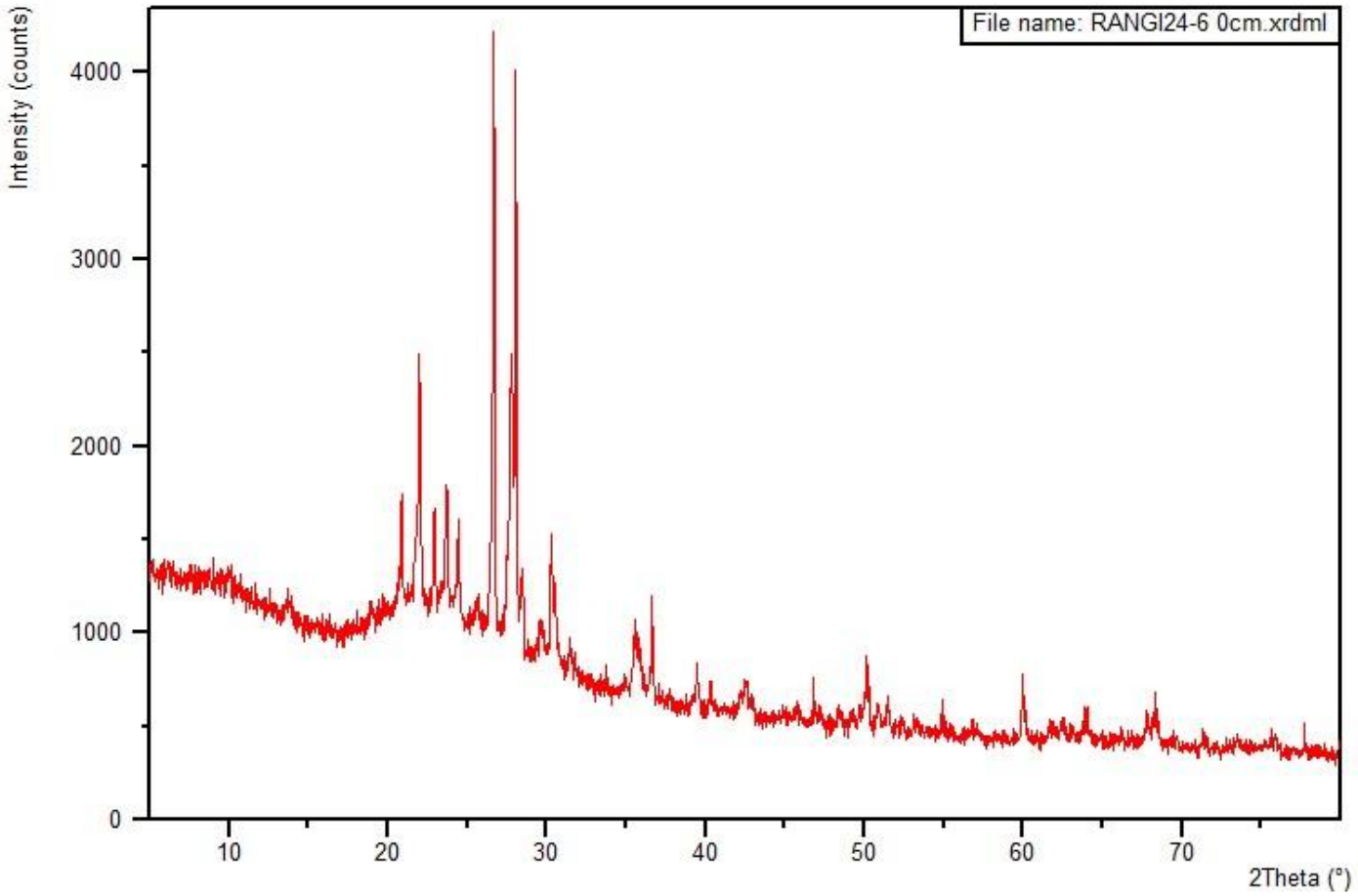
File name: RANGI24-6 0cm.xrdml
Intensity (counts)
4000
3000
2000
1000
0
10
20
30
40
50
60
70
2Theta (°)

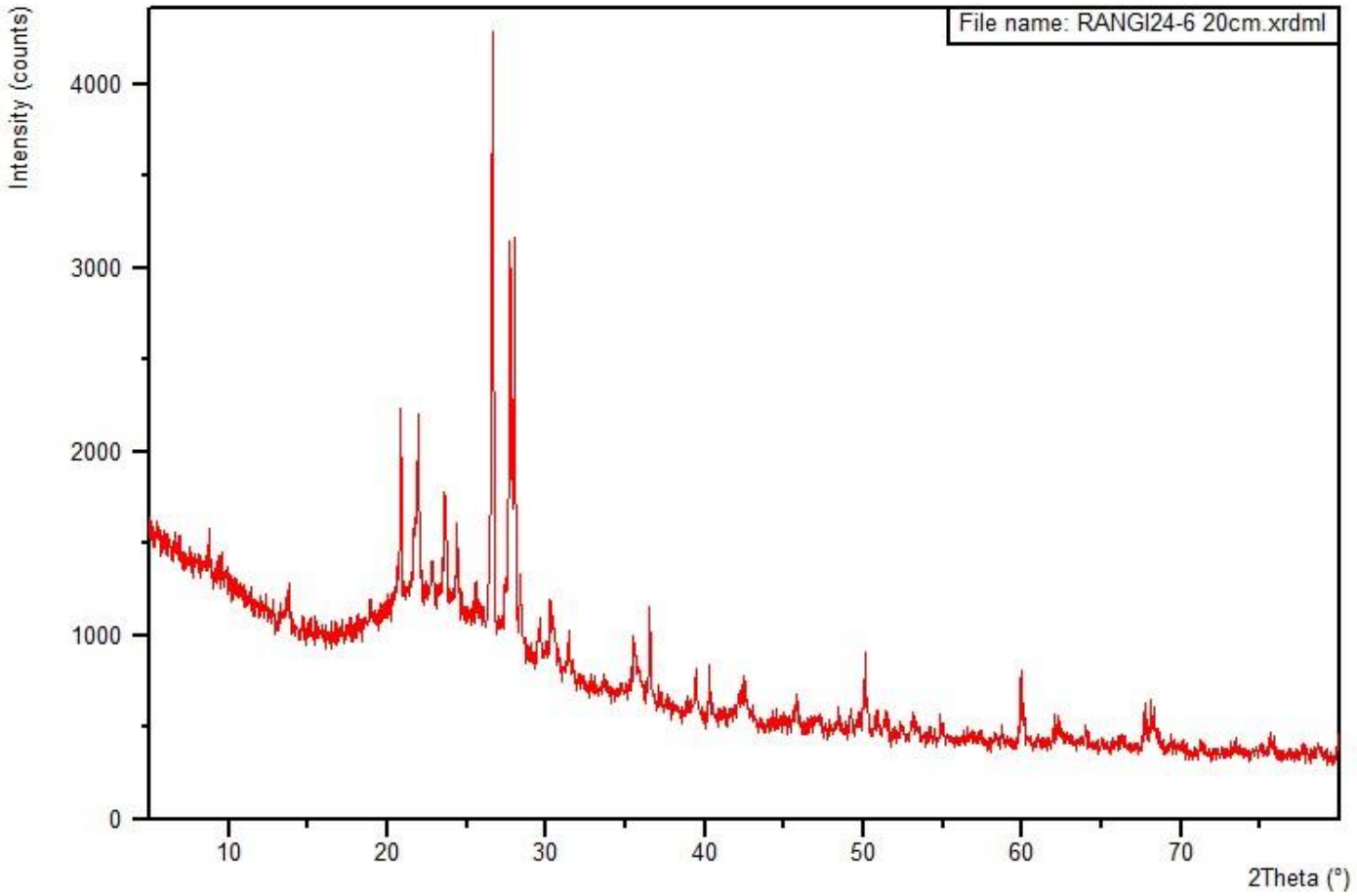
File name: RANGI24-6 20cm.xrdml
Intensity (counts)
4000
3000
2000
1000
0
10
20
30
40
50
60
70
2Theta (°)

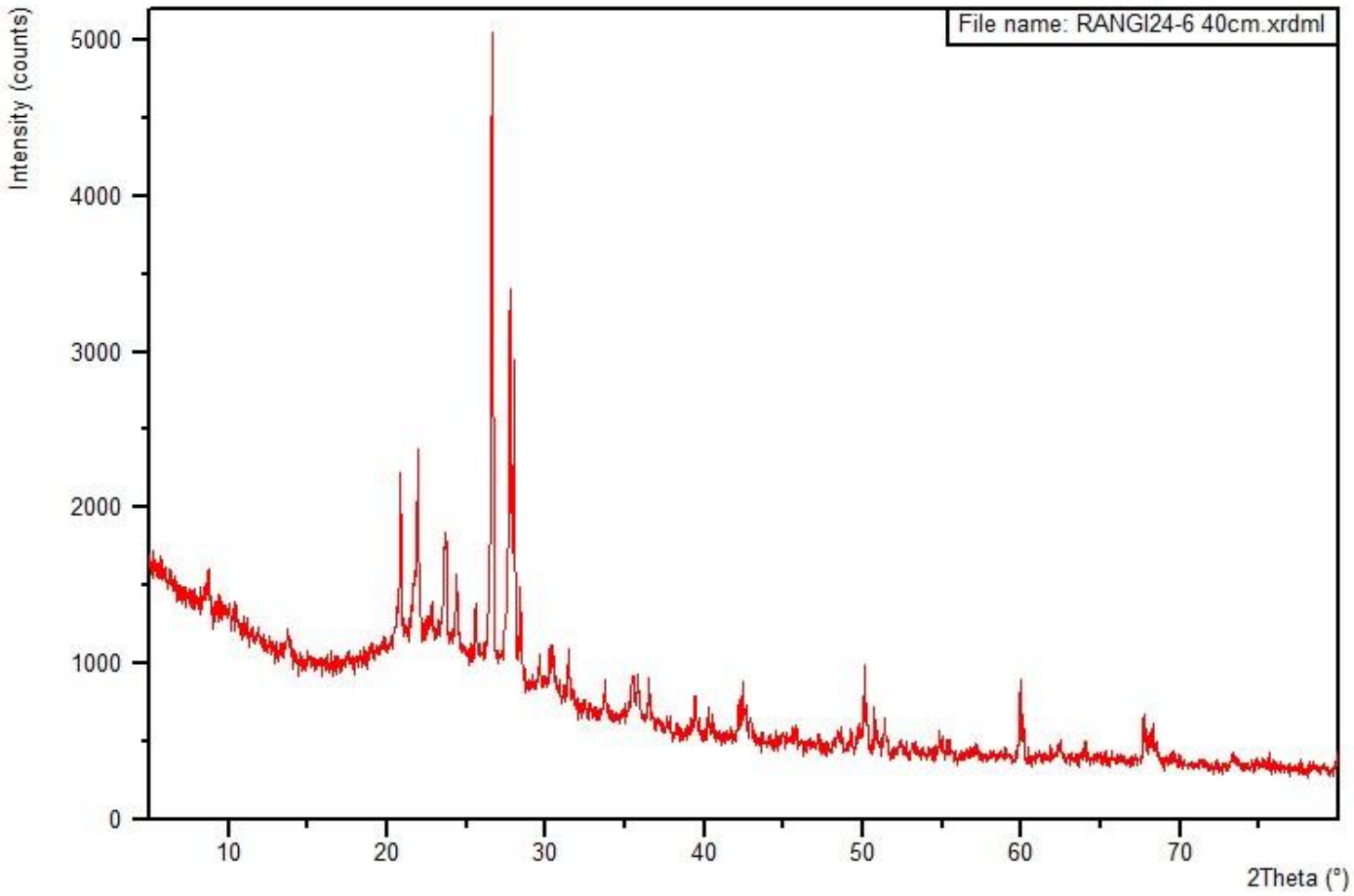
File name: RANGI24-6 40cm.xrdml
Intensity (counts)
5000
4000
3000
2000
1000
0
10
20
30
40
50
60
70
2Theta (°)

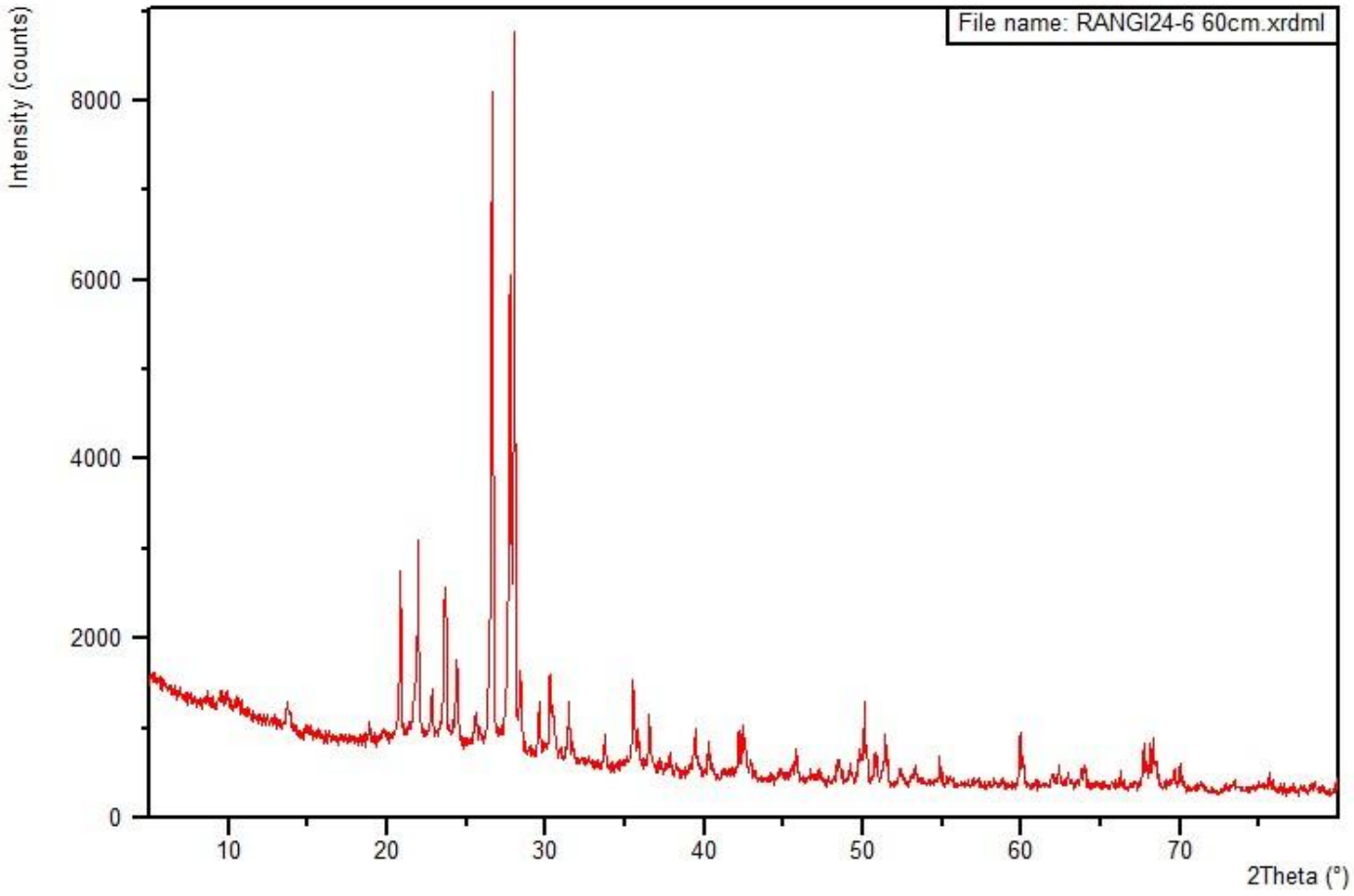
File name: RANGI24-6 60cm.xrdml
Intensity (counts)
8000
6000
4000
2000
0
10
20
30
40
50
60
70
2Theta (°)

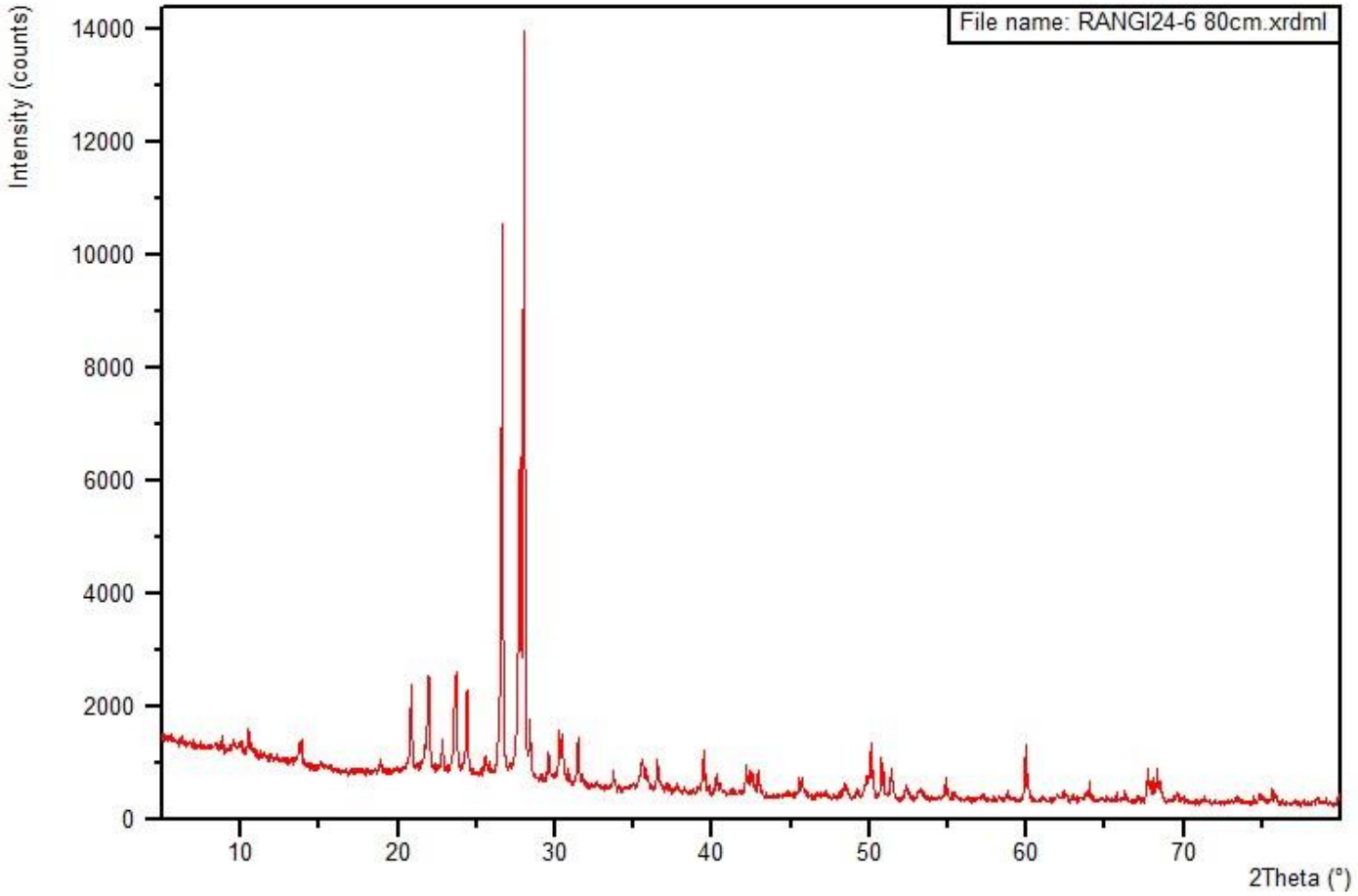
File name: RANGI24-6 80cm.xrdml
Intensity (counts)
14000
12000
10000
8000
6000
4000
2000
0
10
20
30
40
50
60
70
2Theta (°)

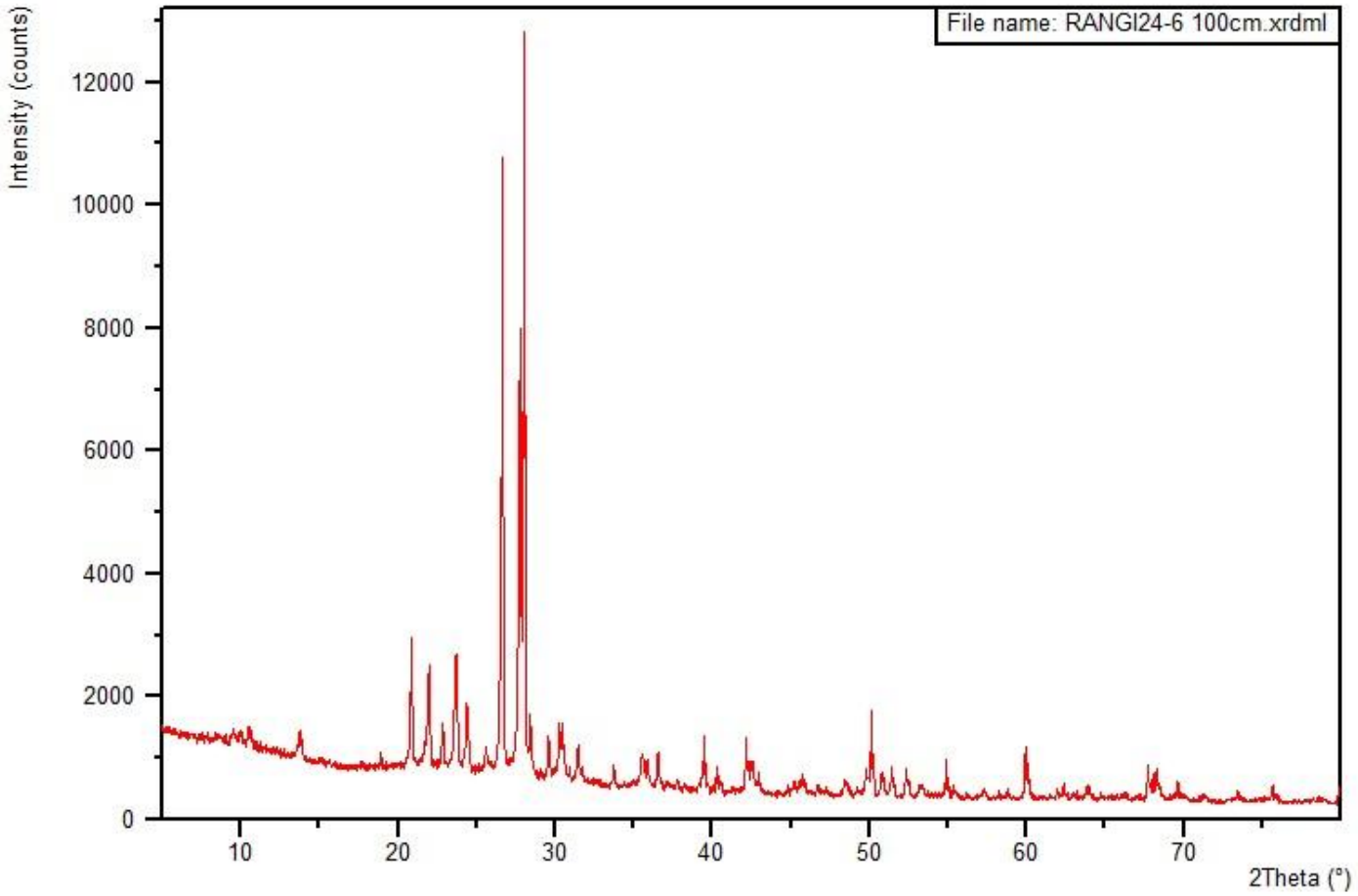
File name: RANGI24-6 100cm.xrdml
Intensity (counts)
12000
10000
8000
6000
4000
2000
0
10
20
30
40
50
60
70
2Theta (°)

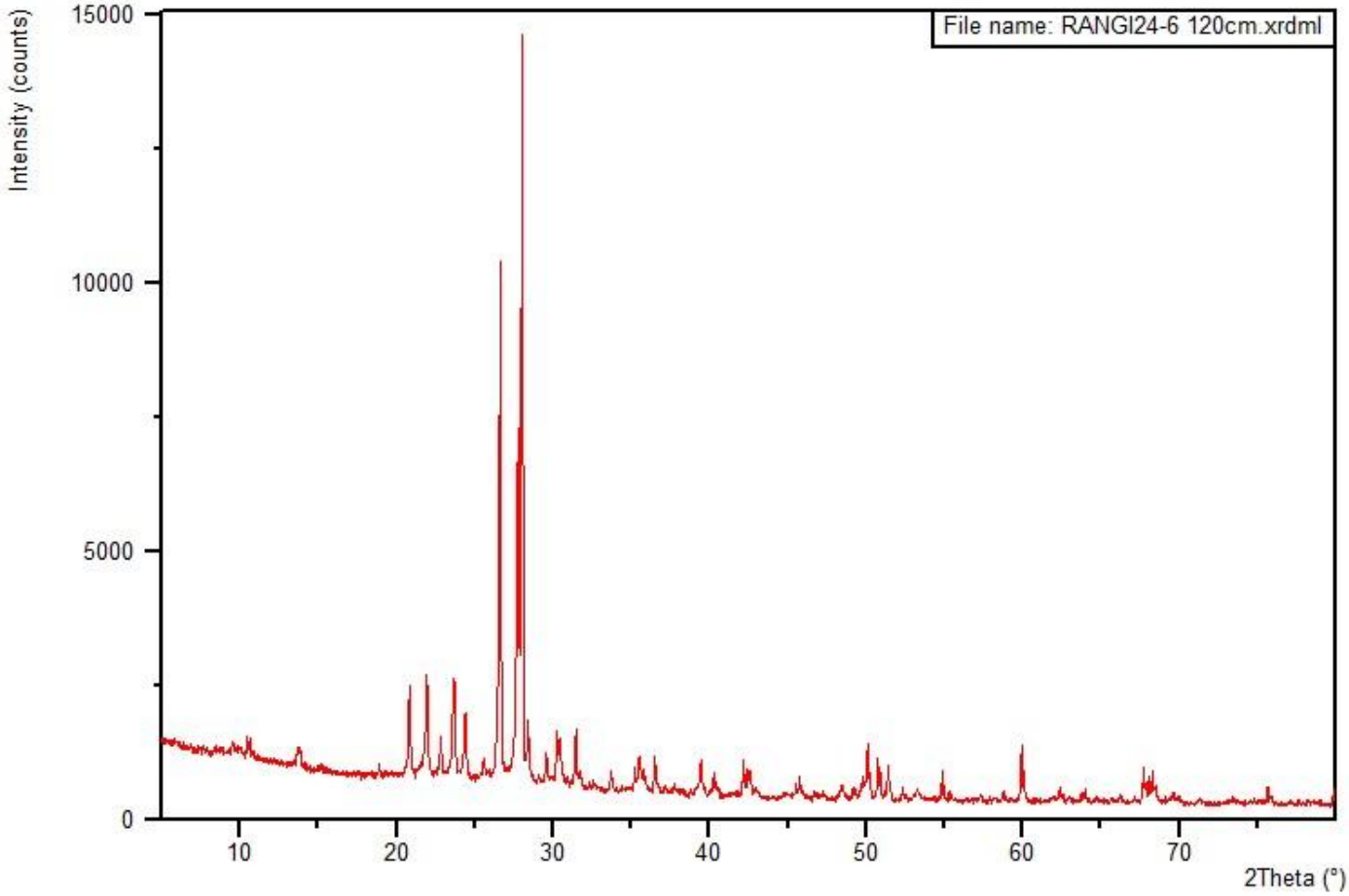
File name: RANGI24-6 120cm.xrdml
Intensity (counts)
15000
10000
5000
0
10
20
30
40
50
60
70
2Theta (°)

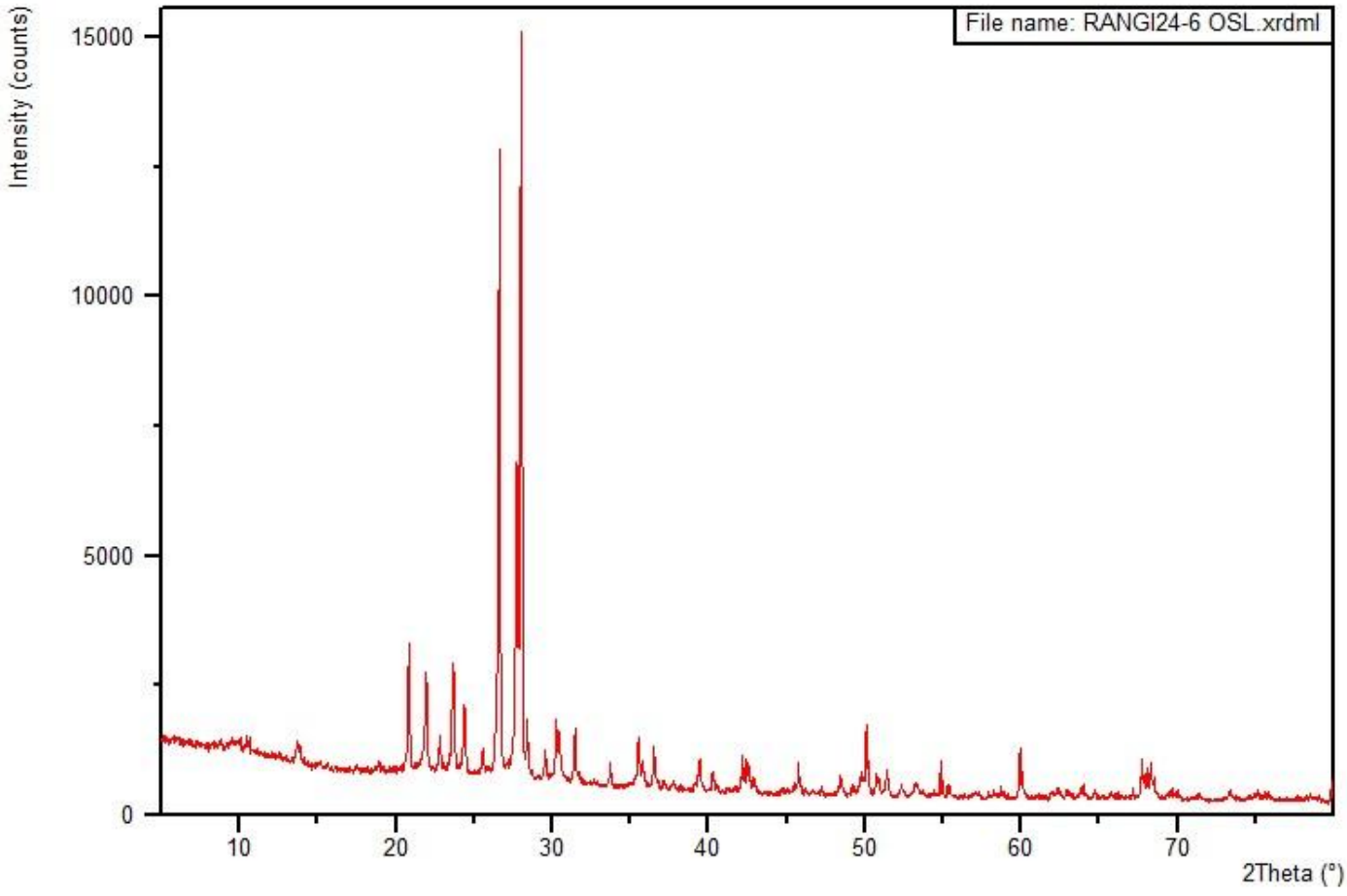
File name: RANGI24-6 OSL.xrdml
Intensity (counts)
15000
10000
5000
0
10
20
30
40
50
60
70
2Theta (°)

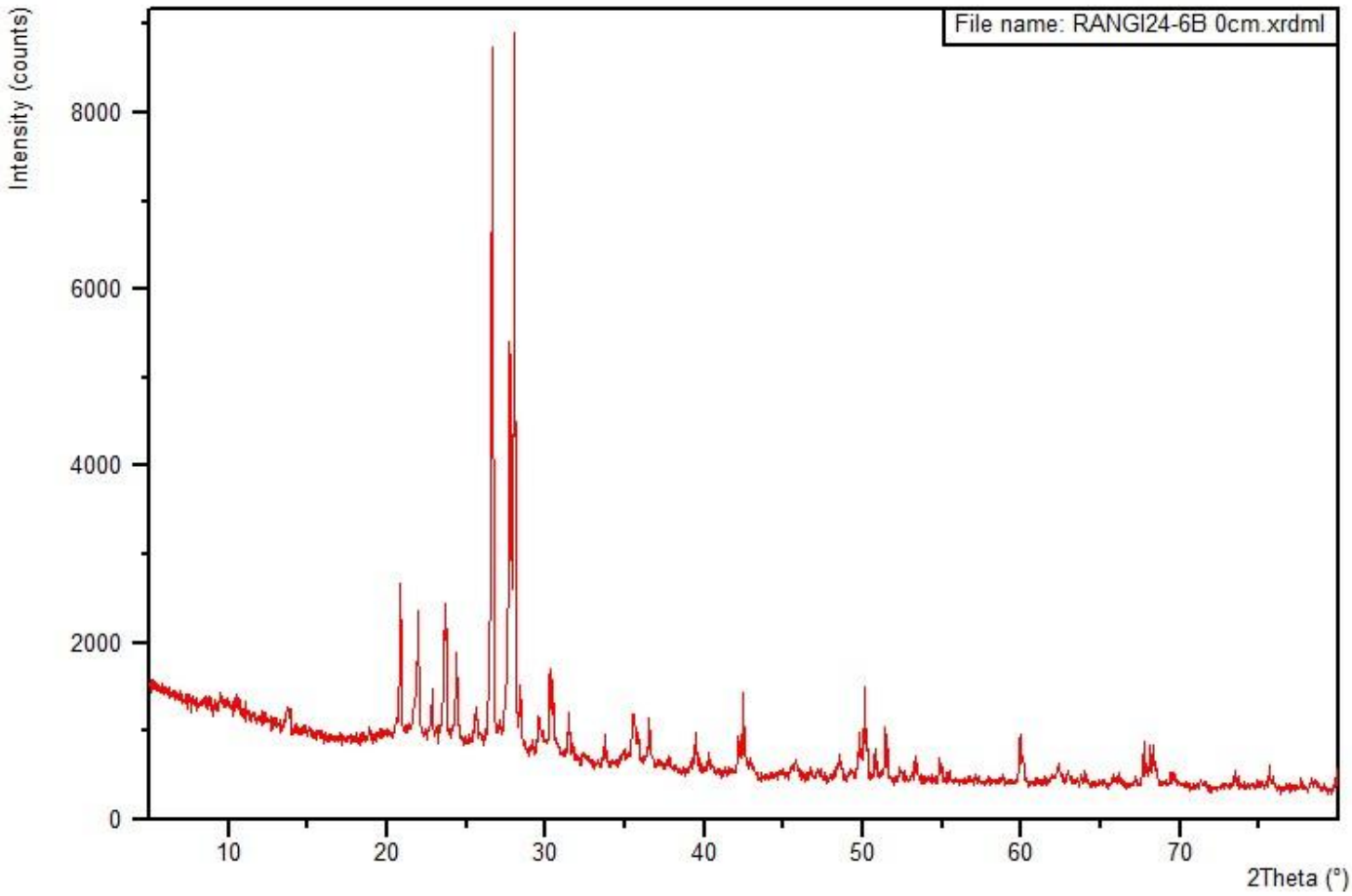
File name: RANGI24-6B 0cm.xrdml
Intensity (counts)
8000
6000
4000
2000
0
10
20
30
40
50
60
70
2Theta (°)

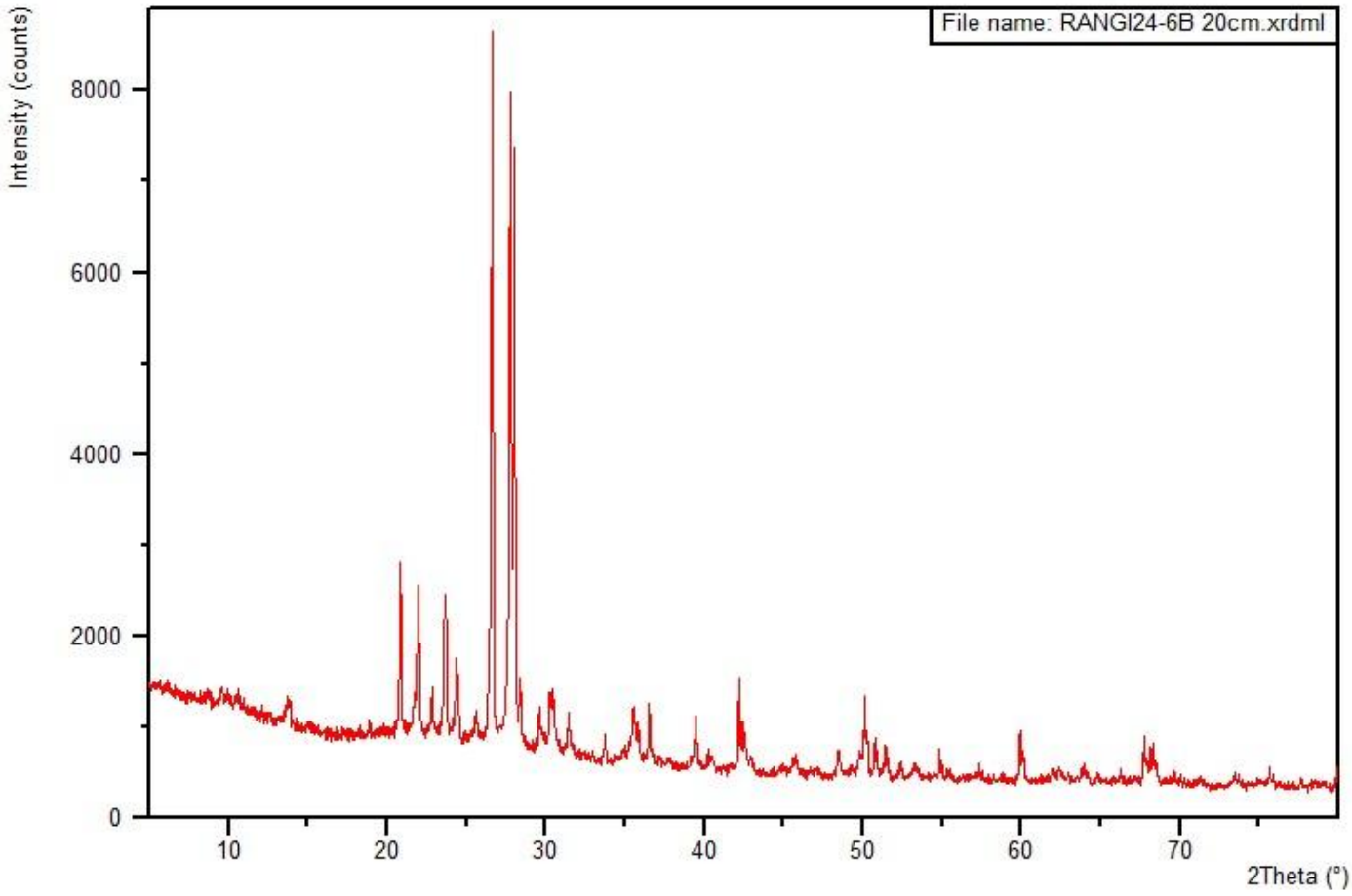
File name: RANGI24-6B 20cm.xrdml
Intensity (counts)
8000
6000
4000
2000
0
10
20
30
40
50
60
70
2Theta (°)

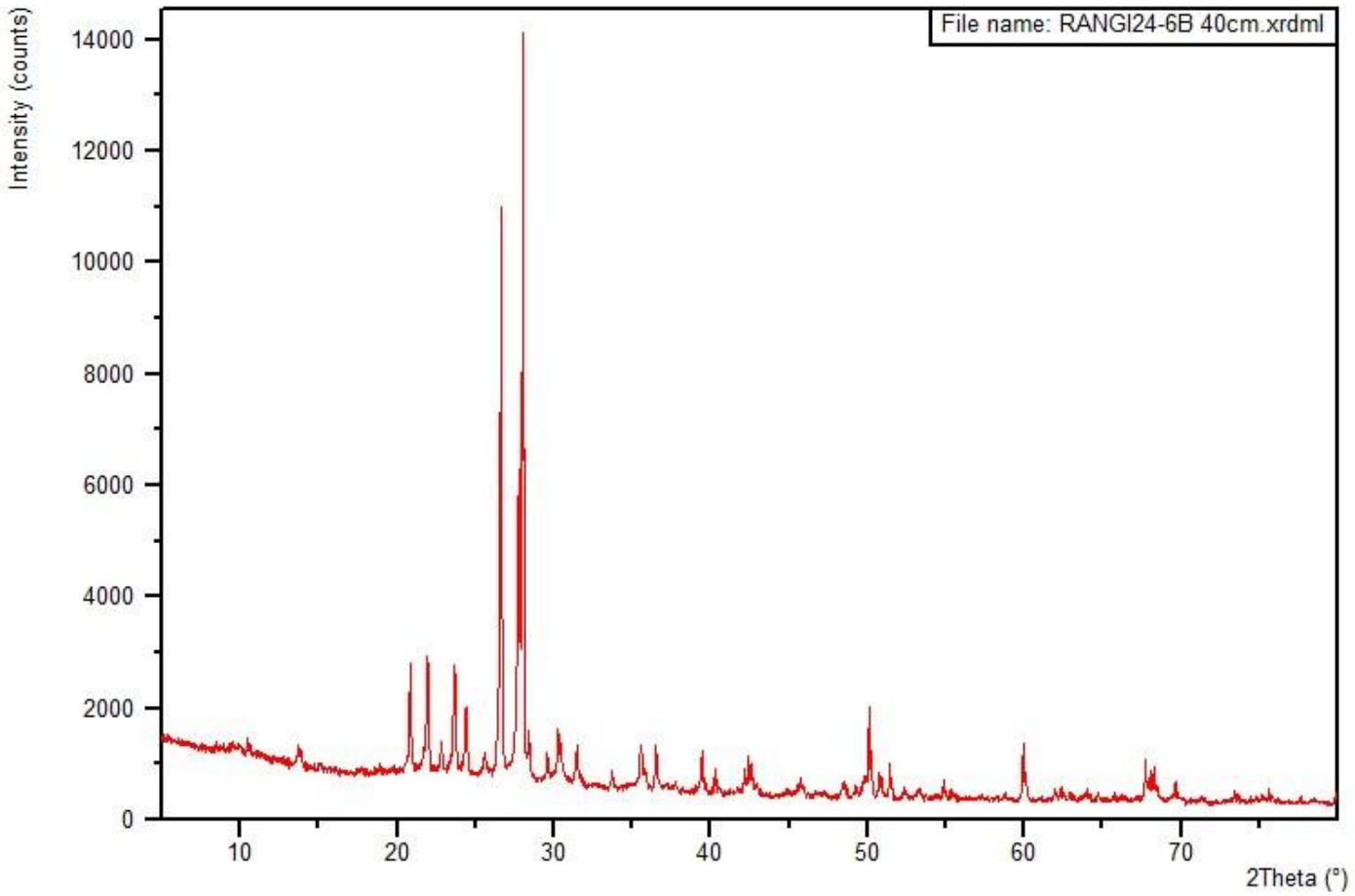
File name: RANGI24-6B 40cm.xrdml
Intensity (counts)
14000
12000
10000
8000
6000
4000
2000
0
10
20
30
40
50
60
70
2Theta (°)

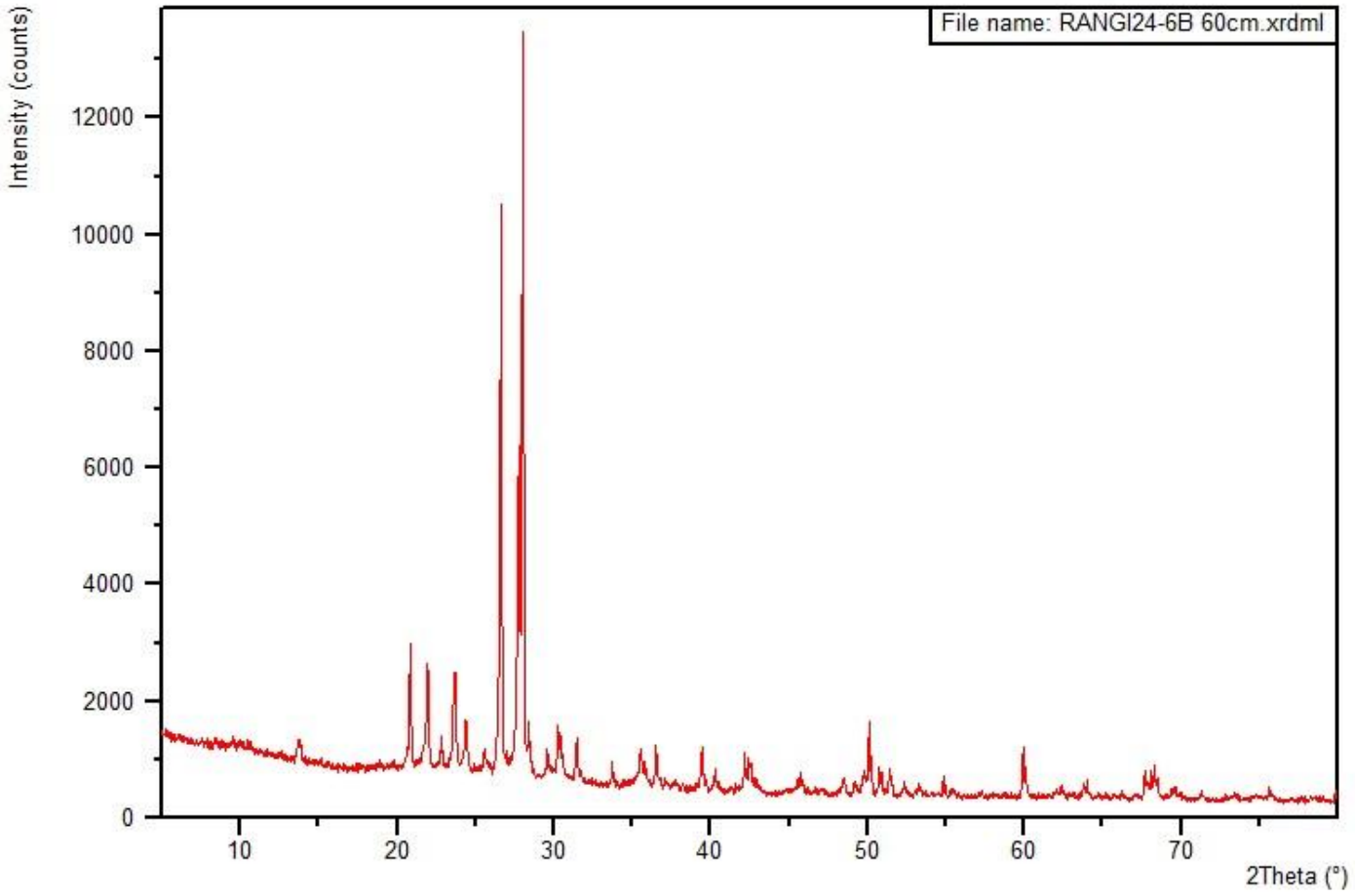
File name: RANGI24-6B 60cm.xrdml
Intensity (counts)
12000
10000
8000
6000
4000
2000
0
10
20
30
40
50
60
70
2Theta (°)

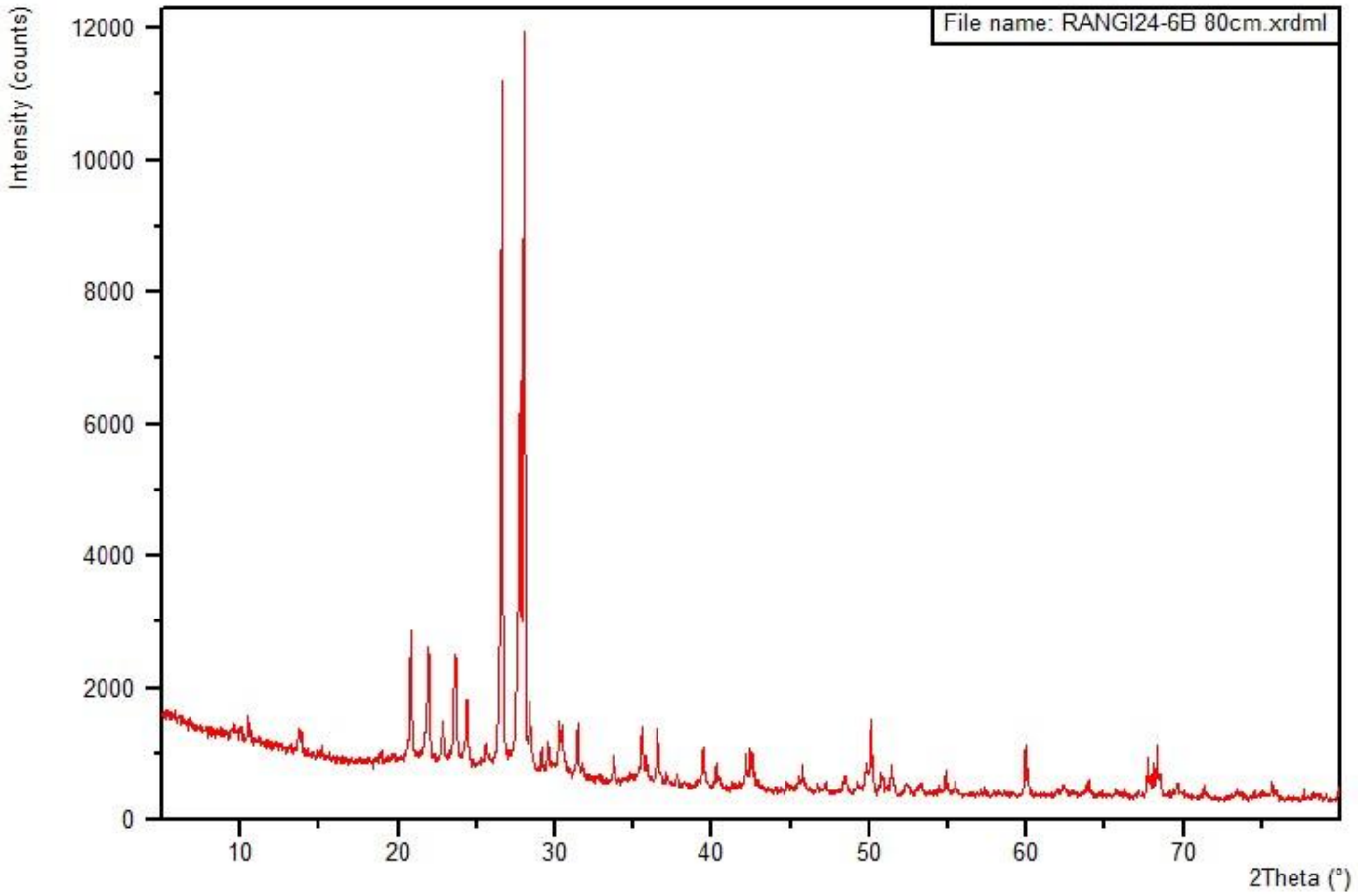
File name: RANGI24-6B 80cm.xrdml
Intensity (counts)
12000
10000
8000
6000
4000
2000
0
10
20
30
40
50
60
70
2Theta (°)

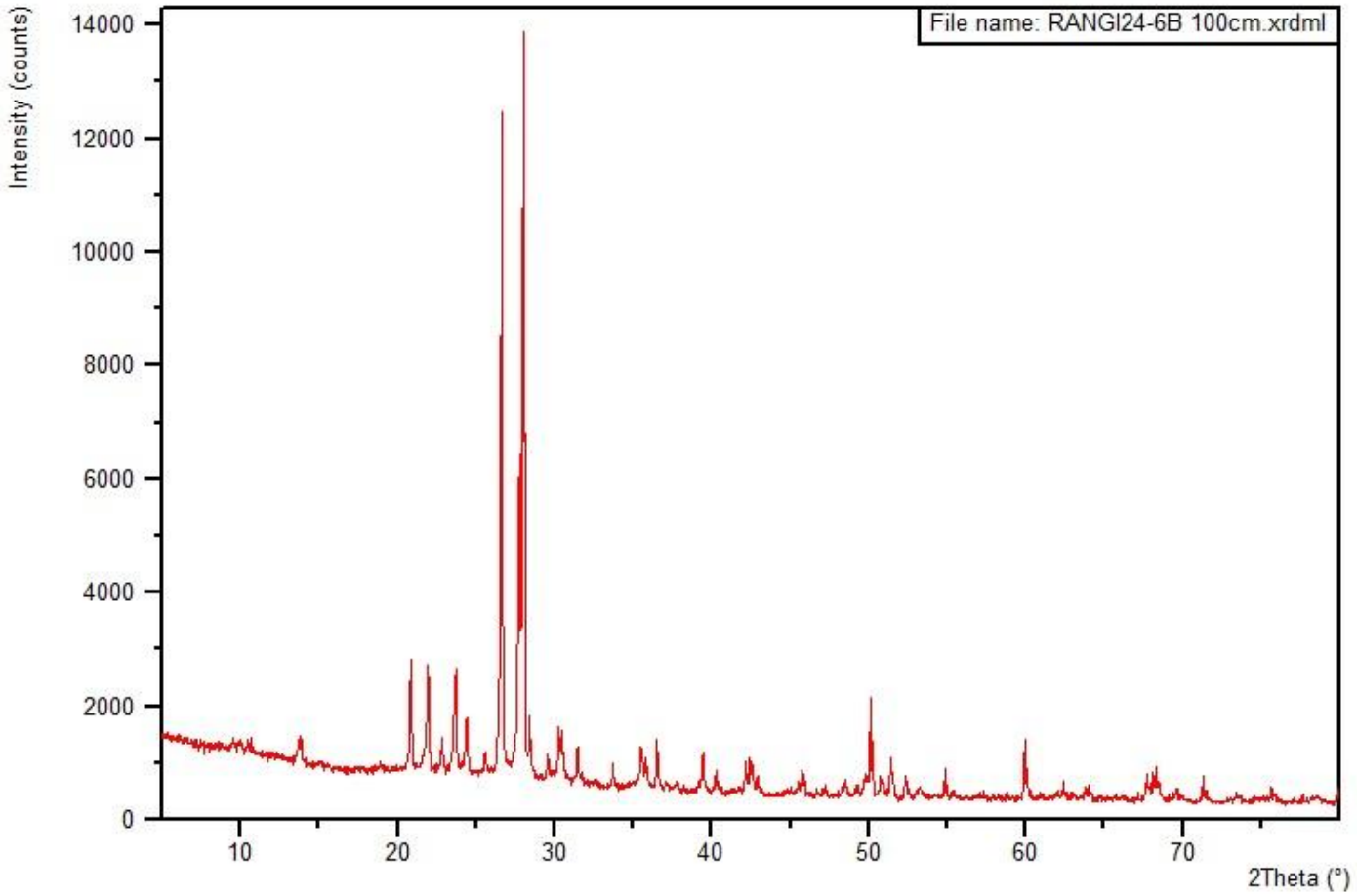
File name: RANGI24-6B 100cm.xrdml
Intensity (counts)
14000
12000
10000
8000
6000
4000
2000
0
10
20
30
40
50
60
70
2Theta (°)

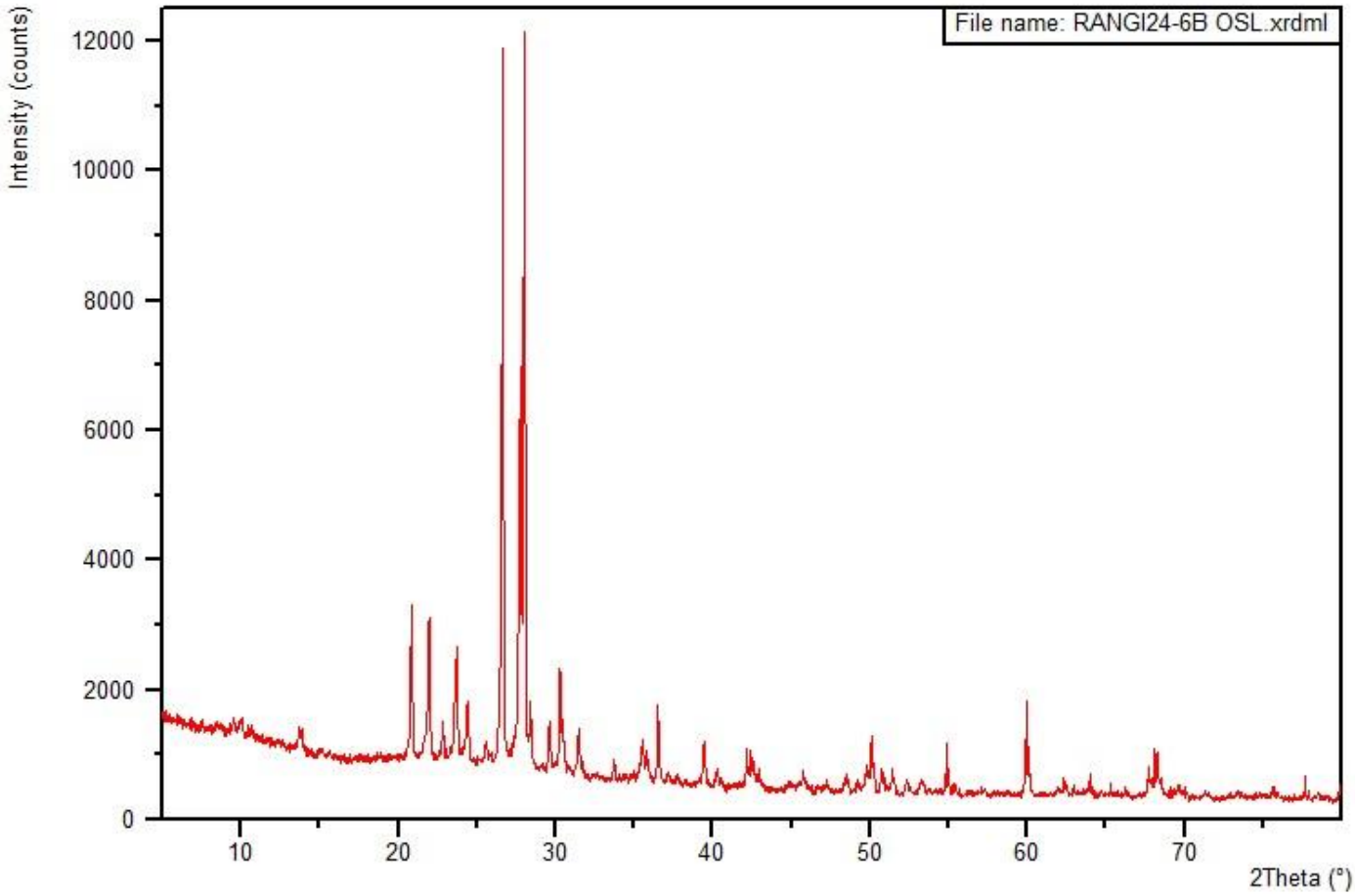
File name: RANGI24-6B OSL.xrdml
Intensity (counts)
12000
10000
8000
6000
4000
2000
0
10
20
30
40
50
60
70
2Theta (°)

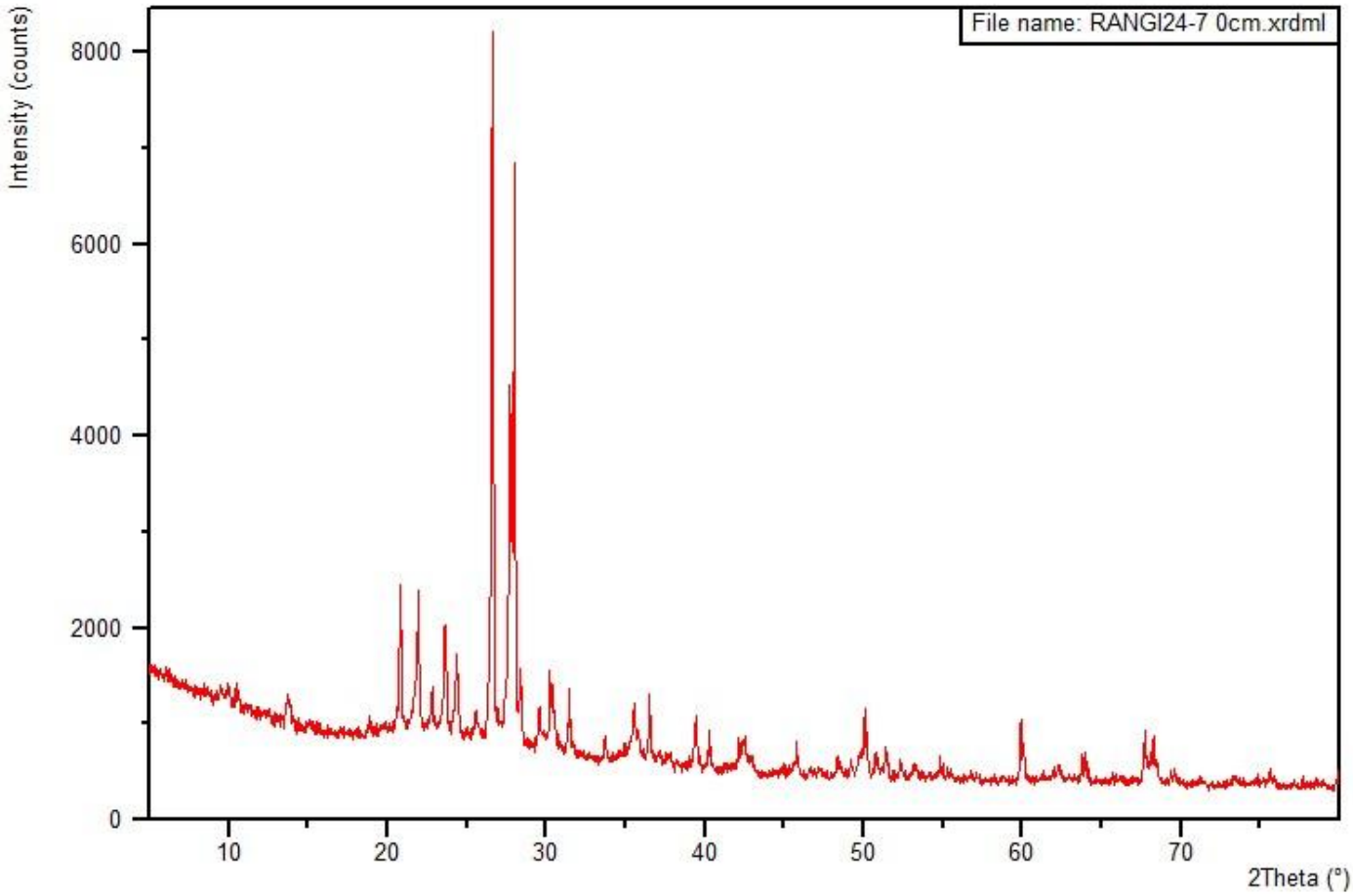
File name: RANGI24-7 0cm.xrdml
Intensity (counts)
8000
6000
4000
2000
0
10
20
30
40
50
60
70
2Theta (°)

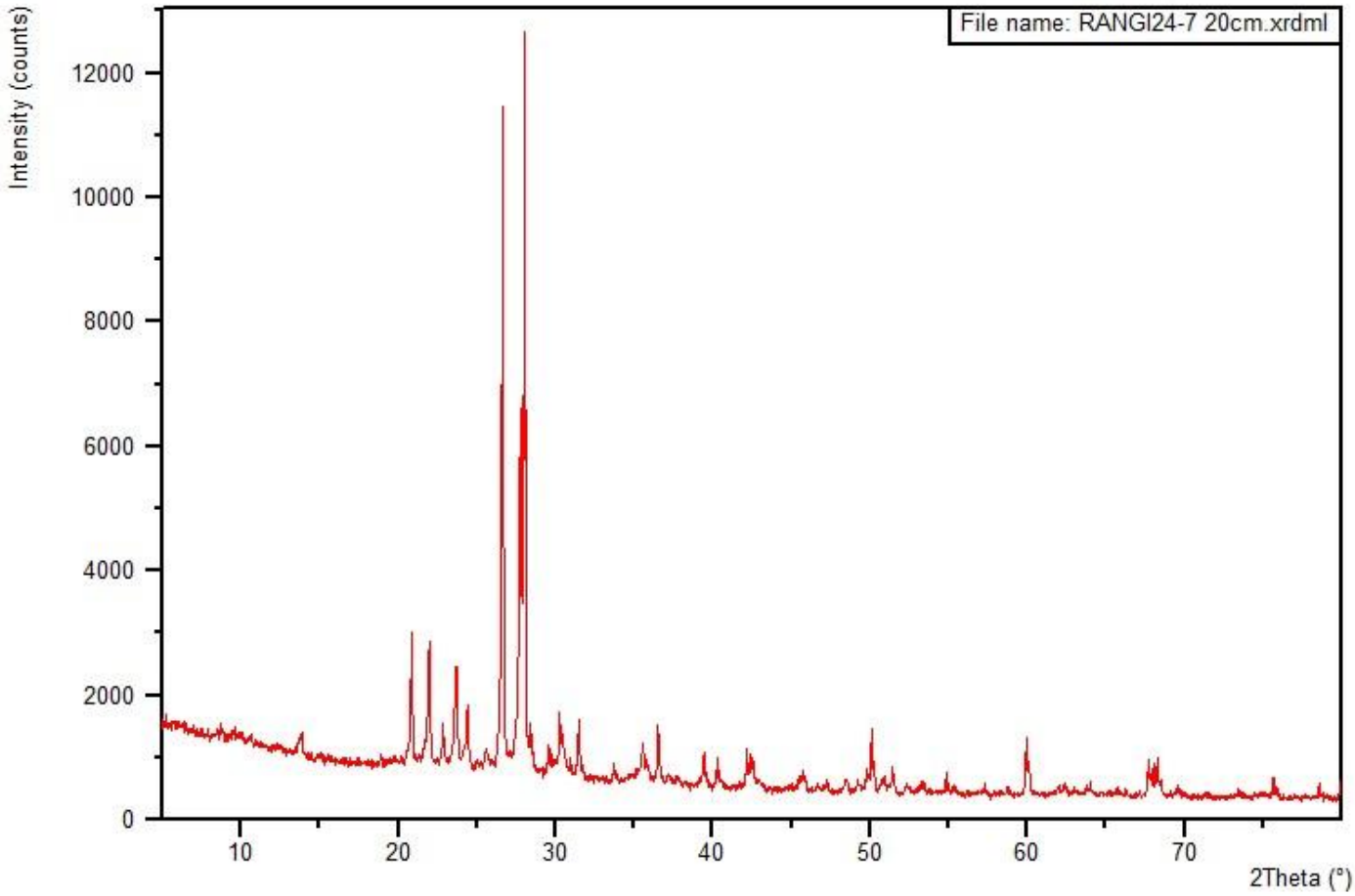
File name: RANGI24-7 20cm.xrdml
Intensity (counts)
12000
10000
8000
6000
4000
2000
0
10
20
30
40
50
60
70
2Theta (°)

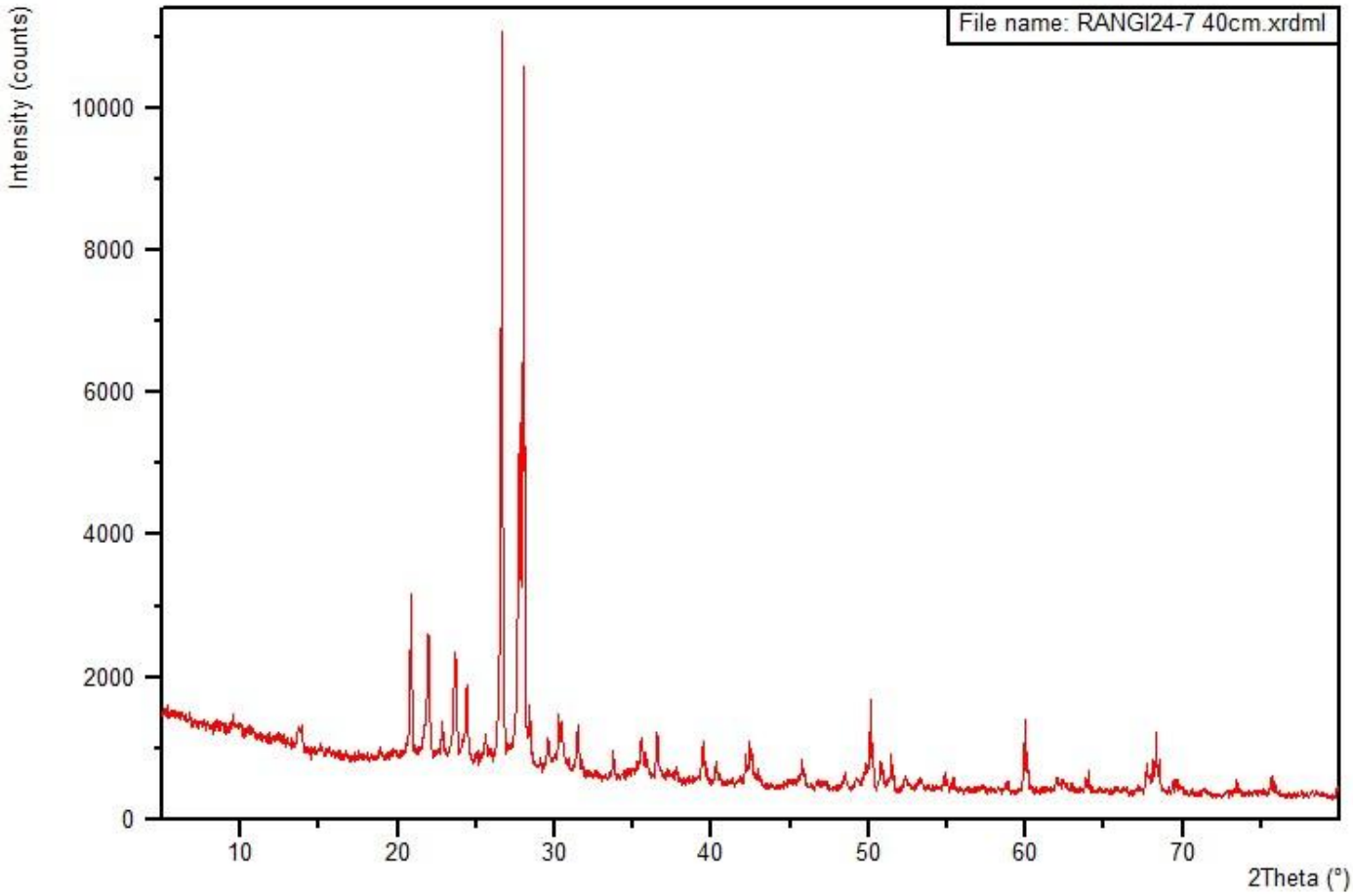
File name: RANGI24-7 40cm.xrdml
Intensity (counts)
10000
8000
6000
4000
2000
0
10
20
30
40
50
60
70
2Theta (°)

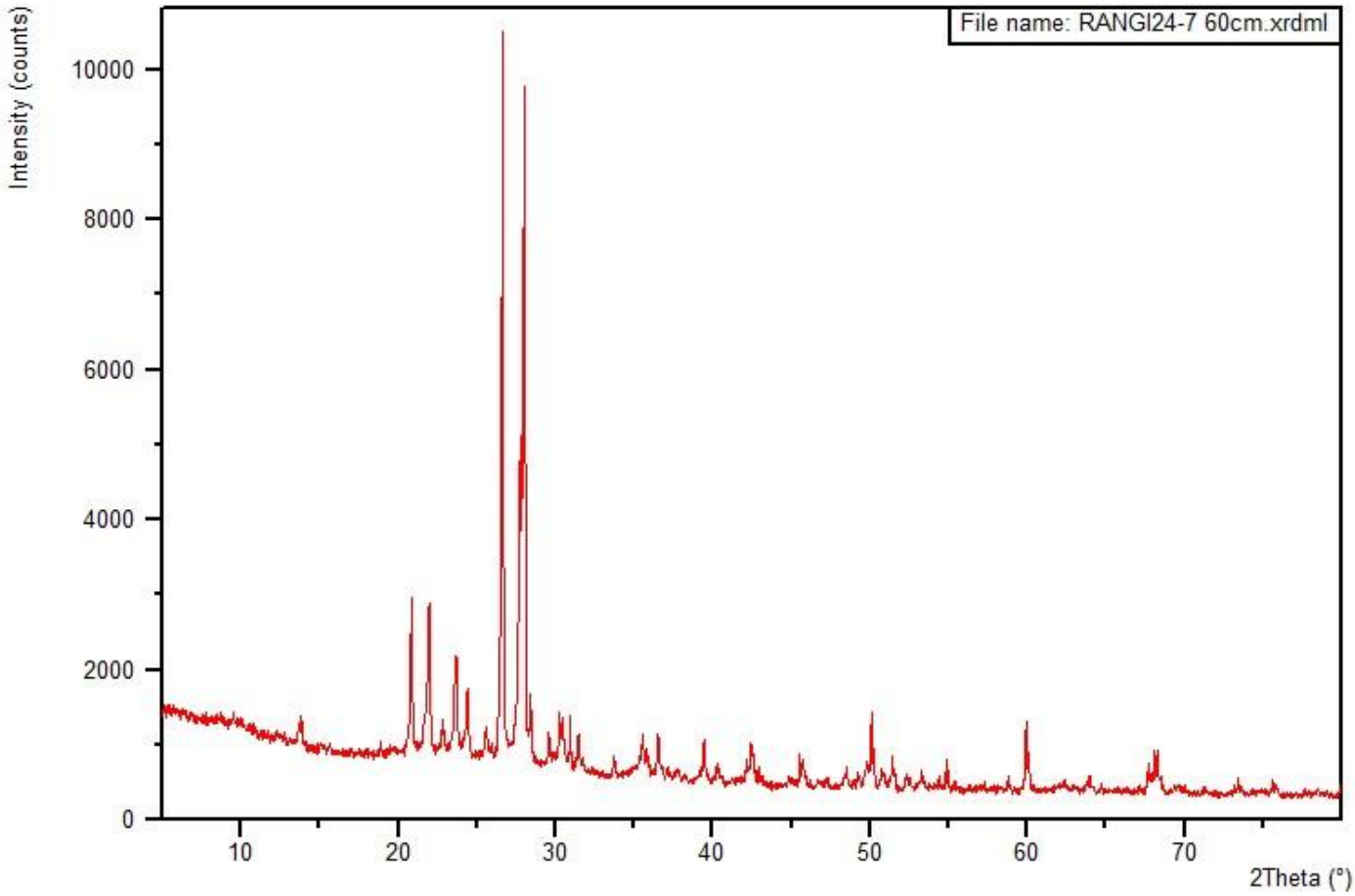
File name: RANGI24-7 60cm.xrdml
Intensity (counts)
10000
8000
6000
4000
2000
0
10
20
30
40
50
60
70
2Theta (°)

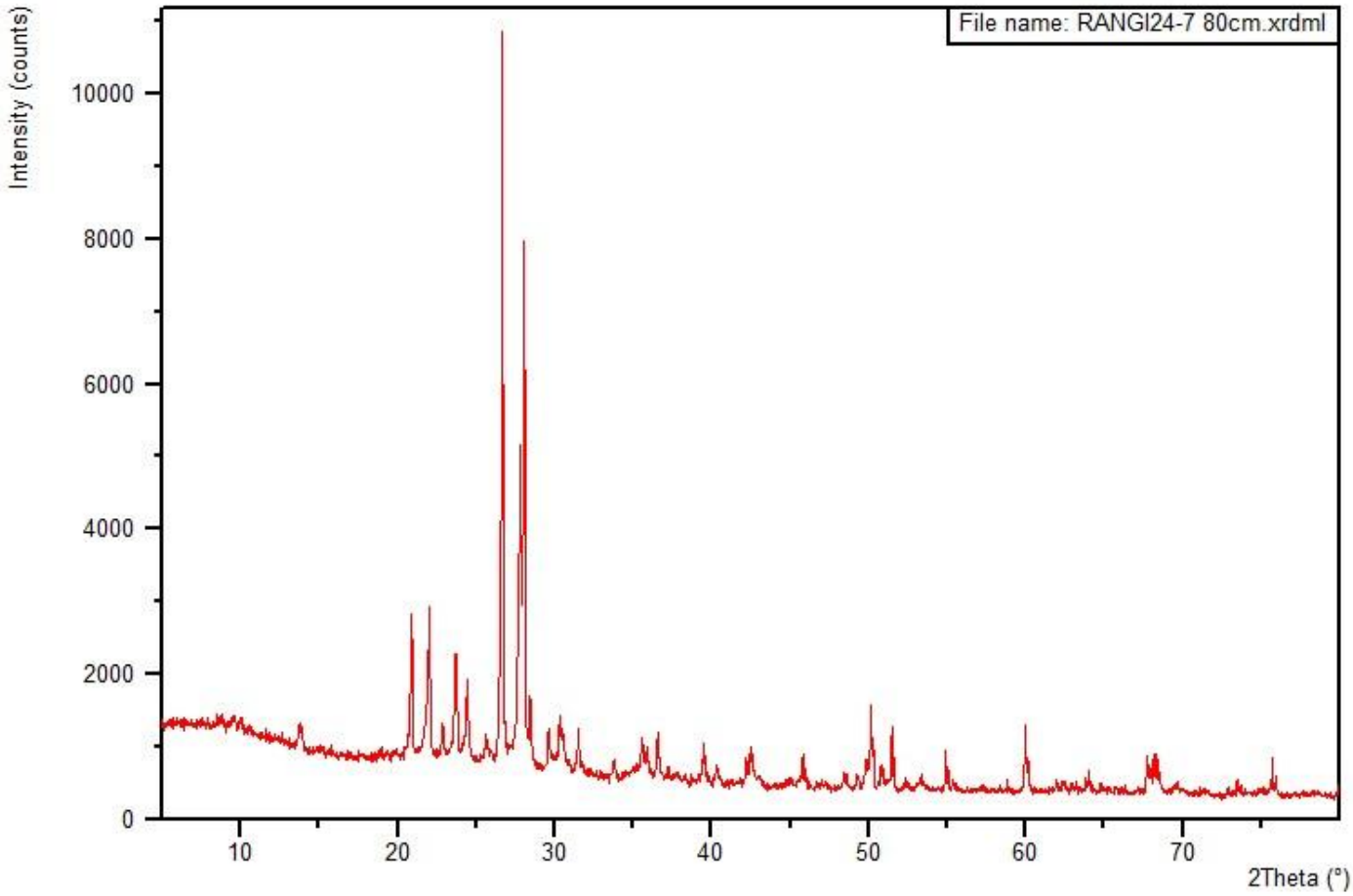
File name: RANGI24-7 80cm.xrdml
Intensity (counts)
10000
8000
6000
4000
2000
0
10
20
30
40
50
60
70
2Theta (°)

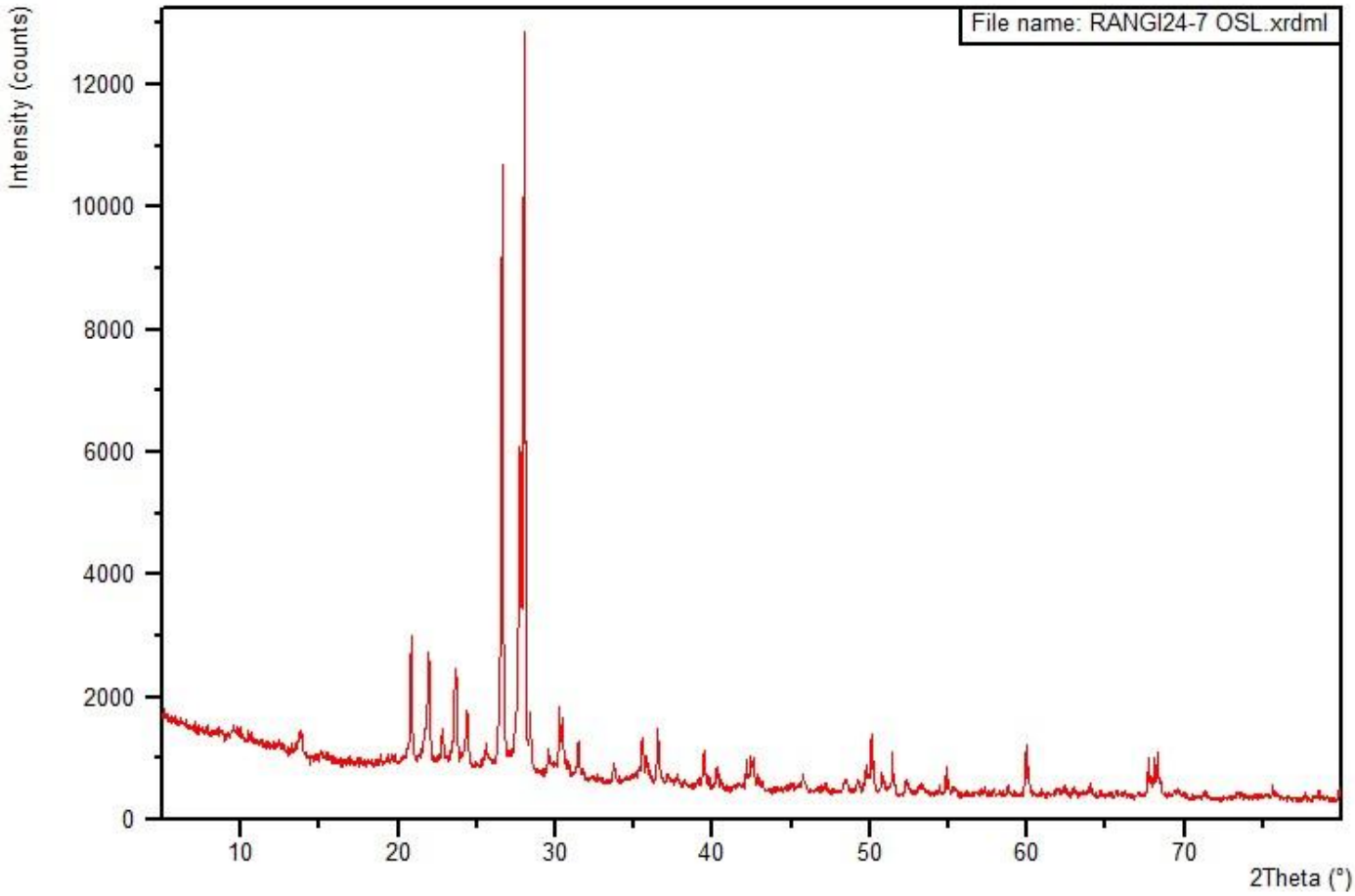
File name: RANGI24-7 OSL.xrdml
Intensity (counts)
12000
10000
8000
6000
4000
2000
0
10
20
30
40
50
60
70
2Theta (°)

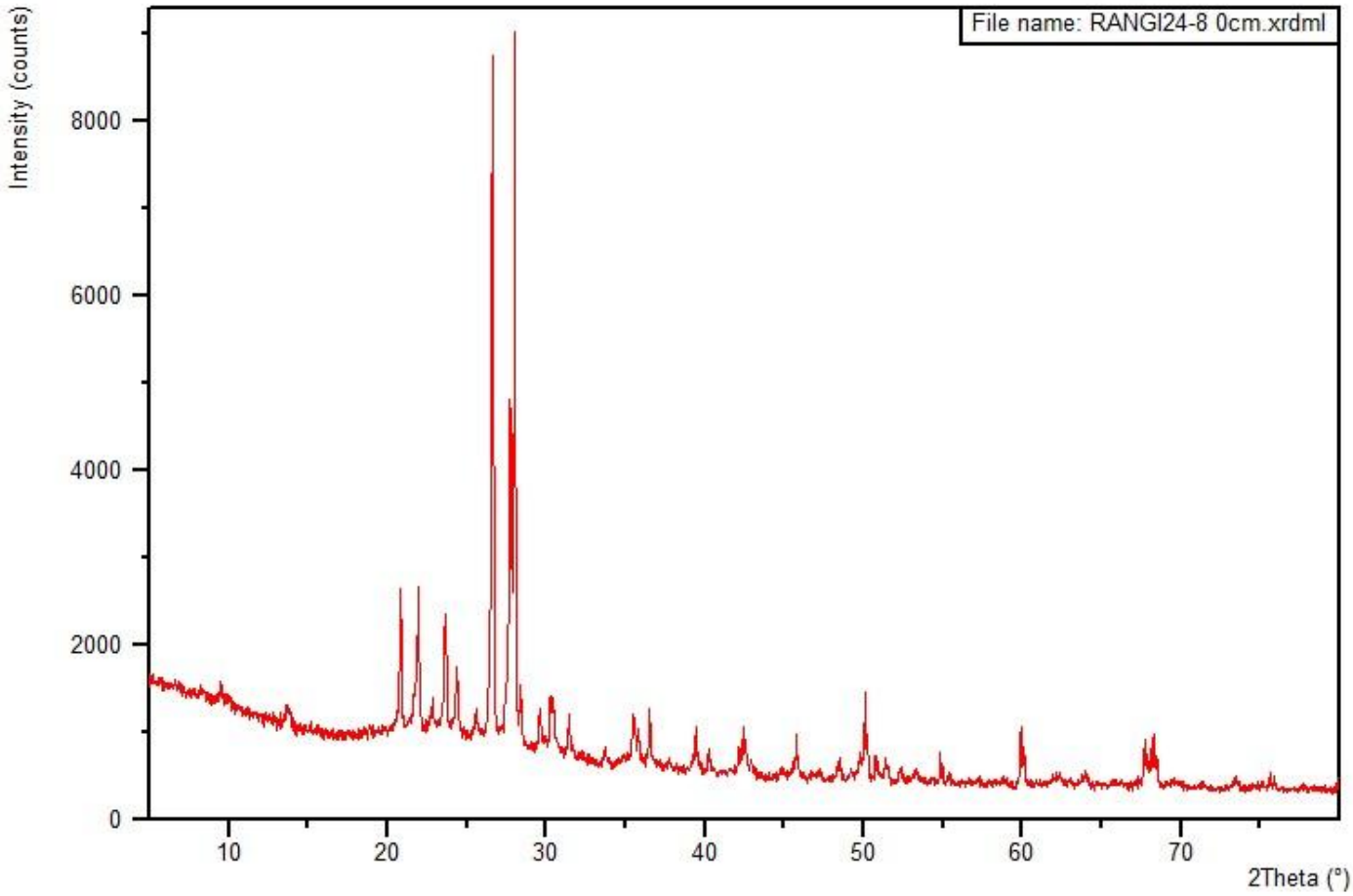
File name: RANGI24-8 0cm.xrdml
Intensity (counts)
8000
6000
4000
2000
0
10
20
30
40
50
60
70
2Theta (°)

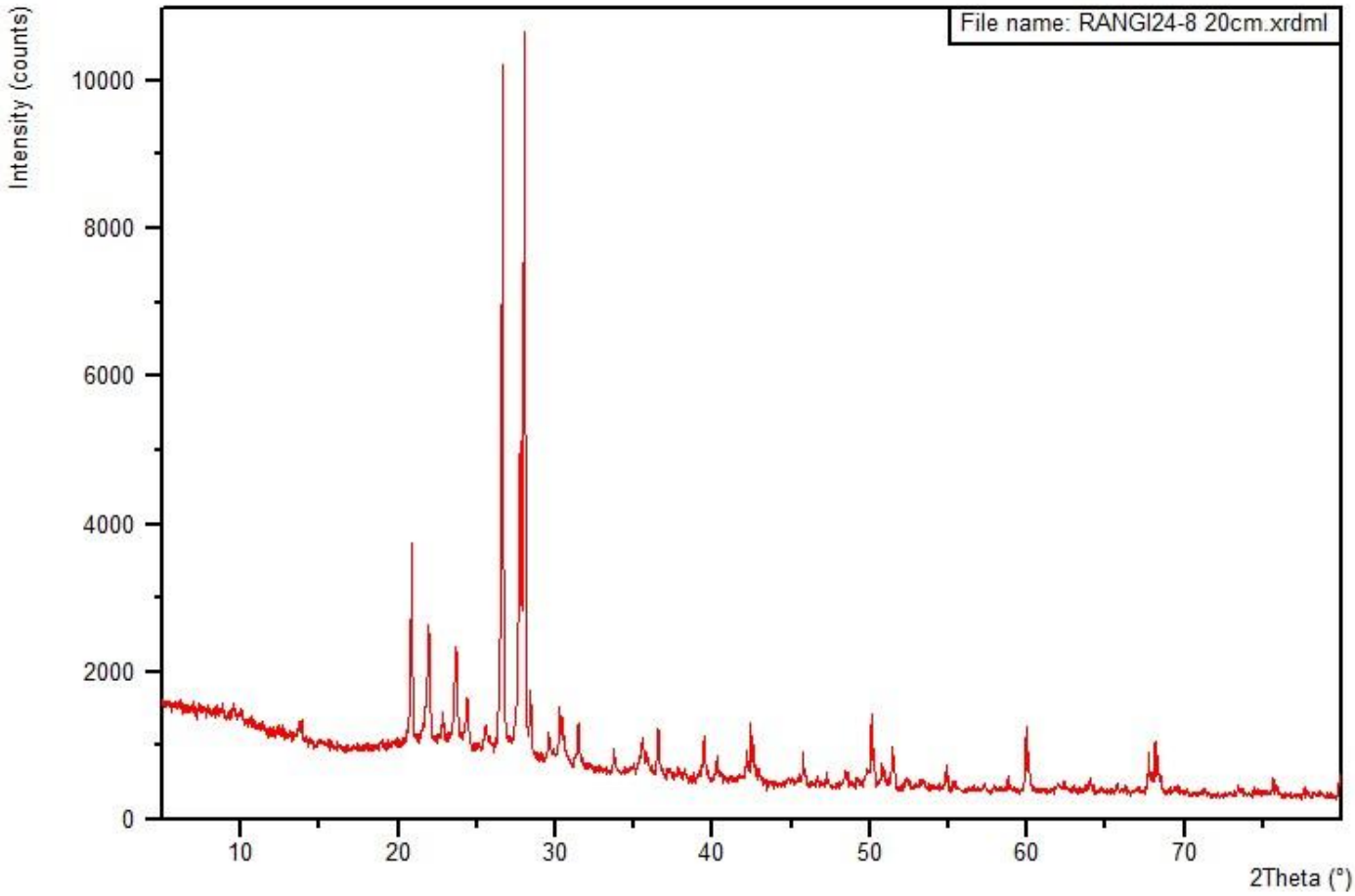
File name: RANGI24-8 20cm.xrdml
Intensity (counts)
10000
8000
6000
4000
2000
0
10
20
30
40
50
60
70
2Theta (°)

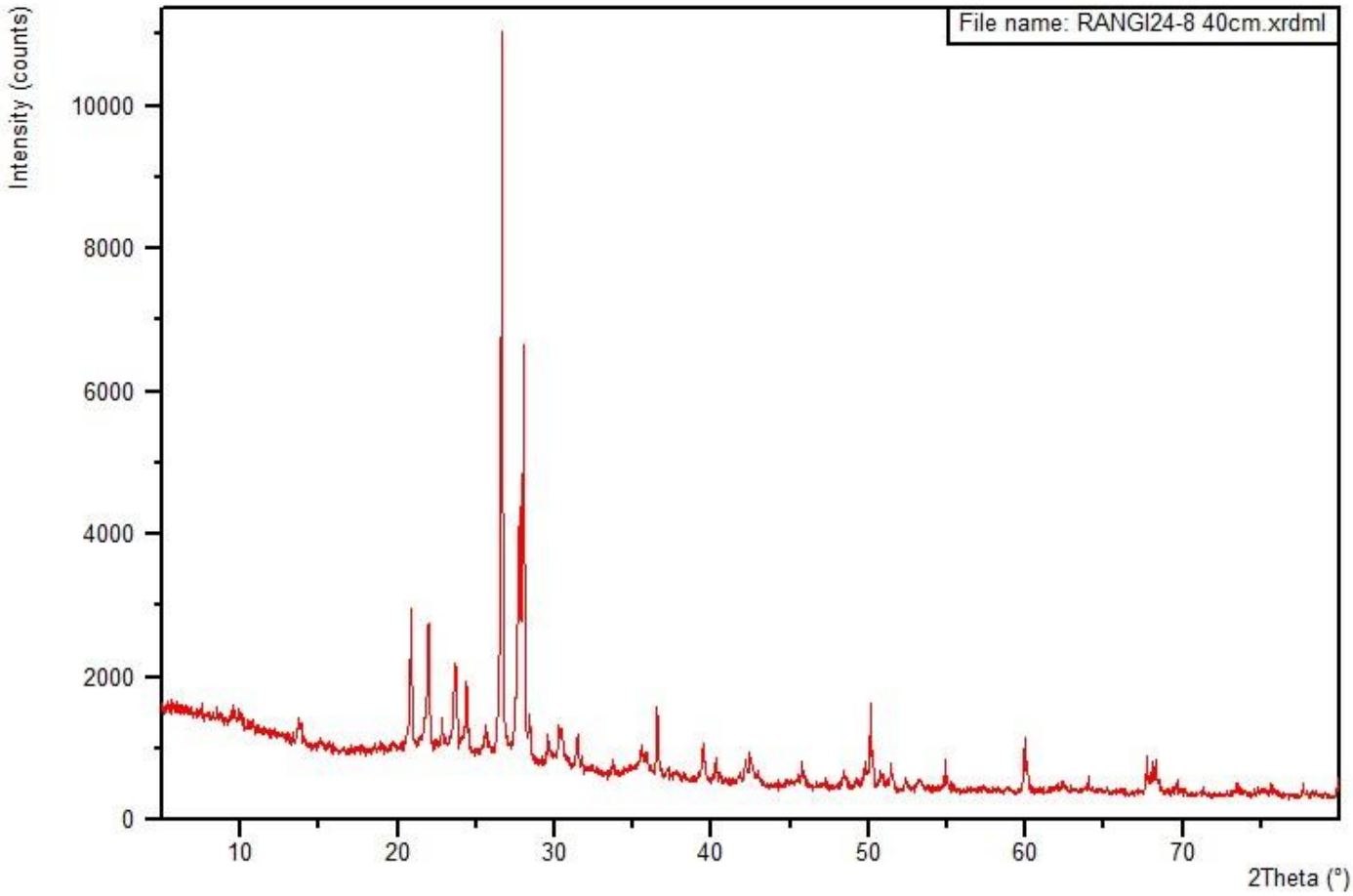
File name: RANGI24-8 40cm.xrdml
Intensity (counts)
10000
8000
6000
4000
2000
0
10
20
30
40
50
60
70
2Theta (°)

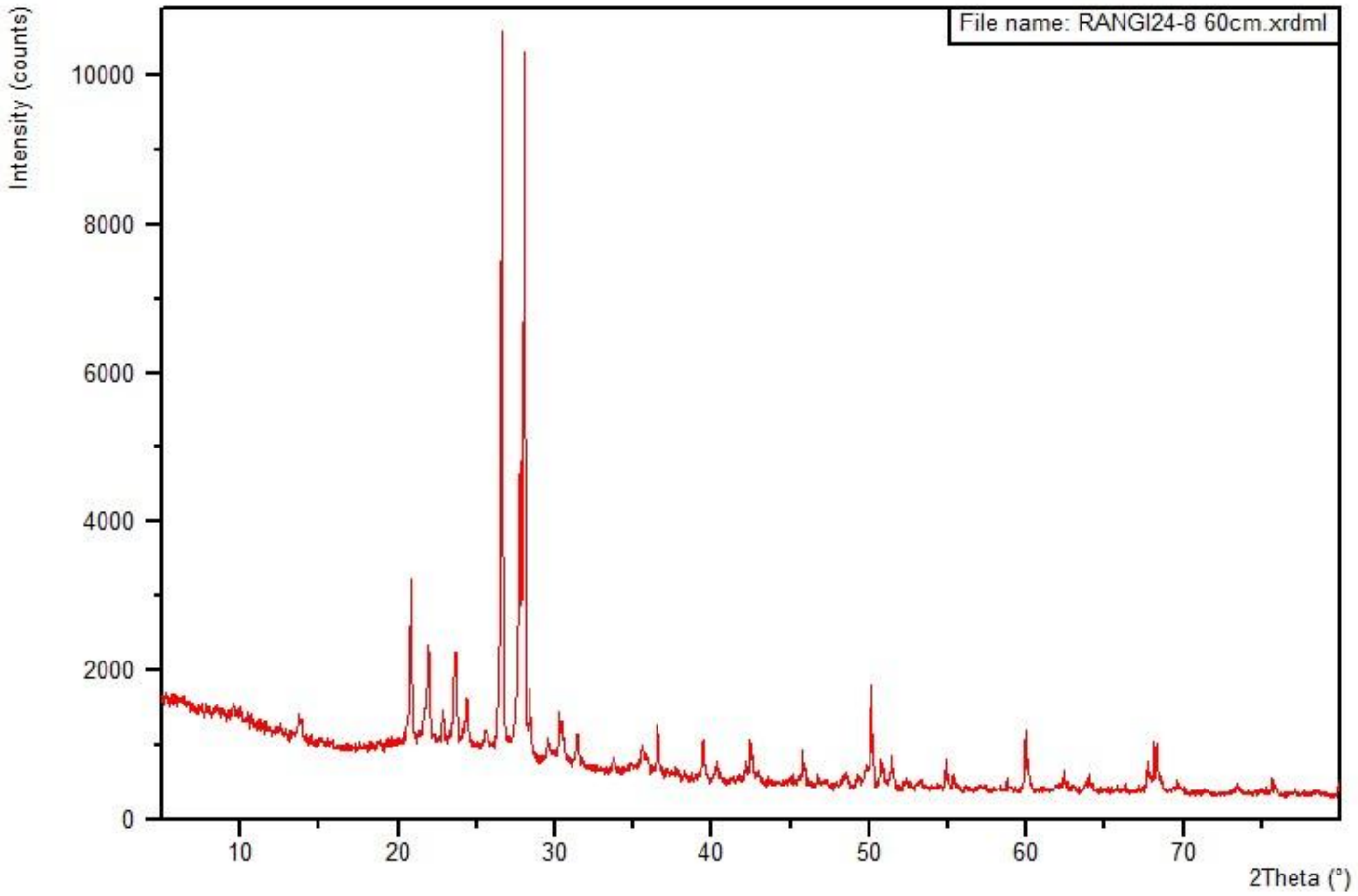
File name: RANGI24-8 60cm.xrdml
Intensity (counts)
10000
8000
6000
4000
2000
0
10
20
30
40
50
60
70
2Theta (°)

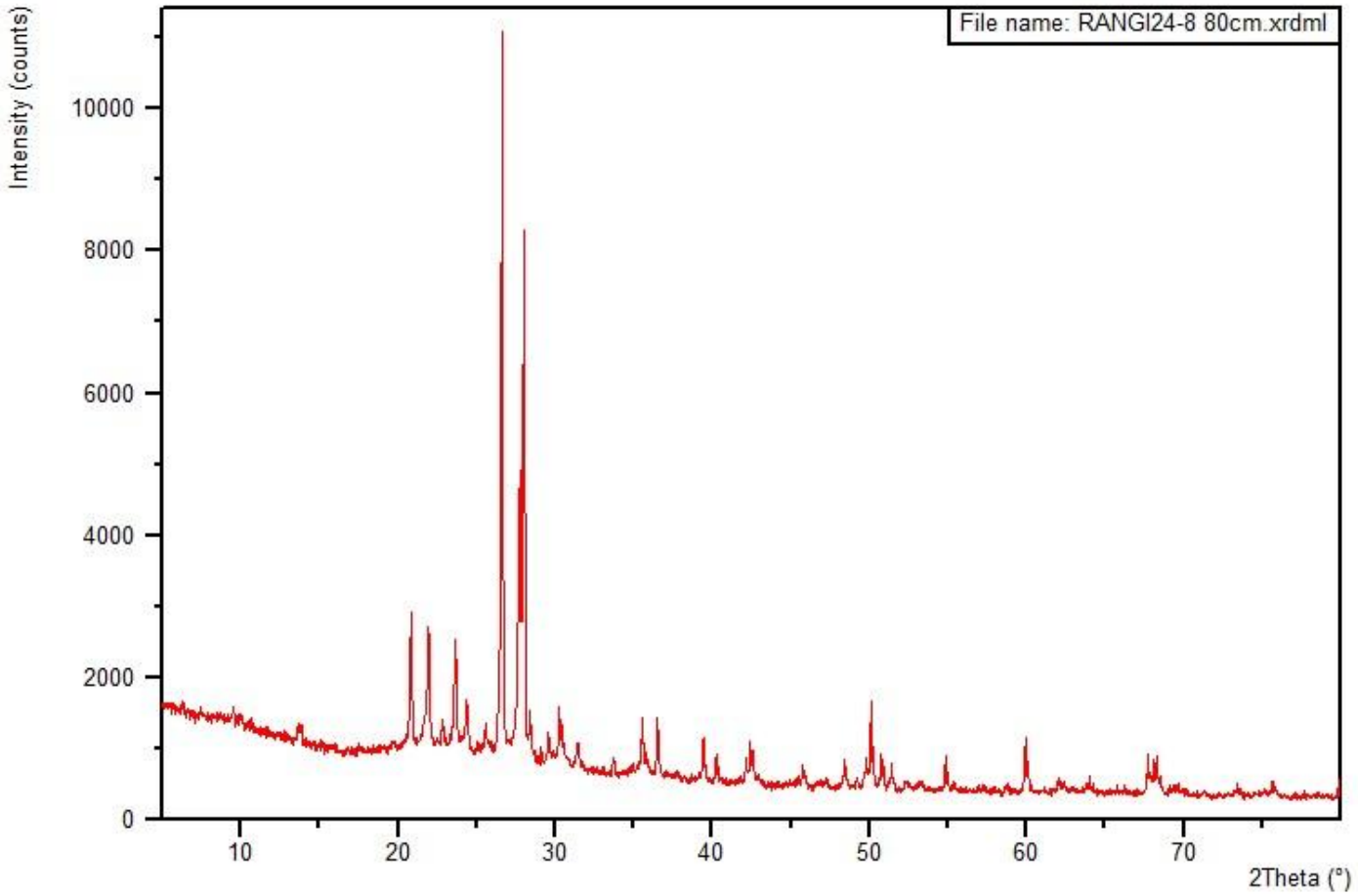
File name: RANGI24-8 80cm.xrdml
Intensity (counts)
10000
8000
6000
4000
2000
0
10
20
30
40
50
60
70
2Theta (°)

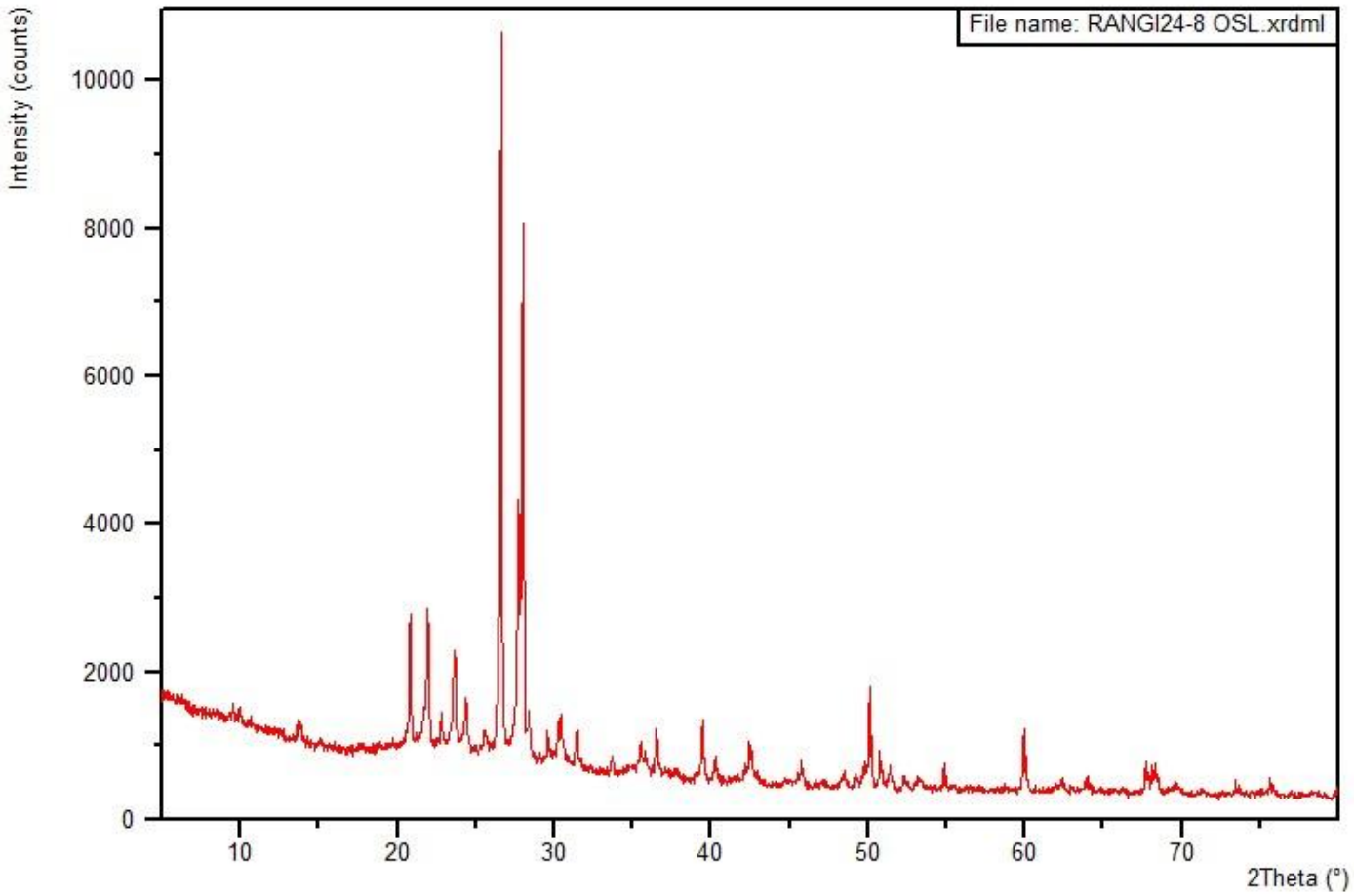
File name: RANGI24-8 OSL.xrdml
Intensity (counts)
10000
8000
6000
4000
2000
0
10
20
30
40
50
60
70
2Theta (°)

Appendix K: Qualitative XRD Interpretation

Sample Name	Sample Depth	Minerals Present Based on XRD		
		Quartz	Plagioclase	Mica(?)
COAST 1	**0cm**	✓	✓	✓
COAST 2	**0cm**	✓	✓	✓
COAST 3	**0cm**	✓	✓	✓
COAST 4	**0cm**	✓	✓	✓
COAST 5	**0cm**	✓	✓	
COAST 6	**0cm**	✓	✓	
RANGI24-1	**20cm**	✓	✓	
RANGI24-1	**40cm**	✓	✓	
RANGI24-1	**TAUPO**	✓	✓	
RANGI24-1	**60cm**	✓	✓	
RANGI24-1	**80cm**	✓	✓	
RANGI24-1	**100cm**	✓	✓	
RANGI24-1	**120cm**	✓	✓	
RANGI24-1	**140cm**	✓	✓	
RANGI24-1	**160cm**	✓	✓	
RANGI24-1	**180cm**	✓	✓	
RANGI24-1	**200cm**	✓	✓	✓
RANGI24-1	**220cm**	✓	✓	
RANGI24-1	**OSL**	✓	✓	
RANGI24-2	**20cm**	✓	✓	
RANGI24-2	**40cm**	✓	✓	
RANGI24-2	**60cm**	✓	✓	
RANGI24-2	**80cm**	✓	✓	
RANGI24-2	**100cm**	✓	✓	
RANGI24-2	**120cm**	✓	✓	
RANGI24-2	**140cm**	✓	✓	
RANGI24-2	**160cm**	✓	✓	
RANGI24-2	**180cm**	✓	✓	
RANGI24-2	**200cm**	✓	✓	
RANGI24-2	**220cm**	✓	✓	
RANGI24-2	**OSL**	✓	✓	
RANGI24-3	**0cm**	✓	✓	
RANGI24-3	**20cm**	✓	✓	
RANGI24-3	**40cm**	✓	✓	✓
RANGI24-3	**60cm**	✓	✓	
RANGI24-3	**80cm**	✓	✓	
RANGI24-3	**100cm**	✓	✓	
RANGI24-3	**120cm**	✓	✓	
RANGI24-3	**140cm**	✓	✓	
RANGI24-3	**160cm**	✓	✓	
RANGI24-3	**OSL**	✓	✓	
RANGI24-4	**20cm**	✓	✓	
RANGI24-4	**40cm**	✓	✓	
RANGI24-4	**60cm**	✓	✓	

RANGI24-4	**80cm**	✓	✓		
RANGI24-4	**100cm**	✓	✓		
RANGI24-4	**120cm**	✓	✓		
RANGI24-4	**140cm**	✓	✓		
RANGI24-4	**OSL**	✓	✓		
RANGI24-5	**0cm**	✓	✓		
RANGI24-5	**20cm**	✓	✓		
RANGI24-5	**40cm**	✓	✓		
RANGI24-5	**60cm**	✓	✓		
RANGI24-5	**80cm**	✓	✓		
RANGI24-5	**100cm**	✓	✓	✓	
RANGI24-5	**120cm**	✓	✓		
RANGI24-5	**OSL**	✓	✓		
RANGI24-5	**OUTCROP**	✓	✓		
RANGI24-6	**0cm**	✓	✓		
RANGI24-6	**20cm**	✓	✓	✓	
RANGI24-6	**40cm**	✓	✓	✓	
RANGI24-6	**60cm**	✓	✓		
RANGI24-6	**80cm**	✓	✓		
RANGI24-6	**100cm**	✓	✓		
RANGI24-6	**120cm**	✓	✓		
RANGI24-5	**OSL**	✓	✓		
RANGI24-6B	**0cm**	✓	✓	✓	
RANGI24-6B	**20cm**	✓	✓		
RANGI24-6B	**40cm**	✓	✓		
RANGI24-6B	**60cm**	✓	✓		
RANGI24-6B	**80cm**	✓	✓		
RANGI24-6B	**100cm**	✓	✓		
RANGI24-6B	**OSL**	✓	✓	✓	
RANGI24-7	**0cm**	✓	✓		
RANGI24-7	**20cm**	✓	✓	✓	
RANGI24-7	**40cm**	✓	✓		
RANGI24-7	**60cm**	✓	✓		
RANGI24-7	**80cm**	✓	✓	✓	
RANGI24-7	**OSL**	✓	✓		
RANGI24-8	**0cm**	✓	✓		
RANGI24-8	**20cm**	✓	✓		
RANGI24-8	**40cm**	✓	✓		
RANGI24-8	**60cm**	✓	✓		
RANGI24-8	**80cm**	✓	✓		
RANGI24-8	**OSL**	✓	✓		

Appendix L: Grainsize Summary Statistics

Name	Depth	Measurement Date & Time	Dx (10)	Dx (50)	Dx (90)	Laser Obscuration	D [4,3]	D [3,2]	Residual	Weighted Residual
Coast 1	**0cm**	30/01/2025 9:40	247	437	754	8.05	471	350	0.63	0.62
Coast 2	**0cm**	30/01/2025 9:49	352	666	1180	8.37	713	261	0.65	0.67
Coast 3	**0cm**	30/01/2025 9:59	509	824	1380	7.7	894	775	1.33	1.25
Coast 4	**0cm**	30/01/2025 10:12	286	514	904	12	558	456	0.66	0.62
Coast 5	**0cm**	30/01/2025 10:19	342	589	967	12.99	620	265	0.53	0.52
Coast 6	**0cm**	30/01/2025 10:27	223	399	741	9.09	446	365	0.45	0.42
RANGI24-1	**20cm**	30/01/2025 10:36	4.3	185	780	14.96	298	11.3	0.23	0.45
RANGI24-1	**40cm**	30/01/2025 10:44	8.89	84.9	396	16.96	165	18.1	0.17	0.29
RANGI24-1	**40cm**	30/01/2025 14:07	5.34	50	531	14.72	185	12.7	0.19	0.39
RANGI24-1	**60cm**	30/01/2025 10:52	9.01	274	972	14.96	401	20.3	0.22	0.32
RANGI24-1	**80cm**	5/02/2025 9:57	14.2	157	427	15.11	193	24.6	0.34	0.38
RANGI24-1	**100cm**	30/01/2025 11:00	6.33	136	437	15.27	183	15.8	0.19	0.33
RANGI24-1	**120cm**	30/01/2025 11:09	6.44	178	876	18.21	335	16.2	0.2	0.35
RANGI24-1	**140cm**	30/01/2025 11:17	41.5	402	720	15.83	411	27.6	0.38	0.41

RANGI24-1	**160cm**	30/01/2025 11:25	222	418	717	14.83	441	137	0.49	0.51
RANGI24-1	**180cm**	30/01/2025 11:34	212	420	727	12.7	442	186	0.4	0.4
RANGI24-1	**200cm**	30/01/2025 11:42	233	418	705	12.36	442	251	0.36	0.35
RANGI24-1	**220cm**	30/01/2025 11:50	238	422	724	13.69	453	364	0.63	0.6
RANGI24-2	**20cm**	30/01/2025 11:58	4.07	80.7	604	17.32	212	10.8	0.23	0.45
RANGI24-2	**40cm**	30/01/2025 12:05	7.32	182	975	15.98	363	17	0.23	0.36
RANGI24-2	**60cm**	5/02/2025 10:05	6.56	126	565	15.86	220	15.3	0.16	0.33
RANGI24-2	**80cm**	5/02/2025 10:13	16.3	211	628	17	275	27.8	0.17	0.23
RANGI24-2	**100cm**	5/02/2025 10:20	8.5	129	494	16.37	203	18.1	0.14	0.27
RANGI24-2	**120cm**	30/01/2025 14:16	12.6	114	337	16.15	149	22.4	0.19	0.27
RANGI24-2	**140cm**	30/01/2025 12:14	14.2	409	950	18.61	454	28	0.21	0.28
RANGI24-2	**160cm**	30/01/2025 12:23	189	354	632	12.88	382	193	0.31	0.32
RANGI24-2	**180cm**	30/01/2025 12:31	213	384	663	12.71	413	302	0.52	0.5
RANGI24-2	**200cm**	30/01/2025 14:24	206	369	636	10.74	396	293	0.54	0.52
RANGI24-2	**220cm**	30/01/2025 12:39	208	359	610	13.77	386	313	0.52	0.49
RANGI24-3	**0cm**	30/01/2025 14:32	5.9	207	582	15.62	252	14.6	0.22	0.36

RANGI24-3	**20cm**	5/02/2025 10:27	7.78	233	676	15.92	291	17.5	0.26	0.36
RANGI24-3	**40cm**	30/01/2025 12:47	7.35	217	524	16.76	239	16.7	0.23	0.34
RANGI24-3	**60cm**	5/02/2025 10:35	58	278	525	17.1	323	43.7	0.39	0.4
RANGI24-3	**80cm**	30/01/2025 14:40	143	278	463	17.7	287	79	0.35	0.37
RANGI24-3	**100cm**	30/01/2025 12:55	162	284	458	14.14	294	65.8	0.35	0.36
RANGI24-3	**120cm**	30/01/2025 13:42	168	323	561	17.09	341	116	0.39	0.4
RANGI24-3	**140cm**	30/01/2025 14:48	183	348	604	18.34	369	139	0.34	0.35
RANGI24-3	**160cm**	30/01/2025 13:51	162	266	429	16.05	281	232	0.5	0.49
RANGI24-4	**20cm**	30/01/2025 13:59	6.03	165	665	17.64	260	14.4	0.2	0.35
RANGI24-4	**40cm**	5/02/2025 10:42	9.3	234	658	16.32	289	19.4	0.21	0.31
RANGI24-4	**60cm**	5/02/2025 10:50	139	295	504	16.05	306	51.5	0.33	0.33
RANGI24-4	**80cm**	30/01/2025 14:56	190	327	536	15.19	343	160	0.43	0.44
RANGI24-4	**120cm**	30/01/2025 15:04	205	349	570	14.65	367	187	0.43	0.44
RANGI24-4	**140cm**	30/01/2025 15:12	167	284	466	14.67	300	190	0.43	0.44
RANGI24-5	**0cm**	5/02/2025 10:59	11.6	265	615	16.64	297	21.6	0.25	0.32
RANGI24-5	**20cm**	30/01/2025 15:19	6.35	169	620	20.09	246	14.2	0.2	0.35

RANGI24-5	**40cm**	30/01/2025 15:27	29.7	292	538	18.42	302	39.6	0.33	0.34
RANGI24-5	**60cm**	30/01/2025 15:35	139	304	521	20.56	314	66.7	0.28	0.28
RANGI24-5	**80cm**	30/01/2025 15:43	153	332	564	19.49	342	87.8	0.32	0.33
RANGI24-5	**100cm**	30/01/2025 15:51	187	347	598	12.27	368	126	0.31	0.34
RANGI24-5	**120cm**	30/01/2025 15:59	167	314	530	19.63	327	100	0.37	0.38
RANGI24-5	**OUTCROP**	30/01/2025 16:07	184	313	543	13.02	340	210	0.47	0.47
RANGI24-6	**0cm**	30/01/2025 16:15	7.8	201	650	17	270	15.6	0.21	0.34
RANGI24-6	**20cm**	30/01/2025 16:23	7.06	226	981	17.43	380	16.3	0.2	0.35
RANGI24-6	**40cm**	30/01/2025 16:30	7.23	196	751	18.28	306	16.6	0.22	0.35
RANGI24-6	**60cm**	30/01/2025 16:38	21.1	278	510	19.42	282	35	0.29	0.32
RANGI24-6	**80cm**	30/01/2025 16:46	143	300	514	15.83	312	77.4	0.35	0.37
RANGI24-6	**100cm**	31/01/2025 10:39	167	287	470	16.01	301	132	0.35	0.35
RANGI24-6	**120cm**	31/01/2025 10:46	162	285	481	19.69	303	141	0.38	0.38
RANGI24-6B	**0cm**	31/01/2025 10:53	13	269	512	17.29	277	20.7	0.37	0.41
RANGI24-6B	**20cm**	31/01/2025 11:01	33.7	291	557	17.76	314	32.2	0.41	0.43
RANGI24-6B	**40cm**	31/01/2025 11:09	195	323	516	14.68	339	222	0.46	0.46

RANGI24-6B	**60cm**	31/01/2025 11:17	190	329	541	14.27	345	167	0.42	0.43
RANGI24-6B	**80cm**	31/01/2025 11:24	184	313	499	10.75	324	151	0.37	0.37
RANGI24-6B	**80cm**	31/01/2025 11:33	183	305	495	15.84	321	181	0.41	0.41
RANGI24-7	**0cm**	5/02/2025 11:07	40.3	277	499	16	283	36.8	0.37	0.38
RANGI24-7	**20cm**	31/01/2025 11:40	186	306	485	16.22	318	160	0.46	0.48
RANGI24-7	**40cm**	31/01/2025 11:49	194	321	507	17.84	334	177	0.46	0.47
RANGI24-7	**60cm**	31/01/2025 11:56	216	367	607	15.43	388	226	0.48	0.48
RANGI24-7	**80cm**	31/01/2025 12:04	212	364	611	13.14	388	252	0.47	0.47
RANGI24-8	**0cm**	31/01/2025 12:11	171	365	680	12.47	396	131	0.39	0.41
RANGI24-8	**0cm**	31/01/2025 12:19	187	334	574	12.34	357	215	0.4	0.4
RANGI24-8	**20cm**	31/01/2025 12:19	187	334	574	12.34	357	215	0.4	0.4
RANGI24-8	**40cm**	31/01/2025 12:26	159	303	548	15.19	329	132	0.4	0.41
RANGI24-8	**40cm**	31/01/2025 12:33	172	316	554	20.52	340	186	0.35	0.35
RANGI24-8	**60cm**	31/01/2025 12:33	172	316	554	20.52	340	186	0.35	0.35
RANGI24-8	**80cm**	31/01/2025 12:41	179	354	653	12.08	386	175	0.33	0.34

Appendix M: Full Grainsize Dataset

Sample Name	Coast 1	Coast 2	Coast 3	Coast 4	Coast 5	Coast 6
0.05	0	0	0	0	0	0
0.06	0	0	0	0	0	0
0.12	0	0	0	0	0	0
0.24	0	0	0	0	0	0
0.49	0	0	0	0	0	0
0.98	0	0	0	0	0	0
2	0	0.2	0	0	0.11	0
3.9	0	0.43	0	0	0.44	0
7.8	0.25	0.46	0	0	0.52	0
15.6	0.07	0.5	0	0	0.43	0
31	0.12	0.1	0	0	0.09	0
37	0.14	0.04	0	0	0.11	0
44	0.16	0.09	0	0.08	0.15	0
53	0.14	0.15	0	0.11	0.18	0
63	0.09	0.21	0	0.11	0.19	0
74	0.01	0.31	0	0.09	0.2	0
88	0	0.36	0	0	0.14	0
105	0	0.32	0	0	0.04	0
125	0.11	0.16	0	0.03	0	0.65
149	0.98	0	0	0.35	0	2.21
177	2.66	0.09	0	1.27	0	4.57
210	5.9	0.71	0	3.48	0.69	8.23
250	9.69	2.12	0	6.54	2.62	11.78
300	10.89	3.61	0.41	8.21	4.86	11.86
350	15.29	7.59	2.71	13.02	10.36	14.93
420	15.13	10.35	6.14	14.32	13.7	13.57
500	13.31	12.29	10.04	14.04	15.33	11.12
590	11.77	15.37	16.07	14.23	17.32	9.29
710	7.6	13.64	16.55	10.56	13.69	5.88
840	4.47	12.21	16.56	7.69	10.41	3.62
1000	1.23	9.21	13.4	4.39	6.11	1.77
1190	0	6.12	9.25	1.42	2.19	0.49
1410	0	2.95	5.33	0.06	0.11	0.02
1680	0	0.45	2.45	0	0	0
2000	0	0	0.93	0	0	0
2380	0	0	0.17	0	0	0
2830	0	0	0	0	0	0
3360	0	0	0	0	0	0

RANGI2 4-1 20cm	RANGI2 4-1 40cm	RANGI2 4-1 60cm	RANGI2 4-1 80cm	RANGI2 4-1 100cm	RANGI2 4-1 120cm	RANGI2 4-1 140cm	RANGI2 4-1 160cm	RANGI2 4-1 180cm	RANGI2 4-1 200cm	RANGI2 4-1 220cm
0	0	0	0	0	0	0	0	0	0	0
0	0	0.24	0	0	0.13	0	0	0	0	0
0	0	0.48	0	0	0.28	0	0	0	0	0
0	0.04	0.82	0	0	0.54	0	0	0	0	0
0.23	0.28	1.18	0	0	0.87	0	0	0	0	0
0.86	0.61	1.66	0	0	1.34	0	0	0	0	0
1.53	0.94	2.2	0	0	1.88	0	0	0	0	0
2.34	1.26	2.88	0	0.06	2.54	0.72	0.57	0.58	0.09	0.54
3.33	1.55	3.67	0.03	0.39	3.27	3.47	3.35	3.62	2.95	3.51
4.19	1.73	4.36	0.56	1.02	3.86	6.47	6.57	7.04	6.62	6.9
5.51	2.17	5.62	1.91	2.08	4.88	10.39	10.97	11.25	11.13	11.16
5.59	2.29	5.73	3.21	3.1	4.82	11.91	13.04	12.88	13.31	13.08
6.09	2.82	6.39	4.8	4.47	5.23	13.53	15.15	14.63	15.55	15.2
6.14	3.39	6.67	6.33	5.81	5.36	13.57	15.44	14.71	15.93	15.63
4.58	3.2	5.22	6.23	5.67	4.18	9.58	10.97	10.41	11.4	11.34
4.5	3.92	5.36	7.81	7	4.39	8.52	9.7	9.31	10.14	10.31
3.32	3.65	4.18	7.5	6.57	3.59	5.29	5.89	5.83	6.2	6.51
2.3	3.26	3.1	6.98	5.91	2.9	2.57	2.7	2.9	2.87	3.18
1.74	2.94	2.47	6.49	5.34	2.52	1.14	1.08	1.36	1.15	1.35
1.41	2.66	2.08	5.9	4.75	2.3	0.36	0.23	0.5	0.25	0.32
1.26	2.39	1.85	5.04	4.01	2.15	0.13	0	0.23	0	0
1.28	2.34	1.83	4.41	3.52	2.17	0.23	0.06	0.31	0	0
1.33	2.37	1.8	3.64	2.97	2.18	0.41	0.19	0.45	0.13	0.11
1.3	2.37	1.67	2.89	2.43	2.08	0.48	0.27	0.48	0.2	0.18
1.47	2.8	1.76	2.7	2.37	2.29	0.54	0.32	0.49	0.24	0.21
1.69	3.39	1.84	2.52	2.33	2.5	0.54	0.3	0.42	0.24	0.2
1.71	3.48	1.68	2.09	2.05	2.33	0.45	0.22	0.29	0.17	0.15
1.92	3.8	1.7	1.96	2.03	2.36	0.44	0.18	0.22	0.14	0.1
9.13	15	6.72	6.27	7.65	8.54	1.81	0.68	0.74	0.44	0
9.22	11.19	5.9	4.35	6.75	6.92	1.84	0.8	0.68	0.51	0
6.87	6.82	4.09	2.75	5.2	5.2	1.76	0.72	0.49	0.33	0
4.53	3.91	2.58	1.78	3.53	3.47	1.64	0.56	0.2	0	0
2.94	2.38	1.49	1.27	2.09	2.12	1.3	0.04	0	0	0
1.7	1.03	0.75	0.58	0.89	0.81	0.92	0	0	0	0
0	0	0	0	0	0	0	0	0	0	0
0	0	0	0	0	0	0	0	0	0	0
0	0	0	0	0	0	0	0	0	0	0
0	0	0	0	0	0	0	0	0	0	0

RANGI2 4-2 20cm	RANGI2 4-2 40cm	RANGI2 4-2 60cm	RANGI2 4-2 80cm	RANGI2 4-2 100cm	RANGI2 4-2 120cm	RANGI2 4-2 140cm	RANGI2 4-2 160cm	RANGI2 4-2 180cm	RANGI2 4-2 200cm	RANGI2 4-2 220cm
0	0	0	0	0	0	0	0	0	0	0
0	0	0	0	0	0	0	0	0	0	0
0	0	0	0	0	0	0	0	0	0	0
0	0	0	0	0	0	0	0	0	0	0
0	0.49	0.07	0	0	0	0.34	0	0	0	0
0	1.73	0.25	0.02	0.15	0	1.4	0	0	0	0
0.19	2.96	0.53	0.35	0.46	0	2.61	0	0	0	0
1	4.16	0.95	1.14	0.81	0	4.1	0	0.01	0	0
2.06	5.2	1.58	2.17	1.25	0.02	5.87	1.47	2.07	1.33	0.8
3.03	5.56	2.28	3.26	1.71	0.22	7.27	4.1	5.19	4.27	3.5
4.28	6.15	3.37	4.79	2.46	0.73	9.25	7.52	9.13	8.11	7.19
4.51	5.03	3.92	5.38	2.91	1.47	8.83	9.98	11.58	10.92	10.36
5.02	4.61	4.83	6.42	3.77	2.58	9	12.92	14.35	14.06	13.98
5.21	4.05	5.56	7.18	4.68	3.93	8.4	14.89	15.73	15.9	16.42
4.07	2.81	4.87	6.17	4.56	4.48	5.7	12.4	12.29	12.8	13.65
4.27	2.86	5.58	7.06	5.81	6.29	5.17	12.91	11.99	12.81	13.88
3.47	2.45	4.92	6.3	5.77	6.69	3.55	9.65	8.28	9.07	9.88
2.79	2.28	4.24	5.55	5.67	6.86	2.35	6.05	4.63	5.24	5.62
2.44	2.32	3.8	5.05	5.59	6.84	1.78	3.51	2.36	2.76	2.84
2.25	2.44	3.48	4.61	5.46	6.65	1.48	1.55	0.83	1.02	0.96
2.15	2.5	3.15	4.02	5.06	6.07	1.31	0.35	0.1	0.14	0.1
2.18	2.56	3	3.61	4.72	5.6	1.26	0.04	0	0	0
2.19	2.48	2.79	3.03	4.11	4.89	1.16	0.01	0.03	0.03	0
2.08	2.24	2.47	2.39	3.34	4.05	1.01	0.09	0.17	0.17	0.03
2.28	2.33	2.55	2.18	3.11	3.9	1	0.17	0.25	0.26	0.12
2.53	2.44	2.65	1.94	2.82	3.69	1	0.24	0.27	0.3	0.18
2.45	2.23	2.42	1.54	2.26	3.03	0.9	0.22	0.21	0.23	0.17
2.6	2.27	2.47	1.4	2.07	2.74	0.92	0.19	0.15	0.18	0.15
10.71	8.52	9.36	4.72	6.76	7.62	3.8	0.51	0.1	0.18	0.15
9.57	6.83	7.49	3.74	5.25	4.51	3.68	0.59	0.29	0.23	0
7.05	4.7	4.98	2.64	3.92	3.04	3.01	0.56	0	0	0
4.76	3.03	3.23	1.72	2.81	2.1	2.1	0.07	0	0	0
3.18	1.86	2.23	1.11	1.85	1.5	1.32	0	0	0	0
1.69	0.91	1	0.5	0.86	0.49	0.42	0	0	0	0
0	0	0	0	0	0	0	0	0	0	0
0	0	0	0	0	0	0	0	0	0	0
0	0	0	0	0	0	0	0	0	0	0
0	0	0	0	0	0	0	0	0	0	0

RANGI24-3 0cm	RANGI24-3 20cm	RANGI24-3 40cm	RANGI24-3 60cm	RANGI24-3 80cm	RANGI24-3 100cm	RANGI24-3 120cm	RANGI24-3 140cm	RANGI24-3 160cm
0	0	0	0	0	0	0	0	0
0	0	0	0.17	0	0	0	0	0
0	0	0	0.29	0	0	0	0	0
0	0	0	0.39	0	0	0	0	0
0	0	0	0.42	0	0	0	0	0
0.01	0.35	0	0.37	0	0	0	0	0
0.22	0.98	0	0.22	0	0	0	0	0
0.83	1.65	0.06	0.13	0	0	0	0	0
1.68	2.52	0.86	0.34	0	0	0.22	0.69	0
2.68	3.38	1.94	1.16	0.04	0	2.2	3.36	0
4.21	4.77	3.64	3	1.71	1.44	5.21	6.96	0.26
5.11	5.4	5.1	5.41	4.93	4.73	8.34	9.93	3.41
6.48	6.63	7.02	8.66	9.04	9.27	12.05	13.2	7.52
7.6	7.63	8.66	11.9	13.41	14.26	15.01	15.34	12.52
6.7	6.64	7.84	11.7	13.77	14.87	13.28	12.73	14.17
7.6	7.42	8.87	13.86	16.5	17.71	14.29	13.11	18.26
6.47	6.18	7.36	11.78	13.86	14.53	10.9	9.64	16.46
5.12	4.73	5.46	8.6	9.67	9.59	6.88	5.91	12.41
4.07	3.63	4	5.81	6.04	5.53	3.95	3.36	8.3
3.14	2.72	2.76	3.23	2.88	2.29	1.69	1.44	4.3
2.33	2.01	1.86	1.23	0.74	0.43	0.35	0.32	1.28
1.94	1.77	1.56	0.42	0.09	0.03	0.03	0.03	0.19
1.66	1.66	1.5	0.23	0	0	0.03	0.02	0
1.46	1.57	1.5	0.39	0.06	0	0.19	0.16	0
1.53	1.72	1.72	0.65	0.23	0.09	0.34	0.28	0
1.62	1.85	1.92	0.87	0.39	0.25	0.44	0.35	0.02
1.49	1.67	1.79	0.82	0.44	0.31	0.4	0.3	0.13
1.52	1.65	1.79	0.75	0.46	0.34	0.35	0.25	0.19
6.22	5.99	6.58	2.06	1.59	1	1.08	0.65	0.58
6.18	5.46	5.77	1.73	1.68	0.96	1.26	0.78	0
4.93	4.17	4.29	1.3	1.45	1	1	0.7	0
3.55	2.85	2.96	0.96	0.89	0.74	0.5	0.47	0
2.35	1.99	2.11	0.71	0.14	0.4	0	0	0
1.32	1.01	1.06	0.42	0	0.23	0	0	0
0	0	0	0	0	0	0	0	0
0	0	0	0	0	0	0	0	0
0	0	0	0	0	0	0	0	0
0	0	0	0	0	0	0	0	0

RANGI24-4 20cm	RANGI24-4 40cm	RANGI24-4 60cm	RANGI24-4 80cm	RANGI24-4 120cm	RANGI24-4 140cm
0	0	0	0	0	0
0	0	0	0	0	0
0	0	0	0	0	0
0	0	0	0	0	0
0	0.1	0	0	0	0
0.03	0.44	0	0	0	0
0.54	0.86	0	0	0	0
1.47	1.42	0	0	0	0
2.62	2.24	0	0.01	0.12	0
3.7	3.19	0.66	1	1.96	0.03
5.16	4.77	3.29	4.52	6.1	1.73
5.45	5.62	6.47	8.33	9.98	5.07
6.11	6.98	10.5	12.88	14.29	9.37
6.35	7.96	14.22	16.61	17.31	13.99
4.95	6.75	13.48	14.83	14.53	14.45
5.13	7.29	15.23	15.75	14.64	17.42
4.09	5.84	12.13	11.56	10.14	14.75
3.19	4.27	8.03	6.72	5.42	10.38
2.71	3.19	4.85	3.42	2.5	6.55
2.46	2.4	2.25	1.16	0.7	3.15
2.32	1.91	0.58	0.13	0.04	0.82
2.35	1.84	0.07	0	0	0.1
2.34	1.88	0.04	0.01	0	0
2.19	1.85	0.3	0.09	0.03	0
2.34	2.05	0.56	0.18	0.11	0.07
2.49	2.21	0.74	0.26	0.18	0.19
2.29	2	0.66	0.26	0.19	0.23
2.32	1.97	0.56	0.24	0.18	0.25
8.55	6.83	1.37	0.58	0.43	0.59
6.83	5.31	1.23	0.56	0.43	0.42
5.02	3.71	1	0.55	0.49	0.43
3.46	2.51	0.8	0.33	0.23	0
2.22	1.76	0.58	0	0	0
1.32	0.84	0.38	0	0	0
0	0	0	0	0	0
0	0	0	0	0	0
0	0	0	0	0	0
0	0	0	0	0	0

RANGI24-5 0cm	RANGI24-5 20cm	RANGI24-5 40cm	RANGI24-5 60cm	RANGI24-5 80cm	RANGI24-5 100cm	RANGI24-5 120cm	RANGI24-5 OUTCROP
0	0	0	0	0	0	0	0
0	0	0	0	0	0	0	0
0	0	0	0	0	0	0	0
0	0	0	0	0	0	0	0
0.07	0	0	0	0	0	0	0
0.25	0.03	0	0	0	0	0	0
0.52	0.5	0	0	0	0	0	0
0.98	1.24	0	0	0	0	0	0.1
1.78	2.14	0.19	0.03	0.14	0.62	0.04	0.6
2.86	3.02	1.85	0.98	1.96	3.21	1.12	1.79
4.71	4.29	4.33	3.97	5.67	6.75	4.28	4.22
6.1	4.77	6.95	7.18	9.08	9.81	7.62	7.17
8.07	5.72	10.15	11.1	12.93	13.28	11.71	11.1
9.68	6.46	12.87	14.51	15.68	15.64	15.25	14.84
8.53	5.54	11.68	13.34	13.3	13.08	13.94	14.13
9.4	6.16	12.97	14.73	13.62	13.43	15.26	16.09
7.54	5.16	10.31	11.47	9.7	9.73	11.7	12.88
5.31	4.03	6.96	7.38	5.49	5.74	7.27	8.4
3.64	3.23	4.36	4.31	2.75	3.06	4.03	4.82
2.27	2.6	2.2	1.9	0.93	1.15	1.59	1.94
1.34	2.16	0.73	0.44	0.1	0.16	0.26	0.29
1.07	2.07	0.26	0.05	0	0	0	0
1.09	2.09	0.29	0.02	0.11	0.08	0	0
1.17	2.05	0.49	0.19	0.27	0.2	0.06	0
1.42	2.31	0.73	0.39	0.43	0.31	0.23	0
1.63	2.57	0.9	0.56	0.57	0.37	0.37	0.03
1.53	2.42	0.83	0.55	0.55	0.31	0.38	0.16
1.53	2.46	0.78	0.53	0.54	0.26	0.37	0.2
5.44	8.84	2.76	1.83	2.04	0.68	1.22	0.59
4.4	6.64	2.88	1.86	1.96	0.77	1.41	0.23
3.07	4.49	2.2	1.42	1.39	0.72	1.22	0.38
2.15	3.2	1.31	0.85	0.74	0.59	0.65	0.05
1.58	2.37	0.7	0.27	0.04	0.04	0.03	0
0.85	1.43	0.32	0.13	0	0	0	0
0	0	0	0	0	0	0	0
0	0	0	0	0	0	0	0
0	0	0	0	0	0	0	0
0	0	0	0	0	0	0	0

RANGI 24-6 0cm	RANGI 24-6 20cm	RANGI 24-6 40cm	RANGI 24-6 60cm	RANGI 24-6 80cm	RANGI 24-6 100cm	RANGI 24-6 120cm	RANGI 24-6B 0cm	RANGI 24-6B 20cm	RANGI 24-6B 40cm	RANGI 24-6B 60cm	RANGI 24-6B 80cm
0	0	0	0	0	0	0	0	0	0	0	0
0	0.33	0.06	0	0	0	0	0	0	0	0	0
0	0.63	0.19	0	0	0	0	0	0	0	0	0
0	1	0.37	0	0	0	0	0	0.02	0	0	0
0.02	1.35	0.61	0	0	0	0	0	0.1	0	0	0
0.4	1.74	0.95	0	0	0	0	0	0.16	0	0	0
0.97	2.09	1.35	0	0	0	0	0	0.23	0	0	0
1.54	2.52	1.87	0	0	0	0	0	0.4	0	0	0
2.26	3.01	2.55	0.04	0.1	0	0.04	0.21	0.93	0	0.04	0
2.96	3.47	3.26	0.99	1.21	0.3	0.62	1.56	2	0.7	1.19	0.48
4.16	4.49	4.5	3.62	3.54	1.91	2.35	3.54	4.11	3.66	4.73	2.73
4.75	4.73	4.95	6.31	6.65	4.96	5.26	5.76	6.4	7.66	8.47	6.24
5.92	5.51	5.85	9.58	10.62	9.41	9.34	8.71	9.48	12.7	12.95	11
6.92	6.05	6.43	12.42	14.27	14.24	13.66	11.51	12.31	17.13	16.59	15.71
6.12	5.02	5.28	11.46	13.46	14.77	13.98	10.98	11.51	15.73	14.74	15.39
6.93	5.41	5.66	12.87	15.14	17.64	16.79	12.73	13.08	16.81	15.56	17.48
5.87	4.38	4.58	10.34	11.95	14.59	14.17	10.59	10.62	12.22	11.34	13.65
4.58	3.31	3.53	7.07	7.75	9.78	9.95	7.53	7.3	6.84	6.5	8.45
3.59	2.6	2.87	4.49	4.53	5.75	6.25	4.94	4.62	3.27	3.25	4.54
2.75	2.07	2.41	2.3	1.97	2.45	2.99	2.63	2.32	0.98	1.07	1.65
2.1	1.69	2.09	0.79	0.43	0.49	0.77	0.91	0.72	0.08	0.11	0.21
1.88	1.6	2.03	0.31	0.04	0.04	0.1	0.26	0.19	0	0	0
1.82	1.57	1.99	0.36	0.02	0	0	0.19	0.21	0	0.02	0
1.78	1.53	1.89	0.6	0.2	0	0.04	0.39	0.44	0.03	0.12	0
2.03	1.73	2.08	0.92	0.4	0	0.16	0.68	0.7	0.13	0.23	0.06
2.31	1.99	2.3	1.18	0.58	0.14	0.3	0.94	0.9	0.24	0.33	0.19
2.22	1.97	2.2	1.13	0.56	0.22	0.33	0.93	0.83	0.27	0.32	0.24
2.27	2.11	2.29	1.1	0.53	0.27	0.34	0.92	0.77	0.26	0.29	0.25
8.03	8.49	8.65	3.66	1.64	0.97	0.87	3.23	2.44	0.6	0.72	0.63
5.82	6.79	6.63	3.27	1.83	0.89	0.72	3.26	2.35	0.4	0.66	0.48
3.89	4.59	4.56	2.5	1.53	0.81	0.67	2.7	1.84	0.28	0.57	0.49
2.68	3.08	3.04	1.56	0.85	0.36	0.3	2.06	1.35	0	0.21	0.12
1.99	2.1	2.03	0.8	0.19	0	0	1.7	1.03	0	0	0
1.44	1	0.96	0.34	0	0	0	1.15	0.65	0	0	0
0	0	0	0	0	0	0	0	0	0	0	0
0	0	0	0	0	0	0	0	0	0	0	0
0	0	0	0	0	0	0	0	0	0	0	0
0	0	0	0	0	0	0	0	0	0	0	0

RANGI24-7 0cm	RANGI24-7 20cm	RANGI24-7 40cm	RANGI24-7 60cm	RANGI24-7 80cm	RANGI24-8 0cm	RANGI24-8 20cm	RANGI24-8 40cm	RANGI24-8 60cm	RANGI24-8 80cm
0	0	0	0	0	0	0	0	0	0
0	0	0	0	0	0	0	0	0	0
0	0	0	0	0	0	0	0	0	0
0	0	0	0	0	0	0	0	0	0
0	0	0	0	0	0	0	0	0	0
0	0	0	0	0	0	0	0	0	0
0	0	0	0	0	0.07	0	0	0	0
0	0	0	0	0	0.92	0	0.13	0	0.32
0.01	0	0	0.55	0.7	2.66	0.34	0.72	0.21	2.19
0.73	0.02	0.27	3.38	3.51	4.81	2.59	1.97	2.12	4.46
3.21	2.09	3.05	7.33	7.36	8.07	5.78	4.34	4.93	7.72
5.93	6.22	7.51	10.93	10.7	10.08	8.9	6.94	7.88	9.79
9.37	11.35	12.72	14.91	14.43	12.56	12.61	10.36	11.51	12.36
12.55	16.42	17.37	17.4	16.85	14.01	15.51	13.55	14.59	14.04
11.91	16.02	16.05	14.06	13.8	11.29	13.59	12.8	13.28	11.67
13.6	17.9	17.13	13.66	13.72	11.43	14.54	14.73	14.77	12.26
11.08	13.59	12.36	9.01	9.42	8.3	11.01	12.16	11.75	9.37
7.69	7.99	6.79	4.45	4.98	5.05	6.86	8.53	7.88	6.14
4.99	4.01	3.14	1.83	2.25	2.9	3.87	5.49	4.86	3.8
2.71	1.29	0.87	0.4	0.58	1.32	1.59	2.8	2.33	1.88
1.14	0.12	0.05	0	0	0.43	0.28	0.85	0.63	0.57
0.65	0	0	0	0	0.24	0	0.13	0.09	0.09
0.66	0	0	0	0	0.34	0.02	0.02	0.02	0.02
0.83	0	0	0.04	0.04	0.47	0.12	0.14	0.13	0.17
1.09	0.07	0.08	0.14	0.14	0.58	0.23	0.33	0.29	0.3
1.25	0.22	0.21	0.22	0.21	0.61	0.31	0.49	0.41	0.39
1.08	0.28	0.26	0.21	0.21	0.47	0.28	0.46	0.38	0.33
0.95	0.3	0.27	0.19	0.19	0.37	0.23	0.4	0.31	0.26
2.54	0.77	0.68	0.46	0.33	0.96	0.5	0.83	0.56	0.54
1.98	0.54	0.51	0.41	0.32	0.89	0.49	0.74	0.53	0.58
1.49	0.52	0.49	0.38	0.27	0.67	0.34	0.65	0.47	0.51
1.14	0.28	0.2	0.05	0	0.47	0	0.45	0.06	0.23
0.85	0	0	0	0	0.03	0	0	0	0
0.54	0	0	0	0	0	0	0	0	0
0	0	0	0	0	0	0	0	0	0
0	0	0	0	0	0	0	0	0	0
0	0	0	0	0	0	0	0	0	0
0	0	0	0	0	0	0	0	0	0

RANGI24-1 OSL	RANGI24-2 OSL	RANGI24-3 OSL	RANGI24-4 OSL	RANGI24-5 OSL	RANGI24-6 OSL	RANGI24-6B OSL	RANGI24-7 OSL	RANGI24-8 OSL
0	0	0	0	0	0	0	0	0
0	0	0	0	0	0	0	0	0
0	0	0	0	0	0	0	0	0
0	0	0	0	0	0	0	0	0
0	0	0	0	0	0	0	0	0
0	0	0	0	0	0	0	0	0
0	0	0	0	0	0	0	0	0
0.92	0	0	0	0	0	0	0	0.2
4.46	0	0.07	1.1	0	0.12	0.19	0	1.81
8.22	0.37	1.51	4.32	0.18	1.88	1.2	0.69	3.89
12.87	3.2	5.39	8.61	1.34	5.86	3.78	3.76	7.06
14.46	7.28	9.26	11.87	4.26	9.61	7.41	8.12	9.48
16.14	12.06	13.72	15.28	8.88	13.88	12.06	13.62	12.54
15.81	16.43	17.16	16.99	14.28	17.05	16.3	18.39	14.85
10.7	15.47	14.93	13.16	15.46	14.65	15.27	16.69	12.79
8.96	17.17	15.55	12.44	18.89	15.17	16.79	17.36	13.7
4.98	13.22	11.21	8.06	15.78	10.88	12.71	12.01	10.52
1.9	8.16	6.36	3.98	10.5	6.12	7.56	6.05	6.74
0.54	4.4	3.14	1.68	6	2.98	3.87	2.45	3.92
0.04	1.62	1	0.4	2.38	0.91	1.29	0.5	1.67
0	0.2	0.09	0	0.4	0.06	0.13	0	0.3
0	0	0	0	0.02	0	0	0	0
0	0	0	0.01	0	0	0	0	0
0	0	0	0.1	0	0	0	0	0
0	0	0	0.16	0	0	0	0	0
0	0	0.09	0.2	0	0.12	0	0	0.1
0	0.05	0.13	0.18	0	0.17	0.05	0	0.14
0	0.12	0.15	0.15	0.07	0.18	0.12	0	0.14
0	0.24	0.24	0.43	0.6	0.36	0.52	0.25	0.15
0	0	0	0.48	0.46	0	0.37	0.1	0
0	0	0	0.38	0.44	0	0.36	0	0
0	0	0	0	0.05	0	0	0	0
0	0	0	0	0	0	0	0	0
0	0	0	0	0	0	0	0	0
0	0	0	0	0	0	0	0	0
0	0	0	0	0	0	0	0	0
0	0	0	0	0	0	0	0	0
0	0	0	0	0	0	0	0	0

Appendix N: Lithological Profiles

Lithological profiles of hand-auger “cores” from the Rangitāiki Plains.

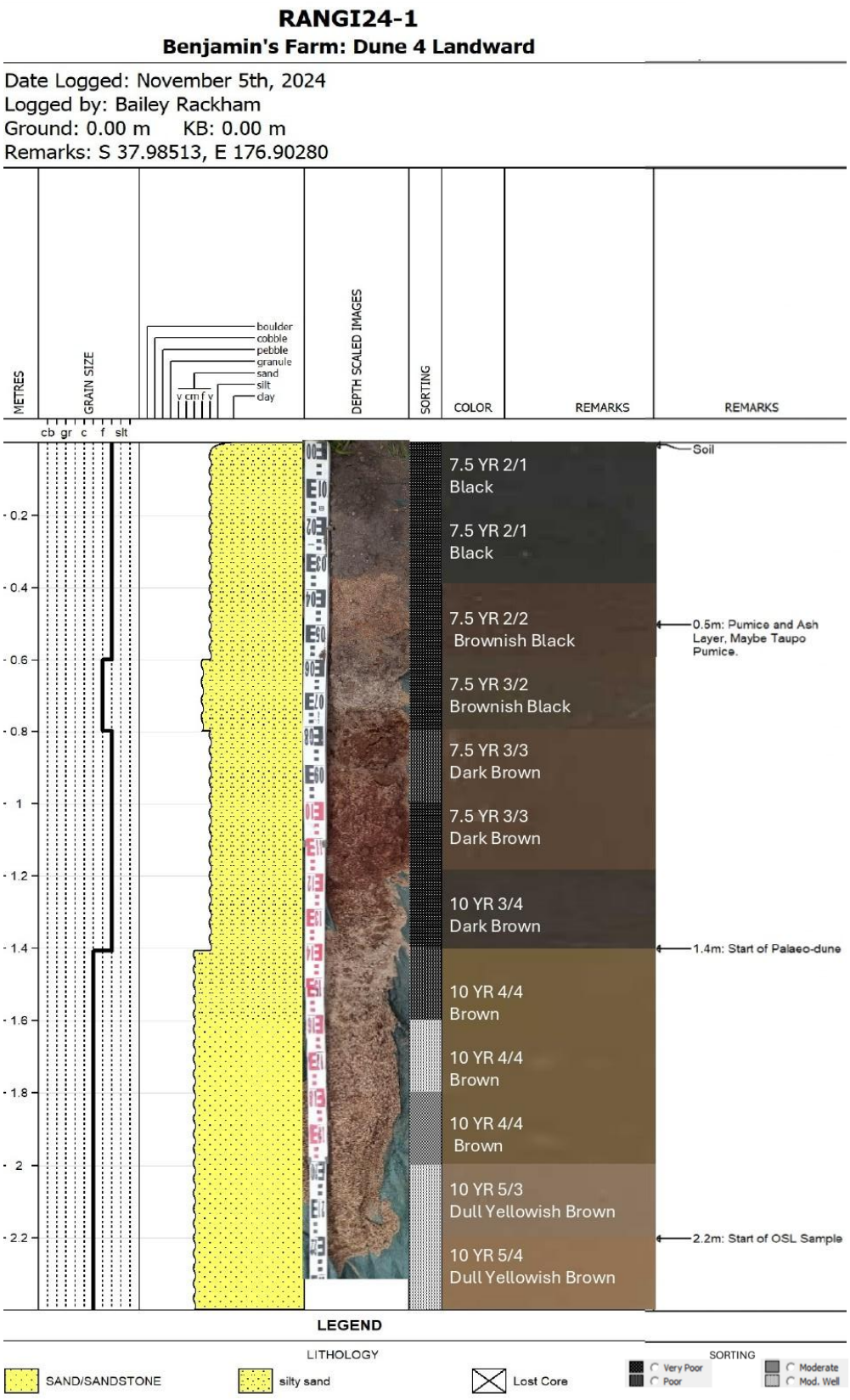

RANGI24-1

Benjamin's Farm: Dune 4 Landward

Date Logged: November 5th, 2024
Logged by: Bailey Rackham
Ground: 0.00 m KB: 0.00 m
Remarks: S 37.98513, E 176.90280

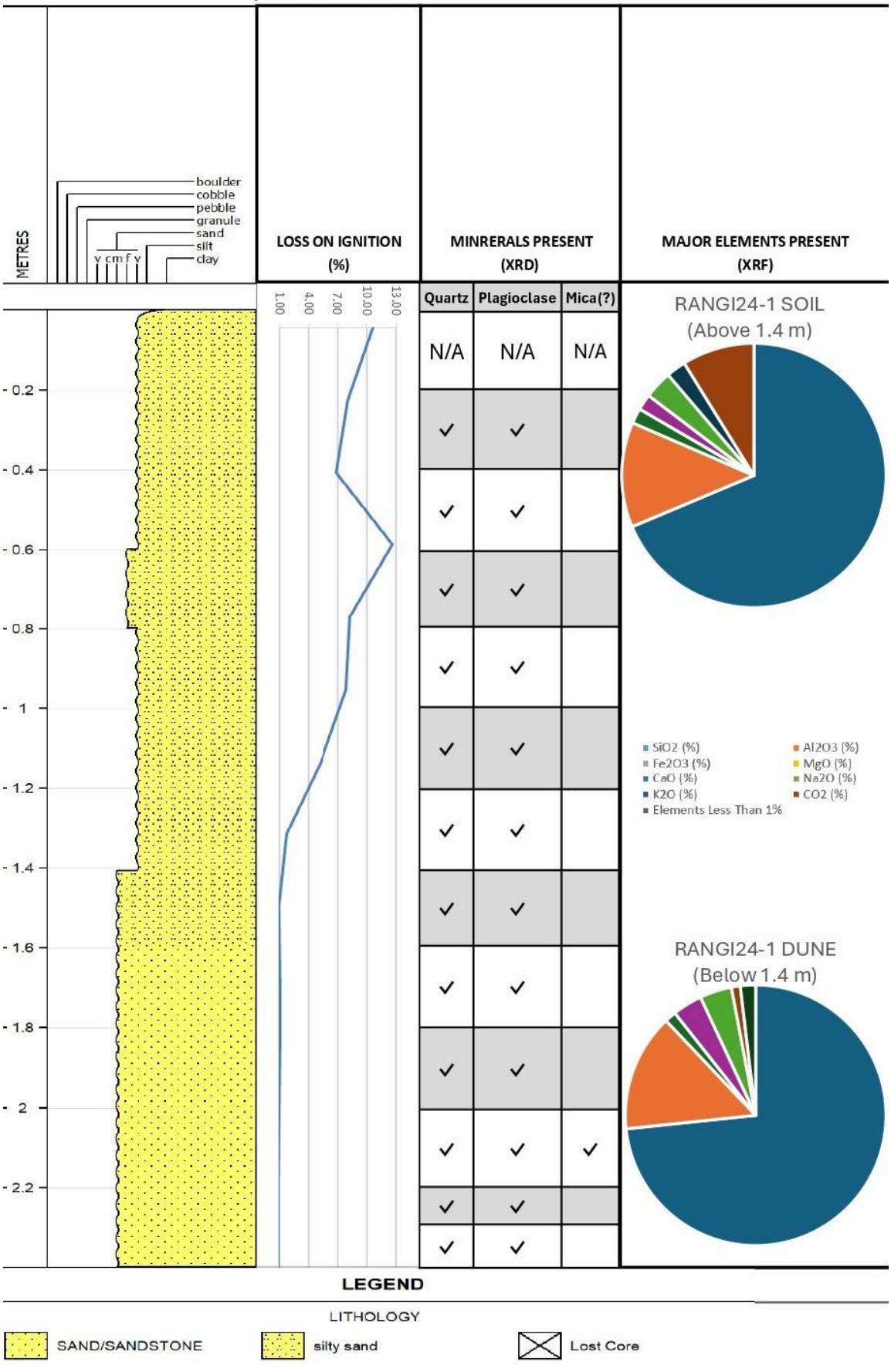

LEGEND

LITHOLOGY

SAND/SANDSTONE silty sand Lost Core

RANGI24-2

Benjamin's Farm: Dune 4 Seawards

Date Logged: November 5th, 2024
Logged by: Bailey Rackham
Ground: 0.00 m KB: 0.00 m
Remarks: S 37.98009, E 176.90752

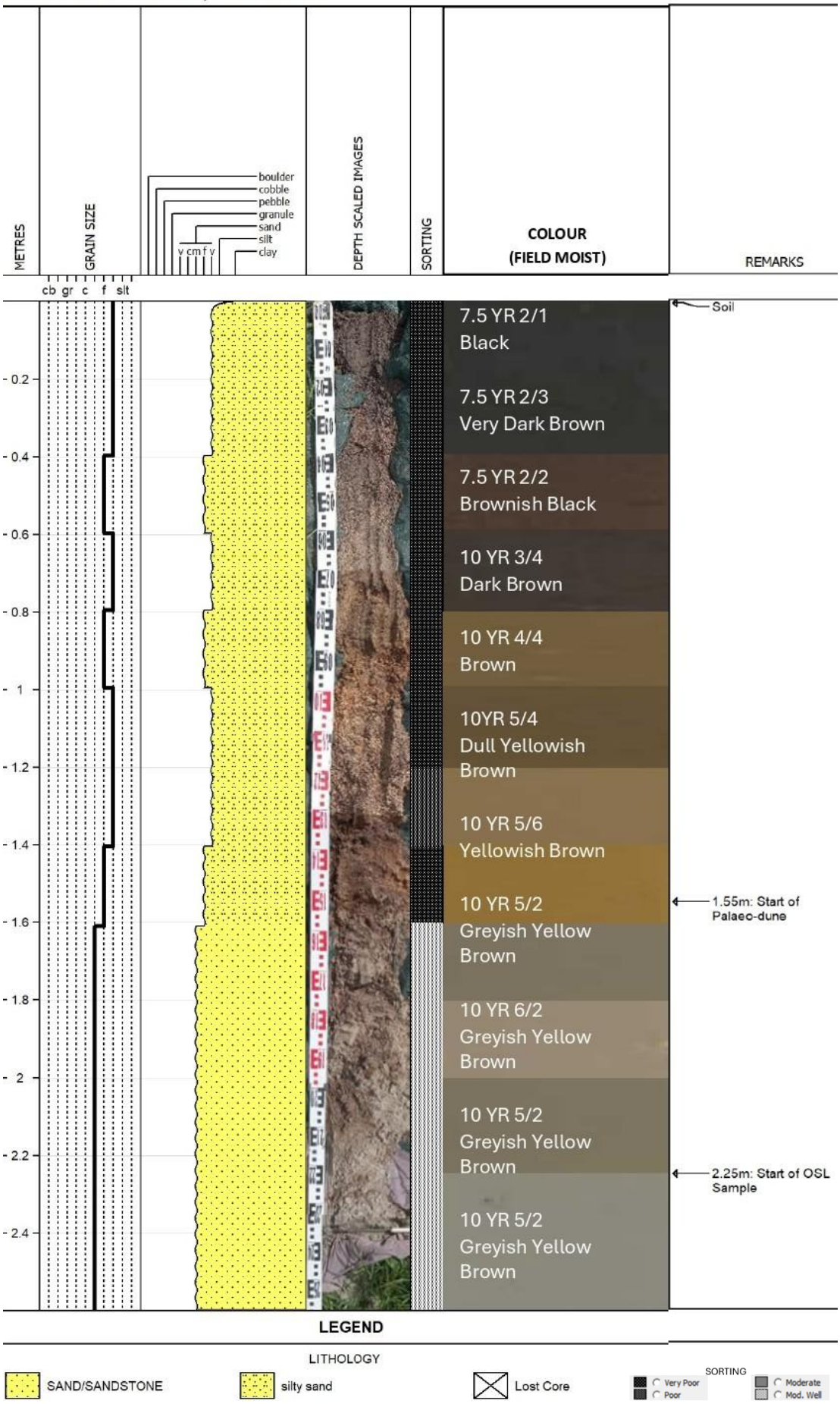

LEGEND

LITHOLOGY

SAND/SANDSTONE | silty sand | Lost Core

SORTING: Very Poor, Poor, Moderate, Mod. Well

RANGI24-2

Benjamin's Farm: Dune 4 Seawards

Date Logged: November 5th, 2024
Logged by: Bailey Rackham
Ground: 0.00 m KB: 0.00 m
Remarks: S 37.98009, E 176.90752

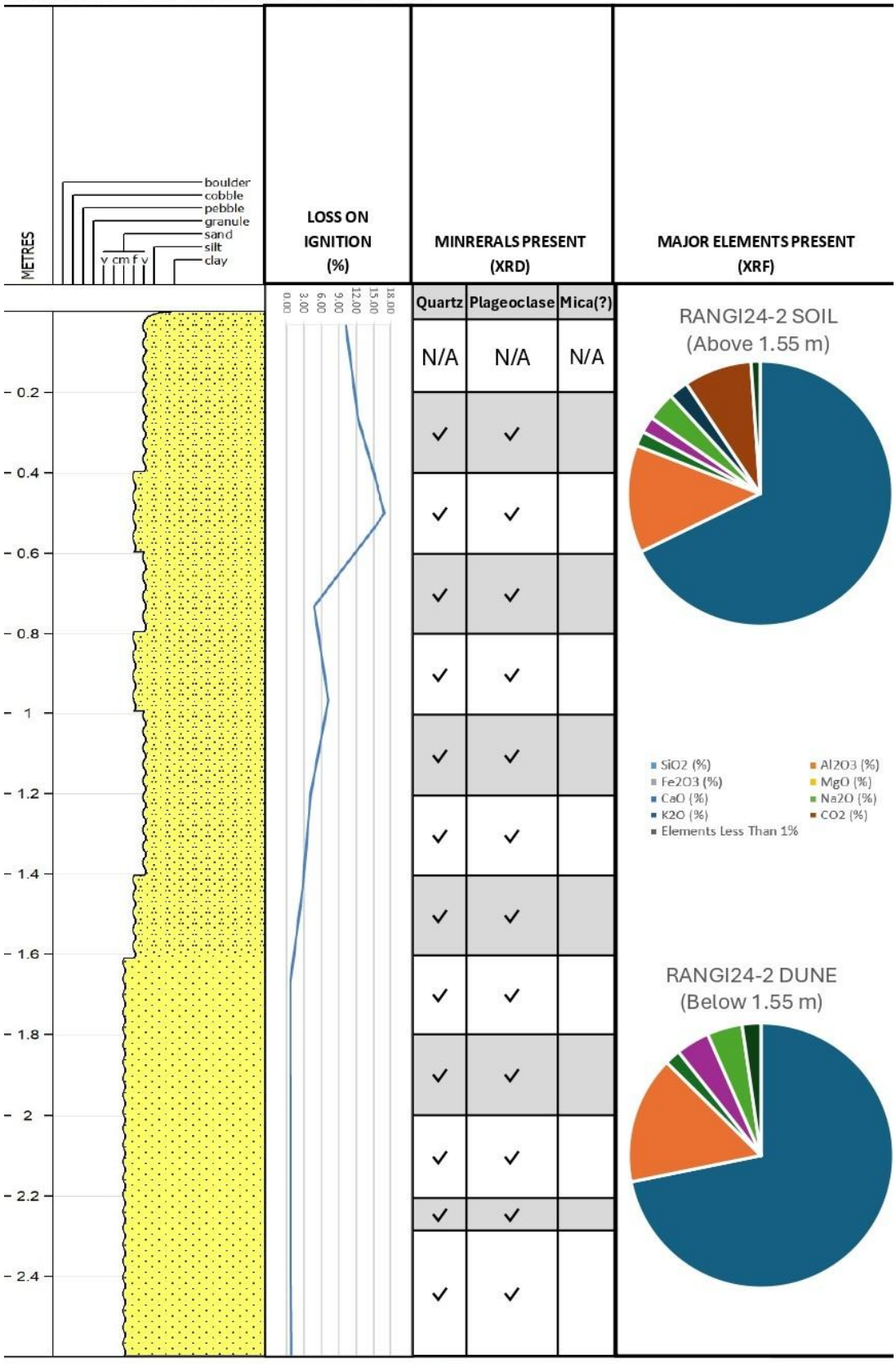

LEGEND

LITHOLOGY

SAND/SANDSTONE | silty sand | Lost Core

RANGI24-3

Robert's Farm: Dune 3 Landwards

Date Logged: November 6th, 2024
Logged by: Bailey Rackham
Ground: 0.00 m KB: 0.00 m
Remarks: S 37.96970, E 176.90828

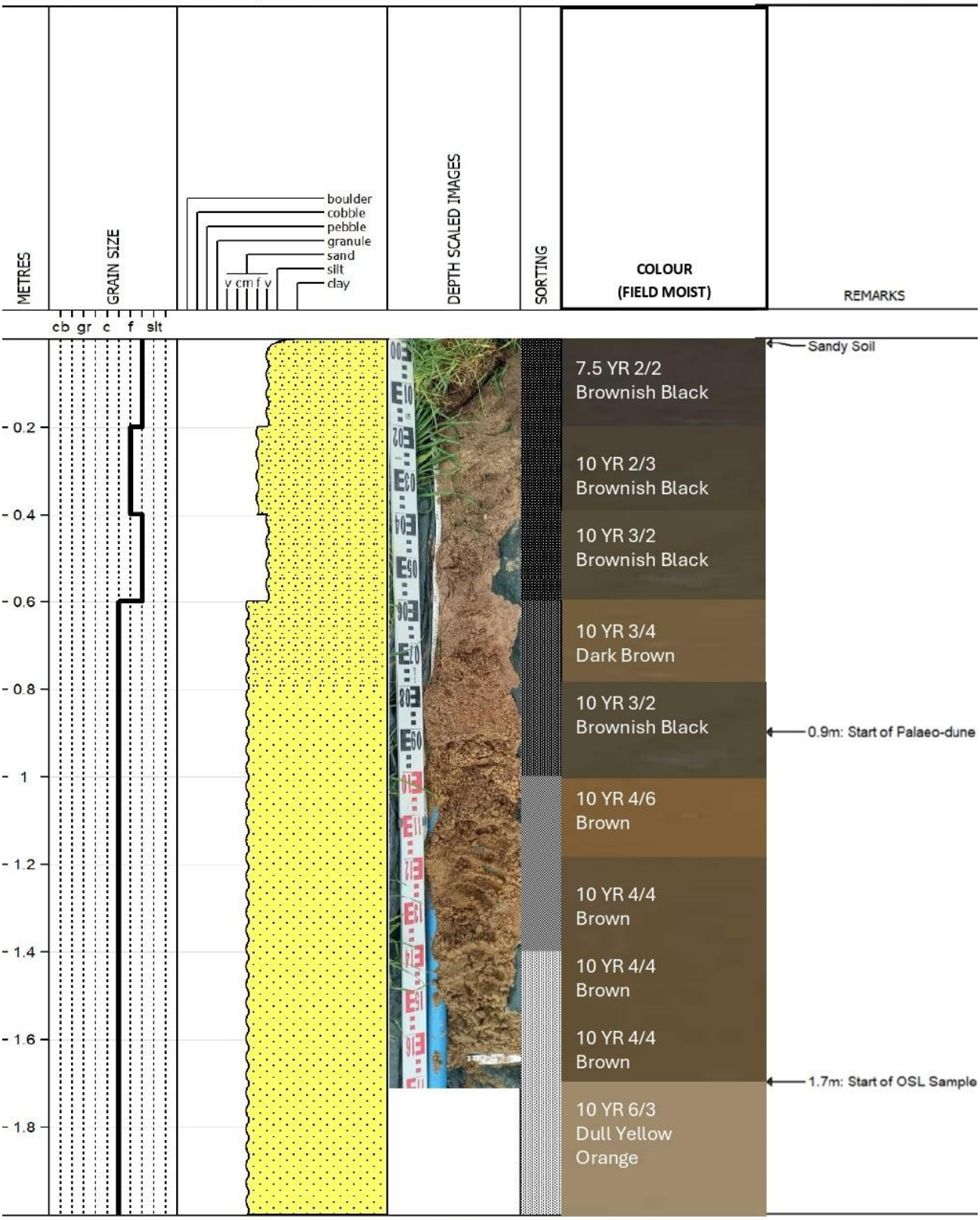

LEGEND

LITHOLOGY

SAND/SANDSTONE

silty sand

Lost Core

SORTING

Very Poor
Poor
Moderate
Mod. Well

RANGI24-3

Robert's Farm: Dune 3 Landwards

Date Logged: November 6th, 2024
Logged by: Bailey Rackham
Ground: 0.00 m KB: 0.00 m
Remarks: S 37.96970, E 176.90828

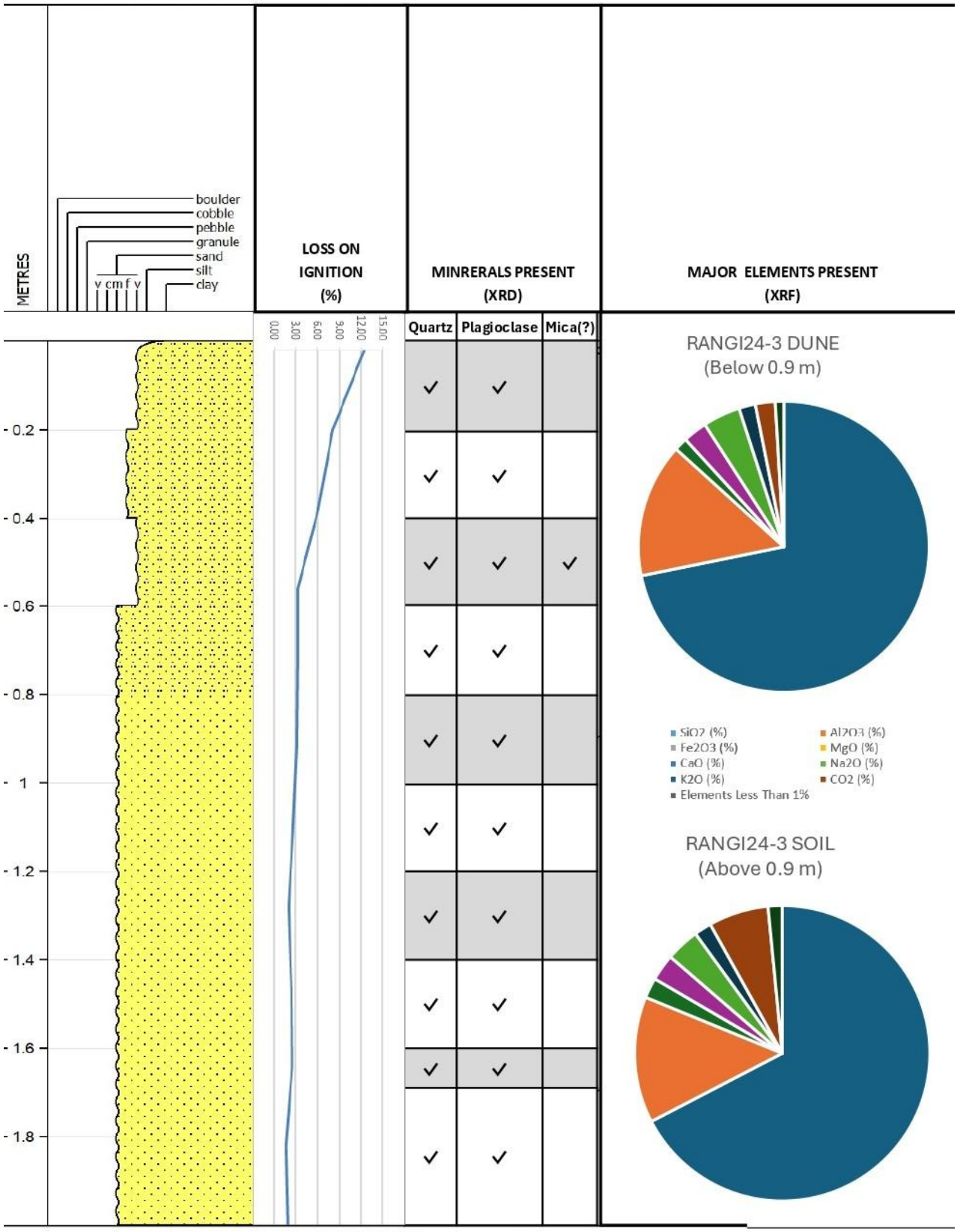

LEGEND

LITHOLOGY

SAND/SANDSTONE | silty sand | Lost Core

RANGI24-4

Scottie's Farm (Dune 3 Seaward)

Date Logged: November 5th, 2024
Logged by: Bailey Rackham
Ground: 0.00 m KB: 0.00 m
Remarks: S 37.97131, E 176.92822

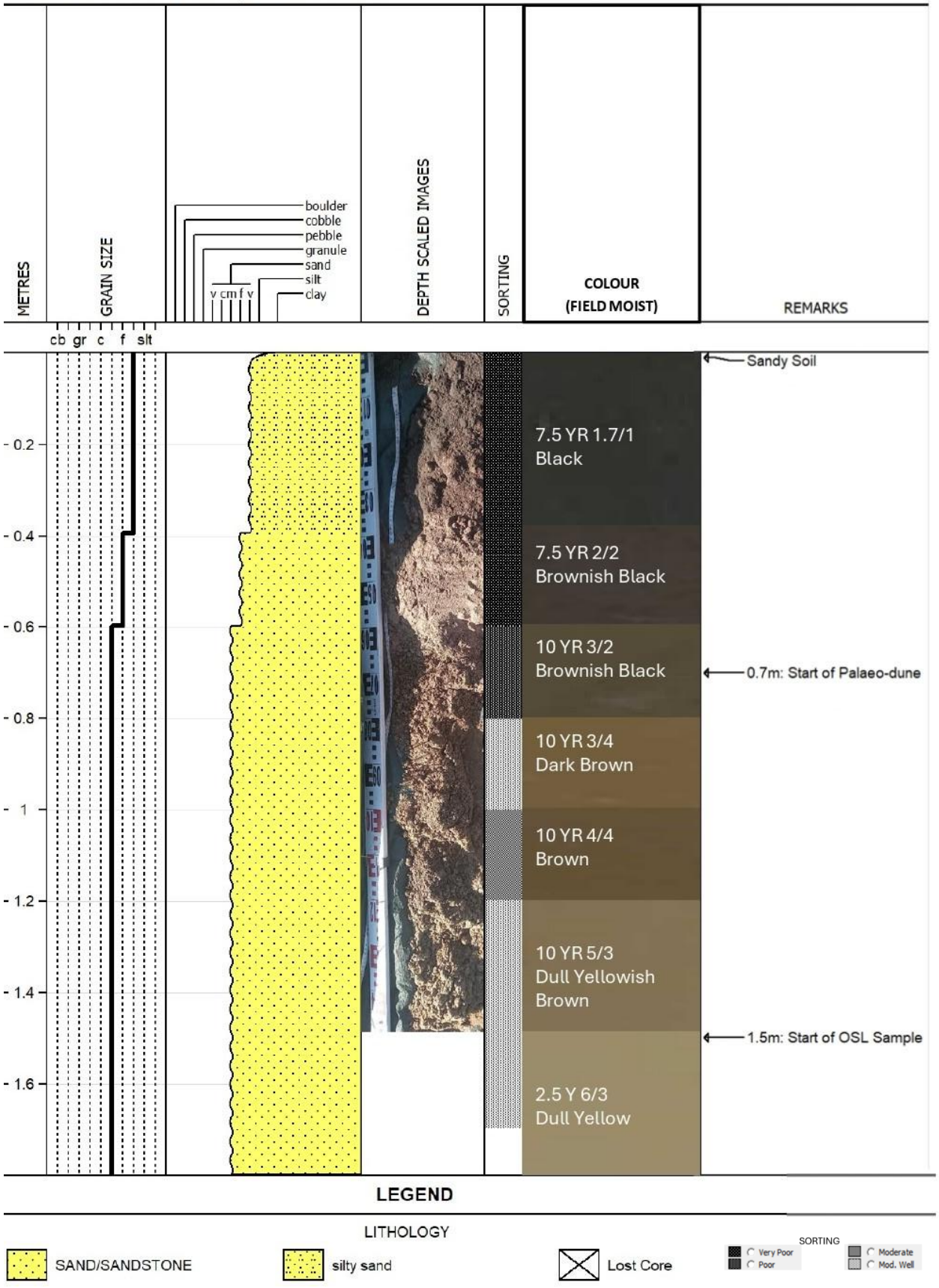

LEGEND

LITHOLOGY

SAND/SANDSTONE | silty sand | Lost Core

SORTING: Very Poor, Poor, Moderate, Mod. Well

RANGI24-4

Scottie's Farm (Dune 3 Seaward)

Date Logged: November 5th, 2024
Logged by: Bailey Rackham
Ground: 0.00 m KB: 0.00 m
Remarks: S 37.97131, E 176.92822

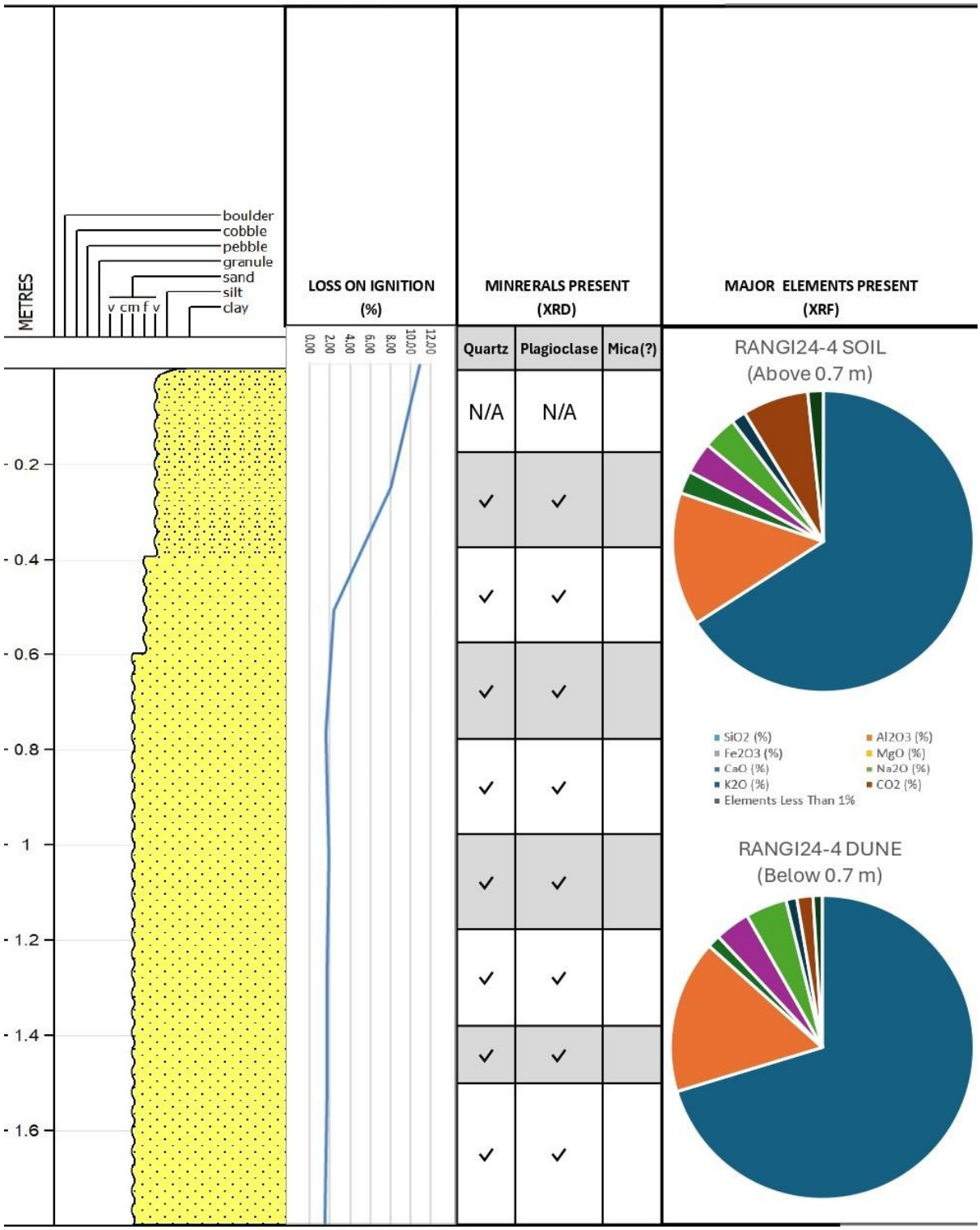

LEGEND

LITHOLOGY

SAND/SANDSTONE | silty sand | Lost Core

RANGI24-5

Gerald's Farm (Dune 2 Landward)

Date Logged: November 6th, 2024
Logged by: Bailey Rackham
Ground: 0.00 m KB: 0.00 m
Remarks: S 37.9618929, E 176.9140622

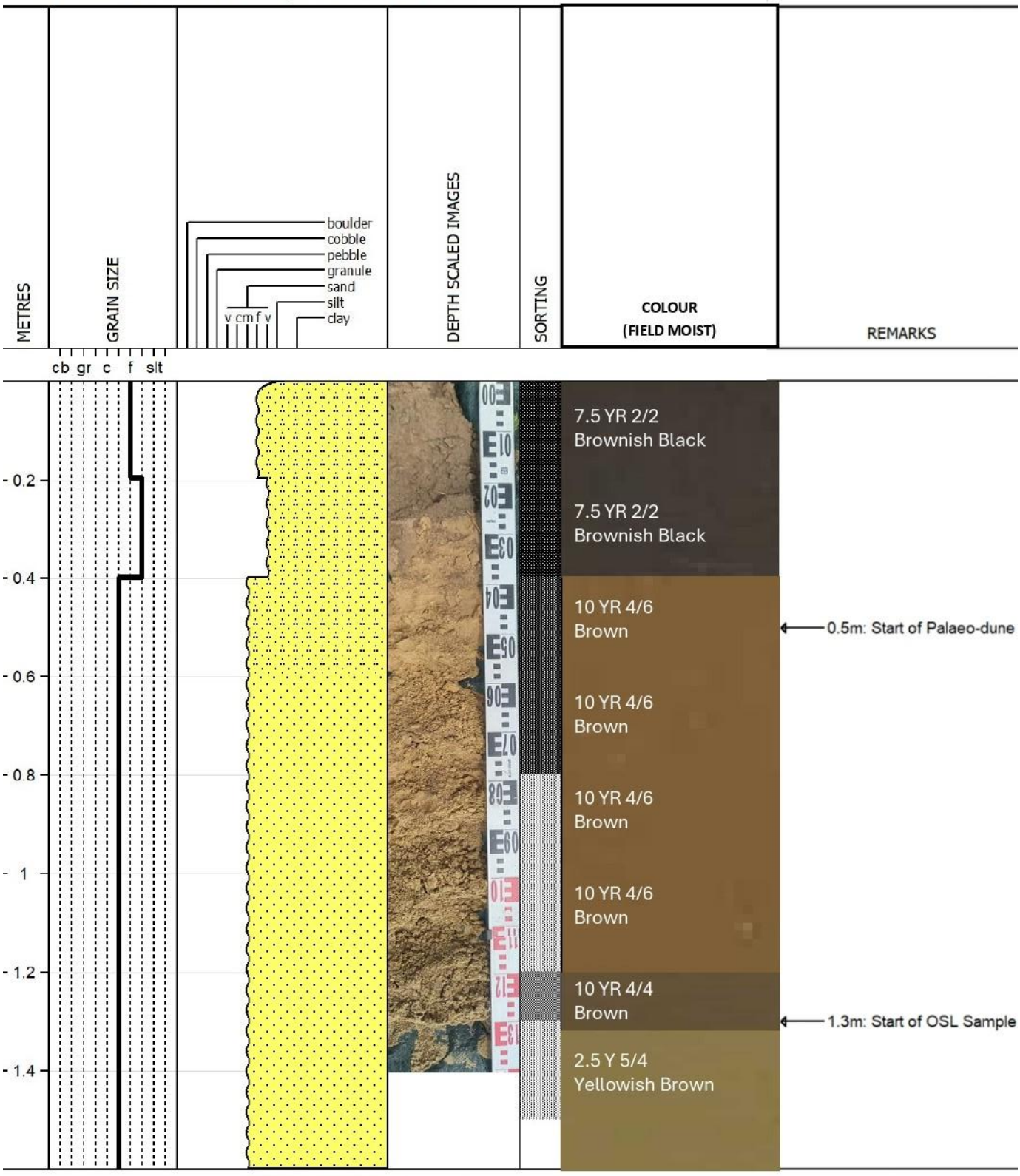

LEGEND

LITHOLOGY

SAND/SANDSTONE

silty sand

Lost Core

SORTING

Very Poor
Poor
Moderate
Mod. Well

RANGI24-5

Gerald's Farm (Dune 2 Landward)

Date Logged: November 6th, 2024
Logged by: Bailey Rackham
Ground: 0.00 m KB: 0.00 m
Remarks: S 37.9618929, E 176.9140622

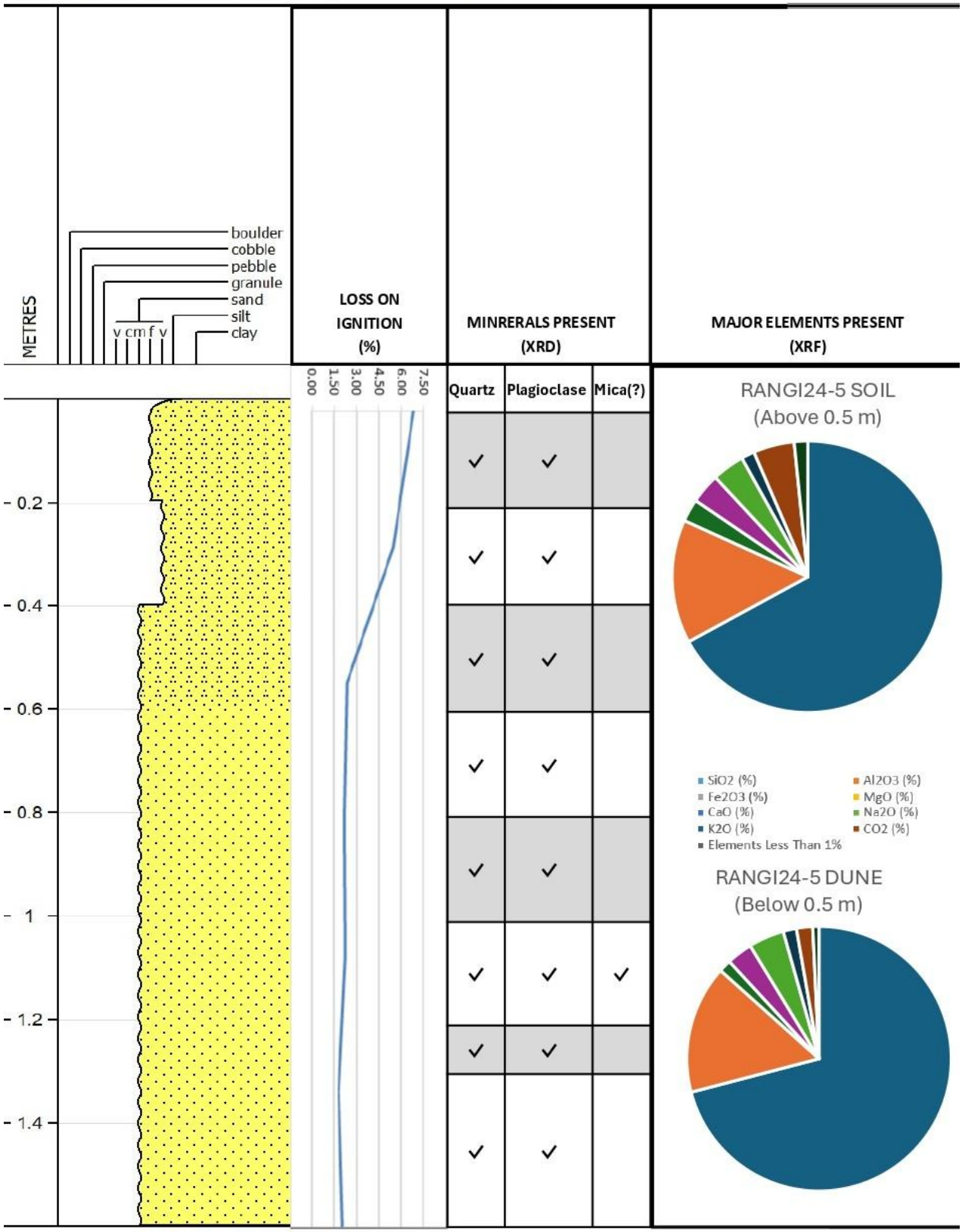

LEGEND

LITHOLOGY

SAND/SANDSTONE

silty sand

Lost Core

RANGI24-6

Gerald's Farm (Dune 2 Seaward)

Date Logged: November 6th, 2024
Logged by: Baile Rackham
Ground: 0.00 m KB: 0.00 m
Remarks: S 37.9570788, E 176.9142161

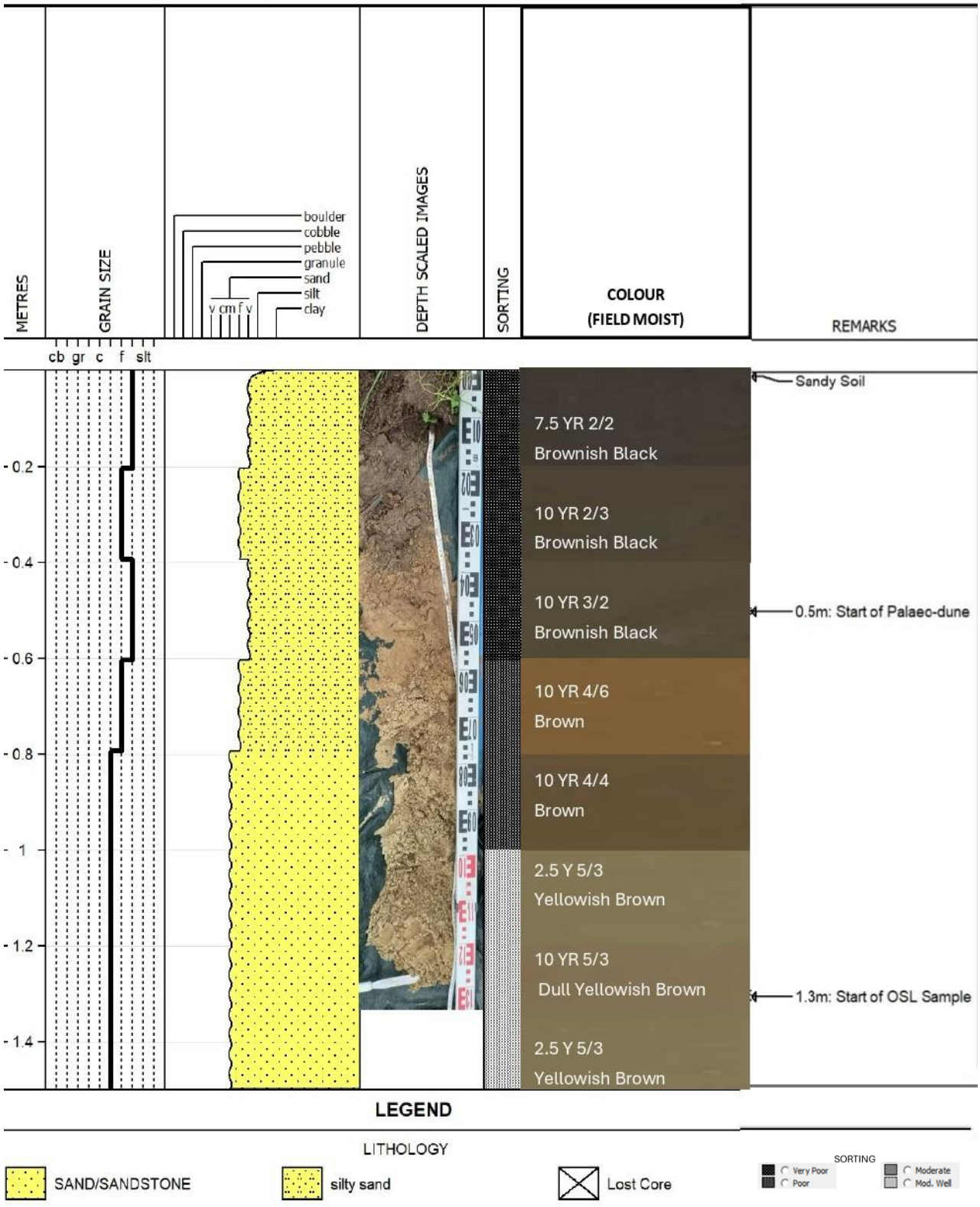

LEGEND

LITHOLOGY

SAND/SANDSTONE

silty sand

Lost Core

SORTING

Very Poor
Poor
Moderate
Mod. Well

RANGI24-6

Gerald's Farm (Dune 2 Seaward)

Date Logged: November 6th, 2024
Logged by: Baile Rackham
Ground: 0.00 m KB: 0.00 m
Remarks: S 37.9570788, E 176.9142161

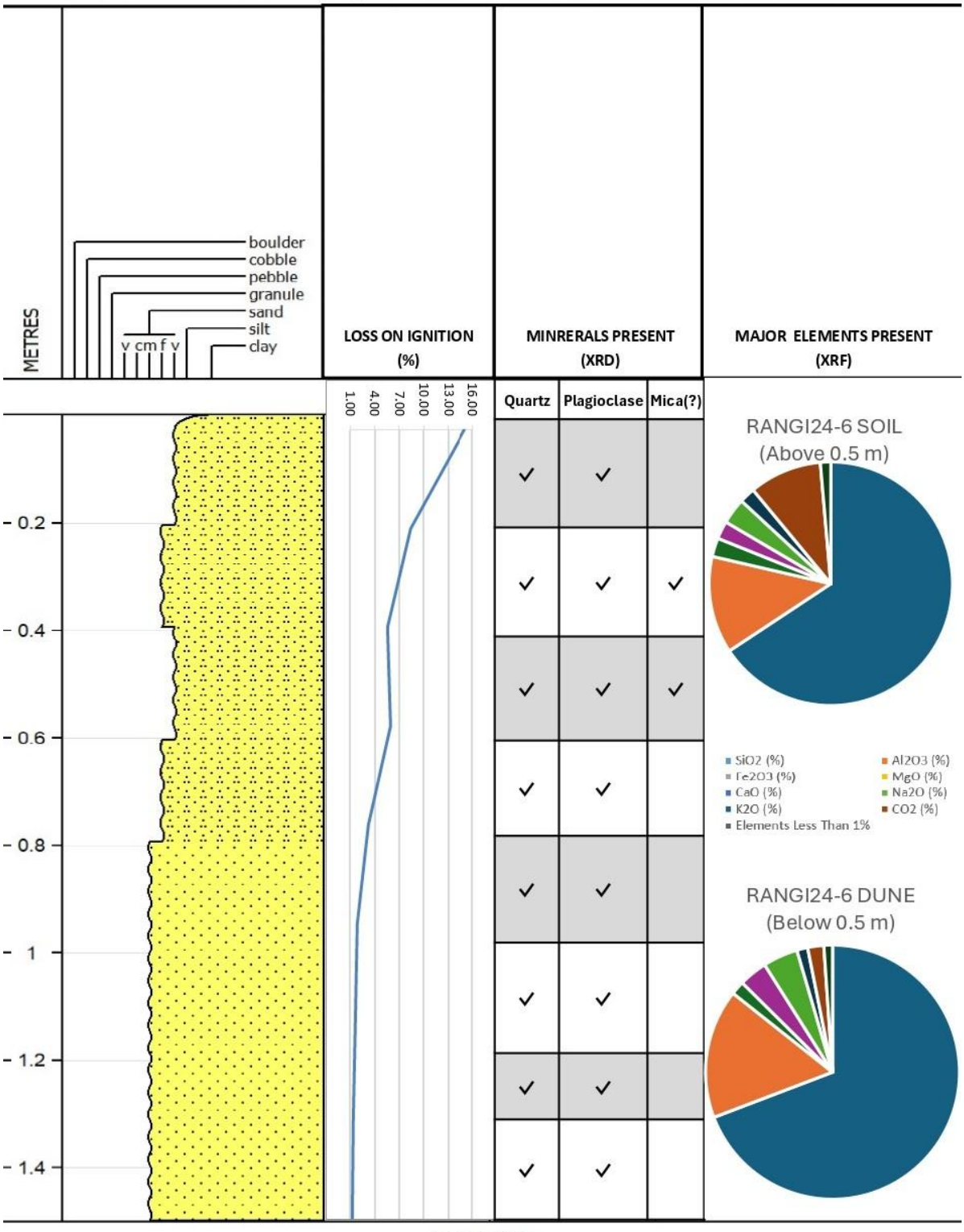

LEGEND

LITHOLOGY

SAND/SANDSTONE | silty sand | Lost Core

RANGI24-6B

Julians Berry Farm and Cafe (Dune 1.5)

Date Logged: November 6th, 2024
Logged by: Bailey Rackham
Ground: 0.00 m KB: 0.00 m
Remarks: S 37.94746, E 176.94490

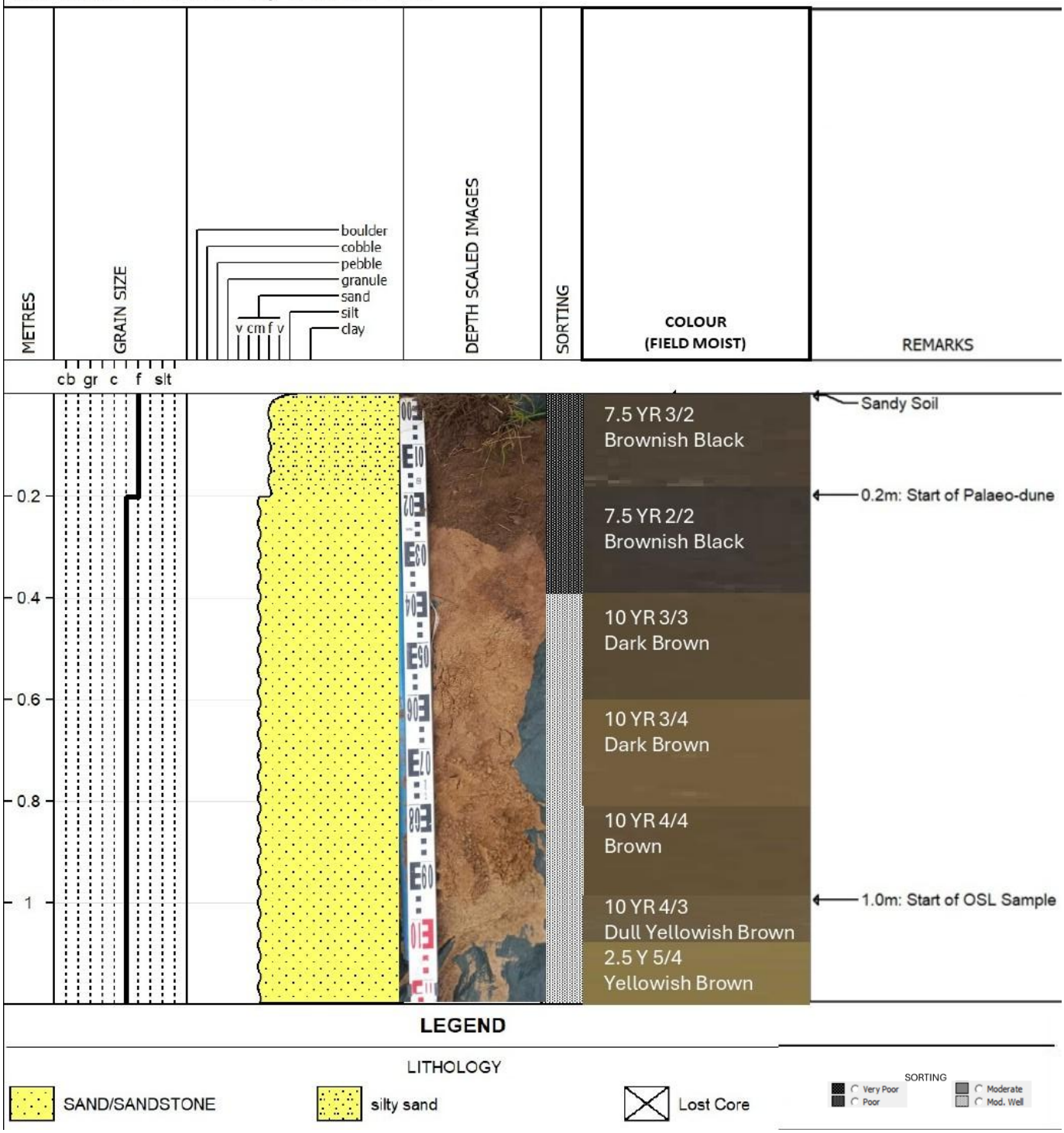

LEGEND

LITHOLOGY

SAND/SANDSTONE

silty sand

Lost Core

SORTING

Very Poor
Poor
Moderate
Mod. Well

RANGI24-6B

Julians Berry Farm and Cafe (Dune 1.5)

Date Logged: November 6th, 2024
Logged by: Bailey Rackham
Ground: 0.00 m KB: 0.00 m
Remarks: S 37.94746, E 176.94490

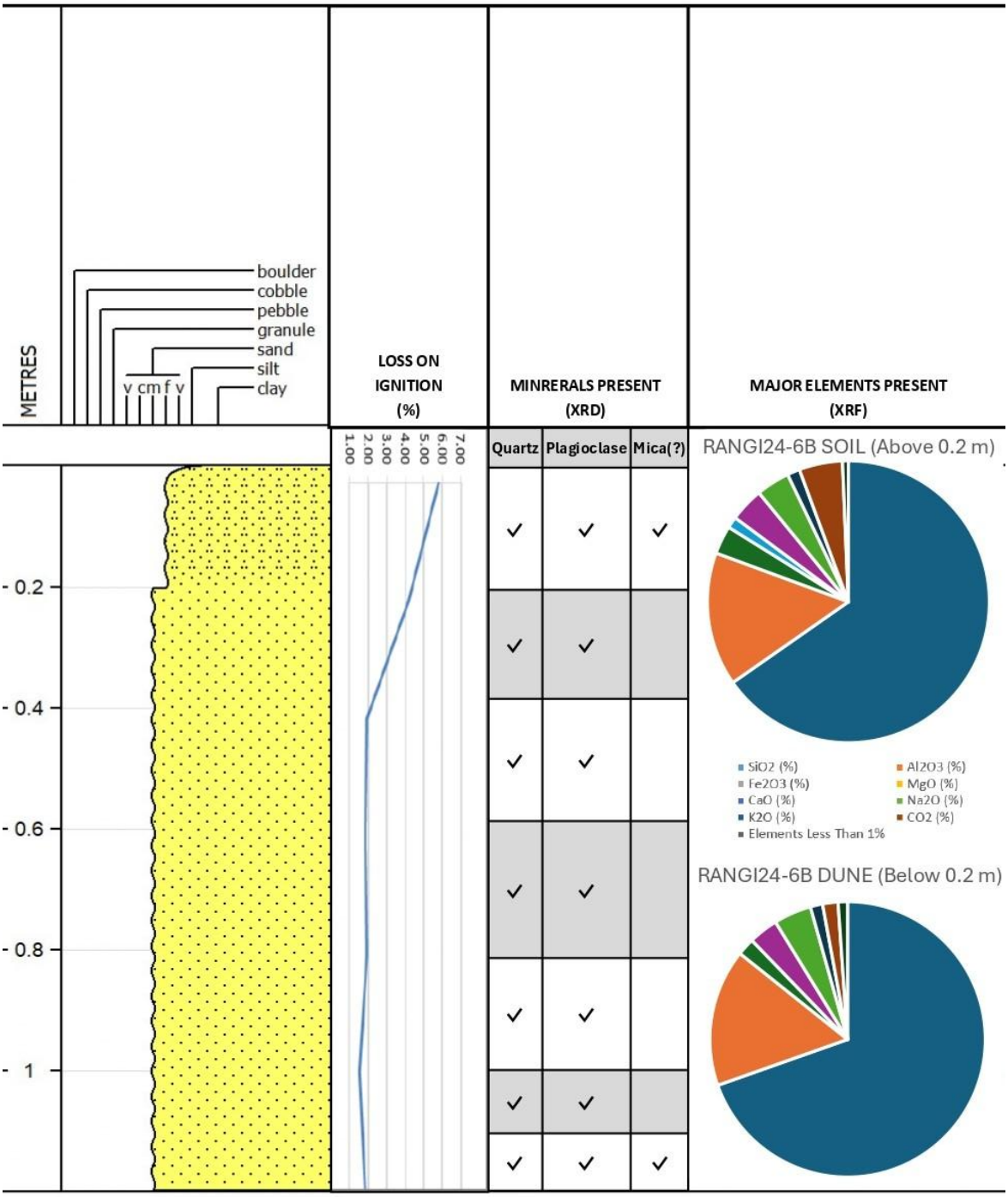

LEGEND

LITHOLOGY

SAND/SANDSTONE
silty sand
Lost Core

RANGI24-7

Whakatane Golf Course (Dune 1 Landward)

Date Logged: November 6th, 2024
Logged by: Bailey Rackham
Ground: 0.00 m KB: 0.00 m
Remarks: S 37.92847, E 176.93378

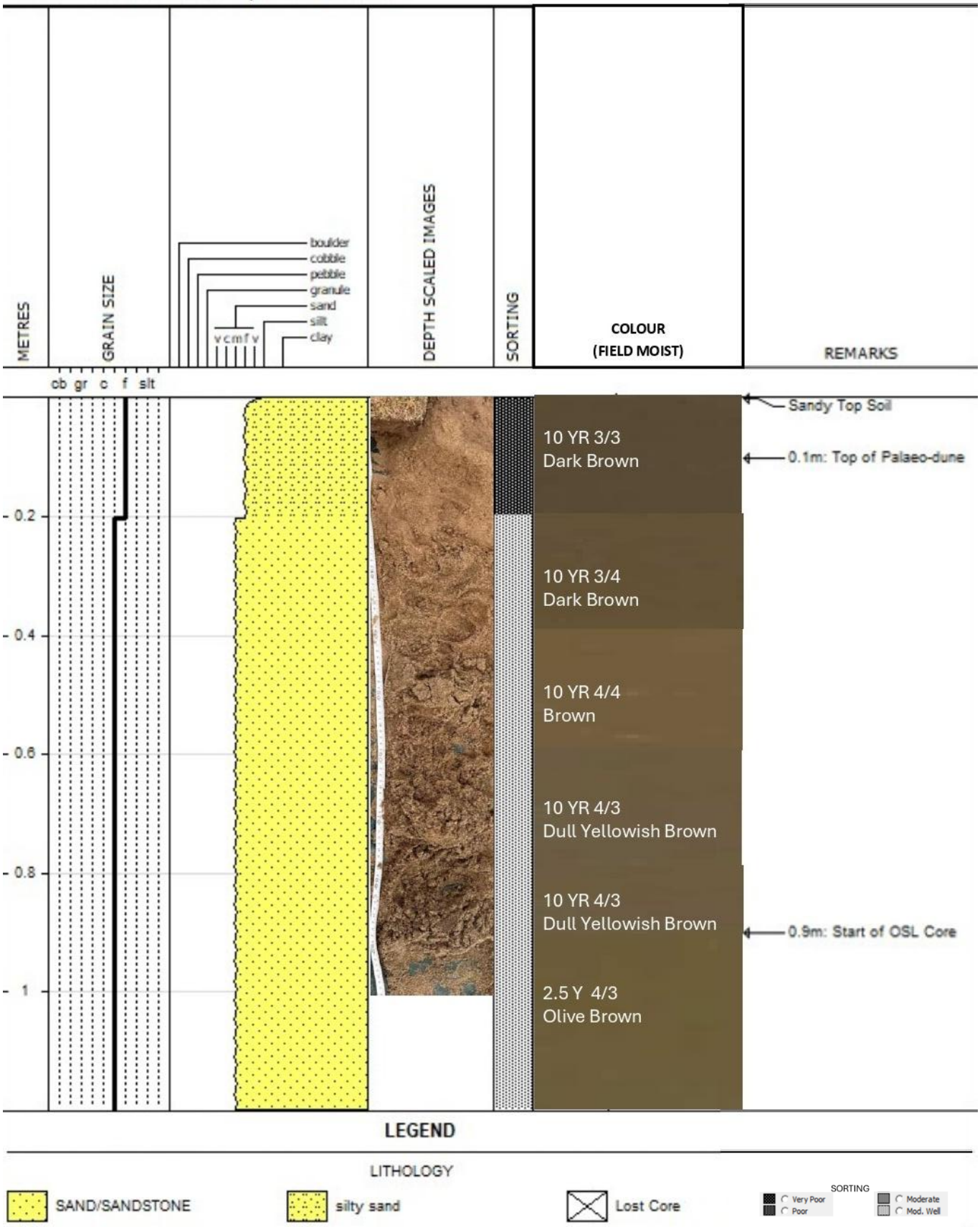

LEGEND

LITHOLOGY

SAND/SANDSTONE | silty sand | Lost Core

SORTING: Very Poor, Poor, Moderate, Mod. Well

RANGI24-7

Whakatane Golf Course (Dune 1 Landward)

Date Logged: November 6th, 2024
Logged by: Bailey Rackham
Ground: 0.00 m KB: 0.00 m
Remarks: S 37.92847, E 176.93378

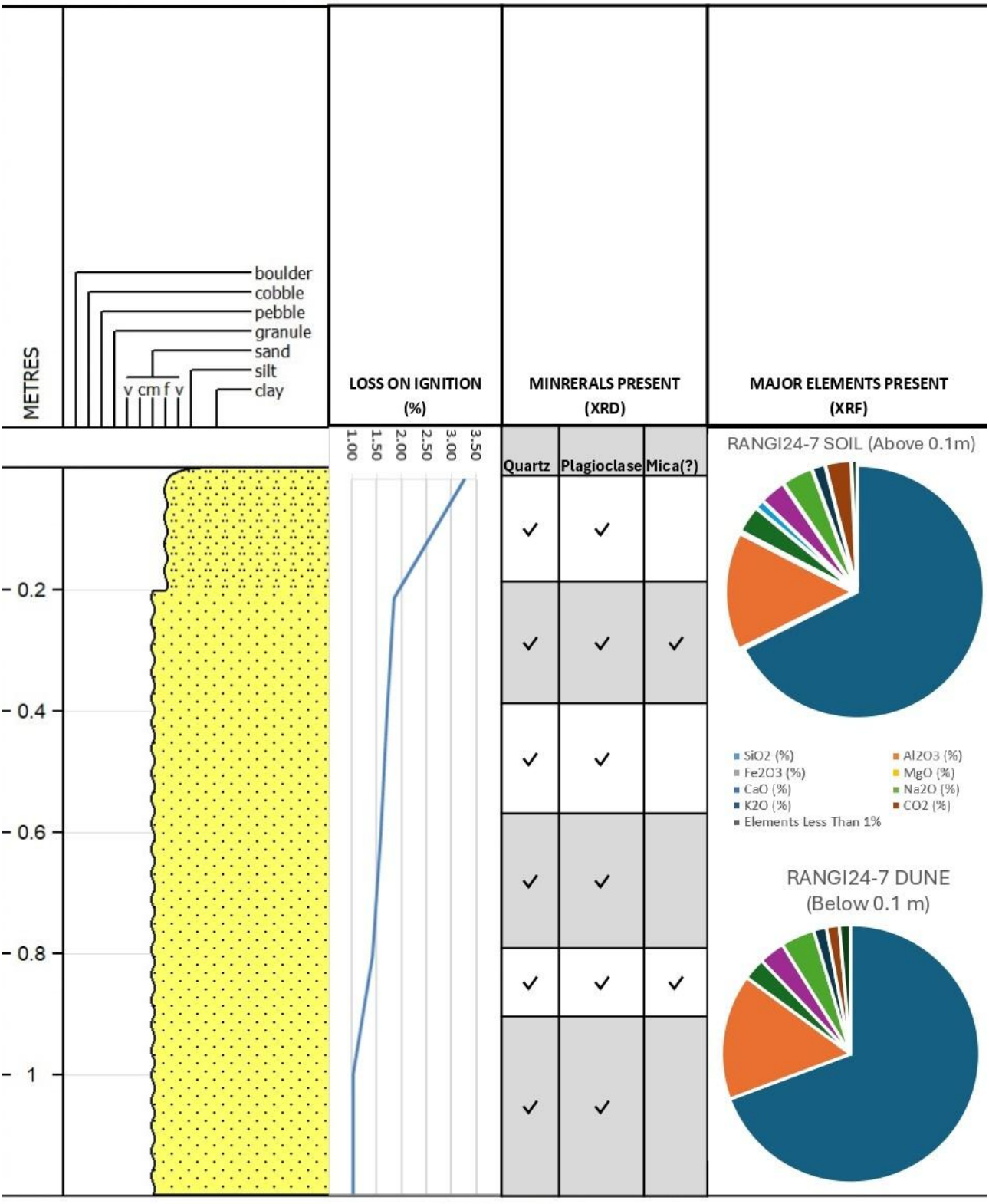

LEGEND

LITHOLOGY

SAND/SANDSTONE

silty sand

Lost Core

RANGI24-08

Airport: Dune 1 Seaward

Date Logged: February 28, 2025
Logged by: Bailey Rackham
Ground: 0.00 m KB: 0.00 m
Remarks: S 37.91532, E176.90518

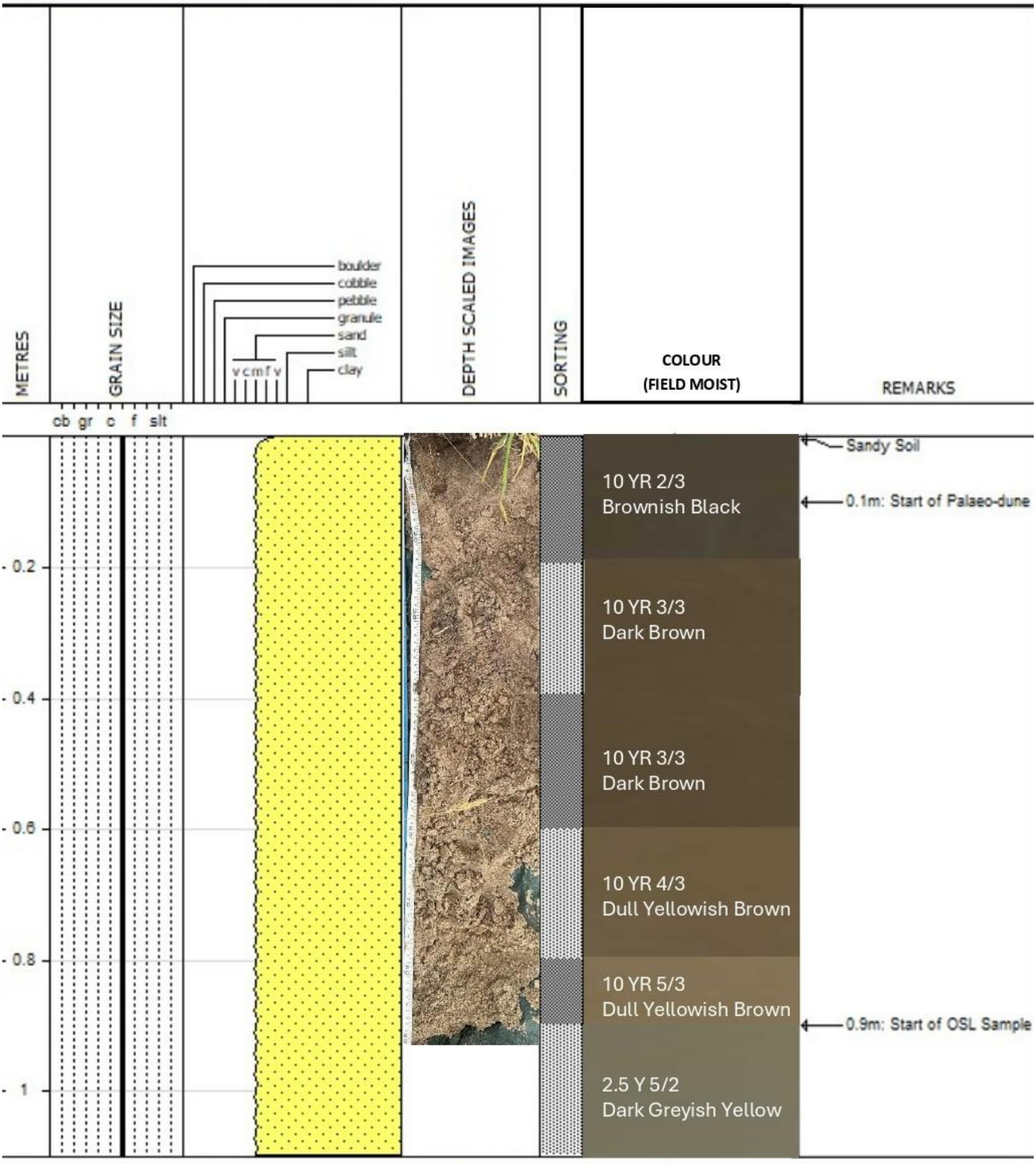

LEGEND

LITHOLOGY

SAND/SANDSTONE

Lost Core

SORTING

Very Poor
Poor
Moderate
Mod. Well

RANGI24-08

Airport: Dune 1 Seaward

Date Logged: February 28, 2025
Logged by: Bailey Rackham
Ground: 0.00 m KB: 0.00 m
Remarks: S 37.91532, E176.90518

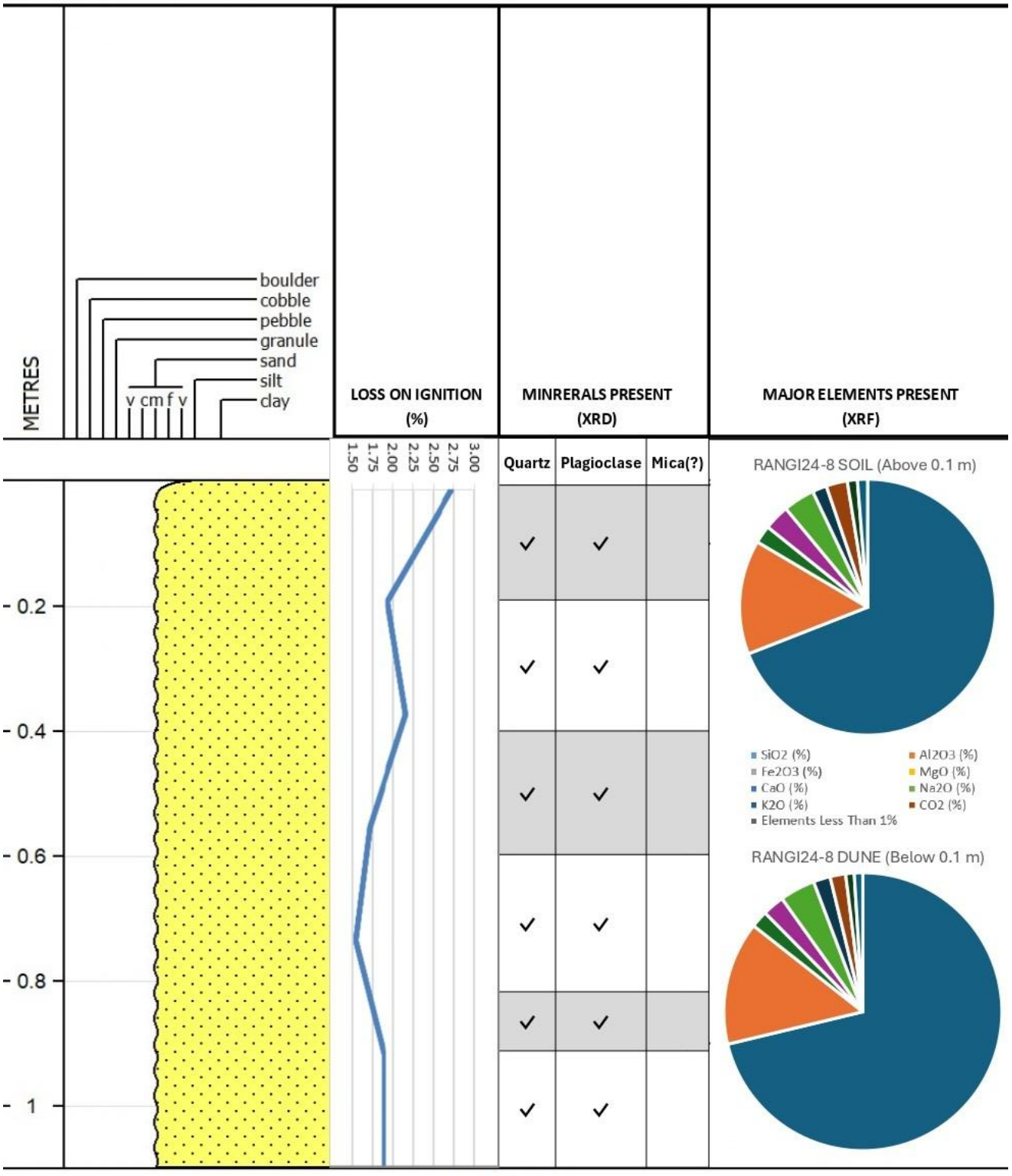

LEGEND

LITHOLOGY

SAND/SANDSTONE

Lost Core

Appendix O: Bay of Plenty Regional Council (2025)

Location of CCS monitoring sites. Coastal Morphology data from 1990 to 2025 available from the Bay of Plenty Regional Council on request.

Site	Longitude	Latitude
CCS12	177 00 04.84147 E	37 56 34.64315 S
CCS13	176 58 43.89086 E	37 56 05.70378 S
CCS14	176 56 32.51080 E	37 55 15.48584 S
CCS15	176 54 24.26831 E	37 54 49.37305 S
CCS16	176 53 29.38424 E	37 54 40.18963 S
CCS17	176 52 16.31402 E	37 54 25.80916 S
CCS18	176 49 13.40575 E	37 53 38.74011 S
CCS19	176 47 43.27889 E	37 53 28.84883 S
CCS20	176 46 08.36496 E	37 53 15.07212 S
CCS21	176 45 03.24324 E	37 53 02.10611 S